Continuous-time Markov Modelling of the Effects of Treatment Regimens on HIV/AIDS Immunology and Virology

Shoko Claris (2015251768)

June, 2019

Continuous-time Markov Modelling of the Effects of Treatment Regimens on HIV/AIDS Immunology and Virology

by

Shoko Claris (2015251768)

A thesis submitted to the
University of the Free State
in fulfilment of the requirements for the degree
of
PHILOSOPHIAE DOCTOR
in
STATISTICS
(APPLIED)

Thesis promoter: Dr Delson Chikobvu

UNIVERSITY OF THE FREE STATE
FACULTY OF NATURAL AND AGRICULTURAL SCIENCES
DEPARTMENT OF MATHEMATICAL STATISTICS AND ACTUARIAL SCIENCE
BLOEMFONTEIN, SOUTH AFRICA

Declaration - Plagiarism

I, Shoko Claris (2015251768), declare that

1. The research reported in this thesis, except where otherwise indicated, is my original research.
2. This thesis has not been submitted for any degree or examination at any other university.
3. This thesis does not contain other persons' data, pictures, graphs or other information, unless specifically acknowlegded as being sourced from other persons.
4. This thesis does not contain other persons' writing, unless specifically acknowledged as being sourced from other researchers. Where other written sources have been quoted, then
   (a) their words have been re-written but the general information attributed to them has been referenced, or
   (b) where their exact words have been used, then their writing has been placed in italics and referenced.
5. This thesis does not contain text, graphics or tables copied and pasted from the internet, unless specifically acknowledged, and the source being detailed in the thesis and in the reference sections.

Shoko Claris (2015251768) Date

Disclaimer

This document describes work undertaken as a PhD programme of study at the University of the Free State. All views and opinions expressed therein remain the sole responsibility of the author, and do not necessarily represent those of the institution.

Science is the knowledge of consequences, and dependence of one fact upon another.
Thomas Hobbes

Abstract

As the Human immunodeficiency virus (HIV) enters the human body, its main target is the CD4+ cell, which it turns into a factory that produces millions of other HIV particles, thus compromising the immune system and resulting in opportunistic infections, for example tuberculosis (TB). Combination Anti-retroviral therapy (cART) has become the standard of care for patients with HIV infection and has led to the reduction in acquired immunodeficiency syndrome (AIDS) related morbidity and mortality, an increase in CD4+ cell counts and a decrease in viral load count to undetectable levels. In modelling HIV/AIDS progression in patients, researchers mostly deal with either viral load only or CD4+ cell counts only, as they expect these two variables to be collinear. The purpose of this study is to fit a continuous-time Markov model that best describes mortality of HIV infected patients on cART by eventually including both CD4+ cell counts monitoring and viral load monitoring in a single model after treating for collinearity of these variables using the Principal Component approach. A cohort of 320 HIV infected patients on cART followed up at a Wellness Clinic in Bela Bela, South Africa, is used in this thesis. These patients are administered with a triple therapy of two nucleoside reverse transcriptase inhibitor (NRTIs) and one non-nucleoside reverse transcriptase inhibitor (NNRTI).

The thesis is divided into five sections. In the first section, a continuous-time homogeneous Markov model based on CD4+ cell count states is fitted. The model is used to analyse the effects of tuberculosis (TB) co-infection on the immunologic progression of HIV/AIDS patients on cART. TB co-infection was of interest because it is an opportunistic infection that takes advantage of the compromised immune system. Results from this section showed that once TB is diagnosed prior to treatment initiation and managed, mortality rates are reduced. However, if TB is diagnosed during the course of treatment, it increases the rates of immune deterioration in patients, leading to high rates of mortality. Therefore, this section proposes the need for routine TB screening before treatment initiation and at every stage of the follow-up period, to avoid loss of lives.

The goal of cART is not only to boost the immune system but also to suppress the viral load to undetectable levels. Thus, in the second section, a non-homogeneous continuous-time Markov model based on viral load states is fitted. This model helped in revealing possibilities of viral rebound among patients on cART. Although there were no significant gender differences on HIV/AIDS virology, the model explained the progression of patients better than the model based on CD4+ cell count fitted in the first section.

In the third section, determinants of viral rebound are analysed. Viral rebound was notable mainly after patients had attained a viral load suppressed to the levels between 50 copies/mL and 10 000 copies/mL. The major attributes of viral rebound were non-adherence, lactic acid, resistance to treatment, and different combination therapy such as AZT-3TC-LPV/r and FTC-TDF-EFV. This section suggests the need to closely monitor HIV patients to ensure attainment of undetectable viral load (below 50 copies/mL) during the first six months of treatment uptake, as this reduces chances of viral rebound, leading to life gain by HIV/AIDS patients.

The fourth section compares the use of viral load count and CD4+ cell count in monitoring HIV/AIDS disease progression on patients receiving cART in order to establish the superiority of viral load over CD4+ cell count. This was done by fitting two separate models, one for CD4+ cell count states and the other one for viral load states. Comparison of the fitted models were based on percentage prevalence plots for the fitted model and for the observed data and likelihood ratio tests. The test confirmed that viral load monitoring is superior compared to CD4+ cell count monitoring. Viral load monitoring is very good at detecting virologic failure, thereby avoiding unnecessary switches of treatment lines. However, this section suggests the use of both CD4+ cell count monitoring and viral load monitoring because CD4+ cell count monitoring helps in managing possibilities of the development of opportunistic infections.

In the fifth section, continuous-time homogeneous Markov models are fitted, including both CD4+ cell count monitoring and viral load monitoring in one model. Since these variables are assumed to be collinear, principal component analysis was used to treat for the collinearity among these two variables. The models are fitted in such a way that when Markov states are based on CD4+ cell count, the principal component of viral load is included as a covariate, and when the Markov states are based on viral load, the principal component of CD4+ cell count is included as a covariate. Results from the models show an improvement in the power of the continuous-time Markov model to explain and predict mortality when both CD4+ cell count and viral

load routine monitoring are included in one model.

Key Words: HIV / AIDS progression; virology; immunology; continuous-time Markov process; principal component analysis; viral rebound; Longitudinal data.

Acknowledgements

This work was carried out in the Department of Mathematical Statistics and Actuarial Sciences at the University of the Free State. Foremost, I would like to thank my supervisor Dr. Delson Chikobvu for his encouragement, support, and advice throughout the years, and for creating an inspiring environment where I could follow my own ideas. Thank you for giving me the opportunity to carry out this project.

This study would not have been a success without the assistance of the Microbiology Department at the University of Venda, in providing the secondary data, through Professor Pascal O. Bessong. We also thank the participants of the study.

I am grateful to my husband Munashe Shoko and my daughters, Zandile, Anenyasha and Matidashe for their patience, support and motivation throughout the study period. To my daughters, I would like to say, "Mama is building a legacy for you." Finally and most importantly, I wish to thank God for giving me the strength and courage to continue with the studies regardless of the difficulties along the way.

Contents

List of Figures

List of Tables

Abbreviations

3TC	lamivudine
ABC	abacavir
AIDS	acquired immunodeficiency syndrome
AZT	zidovudine (also known as ZDV)
cART	combination antiretroviral therapy
CD4	Tlymphocyte cell bearing CD4 receptor
d4T	stavudine
ddI	didanosine
DNA	deoxyribonucleic acid
EFV	efavirenz
FTC	emtricitabine
HIV	human immunodeficiency virus
LPV	lopinavir
LPV/r	lopinavir/ritonavir
NFV	nelfinavir
NNRTI	non-nucleoside reverse-transcriptase inhibitor
NRTI	nucleoside reverse-transcriptase inhibitor
NVP	nevirapine
PCA	principal component analysis
PI	protease inhibitor
RNA	ribonucleic acid
TB	tuberculosis
TDF	tenofovir disoproxil fumarate
UNAIDS	Joint United Nations Programme on HIV/AIDS
AIC	Akaike Information Criterion
CD4BL	Cluster Difference 4 Baseline
LA	Lactic acidosis
MSM	Multi-state modelling
NA	non-adherence
PWC	Piece-wise constant
RTI	Reverse Transcriptase Inhibitors

Research Output

A list of research output from this thesis is given below.

Peer-reviewed Journal Publications

1. Shoko C. and Chikobvu D. Time-homogeneous Markov process for HIV/AIDS progression under a combination treatment therapy: cohort study, South Africa. *Theoretical Biology and Medical Modelling* (2018) 15:3. DOI: 10.1186/s12976-017-0075-4

2. Shoko C and Chikobvu D. Determinants of Viral Load Rebound on HIV/AIDS Patients Receiving Antiretroviral Therapy: Results from South Africa. *Theoretical Biology and Medical Modelling* (2018) 15:10. Doi: 10.1186/s12976-018-0082-0

3. Shoko C and Chikobvu D. A superiority of viral load over CD4 cell count when predicting mortality in HIV patients on therapy. *BMC Infectious Disease.* (2019) 19:169. DOI: 10.1186/s12879-019-3781-1

4. Chikobvu D and Shoko C. A Markov Model to estimate Mortality due to HIV/AIDS using CD4 cell counts based states and viral load: A Principal Component Analysis approach. *Biomedical Research* 2018; 29 (15): 3090-3098

5. Shoko C, Chikobvu D and Pascal O. Bessong. A Markov Model to estimate Mortality due to HIV/AIDS using viral load levels based states and CD4 cell counts: A Principal Component Analysis approach. *Infectious Disease and Therapy* (2018), 2 November 2018. Doi: 10.1007/s40121-018-0217-y.

6. Shoko C, Chikobvu D and Bessong P.O. A Comparison of the Time Homogeneous and Time Non-homogeneous Markov models for monitoring HIV/AIDS progression based on viral load: Results from Patients on ART. *Biomedical Research Journal* 2019; 30 (5): 786-795.

7. Shoko C, Chikobvu D and Bessong P.O. A Markov model for the effects of virologic failure on HIV/AIDS progression in TB co-infected patients receiving antiretroviral therapy in a rural clinic in northern South Africa. *South African Medical Journal*. *(Accepted on the 8th July 2019)*

Conference Presentations

1. Chikobvu D and Shoko C. A Markov Model to estimate Mortality due to HIV/AIDS using CD4 cell counts based states and viral load: A Principal Component Analysis approach. Conference, South African Statistics Association, 26-30 November 2018. University of South Africa

Chapter 1

Introduction

1.1 Background of the study

The Joint United Nations Programme on human immunodeficiency virus/acquired immunodeficiency syndrome (HIV/AIDS) (UNAIDS) estimates show that approximately 35 million people globally are living with HIV, and tens of millions have died of AIDS-related illnesses by the end of 2014. Although Sub-Saharan Africa constitute a small fraction of the world population, approximately 68% of the HIV/AIDS cases have been reported in Sub-Saharan Africa (UNAIDS, 2013). In Sub-Saharan Africa, 23.4 million people were HIV positive by 2011 (UNAIDS, 2012). South Africa was leading with 5.6 million, followed by Nigeria with 3 million HIV positive individuals.

In 2016 UNAIDS provided estimates of global, regional and country-specific progress against the 90-90-90 target. Basic indicators have been used to monitor progress towards these targets. The indicators are as follows: (i) 90% of all people living with HIV should know their HIV status; (ii) 90% of all people who know their HIV status should access treatment; and (iii) 90% of all people on treatment should have suppressed viral load. Indicators (ii) and (iii) give information on the percentage of people living with HIV. If the coverage of treatment target is calculated relative to people living with HIV, this is typically called "the HIV treatment cascade" (Myhre and Sifris, 2018). Using this cascade, the 90-90-90 target translates to 81% coverage of anti-retroviral therapy (ART) and 73% of people achieving viral suppression by 2020.

New global efforts have been implemented to address the challenges caused by the HIV epidemic. Some of the efforts include introduction of ART in 1996, use of condoms, HIV/AIDS awareness campaigns, counselling, to mention but a few (Coates et al., 2008). However, because of the stigma associated with HIV/AIDS, many peo-

ple still do not want to get tested. Coupled with the inaccessibility of treatment, prevention and care, HIV has remained a challenge in the Sub-Saharan Africa region (Kharsany and Karim, 2016).

South Africa has one of the worst epidemics of HIV in the world (UNAIDS, 2010). Studies show that one in every five people in the world with HIV infection lives in South Africa (Moorhouse et al., 2016). Thus, if the world is going to end the AIDS epidemic, then South Africa has a big role to play. The South African government has agreed to provide ART to all people infected with HIV, irrespective of the CD4 cell count (hit early and hit hard policy). A study by Williams et al. (2017) suggested that South Africa is on the road to reducing HIV incidence and AIDS-related mortality substantially by 2030. South Africa has the best HIV surveillance system (Ingram, 2007; Swanevelder et al., 1998) and has one of the highest levels of ART provision (UNAIDS, 2010).

The current levels of ART provision in South Africa have reduced prevalence of HIV among those on ART by 1.9 million, averted 259 thousands of new infections and 428 thousands deaths (Williams et al., 2010). Although ART substantially reduces the risks of developing active tuberculosis (TB) by 60%, people on ART are still at greater risks of developing active TB than those who are not infected with HIV (Williams et al., 2010).

South Africa should be committed to getting as many people onto ART, while ensuring high levels of adherence and suppression of viral load counts to end AIDS in South Africa by 2030 (Williams et al., 2017). In addition to that, South Africa should ensure good patient monitoring, support and routinely collect data to monitor progress of HIV/AIDS patients.

Monitoring of the progress of HIV infected patients involves gathering routine data on CD4 cell count and viral load count. In the year 2000, there were uncertainties regarding the use of either CD4 cell markers or viral load markers in controlled trials (Erb et al., 2000).

Although the viral load count is very expensive to measure, it is the most useful in measuring the effectiveness of ART after initiation. Some researchers argue that lack of viral load count monitoring leads to delayed and unnecessary switches to second line therapy, resulting in development of resistance to treatment and limitations to treatment options (Salazar-Vizcaya et al., 2014). Other researchers argue that viral load count appears to be the best predictor of long-term clinical outcome, whereas

CD4 cell count predicts clinical progression and survival in the shorter term (Erb et al., 2000). Brennan et al. 2013, in their research to determine the interplay between CD4 cell count and viral load count, argued that long-term virological suppression plays an important role in ensuring the recovery of CD4 cell count to levels that reduce the risk of opportunistic infection and increase life expectancy.

In this study, both viral load count and/or CD4 cell count are used in assessing, monitoring and management of patients receiving ART. Continuous-time Markov models with states based on either CD4 cell count or viral load count are used. Factors associated with viral rebound, effects of TB co-infection on HIV progression, superiority of viral load count over CD4 cell count in HIV/AIDS monitoring, and the Principal Component Approach (PCA) to the inclusion of both CD4 cell count and viral load count monitoring in one Markov model are assessed.

1.2 Statement of the problem

Mathematical models have been extensively used in research into the epidemiology of HIV/AIDS because they play an important role in improving our understanding of major factors contributing to the spread of this virus (Moysis et al., 2016; Cassels et al., 2008; Waziri et al., 2012; Rivadeneira et al., 2012; Duffin and Tullis, 2002). It has also been argued that multi-state stochastic models are useful tools for studying complex dynamics such as chronic disease, and also in determining factors associated with the progression between different stages of the disease (Naresh et al., 2006; Dessie, 2014).

Progression of HIV at individual level is fully described by the interaction between CD4 cell count and the HIV ribonucleic acid (RNA). However, for most of the studies, states of the Markov processes are mostly based on either simulated data or CD4 cell counts. This thesis uses either CD4 cell counts and/or viral load count in assessing, monitoring and management of treatment of HIV infected patients. The superiority of viral load count monitoring over CD4 cell count monitoring is analysed. In addition, determinants of viral rebound in HIV infected patients are assessed. The thesis further addresses the collinearity problem between viral load count monitoring and CD4 cell count monitoring. The problem is addressed by including both variables in one model, after Principal Component Analysis is used to treat for collinearity and this also improves the efficiency of the model, thus giving a better prediction of mortality.

In this research, a continuous-time-homogeneous Markov jump process is used to

model the progression of HIV/AIDS patients. HIV/AIDS progression is based on either viral load count states (measured in copies/mL) or CD4 cell counts states (measured in copies/mm^3), followed by the end point (absorbing state), which is death. The inclusion of both the viral load count monitoring and/or CD4 cell counts monitoring in the same model, makes this research different from previous studies.

1.2.1 Study aim and objectives

The major aim of this study is to develop a model that allows inclusion of either CD4 cell count or viral load count, or both, to monitor HIV/AIDS patients on ART. Effects of TB co-infection on HIV immunology and virology are assessed. The determinants of viral rebound on HIV virology are also assessed. The Principal Component Analysis (PCA) is used to treat for collinearity among CD4 cell count and viral load count and thus, improving the efficiency of the model. The objectives are:

1. To fit a time-homogeneous Markov model that assesses the effects of TB co-infection on HIV/AIDS immunological progression.
2. To fit a time-inhomogeneous Markov model that explains HIV/AIDS virological progression.
3. To fit a continuous-time homogeneous Markov model for the determinants of viral rebound on HIV/AIDS patients receiving different treatment combinations in South Africa.
4. To fit continuous-time homogeneous Markov models to analyse the superiority of viral load count monitoring over CD4 cell counts monitoring of HIV/AIDS progression in infected patients.
5. To fit a time-homogeneous Markov model that predicts mortality in a more efficient way by including both viral load count and CD4 cell counts variables after using the PCA to treat for collinearity of CD4 cell count and viral load count.

1.3 Significance of the study

The knowledge of HIV/AIDS virology and immunology helps in understanding the treatment mechanism of the HIV/AIDS disease. This leads to increased life expectancy of infected patients, achieving suppressed viral load count to undetectable levels, maintaining undetectable viral load count, reduction of viral rebound, reduction of HIV/AIDS morbidity and mortality, and consequently eradicating HIV from the human population. Within the first 3 months of treatment uptake, most

HIV/AIDS patients achieve an undetectable viral load but they take long to achieve normal CD4 cell counts. Therefore, there is need to monitor both viral load count and CD4 cell counts for patients on treatment and not to completely rely on one variable. A continuous-time Markov modelling approach to multi-state modelling plays an important role in determining the drivers of viral load count rebound or immune suppression in every state of HIV/AIDS progression.

1.4 Contributions

The major contribution of this thesis is in applying mathematical techniques in modelling HIV/AIDS progression based on either CD4 cell counts or viral load monitoring using longitudinal data collected from a Wellness clinic in Bela Bela, South Africa. Results from the analysis help to inform stakeholders on the best ways of monitoring and management of combination anti-retroviral therapy (cART) to improve lives of HIV/AIDS patients. The contributions are:

1. Modelling the effects of TB co-infection on HIV immunology. This is done using continuous-time homogeneous Markov processes with states defined using CD4 cell counts. Although Markov models based on CD4 cell counts is a common approach in HIV/AIDS modelling, this is clinically unique in that TB co-infection is included as a covariate.

2. Very few studies used the non-homogeneous continuous-time approach to Markov modelling of HIV/AIDS progression, and in particular, the use of viral load monitoring is rare, mainly due to unavailability of data. Non-homogeneous models reveal the interval in which viral rebound occurs. This thesis develops a non-homogeneous Markov model with states defined virologically. This is done using the piece-wise constant transition rate approach.

3. In developing countries, the nucleosides reverse transcriptase inhibitors (NRTIs) class are widely used because of their low production costs. For this study, patients are administered with a triple therapy of two NRTIs and one non-nucleoside reverse transcriptase inhibitor (NNRTI). However, patients treated with NRTIs develop varying degree of toxicity after long-term therapy, leading to virologic rebound. In this thesis, a Markov process is used to assess the determinants of viral rebound on patient receiving cART. These determinants include cART, non-adherence, lactic acidosis and peripheral neuropathy, among others.

4. Application of continuous-time Markov modelling in assessing the superiority of viral load over CD4 cell counts in monitoring and management of

HIV/AIDS disease progression on patients receiving combination anti-retroviral therapy (cART) is done. Most countries, especially in Sub-Saharan Africa, rely on CD4 cell count monitoring of HIV progression. This has led to unnecessary switching of treatment line, which then causes drug resistance and limitations of treatment options. This thesis addresses the uncertainties regarding the use of either viral load or CD4 cell count in monitoring HIV/AIDS progression in controlled trials.

5. Most studies on HIV progression rely on either CD4 cell count or viral load counts only to monitor and manage cART because of the collinearity between these two variables. This thesis is unique in that both CD4 cell count and viral load counts variables are used in one model, and collinearity between these two variables is treated for using the Principal Component Analysis (PCA).

1.5 Thesis layout

Given the background and the objectives, the rest of this thesis is organised as follows: **Chapter 2** explores the literature on HIV/AIDS modelling. Findings from previous researchers are highlighted and their differences from the current studies are discussed.

Chapter 3 gives an overview of the methodology on continuous-time Markov modelling. It demonstrates how the basic parameters are computed, including the maximum likelihood estimation of these basic parameters. Techniques used in the selection of the best Markov model are also discussed. Important theorems, their proofs and examples are given.

In **Chapter 4**[1], a continuous-time Markov model based on CD4 cell count states is fitted to assess the effects of TB co-infection on HIV/AIDS progression. The virus causes severe depletion of the immune system/severe reduction in CD4+ T-cells. This leaves the infected person exposed to co-infections which, among others, include TB co-infection. This justifies the use of CD4-based states in modelling HIV progression for TB co-infected patients. However, CD4 cell count monitoring has got its shortcoming, that of failing to detect virologic failure leading to unnecessary treatment switches.

[1]Time-homogeneous Markov process for HIV/AIDS progression under a combination treatment therapy: cohort study, South Africa. *Theoretical Biology and Medical Modelling* (2018) 15:3. DOI: 10.1186/s12976-017-0075-4

To address the above shortcoming, in **Chapter 5**[2], a time inhomogeneous Markov model for HIV/AIDS virological progression is fitted. The model fitted in **Chapter 5** helps to detect virologic failure/rebound on patients receiving combination antiretroviral therapy (cART).

In **Chapter 6**[3], the determinants of viral rebound in HIV/AIDS patients are analysed. Although, the models based on viral load counts monitoring are very good at detecting virologic failure, these models have a weakness of failure to explain mortality of HIV/AIDS patients. In order to come up with a model that guides decision making, CD4 cell count based model is compared with the viral load based model in **Chapter 7**[4].

In **Chapter 7**, the superiority of viral load count levels monitoring over CD4 cell count monitoring is assessed by fitting two continuous-time Markov models, one based on CD4 cell count and the other one based on viral load count levels, and comparison of these models is based on the plots of observed versus expected percentage prevalences. Although likelihood ratio tests and the plots of observed versus the fitted model revealed that viral load count monitoring is superior, the model for viral load monitoring fails to explain the effects of gender on progression of HIV patients. Thus, in **Chapters 8**[5] and **9**[6], including both CD4 cell count and viral load count in one model is proposed so that the mortality of patients is better explained and also to address the effect of gender differences on the progression of HIV.

In **Chapters 8** and **9**, both CD4 cell count and viral load levels monitoring are used in one model and the collinearity between these variables is treated for using the PCA. In **Chapter 8**, the states are CD4 cell count based and the Principal Component of viral load count levels is used as a covariate, and in **Chapter 9**, viral load count states are used and CD4 cell count is used as a covariate. The models in **Chapters 8** and **9** explain mortality better than the models with ether CD4 cell count alone or viral load count alone.

[2] A Comparison of the Time Homogeneous and Time Non-homogeneous Markov models for monitoring HIV/AIDS progression based on viral load: Results from Patients on ART. *Biomedical Research*

[3] Determinants of Viral Load Rebound on HIV/AIDS Patients Receiving Antiretroviral Therapy: Results from South Africa. *Theoretical Biology and Medical Modelling* (2018) 15:10. Doi: 10.1186/s12976-018-0082-0

[4] A superiority of viral load over CD4 cell count when predicting mortality in HIV patients on therapy. *BMC Infectious Disease.* (2019) 19:169. DOI: 10.1186/s12879-019-3781-1

[5] A Markov Model to estimate Mortality due to HIV/AIDS using CD4 cell counts based states and viral load: A Principal Component Analysis approach. *Biomedical Research* 2018; 29 (15): 3090-3098

[6] A Markov Model to estimate Mortality due to HIV/AIDS using viral load levels based states and CD4 cell counts: A Principal Component Analysis approach. *Infectious Disease and Therapy* (2018), 2 November 2018. Doi: 10.1007/s40121-018-0217-y.

Finally, **Chapter 10** discusses the findings, concludes the study, and highlights possibilities for future research.

Chapter 2

Literature Review

2.1 Introduction

In this chapter, a literature overview of the key aspects of the study is explored. The origin of HIV, HIV pathogenesis which is defined immunologically (based on CD4-T cells) and virologically (based on HIV RNA), the interplay between cART and HIV/AIDS progression, and relevant studies in the modelling of HIV/AIDS progression from previous research are reviewed.

2.2 Origin of HIV/AIDS

The human immunodeficiency virus (HIV), the virus that causes acquired immunodeficiency syndrome (AIDS), originated from non-human primates in the Democratic Republic of Congo around the 1920s (Faria et al., 2014; Sharp and Harn, 2011). AIDS is caused by two lentiviruses, human immunodeficiency virus types 1 and 2 (HIV-1 and HIV-2 respectively) (Sharp and Harn, 2011; Kandathil et al., 2005; Rambaut et al., 2004). The global pandemic originated in the emergence of one specific strain, HIV-1 subgroup M (main), in Lepoldville in the Belgian Congo (now Kinshasa in the Democratic Republic of Congo) between 1915 and 1941 (Lihana et al., 2012; Sharp and Harn, 2011; Worobey et al., 2008).

HIV/AIDS was clinically defined in the early 1980s and by that time approximately between 100 000 and 300 000 people across all continents could have been infected (Mann, 1989) and it gained prominence in the international community as a disease of the young homosexual men (Greene, 2007). AIDS was first recognised as a new disease when a number of homosexual men succumbed to unusual opportunistic infections and rare malignancies (Greene, 2007; Sharp and Harn, 2015). In South Africa, HIV/AIDS entered simultaneously through homosexual and heterosexual

populations (Schneider and Stain, 2001).

When anti-retroviral drugs were first introduced, therapy was delayed because of side effects, a limited understanding of the drug toxicities, and concerns over drug resistance. However, anti-retroviral therapy (ART) has improved dramatically over the last 10 to 15 years and people on ART can now expect to live out a normal life (Gouws, 2011).

Mathematical models are very useful in facilitating the understanding of the complex dynamics of many biomedical systems such as epidemiology, ecology and virology (Xie et al., 2017). Epidemiology is the cornerstone of public health that informs policy decisions and evidence-based practice by identifying risk factors of diseases and targets for prevention health care (Frerot et al., 2018). It involves studying the patterns, causes and effects of health and disease conditions in defined populations (Gouda and Powles, 2014).

Mathematical models help to improve understanding of disease dynamics such as HIV/AIDS, by providing alternative ways to study the effects of different drugs (Heesterbeek et al., 2015). For example, studying the dynamics between HIV RNA and CD4+ cellular populations.

In particular, stochastic processes are very important in modelling HIV/AIDS because real life is stochastic rather than deterministic (Clemencon et al., 2008). The randomness both in the different states of the infection and in the time spend in each state, the randomness in the evolution of the infection taking into account the ages of patients, are a resemblance of stochastic processes.

2.3 HIV pathogenesis

Knowledge of the principal mechanism of viral pathogenesis, namely binding of the retrovirus to the gp120 protein in the CD4 cell, the entry of the HIV RNA into the target cell, the reverse transcriptase of the HIV RNA to HIV DNA, the integration of the HIV DNA with that of the host, the viral regulatory processes meditated through regulatory proteins and the reaction of the viral protease in cleaving viral proteins into mature products, have led to the design of drugs (chemotherapeutic agents) that help to control the reproduction of HIV (Yadavalli et al., 2009). The anti-retroviral drugs are designed in such a way that they inhibit all these stages, in particular the reverse transcriptase inhibitors (non-nucleosides) and the protease inhibitors (saquinavir), thereby reducing the viral load count substantially (Sanchez

et al., 2006).

The progression of HIV/AIDS in patients on cART varies from individual to individual due to a number of factors that include gender, age, CD4 cell count at baseline, viral load count at baseline, non-adherence to treatment, development of adverse effects like peripheral neuropathy and lactic acid, development of TB co-infection before treatment commencement or during the course of treatment uptake, change of treatment line or treatment regimen, among others. Despite these individual variations, the course of HIV infection follows, generally, an exponentially increasing pattern in viral load count in the first 3 to 6 weeks following infection (Alizon and Magnus, 2013). This marks the early phase of HIV infection referred to as the primary infection phase or the initial phase.

After the initial high infection phase, HIV infection exhibits a long asymptomatic (chronic) phase of approximately up to 10 years, known as the incubation period (Yadavalli et al., 2009). During this incubation period, a patient looks well, leading to a significant contribution to the spread of the epidemic within a community. With the onset of a cellular immune response, viral load count decreases and settles at a constant value for several years. At this phase, there is a rapid turnover of infected CD4 cells and it is this cellular and the humoral immune response that keep the viral load count to a constant level, referred to as a viral set point (Alizon and Magnus, 2013). During this period, the within host CD4 cells decrease because they are the target of the virus.

The third phase is called the AIDS phase. This phase is characterised by a dramatic loss in CD4 cells and a strong increase of the viral load count (Alizon and Magnus, 2013). At this phase, the CD4 cell count in the blood falls below 200 cells per mm^3 of blood. The AIDS phase often coincides with a shift in the virus population and the emergence of virus strains that are able to use CXCR4 co-receptors (instead of CCR5 co-receptors) and thus, a wider range of immune cells become susceptible to the virus. Due to fragility in the immune system, a person suffers from a variety of opportunistic infections such as TB, diarrhoea, pneumonia and many others. Furthermore, within host genetic diversity tends to decrease during this phase.

The progression of HIV/AIDS infection is divided into three stages as shown in Figure 2.1 below.
Clinical markers such as CD4 cell count and viral load count provide information about the progression of HIV/AIDS in infected individuals (Yadavalli *et al.*, 2009). As a result, the pathogenesis of HIV can be predicted by the two basic factors. These

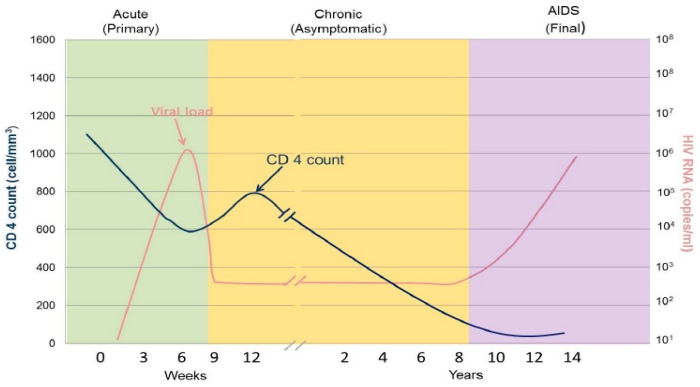

Figure 2.1 – *An illustration of the different stages of HIV infection. Source: Manoto SL., Lugongolo M., Govender U. and Mthunzi-Kufa P. Point of Care Diagnostics for HIV in Resource Limited Settings: An Overview. Medicina 2018, 54, 3; doi:10.3390/medicina54010003*

factors are immunological factors, based on CD4 cells and the virological factors, based on the HIV RNA (that is, viral load count). These factors, combined together, can give us a clear picture as to how HIV/AIDS evolves within an individual as well as within the community.

2.3.1 Immunological factors

The CD4 cells are fundamental to the development of immune responses to infection. As a result of HIV infection, the CD4 cells are destroyed. The depletion of the CD4 cells severely limits the host response capacity (Portela and Simpson, 1997; Langford et al., 2007). According to the United States Department of Health and Human Resources (DHHR), commencement of anti-retroviral treatment is based on the CD4 cell count. Currently the World Health Organisation (WHO) stage baseline upon initiation of therapy is at 500 cells per mm^3 of blood plasma or below (COHERE in EuroCoord, 2012). However, concern about resistance (Richman et al., 2004), inadequate adherence (Paterson et al., 2000) and toxic effects (Carr et al., 1998), led to a shift to delay initiation of treatment until later stages of HIV disease. The immunological recovery is largely dependent on baseline CD4 cell count and as a result, the timing of cART initiation is important in order to maximise the CD4 cell response to therapy (Battegay et al., 2006). Some studies have shown that initiation of treatment at higher CD4 cell count maximises the response to therapy (Kranzer et al., 2010).

The influence of CD8 T-lymphocyte on HIV progression is also of considerable interest, as cytotoxic T-lymphocytes (CTLs) are the main effector cells of the specific cellular response. Activated by CD4+ T-helper cells, the anti-HIV specific CD8+ T-

cells have a crucial role to play in the control of viremia. The population of these cells increases in response to the ongoing viral replication (Langford et al., 2007; Portela and Simpson, 1997). According to the research by Langton et al. (2007), low absolute numbers of HIV-specific CD8+ T-cells correlate with poor survival outcomes in both ART-naive and experienced patients, providing evidence of the CTL response. Lower CD4 cell counts are highly associated with greater risk of disease progression.

2.3.2 Virological factors

When the HIV RNA enters the human body, it is attracted to the cell with appropriate CD4+ receptor molecule, where it attaches itself to the susceptible cell membrane. This process is facilitated by the proteins gp41 and gp120, that are present in the cell membrane (Portela and Simpson, 1997; Mbogo, 2013). The virus then transfuses the viral RNA and other important proteins into the host cell, where the viral RNA is reverse transcribed into the DNA, which then integrates with the host cell's DNA. At this stage the virus commandeers the mechanisms of the cell to start producing copies in the form of poly-protein which are cut into proteins using protease. Finally, the viral RNA and these proteins assemble near the cell membrane and bud out, ready to infect other CD4 cells. The process of budding out causes the depletion of the CD4 cells.

According to the report on CD4 cell count and viral load count levels monitoring of 2011, viral load count level is the best indicator of the level of HIV activity in the patient's body (UNAIDS, 2011) and also the single most predictor of HIV transmission (Kranzer et al., 2013). Thus, a person with very high viral load count levels is highly infective, whereas a patient with undetectable viral load count may not be infective. In the United States, they most commonly use HIV viral load count to monitor the success or failure of ART (Hirchhorn et al., 2005). Just like the CD4 cell count, the viral load count level can also be used to determine the progression of HIV and to manage cART. Therefore, viral load response is also used as a surrogate marker of efficacy in ART drug trials and in clinical practice. Virologic response to treatment varies widely, as do the definitions and patterns or virological response and success (Hirschorn et al., 2005).

Once an individual has been diagnosed with HIV and has reached the stage of the infection, that individual is introduced to cART. cART has the advantages of suppressing viral replication at different stages of the HIV life cycle, leading to the reduction of plasma viremia often below the level of detectability by commercially available tests. However, changes in technological advances over time have decreased the

lower limit of detection from under 10 000 copies/mL to less than 20 copies/mL (Hirschhorn, *et al.*, 2005). In this thesis a limit of detection of 50 copies/mL is used.

The virological response to cART varies from individual to individual. The range of possible virologic responses to cART include failure to ever see a virologic response, any decline without achieving suppression, decline followed by rebound, ever achieving suppression, durable suppression over time, suppression with rare or very low viral blips, intermittent suppression with higher level rises in viral load count, and loss of suppression after it has been achieved.

Although the ideal outcome of treatment is viral load count suppression below the level of detection, virologic response to cART varies widely as do the definitions and patterns of virologic response used in guidelines and studies. However, it is important to note that, not everyone on cART can reach viral load suppression due to the following factors: viral resistance, poor adherence, poor absorption, altered bio-availability, drug-drug interactions, and co-morbid illness. These might derail progress towards the 90-90-90 treatment targets set by UNAIDS (2013). That is, by 2020, 90% of HIV infected patients will be diagnosed, 90% of the diagnosed will be on cART and 90% of those receiving cART will have the virus suppressed as mentioned earlier on in Chapter 1.

2.4 The interplay between HAART and HIV RNA population growth

The development of Highly Active Antiretroviral Therapy (HAART) has substantially reduced the death rate from HIV (Palella et al., 1998). HAART reduces viral load count levels of circulating HIV by blocking replication at multiple points in the virus life cycle (Cole et al., 2007), resulting in an increase in CD4 cell counts and increased life expectancy of individuals infected with HIV. This has made CD4 cell counts and viral load counts the fundamental laboratory markers regularly used for patient management (Mathieu et al., 2007), in addition to predicting HIV/AIDS disease progression or treatment outcomes (Hoffman et al., 2010).

Treatment of HIV/AIDS includes a combination therapy to attack the virus at different stages of its life cycle and medication to treat the opportunistic infections that occur with the compromising of the immune system by HIV. The introduction of cART has led to the dramatic reduction in morbidity and mortality (Simon and Ho, 2003; Libin *et al.*, 2007; Shiri, 2011) at both individual level and population level

(Kranzer *et al.*, 2010).

In South Africa, the anti-retroviral therapy available at present is the nucleotides reverse transcriptase inhibitors (NRTIs) class which includes, among others, zidovudine (AZT), didanosine (ddI), lamivudine (3TC) and stavudine (d4T) (Thaker and Snow, 2003). Other NRTIs include abacavir (ABC), tenofovir (TDF) and Emtricitabine (FTC) (Prosperi et al., 2009). NRTIs are most preferred for HIV/AIDS patients in low income countries (Munderi, 2010) because of their low production costs (Kore and Waghmare, 2012).

However, patients treated with NRTIs develop varying degrees of myopathy or neuropathy after long-term therapy (Currier, 2007). AZT causes myopathy, ddI and 3TC cause neuropathy, d4T causes neuropathy or myopathy and lactic acidosis (LA). Studies show that d4T appears to cause lactic acidosis (LA) more frequently than ddI or AZT (Dalakas, 2001; Kore and Waghmare, 2012). In developed countries, d4T is no longer favoured as a consequence of both short-term toxicity (lactic acidosis) and long-term toxicity (lipoatrophy and neurophathy) (Kore and Waghmare, 2012). Neuropathy is long-term in the sense that it is usually associated with late stages of HIV disease as indicated by the presence of opportunistic infections (Simpson, 2002). Thus, it is highly associated with low CD4 cell count and high HIV viral load levels.

Science literature has successfully established the efficiency of cART in controlling HIV. However, its effectiveness depends particularly on the adherence of patients to cART (Silva et al., 2015). Adherence can be defined as the extent to which a person uses a medication according to medical recommendations, inclusive of time, dosing, and consistency (Chaiyachati et al., 2014). Non-adherence results in antiretroviral agents not being able to maintain sufficient concentration to suppress HIV RNA replication in infected cells and to lower the plasma viral load count levels (Chesney, 2000). Poor adherence also accelerates drug-resistant HIV (Chesney, 2000; Chaiyachati et al., 2014).

The development of drug-resistant variants in HIV/AIDS patients under ART makes it difficult to completely eradicate the virus (Hirchhorn et al., 2005). This results in virologic rebound and eventual disease progression (Hirchhorn et al., 2005). But, with proper adherence to treatment, cART has the potential to suppress viral replication, often below the level of detection by commercially available tests (Saint-Pierre et al., 2003).

Although CD4 cell count is a cheaper way of monitoring HIV/AIDS progression for patients on cART, based on the above discussion, its effectiveness, single-handedly, cannot be justified since the major aim of cART is to suppress the viral load. This makes viral load the primary predictor of HIV/AIDS progression within an individual and, consequently, HIV transmission between individuals. Then CD4 cell count comes in to monitor potential development of opportunistic infection.

However, relatively fewer HIV modelling studies include a detailed description of the dynamics of HIV viral load count along stages of HIV disease progression (Case et al., 2012; Herbeck et al., 2014). This could be due to the unavailability of data on viral load, particularly from low- and middle-income countries that have historically relied on monitoring CD4 cell counts for patients on ART because of higher costs of viral load count testing (Lecher et al., 2016). However, sometimes both CD4 cell counts and viral load count information is available.

2.5 Modelling HIV/AIDS progression

Mathematical models have proved to be valuable in the understanding of the dynamics of many biological processes that include epidemiology, ecology, virology and many others. Hence these models contribute to improving the understanding of HIV dynamics such as viral transmission, multiple viral transmission within the host, disease progression and the interplay between viral population growth and drugs or immune responses (Rong et al., 2007; Srivastava et al., 2008; Shiri, 2011). The models allow the description of biological systems in terms of hazards or rates of the process (Shiri, 2011). They also help in the derivation of important insights into the pathogenesis interaction between HIV RNA and CD4+ T-cells.

Mathematical models have been extensively used in research into the epidemiology of HIV/AIDS because they play an important role in improving our understanding of major factors contributing to the spread of this virus. It has also been argued that multi-state stochastic models are useful tools for studying complex dynamics such as chronic disease, and also in determining factors associated with the progression between different stages of the disease (Naresh et al., 2006; Dessie, 2014). The viral evolution in the presence of cART is a stochastic process following a Markov chain of events, with the possibility of forward and backward (bi-directional) transition between states. This is different from the natural viral evolution (which is uni-directional) which follows a Poisson distribution.

However, for most of these studies, states of the Markov processes are based on CD4

cell counts. For example, Titus (2016) analysed HIV dynamics using a discrete-time Markov chain model based on simulated CD4 cell count states. When dealing with real data, the use of a discrete-time Markov model may not apply since the exact time of transitions may not be known. Transitions are assumed to have taken place between observation times, resulting in interval censored data which can easily be handled by continuous-time Markov processes.

Alizon and Magnus (2012) also emphasised the importance of mathematical models in estimating parameters associated with the infection, such as death rate of infected CD4 cells or HIV RNA production rate from longitudinal data. They also highlighted that mathematical models are used to compare hypotheses by estimating parameters for each model, then performing a likelihood ratio test.

Due to their importance in related fields such as biology, mathematical models have been used extensively in the field of medicine to analyse disease progression within a community (deterministic models) or within an individual (stochastic models). However, when modelling biological phenomena, stochastic models are preferred compared to deterministic models, because real life is stochastic. Mathematical models can take many forms, including, but not limited to, dynamic systems, statistical models and differential equations (Charlebois et al., 2007). However, most of the models have been developed from simulated data. Hence there is need to apply these models on real data collected from HIV infected individuals on cART.

As the HIV/AIDS progresses in an individual, there is random movement between states. Stochastic models are very good at handling these random variables. Stochastic processes also allow modelling the effects of covariates such as stages of infection, virus subtype, presence of STIs, sexual practices, condom use, religion, education, age, gender and genes on transition intensities. In particular, continuous-time homogeneous Markov models are usually used to model the evolution in chronic diseases (Saint-Pierre, 2003). Continuous-time homogeneous Markov models have been used since early in the epidemic to model disease progression of HIV/AIDS patients, and there has been some recent renewed interest in the use of these models.

Longini et al. (1989) used a 5-state Markov model based on the clinical indicators of the HIV disease progression. Alioum et al. (1998) estimated the effects of gender, age, mode of transmission and ART on HIV progression using a 3-state Markov model. Reddy (2011) carried out a research, using data from South Africa, almost similar to that of Alioum et al. However, Reddy used a 5-state Markov model with four CD4 cell count based transient states, followed by the absorbing state, cART ini-

tiation. Reddy's model is characterised by high rates of immune deterioration since the study was carried out on patients not receiving cART.

Binquet et al. (2009) used a multi-state Markov model to analyse the impact of gender, intravenous drug use, weight loss, low haemoglobin, CD8 cell count and viral load count on HIV evolution in the era of highly active anti-retroviral therapy (HAART) (Binquet et al., 2009). Recently, Grover et al. (2013) assessed the impact of ART using a 5-staged multistate Markov model and went further to examine the effects of explanatory variables: age, sex and mode of transmission on the transition rates.

Estill et al. (2012) investigated the benefits of viral load count routine monitoring for reducing HIV transmission. They developed a stochastic mathematical model representing 1000 simulations for both CD4 cell count and viral load routine monitoring. Their findings revealed that viral load routine monitoring reduces both cohort viral load count and transmissions by 31%. Goshu and Getahun (2013) used a semi-Markov process to model the progression of HIV/AIDS. They used five CD4 cell counts classified states. They concluded that transition probabilities from a given state to the next worse state increase with time, get to an optimum level at a given time and then decrease with increasing time. In a recent research, Osisiogu and Nwosu (2015), also used the same states as Goshu and Getahun (2013). However, they used a non-stationary Markov chain approach. They examined a cohort from Nnamdi Azikiwe University Teaching Hospital with a follow-up in their CD4 cell counts of the HIV/AIDS patients. Their main finding was that low CD4 cell counts do not generally imply faster rates of patient absorption but, rather, the age of the patient is a relevant factor.

Lee et al. (2014) investigated the most vulnerable racial minority races (African Americans) in the United States and the Caucasians in order to predict the trends of the HIV/AIDS epidemic using a Markov chain analysis. They predicted, from these races, the number of people living with HIV, and mortality due to HIV/AIDS. They observed a stable number of deaths over the years in both races.

Grover et al. (2013) assessed the effects of anti-retroviral therapy on 580 AIDS patients from an ART centre in New Delhi. They used a 5-stage multi-state Markov model to estimate transition intensities and transition probabilities. The states of their model were based on CD4 cell count as follows: state 1 (> 500), state 2 (351 to 500), state 3 (200 to 350), state 4 (< 200) and state 5 (death). They further examined the effects of covariates: age, gender and mode of transmission on transition inten-

sities using a Cox proportional hazards model.

Dessie (2014) used a Markov model based on CD4 cell count to determine the factors associated with the progression between different stages of the disease for individuals on anti-retroviral therapy (ART).

Rose et al. (2015) investigated the analysis of viral load. They developed two frameworks: the single measure viral load count and the repeated measure viral load. Their findings indicated that the repeated measure viral load count has more precision than the single measure viral load count because it utilises all available viral load count data, has more statistical power, and also avoids subjectivity of defining a "window period". Thus, in this study, a repeated measure viral load count monitoring and management using a Markov stochastic model as proposed by Rose and others is used.

In this thesis, both CD4 cell counts and viral load random variables are used to monitor HIV/AIDS progression. A continuous-time homogeneous Markov process is used to model the progression of HIV/AIDS patients. HIV/AIDS progression is defined based on five viral load states, measured in copies/mL, followed by the end point, death. More importantly, among the determinants of HIV/AIDS, both the viral load counts and CD4 cell counts are included in the same model, thus making this research different from previous studies. The CD4 cell count covariate is included and the effect of collinearity with viral load count is corrected for using the Principal Component Approach. In addition to that, effects of non-adherence to treatment, viral load count at baseline (VLBL), age and gender on transition intensities, is assessed. Transitions between the viral load count states is considered to be bi-directional using data recorded from a cohort of 320 HIV+ patients from a wellness clinic in Bela Bela, South Africa.

In the next chapter, the methods used in the thesis are discussed.

Chapter 3

Methodology

This chapter discusses methods and data used in the analysis of the thesis.

3.1 Introduction

The Markov model is named after the Russian mathematician, Andrey Markov (1856-1922) and it represents a general category of processes called stochastic processes. According to Mullins and Weisman (1996), Markov processes are characterised by six basic attributes. These attributes are states, stages, actions, rewards, transitions and constraints. Mullins and Weisman (1996) defined these attributes as follows:

States of a Markov model describe the complete set of mutually exclusive conditions under which the system operates. In medicine, these states represent various levels of disease progression. States can be transient or absorbing. If a state is transient, then once entered, it can be exited with certainty. Absorbing states are such that once entered, there is no escape. For example, sick and death states represent a transient state and an absorbing state, respectively.

Stages of a Markov process are the points in time in which observations of the system are made and data are collected. From each stage, action may be taken and this may be state specific. In terms of disease, this action may involve drug regimen change, performing surgery, dietary modification, or no action at all.

A series of observations made to the system helps to maximise potential benefits or rewards. These rewards can be a speedy recovery, extended years of life, or improved quality of life. A Markov process results in a sequence of rewards that vary from state to state.

State transitions, also known as the laws of motion, describe the likelihood of being in a particular state at some future time, given the current state. The laws of motion determine the probability distribution of the Markov random variable. In a Markov process, constraints are introduced in order to simplify and generalise the progression of the disease states. For example, progression of HIV in the presence of cART, a common constraint is that transitions are bi-directional.

A Markov jump model is useful when a decision problem involves risk that is continuous over time, when the timing of events is important and when important events may happen once or more than once (Sonnenberg and Beck, 1993), for example, risk of mortality in any person, whether sick or healthy. Markov jump models assume that a patient is always in one of a finite number of discrete states, called Markov states. Thus, states of a Markov model are mutually exclusive. All events are modelled as transitions from one state to another. Each state is assigned a utility and the contribution of this utility to the overall prognosis depends on the length of time spent in each state. For example, for a patient who is HIV positive, these states could be HIV+ (CD4 cell count above 200 cells/mm^3), AIDS (CD4 cell count below 200 cells/mm^3) and Dead. Markov models are ideal for use in studies of HIV/AIDS because they estimate the rates of transition between multiple disease states while allowing for the possible reversibility of some states (Hubbard and Zhou, 2011). The time horizon is divided into continuous equal increments of time, called Markov cycles. During each cycle, a patient makes transitions from one state to another or remains in the same state.

3.2 Markov models: An overview

The materials in this section are in the literature (Cox and Miller, 1965; Chiang, 1968; Kay, 1986). The Markov property can be defined formally as follows:
Definition 1 (*Markov property*): A one-parameter sequence of random variables $X(1), X(2), X(3), ...$ is a Markov process with respect to the filtration $\{\boldsymbol{F}\}_t$ when $X(t)$ is adapted to the filtration (that is, the natural history of the process), and, for any $t > s$, $X(t)$ is independent of $\{\boldsymbol{F}\}_s$ given $X(s)$. Thus, the Markov assumption is that future evolution only depends on the current state. That is, the transition intensities are independent of the history of the process. This can be expressed mathematically as follows:

$$P\left\{X(t) = j|\boldsymbol{F}_{X(s)}\right\} = P\left\{X(t) = j|X(s)\right\} \quad (Markov\ property)$$

Definition 2 (Stochastic process in continuous-time): A stochastic process in continuous-time is a collection of random variables, $(X_c(t))_{t\geq 0}$, indexed by the positive real line $[0, \infty)$. The positive value of $(X_c(t))_{t\geq 0}$ is called the state space, S, of the process. c stands for the number of discrete states available.

A Markov process is a stochastic extension of a finite state automaton. In a Markov process, state transitions are probabilistic in nature. At each time step, the system is considered to be in only one state and these states are mutually exclusive. A Markov process is also known for its memoryless property, that is, the future evolution of the process only depends on the present state of the process and not on its history or filtration $\{\boldsymbol{F}\}_t$. This implies that, in terms of transition intensity $q_{ij}(t)$:

$$q_{ij}(t, \boldsymbol{F}_t) = q_{ij}(t) = \lim_{\Delta t \to 0} \frac{P(X_c(t + \Delta t) = j | X_c(t) = i)}{\Delta t} \tag{3.1}$$

where $X_c(t + \Delta t)$ is the future evolution after a very small increment in time (Δt) given by Δt, $X_c(t)$ is the present state, i is the state occupied at time t, j is the state occupied at time $t + \Delta t$ and $\{\boldsymbol{F}\}_t$ is the history of the process. c is the number of discrete states available.

$$Q(t) = \begin{pmatrix} q_{11}(t) & q_{12}(t) & \cdots & q_{1c}(t) \\ q_{21}(t) & q_{22}(t) & \cdots & q_{1c}(t) \\ \vdots & \vdots & \ddots & \vdots \\ q_{c1}(t) & q_{c2}(t) & \cdots & q_{cc}(t) \end{pmatrix} \tag{3.2}$$

The likelihood for a Markov jump model with discrete observations, assuming the censoring was uninformative, can be expressed simply as a product of transition probabilities, that is:

$$L = \Pi_{i=0}^{N-1} P_{x_i, x_{i+1}}(t_i, t_{i+1}) \tag{3.3}$$

where N represents the number of jumps made by the process as it makes transition from state i to state $i + 1$ and $P_{x_i, x_{i+1}}$ is the transition probability from state i to state $i + 1$ for $i, i + 1 \in X_c$, the state space. The transition probability matrix of a Markov model satisfies the forward Kolmogorov differential equations:

$$P'(t_1, t) = P(t_1, t)Q(t) \tag{3.4}$$

$P'(t_1, t)$ is the derivative of $P(t_1, t)$ with respect to time, t subject to initial conditions $P(0) = P(t_1, t_1) = I$ where $P(t_1, t)$ is the probability matrix with (i, j) entry $P_{ij}(t_1, t)$ and $Q(t)$ is the transition rate (transition intensity or infinitesimal generator) matrix. The words rate and intensity will be used interchangeably.

3.2.1 The time-homogeneous Markov jump model

Definition 3 (Continuous Time-Homogeneous Markov models with a discrete state space): A Markov jump model on a finite or countable set, S, is a family of random variables $\{X_c(t)\}_{t\geq 0}$ (right continuous), on a probability space $\{\Omega, \boldsymbol{F}_{X_c(s)}, P\}$. $\boldsymbol{F}_{X_c(s)}$ denotes all the information pertaining to the history of X_c up to $s < t$. According to continuous-time homogeneous Markov jump process, individuals transition independently among states. This means we can assume that the transition intensities are constant over time, that is, the transition intensities are independent of t (Chiang, 1968; Kay, 1986). Thus, for the time-homogeneous Markov jump model we have:

$$Q(t) = Q, \quad \forall t \tag{3.5}$$

and Q is a $c \times c$ transition rate matrix and becomes:

$$Q = \begin{pmatrix} q_{11} & q_{12} & \cdots & q_{1c} \\ q_{21} & q_{22} & \cdots & q_{1c} \\ \vdots & \vdots & \ddots & \vdots \\ q_{c1} & q_{c2} & \cdots & q_{cc} \end{pmatrix} \tag{3.6}$$

for some constant matrix Q. This implies that sojourn time with a particular state, i, has an exponential distribution with rate parameter $-q_{ii} = \lambda_i = \sum_{i \neq j} q_{ij}$ where q_{ij} is the $(i, j)^{th}$ entry of Q. Thus, transition probabilities only depend on the interval between times t_1 and t_2 and not on t_1 itself.

Derivation of the Chapman-Kolmogorov equations

Theorem 1 (Chapman-Kolmogorov equations): Transition probabilities for a continuous-time homogeneous Markov process satisfy the Chapman-Kolmogorov equations (Isham, 2009; Nielsen, 2009):

$$\forall s, t \geq 0, \forall i, j \in S : P_{ij}(t + s) = \sum_{l \in S} P_{il}(s) \cdot P_{lj}(t) \tag{3.7}$$

since the state space is finite ($|S| < \infty$) then $P(t) = \{P_{ij}(t)\}_{i,j \in S}$ may be regarded as a matrix for any fixed $t \geq 0$ and the Chapman-Kolmogorov equations may be expressed in matrix notation $P(t) = \{P_{ij}(t)\}$ such that $P(t+s) = P(t) \cdot P(s)$. According to Longini and Hudgens (2003), this means that the family $\{P(t) : t \geq 0\}$ forms a semi-group.

Proof (Nielson, 2009): For $i, j \in S,\ \ 0 \leq s < t$ and any $0 \leq u$ we have;

$$
\begin{aligned}
& P_{ij}(t+s) \\
= \ & P(X(t+s+u) = j | X(u) = i) \\
= \ & \sum_{l \in S} P(X(t+s+u) = j, X(s+u) = l, X(u) = i) \cdot P(X(s+u) = l | X(u) = i) \\
= \ & \sum_{l \in S} P(X(t+s+u) = j | X(s+u) = l) \cdot P(X(s+u) = l | X(u) = i) \ \ (Memoryless\ property) \\
= \ & \sum_{l \in S} P_{lj}((t+s+u) - (s+u)) \cdot P_{il}((s+u) - (u)) \\
= \ & \sum_{l \in S} P_{il}(s) \cdot P_{lj}(t)
\end{aligned}
$$

Definition 4 (*Infinitesimal transition probabilities*): For a continuous-time Markov jump process, transition probabilities are referred to as infinitesimal transition probabilities because they are valid over a sufficiently small time Δt. Let T_i denote the amount of time the process stays in state i after entering state i, which is exponentially distributed with parameter λ_i, we define $j \neq i$ such that:

$$p_{ij} = P\left\{X_c(T_i) = j | X_c(0) = i\right\}$$

to be the probability that the process makes a transition to state j after leaving state i. Define $q_{ij} = \lambda_i p_{ij}$ (or $p_{ij} = \frac{q_{ij}}{\lambda_i}$) since T_i is exponential with parameter λ_i, we have that:

$$P\{T_i \geq \Delta t\} = e^{-\lambda_i \cdot \Delta t} \tag{3.8}$$

representing the probability of remaining in state i over a small interval Δt.

$$P\left\{T_i < \Delta t\right\} = 1 - e^{-\lambda_i \cdot \Delta t} \doteq 1 - (1 - \lambda_i \cdot \Delta t + o(t)) = \lambda_i \cdot \Delta t + o(\Delta t), \ \ as \ \ \Delta t \to 0$$

is the probability of leaving state i. Thus, we have:

$$\begin{aligned} P\{X_c(\Delta t) = j | X_c(0) = i\} &\doteq P\{T_i < \Delta t, X_c(T_i) = j | X_c(0) = i\} + o(\Delta t) \\ &= \lambda_i \cdot \Delta t \cdot p_{ij} + o(\Delta t) \\ &= q_{ij}\Delta t + o(\Delta t) \end{aligned}$$

p_{ij} is the probability of entering state j after leaving state i as $\Delta t \to 0$, the $o(\Delta t)$ in the first equality represents the probability of seeing two or more jumps in the time window $[0, \Delta t]$. Therefore, q_{ij} yields the local rate or intensity of transitioning from state i to state j. Explicitly, $i \in S$ such that:

$$\sum_{j \neq i} q_{ij} = \sum_{j \neq i} \lambda_i p_{ij} = \lambda_i.$$

This implies that

$$p_{ij} = \frac{q_{ij}}{\lambda_i} = \frac{q_{ij}}{\sum_{j \neq i} q_{ij}}.$$

This implies that $q_{ij} = \lambda_i p_{ij}$.
Alternatively, we also have:

$$\begin{aligned} P\{X_c(\Delta t) = i | X_c(0) = i\} &= 1 - \sum_{j \neq i} P\{X_c(\Delta t) = j | X_c(0) = i\} \\ &= 1 - \sum_{j \neq i} q_{ij} \cdot \Delta t + o(\Delta t) \\ &= 1 - \lambda_i \Delta t \cdot \sum_{j \neq i} p_{ij} + o(\Delta t) \\ &= 1 - \lambda_i \cdot \Delta t + o(\Delta t) \quad (since \sum_{j \neq i} p_{ij} = 1) \end{aligned}$$

Theorem 2 (Infinitesimal Generator of a continuous-time Markov process): The transition intensities for the infinitesimal generator matrix of a continuous-time Markov jump process $(X_c(t))_{t \geq 0}$ are derived from the transition probabilities $P(t) = (P_{ij}(t))_{i,j \in S}$ as the limits (Wu, 2015):

$$lim_{\Delta t \to 0+} \frac{P_{ii}(t) - 1}{\Delta t} = q_{ii} = -\lambda_i, \quad for\ i = j$$

$$lim_{\Delta t \to 0+} \frac{P_{ij}(t)}{\Delta t} = q_{ij}, \ \ i \neq j$$

Kolmogorov forward equations are a system of differential equations governing the

behaviour of the probabilities $P_{ij}(t)$. Thus we have:

$$\begin{aligned} P'_{ij}(t) &= \lim_{\Delta t \to 0} \frac{P_{ij}(t+\Delta t) - P_{ij}(t)}{\Delta t} \\ &= \lim_{\Delta t \to 0} \frac{1}{\Delta t} \left(P\left\{X_c(t+\Delta t) = j | X_c(0) = i\right\} - P\left\{X_c(t) = j | X_c(0) = i\right\} \right) \\ &= \lim_{\Delta t \to 0} \frac{1}{\Delta t} \left(\sum_{l \in S} P\left\{X_c(t+\Delta t) = j | X_c(t) = j, X_c(0) = i\right\} - P\left\{X_c(t) = j | X_c(0) = i\right\} \right) \end{aligned}$$

However,

$$\begin{aligned} & \sum_{l \in S} P\left\{X_c(t+\Delta t) = j | X_c(t) = l, X_c(0) = i\right\} \\ = \; & P\left\{X_c(t+\Delta t) = j | X_c(t) = j, X_c(0) = i\right\} P\left\{X(t) = j | X_c(0) = i\right\} \\ + \; & \sum_{l \neq j} P\left\{X_c(t+\Delta t) = j | X_c(t) = l, X_c(0) = i\right\} P\left\{X_c(t) = l | X_c(0) = i\right\} \\ = \; & (1 - \lambda_j \cdot \Delta t) P_{ij}(t) + \sum_{l \neq j} q_{lj} \cdot \Delta t \cdot P_{il}(t) + o(\Delta t) \end{aligned}$$

and so:

$$\begin{aligned} P'_{ij}(t) &= \lim_{\Delta t \to 0} \frac{1}{\Delta t} \left(1 - \lambda_j \Delta t - 1\right) P_{ij}(t) + \sum_{l \neq j} q_{lj} \cdot \Delta t \cdot P_{il}(t) + o(\Delta t) \\ &= -\lambda_j P_{ij}(t) + \sum_{l \neq j} q_{lj} P_{il}(t) \end{aligned}$$

Thus:

$$\begin{aligned} P'_{ij}(t) &= -\lambda_j P_{ij}(t) + \sum_{l \neq j} P_{il}(t) q_{lj} = P_{ij}(t) q_{jj} + \sum_{l \neq j} P_{il}(t) q_{lj} \;\; (since \;\; -\lambda_j = q_{jj}) \\ &= \sum_{l \in S} P_{il}(t) q_{lj} = P(t) \cdot Q \end{aligned} \tag{3.9}$$

with the restriction that $\sum_{l \in S} q_{lj} = 0$ and $q_{lj} > 0$ whenever $l \neq j$. Thus, it follows immediately that $q_{jj} = -\sum_{l \in S} q_{lj}$ for $l \neq j$. Therefore, we can write that

$$P\left[X\left(t+\Delta t\right) = j | X\left(t\right) = l\right] = \begin{cases} q_{lj} \cdot \Delta t + o(\Delta t); & if \;\; l \neq j \\ 1 - \lambda_l \cdot \Delta t + o(\Delta t); & if \;\; l = j \\ o(\Delta t); & otherwise \end{cases}$$

where $o(\Delta t)$ is defined such that $\lim_{\Delta t \to 0} \frac{o(\Delta t)}{\Delta t} = 0$. The above result will be used to derive the forward and backward Kolmogorov differential equations. This can also

be seen as an alternative proof of $P'(t) = P(t) \cdot Q$.

Deriving the Kolmogorov forward equation

(See Longini and Hudgens (2003) for a similar proof). The derived results are highlighted again.

$$P\left[X\left(t+\Delta t\right)=j|X\left(t\right)=l\right]=\begin{cases} q_{lj}\cdot\Delta t+o(\Delta t); & if\ \ l\neq j \\ 1-\lambda_l\cdot\Delta t+o(\Delta t); & if\ \ l=j \\ o(\Delta t); & otherwise \end{cases}$$

leads to the Kolmogorov forward equation:

$$\frac{d}{dt}P_{ij}(t)=\sum_{l\in S}P_{il}(t)q_{lj}=P(t)\cdot Q,\ \ for\ \ all\ \ i,j. \tag{3.10}$$

The Kolmogorov forward differential equation is derived from:

$$\begin{aligned} P_{ij}(t+\Delta t) &= \sum_{l\in S}P_{il}(t)P_{lj}(\Delta t)\ \ (substitute\ \ s=\Delta t\ in\ equation\ \ 3.7) \\ &= P_{ij}(t)P_{jj}(\Delta t)+\sum_{l\neq j}P_{il}(t)P_{lj}(\Delta t) \\ &= P_{ij}(t)(1+q_{jj}\cdot\Delta t+o(\Delta t))+\sum_{l\neq j}P_{il}(t)(q_{lj}\cdot\Delta t+o(\Delta t)) \\ &= \sum_{l\neq j}P_{il}(t)q_{lj}\cdot\Delta t+P_{ij}(t)q_{jj}\cdot\Delta t+P_{ij}(t)+o(\Delta t) \\ &= P_{ij}(t)+\sum_{l\in S}P_{il}(t)q_{lj}\cdot\Delta t+o(\Delta t) \end{aligned} \tag{3.11}$$

Rearranging to derive the forward differential equation gives:

$$\frac{P_{ij}(t+\Delta t)-P_{ij}(t)}{\Delta t}=\sum_{l\in S}P_{il}(t)q_{lj}+\frac{o(\Delta t)}{\Delta t} \tag{3.12}$$

Taking the limits as $\Delta t \longrightarrow 0$ gives the desired result:

$$P'_{ij}(t)=\sum_{l\in S}P_{il}(t)q_{lj}=P(t)\cdot Q. \tag{3.13}$$

as before since $\lim_{h\to 0} \frac{0(\Delta t)}{\Delta t} = 0$.
This is the Kolmogorov forward equation for the process. In the biology literature, this system of equations is termed the *chemical master equation* (Serfozo, 2009).

Deriving the Kolmogorov backward equation

(See Longini and Hudgens (2003) for a similar proof) For a time-homogeneous case, the Kolmogorov backward differential equation can be written in matrix form as:

$$P'(t) = Q \cdot P(t).$$

The Kolmogorov backward equation is derived from Equation (3.7) by substituting $s = \Delta t$ as follows:

$$P_{ij}(t + \Delta t) = \sum_{l \in S} P_{il}(\Delta t) P_{lj}(t).$$

Now, since:

$$P_{il}(\Delta t) = q_{il} \cdot \Delta t + o(\Delta t), \quad for \ \ l \neq i$$

and:

$$\begin{aligned} P_{ii}(\Delta t) = 1 - \sum_{l \neq j} P_{il}(\Delta t) &= 1 - \sum_{l \neq j} q_{lj} \cdot \Delta t + o(\Delta t) \\ &= 1 + q_{ii} \cdot \Delta t + o(\Delta t) \quad (since \ \ q_{ii} = -\sum_{i \neq j} q_{ij} = -\lambda_i) \\ &= 1 - \lambda_i \cdot \Delta t + o(\Delta t) \end{aligned}$$

we have:

$$\begin{aligned} P_{ij}(t + \Delta t) &= \sum_{l \in S} P_{il}(\Delta t) P_{lj}(t) && (3.14) \\ &= \sum_{l \neq j} P_{il}(\Delta t) P_{lj}(t) + P_{ii}(\Delta t) P_{ij}(t) && (3.15) \\ P_{ij}(t + \Delta t) &= \sum_{l \neq j} \Delta t \cdot q_{il} P_{ij}(t) + (1 + \Delta t \cdot q_{ii}) P_{ij}(t) + o(\Delta t) \\ &= P_{ij}(t) + \sum_{l \in S} q_{il} P_{lj}(t) \cdot \Delta t + o(\Delta t). \end{aligned}$$

If we then take $P_{ij}(t)$ term to the left-hand side, divide by Δt and then taking limits as $\Delta t \to 0$ we obtain the differential equation:

$$\begin{aligned} \frac{P_{ij}(t+\Delta t) - P_{ij}(t)}{\Delta t} &= \sum_{l \in S} q_{il} P_{lj}(t) + \frac{o(\Delta t)}{\Delta t} \\ &= P'_{ij}(t) = \sum_{l \in S} q_{il} P_{lj}(t), \quad for \ \ all \ \ i, j \end{aligned}$$

or, equivalently in matrix notation:

$$P'(t) = Q \cdot P(t).$$

3.3 The time-homogeneous HIV, AIDS, DEATH (HAD) Model

Consider the following HIV, AIDS, DEATH (HAD) model with the given transition rates. The state space is $S = \{H, A, D\}$. These states are based on CD4 cell counts as follows:

$$CD4\, level = \begin{cases} H; & CD4 \geq 200 \quad (HIV\ state) \\ A; & CD4 < 200 \quad (AIDS\ state) \\ D; & DEATH state \end{cases}$$

CD4 state H represents CD4 cell counts above 200 cells/mm^3, state A represents the AIDS defining state which is characterised by CD4 cell counts below 200 cells/mm^3 and state D is the DEATH state that can be reached from either state H or state A. At each stage, an individual is expected to be in either state A, state H or state D. The states H, A and D are mutually exclusive. States H, A and D are defined for patients receiving anti-retroviral therapy, such that the transitions between states are bi-directional due to adherence or non-adherence to treatment.

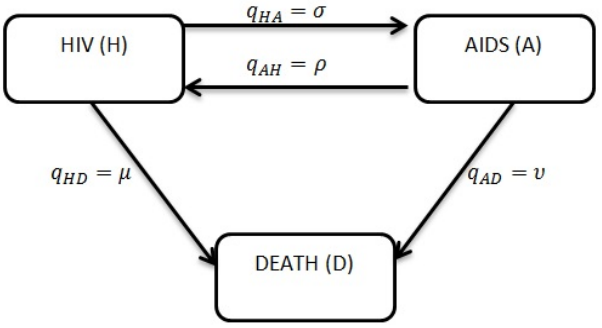

The transition rate from the AIDS state to the DEATH state is denoted by ν. A life

may be in the HIV state or the AIDS state on a number of separate occasions before making the one-way transition to the death state. Alternatively, the life may pass from the HIV state to the DEATH state without ever having been in the AIDS state.

Using the notations of the HAD model, expression for $q_{AH},\ q_{HH},\ q_{HA},\ q_{HD},\ q_{AD},\ q_{AA}$ and q_{DD} can be given as follows:
$q_{AH} = \rho,\ q_{HH} = -(\sigma + \mu) = -\lambda_H,\ q_{DD} = -\lambda_D = 0,\ q_{HA} = \sigma,\ q_{HD} = \mu,\ q_{AD} = \nu,\ q_{AA} = -(\rho + \nu) = -\lambda_A$.
The generator matrix for the HAD model is:

$$Q = \begin{pmatrix} q_{HH} & q_{HA} & q_{HD} \\ q_{AH} & q_{AA} & q_{AD} \\ q_{DH} & q_{DA} & q_{DD} \end{pmatrix} = \begin{pmatrix} -\sigma - \mu & \sigma & \mu \\ \rho & -\rho - \nu & \nu \\ 0 & 0 & 0 \end{pmatrix} \tag{3.16}$$

Here the order of the states has been taken to be H, A then D.
Example 1

For the HIV, AIDS, DEATH (HAD) model, the differential equation for $P_{HH}(t)$ can be defined by using the general forward equation as a template. This gives:

$$\begin{aligned} P'_{HH}(t) &= \sum_{L \in S} P_{HL}(t) q_{LH}, \quad for\ L = H, A, D \\ &= P_{HH}(t) q_{HH} + P_{HA}(t) q_{AH} + P_{HD}(t) q_{DH}. \end{aligned} \tag{3.17}$$

Now substituting it for transition rates, we have:

$$P'_{HH}(t) = -P_{HH}(t)(\sigma + \mu) + P_{HA}(t)\rho = -P_{HH}\lambda_H + P_{HA}(t)\rho. \tag{3.18}$$

The Kolmogorov forward equation for the transition probability $P_{HA}(t)$ is:

$$\begin{aligned} P'_{HA}(t) &= \sum_{L \in S} P_{HL}(t) q_{LA}, \quad for\ \ L = H, A, D \\ &= P_{HH}(t) q_{HA} + P_{HA}(t) q_{AA} + P_{HD}(t) q_{DA} \\ &= P_{HH}(t)\sigma - P_{HA}(t)(\rho + \nu) = P_{HH}(t)\sigma - P_{HA}(t)\lambda_A. \end{aligned}$$

Example 2:
For the time-homogeneous HAD model, Kolmogorov's backward differential equa-

tion for $P_{HH}(t)$ can be obtained using the general backward equation as a template. This gives:

$$\begin{aligned} P'_{HH}(t) &= \sum_{L \in S} q_{HL} P_{LH}(t), \quad for \;\; L = H, A, D \\ &= q_{HH} P_{HH}(t) + q_{HA} P_{AH}(t) + q_{HD} P_{DH}(t). \end{aligned} \tag{3.19}$$

Now substituting in the transition rates, we have:

$$P'_{HH}(t) = -(\sigma + \mu) P_{HH}(t) + \sigma P_{AH}(t) = -\lambda_H P_{HH}(t) + \sigma P_{AH}. \tag{3.20}$$

The backward equation for the transition probability $P_{HA}(t)$ is given by:

$$\begin{aligned} P'_{HA}(t) &= q_{HH} P_{HA}(t) + q_{HA} P_{AA}(t) + q_{HD} P_{DA}(t) \\ &= -(\sigma + \mu) P_{HA}(t) + \sigma P_{AA}(t) = -\lambda_H P_{HA}(t) + \sigma P_{AA}(t). \end{aligned} \tag{3.21}$$

3.3.1 Solution to the Kolmogorov forward differential equation

Theorem 3 (Kolmogorov forward equations):

For a continuous-time Markov jump process, $\{X_c(t)\}_{t \geq 0}$, with transition intensity $Q = \{q_{ij}\}_{i,j \in S}$ and transition probability $\{P_{ij}(t)\}_{i,j \in S}$ it always holds that the solution to:

$$\begin{aligned} P'(t) &= \sum_{l \in S} P_{il}(t) q_{lj} \\ &= P_{ij}(t) q_{jj} + \sum_{l \neq j} P_{il}(t) q_{lj} \\ &= P(t) \cdot Q \end{aligned} \tag{3.22}$$

is:

$$P(t) = exp(-\lambda_j t)\delta_{ij} + \int_0^t \sum_{l \neq j} P_{il}(t - v) \cdot q_{lj} \cdot exp(-\lambda_j(v)) dv.$$

To prove this theorem, we start from the solution and we show that the stochastic differential equation holds. (See Serfozo (2009) for a similar proof).

Proof:

Since $X_c(s) = j$, then by minimal construction, the waiting time to the final jump follows an exponential distribution with the rate $\lambda_j = -q_{jj}$ and therefore the solution

is written as given.

$$P(t) = exp(-\lambda_j t)\delta_{ij} + \int_0^t \sum_{l \neq j} P_{il}(t-v) \cdot q_{lj} \cdot exp(-\lambda_j(v))dv$$

with change of variables $u = t - v$ the equation becomes:

$$\begin{aligned} P_{ij}(t) &= exp(-\lambda_j t)\delta_{ij} + \int_0^t \sum_{l \neq j} P_{il}(u) \cdot q_{lj} \cdot exp(-\lambda_j(t-u))du \\ &= exp(-\lambda_j t)\delta_{ij} + \int_0^t \sum_{l \neq j} P_{il}(u) \cdot q_{lj} exp(\lambda_j u) \cdot exp(-\lambda_j t)du \\ &= [\delta_{ij} + \int_0^t \sum_{l \neq j} P_{il}(u) \cdot q_{lj} exp(\lambda_j u)du] \cdot exp(-\lambda_j t) \end{aligned} \tag{3.23}$$

where $\delta_{ij} = 0, i \neq j$, and $\delta_{jj} = 1$. The integral is continuous in t since its integrand is bounded on finite intervals, and so $P_{ij}(t)$ is continuous. Then the integrand is continuous and so the derivative of the integrand exists, which implies that $P_{ij}(t)$ is differentiable in t. Now, taking derivatives gives:

$$\begin{aligned} P'_{ij}(t) &= [\delta_{ij} + \int_0^t \sum_{l \neq j} P_{il}(u) \cdot q_{lj} \cdot exp(\lambda_j u)du] \cdot [-\lambda_j exp(-\lambda_j t)] \\ &+ \sum_{l \neq i} P_{il}(t) \cdot q_{lj} \cdot exp(\lambda_j t) \cdot exp(-\lambda_j t) \qquad (product\ \ rule) \\ &= P_{ij}(t)(-\lambda_j) + \sum_{l \neq j} P_{il}(t) q_{lj} \quad (since\ \ q_{jj} = -\lambda_j) \\ &= P_{ij}(t) q_{jj} + \sum_{l \neq j} P_{il}(t) q_{lj} \\ &= \sum_{l \in S} P_{il}(t) q_{lj} \\ &= P(t) \cdot Q \end{aligned} \tag{3.24}$$

3.3.2 Solution to the Backward differential equation

Theorem 4 (Backward differential equations): For a continuous-time Markov jump process, $\{X_c(t)\}_{t \geq 0}$, with transition intensity $Q = \{q_{ij}\}_{i,j \in S}$ and transition probability $\{P_{ij}(t)\}_{i,j \in S}$ it always holds that the solution to:

$$P'_{ij}(t) = \sum_{l \in S} q_{il} P_{lj}(t) = q_{ii} P_{ij}(t) + \sum_{l \neq i} q_{il} P_{lj}(t) = Q \cdot P(t)$$

is:

$$P_{ij}(t) = \delta_{ij} exp(-\lambda_i t) + \int_0^t \sum_{l \neq i} exp(-\lambda_i(u)) q_{il} P_{lj}(t-u) du. \tag{3.25}$$

To prove this theorem, we start from the solution and we show that the stochastic differential equation holds (Serfozo, 2009).

Proof:

Since $X_c(s) = i$, then by minimal construction, the waiting time to the first jump follows an exponential distribution with rate parameter $\lambda_i = -q_{ii}$ and therefore the solution is written as given. (See Serfozo (2009) for a similar proof):

$$P_{ij}(t) = \delta_{ij} exp(-\lambda_i t) + \int_0^t \sum_{l \neq i} exp(-\lambda_i u) q_{il} P_{lj}(t-u) du, \tag{3.26}$$

with change of variables $v = t - u$ such that Equation (3.23) becomes:

$$\begin{aligned} P_{ij}(t) &= \delta_{ij} exp(-\lambda_i t) + \int_0^t \sum_{l \neq i} exp(-\lambda_i (t-v)) q_{il} P_{lj}(v) dv \\ &= exp(-\lambda_i t)[\delta_{ij} + \int_0^t \sum_{l \neq i} exp(\lambda_i v) q_{il} P_{lj}(v) dv] \end{aligned}$$

where $\delta_{ij} = 0, i \neq j$, and $\delta_{ii} = 1$. The integral is continuous in t since its integrand is bounded on finite intervals, and so $P_{ij}(t)$ is continuous. Then the integrand is continuous and so the derivative of the integrand exists, which implies that $P_{ij}(t)$ is differentiable in t. Now, taking derivatives gives:

$$\begin{aligned} P'_{ij}(t) &= -\lambda_i exp(-\lambda_i t)[\delta_{ij} + \int_0^t \sum_{l \neq i} exp(\lambda_i v) q_{il} P_{lj}(v) dv] \\ &+ \sum_{l \neq j} exp(-\lambda_i t) \cdot exp(\lambda_i t) q_{il} P_{lj}(t) \ \ (product\ rule) \\ &= -\lambda_i P_{ij}(t) + \sum_{l \neq j} q_{il} P_{lj}(t) \\ &= q_{ii} P_{ij}(t) + \sum_{l \neq j} q_{il} P_{lj}(t) \quad (since\ q_{ii} = -\lambda_i) \\ &= \sum_{l \in S} q_{il} P_{lj}(t) \\ &= Q \cdot P(t). \end{aligned} \tag{3.27}$$

Using the matrix notation, the Kolmogorov forward differential equation and the Backward differential equation respectively are:

$$P'(t) = P(t) \cdot Q \quad and \quad P'(t) = Q \cdot P(t).$$

The matrix $Q = \{q_{ij}\}$ is the infinitesimal generator of the semi-group $P(t)$.

Example 3

The above HAD model can be extended to accommodate more states as follows: Consider HIV/AIDS patients on cART, with transitions between viral load (measured in copies/mL) defined states. We have the first five transient states followed by the 6^{th} state which is absorbing (death) defined as follows:

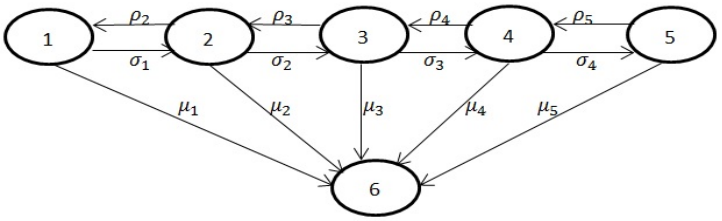

The states are defined as follows, where VL stands for the viral load level of a patient:

$$Viral\ load\ levels\ (X_v(t)) = \begin{cases} 1, & VL < 50 \\ 2, & 50 \leq VL < 10\,000 \\ 3, & 10\,000 \leq VL < 100\,000 \\ 4, & 100\,000 \leq VL < 500\,000 \\ 5, & VL \geq 500\,000 \\ 6, & DEATH. \end{cases}$$

Thus, for a patient in state $w = 1, ..., 5$ we define transitions from state w as follows: let σ representing viral rebound from state w to state $w + 1$ or birth (protease) of new viral particles into the circulating blood, ρ representing suppression from state w to state $w - 1$ or death of viral particles due to treatment effect, and μ representing absorption from state w or death of an infected individual. This description of transitions is in line with the "general birth and death process" by Longini and Hudgen (2003). All the transitions from state w are illustrated below (except for states 1 and 5).

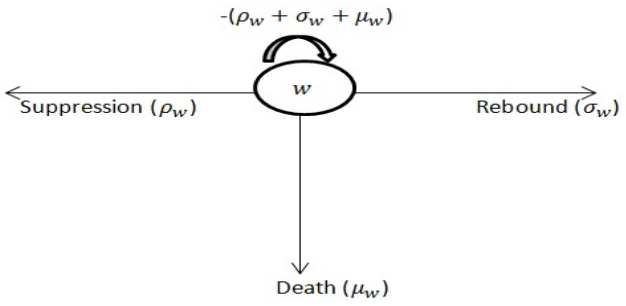

Thus from the model

$$q_{wj} = \begin{cases} \sigma_w; & if\ \ j = w+1,\ for\ w = 1,2,3,4 \\ \rho_w; & if\ \ j = w-1,\ for\ w = 2,3,4,5 \\ \mu_w; & if\ \ j = death \\ -(\sigma_w + \rho_w + \mu_w); & if\ \ j = w,\ for\ ww = 2,3,4 \\ -(\sigma_w + \mu_w); & if\ \ j = 1,\ and\ \ w = 1 \\ -(\rho_w + \mu_w); & if\ \ j = 5,\ and\ \ w = 5 \\ 0; & otherwise. \end{cases} \tag{3.28}$$

The forward differential equation for the transition probability from a viral load state w to the same viral load state, $P_{ww}(t)$, is given by:

$$\begin{aligned} P'_{ww}(t) &= \sum_{l \in X} P_{wl}(t) q_{lw}(t); \qquad for\ \ l = w, w-1, w+1, D,\ \ w = 2,3,4 \\ &= P_{ww}(t)q_{ww} + P_{w,w-1}(t)q_{w-1,w} + P_{w,w+1}(t)q_{w+1,w} + P_{w,D}(t)q_{D,w} \\ &= -(\sigma_w + \rho_w + \mu_w)P_{ww}(t) + \sigma_w P_{w,w-1}(t) + \rho_w P_{w,w+1}(t)\ \ (since\ q_{Dw} = 0) \\ P'_{11}(t) &= -(\sigma_1 + \mu_1)P_{11}(t) + \rho_2 P_{12}(t); \qquad for\ \ w = 1 \\ P'_{55}(t) &= -(\rho_5 + \mu_5)P_{55}(t) + \sigma_4 P_{54}(t); \qquad for\ \ w = 5. \end{aligned}$$

The backward differential equation for the transition probability from a viral load state w to the same viral load state, $P_{ww}(t)$, is given by:

$$\begin{aligned} P'_{ww}(t) &= \sum_{l \in X} q_{wl} P_{lw}(t); \qquad for\ \ l = w, w-1, w+1, D,\ \ w = 2,3,4 \\ &= q_{ww}P_{ww}(t) + q_{w,w-1}P_{w-1,w}(t) + q_{w,w+1}P_{w+1,w}(t) + q_{w,D}P_{D,w}(t) \\ &= -(\sigma_w + \rho_w + \mu_w)P_{ww}(t) + \rho_w P_{w-1,w}(t) + \sigma_w P_{w+1,w}(t)\ \ (since\ P_{D,w}(t) = 0) \\ P'_{11}(t) &= -(\sigma_1 + \mu_1)P_{11}(t) + \sigma_1 P_{21}(t); \qquad for\ \ w = 1 \\ P'_{55}(t) &= -(\rho_5 + \mu_5)P_{55}(t) + \rho_5 P_{45}(t); \qquad for\ \ w = 5. \end{aligned}$$

3.3.3 Maximum Likelihood estimators

From the HAD model defined earlier:

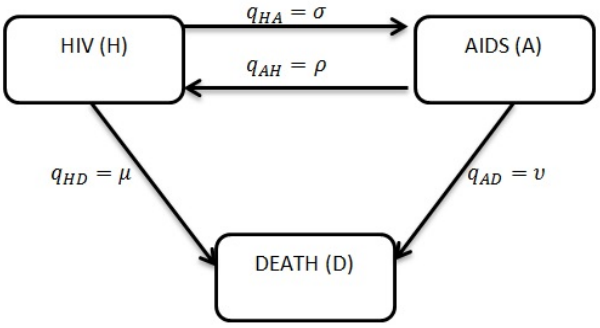

Let:
T_{Hi} = Waiting time of the i^{th} life in the HIV state,
T_{Ai} = Waiting time of the i^{th} life in the AIDS state,
S_i = Number of transitions HIV $\rightarrow$ AIDS by the i^{th} life,
R_i = Number of transitions AIDS $\rightarrow$ HIV by the i^{th} life,
D_i = Number of transitions HIV $\rightarrow$ Death by the i^{th} life, and
U_i = Number of transitions AIDS $\rightarrow$ Death by the i^{th} life.

We also need to define totals $T_H = \sum_{i=1}^{N} T_{Hi}$, $T_A = \sum_{i=1}^{N} T_{Ai}$, $S = \sum_{i=1}^{N} S_i$, $R = \sum_{i=1}^{N} R_i$, $D = \sum_{i=1}^{N} D_i$, *and* $U = \sum_{i=1}^{N} U_i$
Using the lower case symbols for the observed samples, it can be shown (based on the ideas from Serfozo, 2009) that the likelihood for the parameters, μ, ν, σ, ρ, for the HAD model in Example 1 is given by:

$$\begin{aligned} L(\mu,\nu,\sigma,\rho) &= \Pi_{i=1}^{N} e^{-(\mu+\sigma)T_{Hi}} e^{-(\nu+\rho)T_{Ai}} \mu^{d_i} \nu^{u_i} \sigma^{s_i} \rho^{r_i} \\ &= e^{-(\mu+\sigma)\sum T_{Hi}} e^{-(\nu+\rho)\sum T_{Ai}} \mu^{\sum d_i} \nu^{\sum u_i} \sigma^{\sum s_i} \rho^{\sum r_i} \\ &= e^{-(\mu+\sigma)T_H} e^{-(\nu+\rho)T_A} \mu^{d} \nu^{u} \sigma^{s} \rho^{r}, \end{aligned} \tag{3.29}$$

where $d = \sum d_i$, $u = \sum u_i$, $s = \sum s_i$, $r = \sum r_i$.
The likelihood function $L(\mu, \nu, \sigma, \rho)$ for the i^{th} life reflects:

- the probability of the life remaining in the HIV state for total time T_{Hi} and in the AIDS state for time T_{Ai}, giving the factors $e^{-(\mu+\sigma)T_{Hi}}$ and $e^{-(\nu+\rho)T_{Ai}}$ respectively.
- the probability of the life making the relevant number of transitions between states giving the factors $\mu^{d_i}, \nu^{u_i}, \sigma^{s_i}$ and ρ^{r_i}.

The likelihood factorises into functions of each parameter of the form $e^{-\mu T_A}\mu^d$:

$$\begin{aligned} L(\mu,\nu,\sigma,\rho) &= e^{-(\mu+\sigma)T_H}e^{-(\nu+\rho)T_A}\mu^d\nu^u\sigma^s\rho^r \\ &= \left(e^{-\mu T_H}\mu^d\right)\times\left(e^{-\sigma T_H}\sigma^s\right)\times\left(e^{-\nu T_A}\nu^u\right)\times\left(e^{-\rho T_A}\rho^r\right). \end{aligned} \tag{3.30}$$

So the log-likelihood is:

$$\log L = -(\mu+\sigma)T_H - (\nu+\rho)T_A + d\log\mu + u\log\nu + s\log\sigma + r\log\rho. \tag{3.31}$$

Differentiating this with respect to each of the four parameters gives:

$$\begin{aligned} \frac{\partial\log L}{\partial\mu} &= -T_H + \frac{d}{\mu}, & \frac{\partial\log L}{\partial\nu} &= -T_A + \frac{u}{\nu} \\ \frac{\partial\log L}{\partial\sigma} &= -T_H + \frac{s}{\sigma}, & \frac{\partial\log L}{\partial\rho} &= -T_A + \frac{r}{\rho}. \end{aligned}$$

Setting each of the derivatives to 0 and solving the resulting equations, we see that:

$\hat{\mu} = \frac{d}{T_H}, \quad \hat{\nu} = \frac{u}{T_A}, \quad \hat{\sigma} = \frac{s}{T_H}, \quad \hat{\rho} = \frac{r}{T_A}.$

When there is more than one parameter to be estimated, the second order condition to check for maxima is that the Hessian matrix is negative definite, or equivalently, the eigenvalues of the Hessian matrix are all negative. The Hessian matrix is the matrix of the second derivatives. So in this case we consider the matrix:

$$\begin{pmatrix} \frac{\partial^2\ln L}{\partial\mu^2} & \frac{\partial^2\ln L}{\partial\mu\partial\nu} & \frac{\partial^2\ln L}{\partial\mu\partial\sigma} & \frac{\partial^2\ln L}{\partial\mu\partial\rho} \\ \frac{\partial^2\ln L}{\partial\nu\partial\mu} & \frac{\partial^2\ln L}{\partial\nu^2} & \frac{\partial^2\ln L}{\partial\nu\partial\sigma} & \frac{\partial^2\ln L}{\partial\nu\partial\rho} \\ \frac{\partial^2\ln L}{\partial\sigma\partial\mu} & \frac{\partial^2\ln L}{\partial\sigma\partial\nu} & \frac{\partial^2\ln L}{\partial\sigma^2} & \frac{\partial^2\ln L}{\partial\sigma\partial\rho} \\ \frac{\partial^2\ln L}{\partial\rho\partial\mu} & \frac{\partial^2\ln L}{\partial\rho\partial\nu} & \frac{\partial^2\ln L}{\partial\rho\partial\sigma} & \frac{\partial^2\ln L}{\partial\rho^2} \end{pmatrix} = \begin{pmatrix} -\frac{d}{\mu^2} & 0 & 0 & 0 \\ 0 & -\frac{u}{\nu^2} & 0 & 0 \\ 0 & 0 & -\frac{s}{\sigma^2} & 0 \\ 0 & 0 & 0 & -\frac{r}{\rho^2} \end{pmatrix}$$

Since this is a negative definite matrix, the maximum likelihood estimates for μ,ν,σ,ρ are:

$\hat{\mu} = \frac{d}{T_H}, \quad \hat{\nu} = \frac{u}{T_A}, \quad \hat{\sigma} = \frac{s}{T_H}, \quad \hat{\rho} = \frac{r}{T_A}.$

The maximum likelihood estimators are therefore as given:

$\tilde{\mu} = \frac{D}{T_H}, \quad \tilde{\nu} = \frac{U}{T_A}, \quad \tilde{\sigma} = \frac{S}{T_H}, \quad \tilde{\rho} = \frac{R}{T_A}.$

This represents a special case of a more general result.

The Interevent time

A new random variable T_i is now defined.
Theorem 5: The inter-event time, T_i, is a continuous random variable for the time to the next event given the process is in state i. T_i has an exponential distribution following from the Markov's "memoryless property".

Proof (See Berestycki and Sousi (2017) for a similar proof):
Once the process enters state $i \in S$ one can determine how long the process remains in state i as follows: Suppose $X(0) = i$ and letting T_i denote the time the system transition away from state i. The distribution of T_i is obtained by letting $s, t \geq 0$ and consider;

$$\begin{aligned}
& P\{T_i > s+t | T_i > s\} \\
= \; & P\{X_c(r) = i \; for \; r \in [0, s+t] | X_c(r) = i \; for \; r \in [0, s]\} \\
= \; & P\{X_c(r) = i \; for \; r \in (s, s+t] | X_c(r) = i \; for \; r \in [0, s]\} \\
= \; & P\{X_c(r) = i \; for \; r \in (s, s+t] | X_c(s) = i\} \; (Markov \; property) \\
= \; & P\{X_c(r) = i \; for \; r \in (0, t] | X_c(0) = i\} \; (time - homogeneity) \\
= \; & P\{T_i > t\}.
\end{aligned}$$

Hence, T_i satisfies the loss of memory property and therefore it is exponentially distributed with parameter $-q_{ii} = \lambda_i = \sum_{j \neq i} q_{ij}$ where q_{ij} is the (i, j) entry of Q. Thus, $P\{T_i > s+t | T_i > s\} = P_{ii}(t) = e^{-\lambda_i t}$.

The mean inter-event time, also called the expected holding time in each state or the mean sojourn time, describes the average time an individual spends in each state in a single stay before he/she makes a transition to another state. It can also be shown that $E(T_i) = \frac{1}{\lambda_i}$. This is simply an exponential mean with parameter λ_i. This implies that the higher the rate λ_i, representing the rate out of state i, the smaller the expected time for the transition to occur.

Example 4:
Consider the two-decrement model, in which the transition intensities are constant. We show:

1. $P_{11}(t) = e^{-(q_{12}+q_{13})\cdot t} = e^{-\lambda_1 \cdot t}$ where $\lambda_1 = (q_{12} + q_{13})$

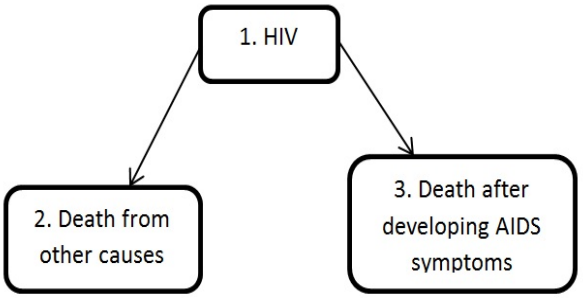

2. $P_{12}(t) = \frac{q_{12}}{q_{12}+q_{13}}[1 - e^{-(q_{12}+q_{13})\cdot t}] = \frac{q_{12}}{\lambda_1} \cdot [1 - e^{-\lambda_1 \cdot t}]$
3. $P_{13}(t) = \frac{q_{13}}{q_{12}+q_{13}}[1 - e^{-(q_{12}+q_{13})\cdot t}] = \frac{q_{13}}{\lambda_1} \cdot [1 - e^{-\lambda_1 \cdot t}]$

Proof:

1.

$$\begin{aligned} & P_{11}(t+\Delta t) \\ = \; & P_{11}(t)P_{11}(\Delta t) = P_{11}(t)(1 - \lambda_1 \cdot \Delta t + o(\Delta t)) \\ = \; & P_{11}(t)(1 - (q_{12}+q_{13}) \cdot \Delta t + o(\Delta t)) \quad (since\ \lambda_1 = (q_{12}+q_{13}) = -q_{11}) \\ = \; & P_{11}(t) - (q_{12}+q_{13}) \cdot P_{11}(t) \cdot \Delta t + o(\Delta t) \end{aligned}$$

Subtracting $P_{11}(t)$ from both sides and dividing both sides by Δt yields.

$$\frac{P_{11}(t+\Delta t) - P_{11}(t)}{\Delta t} = -(q_{12}+q_{13}) \cdot P_{11}(t) + \frac{o(\Delta t)}{\Delta t}. \tag{3.32}$$

Taking limits as $\Delta t \to 0$

$$P'_{11}(t) = -(q_{12}+q_{13}) \cdot P_{11}(t) = -\lambda_1 P_{11}(t). \tag{3.33}$$

Finding the solution to the differential equation gives:

$$\begin{aligned}
\frac{P'11(t)}{P_{11}(t)} &= -(q_{12}+q_{13}) \\
\frac{d}{dt}\ln P_{11}(t) &= -(q_{12}+q_{13}) \\
\int_0^t \frac{d}{dr}\ln P_{11}(r)dr &= -\int_0^t (q_{12}+q_{13})dr \\
\ln P_{11}(r)|_0^t &= -(q_{12}+q_{13})r|_0^t \\
\ln P_{11}(t) - \ln P_{11}(0) &= -(q_{12}+q_{13})(t-0) \\
\ln P_{11}(t) - \ln 1 &= -(q_{12}+q_{13})\cdot t \\
P_{11}(t) &= e^{-(q_{12}+q_{13})\cdot t} = e^{-\lambda_1 \cdot t} \ \ (since\ \lambda_1 = q_{12}+q_{13}).
\end{aligned}$$

2.

$$\begin{aligned}
& P_{12}(t+\Delta t) \\
= \ & P_{11}(t)P_{12}(\Delta t) + P_{12}(t)P_{22}(\Delta t) \\
= \ & P_{11}(t)(q_{12}\cdot\Delta t + o(\Delta t)) + P_{12}(t)(1-\lambda_2\cdot\Delta t + o(\Delta t)) \ \ (since\ \lambda_2 = -q_{22}) \\
= \ & P_{11}(t)q_{12}\cdot\Delta t + P_{12}(t) + P_{12}(t)q_{22}\cdot\Delta t + o(\Delta t) \ \ (since\ \lambda_2 = -q_{22} = 0).
\end{aligned}$$

Subtracting $P_{12}(t)$ and dividing both sides by Δt

$$\begin{aligned}
P_{12}(t+\Delta t) - P_{12}(t) &= P_{11}(t)q_{12}\cdot\Delta t + P_{12}(t)\cdot 0\cdot\Delta t + o(\Delta t) \\
\frac{P_{12}(t+\Delta t) - P_{12}(t)}{\Delta t} &= P_{11}(t)q_{12} + \frac{o(\Delta t)}{\Delta t} \\
P'_{12}(t) &= P_{11}(t)q_{12} \quad (taking\ limits\ \ as\ \ \Delta t \to 0) \\
P'12(t) &= e^{-(q_{12}+q_{13})\cdot t}q_{12} \ \ (since\ P_{11}(t) = e^{-(q_{12}+q_{13})\cdot t}) \\
\int_0^t P'_{12}(r)dr &= q_{12}\int_0^t e^{-(q_{12}+q_{13})\cdot r}dr \\
P_{12}(r)|_0^t &= \frac{q_{12}}{-(q_{12}+q_{13})}e^{-(q_{12}+q_{13})\cdot r}|_0^t \\
P_{12}(t) - P_{12}(0) &= \frac{q_{12}}{-(q_{12}+q_{13})}[e^{-(q_{12}+q_{13})\cdot t} - 1] \\
P_{12}(t) - 0 &= \frac{q_{12}}{q_{12}+q_{13}}[1 - e^{-(q_{12}+q_{13})\cdot t}] \\
P_{12}(t) &= \frac{q_{12}}{\lambda_1}[1 - e^{-\lambda_1\cdot t}]
\end{aligned} \tag{3.34}$$

3.

$$\begin{aligned} & P_{13}(t+\Delta t) \\ = \; & P_{11}(t)P_{13}(\Delta t) + P_{13}(t)P_{33}(\Delta t) \\ = \; & P_{11}(t)(q_{13}\cdot\Delta t + o(\Delta t)) + P_{13}(t)(1-\lambda_3\cdot\Delta t + o(\Delta t)) \\ = \; & P_{11}(t)q_{13}\cdot\Delta t + P_{13}(t) + P_{13}(t)q_{33}\cdot\Delta t + o(\Delta t) \;\; (since\ q_{33} = -\lambda_3). \end{aligned}$$

Subtracting $P_{13}(t)$ and dividing both sides by Δt

$$\begin{aligned} P_{13}(t+\Delta t) - P_{13}(t) &= P_{11}(t)q_{13}\cdot\Delta t + P_{13}(t)\cdot 0\cdot\Delta t + o(\Delta t) \;\; (since\ \lambda_3 = -q_{33} = 0) \\ \frac{P_{13}(t+\Delta t) - P_{13}(t)}{\Delta t} &= P_{11}(t)q_{13} + \frac{o(\Delta t)}{\Delta t} \\ P'_{13}(t) &= P_{11}(t)q_{13} \quad (taking\ limits\ \ as\ \ \Delta t\to 0) \\ P'13(t) &= e^{-(q_{12}+q_{13})\cdot t}q_{13} \;\; (since\ P_{11}(t) = e^{-(q_{12}+q_{13})\cdot t}) \\ \int_0^t P'_{13}(r)dr &= q_{13}\int_0^t e^{-(q_{12}+q_{13})\cdot r}dr \\ P_{13}(r)|_0^t &= \frac{q_{13}}{-(q_{12}+q_{13})}e^{-(q_{12}+q_{13})\cdot r}|_0^t \\ P_{13}(t) - P_{13}(0) &= \frac{q_{13}}{-(q_{12}+q_{13})}[e^{-(q_{12}+q_{13})\cdot t} - 1] \\ P_{13}(t) - 0 &= \frac{q_{13}}{q_{12}+q_{13}}[1 - e^{-(q_{12}+q_{13})\cdot t}] \\ P_{13}(t) &= \frac{q_{13}}{\lambda_1}[1 - e^{-\lambda_1\cdot t}] \end{aligned}$$

Summary of the three results:
Some intuitive results are arrived at:

1. $e^{-(q_{12}+q_{13})\cdot t}$ gives the probability of remaining in the same state (state 1 only).
2. $1 - e^{-(q_{12}+q_{13})\cdot t}$ is the probability of leaving state 1.
3. The fraction $\frac{q_{12}}{q_{12}+q_{13}}$ is the probability of entering state 2 conditional on the probability of having left state 1.
4. The fraction $\frac{q_{13}}{q_{12}+q_{13}}$ is the probability of entering state 3 conditional on the probability of having left state 1.

$$\begin{aligned}
\therefore P_{12}(t) &= [1-e^{-(q_{12}+q_{13})\cdot t}]\frac{q_{12}}{q_{12}+q_{13}} = [1-e^{-\lambda_1 \cdot t}]\cdot\frac{q_{12}}{\lambda_1} \\
&= P(leaving\ \ state\ 1)\times P(entering\ \ state\ 2) \\
P_{13}(t) &= [1-e^{-(q_{12}+q_{13})\cdot t}]\frac{q_{13}}{q_{12}+q_{13}} = [1-e^{-\lambda_1 \cdot t}]\cdot\frac{q_{13}}{\lambda_1} \\
&= P(leaving\ \ state\ 1)\times P(entering\ \ state\ 3).
\end{aligned} \tag{3.35}$$

Note that the holding time in state 1 is an exponential random variable with a parameter $\lambda_1 = q_{12} + q_{13}$. The probability that the process enters state 2 after leaving state 1 is:
$\frac{q_{12}}{q_{12}+q_{13}} = \frac{q_{12}}{\lambda_1} = p_{12}$
and the probability that the process enters state 3 after leaving state 1 is:
$\frac{q_{13}}{q_{12}+q_{13}} = \frac{q_{13}}{\lambda_1} = p_{13}$.
Thus, the process can be simulated by sequentially computing holding times and transitions.

3.3.4 Mean time to absorption

According to Fennell *et al.* (2016) the mean time to absorption in a continuous-time Markov jump process is obtained by first motivating the one-dimensional case as follows: Let T be the random variable for the time to absorption with exponential density function $f(t) = \lambda e^{-\lambda t}$ and corresponding moment generating function

$$\begin{aligned}
m(z) &= E[e^{zt}] \\
m(z) &= \lambda\int_0^\infty e^{-(\lambda-z)t}dt = \frac{\lambda}{\lambda-z} = \lambda(\lambda-z)^{-1}.
\end{aligned} \tag{3.36}$$

The r^{th} moment of T is then found by evaluating

$$\frac{d^r m(z)}{dz^r}|_{z=0} = r!(\lambda)^{-r}. \tag{3.37}$$

It follows that the mean time to absorption is the mean of the exponential distribution:

$$E(T) = \lambda^{-1}. \tag{3.38}$$

Suppose there are z transient states and one super absorbing state such that the

infinitesimal generator V is a $(z \times 1) \times (z \times 1)$ matrix which can be partitioned as follows:

$$V = \begin{pmatrix} \mathbf{Q} & \mathbf{R} \\ \mathbf{0} & 0 \end{pmatrix}$$

where $\mathbf{Q}$ is the $z \times z$ infinitesimal generator among the transient states. Define $z \times 1$ vector $\mathbf{f}(t) = [f_1(t), f_2(t), ..., f_z(t)]^T$ where $f_i(z)$ is the time to absorption density from state i such that $\mathbf{f}(t) = e^{\mathbf{Q}t}\mathbf{R}$. Then, the matrix moment generating function is given by:

$$M(z) = \int_0^\infty e^{zt}\mathbf{f}(t)dt = \int_0^\infty e^{zt}e^{\mathbf{Q}t}dt\mathbf{R} = -\left(\mathbf{Q} + z\mathbf{I}\right)^{-1}\mathbf{R} \tag{3.39}$$

from which we can obtain the r^{th} moment;

$$\mathbf{M}_r = (-1)^r r!\mathbf{Q}^{-1}\mathbf{C} \tag{3.40}$$

$$\mathbf{M}_1 = -\mathbf{Q}^{-1}\mathbf{C} \tag{3.41}$$

3.3.5 Inference: Maximum likelihood estimation (MLE) of transition intensities

Kalbfleisch and Lawless (1985) and Kay (1986) proposed maximum likelihood methods for the analysis of panel data under continuous-time Markov jump models. Using Equation (3.25) of Example 3, the observation takes the form $s_w = n_{w,w+1}$, rate of viral rebound from state w to $w+1$ or birth of viral particles; $r_w = n_{w,w-1}$, rate of viral suppression from state w or death of viral particles; $d_w = n_{w,6}$ the rate of absorption from w to death of an infected person; and T_w the total time spent in state w. Then, the likelihood function for the parameters, ρ_w, μ_w and σ_w, in example 3 is given by:

$$\begin{aligned}
L &= \Pi_{i=1}^N e^{-(\mu_1+\sigma_1)T_{1i}}e^{-(\mu_2+\sigma_2+\rho_2)T_{2i}}e^{-(\mu_3+\sigma_3+\rho_3)T_{3i}}e^{-(\mu_4+\sigma_4+\rho_4)T_{4i}}e^{-(\rho_5+\mu_5)T_{5i}} \\
&\times \mu_1^{d_{1i}} \times \sigma_1^{s_{1i}} \times \mu_2^{d_{2i}} \times \rho_2^{r_{2i}} \times \sigma_2^{s_{2i}} \times \mu_3^{d_{3i}} \times \rho_3^{r_{3i}} \times \sigma_3^{s_{3i}} \times \mu_4^{d_{4i}} \times \rho_4^{r_{4i}} \times \sigma_4^{s_{4i}} \times \mu_5^{d_{5i}} \times \rho_5^{r_{5i}} \\
&= e^{-(\mu_1+\sigma_1)\sum T_{1i}}e^{-(\mu_2+\sigma_2+\rho_2)\sum T_{2i}}e^{-(\mu_3+\sigma_3+\rho_3)\sum T_{3i}}e^{-(\mu_4+\sigma_4+\rho_4)\sum T_{4i}}e^{-(\rho_5+\mu_5)\sum T_{5i}} \\
&\times \mu_1^{\sum d_{1i}} \times \sigma_1^{\sum s_{1i}} \times \mu_2^{\sum d_{2i}} \times \rho_2^{\sum r_{2i}} \times \sigma_2^{\sum s_{2i}} \times \mu_3^{\sum d_{3i}} \times \rho_3^{\sum r_{3i}} \times \sigma_3^{\sum s_{3i}} \times \mu_4^{\sum d_{4i}} \\
&\times \rho_4^{\sum r_{4i}} \times \sigma_4^{\sum s_{4i}} \times \mu_5^{\sum d_{5i}} \times \rho_5^{\sum r_{5i}}.
\end{aligned}$$

If we define $s_j = \sum s_{ji}$, $r_j = \sum r_{ji}$, $d_j = \sum d_{ji},$, $T_j = \sum T_{ji}$ for $j = 1, ..., 5$ then:

$$
\begin{aligned}
L &= e^{-(\mu_1+\sigma_1)T_1} e^{-(\mu_2+\sigma_2+\rho_2)T_2} e^{-(\mu_3+\sigma_3+\rho_3)T_3} e^{-(\mu_4+\sigma_4+\rho_4)T_4} e^{-(\rho_5+\mu_5)T_5} \\
&\times \mu_1^{d_1} \times \sigma_1^{s_1} \times \mu_2^{d_2} \times \rho_2^{r_2} \times \sigma_2^{s_2} \times \mu_3^{d_3} \times \rho_3^{r_3} \times \sigma_3^{s_3} \times \mu_4^{d_4} \times \rho_4^{r_4} \times \sigma_4^{s_4} \times \mu_5^{d_5} \times \rho_5^{r_5} \\
L &= \left(e^{-\mu_1 T_1} \mu_1^{d_1}\right) \left(e^{-\sigma_1 T_1} \sigma_1^{s_1}\right) \left(e^{-\mu_2 T_2} \mu_2^{d_2}\right) \left(e^{-\rho_2 T_2} \rho_2^{r_2}\right) \left(e^{-\sigma_2 T_2} \sigma_2^{s_2}\right) \left(e^{-\mu_3 T_3} \mu_3^{d_3}\right) \\
&\times \left(e^{-\rho_3 T_3} \rho_3^{r_3}\right) \left(e^{-\sigma_3 T_3} \sigma_3^{s_3}\right) \left(e^{-\mu_4 T_4} \mu_4^{d_4}\right) \left(e^{-\rho_4 T_4} \rho_4^{r_4}\right) \left(e^{-\sigma_4 T_4} \sigma_4^{s_4}\right) \\
&\times \left(e^{-\mu_5 T_5} \mu_5^{d_5}\right) \left(e^{-\rho_5 T_5} \rho_5^{r_5}\right) \\
\ln L &= (-\mu_1 T_1 + d_1 \ln \mu_1) + (-\sigma_1 T_1 + s_1 \ln \sigma_1) + (-\mu_2 T_2 + d_2 \ln \mu_2) \\
&+ (-\rho_2 T_2 + r_2 \ln \rho_2) + (-\sigma_2 T_2 + s_2 \ln \sigma_2) + (-\mu_3 T_3 + d_3 \ln \mu_3) \\
&+ (-\sigma_3 T_3 + s_3 \ln \sigma_3) + (-\rho_3 T_3 + r_3 \ln \rho_3) + (-\mu_4 T_4 + d_4 \ln \mu_4) \\
&+ (-\sigma_4 T_4 + s_4 \ln \sigma_4) + (-\rho_4 T_4 + r_4 \ln \rho_4) + (-\mu_5 T_5 + d_5 \ln \mu_5) \\
&+ (-\rho_5 T_5 + r_5 \ln \rho_5)
\end{aligned}
\tag{3.42}
$$

Differentiating and equating the derivatives to zero leads to:

$$\begin{aligned}
\frac{\partial \ln L}{\partial \mu_1} &= -T_1 + \frac{d_1}{\mu_1} \Rightarrow \hat{\mu}_1 = \frac{d_1}{T_1}, \\
\frac{\partial \ln L}{\partial \sigma_1} &= -T_1 + \frac{s_1}{\sigma_1} \Rightarrow \hat{\sigma}_1 = \frac{s_1}{T_1}, \\
\frac{\partial \ln L}{\partial \mu_2} &= -T_2 + \frac{d_2}{\mu_2} \Rightarrow \hat{\mu}_2 = \frac{d_2}{T_2}, \\
\frac{\partial \ln L}{\partial \rho_2} &= -T_2 + \frac{r_2}{\rho_2} \Rightarrow \hat{\rho}_2 = \frac{r_2}{T_2}, \\
\frac{\partial \ln L}{\partial \sigma_2} &= -T_2 + \frac{s_2}{\sigma_2} \Rightarrow \hat{\sigma}_2 = \frac{s_2}{T_2}, \\
\frac{\partial \ln L}{\partial \mu_3} &= -T_3 + \frac{d_3}{\mu_3} \Rightarrow \hat{\mu}_3 = \frac{d_3}{T_3}, \\
\frac{\partial \ln L}{\partial \rho_3} &= -T_3 + \frac{r_3}{\rho_3} \Rightarrow \hat{\rho}_3 = \frac{r_3}{T_3}, \\
\frac{\partial \ln L}{\partial \sigma_3} &= -T_3 + \frac{s_3}{\sigma_3} \Rightarrow \hat{\sigma}_3 = \frac{s_3}{T_3}, \\
\frac{\partial \ln L}{\partial \mu_4} &= -T_4 + \frac{d_4}{\mu_4} \Rightarrow \hat{\mu}_4 = \frac{d_4}{T_4}, \\
\frac{\partial \ln L}{\partial \rho_4} &= -T_4 + \frac{r_4}{\rho_4} \Rightarrow \hat{\rho}_4 = \frac{r_4}{T_4}, \\
\frac{\partial \ln L}{\partial \sigma_4} &= -T_4 + \frac{s_4}{\sigma_4} \Rightarrow \hat{\sigma}_4 = \frac{s_4}{T_4}, \\
\frac{\partial \ln L}{\partial \mu_5} &= -T_5 + \frac{d_5}{\mu_5} \Rightarrow \hat{\mu}_5 = \frac{d_5}{T_5}, \quad and \\
\frac{\partial \ln L}{\partial \rho_5} &= -T_5 + \frac{r_5}{\rho_5} \Rightarrow \hat{\rho}_5 = \frac{r_5}{T_5}.
\end{aligned}$$

In general

$$\begin{aligned}
\hat{\mu_w} &= \frac{d_w}{T_w}, \\
\hat{\sigma_w} &= \frac{s_w}{T_w}, \ and \\
\hat{\rho_w} &= \frac{r_w}{T_w}.
\end{aligned}$$

A more compact proof is as follows:
The components of the likelihood are as follows:

1. Remaining in state w. The likelihood becomes:

$$\exp\{-\sum_{w=1}^{5}(\rho_w + \mu_w + \sigma_w)T_w - \rho_1 T_1 - \sigma_5 T_5\}$$

$\rho_1 T_1$ and $\sigma_5 T_5$ are subtracted since they are missing from the first and last terms respectively.

2. Entering state $w+1$. The likelihood becomes:

$$\begin{aligned} & \exp\{-\sum_{w=1}^{5}(\rho_w+\mu_w+\sigma_w)T_w-\rho_1 T_1-\sigma_5 T_5\}\times\sigma_1^{s_1}\sigma_2^{s_2}\sigma_3^{s_3}\sigma_4^{s_4} \\ = \quad & \exp\{-\sum_{w=1}^{5}(\rho_w+\mu_w+\sigma_w)T_w-\rho_1 T_1-\sigma_5 T_5\}\Pi_{w=1}^{4}\sigma_w^{s_w} \end{aligned}$$

3. Entering state $w-1$. The likelihood becomes:

$$\begin{aligned} & \exp\{-\sum_{w=1}^{5}(\rho_w+\mu_w+\sigma_w)T_w-\rho_1 T_1-\sigma_5 T_5\}\times\rho_2^{r_2}\rho_3^{r_3}\rho_4^{r_4}\rho_5^{r_5} \\ = \quad & \exp\{-\sum_{w=1}^{5}(\rho_w+\mu_w+\sigma_w)T_w-\rho_1 T_1-\sigma_5 T_5\}\Pi_{w=2}^{5}\rho_w^{r_w} \end{aligned}$$

4. Entering state D. The likelihood becomes:

$$\begin{aligned} & \exp\{-\sum_{w=1}^{5}(\rho_w+\mu_w+\sigma_w)T_w-\rho_1 T_1-\sigma_5 T_5\}\times\mu_1^{d_1}\mu_2^{d_2}\mu_3^{d_3}\mu_4^{d_4}\mu_5^{d_5} \\ = \quad & \exp\{-\sum_{w=1}^{5}(\rho_w+\mu_w+\sigma_w)T_w-\rho_1 T_1-\sigma_5 T_5\}\Pi_{w=1}^{5}\mu_w^{d_w} \end{aligned}$$

The components can be put together and the likelihood would be written as:

$$L = \exp\{-\sum_{w=1}^{5}(\rho_w + \mu_w + \sigma_w)T_w - \rho_1 T_1 - \sigma_5 T_5\}\Pi_{w=1}^{4}\sigma_w^{s_w}\Pi_{w=2}^{5}\rho_w^{r_w}\Pi_{w=1}^{5}\mu_w^{d_w} \tag{3.43}$$

$$\begin{aligned}
\ln L &= l = -\sum_{w=1}^{5}(\rho_w + \mu_w + \sigma_w)T_w - \rho_1 T_1 - \sigma_5 T_5 \\
&+ \sum_{w=1}^{5}(s_w \ln\sigma_w + r_w \ln\rho_w + d_w \ln\mu_w) - s_5 \ln\sigma_5 - r_1 \ln\rho_1 \\
l &= \sum_{w=1}^{5}(-\rho_w T_w + r_w \ln\rho_w - \mu_w T_w + d_w \ln\mu_w - \sigma_w T_w + s_w \ln\sigma_w) \\
&- (\rho_1 T_1 + r_1 \ln\rho_1 + \sigma_5 T_5 + s_5 \ln\sigma_5)
\end{aligned} \tag{3.44}$$

The score functions are:

$$\begin{aligned}
\frac{\partial l}{\partial \rho_w} &= \frac{r_w}{\rho_w} - T_w, \\
\frac{\partial l}{\partial \mu_w} &= \frac{d_w}{\mu_w} - T_w, \ and \\
\frac{\partial l}{\partial \sigma_w} &= \frac{s_w}{\sigma_w} - T_w.
\end{aligned}$$

Resulting in the MLEs $\hat{\rho}_w = \frac{r_w}{T_w}$, $\hat{\mu}_w = \frac{d_w}{T_w}$, $\hat{\sigma}_w = \frac{s_w}{T_w}$ for $w = 1, 2, \ldots, 5$ representing transitions out of state w.

The Hessian matrix can be shown to be negative definite. This confirms the estimates to be maximum likelihood.

3.3.6 Estimation of non-homogeneous continuous-time Markov jump processes

Modelling the non-homogeneous Markov jump model can easily be done using a piecewise constant intensities approach. This involves the inclusion of time-dependent covariates in a Markov model, making it easier to deal with non-homogeneous Markov jump models. This approach, according to Saint-Pierre et al. (2003), partitions the time axis into r continuous and disjoint intervals, $[\tau_{(l-1)}, \tau_l)$ where $l = 1, ..., r+1$ and $\tau_{(r+1)} = \infty$ and assuming constant transition intensities in different time intervals. Consider a vector $\mathbf{z}^*(t) = (z_0^*(t), z_1^*(t), ..., z_r^*(t))'$ of artificially time-dependent covariates defined as:

$z_0^*(t) = 0, \forall t$ and:

$$z_l^*(t) = \begin{cases} 0; & \tau_0 \leq t < \tau_l \\ 1; & t \geq \tau_l \end{cases}$$

Where $l = 1, \ldots, r$ disjoint intervals. The model with transition intensities is as follows:

$$q_{ij}(t|\mathbf{z}^*(t)) = q_{ij}^{(0)} exp\{\beta'_{ijz^*}\mathbf{z}^*(t)\}, i \neq j \tag{3.45}$$

This approach to non-homogeneity in a Markov jump process is a step-wise method that assumes constant transition intensities in different time intervals. The parameters of this model are the baseline transition intensities $q_{ij}^{(0)}$ which represent transition intensities in the interval $[\tau_0, \tau_1)$ and the vector of regression coefficient β_{ijz^*} associated with artificially time-dependent covariates z^*.

The effect of covariates $(\mathbf{y})$ on the transition rates is modelled using the proportional intensities model. The intensity matrix $Q(\mathbf{y})$ for each interval now depends on a vector $\mathbf{y}$ defined as follows:

$$y(t) = \begin{cases} 0; & if\ \ covariate\ \ attribute\ \ is\ \ not\ \ present, \\ 1; & if\ \ covariate\ \ attribute\ \ is\ \ present \end{cases}$$

The entry of $Q(\mathbf{y})$ is given by:

$$q_{ij}(y_x(t)) = q_{ij}^{(0)} exp\left(\beta'_{ijy}\mathbf{y}(t)\right) \tag{3.46}$$

define the transition intensity from state i to state j for patient x at observation time t for each interval. For the full model that combines the time-dependent effect and the effect of the covariate $\mathbf{y}$ as the initial marker of HIV infection, equations (3.45) and (3.46) are combined as follows:

$$q_{ij}(t|\mathbf{z}^*(t), y_x(t)) = q_{ij}^{(0)} exp\left[\left\{\beta'_{ijz^*}\mathbf{z}^*(t) + \beta'_{ijy}\mathbf{y}(t)\right]\right\} \quad , i \neq j \tag{3.47}$$

The parameters $q_{ij}^{(0)}$ are the baseline transition intensities for intervals $[\tau_0, \tau_1)$, β_{ijz^*} is the log-linear effect of the artificial time-depended covariate and β_{ijy} is the vector of regression coefficients associated with the other covariates defined by $\mathbf{y}$.

Computing $P(0, t_i)$ for a t_i in segment τ_l entails multiplying all the transition matrices across the various intervals as shown below:

$$P(0, t_i) = \left[\Pi_{l=1}^{l-1} P^{(b)}(\Pi_b)\right] P^{(l)}\left(\tau_{(l-1)}, \tau_j\right) \tag{3.48}$$

where $P^{(b)}$ is the transition probability matrix obtained using $q_{ij}^{(b)}$ for the b^{th} segment denoted by τ_b. If subjects are observed on an equal spaced grid and segments are divided up along these time points, then $P_{ij}(0, t_i)$ would simply be the $(ij)^{th}$ element of the matrix in the above equation. When data is not equally spaced, then observations would be considered missing at the breakpoints. To resolve this, a model that accounts for all possible pathways between the last observed state in the segment b_{l-1} and the first observation in segment b_0 was suggested. For example, if a breakpoint t' is created between two points t_j and t_k, then via Chapman-Kolmogorov equations, the likelihood contribution from interval (t_j, t_k) for individual x can be found as:

$$L_x = \sum_{l=1}^{k} P_{il}^{(1)}\left(t_j, t'\right) P_{lj}^{(2)}(t', t_k) \tag{3.49}$$

for states i, j.

3.3.7 Incorporation of covariates in a continuous-time Markov model

Collection of longitudinal data on states occupied by a process includes measurement of some covariates. In monitoring HIV/AIDS progression based on CD4 cell count and/or viral load monitoring, these covariates are analysed together with gender, age, drug regimen, TB screening, development of any form of reaction to treatment (eg. lactic acid, peripheral neuropathy), non-adherence to treatment, and others. There is need to study the effects of these covariates to the intensity matrix Q in the Markov model. This is done by assuming a proportional intensities regression model. Thus, according to Cox and Miller (1968), modelling the transition intensities as:

$$q_{ij}(\mathbf{Z}) = q_{ij}^{(0)} exp(\beta_{ij}' \mathbf{Z}) \qquad i \neq j \tag{3.50}$$

where $\mathbf{Z}$ is an $k-$dimensional vector of covariates, β_{ij} is a vector of k regression

parameters relating to the instantaneous rate of transitions from state i to state j to the covariates and $q_{ij}^{(0)}$ is the baseline intensity relating to the transition from state i to state j. The resulting transition intensity matrix, $Q(\mathbf{Z})$ for a subject with vector of covariates $\mathbf{Z}$ with element $q_{ij}(\mathbf{Z})$, can be used in the equation:

$$\lim_{\Delta t \to 0+} \frac{P_{ij}(t + \Delta t)}{\Delta t} = q_{ij}(t),\ i \neq j \tag{3.51}$$

to compute a transition probability matrix $P(t|\mathbf{Z})$ whose elements $P_{ij}(t|\mathbf{Z})$ contribute to the likelihood function. The log-linear model for the Markov rates $q_{ij}(\mathbf{Z})$ is chosen primarily for analytical convenience and because this model has the attractive feature of yielding non-negative transition intensities for any $\mathbf{Z}$ and β_{ij}. Modelling on related scales such as the log-hazard makes it possible to study the way the baseline probabilities are modified by covariates. The log-linear model is nearly additive, thus making it possible to interpret the values of the coefficient $\beta_{ij,k}$.

3.4 Diagnostic methods for Markov Models

Titman (2007) suggested a number of methods that can be used as diagnostic tools for the fitted Markov models. He classified the methods into two groups, the formal methods and the informal methods. The formal methods include the use of the log-likelihood ratio tests (LRT) and the Pearson's chi-squared test. The log-likelihood ratio test is used to compare two different fitted models, for example, a Markov model without covariates and a Markov model with covariates. The Pearson's chi-squared test is used to compare prevalence counts by the use of observed and expected frequencies. The informal methods use graphs to compare the fitted model with the observed data and does not involve calculations such as of likelihood ratio's.

3.4.1 Testing the Markov assumption

The Markov assumption is that future state of a process only depends on the current state and is independent of the past. The method by Kay (1986) as cited by Titman (2007) involves creating data for the exact transition times between states using interpolation when the data is completed and a test is performed, for example, given an illness-death model with two communicating states, 1 and 2, and death being the absorbing state. By letting t_2 be the time spent in state 2 during the last sojourn in state 1, we can fit the model for intensity, $q_{12} = q_{12}^{(0)} exp(\beta t_2)$ and test the hypothesis, $H_0 : \beta = 0$. This hypothesis will assess the assumption that the transition rate to

death from state 1 is unaffected by the previous sojourn time.

3.4.2 Testing the homogeneity assumption

The homogeneity assumption is that the transition intensities are constant throughout time, that is, $q_{ij}(t) = q_{ij}$. This assumption is tested using piecewise constant transition intensities using a formal likelihood ratio test for the independence of the two models. The fitted parametric time-dependent will be of the form $q_{ij}(t) = q_{ij}^{(0)} exp(-\lambda t)$ and perform a likelihood ratio test on the hypothesis $H_0 : \lambda = 0$.

Likelihood ratio test (LRT)

Suppose,

$$LRT = -2\log_e\left(\frac{L_s(\hat{\theta})}{L_g(\hat{\theta})}\right), \tag{3.52}$$

is the ratio of two likelihood functions, for a simpler model (s) with fewer parameters and the general model (g). The test statistic is asymptotically distributed as a chi-square random variable, with degrees of freedom equal to the number of parameters between the two models. The likelihood ratio test can be done provided the simpler model is a special case of the complex model.
The LRT can also be presented in terms of deviance, that is,

$$\begin{aligned} LRT &= -2(\log_e(L_s) - \log_e(L_g)) \\ &= -2\log_e(L_s) + 2\log_e(L_g) \\ &= deviance_s - deviance_g. \end{aligned}$$

Thus, LRT can be computed as a difference between the deviance for the two fitted models. For this research the LRT is also going to be used to compare the homogeneous model with covariates and the homogeneous model without covariates.

3.4.3 Contingency table based methods

This method provides an assessment of the overall fit of the assumed model. Kalbfleisch and Lawless (1985) dealt with balanced observation with categorical covariates. They fitted the model by considering observed and expected transition frequencies either through likelihood ratio test or asymptotically equivalent Pearson chi-squared statistic. However, Chen and Chen (2003) argue that Pearson chi-square has low power,

particularly when the degrees of freedom are very large and that the asymptotic null distribution cannot be applied when the counts in table are small.

3.4.4 Akaike Information Criteria

Akaike information criterion (AIC) compares the quality of a set of substantial models to each other. It does so by ranking the fitted models from best to worst and the best model will be the one with the lowest AIC. The AICs for any given model are defined as:

$$AIC = -2 \times \log(likelihood) + 2k \tag{3.53}$$

where k is the number of model parameters (the number of variables in the model plus the intercept). $\log(likelihood)$ is a measure of model fit. The higher the number of parameters in the model, the better the fit. This is usually obtained from statistical output. The model with the lowest AIC is considered as the better model.

3.4.5 Convergence of a Time-Homogeneous Markov Model

If a Markov model fails to converge, optimisation criteria results in a failure to calculate standard errors leading to the exclusion in the calculation of confidence intervals for the estimated parameters. After running the analysis for suffixes: using the "msm" package in R, the statistical package gives a warning; optimisation has probably not converged to the maximum likelihood. Thus, to ensure that the model converges, a scaling factor is used to normalise the likelihood and to prevent the overflow within the optimisation process.

3.5 Data

3.5.1 Compliance with Ethics Guidelines

The procedures used in this study were approved by the Research Ethics Committee of the University of Venda, South Africa (Protocol number SMNS/13/MBY/01/0625), in accordance with the 1964 Helsinki declaration and its subsequent amendments. Additionally, permission to access health facilities was obtained from the Limpopo Provincial Department of Health, South Africa, and the collaborating health facilities. Informed consent was obtained from the study participants prior to their involvement, and the data obtained were stripped of personal identifiers to ensure the anonymity and confidentiality of participants.

3.5.2 Data description

This study includes data from a heterogeneous group of 319 HIV infected patients on combination anti-retroviral therapy (cART) who fulfilled the entry criteria from a longitudinal cohort of 1092 HIV-infected patients followed up at a Wellness clinic in Bela Bela, South Africa, from year 2005 to year 2009. These patients were observed at enrolment and followed up after the first and second 3 months of treatment uptake and after every 6 months thereafter. The longitudinal data from the 320 HIV/AIDS patients who were on follow-up yielded 2 259 observations. Patients were eligible for inclusion if they had a routinely reported viral load and if they were 15 years and older. The ages of the patients ranged from 15 years to 77 years. Children born to HIV-infected patients were not included in the study. From the 320 patients selected for study, females constituted 70% and males constituted 30%. 172 patients were aged 45 and below, and 72 were over 45 years of age. From these patients, 267 had a baseline viral load above 10 000 copies/mL, 49 had a baseline viral load (VLBL) below 10 000 copies/mL and 3 had missing viral load baseline. Approximately 70% of these patients had a baseline CD4 (CD4BL) cell count below 200 cells/mm^3 (AIDS defining stage). At treatment initiation the variables age, VLBL and CD4BL are described in Table 3.1 as follows:

Table 3.1: Descriptive statistics for the baseline variables: Age, viral load and CD4 cell count

	Age (years)	VLBL (copies/mL)	CD4BL (cells/mm^3
Minimum	15	$<$ 50 (undetectable)	16
First Quartile	32	21 334	38
Median	39	67 995	116
Mean	40.62	138 208	156
Third Quartile	47	201 445	206
Maximum	77	$>$ 500 000	1 202

For each visit time, blood samples were obtained for each patient and stored frozen until assayed. Plasma HIV RNA was measured using an amplicator HIV-1 monitor assay kit which has a limit of sensitivity ranging from 50 copies/mL to 500 000 copies/mL.

At $t = 0$, the regimens that were mostly administered to patients were the triple combination therapy, d4T-3TC-EFV (208 patients) and d4T-3TC-NVP (92 patients). d4T and 3TC represent Stavudine and Lamivudine, respectively, which fall under nucleoside reverse transcriptase inhibitors (NRTI) class. EFV and NVP stand for Efavirenz and Nevirapine, respectively, and are from the non-nucleoside reverse transcriptase

inhibitors (NNRTI) class. In patients who showed some signs of non-adherence, D4T was substituted with AZT (Zidovudine). A switch from d4T-3TC-EFV to AZT-3TC-EFV was most common, rising from 10 patients in the first 6 months to 92 patients in 30 months (2 and half years). During the same period, the number of patients who switched from d4T-3TC-NVP to AZT-3TC-NVP rose from 6 to 45. After one year of treatment uptake, one patient was introduced to FTC-TDF-EFV and after three and half years, the frequency increased to 10 patients. Another combination of FTC-TDF-NVP was also introduced to 3 patients after 2 years and the number rose to 7 after 3 years. The drug regimens that were mostly administered during the first three and half years are summarised in Table 3.2 below:

Table 3.2: Treatment regimen administered to the patients i the first 3.5 years of treatment follow-up

Drug/t	**0**	**0. 25**	**0.5**	**1**	**1.5**	**2**	**2.5**	**3**	**3.5**
1	208	191	165	140	94	44	18	5	3
2	92	73	70	62	35	23	7	1	0
3	2	3	10	20	50	77	92	88	60
4	3	6	6	14	35	36	45	35	31
5	0	0	0	1	1	3	8	10	10
6	0	0	0	0	0	3	5	7	3
7	2	2	1	2	5	4	2	2	1

KEY: **1**:-d4T-3TC-EFV, **2**:-d4T-3TC-NVP, **3**:-AZT-3TC-EFV, **4**:-AZT-3TC-NVP, **5**:-FTC-TDF-EFV, **6**:-FTC-TDF-NVP, **7**:-d4T-3TC-LPV/r, **t** represents time in years post treatment commencement.

During the course of the study, HIV/AIDS progression was assessed based on CD4 cell count routine monitoring (CD4) and viral load routine monitoring (VL). In this thesis, continuous-time Markov models are based on either CD4 cell count states or viral load count states. These variables are time-dependent and are defined as follows:

$$CD4\ cell\ count\ levels(X_c(t)) = \begin{cases} 1; & CD4 > 800 \\ 2; & 500 < CD4 \leq 800 \\ 3; & 350 < CD4 \leq 500 \\ 4; & CD4 < 350 \\ 5; & Death. \end{cases}$$

$$Viral\ load\ levels(X_v(t)) = \begin{cases} 1; & VL < 50 \\ 2; & 50 \leq VL < 10\,000 \\ 3; & 10\,000 \leq VL < 100\,000 \\ 4; & 100\,000 \leq VL < 500\,000 \\ 5; & VL \geq 500\,000 \\ 6; & Dead. \end{cases}$$

where VL stands for viral load.
During the course of treatment, patients are expected to transition in both CD4 cell count states and viral load count states. For example, for the data defined above, transitions in the first 2 years of treatment, CD4 cell count and viral load counts for each state are distributed in Table 3.3 as follows:

Table 3.3: Transition intensities in the first 2 years of treatment follow-up

	$X_c(t)$					$X_v(t)$					
t (years)	**1**	**2**	**3**	**4**	**5**	**1**	**2**	**3**	**4**	**5**	**6**
0	3	8	11	298	0	4	43	134	106	32	0
0.25	6	16	39	228	24	155	123	6	4	4	24
0.5	13	30	42	195	11	214	48	13	2	3	11
1	16	38	49	154	7	208	37	9	2	1	7
1.5	24	44	66	102	7	186	39	8	3	0	7
2	25	64	47	80	5	178	26	10	2	0	5

The information presented in the above table shows that once HIV/AIDS patients are on treatment, viral load responds faster to treatment compared to CD4 cell count, such that within the first 0.25 years of treatment, the majority of the patients had viral load suppressed to undetectable levels. Although there are some transitions among the CD4 cell count states, transitions to better CD4 cell count states was slow.

Checking for the linear regression assumption between time and either Viral load or CD4 cell count

In this thesis, viral load count is expected to decrease with time and the CD4 cell count is expected to increases with time for HIV/AIDS patients on cART, as discussed above. Thus, diagnostic plots are drawn to check the linear regression assumption between the explanatory variable (either viral load count or CD4 cell count) and the predictor (time). Diagnostic plots help to check whether fitted models fit well with the observed data. This is done using residuals. Residuals can reveal

unexplained patterns in the observed data by the fitted model and help in improving the model in an explanatory way (Bommae, 2015). Plot of residuals versus fitted would show if residuals have non-linear patterns. Uniformly spread residuals around a horizontal line without an evident pattern is an indication that we have a good relationship. A normal Q-Q plot shows if residuals are normally or exponentially distributed, or whether the residuals deviate from normality. Scale location plot shows if the residuals are spread equally along the ranges of predictors. This helps in checking the assumption of variability. Residuals versus Leverage plot helps to find influential cases (subjects), if any. In some cases, extreme value cases may not be influential in determining the regression line.

In Figure 3.1 and Figure 3.2 below, plots of residuals versus fitted model, normal Q-Q plots, scale location plots and residuals versus leverage plots are shown.

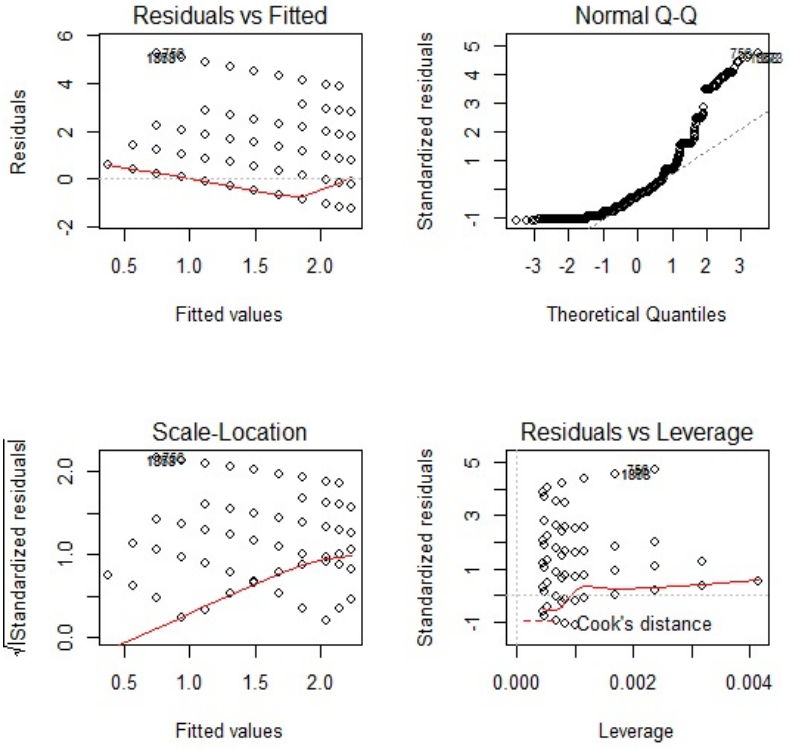

Figure 3.1 – *Diagnostic Plots for the linear regression model of time on viral load counts*

The Residuals versus fitted plot in Figure 3.1 indicates a non-linear relationship. The normal Q-Q plot shows deviation from normality. For the Scale location plot,

the smooth line is not horizontal, indicating no homoscedacity among the residuals. Overall, the diagnostic plots showed that the fitted model violates the linear regression assumption. This is further explored in Chapter 5, where a non-homogeneous model is fitted.

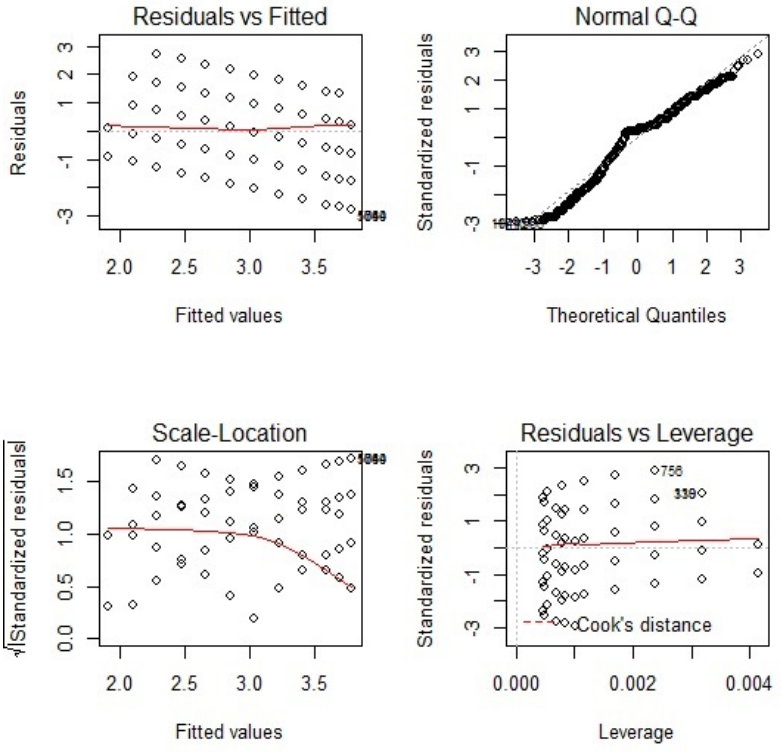

Figure 3.2 – *Diagnostic Plots for the linear regression model of time on CD4 cell count states*

Residuals versus fitted plot in Figure 3.2 shows residuals that are equally spread around the horizontal line. This shows that the model explains better the linear relationship between CD4 cell count states and time (years). The Normal Q-Q plot shows residuals that are in a straight dashed line. This indicates that the residuals are normally distributed. The Scale location plot shows a horizontal line with uniformly (randomly) spread points, thus revealing homoscedasticity of residuals.

Besides CD4 cell count and viral load monitoring at follow-up times, a number of other factors were noted. These included non-adherence to treatment, treatment change, treatment line, resistance to treatment and other factors that are of interest, depending on the chapter under consideration. Patients who had problems in adherence to treatment were those who were intolerant to the treatment combination

and those who failed to reach viral suppression. Change of treatment line was based on treatment failure, toxicity, patient intolerance to the combination therapy, or inability of the patient to adhere to treatment and viral rebound. From these patients, 36 showed some signs of non-adherence to treatment.

In this thesis, viral load below 50 copies/mL is defined as undetectable viral load, and the progression of HIV/AIDS is defined either by change in viral load level or change in CD4 cell count level. The viral load levels are divided into 5 transient states, and the sixth state being the absorbing state, death. The CD4 cell count levels are divided into 4 transient states and the fifth state is the death state. The viral load states, CD4 cell count states and other factors that are likely to determine change in either viral load/CD4 cell count levels are defined in the next sub-section.

3.5.3 Variable coding

In this thesis, variables are coded as shown below:

$$Non-adherence\,to\,treatment(NA) = \begin{cases} 1; & Yes \\ 0; & No \end{cases} \tag{3.54}$$

$NA = 1$ means intolerant to treatment combination and this might result in change of treatment combination. $NA = 0$ means that the patient is tolerant to treatment and can continue with treatment.

$$CD4\,cell\,count\,at\,baseline\,(CD4BL) = \begin{cases} 1; & \leq 200\,cells/mm^3 \\ 0; & > 200\,cells/mm^3 \end{cases} \tag{3.55}$$

CD4 cell count less than or equal to 200 cells/mm^3 represents HIV-infected patients in the AIDS defining state.

$$Gender = \begin{cases} 1; & male \\ 0; & female \end{cases} \tag{3.56}$$

Males constituted 30% of the patients and females constituted 70%.

$$Age = \begin{cases} 1; & 15 \leq\ Age\ \leq 45\,years \\ 0; & > 45\,years \end{cases} \tag{3.57}$$

$$Baseline\ viral\ load\ (VLBL) = \begin{cases} 1; & > 10\,000\ \ copies/mL \\ 0; & \leq 10\,000\ \ copies/mL \end{cases} \tag{3.58}$$

Patients who initiated therapy with baseline viral load below 10 000 copies/mL were in a better HIV disease state than those who initiated therapy with baseline viral load above 10 000 copies/mL.

In this thesis, variables are coded as indicated in equations (3.54) to (3.58). In the event that a different coding is used, this will be indicated in the relevant chapters. Any additional variables will also be indicated in relevant chapters, and coding will be done accordingly.

3.6 Concluding Remarks

In this chapter, the theory of Markov jump processes has been explored. An HIV, AIDS and Death (HAD) model for HIV/AIDS patients on combination anti-retroviral therapy was developed. Based on the HAD model, Kolmogorov forward and backward differential equations were constructed. The model was extended to cater for more states. The MLEs of model parameters were obtained. A description of the data used for analysis was given with some linear relationships between the variables of interest, CD4 cell count and viral load, with time, established.

In the next chapter, a continuous-time homogeneous Markov model is fitted using the methods discussed in this chapter.

Chapter 4

Time-homogeneous Markov process for HIV/AIDS immunology under a combination treatment therapy

4.1 Introduction

The number of CD4 T-cells in one's body determines how strong or weak the immune system is in fighting infections (Cichocki, 2018). The HIV targets the CD4 T-cell by invading it and turning it into a factory that produces millions of HIV RNA particles (Moncivaiz and Alexander, 2018). In the process, the CD4 T-cells are destroyed and this leads to the compromising of the immune system, making it more susceptible to infections by pathogens, leading to the development of opportunistic infections that include TB (Chinen and Shearer, 2002). The need to address the factors associated with immune compromisation (including TB co-infection) on HIV infected patients receiving cART has prompted the development of this chapter. Analysis of HIV disease history based on CD4 cell count states and death/loss to follow-up in a single model is done.

Most studies use Kaplan-Meier analysis and Cox proportional hazards regression models (Cingolani et al., 2012; Ndumbi et al., 2014; Phillips et al., 2001). Kaplan-Meier survival methods and Cox proportional hazards regression are commonly employed tools to model mortality and time to viral suppression and/or subsequent rebound and occasionally used to model time to CD4 cell recovery (Babiska et al, 2015). However, survival models are not appropriate for all studies, particularly in

the presence of competing risks and when multiple or recurrent outcomes are of interest (Zhang, 2017).

In medical research, the state of the patient at observation time is the only thing known with certainty (Jackson, 2019). The researcher may know the time interval in which a transition has occurred, but not the exact time (Lawless and Rad, 2015). Thus, homogeneous Markov models which are interval-censored can handle such data (Gibson, 2008). In particular, when modelling HIV/AIDS progression, Markov models are relatively straightforward to analyse both CD4 cell count stages and death or loss to follow-up within a single model, which survival models fail to do (Longini et al., 1989). Thus, Markov models can accommodate censored data, competing risks (informative censoring), multiple outcomes, recurrent outcomes, frailty and non-constant survival probabilities (Abner et al., 2014). As the multi-outcomes evolve over time, history is naturally generated containing information on previous visits, time of entry into various states, and the length of stay in states (Jackson, 2019). These states are mutually exclusive, that is, at any given time, the process can only be in one and only one state.

Markov models are favourable to the modelling of diseases in particular cases where the disease is grouped into a set of exhaustive and mutually exclusive health states, thereby forming a multi-state model (Foucher et al., 2005). Markov models are used to examine the conditions of the stochastic processes at various stages, categorisation of the conditions, and examination of the external influences (including TB co-infection) on the stochastic processes (Mullins, 1996).

Continuous-time homogeneous Markov models have been used to model disease progression of HIV/AIDS patients, and there has been some recent renewed interest in the use of these models (Lee et al., 2014).

Although most of the studies on HIV progression use Markov models approach with states based on CD4 cell count (Longini et al., 1989; Alioum et al., 1998; Binquet et al., 2009; Grover et al., 2013), none of these studies included the effects of TB co-infection on the disease progression.

In this chapter, a 7-staged continuous-time Markov model is used to assess the disease progression of HIV/AIDS patients receiving cART from a clinic in Bela-Bela, South Africa. The first 5 stages are based on CD4 cell counts and the end points are either death or withdrawal from study. In addition to the gender and age differences in HIV/AIDS progression, the effects of having TB as the initial marker of

HIV/AIDS, developing TB during the course of treatment, developing some adverse effects to treatment (Reaction), CD4 cell count at baseline and viral load at baseline, are assessed. Though Markov models based on CD4 cell counts is a common approach in HIV/AIDS modelling, this chapter is unique clinically, in that tuberculosis (TB) co-infection is included as a covariate.

The transition intensities, probabilities and the distribution functions associated with the times are the basic building blocks of the Markov processes (Halim, 1996). For a continuous-time Markov model, transitions are exponentially distributed and can occur at any (real-valued) time instant, for example, time until death, and waiting time before moving to another state (Whitt, 2013). For a time-homogeneous Markov jump process, the holding time in state i is modelled using the exponential distribution (Cox and Miller, 1965).

Transition probabilities for continuous-time homogeneous models only depend on the difference between the two observation times (Meira Macado et al., 2009). That is, for all $t \geq 0$ the probability of moving from state i to state j is given by:

$$\begin{aligned} P_{ij}(s,t) &= P(X(t) = j|F(s)) = P(X(t) = j|X(s) = i) \\ &= P(X(t-s) = j|X(0) = i), \forall t \geq 0, t > s. \end{aligned} \tag{4.1}$$

This is the Markov property, where $F(s)$ is the natural Filtration of the stochastic process. $P(X(t) = j|F(s))$, therefore, represents the probability that the stochastic process $X(t)$ is in state j at time t given the history of the process up to time s. The Markov property implies that all the history of the process is contained in the state currently occupied, $X(s) = i$. The transition probabilities of a continuous time homogeneous Markov process $X(t), t \geq 0$ is given by:

$$P_{ij}(t) = P(X(t) = j|X(0) = i) \tag{4.2}$$

The equations obey the Chapman-Kolmogorov equations:

$$P_{ij}(t+s) = \sum_{k \in X} P_{il}(t) P_{lj}(s), \forall t > 0 \tag{4.3}$$

In this chapter, HIV progression is described, using the theory of continuous time Markov processes, and using real data on an evolving disease such as AIDS. The effects of covariates, including TB, on baseline transition rates, is considered. Models

with and without covariates are fitted and compared using the likelihood ratio test.

The next section explores the methods of Markov modelling used in this chapter and an illustrative case study on HIV progression is given. In this section, data used in the analysis is highlighted and we explain formulation of the model based on the data. This is followed by a section on the results and discussions. The final section concludes on the findings from this chapter.

4.2 The continuous-time homogeneous Markov model

Formulation of the continuous-time Markov models is done by considering transition probabilities over narrow interval of time Δt. In this study, $\Delta t = \frac{1}{2}$ year, making it appropriate to assume that transition rates over these intervals are constant. These transition rates, also known as transition intensities or forces of transition, are the fundamental concept in continuous time Markov jump processes. They can take values greater than 1, unlike probabilities. In order to differentiate the transition probabilities and avoid technical problems with mathematics, the assumption is that the functions $P_{ij}(t)$ are continuously differentiable and are subject to the initial condition (Nielsen, 2009).

$$P_{ij}(0) = \delta_{ij} = \begin{cases} 0 & , i \neq j, \\ 1 & , i = j. \end{cases} \tag{4.4}$$

δ_{ij} is a Kronecker delta, $P_{ii}(0) = 1$ means that at $t = 0$ the system maintains its original state and $P_{ij}(0) = 0$ means that there is no change of state when no time elapses. The force of transition from state i to j is defined as:

$$q_{ij} = P'_{ij}(t)|_{t=0} = \lim_{\Delta t \to 0} \frac{P_{ij}(\Delta t) - \delta_{ij}}{\Delta t} \tag{4.5}$$

q_{ij}, for $i = 1, \ldots, 5$ and $j = 1, \ldots, 7$, does not vary over time and satisfies the following conditions: $\sum_{j \in X} q_{ij} = 0$ and $q_{ij} = -\sum_{i \neq j} q_{ij}$. Once the transition intensities are known, the transition probabilities can be obtained by solving a system of differential equations known as the Kolmogorov's forward equation subject to the initial conditions stated in Equation (4.4). The Kolmogorov's forward equation is as follows:

$$P'_{ij}(t) = \sum_{l \in S} P_{il}(t) q_{lj}, \forall i, j \tag{4.6}$$

where l is a state that the system can pass through as it makes a transition from state i to state j and S is the state space. The time homogeneous models are fitted for this data to assess effectiveness of the treatment by comparing the forward transition and the reverse transitions. This, then, leads to building of models that allow transitions in both directions.

4.3 Data description

Although the whole data set was obtained from HIV patients on combination antiretroviral therapy (cART) from a Wellness clinic in Bela Bela, South Africa, as described in Chapter 3, the dataset used in this Chapter is different from the data set used in all the other Chapters. In this Chapter a sample of 319 HIV patients with TB co-infection and routinely collected CD4 cell counts is extracted and used for analysis. Two hundred and twenty-seven of these patients were females and 92 were males at treatment commencement $(t = 0)$. After 3 years of treatment uptake, 173 females and 71 males were remaining in the study. Thirty-eight females had died and 16 withdrew and their status was not known after 3 years of treatment up take. Nineteen of the males died during the first three years and two had withdrawn and it was not known whether they were alive or dead. A 2-year old (subject 81) together with subject 82 were detected by the residuals plot as an outlier and it was removed from the analysis, meaning that the remaining 317 patients were used for analysis. About 50% and 65% of the female and male deaths, respectively, occurred during the first 6 months of treatment uptake. The interquartile range of patient ages is (33; 47.5), years with a mean and median age of 39.53 and 40 years, respectively. The ages were negatively skewed (skew =-0.24) which means that there were more younger patients than older patients in this cohort.

At time t = 0 there were 242 individuals with CD4 baseline (CD4BL) cell count below 200, 59 individuals with CD4 cell count between 200 and 350, 11 individuals with CD4 cell count between 350 and 500, 6 individuals with CD4 cell count between 500 and 750 and 1 individual with CD4 cell count above 750. At t = 0 the CD4 cell count had a mean of 156 cells/mm^3, a median of 116 cell/mm^3 and the maximum CD4 cell count was 1202 cells/mm^3. The mean viral load baseline (VLBL) for these patients was 105 573.35 copies/mm^3 and it ranged from 56 to 818 600 copies/mm^3. The me-

dian viral load was 58 523 copies/mm^3. From these individuals, 155 had a WHO stage baseline (WSBL) of 4, which is related to severe HIV symptoms. WSBL is the categorisation of HIV/AIDS at baseline basing on the clinical markers as defined by World Health Organisation (WHO).

Although some individuals developed TB (DTB) during the course of treatment, 109 patients had TB as an initial marker of HIV. From the individuals who had TB before (TBB4) commencement of anti-retroviral therapy (ART), 66 had a CD4 cell count baseline below 200 cells/mm^3, 20 had a CD4 cell count baseline between 200 and 350 cells/mm^3, 2 had CD4 cell count baseline between 350 and 500 cells/mm^3, 2 between 500 and 750 cells/mm^3 and 19 had unknown CD4 cell count baseline. These patients completed their TB treatment before commencement of ART. Fifty-two patients developed TB during the treatment period, and 12 of these patients had TB before commencement of treatment. During the first 6 months of treatment uptake, 35 patients died and from these deaths, only five were attributed to having TB before commencement of ART.

A combination therapy was administered to all HIV-infected individual in the cohort. The therapeutic intervention inhibits the actions of reverse transcriptase enzyme and/or protease of new infectious free HIV by the HIV-infected cell. The drug regimens at $t = 0$ were mainly a combination of d4T-3TC-EFV (administered to 207 patients) and d4T-3TC-NVP (administered to 83 patients). The second line regimens were mainly a combination of AZT-3TC-EFV/NVP and were given to patients who developed some adverse reaction. These second line regimens were frequently used from 2 to 4 years post-treatment commencement. The therapeutic intervention lowers the number of infectious free virus particles in the circulation, and in some cases to beyond detection. This results in a reduction in the density of infected cells, causing a rise in the CD4 cell count of infected individuals. So generally the CD4 cell count of an individual receiving therapeutic intervention is expected to rise to well above 500 cell/mm^3, assuming a proper adherence to treatment is done. Hence the use of increase in CD4 cell count as the marker of efficacy of treatment was adopted.

During the course of treatment, some individuals developed some adverse reaction (React) to treatment. For these individuals, the adverse reactions were treated and drugs administered to them were changed. Change of treatment was also based on the viral load monitoring.

For the purpose of analysis, the variables are coded as follows:

$$React\ to\ Treatment\ (React) = \begin{cases} 1; & if\ Yes \\ 0; & if\ No \end{cases}$$

$$TB\ Before\ Enrolment\ (TBB4) = \begin{cases} 1; & if\ Yes \\ 0; & if\ No \end{cases}$$

$$Develop\ active\ TB\ (DTB) = \begin{cases} 1; & if\ Yes \\ 0; & if\ No \end{cases}$$

$$Viral\ Load\ Baseline\ (VLBL) = \begin{cases} 1; & \geq 10\,000 \\ 0; & < 10\,000 \end{cases}$$

$$Age = \begin{cases} 1; & if\ 15 \leq Age \leq 45\ years \\ 0; & Age > 45\ years \end{cases}$$

$$CD4\ cell\ count\ at\ baseline\ (CD4BL) = \begin{cases} 1; & \leq 350\ cells/mm^3 \\ 0; & > 350\ cells/mm^3 \end{cases}$$

$$WHO\ Stage\ Baseline\ (WSBL) = \begin{cases} 1; & if\ WSBL = 4 \\ 0; & otherwise \end{cases}$$

$$Gender = \begin{cases} 1; & if\ Male \\ 0; & if\ Female \end{cases}$$

4.4 Model formulation

The model is formulated based on the standard model proposed by Goshu and Getahum (2013). At any time $t + \Delta t$, the state of an HIV-infected individual is defined based on the CD4 cell count level or whether the individual is dead or is lost to follow up (withdrawn) as follows:

State 1-$CD4 \geq 750$	**State 2**-$500 \leq CD4 < 750$
State 3-$350 \leq CD4 < 500$	**State 4**-$200 \leq CD4 < 350$
State 5-$CD4 < 200$	**State 6**-Death
State 7-Withdrawal	

Basing on these seven states, progression of HIV positive individuals on treatment is defined by the state diagram in Figure 4.1 below. The arrows in the diagram show possible transitions between the seven states defined above.

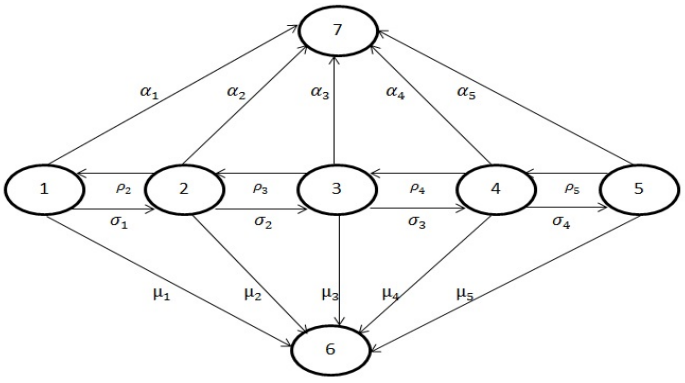

Figure 4.1 – *The State Diagram for HIV Progression of an Individuals on ART*

The information in Figure 4.1 shows that state 6 and 7 are absorbing states, hence there are no transitions out of these states. As HIV progresses in an individual's body, there is a possibility of an individual being in the same state in consecutive visit times.

Basing on the classification above, Table 4.1 summarises transition counts that took place for the whole period of study from 2005 to 2009.

Table 4.1: Transition Counts from 2005 to 2009

	To	1	2	3	4	5	6	7
From	1	69	34	5	1	1	1	1
	2	47	80	37	4	0	2	4
	3	21	79	193	46	9	6	5
	4	0	14	128	203	37	8	9
	5	0	3	26	117	204	42	8

Table 1 shows that, transition counts from state i to $i \pm j$ are higher for all the values in which $j = 1$ than for $j > 1$ where $i, j \in 1, \ldots, 5$. As a result a bidirectional model is proposed, which defines transitions from state i to $i \pm 1$ or from i to $j = 6; 7$.

The model is formulated based on the assumptions that between times $(t, t + \Delta t)$, where Δt is a very small value, there is a transition from any one of the states $i = 1, 2, \ldots, 5$ (transient states) to state $j = 1, 2, \ldots, 7$ defined as follows:

- CD4 cell count of an individual is expected to rise due to the efficacy of treatment at a rate of $q_{i,i-1}$, where $i = 2, 3, 4, 5$;
- Some individuals fail to adhere to treatment therapy. These individuals can move to a state of lower CD4 cell count at a rate of $q_{i,i+1}$, where $i = 1, 2, 3, 4$;
- From any state $i = 1, 2, \ldots, 5$ an infected individual can die (state 6) at a rate of q_{i6};
- An individual in state $i = 1, 2, \ldots, 5$ can decide to withdraw (state 7) at a rate of q_{i7};
- An individual can remain in the same state at a rate of $q_{ii} = -\lambda_i = -(q_{i,i-1} + q_{i,i+1} + q_{i6} + q_{i7})$ for $i = 2, 3, 4$; $q_{ii} = -\lambda_i = -(q_{i,i+1} + q_{i6} + q_{i7})$ for $i = 1$ and $q_{ii} = -\lambda_i = -(q_{i,i-1} + q_{i6} + q_{i7})$ for $i = 5$. This is based on the fact that the sum of transition rates from any state is equal to zero.

These rates can be represented by the following transition rate matrix $Q(t)$:

$$\begin{pmatrix} q_{11} & q_{12} & 0 & 0 & 0 & q_{16} & q_{17} \\ q_{21} & q_{22} & q_{23} & 0 & 0 & q_{26} & q_{27} \\ 0 & q_{32} & q_{33} & q_{34} & 0 & q_{36} & q_{37} \\ 0 & 0 & q_{43} & q_{44} & q_{45} & q_{46} & q_{47} \\ 0 & 0 & 0 & q_{54} & q_{55} & q_{56} & q_{57} \\ 0 & 0 & 0 & 0 & 0 & 0 & 0 \\ 0 & 0 & 0 & 0 & 0 & 0 & 0 \end{pmatrix} \tag{4.7}$$

where $q_{11} = -(q_{12} + q_{16} + q_{17})$, $q_{22} = -(q_{21} + q_{23} + q_{26} + q_{27})$, $q_{33} = -(q_{32} + q_{34} + q_{36} + q_{37})$, $q_{44} = -(q_{43} + q_{45} + q_{46} + q_{47})$, $q_{55} = -(q_{54} + q_{56} + q_{57}), q_{66} = 0, q_{77} = 0$. Once the transition rate matrix has been obtained, the matrix of transition probabilities can be obtained using Kolmogorov's forward differential equations defined in (4.6). This yields the following forward differential equations for the Markov jump processes:

$$
\begin{aligned}
P'_{i1}(t) &= -(q_{12}+q_{16}+q_{17})P_{i1}(t)+q_{21}P_{i2}(t),\ i=1,2; && (4.8)\\
P'_{i2}(t) &= q_{12}P_{i1}(t)-(q_{21}+q_{23}+q_{26}+q_{27})P_{i2}(t)+q_{32}P_{i3}(t),\ i=1,2,3; && (4.9)\\
P'_{i3}(t) &= q_{23}P_{i2}(t)-(q_{32}+q_{34}+q_{36}+q_{37})P_{i3}(t)+q_{43}P_{i4}(t),\ i=2,3,4; && (4.10)\\
P'_{i4}(t) &= q_{34}P_{i3}(t)-(q_{43}+q_{45}+q_{46}+q_{47})P_{i4}(t)+q_{54}P_{i5}(t),\ i=3,4,5; && (4.11)\\
P'_{i5}(t) &= q_{45}P_{i4}(t)-(q_{54}+q_{56}+q_{57})P_{i5}(t),\ i=4,5; && (4.12)\\
P'_{1j}(t) &= q_{11}P_{1j}+q_{12}P_{2j},\ \ j=6,7; && (4.13)\\
P'_{ij}(t) &= q_{i,i-1}P_{i-1,j}+q_{i,i}P_{i,j}+q_{i,i+1}P_{i+1,j},\ i=2,3,4,\ \ j=6,7; && (4.14)\\
P'_{5j}(t) &= q_{54}P_{4j}+q_{55}P_{5j},\ \ j=6,7. && (4.15)
\end{aligned}
$$

Equations (4.8) to (4.15) represent all the possible transition probabilities from state i, for $i = 1, 2, \ldots, 5$, to state $j = 1, \ldots, 7$. $P_{ij}(t)$ represents the probability that a patient in state i makes a transition to state j and its coefficients represent the transition rates, for example, in equation (4.8), $-(q_{12} + q_{16} + q_{17}) = q_{11}$. These states denoted by i are defined based on the CD4 cell count grouping. So there is a possibility of a backward or forward movement transition between transient states, due to failure or efficacy of treatment, respectively. There is no possible transition from state $i = 6$ and state $i = 7$ because these states are absorbing states where $i = 6$ represents death of an infected individual and state $i = 7$ represents withdrawal from treatment by an infected individual.

The Likelihood estimates of the Model in Figure 4.1

The observation takes the form $s_w = n_{w,w+1}$ rate of viral rebound from state w to $w + 1$ or birth of viral particles; $r_w = n_{w,w-1}$ rate of viral suppression from state w or death of viral particles; $d_w = n_{w,6}$ the rate of absorption from w to death of an infected person; $l_w = n_{w,7}$ the rate of loss to follow-up from w to the withdrawal of an infected person; and T_w the total time spent in state w. Then the likelihood function for the parameters; ρ_w, μ_w, α_w and σ_w. Estimation of the transition intensities is done using the method of maximum likelihood to estimate the transition intensities. The likelihood, L, based on Equation (3.42) and Figure 4.1 is given by:

1. Remaining in state w:

$$\exp\{-\sum_{w=1}^{5}(\rho_w+\mu_w+\sigma_w+\alpha_w)T_w-\rho_1T_1-\sigma_5T_5\}$$

ρ_1T_1 and σ_5T_5 are subtracted since they are missing from the first and last

terms, respectively, of the transient states. This means that there is no possibility of transitions from w to $w-1$ if $w=1$ and there is no possibility of a further immune deterioration (i.e transition from w to $w+1$) if $w=5$.

2. Entering state $w+1$, the likelihood becomes:

$$\exp\{-\sum_{w=1}^{5}(\rho_w+\mu_w+\sigma_w+\alpha_w)T_w-\rho_1T_1-\sigma_5T_5\}\Pi_{w=1}^{4}\sigma_w^{s_w}$$

3. Entering state $w-1$, the likelihood becomes:

$$\exp\{-\sum_{w=1}^{5}(\rho_w+\mu_w+\sigma_w+\alpha_w)T_w-\rho_1T_1-\sigma_5T_5\}\Pi_{w=2}^{5}\rho_w^{r_w}$$

4. Entering state 6 (DEATH state), the likelihood becomes:

$$\exp\{-\sum_{w=1}^{5}(\rho_w+\mu_w+\sigma_w+\alpha_w)T_w-\rho_1T_1-\sigma_5T_5\}\Pi_{w=1}^{5}\mu_w^{d_w}$$

5. Entering state 7 (WITHDRAWAL state), the likelihood becomes:

$$\exp\{-\sum_{w=1}^{5}(\rho_w+\mu_w+\sigma_w+\alpha_w)T_w-\rho_1T_1-\sigma_5T_5\}\Pi_{w=1}^{5}\alpha_w^{l_w}$$

The components can be put together and the likelihood would be written as:

$$L = \exp\{-\sum_{w=1}^{5}(\rho_w+\mu_w+\sigma_w+\alpha_w)T_w-\rho_1T_1-\sigma_5T_5\}\Pi_{w=1}^{4}\sigma_w^{s_w}\Pi_{w=2}^{5}\rho_w^{r_w}\Pi_{w=1}^{5}\mu_w^{d_w}\Pi_{w=1}^{5}\alpha_w^{l_w} \tag{4.16}$$

Maximum likelihood estimates can be derived using methods discussed in Chapter 3. The estimates are:

$\hat{\mu}_w=\frac{d_w}{T_w}$, $\hat{\sigma}_w=\frac{s_w}{T_w}$, $\hat{\rho}_w=\frac{r_w}{T_w}$, $\hat{\alpha}_w=\frac{l_w}{T_w}$

All the analysis is done using the package 'msm' for multi-state modelling in R software. The package was developed by Jackson in 2013.

4.5 Results and discussions

4.5.1 Residual plot for detection of outliers

The plot of residuals for each of the individuals in the study was drawn to identify the outliers (subjects with higher influence) in the data. Once the outliers are identified, they can simply be deleted and the model is re-fitted. According to Titman (2007), residuals for multi-state models can be determined as follows: If n subjects and a parameter vector $\theta \in \Theta$, with maximum likelihood estimator based upon the whole data $\hat{\theta}$. Let $\hat{\theta}_{(j)}$ represent the estimate with subject j deleted. Thus, the quantity $\hat{\theta}_{(j)} - \hat{\theta}$ for $j = 1, \ldots, n$ is of interest. The influence of each point on each parameter can be compared separately and to get a measure of the overall influence of a particular subject we take the scalar quantity:

$$\left(\hat{\theta}_{(j)} - \hat{\theta}\right)' I\left(\hat{\theta}\right)\left(\hat{\theta}_{(j)} - \hat{\theta}\right)$$

where $I(\theta)$ is the observed Fisher information matrix at the maximum likelihood estimates for the full data. Consider the contribution to the score function of each subject evaluated to the maximum likelihood estimate for the full model. Highly influential subjects will have scores of high magnitude. For a single subject, the score residual is given by an analogous scalar measure:

$$U_j\left(\hat{\theta}\right)' I\left(\hat{\theta}\right)^{-1} U_j\left(\hat{\theta}\right)$$

where $U_j\left(\hat{\theta}\right)$ is the vector of first derivatives of the log-likelihood for that subject at maximum likelihood estimates θ. That is, $U\left(\hat{\theta}\right) = \frac{\partial L}{\partial \theta}\left(\hat{\theta}\right)$ is determined using the derivative of the transition probability matrix $P(t)$ with respect to θ. These derivatives were given by Kalbfleisch and Lawless (Titman, 2007). The residuals plot displays the residuals for each subject in the order labelled by subject identifiers. Subjects with a higher influence on the maximum likelihood estimates will have higher score residuals (Jackson, 2013). The plot helps to identify any outliers in the data. Figure 4.2 below shows the plot of residuals.

Results from Figure 4.2 show that patients with ID numbers 81 and 82 are outliers as indicated by their positions from the rest of the patients in the cohort. The corresponding residuals for these values are 1.58315799 and 1.58315999, respectively,

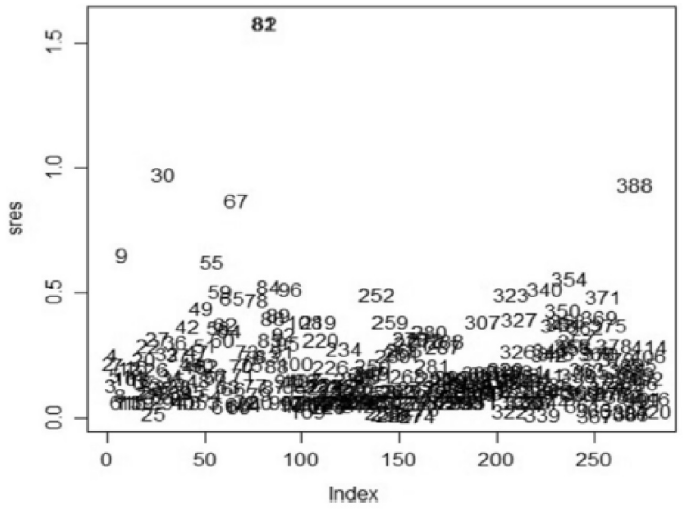

Figure 4.2 – *The score residuals plot for detecting outliers*

compared to the rest of the subjects whose residuals are below 1. Patient number 81 is a 2 year old enrolled whilst in state 1 and maintained the state throughout the study period. Patient number 82 was enrolled whilst in state 5 and, during the third visit, was already in state 1 and maintained it throughout the study period. These patients are excluded from the analysis, leaving us with 317 subjects.

Estimation of transition intensities

Transition intensities for the model with outliers and the model without outliers are estimated in this subsection. The corresponding confidence interval is also given for each transition intensity. The state space is $X_c(t) = \{1, 2, 3, 4, 5, 6, 7\}$. The transition intensities are shown in Table 4.2

The results from Table 4.2 show narrow confidence intervals, which is an indication that the suggested continuous-time Markov model gives a precise estimate of the data. Results from Table 4.2 show that transitions to better CD4 cell count states are higher than transitions to worse off CD4 cell count states, which is an indication of efficacy of ART. The model with outliers has a higher log-likelihood than the model without outliers as expected, since the model with outliers has a greater dimension.

Table 4.2: Transition intensities and their corresponding confidence intervals for the model with and the model without outliers

	With outliers	Without outliers
q_{12}	0.982 (0.669,1.441)	0.887 (0.636,1.239)
q_{16}	0.118 (0.068,0.204)	0.102 (0.054,0.191)
q_{17}	0.115 (0.066,0.201)	0.142 (0.084,0.239)
q_{21}	0.687 (0.481,0.981)	0.518 (0.372,0.722)
q_{23}	0.426 (0.313,0.579)	0.496 (0.373,0.659)
q_{26}	0.073 (0.041,0.130)	0.081 (0.047,0.140)
q_{27}	0.026 (0.009,0.073)	0.038 (0.017,0.085)
q_{32}	0.437 (0.361,0.531)	0.423 (0.345,0.519)
q_{34}	0.338 (0.264,0.434)	0.332 (0.261,0.424)
q_{36}	0.027 (0.013,0.059)	0.015 (0.005,0.044)
q_{37}	0.030 (0.016,0.057)	0.031 (0.017,0.058)
q_{43}	0.552 (0.469,0.650)	0.518 (0.439,0.612)
q_{45}	0.224 (0.169,0.298)	0.252 (0.194,0.329)
q_{46}	0.036 (0.017,0.076)	0.003 (0.015,0.074)
q_{47}	0.038 (0.023,0.065)	0.054 (0.035,0.083)
q_{54}	0.548 (0.465,0.646)	0.516 (0.436,0.612)
q_{56}	0.090 (0.062,0.132)	0.091 (0.063,0.131)
q_{57}	0.036 (0.021,0.061)	0.029 (0.016,0.052)
-2xLL	3969.72	3941.971

A further analysis on the transition intensities was also done for each of the baseline CD4 cell count (CD4BL) and baseline WHO clinical stage (WHOSBL) levels coded as follows:

$$CD4BL = \begin{cases} 1; & CD4 > 750 \\ 2; & 500 < CD4 \leq 750 \\ 3; & 350 < CD4 \leq 500 \\ 4; & 200 < CD4 \leq 350 \\ 5; & CD4 \leq 200 \end{cases}$$

and;

$$WHOSBL = \begin{cases} 1; & Asymptomatic \\ 2; & Mild\ symptoms \\ 3; & Advanced\ symptoms \\ 4; & Severe\ symptoms \end{cases}$$

The results are shown in Appendix A2 and A3 for CD4BL and WHOSBL respectively. The results from Appendix A2 show that transition rates to CD4 cell count recovery (given by state 2 to state 1, state 3 to state 2, state 4 to state 3 or state 5 to state 4) were high for patients who initiated therapy when their CD4 cell count baseline level was well above 350 per mm^3. These rates of CD4 cell count recovery decrease with decreasing CD4 cell count at treatment initiation, with a baseline CD4

cell count below 200 per mm^3 recording the lowest rates of CD4 cell count recovery. The results from Appendix A3 show that regardless of the WHO stage baseline, transition rates to CD4 cell count recovery are higher than transition rates to CD4 cell count deterioration. The rates of CD4 cell count recovery are the highest for transitions from state 5 to state 4. Transition rates to state 6 (death) are the highest for those individuals who had severe HIV symptoms (WHOSBL = 4) and these intensities decrease as the symptoms decrease from severe to asymptomatic levels.

4.5.2 Expected holding times

The expected holding time in each state, also known as the mean sojourn time, describes the average time an individual spends in each state in a single stay before he/she makes a transition to another state. The mean sojourn time in each state i, for $i = 1, 2, \ldots, 5$, is estimated as $E(T_i) = \frac{1}{\lambda_i}$, where $\lambda_i = \sum_{i \neq j} q_{ij}$ is the total force of transition out of state i. For example, the expected holding time in state 1 is $1/(0.887 + 0.1016 + 0.1418) \approxeq 0.8844$ years as shown in Table 4.3 below:

Table 4.3: Expected holding times (years) in each state

i	Estimates	SE	L	U
1	0.884	0.126	0.669	1.170
2	0.883	0.092	0.720	1.082
3	1.248	0.096	1.073	1.452
4	1.207	0.079	1.020	1.332
5	1.573	0.115	1.362	1.816

Results from Table 4.3 show estimates of the holding time, the standard error (SE), the lower bound (L) and the upper bound (U) for each of the transient state i. From the results, if an individual is in state 5 (corresponding to a CD4 cell count below 200 cells/mm^3), he/she spends more time in that state before making a transition to other states. This could be due the time taken by an individual to respond to treatment since state 5 is the worst state in HIV/AIDS progression, for a patient who is still alive.

4.5.3 Computation of the probability of each state being next given that i is the initial state

This is when a Markov process is observed at the times it makes transitions to a new state. In other words, the probability of each state being next is a stochastic matrix R of probabilities where each row sums to one, on the state space $X_c(t)$, which gives the conditional probability of the next state (state j) an individual goes to after leaving state i for $i \neq j$. If $q_{ii} > 0$ then, given that there is a jump to a different

state, it means we never stay in state i. We make a jump out, resulting in having $R_{ii} = 0$ and if $q_{ii} = 0$, then we never leave state i, meaning that $R_{ii} = 1$ (States 6 and 7). The computed matrix of probabilities of each state being next, together with the mean sojourn times in each state, fully define a continuous-time Markov model (Jackson, 2013). This is a more intuitively meaningful description of a model than the transition intensity matrix. The matrix for the probabilities that the next state after state i is state j is approximated as $p_{ij} = \frac{q_{ij}}{\lambda_i}$, for each i and j such that $i \neq j$. q_{ij} is the force of transition from state i to state j and q_{ii} is the total force of transition out of state i. For example, $p_{12} = \frac{q_{12}}{\lambda_1} = \frac{0.8872}{0.8872+0.1016+0.1418} = 0.7847$, as shown in the matrix below. The results are shown Table 4.4 below:

Table 4.4: Probability of each State being next (R_{ij})

	To	1	2	3	4	5	6	7
From	1	0	0.785	0	0	0	0.090	0.125
	2	0.458	0	0.438	0	0	0.072	0.033
	3	0	0.528	0	0.415	0	0.018	0.039
	4	0	0	0.604	0	0.294	0.039	0.063
	5	0	0	0	0.812	0	0.143	0.045
	6	0	0	0	0	0	1	0
	7	0	0	0	0	0	0	1

The results from Table 4.4 show that $R_{i,i-1} > R_{i,i+1}$, which shows that the probability of jumping to a better state is higher than the probability of jumping to a worse state. This is more pronounced for individuals in state 5, where the probability of jumping to state 4 (recovery) is 0.8123, which is very high compared to the probability of making a jump to state 6. This is an indication of the effectiveness of treatment. Probability of the death state being next is the highest for those patients with CD4 cell counts less than 500 cells/mm^3. These probabilities increase with the decreasing number of CD4 cell counts. Thus, progression to death is higher on patients with lower CD4 cell counts than patients with higher CD4 cell counts.

4.5.4 Forecast of the total length of stay in each state

We need to forecast the total time spent in the good states and the bad states by individuals who are on HIV treatment before death or withdrawal from the study. Estimates of the forecasted total lengths of time spent in each state j between two future time points t_1 and t_2 are estimated using the formula: $L_j = \int_{t_1}^{t_2} P_{ij}(t)dt$ where i is the state at the start of the process, which defaults to 1. The results are shown below:

State 1	State 2	State 3	State 4	State 5	State 6	State 7
8.989	8.806	7.767	3.520	1.154	Inf	Inf

The results show that each individual is forecasted to spend approximately 8.99 half years in state 1, 8.8 half years in state 2, 7.77 half years in state 3, 3.52 half years in state 4, and finally 1.153 half years in state 5. These results show that HIV positive individuals on treatment are expected to spend more time in good states compared to the time spent in bad states.

4.5.5 Percentage prevalence for the model without covariates.

Using the fitted time-homogeneous Markov model, the percentage prevalence were plotted to compare the expected values with the observed values. The results are shown in Figure 4.3 below:

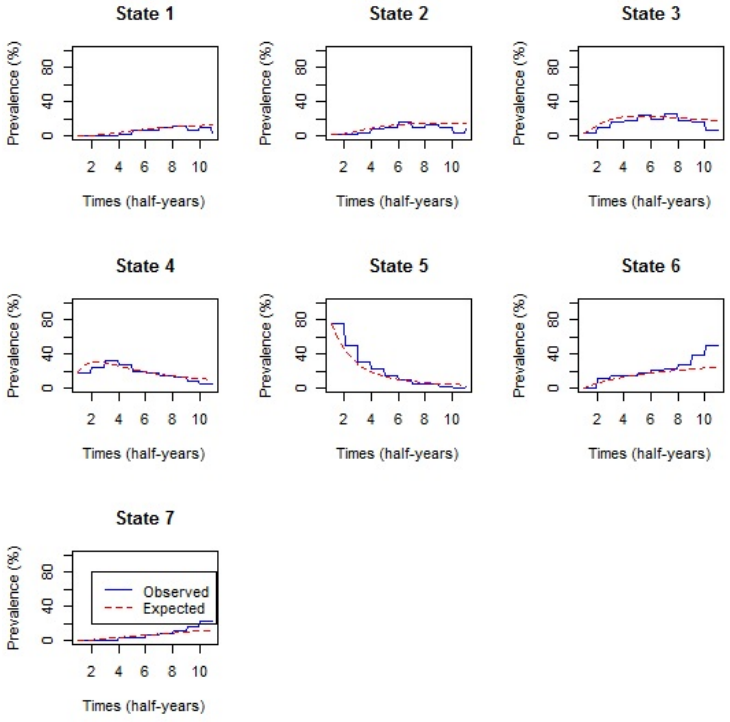

Figure 4.3 – *Comparison of observed and expected prevalence from the time-homogeneous model without covariates*

The results from Figure 4.3 show that for the state $i = 1, \ldots, 6$ the expected prevalence fit the observed data perfectly well, except for the withdrawal state, where the expected prevalence overestimate the observed. The plots further show a sharp decrease on state 5 percentage prevalence with the fitted model underestimating the observed data up to time = 7 half years. The percentage prevalence for the death

state is increasing at a slow rate and from time = 2 half years to time = 8 half years, the percentage prevalence is stable.

4.5.6 Effects of covariates on transition intensities

A continuous-time Markov model for the effects of covariates: Age, CD4 cell count at baseline (CD4BL), viral load at baseline (VLBL), WHO stage at baseline (WSBL), Reaction to treatment, Development of active TB whilst on treatment (DTB), TBB4 and Gender, is fitted. Identification of covariates that have a significant contributory effect is done by comparing the model with all covariates with the model ith one covariate (at a time) removed and performing the likelihood ratio test in comparison to the model without covariates. All the other variables proved to have significant effect to the progression, except for the variable gender which could not be eliminated because of its demographic importance. The baseline transition intensities $\left(q_{ij}^{(0)}\right)$ relate to the transitions from state i to state j. Baseline transition intensities and linear effect of each of the covariates are estimated and the results are shown in Table 4.5 and Appendix A1, respectively. The fitted time homogeneous model with covariates has $-2 \times LL = 3699.259$, which represents an improvement of 242.712 compared to the model without covariates. A Likelihood ratio test is performed to compare the two nested models that were fitted, the one without covariates and the other with covariates. The value of the $LRT = -2log_e\left(\frac{L_s(\hat{\theta})}{L_g(\hat{\theta})}\right)$ where $L_s(\hat{\theta})$ is the simple model (no covariates) and $L_g(\hat{\theta})$ is the general model (with covariates). A likelihood ratio test statistic of 1770.618 is compared to a χ^2 distribution with 144 degrees of freedom. The test was performed and the results are shown below:

Likelihood ratio test	*Preferred model*	*LRT statistic*	*Df*	*p-value*
with covariates vs without covariates	*with.covariates*	*1770.186*	*144*	10^{-4}

The results show that the model with covariates fits significantly better than the model without covariates.

Hazard ratios of covariates on transition intensities

In this section, the hazard ratios for each of the covariates: VLBL:- viral load baseline, DTB:- develop TB during treatment period, TBB4:- develop TB before treatment, Gender, React:-reaction to treatment, CD4BL:- CD4 baseline, WSBL:- WHO stage baseline and Age are estimated. The relationship between these covariates and the transition intensities is defined by the following equation:

$$q_{ij}(\mathbf{Z}) = q_{ij}^{(0)} exp\left(\beta_{ij}'\mathbf{Z}\right), i \neq j;$$

where $\mathbf{Z} = [VLBL, DTB, TBB4, Gender, React, CD4BL, WSBL, Age]$ is a $k = 8$-dimensional vector of covariates. β_{ij} is a vector of k regression parameters relating the instantaneous rate of transitions from state i to state j to the covariates $\mathbf{Z}$ and baseline intensities $q_{ij}^{(0)}$ for the transitions from state i to state j as shown in Table 4.5 below:

Table 4.5: Baseline intensities and their corresponding confidence intervals for the covariate effects

(i, j)	Intensities (q_{ij})	B.L. Intensities $(q_{ij}^{(0)})$
(1, 2)	0.887 (0.636,1.239)	0.503 (0.428,0.861)
(1, 6)	0.102 (0.054,0.191)	0.020 (0.010,0.464)
(1, 7)	0.142 (0.084,0.239)	0.018 (0.009,0.493)
(2, 1)	0.518 (0.372,0.722)	0.390 (0.385,0.686)
(2, 3)	0.496 (0.373,0.659)	0.444 (0.297,0.555)
(2, 6)	0.081 (0.047,0.140)	0.011 (0.007,0.202)
(2, 7)	0.038 (0.017,0.085)	0.012 (0.001,0.019)
(3, 2)	0.423 (0.345,0.519)	0.376 (0.325,0.501)
(3, 4)	0.332 (0.261,0.424)	0.233 (0.208,0.364)
(3, 6)	0.015 (0.005,0.044)	0.006 (0.004,0.129)
(3, 7)	0.031 (0.017,0.058)	0.010 (0.003,0.315)
(4, 3)	0.518 (0.439,0.612)	0.560 (0.449,0.628)
(4, 5)	0.252 (0.194,0.329)	0.230 (0.152,0.279)
(4, 6)	0.003 (0.015,0.074)	0.007 (0.005,0.421)
(4, 7)	0.054 (0.035,0.083)	0.008 (0.006,0.155)
(5, 4)	0.516 (0.436,0.612)	0.502 (0.445,0.630)
(5, 6)	0.091 (0.063,0.131)	0.020 (0.007,0.146)
(5, 7)	0.029 (0.016,0.052)	0.006 (0.001,3.936)
$-2 \times LL$	3941.971	3699.259

At the bottom of Table 4.5, $-2 \times LL$ represents the -2log-likelihood. Estimates of β_{ij}'s, regression coefficients, were computed and the results are shown in Appendix A1. The regression coefficients can be interpreted similarly to those in the proportional hazards regression model (Cox, 1972). The results are shown in Table 4.6.

The $-2 \times LL$ for the model fitted in Table 4.6 is 3699.259. The results show that the strongest predictor of transition from state 1 to 2 is a negative reaction to treatment, which has a hazard ratio of 4.715. This means that patients who developed some form of reaction were over 4 times more likely to transit from a level of $CD4 \geq 750$ to a level of $500 \leq CD4 < 750$ than patients who did not react to treatment. However, from all the other states, hazard ratios for the patients who reacted to treatment are higher for immune recovery than for immune deterioration.

The strongest predictor of immune deterioration from a CD4 cell count level between 350 and 500 to a CD4 cell count level between 200 and 350 (3 to 4) is developing TB

Table 4.6: Hazard ratios for the covariates on intensities

(i, j)	VLBL	DTB	TBB4	Gender	React	CD4BL	WSBL	Age
(1, 2)	0.69	2.29	0.31	2.04	4.72	1.17	0.55	1.45
(1, 6)	1.57	0.87	1.11	1.55	0.60	1.30	1.11	0.83
(1, 7)	1.01	0.96	1.00	1.26	0.68	0.92	0.56	0.40
(2, 1)	0.48	1.14	0.76	1.33	1.46	1.17	0.74	2.63
(2, 3)	0.92	1.98	0.67	6.46	0.67	1.37	0.26	0.40
(2, 6)	1.12	0.96	1.69	1.45	0.54	0.99	1.16	1.10
(2, 7)	1.30	1.19	1.92	0.93	0.73	1.33	0.79	0.70
(3, 2)	0.68	1.58	1.10	2.35	2.08	0.69	0.75	0.83
(3, 4)	0.42	2.55	0.53	1.04	0.55	1.57	1.06	0.89
(3, 6)	0.92	1.17	2.03	1.20	0.59	1.05	1.32	1.77
(3, 7)	1.34	0.86	2.34	0.72	0.20	1.20	0.54	2.06
(4, 3)	1.52	1.72	0.86	0.61	1.02	0.27	0.84	1.08
(4, 5)	0.74	2.25	1.65	1.36	0.65	1.05	0.46	0.89
(4, 6)	1.31	1.09	1.09	1.59	0.22	1.01	1.40	1.96
(4, 7)	1.56	1.17	1.88	0.58	0.36	1.02	0.52	2.18
(5, 4)	0.51	1.86	1.02	0.81	1.32	0.61	0.40	0.63
(5, 6)	0.92	0.65	0.41	2.10	0.06	1.003	2.09	2.60
(5, 7)	0.97	1.20	0.88	1.19	0.66	0.87	0.40	2.31

during treatment, with a hazard ratio of over 2. Developing TB is also the strongest predictor of immune deterioration from 4 to 5, with a hazard ratio also greater than 2. This means that TB is the major cause of further immune deterioration when the immune system is too weak, hence the recommendation that HIV patients should continuously have their TB status checked. Alternatively, the results reveal that a weak immune system is the major cause for developing TB. Those individuals who had TB before enrolment had the strongest predictor for the transition from state 3 to state 6. These patients are over 2 times more likely to die from state 3 than those who were enrolled without having TB. However, for these individuals, transitions to better states were generally higher than transitions to worse states for almost all states.

A hazard ratio of 6.46 for the predictor variable male shows that males were over 6 times more likely to transit from state 2 to 3 than their female counterparts. The hazard ratios of males from a bad state to a better state are less than 1, which is an indication that males are less likely to respond to treatment compared to females.

The hazard ratios for the transitions to a better state for patients who were enrolled with CD4 cell counts below 350 are less than one, but hazards to worse states are greater than one, an indication that starting treatment when the CD4 cell count levels are below 350 retards immune recovery. The transitions to the death state for individuals who started treatment when they were on the WHO stage of 4 are all more than one, meaning that starting treatment with a WHO stage of 4 is a leading

cause of being absorbed in the death state.

4.5.7 Percentage prevalence for the model with covariates

The prevalence for the model with covariates were plotted to examine areas of poor fit of the time-homogeneous model with covariates. The plots are shown in Figure 4.4.

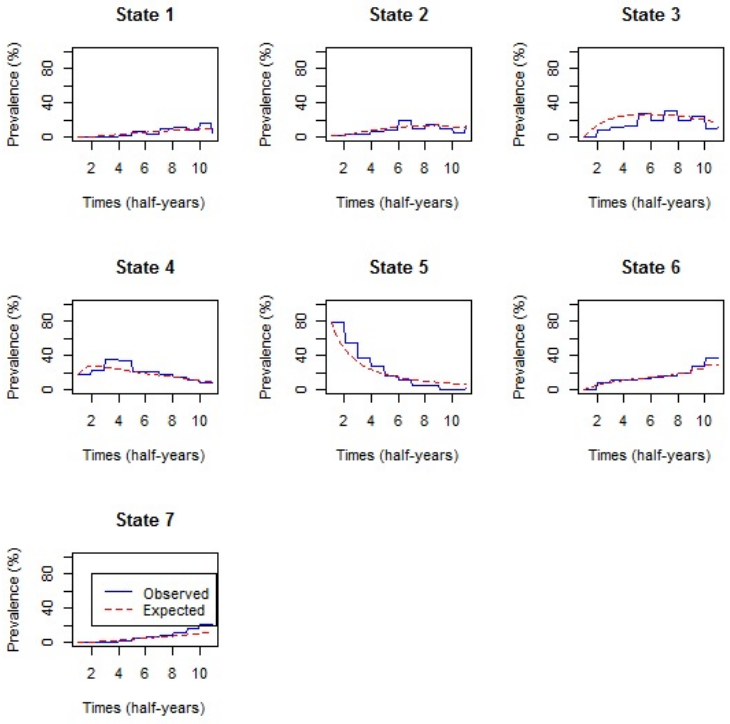

Figure 4.4 – *Comparison of observed and expected prevalence from the time-homogeneous model with covariates*

Figure 4.4 confirms that the inclusion of covariates on the model improves the fitness of the model, since the expected prevalence is now perfectly closer to the observed prevalence for all states than the model without covariates.

4.6 Concluding Remarks

In this chapter, the progression of HIV/AIDS disease in an individual on combination anti-retroviral therapy (cART) follow-up was modelled and described using a continuous-time homogeneous Markov processes. A cohort of 319 HIV-infected patients on cART follow-up at a Wellness Clinic in Bela Bela, South Africa was used. Though Markov models based on CD4 cell counts is a common approach

in HIV/AIDS modelling, this chapter was unique clinically. in that tuberculosis (TB) co-infection was included as a covariate. The method partitioned the HIV infection period into five CD4-cell count intervals followed by the end points: death, and withdrawal from study. The effectiveness of treatment was analysed by comparing the forward transitions with the backward transitions. The effects of reaction to treatment, TB co-infection, gender and age on the transition rates were also examined. The developed models gave a very good fit to the data.

The results show that the strongest predictor of transition from a state of CD4 cell count greater than 750 to a state of CD4 cell count between 500 and 750 is a negative reaction to drug therapy. Developing TB during the course of treatment is the greatest predictor of transitions to states of lower CD4 cell count. Transitions from good states to bad states were higher on male patients than their female counterparts. From some of these findings, this chapter concludes that there is need to monitor adverse reaction to drugs more frequently, screen HIV/AIDS patients for any signs and symptoms of TB and check for factors that may explain gender differences further. The mean sojourn times revealed that patients take longer time in the AIDS defining states (CD4 cell count below 200) before they make transitions to better CD4 cell count states. However, once states of higher CD4 cell counts are achieved, the estimates of total time spent in each state revealed that patients in the cohort spent a greater proportion of their total follow-up time in higher CD4 cell count states. Research has also shown that CD4 cell count rises gradually, despite the suppressed viral load particularly in older patients (Wright et al., 2013). CD4 cell count monitoring also has its shortcoming, that of failing to detect virologic failure, leading unnecessary treatment switches.

Although continuous-time homogeneous Markov models can handle multiple or recurrent outcomes compared to the Kaplan Meier analysis and Cox proportional hazards models, the assumption of constant hazard function is frequently unrealistic (Lange et al., 2015) and puts limitations on the disease history behaviour (Saint-Pierre et al., 2003), especially on HIV/AIDS progression for patients on ART. Some studies have shown that if a patient responds well to treatment and manages to achieve viral load count suppression within the first 6 months, that patient is likely to continue responding well to treatment (Maartens et al., 2012). This goes against the Markov and memoryless properties of the models, thus a limitation in the application of time homogeneous Markov processes.

To address these shortcomings, in the next chapter, a continuous-time non-homogeneous Markov model for HIV/AIDS virological progression is developed. The Markov

model is fitted based on viral load count states.

Appendix A

Appendix A1: Linear effects of covariates on transition intensities

Param.	VLBL	CD4BL	WSBL	React	DTB	TBB4	Gender	Age
β_{12}	-0.37	0.15	-0.59	1.55	0.83	-1.17	0.7118	0.37
β_{16}	0.45	0.27	0.101	-0.52	-0.14	0.11	0.4379	-0.18
β_{17}	0.0071	-0.088	-0.58	-0.39	-0.039	0.00086	0.23	-0.90
β_{21}	-0.73	0.156	-0.31	0.38	0.13	-0.28	0.29	0.97
β_{23}	-0.84	0.31	-1.35	-0.40	0.68	-0.39	1.87	-0.92
β_{26}	0.112	-0.0028	0.150	-0.63	-0.044	0.53	0.37	0.100
β_{27}	0.26	0.29	-0.24	-0.32	0.17	0.65	-0.077	-0.36
β_{32}	-0.39	-0.37	-0.28	0.73	0.46	0.096	0.86	-0.18
β_{34}	-0.86	0.45	0.057	-0.59	0.94	-0.63	0.036	-0.116
β_{36}	-0.085	0.047	0.28	-0.53	0.16	0.71	0.18	0.57
β_{37}	0.29	0.181	-0.24	-1.63	-0.15	0.85	-0.33	0.72
β_{43}	0.42	-1.32	-0.17	0.020	0.54	-0.15	-0.49	0.080
β_{45}	-0.305	0.049	-0.77	-0.43	0.81	0.50	0.31	-0.12
β_{46}	0.27	0.0079	0.34	-1.50	0.087	0.089	0.46	0.67
β_{47}	0.45	0.020	-0.66	-1.01	0.16	0.63	-0.55	0.78
β_{54}	-0.66	-0.501	-0.91	0.27	0.62	0.022	-0.22	-0.46
β_{56}	-0.079	0.0030	0.74	-2.83	-0.43	-0.89	0.74	0.95
β_{57}	-0.028	-0.141	-0.92	-0.41	0.19	-0.13	0.18	0.84

Appendix A2: Transition intensities for each CD4 cell count level at baseline

Transition	2	3	4	5
1 to 2	3.128	6.318	12.760	25.780
1 to 6	0.013	0.020	0.033	0.054
1 to 7	0.039	0.056	0.081	0.116
2 to 1	0.664	0.599	0.541	0.487
2 to 3	0.284	0.405	0.578	0.825
2 to 6	0.018	0.018	0.019	0.020
2 to 7	0.023	0.028	0.034	0.042
3 to 2	0.245	0.166	0.112	0.076
3 to 4	0.275	0.178	0.115	0.075
3 to 6	0.008	0.009	0.010	0.011
3 to 7	0.035	0.033	0.032	0.031
4 to 3	1.399	0.812	0.471	0.273
4 to 5	0.894	0.691	0.535	0.414
4 to 6	0.011	0.001	0.010	0.010
4 to 7	0.050	0.051	0.052	0.054
5 to 4	13.140	5.330	2.162	0.877
5 to 6	0.019	0.017	0.015	0.013
5 to 7	0.375	0.226	0.136	0.082

Appendix A3: Transition for the WHO Stage Baseline Line

Transition	1	2	3	4
1 to 2	0.314	0.129	0.053	0.022
1 to 6	0.004	0.004	0.004	0.004
1 to 7	0.014	0.010	0.008	0.006
2 to 1	0.846	0.876	0.907	0.938
2 to 3	0.125	0.112	0.100	0.090
2 to 6	0.017	0.018	0.019	0.021
2 to 7	0.014	0.129	0.012	0.011
3 to 2	0.812	1.232	1.870	2.839
3 to 4	0.886	1.197	1.617	2.185
3 to 6	0.007	0.008	0.009	0.010
3 to 7	0.031	0.025	0.020	0.016
4 to 3	4.593	5.075	5.607	6.195
4 to 5	1.236	1.024	0.848	0.703
4 to 6	0.014	0.017	0.020	0.023
4 to 7	0.033	0.023	0.016	0.011
5 to 4	67.220	56.630	47.710	40.190
5 to 6	0.039	0.060	0.091	0.139
5 to 7	0.579	0.325	0.183	0.103

Chapter 5

A Comparison of the Time Homogeneous and Time Non-homogeneous Markov models for monitoring HIV virology

5.1 Introduction

The suppression of the viral load from very high levels, greater than 500 000 copies/mL, to undetectable levels due to the effects of cART can be considered as a stochastic process by splitting the progression into various states of the disease, based on the viral load count, including the endpoint, the death state. Stochastic processes allow random movements between viral load states before an HIV/AIDS patient is finally absorbed into the death state (Lee et al., 2014). Patients are monitored only at visit times, resulting in the exact time the transition has occurred not known (Chenand and Zhou, 2011). When transition times are not known and interval censored observations are present, homogeneous and non-homogeneous Markov processes are an important field of research into stochastic processes (Kalbfleisch and Lawless, 1985). A Markov process is a type of stochastic process in which a system changes in a random manner between different states at regular or irregular intervals (Lee et al., 2014).

However, continuous time-homogeneous Markov models are limited by an assumption of constant transition rates that is frequently unrealistic when modelling evolution in chronic diseases (Lange et al., 2014), because they put severe limitations on disease history behaviour (Saint-Pierre et al., 2003). Despite this, most applications

to HIV/AIDS disease assume a homogeneous process where transition probabilities only depend on the elapsed time between observations (Lee et al., 2014; Grover et al., 2013; Mathieu et al., 2007). Gentleman et al. (1994) considered a piece-wise constant transition intensities approach to accommodate non-homogeneity in multi-state models.

Application of non-homogeneous Markov models to study the evolution of HIV allows the researcher to take into account not only the length of the period of the HIV infection, but also the randomness of different states in which the diseases can evolve known as a stochastic process (Ocarn-Riola, 2005). However, non-homogeneity is not treated in survival analysis as extensively as homogeneous models, and in particular for HIV/AIDS disease progression based on viral load count monitoring.

In this chapter, progression of HIV/AIDS is modelled as a piece-wise constant transition intensity approach to form a non-homogeneous Markov process by splitting the progression into various states defined by virologic indicators (viral load count) including the absorbing state, death. The use of Markov models with piece-wise constant transition intensities helps in preserving the tractability of constant intensities (Saint-Pierre et al., 2003).

The next section describes the HIV/AIDS data that is used in this study and also how the model is formulated basing on the data. In section 5.3, we have results and analysis where three different models are fitted and their appropriateness is assessed using the Akaike Information Criteria (AIC), survival probability plots, likelihood ratio tests as well as the plots of percentage prevalence in each state. The last section concludes the findings.

5.2 Data Description

The data that is used in this chapter is described in Section 3.5 of Chapter 3. States of the continuous-time Markov model are based on viral load to assess the effects of time on virology for patients on cART.

At $t = 0$ the regimens that were mostly administered to patients were the triple combination therapy, d4T-3TC-EFV (208 patients) and d4T-3TC-NVP (92 patients) as highlighted in Section 3.5 of Chapter 3. d4T and 3TC represent Stavudine and Lamivudine, respectively, which fall under nucleoside reverse transcriptase inhibitors (NRTI) class. EFV and NVP stand for Efavirenz and Nevirapine, respectively, and are from the non-nucleoside reverse transcriptase inhibitors (NNRTI) class.

In patients who showed some signs of non-adherence, d4T was substituted with AZT (Zidovudine). A switch from d4T-3TC-EFV to AZT-3TC-EFV was most common, rising from 10 patients in the first 6 months to 92 patients in 30 months (2 and half years). During the same period, the number of patients who switched from d4T-3TC-NVP to AZT-3TC-NVP rose from 6 to 45. After one year of treatment uptake, one patient was introduced to FTC-TDF-EFV and after three and half years, the frequency increased to 10 patients. Another combination of FTC-TDF-NVP was also introduced to 3 patients after 2 years and the number rose to 7 after 3 years. AZT-3TC-LPV/r was also administered and at t=0, two patients were administered with this triple combination. Other treatment combinations that were administered include FTC-TDF-NVP, AZT-ddI-LPV/r, d4T-3TC-LPV/r, ddI-d4T-3TC, FTC-TDF-LPV/r. However, these were not frequently administered.

For each visit, viral load count in plasma was also measured. In this chapter, the progression of HIV/AIDS is defined by change in viral load count level. The viral load levels are divided into 5 transient states, and the sixth state being the absorbing state, death, as shown below:

$$Viral\ \ load\ \ levels\ \ (X_v(t)) = \begin{cases} 1; & VL < 50 \\ 2; & 50 \leq VL < 10\,000 \\ 3; & 10\,000 \leq VL < 100\,000 \\ 4; & 100\,000 \leq VL < 500\,000 \\ 5; & VL \geq 500\,000 \\ 6; & Dead \end{cases}.$$

These six states define the HIV/AIDS disease process and are denoted by $X_v(t)$ as shown above. The machine that is used to detect the viral load count used thresholds of [50; 500 000) such that viral load counts below 50 copies $/mL$ is classified as undetectable. The covariates included in the model are non-adherence, CD4 cell count at baseline, gender, and viral load at baseline. These covariates are defined in the previous chapter, except for CD4 cell count at baseline, which from this chapter and in all other Chapters that follow, is coded as follows:

$$CD4\ cell\ count\ at\ baseline\ (CD4BL) = \begin{cases} 1; & \leq 200\ cells/mm^3 \\ 0; & > 200\ cells/mm^3 \end{cases}, \tag{5.1}$$

Table 5.1 provides the number of patients in each viral load defined state from $t = 0$ to t=1.5 years of treatment uptake are shown.

Table 5.1: Number of HIV/AIDS patients in each viral load state from t=0 to t=0.5 years.

	Viral	load	levels	$(X_v(t))$		
	1	2	3	4	5	6
t=0 years	4	43	134	106	32	0
t=0.25 years	155	123	6	4	4	24
t=0.5 years	214	48	13	2	3	11

At treatment initiation, the majority of patients were in state 3, followed by state 4. State 1 had the least number of patients but during the first 0.25 years, it had the highest number of patients, followed by state 2. From $t = 0.25$ to $t = 0.5$ years, the number of patients in state 3 increased from 6 to 13, an indication of viral rebound since the number of patients with higher viral loads levels (state 3 and state 4) reduced collectively only by 3. There is need to investigate the causes of viral load count rebound for HIV/AIDS patients since the patients where on treatment.

5.2.1 Formulation of the non-homogeneous continuous-time Markov model

The non-homogeneous continuous time Markov model is formulated by splitting HIV/AIDS progression into 5 transient states defined by virological marker as shown above.

According to Saint-Pierre et al. (2003) a non-homogeneous Markov model can be constructed using a piece-wise constant approach as follows: Consider the study period $[\tau_{l-1}, \tau_l)$ for $l = 1, \ldots, r+1$, and assumes constant transition intensities in different time intervals. Consider a vector $\mathbf{Z}^*(t) = (Z_1^*(t), Z_2^*(t), \ldots, Z_r^*(t))'$ of artificially time-dependent covariates defined as:

$$Z_0^*(t) = 0; \forall t \ \ and \ \ Z_l^*(t) = \begin{cases} 0; & \tau_0 \leq t < \tau_l \\ 1; & t \geq \tau_l \end{cases} \tag{5.2}$$

for $l = 1, \ldots, r$

The model with transition intensities is as follows:

$$q_{ij}(t|\mathbf{Z}^*(t)) = q_{ij}^{(0)} exp\{(\beta_{ij}^*)'\mathbf{Z}^*(t)\} \tag{5.3}$$

This approach to non-homogeneity in a Markov process is a step-wise method that assumes constant transition intensities in different time-intervals. The parameters of this model are the baseline transition intensities $q_{ij}^{(0)}$, which represent transitions in the interval $[\tau_0, \tau_1)$. β_{ij}^* is a vector of regression coefficients associated with the artificial time-varying covariates. For this model, transition intensities are step-functions of time defined for each interval as follows:

$$q_{ij}(t|\mathbf{Z}^*(t)) = \begin{cases} q_{ij}^{(0)}; & if\ \tau_0 \leq t < \tau_1 \\ q_{ij}^{(1)} = q_{ij}^{(0)} exp\{\beta_{ij,1}^* Z_1^*(t)\}; & if\ \tau_1 \leq t < \tau_2 \\ \vdots & \vdots \\ q_{ij}^{(l)} = q_{ij}^{(0)} exp\{\beta_{ij,1}^* Z_l^*(t) + \beta_{ij,2}^* Z_2^*(t) + \ldots + \beta_{ij,l}^* Z_l^*(t)\}; & if\ t \geq \tau_l \end{cases} \tag{5.4}$$

$for\ l = 1, \ldots, r$
Incorporating the effects of covariates, represented by the vector $\boldsymbol{Z}$, the model becomes:

$$q_{ijl}(t|\mathbf{Z}_l^*(t), \mathbf{Z}) = q_{ij}^{(0)} exp\{(\beta_{ijl}^*)'\mathbf{Z}_l^*(t) + (\beta_{ij})'\mathbf{Z}\} \tag{5.5}$$

where $q_{ij}^{(0)}$ is the baseline transition intensities for the interval $0 \leq t < 0.5$ with covariates set to their means, $\beta_{ij,l}^*$ is the log-linear effect of the l^{th} interval on the baseline transition intensity and $Z_l^*(t)$ is the corresponding artificial time-dependent covariate, β_{ij} is the log-linear effect relating the instantaneous rate of transitions from state i to state j to the covariates $\mathbf{Z}$=[CD4 cell count at baseline (CD4BL),non-adherence (NA),Gender,Viral load count at baseline (VLBL)]

$$q_{ijl}(t|\mathbf{Z}_l^*(t), \mathbf{Z}) = \begin{cases} q_{ij}^{(0)}; & if\ \tau_0 \leq t < \tau_1 \\ q_{ij}^{(1)} = q_{ij}^{(0)} exp\{\beta_{ij,1}^* Z_l^*(t) + \beta_{ij,1} Z_1 + \beta_{ij,2} Z_2 + \ldots + \beta_{ij,k} Z_k\}; & if\ \tau_1 \leq t < \tau_2 \\ \vdots & \vdots \\ q_{ij}^{(l)} = q_{ij}^{(0)} exp\{\beta_{ij,1}^* Z_1^*(t) + \ldots + \beta_{ij,l}^* Z_l^*(t) + \beta_{ij,1} Z_1 + \ldots + \beta_{ij,k} Z_k\}; & if\ t \geq \tau_l \end{cases} \tag{5.6}$$

where $l = 1, 2, \ldots, r$ represents the number of intervals and $k = 1, 2, \ldots, 4$ represents the number of intervals.

5.2.2 Statistical analysis

All the analysis is done using the "msm" package for multi-state modelling for R software developed by Jackson (2013). The process of identifying the appropriate model started off by fitting a time-homogeneous Markov model for the data. The

time homogeneous model converges and has $-2 \times LL$ of 2799.465. From this time-homogeneous model, percentage prevalence in each state is estimated and plotted as shown in Figure 5.1 below:

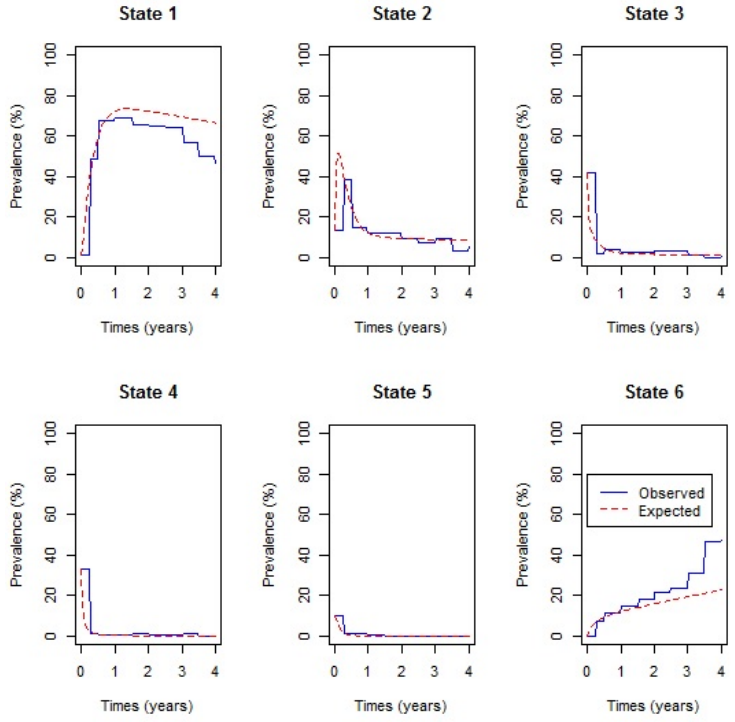

Figure 5.1 – *comparison of the observed and expected percentage Prevalence plot for the time homogeneous Markov model.*

A comparison of the expected and observed percentage prevalence in each state from Figure 5.1 shows that the predicted number of HIV infected individuals who die (State 6) is underestimated by the model from about 1 year of treatment uptake onwards. The number of individuals alive and in state 1 is overestimated by the model from 1 year onwards. Such discrepancies, according to Jackson, indicate a possibility that the transition rates vary with time since the beginning of the process. In this particular case it could be the time on treatment therapy (Jackson, 2016). This calls for the need to fit a Markov process that is non-homogeneous, which can be handled by fitting a piece-wise constant function.

Individuals in this study were followed up after every 6 months, thus a **9**-segment non-homogeneous Markov model with 0.5 year intervals is fitted. Although the **9**-segment model did not converge to maximum likelihood, the prevalence plots for each state in the model helped in revealing intervals with constant transition inten-

sities.

The best piece-wise constant function for the data is investigated by considering different change points. Most of the models did not converge to a maximum likelihood except for the models: 1. with **2**-segments and having a change point at 0.5 years; 2. with **2**-segments and having a change point at 1 year; and 3. with **3**-segments and having change points at 0.5 and 1 year. In the next section, analysis is based on these three models and also the time homogeneous model. This chapter further investigates the effects of covariates: gender, non-adherence and CD4 cell count at baseline on the chosen model.

5.3 Results

For the **2**-segment model, the transition intensities are defined for the following intervals:

$$q_{ij}(t|\mathbf{Z}^*(t)) = \begin{cases} q_{ij}^{(0)}; & if\ \tau_0 \leq t < 0.5 \\ q_{ij}^{(1)} = q_{ij}^{(0)} exp\{\beta_{ij,1}^* Z_1^*(t)\}; & if\ t \geq 0.5 \end{cases} \tag{5.7}$$

where q_{ij}^0 are the baseline transition and $q_{ij,1}$ is the transition intensity matrix for the interval $t \geq 0.5$ years and $\beta_{ij,1}^*$ is the regression coefficient associated with the artificial time-dependent covariate $Z_1^*(t)$. The point estimates of parameters and their corresponding confidence intervals are shown in Table 5.2 below:

The results from Table 5.2 show narrow confidence intervals for transitions from state 1 and from state 2, except for the transition from state 2 to 6 (death). This shows that estimates of transitions from these states are statistically significant. However, most of the point estimates have wide confidence intervals and therefore are not statistically significant. This could be due to the fact that within 6 months of treatment uptake, most patients had made transitions to either state 1 or state 2 as shown by the prevalence plots in Figure 5.1.

Next, estimates of parameters for the **3**-segment non-homogeneous Markov model with half-year and one-year change points, with transition intensities defined for each interval are computed as follows:

Table 5.2: Baseline transition intensities for the 2-segment non-homogeneous model and the time varying log-linear effects. (Confidence Intervals are in brackets)

	Baseline $[q_{ij}^0]$	Log-linear effect $[\beta_{ij1}]$	Hazard Ratios [0.5,Inf)
q_{12}	0.445 (0.360, 0.550)	-1.295 $(-1.814, -0.777)^*$	0.274 (0.163,0.460)
q_{16}	0.053 (0.031, 0.091)	-3.170 $(-4.011, -2.330)^*$	0.041 (0.018,0.097)
q_{21}	2.640 ((2.244, 3.107)	-1.133 $(-1.426, -0.841)^*$	0.322 (0.240,0.431)
q_{23}	1.585 (0. 486, 5.168)	-2.660 (-6.353, 1.033)	0.070 (0.0017, 2.810)
q_{26}	0.002 $(3.7 \times 10^{-6}, 727)$	1.220 (-25.055, 27.495)	3.387 $(1.3 \times 10^{-9}, 8.7 \times 10^{8})$
q_{32}	6.635 (2.158, 20.40)	-3.854 $(-7.347, -0.361)^*$	0.021 (0.0006,0.697)
q_{34}	6.110 (0.015, 2428)	3.010 (-5.893, 11.91)	20.28 (0.0028,149100)
q_{36}	0.144 (0.0018, 11.64)	4.071 (-8.064, 16.21)	58.63 $(0.0003, 1.1 \times 10^{8})$
q_{43}	47.116 (0.137, 16160)	1.387 (-7.123, 9.897)	4.004 (0.0008,19870)
q_{45}	3.772 (0.010, 1356)	-0.849 (-9.605, 7.907)	0.428 (0.000067,2717)
q_{46}	0.02 $(0, 6.8 \times 10^{11})$	2.426 (-194.2,199.1)	11.316 $(4.6 \times 10^{-12}, 2.8 \times 10^{10})$
q_{54}	23.825 (0.089, 6378)	0.649 (-7.528, 8.825)	1.913 (0.0005,6804)
q_{56}	0.035 $(1.3 \times 10^{-9}, 9.3 \times 10^{5})$	2.707 (-26.46, 31.87)	14.99 $(3.2 \times 10^{-10}, 7.0 \times 10^{9})$

-2xLog-Likelihood= 2495.898

$$q_{ij}(t|\mathbf{Z}^*(t)) = \begin{cases} q_{ij}^{(0)}; & if\ \tau_0 \leq t < 0.5 \\ q_{ij}^{(1)} = q_{ij}^{(0)} exp\{\beta_{ij,1}^* Z_1^*(t)\}; & if\ 0.5 \leq t < 1 \\ q_{ij}^{(2)} = q_{ij}^{(0)} exp\{\beta_{ij,1}^* Z_1^*(t) + \beta_{ij,2}^* Z_2^*(t)\}; & if\ t \geq 1 \end{cases}$$

$q_{ij}^{(0)}$ is the baseline transition intensities for the interval $0 \leq t < 0.5$, $\beta_{ij,l}^*$ is the log-linear effect of the $l = (r+1)^{th}$ interval on the baseline transition intensity and $\mathbf{Z}^*(t)$ is the artificial time-dependent covariate. The estimated parameters are shown in Table 5.3 below:

Results from Table 5.3 show an improvement on the estimated parameter values. This is shown by the confidence intervals that are narrower compared to the confidence intervals shown in Table 5.2 for the **2**-segment model. However, transitions to death from either state 2, 3, 4 or state 5 have very wide confidence interval. Only mortality rates from state 1 (undetectable viral load counts) decrease significantly with time as indicated by the narrow confidence intervals and exclusion of zero in

Table 5.3: Hazard ratios and Log-linear effects $(\beta_{ij,r})$ of half-year and one-year changes in time on the baseline transition intensities. (Confidence Intervals are in brackets)

		Hazard Ratios		$\beta_{ij,1}$	$\beta_{ij,2}$
	Baseline$(q_{ij}^{(0)})$	[0.5,1)	[1,Inf)	[0.5,1)	[1,Inf)
q_{12}	0.441 (0.357, 0.546)	0.393 (0.198,0.781)	0.246 (0.145,0.419)	-0.933 (-1.619,-0.248)*	-1.401 (-1.932, -0.870)*
q_{16}	0.057 (0.035, 0.094)	0.040 (0.007,0.233)	0.048 (0.021,0.111)	-3.230 (-5.002,-1.458)*	-3.032 (-3.866, -2.198)*
q_{21}	2.607 (2.208, 3.079)	0.447 (0.275,0.725)	0.289 (0.210,0.400)	-0.806 (-1.289,-0.321)*	-1.240 (-1.562, -0.917)*
q_{23}	1.588 (0.501, 5.036)	0.0836 (0.002,3.404)	0.0692 (0.002,2.540)	-2.482 (-6.188, 1.225)	-2.670 (-6.273, 0.932)
q_{26}	0.00138 (0.001, 2.268)	0.293 (0.048,1.773)	2.111 (0.653,6.827)	-1.227 (-83.617,81.163)	0.747 (-34.965, 36.460)
q_{32}	6.775 (2.264, 10.027)	0.034 (0.010,1.120)	0.020 (0.007,0.61)	-3.376 (-6.866, 0.114)	-3.900 (-7.306, -0.493)*
q_{34}	4.832 (3.571, 6.540)	4.364 (3.462,13.487)	20.097 (2.418, 26.70)	1.474 (-2.907, 5.854)	3.001 (-6.025, 12.026)
q_{36}	0.0585 (0.011, 3.182)	0.799 (0.402,1.589)	61.145 (60.93,61.36)	-0.224 (-35.450,35.002)	4.113 (-9.706, 17.932)
q_{43}	36.307 (2.900, 45.46)	0.688 (0.0691,6.851)	3.951 (0.653,23.91)	-0.374 (-4.975, 4.227)	1.374 (-7.334, 10.082)
q_{45}	0.638 (0.165, 2.467)	0.754 (0.518,10.96)	0.017 (0.0028,1.084)	-0.282 (-2.959, 2.395)	-4.054 (-5.820, 7.712)
q_{46}	0.010 (0.002, 5.081)	2.063 (0.345,12.35)	5.745 (0.997,33.12)	0.724 (-74.748,76.196)	1.748 (-214.14,217.64)
q_{54}	26.276 (18.65, 37.02)	0.090 (0.047,1.703)	5.151 (3.504,7.572)	-2.409 (-5.35, 0.533)	1.639 (-24.07, 27.353)
q_{56}	0.046 (0.011, 1.960)	180.816 (3.766,868.2)	2.298 (0.0002,27.51)	5.198 (-5.582,15.976)	0.832 (-98.36,100.02)
		-2xLog-Likelihood 2485.745			

the confidence intervals.

Presentation of the results from a **2**-segment piece-wise Markov model together with the effects of covariates follows. The model is given below:

$$q_{ijl}(t|\mathbf{Z}^*(t),\mathbf{Z}) = q_{ij}^{(0)} \exp\{(\beta_{ij,l}^*)'\mathbf{Z}_l^*(t) + \beta_{ij}'\mathbf{Z}\}$$

$q_{ij}^{(0)}$ is the baseline transition intensities for the interval $0 \leq t < 0.5$ with covariates set to their means, $\beta_{ij,l}^*$ is the log-linear effect of the l^{th} interval on the baseline transition intensity corresponding to the artificial time-dependent covariate $\mathbf{Z}_l^*(t)$. β_{ij} is the log-linear effect relating the instantaneous rate of transitions from state i to state j to the covariates **Z**=CD4 cell count at baseline (CD4BL), non-adherence (NA), Gender,Viral load count at baseline (VLBL). The results are shown in Table 5.4 below:

The results from Table 5.4 show that during the first 6 months of treatment uptake (baseline) the rates of viral load suppression are higher than the rates of viral re-

Table 5.4: Estimated parameters for the half-year piece-wise Markov model with the Log-linear effects of covariates included. (Confidence Intervals are in brackets)

	Baseline ($q_{ij}^{(0)}$)	CD4BL	NA	Gender	VLBL	[0.5,Inf)
q_{12}	0.515 (0.412,0.643)	0.201 (-0.240,0.642)	0.565 (0.042, 1.088)*	-0.198 (-0.629,0.232)	0.321 (-0.238, 0.879)	-1.163 (-1.69,-0.633)*
q_{16}	0.004 (0.000003,48.1)	0.923 (-0.039,1.884)	-5.245 (-22.225,11.73)	-0.386 (-1.185,0.412)	1.144 (-0.065, 2.353)	-6.079 (-19.38,7.222)
q_{21}	3.021 (2.539,3.593)	0.315 (0.022,0.609)*	-0.978 (-1.395,-0.562)*	-0.034 (-0.330,0.262)	-0.074 (-0.436, 0.288)	-0.994 (-1.295,-0.69)*
q_{23}	1.277 (0.633,2.575)	-0.731 (-2.821,1.358)	0.956 (-0.034,1.947)	0.221 (-0.854,1.295)	-0.212 (-2.554, 2.130)	-1.728 (-3.11,-0.349)*
q_{26}	0.0127 (0.00001,0.114)	1.221 (-1.022,3.463)	-0.909 (-3.657,1.839)	-3.554 (-18.26,11.15)	3.836 (-9.691,17.36)	5.279 (-11.01,21.57)
q_{32}	7.724 (4.081,14.62)	-1.422 (-3.546,0.703)	0.0656 (-0.956,1.087)	0.236) (-0.830,1.302)	-1.476 (-3.788, 0.837)	-2.725 (-3.94,-1.512)*
q_{34}	0.963 (0.253,3.664)	1.714 (-0.749,4.177)	0.882 (-1.430,3.195)	-0.786 (-2.635,1.063)	-0.590 (-4.192, 3.012)	1.023 (-1.659,3.705)
q_{36}	0.0218 (0.00008,58.94)	-0.022 (-3.035,2.992)	-1.477 (-4.606,1.653)	3.454 (-9.17,16.08)	3.362 (-20.82, 27.55)	5.131 (-12.62,22.88)
q_{43}	11.297 (3.569,35.77)	2.047 (0.190,3.903)*	0.530 (-2.012,3.073)	-0.332 (-1.293,0.629)	-0.249 (-3.018, 2.520)	-2.046 (-3.69,-0.398)*
q_{45}	4.325 (0.005,3489)	3.834 (-0.574,8.243)	3.591 (-8.322,15.505)	-2.742 (-12.91,7.427)	3.102 (-15.335, 21.54)	-5.474 (-9.55,-1.402)*
q_{46}	0.166 (0.0004,64.23)	-0.327 (-4.853, 4.199)	-1.186 (-7.007,4.635)	0.587 (-2.433,3.61)	0.360 (-127.3,128.0)	6.455 (-11.13,24.04)
q_{54}	44.854 (0.097,2077)	0.492 (-1.963,2.948)	2.911 (-8.605,14.428)	-2.156 (-11.58,7.266)	-0.078 (-3.581, 3.426)	-1.067 (-3.716,1.581)
q_{56}	0.00899 (0.00009,82100)	0.216 (-58.05,58.48)	-0.0998 (-77.39,77.19)	-0.175 (-53.28,52.93)	-0.305 (-154.9,154.2)	3.530 (-49.91,56.97)

-2xLog(likelihood)= 2390.415; *significant

bound, regardless of the state. The highest transition rates are noted from a viral load above 500 000 copies/mL to a viral load between 100 000 and 499 999 copies/mL. During the first six months most transitions to death occurred from a viral load state between 100 000 and 500 000 copies/mL. This is mainly attributed to initiating treatment with a CD4 cell count at baseline below 200 cells/mm^3.

Having a CD4 cell count at baseline below 200 cells/mm^3 at treatment initiation contributes significantly to increase in viral suppression to undetectable level as shown by a narrow confidence interval and exclusion of zero in the confidence interval. For these patients, there is also a significant increase in the rates of viral suppression from state 4 to state 3. Though not significant, there is reduction in viral suppression from state 3 to state 2.

For non-adherent patients, the results reveal a significant reduction in viral suppression to undetectable levels (state 2 to state 1). Thus, adherence to treatment increases significantly the transition rates to undetectable levels. Non-adherence increases

transitions to viral load rebound from undetectable viral load level (state 1 to state 2). Although some of the estimated parameters are not significant, the results show that non-adherence to treatment contributes more to the increased rates of viral load rebound than viral load suppression.

Males in the study experience a reduction in viral suppression to undetectable levels, but once the undetectable viral load is reached, they have reduced rates of viral rebound. Deaths of males are highly likely to occur from viral load states between 10 000 and 500 000 copies/mL.

The results also show reduction in the rates of transition to better states (viral suppression) for patients who initiated treatment with a viral load level above 10 000 copies/mL. These patients experienced increased transitions to death regardless of the viral load count based state. Thus, starting treatment with a viral load counts above 10 000 copies/mL increases the mortality rates and also accelerates disease progression.

From 6 months (0.5 years) of treatment uptake onwards, most of the transitions between live states are significant, except for the transition from state 3 to state 4, and state 5 to state 4. The results show a significant reduction in the rates of viral suppression to undetectable levels from 6 months onwards but once the undetectable viral load is reached, there is reduction in viral rebound and also reduction in death occurrences. However, if the viral load is still detectable after 6 months, it increases the occurrence of deaths but there is wide margins in the estimated confidence intervals.

5.3.1 Assessment of the Fitted Models

In this subsection, assessment of the fitted models is done using several techniques: prevalence plots, contour plots and estimates of log-likelihoods and Akaike information criteria (AIC). Prevalence plots give a rough indication of the goodness of the fitted models and contours plot the likelihood surface with respect to 2 parameters default to plus or minus 2 standard errors obtained from the Hessian matrix at the maximum likelihood estimate.

In Figure 5.2, Figure 5.3 and Figure 5.4, comparison of the percentage prevalence plots is done for each of the states for the a two-segment non-homogeneous Markov model with change point at 0.5 years, the **2**-segment model with change point at 1 year, and **3**-segment non-homogeneous Markov model, respectively.

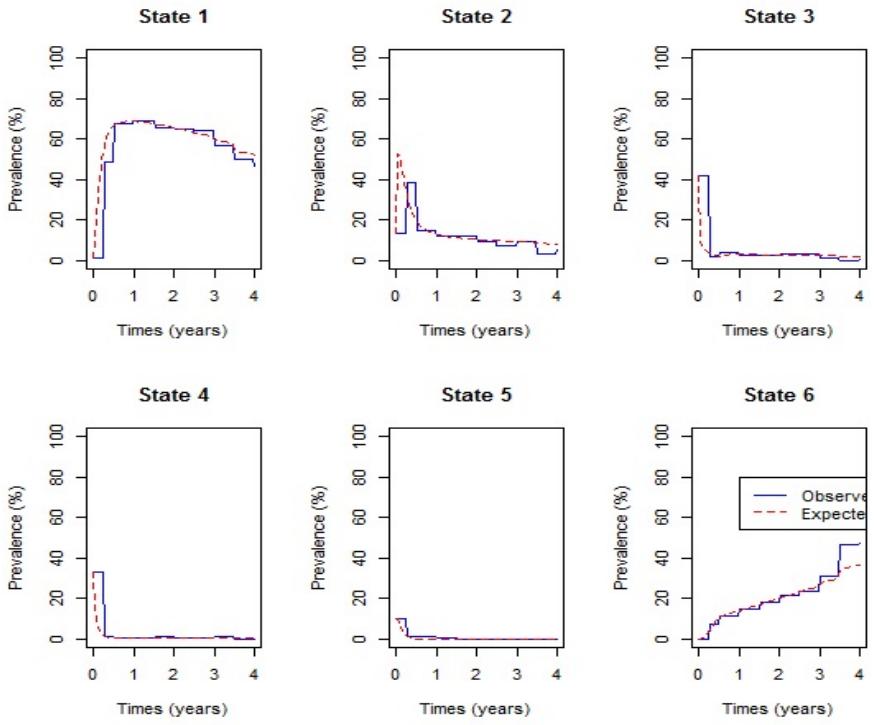

Figure 5.2 – *Percentage Prevalence plots for the 2-segment model with change point at 0.5 years.*

Results from the fitted percentage prevalences (see Figure 5.2, Figure 5.3 and Figure 5.4) show that the fitted models give a perfect fit of the observed data for patients in state 2, 3, 4 and 5. However, the expected percentage prevalence plot for the **2**-segment non-homogeneous continuous-time Markov model with change point at 1 year (see Figure 5.2) overestimates the observed data for patients in state 1. From 3 years onwards, expected percentage prevalence for mortality (state 6) underestimate the observed mortality from all fitted models, although the **2**-segment model with change point at 1 year underestimates mortality from 2 years onwards. Compared to the prevalence plot for the time homogeneous model shown in Figure 5.1, these plots show an improved fit to the observed data.

From all fitted models (Figure 5.2, Figure 5.3 and Figure 5.4), the prevalence of state 1 is down sloping from half a year onwards. This is due to non-adherence to treatment as shown by the results in Table 5.3.

Before computing estimates of AICs, the contours for the fitted models are plotted. These contours help to diagnose any irregularities in the likelihood surface. Thus, they present a graphical visualisation of the fitted surface. For biological data, these

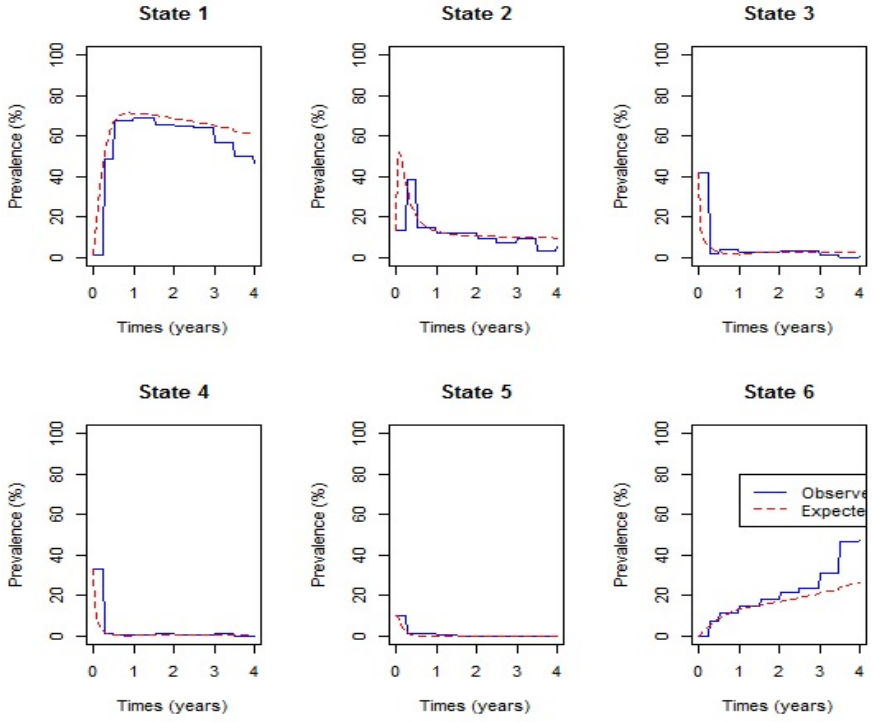

Figure 5.3 – *Percentage Prevalence plots for the* **2***-segment model with change point at 1 year.*

contours are expected to be elliptical. Figure 5.5 below shows contours for the fitted models.

Figure 5.5 shows that contours for the time homogeneous Markov model (top left) are not elliptical but the contour for the three non-homogeneous models are elliptical. This means that the non-homogeneous model gives a better fit to the data, compared to the homogeneous model. However, the contours for the time homogeneous model (top left) and the contours for the **2**-segment with change point at 1 year (top right) are not symmetric, hence the models cannot explain this data fully. The contours for the non-homogeneous models, **2**-segment with change point at 0.5 years (bottom left) and 3-segment with change points at 0.5 and 1 year (bottom right), are both elliptical and evenly distributed contour plots with symmetrical surfaces that peak at the centre (indicated by the white region). Hence these models give an adequate explanation of the data.

Table 5.5 below shows estimates of the $-2 \times LL$, log-likelihoods (LL) are shown in brackets, the degrees of freedom for each of the fitted models and the Akaike information criteria (AIC). The AICs are calculated using the formula; $AIC = -2 \times LL + 2 \times df$. For example, for the homogeneous model $AIC = 2799.465 + 2 \times 13 =$

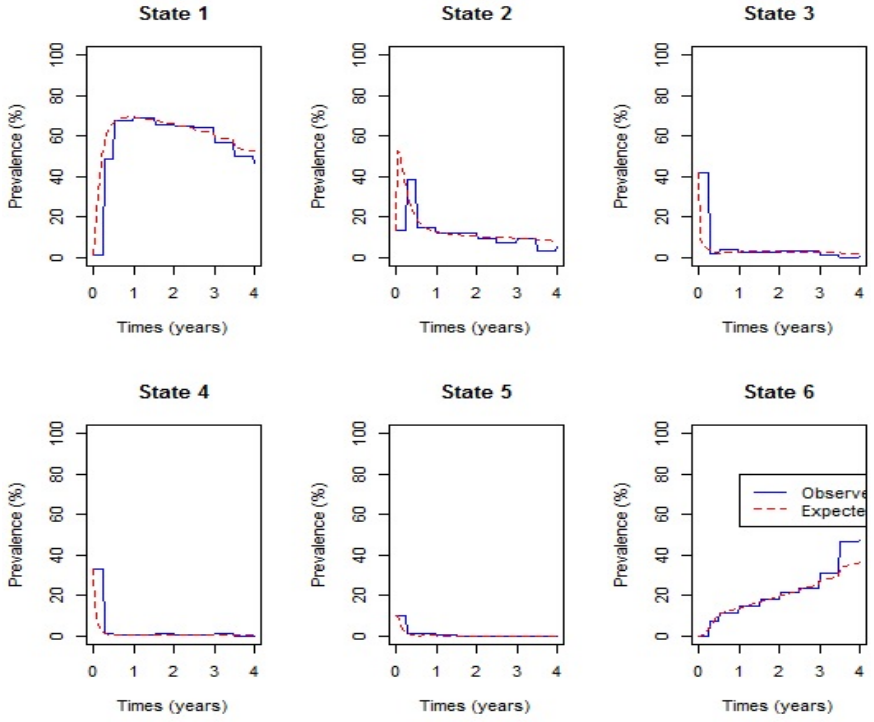

Figure 5.4 – *Percentage Prevalence plots for the the 3-segment model with change points at 0.5 and 1 year.*

2825.465 as shown in the Table 5.5 below:

Table 5.5: Estimated AICs and Log-likelihoods for the fitted models.

	A	B	C	D	E
$-2 \times LL$ Log-Likelihood	2799.465 (-1399.73)	2554.177 (-1277.09)	2495.898 (-1247.95)	2485.745 (-1242.87)	2520.415 (-1260.21)
df	13	26	26	39	65
AIC	2825.465	2606.177	2547.898	2563.745	2390.415

Key:A: Homogeneous Model; B: **2**-segment (1-year change point); C: **2**-segments (0.5-year change point); D: **3**-segments (0.5 and 1-year change points); E: **0.5**-year change point and covariates

The results show that the time homogeneous Markov model has the highest AIC and the lowest log-likelihood, compared to the non-homogeneous Markov models. From the fitted non-homogeneous Markov model, the **3**-segment model with change points at 0.5 and 1 year has the highest log-likelihood compared to all the other fitted models followed by the **2**-segment model with change points at 0.5 years. However, a further assessment basing on the AICs reveals that a **2**-segment model with change points at 0.5 years fits the data better than the **3**-segment model, since it has the lowest AIC. Effects of the covariates were included in the **2**-segment non-homogeneous

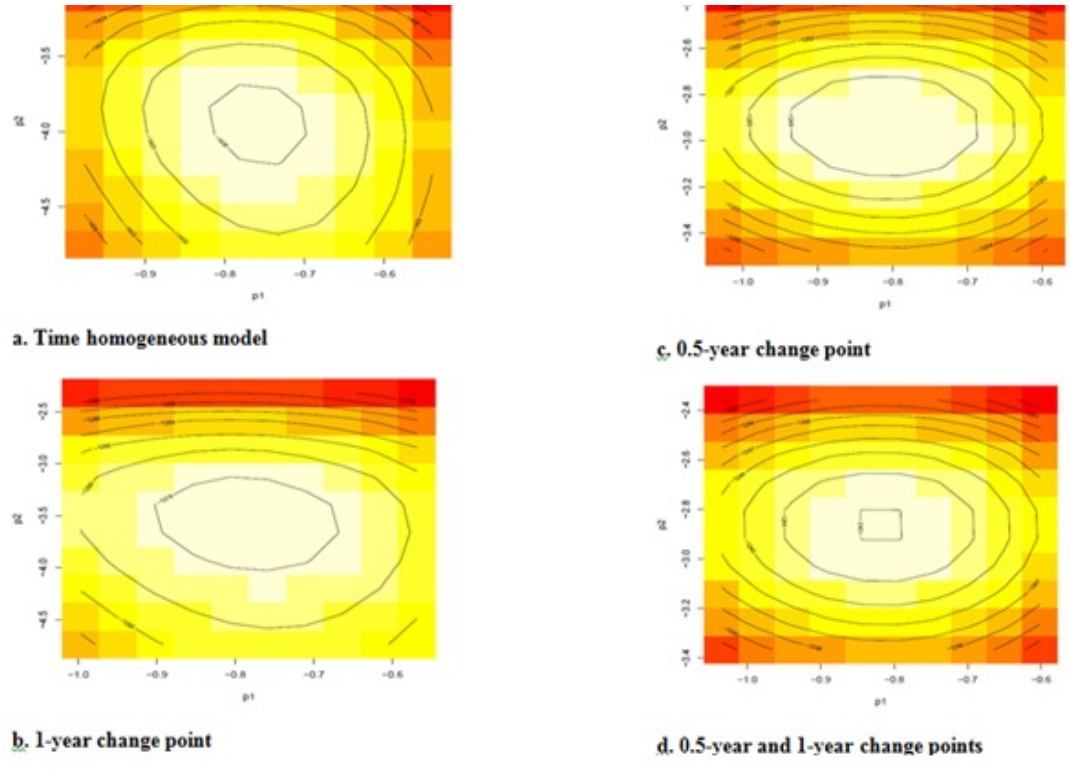

Figure 5.5 – *Contour plots for: (a) the time homogeneous Markov model, (b) the* **2***-segment model with change point at 1 year, (c) the* **2***-segment model with change point at 0.5 years and (d) the* **3***-segment model with change points at 0.5 and 1 year.*

model and the model yielded the lowest AIC.

5.4 Concluding Remarks

In this chapter, a comparison of the time-homogeneous Markov model and the non-homogeneous Markov model to estimate the progression of HIV/AIDS on viral load monitoring, is done. For this model, the expected percentages in state 1 overestimated the observed percentages and the predicted number of individuals who die was underestimated by the model from 1 year of treatment uptake onwards. This indicated the need to fit a non-homogeneous model in which transition intensities are piece-wise constant. Non-homogeneous models with different change points were fitted. However, most of these models did not converge to a maximum likelihood, except for the **2**-segment model with change point at 0.5 years, 2-segment model with change point at 1 year, and **3**-segment model with change points at 0.5 and 1 year. Assessment of the fitted models was done using the percentage prevalence

plots, contour plots, CIs, log-likelihoods and the AICs. The model with the lowest AIC, the 2-segment model with change point at 0.5 years including covariates, was considered as the model that best explains HIV progression in patients on treatment under viral load monitoring for this data set.

This means that HIV/progression is best described by a non-homogeneous Markov model with a change point at 0.5 years. This is mainly influenced by the results from viral load monitoring, which are that, most of the patients on anti-retroviral therapy reach the undetectable viral load within the first 0.5 years of treatment uptake (Silveira et al., 2002). Thus, when monitoring HIV/AIDS patients, one should ensure that viral load suppression is reached, as this reduces mortality rates.

The results also reveal reduction with time in rates of viral suppression to undetectable levels for males and patients who were non-adherent to treatment. However, once the undetectable viral load is reached, there is reduction in viral rebound, particularly from 0.5 years of treatment uptake onwards. The results also show a significant reduction in transitions to death after 0.5 years for patients who have achieved an undetectable viral load despite the challenges of non-adherent.

This chapter also revealed possibilities of viral rebound in patients receiving cART. In the next chapter, determinants of viral rebound on HIV infected patients is analysed using a continuous-time homogeneous Markov model. Among the determinants, cART, treatment line administered, resistance to treatment, lactic acidosis and peripheral neuropathy are included.

Chapter 6

Determinants of Viral Load Rebound on HIV/AIDS Patients Receiving Antiretroviral Therapy

6.1 Introduction

In South Africa, the anti-retroviral therapy available at present are the nucleotides reverse transcriptase inhibitors (NRTIs) class which include: zidovudine (AZT), didanosine (ddI), lamivudine (3TC) and stavudine (d4T) (Thaker and Snow, 2003). Other NRTIs include abacavir (ABC), tenofovir (TDF) and Emtricitabine (FTC) (Prosperi et al., 2009). NRTIs are most preferred for HIV/AIDS patients in low income countries (Munderi, 2010) because of their low production costs (Kore and Waghmare, 2012).

However, patients treated with NRTIs develop varying degrees of myopathy or neuropathy after long-term therapy (Currier, 2007). AZT causes myopathy, ddI and 3TC cause neuropathy, d4T causes neuropathy or myopathy and lactic acidosis (LA). Studies show that d4T appears to cause lactic acidosis (LA) more frequently than ddI or AZT (Dalakas 2001; Kore and Waghmare, 2012). In developed countries d4T is no longer favoured as a consequence of both short-term toxicity (lactic acidosis) and long-term toxicity (lipoatrophy and neurophathy) (Kore and Waghmare, 2012). Neuropathy is long-term in the sense that it is usually associated with late stages of HIV disease as indicated by the presence of opportunistic infections implying that, it is highly associated with low CD4 cell count and high viral load counts (Simpson, 2002).

Science literature has successfully established the efficiency of cART in controlling

HIV. However, its effectiveness depends particularly on the adherence of patients to cART (Silva et al., 2015). Nachega et al. (2011) argued that, although patients and providers should continuously strive for maximum adherence to cART, there is accumulating evidence that each class of antiretroviral therapy has specific adherence-drug resistance relationship characteristics allowing certain regimens to be more flexibility than others. Adherence can be defined as the extent to which a person uses a medication according to medical recommendations, inclusive of time, dosing, and consistency (Chaiyachati et al., 2014). Non-adherence results in anti-retroviral agents not being able to maintain sufficient concentration to suppress HIV replication in infected cells and to lower the plasma viral load count (Chesney, 2000). Poor adherence also accelerates drug-resistant HIV (Chaiyachati et al., 2014; Chesney, 2000).

The development of drug-resistant variants that can develop in HIV/AIDS patients under ART makes it difficult to completely eradicate the virus (Hirchhorn et al., 2005). This results in virological rebound and eventual disease progression (Hirchhorn et al., 2005). But, with proper adherence to treatment, ART has the potential to suppress viral replication, often below the level of detection by commercially available tests (Saint-Pierre et al.,2003). Hirschhorn et al. (2005) also identified the range of possible virologic responses which among failure to ever see a virologic response, decline followed by rebound, ever-achieved suppression, and loss of suppression after it had been achieved. This justifies the importance of viral load as a marker of treatment efficacy.

Stochastic models have proved to be the best when dealing with real-life situations, particularly when modelling biological phenomena such as in-vivo HIV dynamics (Dalal et al. 2008). As the HIV progresses in an individual, there are random movements between states, stochastic models are very good at handling these random variables (Mullins and Weisman, 1996). Stochastic processes also allow modelling the effects of covariates such as age and genetic differences among individuals, level of virulent of an individual, and co-infection with other microbes (Dalal et al., 2008). In particular, continuous-time homogeneous Markov models are usually used to model the evolution in chronic diseases (Gibson, 2008).

6.1.1 The continuous-time homogeneous Markov model for the effects of covariates

Consider a model consisting of $h = 6$ states belonging to the state space $S = 1, 2, \ldots, h = 6$. Consider the i^{th} individual being in some state at time t. Let $X_v(t)$ denote the state

occupied by a randomly chosen individual at time t. Assuming that the individual's movements obey a continuous time-homogeneous Markov process, then for $0 \leq s \leq t$ the $h \times h$ transition probability matrix $P(s,t)$ with entries:

$$P_{ij}(s,t) = P\{X_v(t) = j | X(s) = i\}, \quad i; j = 1, \ldots, h$$

Can be specified in terms of transition intensities

$$q_{ij}(t) = \begin{cases} \lim_{\Delta t \to 0} \frac{P_{ij}(t,t+\Delta t)}{\Delta t}, & i \neq j \\ -\sum_{i \neq j} q_{ij}(t), & i = j. \end{cases} \tag{6.1}$$

where $q_{ij}(t)$ are the entries of the $h \times h$ transition intensity matrix $Q(t)$. Since our model is time-homogeneous we consider $q_{ij}(t) = q_{ij}$ independent of time. $Q = (q_{ij})$ is the transition intensity matrix. For this model, transition probabilities are stationary such that:

$$P(s, s+t) = P(0,t) = P(t)$$

For each of the individuals, covariates are measured. Interest centres on the relationship between the covariates and the transition intensities q_{ij} in the Markov model. Variables associated with the transition intensities are assumed to have a multiplicative effect of the form:

$$q_{ij} = q_{ij}^{(0)} \exp\left(\beta'_{ij,k} \mathbf{Z}_k\right) \tag{6.2}$$

where $\mathbf{Z}$ is the k-dimensional vector of covariates. $\beta_{ij,k}$ is the vector of k regression parameters relating to the instantaneous rate of transition from state i to state j. $q_{ij}^{(0)}$ is the baseline transition intensity relating to the transition from state i to state j.

Equation (6.2) can be written as a log-linear model as shown below:

$$\log\ q_{ij} \quad = \quad \beta_{ij0} + \sum_{k=1}^{p} \beta'_{ij,k} \mathbf{Z}_k \qquad for\ i \neq j, k = 1, 2, \ldots p \tag{6.3}$$

where $\exp(\beta_{ij0}) = q_{ij}^{(0)}$ the baseline transition rates for patients in which the covariates are not mentioned, $\mathbf{Z}_k$ is a k-dimensional vector of covariates and $\beta_{ij,k}$ represents a vector of vector of k regression parameters relating the transition rates from

state i to state j to the covariates $\mathbf{Z}_k$. Maximum likelihood estimates of the baseline transition intensity matrix can be obtained by maximising the likelihood function with respect to the parameter $q_{ij}^{(0)}$.

We let $T_i, i = 1, \ldots, h$, be the total time spent by all individuals in the transient state i before making a transition to state j. We also let $b_{ij}, i; j = 1, \ldots, h$, be the total number of transitions from state i to state j. Then the maximum likelihood estimates of the baseline transition intensities are:

$q_{ij}^{(0)} = \frac{b_{ij}}{T_{ij}} \quad for\ i, j = 1, \ldots, h$

$q_{ij}^{(0)}$ is the baseline hazard rate without (or ignoring) the effects of the covariates. In calculating $q_{ij}^{(0)}$ all β_{ij0} are chosen to be equal to zero, which means that there are no covariates effects. Estimates of β obtained by maximising the partial likelihood function are given by:

$$L(\beta) = \Pi_{k=1}^{n} \left(\frac{\exp(\beta_{ij}' \mathbf{Z}_{kx})}{\sum_{l \in R(t_{ij,k})} (\beta_{ij}' \mathbf{Z}_{kx})} \right)$$

Where $\mathbf{Z}_{kx}$ is the k-dimensional covariate vector for patient x and $R(t_{ij,x})$ is the risk at time t for making a transition from state i to state j.

This chapter explores the effects of treatment toxicity (lactic acidosis (LA) and peripheral neuropathy (PN)), non-adherence (NA), treatment line, CD4 cell count at baseline, viral load baseline and age on the changes in the level of viral load in the plasma cells. The analysis is done using a time-homogeneous Markov model with covariates. In medical research, the state of the patient at observation time is the only thing known with certainty. The researcher may know the time interval in which a transition has occurred, but not the exact time. Thus, time-homogeneous Markov models which are interval censored can handle such data (Gibson, 2008).

In the sections that follow, methods used in analysing the data are explored. This is followed by a section 6.3 on results and discussions. Lastly, in section 6.4 conclusions of the findings is made.

6.2 Longitudinal data from monitored HIV infected patients

The data used in this Chapter is described in Section 3.5. However, in addition to the variables defined in Section 3.5, that is, CD4 baseline, gender, age, viral load baseline and non-adherence to treatment, the effects of different cART, change of cART, development of adverse reactions such as peripheral neuropathy and lactic acidosis on virology are also analysed.

In patients who showed some signs of non-adherence, d4T was substituted with AZT (Zidovudine). A switch from d4T-3TC-EFV (D1) to AZT-3TC-EFV (D2) was most common, rising from 10 patients in the first 6 months to 92 patients in 30 months (2 and half years). During the same period, the number of patients who switched from d4T-3TC-NVP (D3) to AZT-3TC-NVP (D4) rose from 6 to 45. After 1 year of treatment uptake, one patient was introduced to FTC-TDF-EFV (D5) and after three and half years, the frequency increased to 10 patients. Another combination of FTC-TDF-NVP was also introduced to 3 patients after 2 years and the number rose to 7 after 3 years. AZT-3TC-LPV/r (D6) was also administered and at t = 0, two patients were administered with this triple combination. Other treatment combinations that were administered include FTC-TDF-NVP, AZT-ddI-LPV/r, d4T-3TC-LPV/r, ddI-d4T-3TC, FTCTDF- LPV/r. However, these were not frequently administered and hence they were treated as other (D7) combinations for analysis purpose. The table below shows the frequencies for each of the treatment combinations;

Drug	*D1*	*D2*	*D3*	*D4*	*D5*	*D6*	*D7*	*Total*
Frequency	*879*	*461*	*370*	*234*	*56*	*47*	*212*	*2259*

The table shows that d4T-3TC-EFV was the most frequently used drug combination. For each visit, viral load count in the plasma was also measured. In this thesis, if the viral load was below 50 copies/mL it is recorded as undetectable viral load. In this thesis, the progression of HIV/AIDS is defined by change in viral load level. The viral load levels are divided into 5 transient states, and the sixth state being the absorbing state, death. The viral load-based states and other factors that are likely to determine change in viral load levels are defined in the next sub-section.

In this chapter, determinants of viral rebound are assessed from the covariates: age, lactic acidosis, peripheral neuropathy, non-adherence, CD4 at baseline, gender, viral load at baseline, treatment line, and resistance to treatment. For inclusion into the time-homogeneous Markov model, the covariates non-adherence (NA), gender, age and viral load at baseline (VLBL) and CD4 at baseline (CD4BL) are as defined in

Equations (3.54), (3.56), (3.57), (3.58) and (3.55), respectively. Coding of the other covariates is shown below:

$$Lactic\ Acidosis\ (LA) = \begin{cases} 1; & if\ yes \\ 0; & if\ no \end{cases}$$

$$Peripheral\ Neuropathy\ (PN) = \begin{cases} 1; & if\ yes \\ 0; & if\ no \end{cases}$$

$$Treatment\ Change\ (TC) = \begin{cases} 1; & if\ yes \\ 0; & if\ no \end{cases}$$

$$Treatment\ line\ (TL) = \begin{cases} 1; & TL = 1 \\ 0; & TL = 2 \end{cases}$$

$$Resistance\ (Res) = \begin{cases} 1; & if\ yes \\ 0; & if\ NO \end{cases}$$

The states of the continuous-time Markov model are defined as follows:

$$Viral\ load\ levels\ (X_v(t)) = \begin{cases} 1; & VL < 50 \\ 2; & 50 \leq VL < 10\,000 \\ 3; & 10\,000 \leq VL < 100\,000 \\ 4; & 100\,000 \leq VL < 500\,000 \\ 5; & VL \geq 500\,000 \\ 6; & Dead \end{cases} \tag{6.4}$$

Table 6.1 below shows the frequency distributions for each viral load state at $t = 0$ (baseline), $t = 0.25$ years and at $t = 0.5$ years.

Results from Table 6.1 show that at $t = 0$ years most of the patients had a viral load above 10 000 copies/mL. During the first 0.25 years of treatment uptake, the majority of the patients had achieved a suppressed viral load to undetectable levels. These results show possibility of transitions, from state i to state j, between the

Table 6.1: Number of HIV/AIDS patients in each viral load state from $t = 0$ to $t = 0.5$ years.

	Viral	load	levels	$(X_v(t))$		
	1	2	3	4	5	6
$t = 0\ years$	4	43	134	106	32	0
$t = 0.25\ years$	155	123	6	4	4	24
$t = 0.5\ years$	214	48	13	2	3	11

viral load states, $X_v(t)$. In this case $X_v(t) = 1, \ldots, 6$. We assume that the transition rate between states for any subject is governed by some covariates identified above. The effects of the covariates age, lactic acidosis (LA), peripheral neuron (PN), gender, CD4 cell counts at baseline (CD4BL), treatment line (TL), viral load count at baseline (VLBL), treatment change (TC), non-adherence (NA) and resistance to treatment (Res) on transition intensities, q_{ij}, is assessed. The log-linear model linking q_{ij} with the linear effects of covariates is given by:

$$log\ q_{ij} = \beta_{ij0} + \sum_{k=1}^{p} \beta_{ij,k}\mathbf{Z}_k\ for\ i \neq j, i = 1, 2, \ldots, 5;\ j = 1, \ldots, 6\ and\ k = 1, \ldots, 10$$

as defined in Equation (6.2). Thus, the transition intensity for a patient x in this study is given by the model:

$$\begin{aligned} q_{ij} &= q_{ij}^{(0)} \exp(\beta_{ij}^{Age} Age_x + \beta_{ij}^{LA} LA_h + \beta_{ij}^{PN} PN_x + \beta_{ij}^{Gender} Gender_x + \beta_{ij}^{CD4BL} CD4BL_x \\ &+ \beta_{ij}^{TL} TL_x + \beta_{ij}^{VLBL} VLBL_x + \beta_{ij}^{TC} TC_x + \beta_{ij}^{NA} NA_x + \beta_{ij}^{Res} Res_x) \end{aligned} \tag{6.5}$$

For this model, the baseline transition intensities, $q_{ij}^{(0)}$ refer to a patient with age category 0 (over 45 years old), no LA, no PN, Gender = 0 (female), CD4BL = 0 (above 200 cells/mm^3, TL = 0 (second line), VLBL = 0 (over 10 000 copies/μL), no TC, no NA and no resistance. The transition intensities q_{ij}, are presented in rates per year. q_{ij} are the elements of a 6×6 transition intensity matrix Q from a continuous time-homogeneous Markov process. As indicated in Equations (6.2) and (6.3), thus can be represented by the log-linear model:

$$\begin{aligned} \ln\ q_{ij} &= \ln\ q_{ij}^{(0)} + \beta_{ij}^{Age} Age_x + \beta_{ij}^{LA} LA_x + \beta_{ij}^{PN} PN_x + \beta_{ij}^{Gender} Gender_x + \beta_{ij}^{CD4BL} CD4BL_x \\ &+ \beta_{ij}^{TL} TL_x + \beta_{ij}^{VLBL} VLBL_x + \beta_{ij}^{TC} TC_x + \beta_{ij}^{NA} NA_x + \beta_{ij}^{Res} Res_x \end{aligned} \tag{6.6}$$

where β_{ij} represents the log-linear effects of the mentioned covariate on transition intensities from state $i = 1, 2, \ldots, 5$ to state $j = 1, 2, \ldots, 6$ for individual x. Com-

putation of the estimated baseline transition intensities is done by setting all the covariates to their mean.

6.3 Results and discussion

Figure 6.1 is a Box and whiskers plot which shows the distribution of viral load states, defined by equation (6.4), for each and every visit time which is originally considered to be discrete.

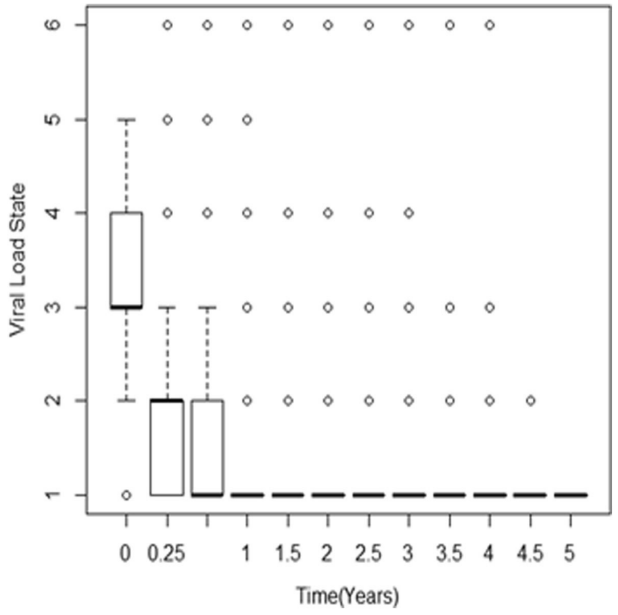

Figure 6.1 – *Box and whiskers diagram for the distribution of viral load levels for each visit time from initiation of therapy to 5 years. Data was collected at discrete time points, that is, at t = 0 years, t = 0.25 years, t = 0.5 years and after every 0.5 years thereafter.*

Figure 6.1 shows that at time equal to zero, there were no cases in state 6 since the state represents the death state. On treatment initiation, the majority of the patients were in state 3, defined by a viral load level between 10 000 and 100 000 copies/mL. After 3 months (0.25 years) the majority of the patients had moved to state 2. This is an indication of viral suppression by the anti-retroviral therapy. From a period of 1 year onwards, the majority of the patients had moved to state 1, a state of undetectable viral load. However, patients whose viral load level is not suppressed throughout the whole period are still notable. There is need to investigate further the factors that are associated with failure of viral load suppression.

Table 6.2: Transition counts.

	To					
	1	2	3	4	5	6
From 1	1109	104	16	2	1	17
2	207	98	21	4	1	8
3	80	63	22	4	0	19
4	45	54	6	2	4	9
5	6	21	0	4	2	7

6.3.1 State table for transition counts

The results from Table 6.2 show that the highest number of deaths was recorded from state 3, which is defined by a viral load level between 10 000 and 100 000 copies/mL. Also to note are the deaths from state 1, defined by suppressed/ undetectable viral load level ($< 50\ copies/mL$). There is need to assess the determinants of deaths from this state because patients in this state have most of the virus particle cleared by the anti-retroviral drug. Estimates of the transition intensities for a continuous time Markov model without the effects of covariates is done first. The transition intensities are estimated based on the assumption that the transition probabilities p_{ij} are known and are given as follows:

$$q_{ij} = q_{ij}^{(0)} \exp(\beta_{ij} t) \ \ for\ i \neq j \tag{6.7}$$

Estimates of the transition intensities are given in Table 6.3 below:

Table 6.3: Transition intensities from a continuous time-homogeneous Markov model.

Intensities	Estimated Intensities	Confidence Interval
q_{12}	0.4687	(0.3787,0.5801)
q_{16}	0.01965	(0.009,0.044)
q_{21}	3.446	(2.983,3.981)
q_{23}	6.195	(2.674,14.36)
q_{26}	0.00004	$(2.34 \times 10^{-39}, 6.382 \times 10^{29})$
q_{32}	34	(15.22,75.93)
q_{34}	4.178	(1.551,11. 25)
q_{36}	1.203	(0.7465,1.940)
q_{43}	23.25	(11.88,45.52)
q_{45}	3.651	(1.174, 11.35)
q_{46}	0.006	$(1.84 \times 10^{-45}, 1.64 \times 10^{40})$
q_{54}	10.640	(5.962,18.97)
q_{56}	1.466	(0.5114,4.202)
$-2 \times LL$	2 799.465	

Results from Table 6.3 show that anti-retroviral therapy plays an important role in slowing down disease progression, particularly for patients in state 3 and state 4.

From state 3, transitions to a better state (state 2) is more than 8 times higher than transitions to the worse state (state 4). For patients in state 4, transition to a better state is more than 6 times transition to the worst state (state 5). However, a patient in state 2 is about twice likely to experience disease progression than recovery. This is a cause for concern, since these patients have lower levels of viral load compared to patients in state 3, 4 and 5. Although transitions to better state are lower than transition to worse state for patients initially in state 2, these patients have the least transition to death compared to deaths from all the other states. This indicates that even though viral suppression is reached, HIV/AIDS patients still experience some viral rebound as supported by Hirschhorn et al. (2005) in their report .

Results from Table 6.3 also show that mortality from state 4 (transition from 4 to 6) is rather too small (less than 0.05) compared to state 3 and state 5. This again is an irregularity in the fitted model which can be addressed by fitting a continuous-time homogeneous Markov model with covariates effects. Thus, in the next section a continuous-time Markov model with covariates is fitted.

6.3.2 Effects of covariates on transition intensities

Maximum likelihood estimation of the baseline transition intensities as well as the log-linear effects for the covariates viral load count at baseline (VLBL), CD4 cell count at baseline (CD4B), age, gender, treatment line (TL), treatment change (TC), non-adherence (NA), lactic acidosis (LA), peripheral neuropathy (PN), resistance to treatment (Res) and triple therapy (Therapy) was done using the "msm" package in R. The log-linear model as indicated in Equation (6.4) is:

$$\begin{aligned}\ln q_{ij} &= \ln q_{ij}^{(0)} + \beta_{ij}^{Age} Age_x + \beta_{ij}^{LA} LA_x + \beta_{ij}^{PN} PN_x + \beta_{ij}^{Gender} Gender_x + \beta_{ij}^{CD4BL} CD4BL_x \\ &+ \beta_{ij}^{TL} TL_x + \beta_{ij}^{VLBL} VLBL_x + \beta_{ij}^{TC} TC_x + \beta_{ij}^{NA} NA_x + \beta_{ij}^{Res} Res_x + \beta_{ij}^{Therapy} Therapy_x\end{aligned}$$

where β_{ij} is the log-linear effects of the mentioned covariate on the baseline transition intensities $q_{ij}^{(0)}$.
On fitting the time-homogeneous model with all the covariates, the model did not converge to a maximum likelihood. As a result, confidence interval for the estimates could not be computed. The covariates effects model was fitted for each of the covariates, one after the other, and it was discovered that treatment line (TL), gender, resistance to treatment (Res) and treatment change (TC) had no significant effects on HIV progression based on viral load levels. As a result, these variables were removed from the model. Results from the model with all covariates are shown in the

appendices.

Table 6.4 shows the estimated baseline transition intensities with covariates set to their mean values in the data. These represent the average intensities for the whole population of given covariates. Table 6.5 shows estimates of log-linear effects of each covariate on transition intensities.

Table 6.4: Baseline transition intensities.

	Baseline intensities	Confidence Interval
q_{12}	0.494	(0.385, 0.634)
q_{16}	0.0000013	$(1.7 \times 10^{-39}, 9.9 \times 10^{26})$
q_{21}	4.008	(3.358, 4.783)
q_{23}	49.74	$(6.2 \times 10^{-17}, 4.0 \times 10^{19})$
q_{26}	0.00007	$(9.0 \times 10^{-13}, 5617)$
q_{32}	535.5	$(6.9 \times 10^{-16}, 4.1 \times 10^{20})$
q_{34}	0.009	$(6.6 \times 10^{-33}, 1.2 \times 10^{28})$
q_{36}	0.0002	$(4.3 \times 10^{-23}, 6.9 \times 10^{14})$
q_{43}	64.37	$(0.000011, 3.8 \times 10^{8})$
q_{45}	0.155	$(6.1 \times 10^{-21}, 3.9 \times 10^{18})$
q_{46}	0.0004	$(2.8 \times 10^{-103}, 1.3 \times 10^{96})$
q_{54}	385.0	$(0.00016, 9.5 \times 10^{8})$
q_{56}	0.0012	$(8.7 \times 10^{-18}, 1.6 \times 10^{13})$

Table 6.4 above shows the baseline transition intensities for the model with covariates. A decreasing trend in the transition rates as the viral load becomes more and more suppressed is portrayed. As a result, the undetectable viral load state (state 1) has the lowest transition rates to death. This result justifies the inclusion of covariates effect in Markov models. The results also show that for patients with a viral load level greater than 2, transition rates to better states are higher than transition rates to worse states. This is quite pronounced for patients initially in state 3, where transition to a better state (state 2) is 535.5 which is quite high compared to transition to the worse state (state 4), which is equal to 0.0090. However, there is a treatment challenge as patients make transitions from state 2. These patients tend to have a viral rebound, resulting in transition to a worse state (state 3) being far much higher than transitions to an undetectable viral load state (state 1). This means that for HIV patients in this cohort, achieving undetectable viral load level was a challenge. In the next table are the effects of age, viral load baseline (VLB), CD4 cell count at baseline (CD4B), non-adherence (NA), peripheral neuropathy (NA), Lactic acidosis (LA) and Triple therapy (Therapy) on transition intensities. Estimates of the confidence intervals are also given.

Results from Table 6.5 below show maximum likelihood estimates of the log-linear effects of the variables on the baseline transition intensities.

Table 6.5: Log-linear effects of Covariate on Baseline Transition Intensities. (Confidence intervals are in brackets)

	Age	VLB	CD4B	NA	PN	LA	Therapy
β_{12}	-0.166 (-0.72,0.39)	0.224 (- 0.55,0.99)	- 0.078 (-0.62,0.46)	0.046 (-0.72,0.81)	- 0.224 (1.04,0.59)	- 0.386 (-1.01,0.24)	- 0.164 (- 0.29,-0.04)
β_{16}	4.904 (-27.45,37.25)	4.387 (-30.94,39.71)	4.373 (-29.56,38.30)	4.844 (-19.60,29.29)	-6.462 (-304.5291.5)	-5.447 (-132,3121)	-0.626 (-10.66,9.41)
β_{21}	-0.377 (- 0.75,-0.01)	-0.369 (-0.96,0.22)	0.330 (-0.03,0.69)	- 1.376 (- 1.94,-0.81)	0.137 (-0.46,0.74)	-0.219 (-0.66,0.23)	-0.268 (- 0.36,-0.174)
β_{23}	0.575 (-1.81,2.96)	6.927 (-9.54,23.39)	- 7.300 (-140.91,26.3)	3.982 (- 13.81,21.77)	1.350 (-1.67,4.37)	6.041 (-10.04,22.11)	0.072 (-0.57,0.71)
β_{26}	-2.304 (- 4.15,-0.46)	4.544 (-29.65,38.73)	6.731 (-26.55,40.01)	- 7.682 (-42.08,26.72)	-8.160 (-44.34,28.01)	-8.035 (- 38.79,22.71)	- 0.113 (- 0.54,0.31)
β_{32}	0.105 (- 2.03,2.24)	5.541 (-10.91,21.99)	-7.484 (-141.21.2)	2.055 (- 15.80,19.91)	0.906 (-1.60,3.41)	5.113 (- 10.99,21.21)	- 0.023 (- 0.64,0.59)
β_{34}	6.347 (-22.04,34.74)	0.959 (-364,366)	6.361 (-24.03,36.75)	- 0.394 (-5.74,4.95)	0.756 (- 2.91,4.43)	- 7.540 (- 96.93,81.85)	0.182 (- 0.36,0.73)
β_{36}	-0.564 (-91.13,90.0)	- 0.576 (-17.82.7)	-0.326 (-100.58,99.9)	-1.740 (-129,126)	-0.028 (-118,8118)	-0.556 (-101.8100)	0.170 (-22.594,22.93)
β_{43}	0.513 (-1.15,2.18)	- 5.237 (-101,91.18)	0.889 (-0.73,2.50)	-0.605 (- 4.51,3.29)	-0.172 (-1.94,1.59)	0.432 (-1.64,2.50)	0.053 (- 0.40,0.51)
β_{45}	1.135 (-95.6,97.88)	1.077 (-182,2184)	-3.177 (-23.95,17.59)	6.334 (- 24.76,37.43)	-4.560 (- 39.83,30.71)	-1.226 (- 28.31,25.8)	0.123 (- 1.48,1.73)
β_{46}	-0.012 (-87.59,87.56)	-0.722 (-1.41,1.41)	-0.552 (-89.7,88.6)	-0.980 (-136,134)	-0.338 (-126,7126)	0.717 (-100,7102)	0.166 (- 7.37,7.70)
β_{54}	-6.221 (-52.9,40.48)	-1.330 (-9.66,7.00)	2.395 (-2.15,6.94)	2.107 (- 21.43,25.6)	-0.578 (- 5.37,4.22)	2.339 (-7.64,12.31)	0.392 (- 0.89,1.68)
β_{56}	0.008 (-85.69,85.71)	3.108 (-29.67,35.89)	- 3.871 (-47.67,39.93)	-2.542 (- 69.13,64.0)	-0.862 (-68.27,66.54)	- 1.611 (- 23.59,20.37)	-0.014 (-9.11,9.08)

$-2 \times LL = 1691.177$

Results from Table 6.5 show that for patients with non-adherence (NA) to treatment, there is a reduction of transitions from a viral load level of 2 (viral load between 50 and 10 000 copies/mL) to a viral load level of 1 (undetectable viral load). For the same group of patients, there is an accelerated rate of transition from state 2 to state 3 (between 10 000 and 100 000 copies/mL). Non-adherence to treatment also causes an accelerated rebound of viral load from state 4 (between 100 000 and 500 000 copies/mL) to state 5 (viral load counts over 500 000 copies/mL). From all the states, the results also show an accelerated viral rebound for patients who developed some resistance to treatment, compared to those who did not. This is shown by very high positive values of β_{ij}'s for cases in which j is a worse state compared to i. Patients with peripheral neuropathy also have accelerated transition rates from state 2 to state 3. Although transition from state 2 to state 1 is accelerated, the rate is slower than that from state 2 to state 3. From the results, it can also be noted that having lactic acidosis (LA) accelerates transition from state 2 to state 3 more than either having peripheral neuropathy or non-adherence.

Patients who enrolled when their CD4 cell count was below 200 cells/mm^3 have higher transition rates from a viral load level between 10 000 and 100 000 copies/mL (state 3) to a viral load counts between 100 000 and 500 000 copies/mL (state 4). Having a viral load baseline level greater than 10 000 copies/mL at enrolment increases viral rebound from state 2 to state 3.

The different treatment combinations give precise estimates of the log-linear effects as shown by the confidence intervals that are narrow. Given the different combination therapy administered to patients, transitions to viral rebound are greater than transitions to viral suppression for patients with viral load states 2 and 3 (viral load counts between 50 and 100 000 copies/mL).

From the different combination therapy that was administered to the patients, d4T-3TC-EFV was the most frequently administered triple therapy with 889 cases, followed by AZT-3TC-EFV and d4T-3TC-NVP and AZT-3TC-NVP with 475, 431 and 279 cases, respectively. Table 6.6 shows the transition intensities for the different drug combinations.

Results from Table 6.6 show narrow confidence intervals for transition intensities from state 1 to 2 (rebound from undetectable viral load to a viral load between 50 and 10 000 copies/mL), state 2 to 6 (deaths from a viral load level between 50 and 10 000 copies/mL) and state 2 to 1 (transition from a viral load between 50 and 10 000 copies/mL to an undetectable viral load levels). This indicates that the continuous

Table 6.6: Transition intensities for various drug combinations on viral load states. (Confidence intervals are in brackets)

	Baseline	D1	D2	D3	D4	D5	D6	D7
q_{12}	0.493 (0.400,0.607)	0.607 (0.458,0.806)	0.515 (0.415,0.64)	0.438 (0.353,0.543)	0.371 (0.281,0.491)	0.315 (0.216,0.460)	0.268 (0.164,0.437)	0.227 (0.124,0.418)
q_{16}	0.001 (0.00004,30.57)	0.002 (0.0001,371)	0.001 (0.00006,26.32)	7.0×10^{-4} (0.00006,821)	0.0004 $(0, 1.7 \times 10^{6})$	2.0×10^{-4} $(0,9.8 \times 10^{9})$	1.1×10^{-4} $(0,8.1\times10^{13})$	5.7×10^{-5} $(0, 7.8 \times 10^{17})$
q_{21}	3.280 (2.82,3.812)	4.613 (3.802,5.596)	3.527 (3.027,4.11)	2.698 (2.289,3.180)	2.063 (1.656,2.57)	1.578 (1.174,2.12)	1.206 (0.83,1.763)	0.923 (0.578,1.472)
q_{23}	6.644 (1.788,24.68)	6.063 (1.422,25.86)	6.516 (1.774,23.92)	7.002 (1.642,29.86)	7.524 (1.21, 46.77)	8.085 (0.792,82.53)	8.688 (0.489,154.4)	9.336 (0.293,297.6)
q_{26}	0.392 (0.279,0.549)	0.452 (0.259,0.79)	0.404 (0.291,0.561)	0.361 (0.216,0.603)	0.322 (0.133,0.779)	0.288 (0.080,1.041)	0.257 (0.047,1.406)	0.230 (0.027,1.906)
q_{32}	38.175 (11.11,131.2)	39.309 (10.41,148.4)	38.414 (11.41,129.3)	37.54 (9.342,150.8)	36.686 (6.223,216.3)	35.85 (3.737,344.0)	35.04 (2.134,575.2)	34.24 (1.187,987.3)
q_{34}	3.161 (1.161,8.61)	2.510 (0.829,7.60)	3.009 (1.124,8.061)	3.608 (1.149,11.33)	4.327 (0.968,19.33)	5.188 (0.745,36.14)	6.220 (0.549,70.43)	7.458 (0.397,140.2)
q_{36}	0.010 (0.00005,212.1)	0.008 (0.00001,59.72)	0.010 (0.000001,681)	0.011 (0.0002,6700)	0.013 (0.0001,1508)	0.016 (0.0003,8987)	0.019 (0.0005,6690)	0.022 (0.0009,5419)
q_{43}	19.868 (10.22,38.61)	18.565 (10.41,33.12)	19.583 (10.73,35.75)	20.66 (8.413,50.72)	21.789 (5.987,79.31)	22.98 (4.128,128.0)	24.24 (2.809,209.2)	25.57 (1.900,344.3)
q_{45}	4.354 (0.513,36.90)	3.723 (0.893,15.53)	4.211 (0.679,26.127)	4.763 (0.209,108.3)	5.388 (0.053,545.4)	6.094 (0.0013,290.2)	6.893 (0.003,1578)	7.797 (0.0007,8679)
q_{46}	0.007 (0.00007,666.4)	0.006 (0.00002,1335)	0.007 (0.00006,710)	0.008 (0.000019 ,3109)	0.009 (0.00001,4305)	0.011 (0.00004,2594)	0.012 (0.00005,28,140)	0.015 (0.00005,4004)
q_{54}	17.711 (3.557,88.2)	10.764 (5.385,21.52)	15.926 (4.35,58.27)	23.56 (1.960,283.2)	34.860 (0.829,147)	51.58 (0.345,7711)	76.31 (0.143,4082)	112.9 (0.059,2168)
q_{56}	0.030 (0.0004,2199)	0.030 (0.0006,14,870)	0.030 (0.0004,2347)	0.030 (0.00004,2153)	0.029 (0.0006,15,210)	0.029 (0.0002,45,560)	0.028 (0.0004,22,650)	0.028 (0.00055,14,060)

Key: D1 = d4T-3TC-EFV, D2 = AZT-3TC-EFV, D3 = d4T-3TC-NVP, D4 = AZT-3TC-NVP, D5 = FTC-TDF-EFV, D6 = AZT-3TC-LPV/r, D7 = Other combinations

time Markov model for the different drug combinations predicts these transitions better, compared to all the other transitions. However, confidence intervals for the deaths from state 1, 3, 4 and 5 are very wide. This could be due to the smaller numbers of deaths for patients in this cohort. Highest rates of mortality are recorded for patients with viral load level between 50 and 10 000 copies/mL, but from all the other states mortality rates are very low.

Overall, the model shows higher transition rates to viral suppression compared to the transitions to viral rebound. For patients with a viral load between 10 000 and 100 000 copies/mL, drug combination d4T-3TC-EFV has the highest transition rates to recovery, followed by the triple combination AZT-3TC-EFV, d4T-3TC-NVP, AZT-3TC-NVP, FTC-TDF-EFV, AZT-3TC-LPV/r, respectively. When the viral load is still above 100 000 copies/mL, the triple combination AZT-3TC-LPV/r gives the best results, followed by FTC-TDF-EFV, AZT-3TC -NVP, d4T-3TC-NVP, d4T-3TC-EFV, d4T-3TC-NVP, AZT-3TC-EFV, in that order. However, for this cohort AZT-3TC-LPV/r was not frequently administered. For patients in state 2, viral rebound to state 3 is greater than viral suppression to undetectable levels and these rates of viral rebound are the highest for patients being administered with triple combinations AZT-3TC-LPV/r and FTC-TDF-EFV.

The Markov process in this study is characterised by successive periods of viral rebound and viral suppression. According to Jackson (2016), we may need to forecast the total time spent in each transient state s, before death. The *msm* function, *totlos.msm*, is used to estimate the total time spent in transient state s between two future time points t_1 and t_2. Jackson (2016) further argued that the defaults to the expected amount of time spent in each transient state s (that is, the state of being HIV infected) between the start of the process ($t = 0$, the present time) and death or a specified future time is obtained as:

$L_s = \int_0^t P(u)_{rs} du$

where $P(u)_{rs}$ is the probability of transition from state r to state s. The value of state r (the state at the start of the process) is by default set to be 1 (the undetectable viral load state). This is calculated using numerical integration. The results are given below.

State 1	*State 2*	*State 3*	*State 4*	*State 5*	*State 6*
18.530	*2.487*	*0.433*	*0.069*	*0.017*	*Infinity*

Thus, the patients are forecasted to spend approximately 18.5 years in a state of

undetectable viral load (state 1) and in the other states patients are expected to spend less than 2.5 years since these are temporal states. This is evidenced by the fact that throughout the 5 year study period, only 17.8% of the patients were reported dead, with 10.9 points occurring during the first 6 months.

6.3.3 Assessment of the fitted model

In order to assess the goodness of fit of the continuous time-homogeneous Markov model for the effects of covariates, the expected percentage prevalence is plotted against the observed percentage prevalence. The prevalence is averaged over the covariates observed in the data. The percentage prevalence is plotted as functions of time for each viral load state. Figures 6.2 and 6.3 show the prevalence plots for the effects of all covariates, including treatment therapy and the model for the effects of treatment therapy, respectively, for each state.

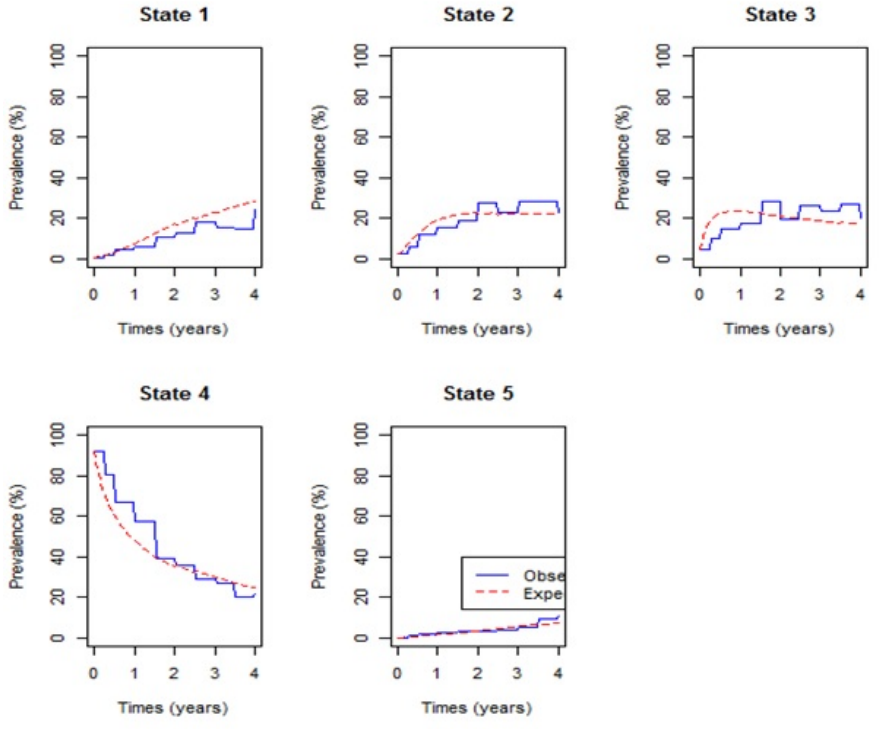

Figure 6.2 – *Comparison of the observed and expected percentage prevalence for the effects of Covariates on viral load levels. Prevalence is averaged over the covariates observed in the data, that is, viral load baseline (VLBL), CD4 baseline (CD4BL), age, non-adherence (NA), lactic acidosis (LA), peripheral neuropathy (PN), and triple therapy (Therapy).*

The results from the plots in Figure 6.2 show a perfect fit of the model to the observed data. In addition to that, the plots show that the percentage prevalence for state 1 increases rapidly in the first year. This shows that under normal treatment,

patients on anti-retroviral therapy attain an undetectable viral load in less than a year post-treatment commencement. For this same state, it also shows that the percentage prevalence becomes stable after a year. Although at $t = 0$ state 1 had the least percentage prevalence, from 1 year onwards, about 80% of the patients had attained an undetectable viral load (state 1). States 2 and 3 had the highest percentage prevalence at $t = 0$, however in less than 6 months of treatment uptake, the percentage prevalence had dropped (Figure 6.3).

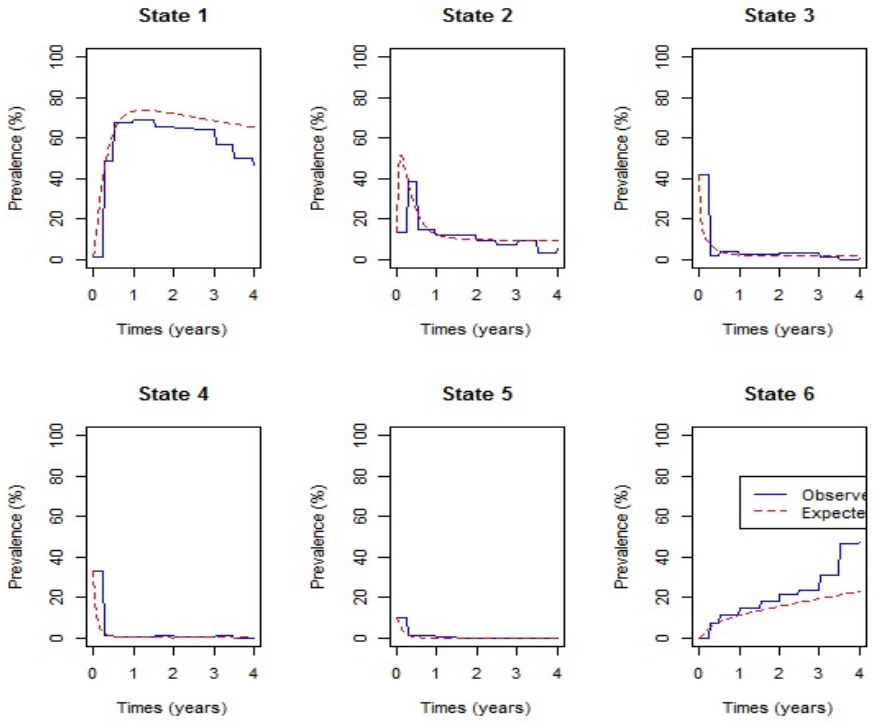

Figure 6.3 – *A comparison of the observed and expected percentage prevalence for the model with different combination therapy. Prevalence is averaged over the different combination therapies observed in the data, that is, D1 = d4T-3TC-EFV, D2 = AZT-3TC-EFV, D3 = d4T-3TC-NVP, D4 = AZT-3TC-NVP, D5 = FTC-TDF-EFV, D6 = AZT-3TC-LPV/r, D7 = Other combinations.*

Results from Figure 6.3 show that if we only consider the effects of treatment therapy without considering the effects of other covariates, the fitted model underestimates death prevalence as well as state 1 prevalence. A likelihood ratio test is also used to compare the fitted models, that is, model without covariates (A), model with all covariates except combination therapy (C), model with all the covariates including the combination therapy (D) and the model for the combination therapy only (B). The results from the likelihood ratio tests and the log-likelihoods of the preferred models are shown below.

Table 6.7: Likelihood ratio tests for the comparison of the fitted models and the -2xLog(likelihood) (-2LL) for the preferred model.

Models Tested	Preferred Model	-2 log LR	df	p	$-2 \times LL$
A and B	B	66.97594	13	< 0.0001	2635. 207
A and C	C	970.1007	78	< 0.0001	1732.082
B and C	C	903.1247	65	< 0.0001	1732.082
C and D	D	40.90497	13	< 0.0001	1691.177

Key: A= model witout covariates; B= model with combination therapy only; C= model with all covariates excluding therapy; D=model with all covariates including combination therapy only

Results from Table 6.7 show that the model with all covariates including the combination therapy, is the best model for this data. This model has the lowest -2xLog(likelihood) (equal to 1691.177) and also the results from the likelihood ratio test are in favour of the model with covariates including combination therapy.

A further assessment of the fitted models is done using the Akaike Information Criteria (AIC). For each model, $AIC = -2 \times log(likelihood) + 2(k)$ where k is the number of parameters in the model. For example, the model with covariates excluding the combination therapy (VLS3.cov.msm) has 26 degrees of freedom and $-2 \times log(likelihood) = 2635.207$, thus, $AIC = 2635.207 + 2 \times 26 = 2687.207$ as shown in Table 6.8 below. The model with the smallest AIC is considered the most efficient for the data. The results are shown in Table 6.8 below.

Table 6.8: AICs for the fitted models.

Model	A	B	C	D
AIC	2728.183	2687.207	1914.082	1899.177

Key: A= model witout covariates; B= model with combination therapy only; C= model with all covariates excluding therapy; D=model with all covariates including combination therapy only

Results from Table 6.8 show that the model with covariates has the smallest AIC. This confirms the results obtained from Table 6.7, that the time-homogeneous Markov model with covariates is the most efficient.

6.4 Concluding Remarks

This chapter developed a continuous-time homogeneous Markov model to assess the effects of adherence to treatment, development of drug toxicity in the form of peripheral neuropathy and lactic acidosis, change in treatment therapy, gender, age, CD4 baseline and viral load baseline and resistance to treatment on transition intensities.

This chapter reveals the major attributes to viral rebound on HIV+ patients, which is notable as patients attain a viral load counts between 50 and 10 000 copies/μL. The major attributes were non-adherence, lactic acid, resistance to treatment, and different combination therapy such as AZT-3TC-LPV/r and FTC-TDF-EFV. However, assuming that the patient was initially in state 1 (the undetectable viral load state) the HIV-infected patient is expected to spend approximately 18.5 years in state 1 before death. This is evidenced by the fact that throughout the 5 year study period only 17.8% of the patients were reported dead, with 10.9 points occurring during the first 6 months.

Before initiation of treatment, patients should be well equipped with information on how anti-retroviral drugs operate, including possibilities of toxicity, in order to reduce chances of non-adherence to treatment. There should also be a good relationship between patient and health-care-giver, to ensure proper adherence to treatment. Uptake of therapy by young patients should be closely monitored by adopting pill counting every time they come for review.

Although the models based on viral load counts monitoring are very good at detecting virologic failure, these models have a weakness of failure to explain mortality of HIV/AIDS patients. In order to come up with a model that guides decision making, a CD4 cell count based model is compared with the viral load count based model in the next chapter. This is done in order to assess the superiority of viral loads monitoring over CD4 cell counts monitoring.

Chapter 7

A superiority of viral load over CD4 cell count when predicting mortality in HIV patients on therapy

7.1 Introduction

CD4 cell count has been deemed an essential component of HIV treatment and care programmes since HIV was identified as a disease compromising the immune system (Ford et al., 2017). Although the World Health Organisation (WHO) has recommended a shift to HIV RNA in monitoring ART, it continues to emphasise CD4 cell count's importance in evaluating disease status at baseline and appropriate care for patients with advanced stages of HIV progression (Ford et al., 2017).

HIV RNA monitoring is most useful in measuring effectiveness of ART in suppressing replication of the virus (UNAIDS, 2016). Some researchers argue that lack of HIV RNA monitoring leads to delayed and unnecessary switches to second line therapy, resulting in development of resistance to treatment and limitations to treatment options (Salazar-Vizcaya et al., 2014). HIV RNA appears to be the best predictor of long-term clinical outcome, whereas CD4 cell count predicts clinical progression and survival in the shorter term (Erb et al., 2000). Brennan et al. (2013), in their research to determine the interplay between CD4 cell count and viral load, further argue that long-term virological suppression plays an important role in ensuring the recovery of CD4 cell count to levels that reduce the risk of opportunistic infection and increase life expectancy.

In the year 2000 there were uncertainties regarding the best use of either CD4 cell count or viral load markers in controlled trials (Erb et al., 2000). Thereafter, attempts have been made by different researchers to try and address these uncertainties. Some of these studies used Cox proportional hazard model and Kaplan Meier curves (Brown et al., 2009; Phillips et al., 2001). Another study to establish the interplay between CD4 cell count, viral load suppression and duration of ART on mortality in a resource limited setting, was carried out using a log-linear model with the Poisson distribution (Miller et al., 2002; Brennan et al., 2013). However, results from these studies were contradictory. Some of the studies show that CD4 cell count monitoring is the best for predicting HIV/AIDS progression (Miller et al., 2002; Brown et al., 2009; Salazar-Vizcaya et al., 2014) while other studies show that viral load monitoring is the best predictor (Hoffman et al., 2010).

Where HIV RNA tests were done, the results cannot be quite reliable due to the highest percentages of missing data caused by limited resources (Hoffman et al., 2010). As a result, some researchers resorted to the use of computer simulated data because HIV RNA tests are very expensive to measure, especially in Southern Africa (Salazar-Vizcaya et al., 2014). In this chapter, data on viral load counts and CD4 cell count monitoring is used. A stochastic Markov approach to multistate modelling is used to investigate the uncertainties regarding the use of viral load counts and CD4 cell count monitoring of HIV/AIDS progression. Multistate modelling is a powerful tool for studying chronic diseases and estimating factors associated with transitions between each stage of progression (Vasconcellos et al., 2013).

In the section that follows, methods used in analysing the data are explained. This is followed by section 7.3, on results and discussions. Lastly, in section 7.4, conclusions of the findings are made.

7.2 Data Description

The data used in this chapter is described in Chapter 3. However, in this chapter, either routinely collected data on CD4 cell count or viral load count is used in fitting continuous-time Markov models. The viral load count states are divided into 5 transient states, and the sixth state being the absorbing state, death. The CD4 cell count states are divided into 4 transient states, and the fifth state is the death state. Change of treatment line was based on treatment failure, toxicity, patient intolerance to the combination therapy or inability of the patient to adhere to treatment and viral rebound. From these patients, 36 showed some signs of non-adherence to treatment.

The viral load states, CD4 cell count states and other factors: age, non-adherence, CD4 cell count at baseline, gender and viral load at baseline, that are likely to determine change in viral load/CD4 cell count levels, are explored. CD4 cell count states and viral load states for the purpose of analysis are coded as follows:

$$CD4\ cell\ count\ levels\ (X_c(t)) = \begin{cases} 1; & CD4 > 800 \\ 2; & 500 < CD4 \leq 800 \\ 3; & 350 < CD4 \leq 500 \\ 4; & CD4 < 350 \\ 5; & Death. \end{cases}$$

$$Viral\ load\ levels\ (X_v(t)) = \begin{cases} 1; & VL < 50 \\ 2; & 50 \leq VL < 10\,000 \\ 3; & 10\,000 \leq VL < 100\,000 \\ 4; & 100\,000 \leq VL < 500\,000 \\ 5; & VL \geq 500\,000 \\ 6; & Dead. \end{cases}$$

For HIV progression based on viral load, the diagram showing possible transitions between states is shown in Example 3 of Chapter 3. The likelihood estimates of the model parameters are also shown in Chapter 3.
In Figure 7.1 below, the possible transitions for the model in which progression is based on CD4 cell count are shown.

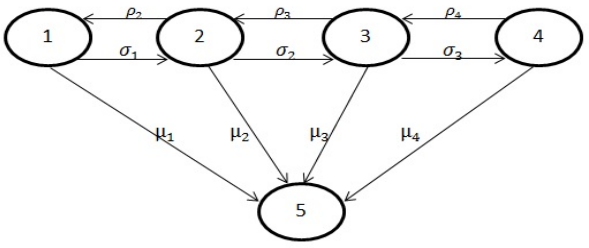

Figure 7.1 – *The State Diagram for HIV Progression based on CD4 cell count for Individuals on ART*

Observations in Figure 7.1 take the form $s_w = n_{w,w+1}$, rate of viral rebound from state w to $w+1$ or birth of viral particles; $r_w = n_{w,w-1}$ rate of viral suppression from state w or death of viral particles; $d_w = n_{w,5}$ the rate of absorption from w to death of an infected person; and T_w the total time spent in state w. Then the likelihood

function for the parameters; ρ_w, μ_w and σ_w. Estimation of the transition intensities is done using the method of maximum likelihood to estimate the transition intensities. The likelihood, L, based on Equation (3.43) and Figure 7.1 is given by:

1. Remaining in state w:

$$\exp\{-\sum_{w=1}^{4}(\rho_w+\mu_w+\sigma_w)T_w-\rho_1T_1-\sigma_4T_4\}$$

   ρ_1T_1 and σ_4T_4 are subtracted since they are missing from the first and last terms, respectively, of the transient states. This means that there is no possibility of transitions from w to $w-1$ if $w=1$ and there is no possibility of a further immune deterioration (i.e transition from w to $w+1$), if $w=4$, $w+1$ becomes the absorbing state representing the DEATH state.

2. Entering state $w+1$. The likelihood becomes:

$$\exp\{-\sum_{w=1}^{4}(\rho_w+\mu_w+\sigma_w+\alpha_w)T_w-\rho_1T_1-\sigma_4T_4\}\Pi_{w=1}^{3}\sigma_w^{s_w}$$

3. Entering state $w-1$. The likelihood becomes:

$$\exp\{-\sum_{w=1}^{4}(\rho_w+\mu_w+\sigma_w+\alpha_w)T_w-\rho_1T_1-\sigma_4T_4\}\Pi_{w=2}^{4}\rho_w^{r_w}$$

4. Entering state 5 (DEATH state). The likelihood becomes:

$$\exp\{-\sum_{w=1}^{4}(\rho_w+\mu_w+\sigma_w+)T_w-\rho_1T_1-\sigma_4T_4\}\Pi_{w=1}^{4}\mu_w^{d_w}$$

The components can be put together and the likelihood would be written as:

$$L = \exp\{-\sum_{w=1}^{4}(\rho_w+\mu_w+\sigma_w)T_w-\rho_1T_1-\sigma_4T_4\}\Pi_{w=1}^{3}\sigma_w^{s_w}\Pi_{w=2}^{4}\rho_w^{r_w}\Pi_{w=1}^{4}\mu_w^{d_w} \tag{7.1}$$

The maximum likelihood estimates are:

$$\hat{\mu}_w = \frac{d_w}{T_w}, \quad \hat{\sigma}_w = \frac{s_w}{T_w}, \quad \hat{\rho}_w = \frac{r_w}{T_w} \tag{7.2}$$

The effects of the categorical variables on the time-dependent variables is assessed using the Markov models:

$$q_{ij(CD4)} = q^{(0)}_{ij(CD4)} exp\left(\beta^{(Age)}_{ij} Age_x + \beta^{(Gender)}_{ij} Gender_x + \beta^{(VLBL)}_{ij} VLBL_x + \beta^{(CD4BL)}_{ij} CD4BL_x + \beta^{(NA)}_{ij} NA_x\right)$$

and

$$q_{ij(VL)} = q^{(0)}_{ij(VL)} exp\left(\beta^{(Age)}_{ij} Age_x + \beta^{(Gender)}_{ij} Gender_x + \beta^{(VLBL)}_{ij} VLBL_x + \beta^{(CD4BL)}_{ij} CD4BL_x + \beta^{(NA)}_{ij} NA_x\right)$$

for CD4 cell count levels and viral load levels, respectively. $q^{(0)}_{ij(CD4)}$ and $q^{(0)}_{ij(VL)}$ are the baseline transition intensities for CD4 cell count states and viral load states respectively. β_{ij} is the log-linear effects of the mentioned covariate on the baseline transition intensities $q^{(0)}_{ij}$.

7.3 Results

The observed prevalence for each of the variables CD4 cell count and viral load were computed in R using the "msm" package for multistate modelling. The observed prevalence are calculated for each CD4 state and viral load state from initiation of treatment ($t = 0$ years) to time equals 4 years. The comparison is based on the transient states for both CD4 cell count and viral load levels. However, since viral load states are more than CD4 cell count states, viral load state 4 and state 5 are combined so that we have an equal number of transient states for both variables. The results are shown in Figure 7.2 below.

Results from Figure 7.2 above show an increase in the number of patients who had their viral load suppressed/undetectable in the first six months of treatment uptake. The plotted figures are also shown at the bottom of each graph. From six months onwards, the number of individuals with suppressed viral load started to decrease. This could be caused by loss of viral suppression, or deaths. The number of patients with CD4 cell count above 800 (CD4 cell count state=1) increases slowly with time. Maartens et al. (2014) also indicated that within 3 months of ART, the plasma viral load decreases to concentrations below the lower limit of detection of available commercial assays in most people. The lower limit for this particular study is 50

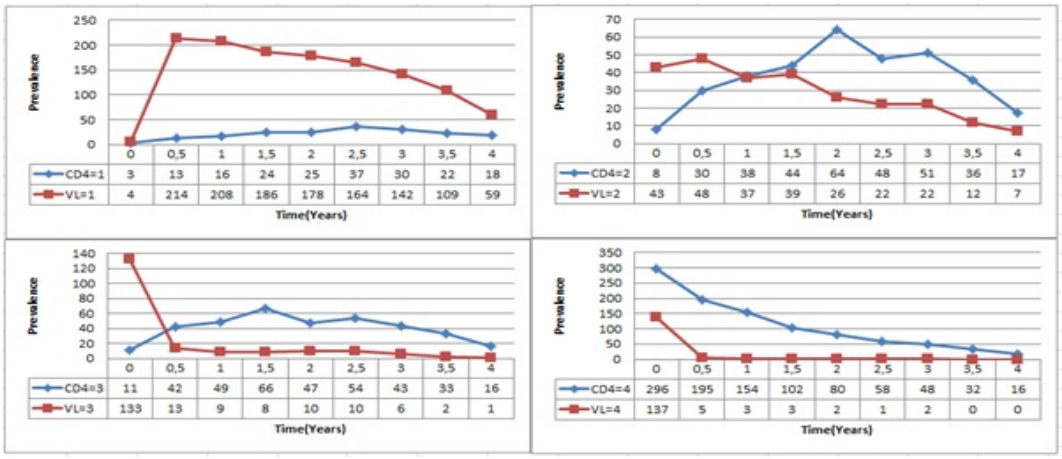

Figure 7.2 – *Comparison of CD4 and Viral load prevalence 4 years post commencement of therapy(Original)*

copies/mL.

From the results, it can also be noted that upon initiation of treatment, the majority of the patients had a viral load state equal to 3, which is associated with between 10 000 and 100 000 copies/mL. After 6 months of ART, the number of patients in this category dropped from 133 to 13, and continued to decrease throughout the study period. The highest number of patients were in the CD4 cell count category 4 which is defined by a CD4 cell count below 350 cells/mm^3. The number of patients in this state continued to decrease throughout the period but at a slower rate than that of viral load levels.

7.3.1 Effects of CD4 levels on Viral load transition intensities

In this sub-section, analysis of the effects of CD4 cell count levels on transition intensities defined by viral load levels is defined by the equation:
$q_{ij(VL)} = q_{ij}^{(0)} \exp(\beta_{ij} \times CD4_c)$
where $q_{ij(VL)}$ is the transition intensity matrix for $i = 1, \ldots, 5$ transient states defined by viral load levels in the plasma cells and $j = 1, \ldots, 6$; β_{ij} is the log-linear effect of CD4 cell count level on the transition intensity $\alpha_{ij(VL)}$ and $c = 1, \ldots, 4$ defines the different levels of CD4 cell count. For this model, transition from i to j where $i > j$ is defined as viral suppression and if $i < j$ it is defined as viral rebound. The values of c define the patient's immunology, such that large values of c are associated with immune deterioration while smaller values of c are associated with immune recovery. $q_{ij}^{(0)}$ is the baseline transition intensity from i to j . The results are shown in Table 7.1 below.

Table 7.1: Effects of changes in CD4 cell count levels on viral load transition intensities

	Baseline	Log-linear	Hazard	CD4L			
q_{ij}	$q_{ij}^{(0)}$	β_{ij}		$c=1$	$c=2$	$c=3$	$c=4$
q_{12}	0.468	0. 245	1. 278	0.269	0.343	0.438	0.560
q_{16}	0.017	0.073	1.076	0.014	0.016	0.017	0.018
q_{21}	3.186	0.061	1.063	2.764	2.943	3.133	3.335
q_{23}	5.659	0.892	2.440	0.788	1.878	4.477	10.673
q_{26}	0.139	1.564	4.778	0.004	0.020	0.092	0.422
q_{32}	30.453	0.868	2.383	4.466	10.405	24. 242	56.481
q_{34}	3.149	-0.0002	0.999	3.177	3.164	3.152	3.140
q_{36}	0.007	-0.144	0.866	0.013	0.010	0.008	0.006
q_{43}	16.964	0.538	1.712	5.056	8.618	14.691	25.044
q_{45}	2. 261	1. 275	3.579	0.118	0.434	1.592	5.844
q_{46}	0.010	-1.728	0.178	0.696	0.106	0.016	0.002
q_{54}	6.5322	1.021	2.776	0.613	1.739	4.931	13.985
q_{56}	0.045	-2.530	0.080	23.735	1.501	0.095	0.006
$-2 \times LL$	2665. 285						

q_{ij}=transition intensities; $q_{ij}^{(0)}$=baseline transition intensities; β_{ij} =log-linear effects; Hazard= hazard ratios; CD4L= CD4 cell count transient states; $-2 \times LL =$ likelihood ratio test

Results from Table 7.1 above show that the rates of viral suppression are higher than the rates of viral rebound for HIV+ patients in state 3 (viral load ranging from 10 000 to below 100 000 copies/mL), state 4 (viral load level ranging from 100 000 to below 500 000 copies/mL) and state 5 (viral load level above 500 000 copies/mL). If a patient is in a viral load level suppressed to state 2 (from 50 to below 10 000 copies/mL), the rates of viral rebound to state 3 are higher than the rates of viral suppression to state 1.

For the viral rebound from state 1 (undetectable viral load) to state 2, the log-linear effect of CD4 cell count level is positive. This indicates that viral rebound from the undetectable level increases as the immune system deteriorates. The increase in transition intensities from 0.2685 at $c = 1$ to 0.5595 at $c = 4$ confirms this result. Although the log-linear effects of CD4 cell count levels on viral rebound and viral suppression from state 2 are both positive, the effect on viral rebound is higher and this also increases as the immune system deteriorates. This means that a patient can reach a suppressed viral load, yet the immune system is still compromised.

The results also show that when the viral load level is 3 and above (viral load level of 10 000 copies/mL and above) mortality rates decrease with immune deterioration and when the viral load level is below 10 000 copies/mL mortality rates increase with immune deterioration. This means that: during the early phases of treatment uptake, when the viral load levels are high and the CD4 cell count levels are still low, there are less chances of death. It is most likely that deaths are caused by viral rebounds due to the compromised immune system.

7.3.2 Effects of viral load levels on CD4 cell count transition intensities

In this sub-section, analysis of the effects of viral load levels on transition intensities defined by CD4 cell count as defined by the equation is done:

$$q_{ij(CD4)} = q_{ij}^{(0)} \exp\left(\beta_{ij} \times VL_v\right)$$

where $q_{ij(CD4)}$ is the transition intensity matrix for $i = 1, \ldots, 4$ transient states defined by CD4 cell count levels and $j = 1, \ldots, 5$, β_{ij} is the log-linear effect of viral load level on the transition intensity $\alpha_{ij(CD4)}$, $v = 1, \ldots, 5$ defines the different levels of viral load. For this model transition where $i > j$ is defined as immune recovery and if $i < j$, it is defined as immune deterioration. The values of v define the patient's virology, such that large values of v are associated with high level of viral load and smaller values of v are associated with suppressed viral load. The results are shown in Table 7.2 below.

Table 7.2: Effects of changes in viral load levels on CD4 cell count transition intensities

	Baseline	Log-linear	Hazard	VL				
q_{ij}	$q_{ij}^{(0)}$	β_{ij}		v=1	v=2	v=3	v=4	v=5
q_{12}	0. 290	-1.415	0. 243	0.716	0.174	0.042	0.010	0.003
q_{15}	0.024	1.279	3.592	0.011	0.038	0.137	0.492	1.767
q_{21}	0.612	0.022	1.027	0.602	0.618	0.635	0.652	0.669
q_{23}	0.843	0. 212	1.236	0.736	0.910	1.125	1.391	1.720
q_{25}	0.004	1.547	4.699	0.002	0.008	0.036	0.168	0.791
q_{32}	1.397	0.201	1.223	1.229	1.502	1.837	2.246	2.745
q_{34}	0.720	0.273	1.314	0.605	0.795	1.044	1.372	1.802
q_{35}	0.128	1.051	2.859	0.065	0.187	0.533	1.524	4.358
q_{43}	0.743	0.023	1.023	0.732	0.749	0.767	0.785	0.803
q_{45}	0.057	0.573	1.774	0.039	0.070	0.124	0.220	0.389
$-2 \times LL$	3308.126							

VL= viral load levels q_{ij} =transition intensities from state i to state j; $q_{ij}^{(0)}$ =baseline transition intensities; β_{ij} =log-linear effects; Hazard= hazard ratios; $-2 \times LL$ = likelihood ratio test.

The results from Table 7.2 show that the rates of immune deterioration are lower than the rates of immune recovery when a patient's CD4 cell count is 500 cells/mm^3 and below (state 3 and state 4). When the CD4 cell count levels are above 500 cells/mm^3 (states 1 and 2), rates of immune deterioration are higher than rates of immune recovery. This is an indication that upon reaching the safe immunological levels, there are certain factors that compromise the immune system. There is need to further investigate the cause.

The negative log-linear effect of viral load levels on the transition from state 1 (CD4 cell count above 800) to state 2 (CD4 cell count more than 500 but less or equal to

800 cells/mm^3) indicates a reduction of immune deterioration from state 1 to state 2 as the levels of viral load in the plasma increase. Mortality rates from all the states are increasing as the viral load levels increase. The highest transitions to death are recorded for patients with viral load levels above 500 000 copies/mL (state 5).

7.3.3 Effects of covariates on CD4 cell count and viral load levels

Effects of covariates Age, Gender, VL baseline (VLBL), CD4 baseline (CD4BL), Non-adherence to treatment (NA) on HIV/AIDS progression defined by the time-dependent variables, CD4 levels or viral load levels, are assessed in this section. The models for the effects of covariates on transition intensities defined by CD4 cell count and viral load are:

$$\begin{aligned} q_{ij(CD4)} &= q^{(0)}_{ij(CD4)} \exp(\beta^{(Age)}_{ij} Age_x + \beta^{(Gender)}_{ij} Gender_x + \beta^{(VLBL)}_{ij} VLBL_x \\ &+ \beta^{(CD4BL)}_{ij} CD4BL_x + \beta^{(NA)}_{ij} NA_x) \end{aligned}$$

and

$$\begin{aligned} q_{ij(VL)} &= q^{(0)}_{ij(VL)} \exp(\beta^{(Age)}_{ij} Age_x + \beta^{(Gender)}_{ij} Gender_x + \beta^{(VLBL)}_{ij} VLBL_x \\ &+ \beta^{(CD4BL)}_{ij} CD4BL_x + \beta^{(NA)}_{ij} NA_x) \end{aligned}$$

respectively. β_{ij} is the log-linear effects of the mentioned covariate on the baseline transition intensities $q^{(0)}_{ij}$.
The results showed that there is no gender variation on the progression of HIV based on viral load levels. This means that change in viral load levels is uniform for both males and females. However, given the time-dependent variable CD4 cell count, the effects of gender is quite significant. Thus, in Table 7.3 below, the effect of gender is only indicated for CD4 cell count levels.

Results from Table 7.3 above show that, for patients in the disease state 2, defined either by CD4 cell count levels or viral load levels, the rates of disease progression to state 3 are higher than the rates of recovery from state 2 to state 1. However, the rate of viral rebound is far much higher than the rate of immune deterioration for patients in state 2.

The results also show a reduction in viral load suppression from state 2 to state 1 and an increased viral rebound from state 2 to state 3 for patients who are 45 years and

Table 7.3: Log-linear effects of age, viral load baseline, CD4 cell count at baseline, gender and non-adherence on baseline transition intensities for CD4 cell count and viral load stages

State	$q_{ij}^{(0)}$		Age		VLBL		CD4BL		Gender	NA	
$i;j$	CD4	VL	CD4	VL	CD4	VL	CD4	VL	CD4	CD4	VL
1;2	0.737	0.496	-1.327	-0.148	-0.144	0.115	-0.464	-0.097	-0.289	-0.232	0.219
1;D	0.0003	0.0001	-0.747	4.495	1.172	3.416	0.916	3.581	0.566	-0.015	4.432
2;1	0.570	4.025	0.344	-0.437	-0.183	-0.370	-0.336	0.326	0.106	0.706	-1.305
2;3	0.752	6.068	-0.093	0.486	0.430	2.433	-0.048	-2.827	0.887	0.969	3.275
2;D	0.003	0.006	4.392	-1.541	4.137	3.473	-0.031	5.259	1.833	-2.219	-5.084
3;2	1.283	62.87	0.286	0.0611	-0.162	0.853	-0.588	-2.978	0.114	0.122	1.926
3;4	0.705	0.208	0.023	5.533	-0.177	1.127	-0.460	5.715	-0.504	0.683	-0.223
3;D	0.0001	0.0008	3.021	-0.283	2.013	-0.369	2.287	0.154	-3.979	5.187	-1.536
4;3	0.792	40.77	0.022	0.483	0.382	-2.688	-1.432	0.802	-0.536	-0.346	-0.734
4;5	0.0005	0.580	-2.012	1.082	3.601	0.789	3.333	-2.222	-5.888	-4.042	4.806
4;6		0.002		0.061		-0.551		-0.420			-0.798
5;4		100.5		-5.066		-1.192		2.105			1.070
5;6		0.040		0.264		1.821		-3.429			-2.092
$-2LL$	2595.89	1767.02									

D=death; Age=1 if ≤ 45 years and 0 otherwise; VLBL=viral load baseline =1 if > 10000copies$/mL$ and 0 otherwise; CD4BL=CD4 cell count at baseline = 1 if ≤ 200 cells/mm^3 and 0 otherwise; Gender= 1 if "male" and 0 if "female"; Non-adherence =1 if "yes" and 0 if "no"; $-2 \times LL =$ likelihood ratio test.

below, compared to those patients over 45 years. The opposite is true when it comes to changes in CD4 cell count levels. These patients, who are 45 years and below, portray an increased immune recovery from state 2 to state 1 and a reduced immune suppression from state 2 to state 3. This means that although young patients experience some challenges in viral load suppression, they have higher chances of cell regeneration than their older counterparts.

Patients who initiated treatment with a viral load baseline above 10 000 copies$/mL$ experience an increased viral rebound and also an increased immune deterioration from state 2 to state 3, and a reduced viral suppression and immune recovery from state 2 to state 1. However, it is interesting to note that if the patient's CD4 cell count at treatment initiation is 200 cells/mm^3 and below, there is increased viral load suppression from state 2 to state 1, and a decreased viral rebound from state 2 to state 3. This emphasises the need for initiation of treatment when the CD4 cell count is low to reduce the chances of reaction to treatment that are associated with long-term treatment uptake.

Patients with non-adherence to treatment have increased viral rebound from state 2 to state 3 and a decreased viral suppression from state 2 to state 1. Non-adherence also causes an increased immune deterioration from state 2 to state 3. This also leads to an increased death rate from a CD4 cell count state of 3. In general, given that a

patient is non-adherent to treatment, there are increased rates of disease progression than recovery.

The results also show that deaths from viral load state 1 (undetectable viral load) are higher for younger patients below the age group of 45 years than their older counterparts. However, for patients who now have normal CD4 cell count, transitions to death are lower in younger patients than older patients. For these younger patients, more deaths are prominent from a CD4 cell count state 2 and 3, compared to the older patients. For younger patients in viral load levels 2 and 3, the opposite is true since lower transitions to death are observed from this data set, compared to the older patients. Thus, although HIV/AIDS patients take a longer time to reach a normal CD4 cell count level than the time taken to reach a suppressed viral load, once a normal CD4 cell count is reached, mortality risks are reduced.

Patients who initially had a viral load baseline of more than 10 000 copies/mL experience higher transitions to death from almost all viral load states, except state 4, and the highest transition to death are noted from state 2. For these individuals with initial viral load baseline above 10 000 copies/mL, the same trend is also notable from all the CD4 cell count states.

Patients with suppressed viral load level who developed some negative reaction to treatment (non-adherent to treatment) show higher transitions to death compared to patients who did not develop any form of negative reaction to treatment.

In the next subsection, prevalence plots for the two Markov models, one in which CD4 cell count is used as a marker of HIV/AIDS progression and the other in which viral load level is used as the marker of the disease progression, are compared. The likelihood ratio test is also used to assess the fitted models.

7.3.4 Assessment of the fitted models

Assessment of the fitted models is done by comparing the expected to the observed percentage prevalence. In Figure 7.3 below, the comparison is based on CD4 cell count monitoring.
Figure 7.3 shows that at treatment initiation, more than 90% of the patients had a CD4 cell count below 200 cells/mm^3 (state 4). As the time on treatment increases, the percentage prevalence for the patients in 4 decreases exponentially to close to 20% after 4 years of treatment administration. For CD4 states 1, 2 and 3, the percentage prevalence at initiation was close to 0% and increased exponentially to more than

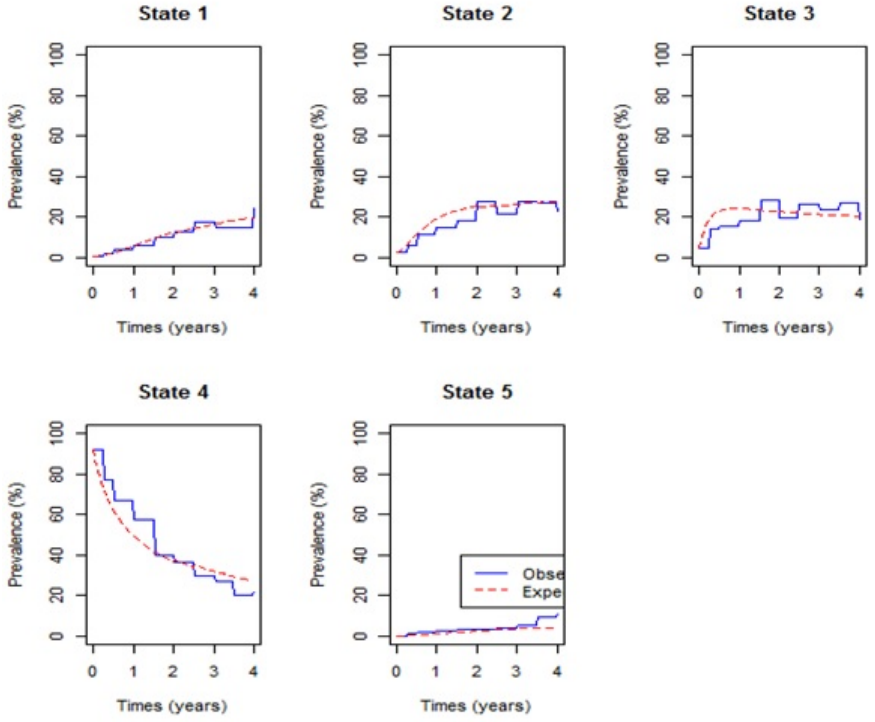

Figure 7.3 – *Percentage prevalence plot for the covariate on HIV/AIDS progression defined by CD4 cell count (Original)*

20% in state 2 and 3 after 2 years of treatment, and slightly above 10% for state 1. Thereafter, the percentage prevalence for all the three states started to decrease, but at a slow rate. Death prevalence increases from 0% to approximately 10% in the first 4 years of treatment uptake. In Figure 7.4 below, comparison of the expected percentage prevalence with the observed percentage prevalence is based on viral load levels.

Figure 7.4 shows that upon initiation of treatment more than 40% of the patients were in viral load state 3. This state had the highest percentage prevalence at start of therapy administration followed by state 4 which had close to 33%. Close to 0% of the patients had undetectable viral load levels (state 1) and this increased at a fast rate to approximately 80% after 1 year of treatment up take. After 1.5 years the percentage prevalence for state 1 became stable, with a slight up and down trend. This could be due to viral rebound or deaths.

The model for viral load states shows a perfect fit for all the states. The model for CD4 cell count states shows a perfect fit only for state 1 percentage prevalence. For state 2 and 3, it overestimates the observed prevalence in the first 2 years of treat-

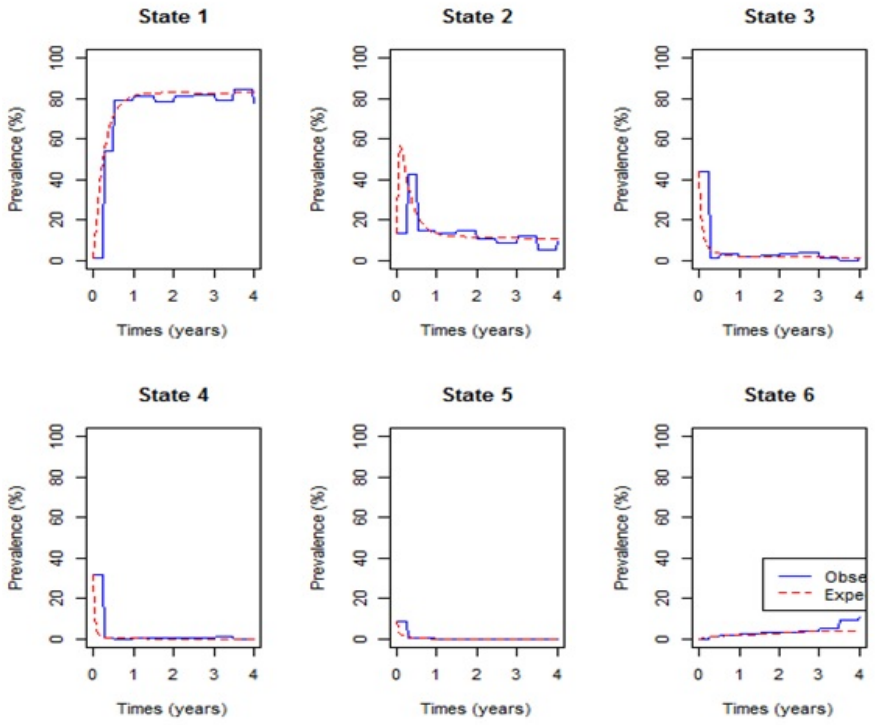

Figure 7.4 – *Percentage prevalence plot for the covariate on HIV/AIDS progression defined by Viral load (Original)*

ment and for state 4, it underestimates the observed in the first 1 and half years of treatment uptake. The fitted model for CD4 cell count states shown in Figure 7.3, underestimates the observed death percentage prevalence slightly for the first 3 and half years and the margin become wider afterwards. In Figure 7.4, the model for viral load states shows a perfect fit of the expected and observed death prevalence in the first 3 and half years, but afterwards it underestimates the observed death prevalence. Thus, the fitted model for viral load states predicts mortality better than the model fitted for CD4 cell count states. This shows that progression of HIV/AIDS for patients on treatment is better explained by the change in viral load levels than the change in CD4 cell count levels.

A likelihood ratio test was also performed to compare HIV/AIDS progression based on CD4 cell count monitoring with progression based on viral load monitoring. The results yield a p-value of 10^{-4} in favour of the Markov model based on viral load monitoring. This, again, confirms that viral load count monitoring is a better marker of HIV/AIDS progression, better than CD4 cell count monitoring. The results are shown below.

Table 7.4: Likelihood ratio test for the superiority of viral load levels monitoring over CD4 cell count monitoring

	$-2 \times logLR$	df	p-value
Viral load-based model	828.869	5	10^{-4}

7.4 Concluding Remarks

The aim of this chapter was to assess the use of the time-dependent variables CD4 cell count and viral load change, in monitoring HIV/AIDS progression on patients receiving anti-retroviral therapy. Effects of covariates such as gender, age, CD4 cell count at baseline, viral load counts at baseline, and non-adherence to treatment, are also considered.

Although viral load monitoring in predicting HIV/AIDS progression gives the clients a measure of understanding, control and motivation to adhere to treatment and understanding their HIV infection (WHO, 2017), basing on the findings, it is recommend to use both viral load levels monitoring, and CD4 cell count monitoring, since viral load level determines the need for treatment change and CD4 cell count helps in monitoring the risk of opportunistic infection (OI) and treatment failure. From this study, one can also conclude that although patients take more time to achieve a normal CD4 cell count and less time to achieve an undetectable viral load level, once the CD4 cell count is normal, mortality risks are reduced. Therefore, both viral load levels monitoring and CD4 cell count monitoring can be used to contribute significantly to the improvement in the life expectancy of patients living with HIV.

However, in this chapter separate time-homogeneous Markov models for either CD4 cell monitoring or viral load levels monitoring where fitted. In the next chapter, a principal component of viral load counts is constructed and included in the continuous-time homogeneous Markov model based on CD4 cell count states, to account for the aspect of mortality which can not be explained by CD4 cell count alone.

Chapter 8

A Markov Model to estimate Mortality due to HIV/AIDS using CD4 cell counts based states and viral load: A Principal Component Analysis approach

8.1 Introduction

Combination anti-retroviral therapy (cART) reduces viral load counts of circulating HIV by blocking replication at multiple points in the virus life cycle (Cole et al., 2007), resulting in an increase in CD4 cell counts and increased life expectancy of individuals infected with HIV. This has made CD4 cell counts and viral load counts the fundamental laboratory markers regularly used for patient management (Mathieu et al., 2007) in addition to predicting HIV/AIDS disease progression or treatment outcomes (Hoffman et al., 2010).

However, although the primary predictor of HIV transmission is the HIV viral load, very few HIV modelling studies include a detailed description of the dynamics of HIV viral load along stages of HIV diseases progression (Case et al., 2012; Herbeck et al., 2014). This could be due to the unavailability of data on viral load counts, particularly from low and middle income countries that have historically relied on monitoring CD4 cell counts for patients on cART, because of higher costs of viral load count testing (Lecher et al., 2016). However, sometimes both CD4 cell counts and viral load information are available. Estill et al. (2012) investigated the benefits

of viral load count routine monitoring for reducing HIV transmission. They developed a stochastic mathematical model representing 1000 simulations for both CD4 cell counts and viral load levels routine monitoring. Their findings revealed that viral load routine monitoring reduces both cohort viral load and transmissions by 31%.

Goshu et al. (2013) used a semi-Markov process to model the progression of HIV/AIDS. They used five CD4 cell counts classified states. They found out that transition probabilities from a given state to the next worse state increase with time, get to an optimum level at a given time and then decrease with increasing time. In a recent research, Osisiogu and Nwosu (2012) also used the same states as Goshu et al. (2013). However, they used a non-stationary Markov chain approach. They examined a Nigerian cohort from Nnamdi Azikiwe University Teaching Hospital with a follow-up in their CD4 cell counts of the HIV/AIDS patients. Their main finding was that low CD4 cell counts do not generally imply faster rates of patient absorption, but, rather, the age of the patient is a relevant factor.

Lee et al. (2014) investigated the most vulnerable racial minority races (African Americans) in the United States and the Caucasians in order to predict the trends of the HIV/AIDS epidemic using a Markov chain analysis. They predicted, from these races, the number of people living with HIV, and mortality count due to HIV/AIDS. They observed a stable number of deaths over the years in both races.

Gurprit et al. (2013) assessed the effects of anti-retroviral therapy on 580 AIDS patients from an ART centre in New Delhi. They used a 5-stage multistate Markov model to estimate transition intensities and transition probabilities. The states of their model were CD4 cell count based as follows: state 1 (> 500), state 2 (351 to 500), state 3 (200 to 350), state 4 (< 200) and state 5 (death). They further examined the effects of covariates age, gender and mode of transmission on transition intensities using Cox proportional hazards model.

Shoko and Chikobvu (2018a) used a continuous time-homogeneous Markov model to analyse the effects of reaction to treatment, TB co-infection, age and gender on transmission intensities. Their model was CD4 cell counts based and they added the death state and loss to follow-up.

In this chapter, a continuous-time homogeneous Markov process is used to model the progression of HIV/AIDS patients. States are classified by the level of sickness based on four CD4 cell counts classifications measured in cells/mm^3, followed by the end point, which is death. More importantly, among the determinants of

HIV/AIDS, both the viral load counts and CD4 cell counts are included in the same model, thus making this research different from previous studies. The viral load count covariate was included and effects of collinearity with CD4 cell count are corrected using the principal component approach. In addition to that, effects of non-adherence to treatment on transition intensities are assessed. Transitions between the CD4 cell counts states is considered to be bi-direction using data recorded from a cohort of 320 HIV+ patients at a wellness clinic in Bela Bela, South Africa.

8.1.1 Continuous-time Markov processes

A stochastic process $X_c(t), t \in [0, \infty)$ defined on a finite state space $C = 1, 2, \ldots, c$ where $X_c(t)$, the disease state of a patient at time t, represents a Markov process if $\forall s, t \geq 0$ and for every $i, j \in C$ such that:

$$P(X_c(t+s) = j | X_c(t) = i, X_c(u) = x_c(u), 0 \leq u < s) = P(X_c(t+s) = j | X_c(t) = i).$$

This implies that a Markov process is memoryless, that is, the future transitions depend on the entire history only through the present state as demonstrated in Chapter 3. Thus, the previous states once occupied by an individual do not matter. These transitions are described using the transition probabilities $(P_{ij}(t))$, and transition intensities (q_{ij}), from state i to state j. The functions $P_{ij}(t)$ are continuously differentiable and are subject to the initial condition:

$$P_{ij}(0) = \delta_{ij} = \begin{cases} 0 & , i \neq j, \\ 1 & , i = j. \end{cases} \tag{8.1}$$

where δ_{ij} is a Kronecker delta, $P_{ij}(0) = 1$, for $i = j$ means the patient's state definitely does not change, with certainty, when no time elapses and $P_{ij}(0) = 0$, for $i \neq j$ means that when no time elapses we are sure that the patient's state cannot change with certainty. The transition intensity is defined as:

$$q_{ij}(t) = P'_{ij}(t)|_{t=0} = lim_{s \to 0} \frac{P_{ij}(t, t+s)}{s}, \ i, j \in C, j \neq i$$

and $q_{ii}(t) = -\sum_{j \neq i} q_{ij}(t)$ for each $i \in C$. In this chapter, transition probabilities depend only on the elapsed time and not on the chronological time. Thus, the Markov process is time-homogeneous, implying that:

$P_{ij}(t, t+s) = P_{ij}(s)$ and $q_{ij}(t) = q_{ij}$

The effect of explanatory variables (covariates) on the transition intensities is modelled using the proportional intensities:

$$q_{ij}(\mathbf{Z}) = q_{ij}^{(0)} exp\left(\beta_{ij}'\mathbf{Z}\right),\ i \neq j \tag{8.2}$$

where $\mathbf{Z}$ is a k-dimensional vector of explanatory variables, β_{ij} is a vector of k regression parameters relating the instantaneous rate of transitions from state i to state j to the covariates $\mathbf{Z}$, and $q_{ij}^{(0)}$ is the baseline transition intensities with covariates set to their means.

8.2 Principal component analysis: Formulation of the orthogonal viral load covariate

Principal component analysis is a technique used to combine highly correlated factors into principal components that are much less correlated with each other. This improves the efficiency of the model. Chifurira and Chikobvu (2014) used a similar approach to construct orthogonal climatic factors which influence rainfall patterns in Zimbabwe.

In this study, the predictive power of CD4 cell counts (I_1) and viral load (I_2) is explored. Two new, uncorrelated factors, I_1^* and I_2^*, can be constructed as follows:
Let $I_1^* = I_1$
Then, we carry out a linear regression analysis to determine the parameters γ_1 and γ_2 in the equation (Chifuria and Chikobvu, 2014):

$$I_2 = -\gamma_1 + \gamma_2 I_1^* + \varepsilon_1$$

γ_1 and γ_2 are the intercept and slope parameters of the regression model, respectively and ε_1 is the 'error' term or residual, which by definition is independent of $I_1^* = I_1$. We then set:

$$I_2^* = \varepsilon_1 = I_2 - (\gamma_1 + \gamma_2 I_1^*)$$

By construction I_2^* is uncorrelated with the viral load values (I_2) since $I_2^* = \varepsilon_1$ is the residual term in the equation. I_2^* in the model explains the component of mortality that cannot be explained by the CD4 cell counts alone (or in the absence of viral load counts). To deal with multi-collinearity of viral load count and CD4 cell count, the orthogonal viral load covariate (residuals) is used. This is done by regressing viral

load count on CD4 cell count and doing the classification below. The residuals from the fitted model are included with the original HIV data to form the new orthogonal covariate, orthogonal viral load (residuals) (VLR). These residuals are coded as: "1" for negative residuals and "0" for positive residuals. Negative orthogonal viral load ("1") represents lower viral load levels than expected for a given CD4 cell count state/level. A continuous-time Markov model for the effects of covariates age, non-adherence (NA), CD4 baseline (CD4BL), and orthogonal viral load (I_2^*) on HIV progression based on CD4 cell counts, is fitted. Instead of using viral load baseline as a covariate, this chapter prefers a routinely observed viral load. Coding of the covariates has been presented earlier in Chapters 3 and 5. In this chapter, the effects of orthogonal viral load which is constructed from a routinely observed variable is preferred, to the effects of viral load at baseline. The "msm" package for multi-state modelling in R developed by Jackson (2013) is used.

8.2.1 Variable coding

For the purpose of this analysis, the orthogonal viral load and the CD4 cell count states are coded as follows:

$$Othogonal\ viral\ load\ variable(I_2^*) = \begin{cases} 1; & negative(lower\ viral\ load\ than\ expected) \\ 0; & otherwise. \end{cases}$$

and

$$CD4\ cell\ count\ levels\ (X_c(t)) = \begin{cases} 1; & CD4 > 800 \\ 2; & 500 < CD4 \leq 800 \\ 3; & 350 < CD4 \leq 500 \\ 4; & CD4 < 350 \\ 5; & Death. \end{cases}$$

8.2.2 Model formulation

Consider a stochastic process $X_c(t), t \in [0, 5)years$ defined on a finite state space $X_c = (1, 2, 3, 4, 5)$ based on CD4 cell counts as defined above. $X_c(t)$ represents the CD4 cell count state of an HIV/AIDS patient at time t. This process represents a Markov process if $\forall s, t \geq 0$ and for every $i, j \in X_c(t)$:

$$P(X_c(t+s) = j | X_c(t) = i, X_c(u) = x_c(u), 0 \leq u < s) = P(X_c(t+s) = j | X_c(t) = i).$$

The above equation implies that a Markov process is memoryless, that is, the future transitions depend on the entire history only through the present state. Formulation of the model is based on the assumption that at $(t = 0)$, an HIV infected individual enters the study with an HIV state defined by CD4 cell count levels. As the patient initiates treatment therapy, the patient is either in state 1, 2, 3 or 4 and these states are mutually exclusive. At time Δt the patient in state i is expected to either maintain his state $(i = 1, 2, 3, 4)$, transition to state of better CD4 cell counts $(i - 1, i \neq 1)$ (or remain at the lowest state), transition to a state of lower CD4 cell counts $(i + 1, i = 1, 2, 3, 4)$ (or remain at the highest state) or absorbed in the death state. These possible transitions are based on the assumption that not all patients initiated into cART recover their CD4 cell counts levels. Some may fail to achieve their normal CD4 cell counts levels due to non-adherence, effect of age as younger patients may not adhere to treatment, and also due to the effect of gender, since the assumption is males have busy schedules and may forget to take medication. However, those who adhere to cART respond well to treatment. Hence the bi-directional model proposed in Figure 8.1 below.

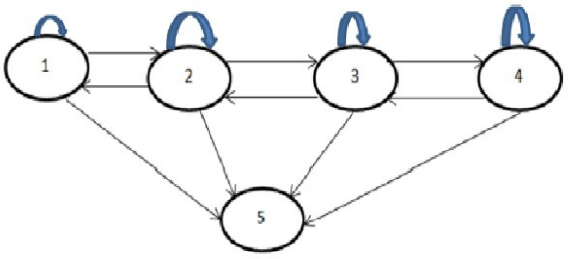

Figure 8.1 – *Diagraph for HIV progression defined by CD4 cell count states followed by the end point, death. a) States 1-4 are transient and there is a possibility of maintaining the same state in 2 or more consecutive visits. b) State 5 is the absorbing state.*

The model in Figure 8.1 is described by a transition intensity matrix $Q = q_{ij}$;

$$Q(t) = \begin{pmatrix} q_{11} & q_{12} & 0 & 0 & q_{15} \\ q_{21} & q_{22} & q_{23} & 0 & q_{25} \\ 0 & q_{32} & q_{33} & q_{34} & q_{35} \\ 0 & 0 & q_{43} & q_{44} & q_{45} \\ 0 & 0 & 0 & 0 & 0 \end{pmatrix} \tag{8.3}$$

The likelihood estimates for the parameters in the model are shown in Equation (7.2) of Chapter 7.

The effect of the above explanatory variables on the transition intensities is modelled using the proportional intensities:

$$q_{ij}(\mathbf{Z}) = q_{ij}^{(0)} exp\left(\beta_{ij}'\mathbf{Z}\right),\ i \neq j \tag{8.4}$$

where $\mathbf{Z}$ is a k-dimensional vector of explanatory variables: "CD4BL, gender, age, non-adherence (NA), orthogonal viral load ("I_2^*")." Thus, the transition intensity for a patient x in this study is given by the model:

$$q_{ij} = q_{ij}^{(0)} exp\left(\beta_{ij}^{(Age)} Age_x + \beta_{ij}^{(Gender)} Gender_x + \beta_{ij}^{(CD4BL)} CD4BL_x + \beta_{ij}^{(NA)} NA_x + \beta_{ij}^{(I_2^*)} I_{2x}^*\right) \tag{8.5}$$

For this model $q_{ij}^{(0)}$, are the baseline transition intensities that refer to a patient with age category 0 (over 45 year old), gender=0 (female), CD4BL=0 (above 200 cells/mm^3, Adherent to treatment and positive I_2^*, β_{ij} is a regression parameter relating the instantaneous rate of transitions from state i to state j to the covariates $\mathbf{Z}$. The transition intensities q_{ij}, are presented in rates per year. q_{ij} are the elements of a 5×5 transition intensity matrix Q from a continuous time-homogeneous Markov process. An important aspect is the inclusion of both CD4BL$_x$ and I_2^* (the orthogonal viral load covariate) derived after curing for collinearity.

8.2.3 Assessment of the fitted models

Based on Equation (8.2) two nested models are fitted. One of the models excludes the effect of the orthogonal viral load and the other includes all covariates including the orthogonal viral load. These models are compared using their Akaike information criteria (AICs), defined as:

$$AIC = -2 \times Log(likelihood) + 2k$$

where $-2 \times Log(likelihood)$ represents the bias, $2k$ represents the variance and k is the number of estimated parameters in the fitted model. The model with the minimum AIC is considered as the better model. Further assessment of the fitted nested models is done using the likelihood ratio test (LRT). The value of the $LRT = -2log_e((L_s(\theta))/(L_f(\theta))$, where $L_s(\theta)$ is the simple model (no viral load orthogonal in the model) and $L_f(\theta)$ is the full model (with the orthogonal viral load covariate

in the model).

8.3 Results

In this section, the combined effect of viral load and CD4 cell counts in the progression of HIV in patients on treatment is analysed. This is done by first fitting a time-homogeneous Markov model for the effects of the covariates CD4 cell count at baseline (CD4BL), Gender, Age and non-adherence to treatment (NA) on HIV/AIDS progression based on CD4 cell count states. Notable is the exclusion of the viral load count covariate in this model. Secondly, a time-homogeneous Markov model for the effects of covariates CD4 cell count at baseline (CD4BL), gender, age, non-adherence to treatment (NA) and the orthogonal viral load covariate is then included in the model. Comparison of these two models is based on their $-2 \times log(likelihood)$, Akaike Information Criteria (AIC), likelihood ratio tests and also the percentage prevalence plots. The results are shown in the following subsections.

CD4 cell counts model and other variables excluding viral load: In this subsection we fit a continuous-time homogeneous Markov model for the effects of non-adherence (NA), CD4 at baseline (CD4BL), age and gender on the progression of HIV defined by the CD4 cell counts states as defined in the model below:

$$q_{ij}(\mathbf{Z}) = q_{ij}^{(0)} exp\left(\beta_{ij}' \mathbf{Z},\right),\ i \neq j, \tag{8.6}$$

where **Z**=(CD4BL, gender, age, NA) is a $k = 4$-dimensional vector of covariates and β_{ij} is a vector of k regression parameters relating the instantaneous rate of transitions from state i to state j to the covariates **Z** and baseline intensities $q_{ij}^{(0)}$ relating to the baseline transition from state i to state j. These states are defined by CD4 cell count and an absorbing state, death. The results are shown in Table 8.1 below.

The -2xLog(likelihood) of the model is 2646.165 and * stands for significant estimates. Also from the table, the first column represents possible transitions from state i to state j, where $i = 1, \ldots, 4$ and $j = 1, \ldots, 5$. The second column represent the baseline transition intensities (with confidence intervals), the third column gives coefficients (with confidence intervals) to represents the effects of non-adherence to treatment, the fourth column gives coefficients (with confidence intervals) to represent the effects of having a CD4 cell count at baseline above 200 cells/mm^3 to HIV progression, the fifth column gives coefficients (with confidence intervals) to represent the effects of having age below 45 years, and lastly the sixth column gives

Table 8.1: Estimated parameters (with 95% confidence intervals in brackets) for the time homogeneous model that excludes the effects of viral load count

State	Baseline ($q_{ij}^{(0)}$)	NA	CD4BL	Age	Gender
2-1	0.561 (0.410, 0.768)*	0.786 (0.008, 1.57)*	-0.411 (-0.938, 0.116)	0.37 (-0.51, 1.25)	0.106 (-0.51, 0.72)
1-2	0.751 (0.486, 1.159)*	0.145 (-1.29, 1.003)	-0.491 (-1.232, 0.25)	-1.309 (-2.57, -0.05)*	-0.0618 (-0.94, 0.817)
3-2	1.27 (1.048, 1.537)*	0.0501 (-0.74, 0.84)	-0.613 (-0.99, -0.23)*	0.277 (-0.15, 0.71)	0.117 (-0.30, 0.54)
2-3	0.711 (0.526, 0.964)*	0.757 (-0.42, 1.94)	-0.0338 (-0.71, 0.64)	0.188 (-0.92, 0.55)	0.737 (0.084, 1.39)*
4-3	0.798 (0.686, 0.929)	0.389 (-0.92, 0.15)	-1.329 (-1.67, -0.99)*	0.0508 (-0.277, 0.38)	-0.463 (-0.79, -0.13)*
3-4	0.691 (0.528, 0.906)*	0.751 (-0.049, 1.55)	-0.522 (-1.15, 0.11)	0.0671 (-0.51, 0.65)	0.516 (-1.13, 0.09)
1-5	0.0005 (0.000006, 4696)	0.058 (-39.9, 39.75)	0.621 (-42.3, 43.6)	-0.607 (-36.1, 34.85)	0.714 (-42.2, 43.6)
2-5	0.00492 (0.00007, 0.330)*	1.629 (-14.36, 11.1)	0.0683 (-2.93, 3.07)	3.702 (-9.11, 16.51)	1.509 (-1.48, 4.50)
3-5	0.00036 (0.000005, 2.44)*	4.48 (-4.15, 13.11)	2.878 (-8.16, 13.9)	2.39 (-9.12, 13.90)	-3.194 (-14.1, 7.7)
4-5	0.0010 (0.00004, 0.276)*	3.35 (-16.4, 9.67)	3.164 (-9.80, 16.1)	-2.065 (-4.31, 0.181)	-5.271 (-18.3, 7.78)

coefficients (with confidence intervals) to represent the effects of gender to HIV progression. The results are as follows:

In Table 8.1 (model that excludes the viral load count), results from the baseline transition intensities show that patients in state 1 (CD4 cell counts above 800 cells/mm^3) are 1502 times more likely to experience immune deterioration to state 2 than being absorbed into the death state. When CD4 cell counts are below 500 cells/mm^3 (states 3 and 4), transitions to better states are more likely to occur than transitions to worse states. However, when CD4 cell counts are above 500 cells/mm^3, the rates of immune deterioration are higher than the rates of immune recovery.

For patients who experienced non-adherence to treatment, transitions from state 2 to state 1, state 3 to state 4, state 3 to state 2 and state 4 to state 3 estimates are relatively precise, as shown by the narrower confidence intervals. The only transition that is significant is from state 2 to state 1. This is shown by the confidence interval that is narrower (zero excluded in the interval) compared to the other transitions. For these non-adherent patients, there is a significant increase in the rate of immune recovery from state 2 to state 1. Although not significant, there is an increase in immune deterioration from state 3 to state 4, and reduction in the rate of immune recovery from state 4.

For the age variable, transitions from state 2 to state 3, state 3 to state 2, state 3 to state 4 and state 4 to state 3 estimates are relatively precise as revealed by the smaller confidence intervals. The only transition that is significant (zero excluded in the interval) is from state 2 to state 1. The results show a significant reduction in immune deterioration once a normal CD4 cell count above 800 cells/mm^3 (state 1) is achieved for the younger patients aged 45 years and below. These younger patients experience reduced immune deterioration from state 2 to state 3 and increased immune deterioration from state 3 to state 4, although these transitions are not statistically significant.

For the other variables, gender and CD4 cell counts at baseline, all the estimated transition intensities between live states are relatively precise since they have narrow confidence intervals. However, for the baseline CD4 cell count, only transitions from state 3 to state 2 and from state 4 to state 3 are significant (zero excluded in the interval). These transitions show a significant reduction in immune deterioration. Males experienced significantly increased immune deterioration from state 2 to state 3, compared to their female counterparts. They also experience a significant reduction in immune recovery from state 4 to state 3.

Overall, the fitted model shows the estimated parameters have relatively wider confidence intervals for the transitions to the death state. This indicates that the estimated parameters are not precisely estimated.

The expected and observed percentage prevalence in each CD4 cell count state and the death state are shown in Figure 8.2 below.
Results from Figure 8.2 show that the expected percentage prevalences give almost a perfect fit of the observed percentage prevalence for state 1 and state 5 (death) in the first 3 years. Thereafter, the number of deaths is slightly underestimated and state 1 prevalence's are slightly overestimated. In the first 2 years observed percentage prevalence in state 2 and 3 is slightly overestimated by the expected percentage prevalence. Percentage prevalence in state 4 is slightly underestimated in the first 2 years and slightly overestimated thereafter by the fitted model.

CD4 cell count model for the viral load principal component: Since the variables CD4 cell count and viral load are expected to be collinear, orthogonality between these variables is achieved by regressing viral load on CD4 cell count as shown in Table 8.2 below.

Multiple R-squared: 0.06015; F-statistic: 130.7 on 1 and 2042 DF, p-value< 0.0001

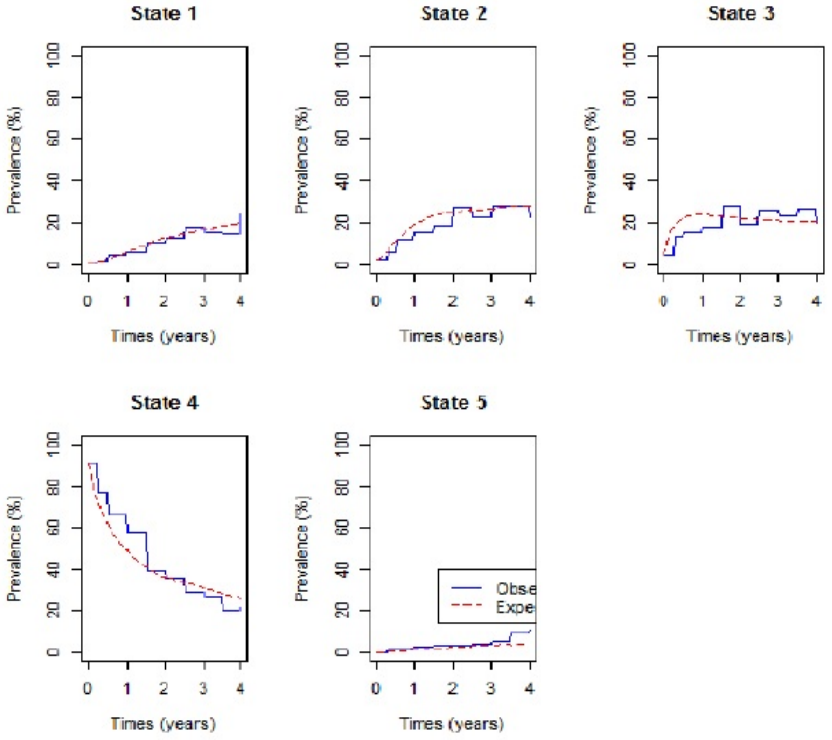

Figure 8.2 – *Observed and expected percentage prevalence in each state for the model with CD4 cell count states without viral load orthogonal. The expected model slightly underestimate mortality after 3 years.*

Table 8.2: Regression of viral load on CD4 cell count

	Estimate	Std.error	t value	$Pr(>\|t\|)$
γ_1(intercept)	55166.91	3136.54	17.59	$< 0.0001^{***}$
γ_2(slope)	-70.963	6.207	-11.43	$< 0.0001^{***}$

The results show a highly significant regression line, suggesting correlation between viral load counts and CD4 cell counts as indicated by a p-value below 0.0001. The residuals from the regression model are then taken to represent another viral load covariate. After extracting the residuals, a linear regression model for the relationship between CD4 cell count an the viral load residuals is fitted.

Since the slope is practically zero, there is practically no correlation (slope =0.0000038) between CD4 cell count and viral load residuals. Thus, the viral load residual covariate is assumed to be orthogonal to the CD4 cell count covariate. Therefore, the orthogonal viral load covariate together with CD4 cell count can now be included in

Table 8.3: Regression of CD4 cell count on the residual viral load

	Estimate	Std.error	t value	$Pr(>\|t\|)$
γ_1(intercept)	397.0	6.919	57.375	$< 0.0001^{***}$
γ_2(slope)	0.0000038	0.000079	0.048	0.961

Multiple R-squared: 0.000001142, Adjusted R-squared: -0.0004886 F-statistic: 0.002332 on 1 and 2042 degrees of freedom, p-value: 0.9615. ***Significant at 5% level

one model. As a result, the orthogonal viral load covariate is coded as follows:

$$Orthogonal\ Viral\ Load\ variable(I_2^*) = \begin{cases} 1, & if\ viral\ load\ residual\ is\ negative \\ 0, & if\ viral\ load\ residual\ is\ positive. \end{cases}$$

The orthogonal viral load covariate and other covariates age, non-adherence, gender and CD4 baseline are then used as covariates for the continuous-time Markov model with states defined by CD4 cell count. The results are shown in Table 8.4 below.

Table 8.4: Parameter effects (with 95% confidence intervals) of age, CD4 at baseline, non-adherence, gender and orthogonal viral load on the transition intensities for the CD4 based Markov model.

State	Baseline	NA	CD4BL	Age	Gender	I_2^*
2-1	0.545	0.765	-0.283	0.613	-0.033	-1.17
	(0.40, 0.74)	(0.034,1.50)*	(-0.78,0.21)	(-0.146,1.37)	(-0.63, 0.56)	(-1.95,-0.39)*
1- 2	0.04	0.15	-0.52	-1.32	-0.08	-4.01
	(0.00,42)	(-1.12,1.42)	(-1.30,0.27)	(-2.66,0.01)	(-1.04, 0.88)	(-18.59,10.56)
3- 2	1.39	0.33	-0.55	0.31	0.17	-0.50
	(1.14,1.72)	(-0.60,1.25)	(-0.94,-0.15)*	(-0.12,0.74)	(-0.27, 0.61)	(-1.07, 0.07)
2-3	0.67	1.12	0.04	-0.08	0.88	0.70
	(0.47,0.94)	(-0.19,2.44)	(-0.65,0.73)	(-0.82,0.65)	(0.20, 1.56)*	(-0.44, 1.85)
4-3	0.83	-0.38	-1.40	0.05	-0.48	-0.07
	(0.71,0.97)	(-0.94,0.19)	(-1.77,-1.03)*	(-0.28,0.39)	(-0.82,-0.14)*	(-0.49, 0.34)
3-4	0.69	0.85	-0.61	0.10	-0.51	0.25
	(0.48,1.02)	(0.02,1.69)*	(-1.29,0.07)	(-0.48,0.69)	(-1.13,0.11)	(-1.31, 1.81)
1-5	0.002	4.37	7.38	2.65	-2.76	7.97
	(0.00,17.1)	(-1.99,10.74)	(-9.15,23.92)	(-14.03,19.33)	(-21.67,16.15)	(-8.96,24.89)
2-5	0.0001	-1.71	-2.54	2.06	4.66	-5.07
	(0.00,131)	(-28.32,24.89)	(-18.23,13.15)	(-15.12,19.24)	(-8.05,17.36)	(-17.16, 7.02)
3-5	0.0001	1.70	1.07	0.38	-1.37	-1.09
	(0.00,2768)	(-36.23,39.64)	(-45.16,47.29)	(-48.26,49.02)	(-48.13,45.38)	(-55.93,53.74)
4-5	0.001	-3.94	3.76	-2.07	-5.76	-1.18
	(0.00,1.05)	(-22.02,14.15)	(-13.53,21.05)	(-4.32,0.19)	(-22.96,11.44)	(-2.98, 0.62)

-2Log(likelihood) = 2554.25; * represents significantly estimated parameters

The results from Table 8.4 (model that includes the viral load count) show that all the covariates in the model give more precise estimates (narrower confidence intervals) of parameters for transitions between live states than the model without the orthogonal viral load covariate (I_2^*). Just like the model without the orthogonal viral load, non-adherent patients experienced a significant increase in immune recovery from

state 2 to state 1. In addition, there is a significant increase in immune deterioration from state 3 to state 4. Although not significant, the inclusion of the orthogonal viral load covariate results in non-adherence to treatment, accelerating death from state 3, although the magnitude is lower than when the orthogonal viral load covariate is excluded.

The estimated parameters for the effects of age on transition intensities have more precise estimates for transition from state 4 to state 5, compared to the other covariates except the orthogonal viral load. The results reveal a reduction of deaths from state 4 for patients aged 45 years and below. Though not significant, the results now show a reduction in immune deterioration from state 1 (CD4 cell count state above 800 cells/mm^3) and an increase in the rate of immune recovery from state 2 to state 1 for younger patients aged 45 years and below. The results generally show a reduction in mortality in cases where the observed viral load is lower than the expected (i.e., negative orthogonal viral load count).

For patients who initiated therapy with CD4 cell counts below 200 cells/mm^3, the rates of immune recovery are reduced. There is a significant reduction in the rates of immune recovery from state 3 to state 2 and from state 4 to state 3.

The continuous-time homogeneous Markov model with the orthogonal viral load component has a lower -2xLog-likelihood than that of the model that excludes the orthogonal viral load component. Next, percentage prevalence for each state for the fitted model are plotted.

Figure 8.3 above shows that if the orthogonal viral load covariate is included, the expected percentage prevalence gives a better estimate of the observed percentage prevalence for the mortality state (state 5), better than the Markov model in which the orthogonal viral load covariate is excluded.

Assessment of the fitted models by performing a likelihood ratio test and calculating estimates of the Akaike Information Criteria (AIC) for each of the fitted models is further done. Results are shown in Table 8.5 below.

Table 8.5: Likelihood ratio test for the model with no orthogonal viral load and the model with orthogonal viral load.

likelihood ratio test.msm	-2×log Likelihood Ratio	df	p
with orthogonal viral load	91.91497	10	< 0.0001

AIC (No orthogonal viral load)=2746.165; AIC (with orthogonal viral load)=2674.25.

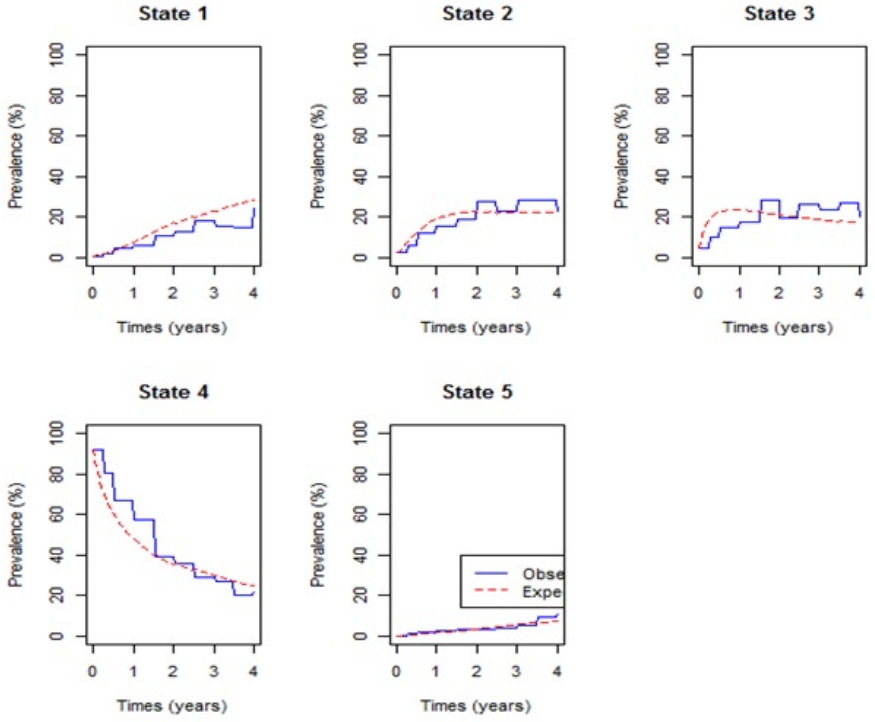

Figure 8.3 – *Percentage prevalence for the continuous-time Markov model defined by CD4 cell count and the orthogonal variable, viral load, included. It shows an improvement in estimating mortality compared to the model without the orthogonal variable.*

A likelihood ratio test for the two nested models has shown that the model with the orthogonal viral load covariate fits the data significantly better than the model with no orthogonal viral load covariate. This is further confirmed by the estimated AICs, which is lower for the model with the orthogonal viral load covariate than that of the model with no orthogonal viral load covariate.

8.4 Concluding Remarks

In this chapter, a time homogeneous Markov model based on CD4 cell count states is developed to explain and predict probability of death from HIV/AIDS. The model was improved by including an orthogonal viral load covariate derived from principal component analysis. Principal component analysis is a technique used to combine highly correlated factors into principal components that are much less correlated with each other. This improves the efficiency of the model. Principal component variables are created by fitting a regression model of viral load count on CD4 cell count. The new orthogonal covariate is included to represent the viral load covariate for the Markov model defined. This viral load covariate helped to explain

a component of mortality/transition, which could not be explained by the CD4 cell count alone.

This study discovered the importance of using both CD4 cell counts and viral load counts in the same model for monitoring progression of HIV/AIDS patients on anti-retroviral therapy. By including both variables, the model has revealed that for given levels of CD4 cell count, there is the possibility of reduction of mortality for patients whose viral load is lower than expected given their CD4 cell count. Progression to death was more pronounced in patients who have achieved normal CD4 cell counts and this is experienced mainly in younger patients, non-adherent patients and also for patients whose initial CD4 cell count was below 200 cells/mm^3. This study will help the researcher to uncover the critical areas of dealing with and correcting for, collinearity when including both CD4 cell count and viral load levels in multistate modelling of HIV/AIDS that many researchers were not able to explore. Thus, a new application of theory and better understanding of the Principal Component Approach when dealing with both CD4 cell count and viral load counts (in the same model) to HIV/AIDS modelling may be arrived at.

In the next chapter, the same methods are used but the continuous-time homogeneous Markov model is based on viral load states and an orthogonal CD4 cell count covariate is constructed and included in the same model.

Chapter 9

A Markov Model to estimate Mortality due to HIV/AIDS using viral load levels-based states and CD4 cell counts: A Principal Component Analysis approach

9.1 Introduction

Rose et al. (2015) investigated frameworks for the analysis of viral load. They came up with two frameworks: the single measure viral load count and the repeated measure viral load count. Their findings indicated that the repeated measure viral load count has more precision than the single measure viral load count because it utilises all available viral load counts data, has more statistical power, and also avoids subjectivity of defining a "window". Thus, in this study, a repeated measure viral load count monitoring and management of HIV/AIDS on patients receiving cART using a Markov stochastic model is proposed.

Markov mathematical models have been extensively used in research into the epidemiology of HIV/ AIDS, because they play an important role in improving our understanding of major factors contributing to the spread of this virus (Titus, 2016). It has also been argued that multi-state stochastic models are useful tools for studying complex dynamics such as chronic disease, and also in determining factors associated with the progression between different stages of the disease (Naresh et al., 2007; Dessie et al., 2014). However, for most of these studies, states of the Markov

processes are based on CD4 cell counts. For example, Titus (2016) analysed HIV dynamics using a discrete-time Markov chain mathematical model based on simulated CD4 cell count states. Dessie (2014) used a CD4 cell count-based Markov model to determine the factors associated with the progression between different stages of the disease for individuals on anti-retroviral therapy (ART).

In this chapter, a continuous time-homogeneous Markov process is used to model the progression of HIV/AIDS patients. HIV/AIDS progression is based on five viral load count states, measured in copies/mL, followed by the end point, death. More importantly, among the determinants of HIV/AIDS, both the viral load counts and CD4 cell counts are included in the same model, thus making this research different from previous studies. The CD4 cell count covariate is included and the effect of collinearity with viral load count is corrected for using the Principal Component Approach. In addition to that, effects of non-adherence to treatment, viral load count at baseline (VLBL), age and gender on transition intensities, are assessed. Transitions between the viral load based states are considered to be bi-directional, thus, allowing forward transitions due to viral rebound and backward transitions due to the therapeutic effects of cART.

9.1.1 Continuous-Time Markov Processes

In this Chapter continuous-time Markov models are constructed as demonstrated in Chapter 8. The only difference is that in this chapter, the transitions intensities and transition probabilities are viral load count based. In the previous chapter, the transition states were CD4 cell count based.

9.2 Data Description

The model is applied to data from a heterosexual group of 320 HIV patients on cART from a Wellness clinic in Bela Bela, South Africa, from 2005 to 2009 as described previously. Patients were eligible for inclusion if they had a routinely reported viral load, routinely collected CD4 cell counts and if they were 15 years and older.

A total of 226 patients had a CD4 cell count at baseline below 200 cells/mm^3 and 96 had a CD4 cell count at baseline above 200 cells/mm^3. During the course of treatment, a number of factors were considered. These include non-adherence to treatment therapy, treatment change, treatment line and resistance to treatment, with 36 showing some signs of non-adherence to treatment, which influenced the need for treatment change.

9.3 Principal Component Analysis: Formulation of the orthogonal CD4 cell variable

Principal Pomponent Analysis is used to construct the orthogonal CD4 cell count using a similar approach as discussed in Chapter 8. In this chapter, the orthogonal variable is constructed from CD4 cell count residuals as follows:

The predictive power of viral load values (I_1) and CD4 cell count values (I_2) is explored. Two new, uncorrelated factors, I_1^* and I_2^*, can be constructed as follows (Chifurira and Chikobvu, 2014):

Let $I_1^* = I_1$

Then, we carry out a linear regression analysis to determine the parameters γ_1 and γ_2 as discussed in Chapter 8. We then set:

$I_2^* = +\varepsilon_1 = I_2 - (\gamma_1 + \gamma_2 I_1^*)$

By construction, I_2^* is uncorrelated with the viral load count values (I_1), since $I_2^* = \varepsilon_1$ is the residual term in the equation. I_2^* in the model explains the component of mortality or HIV/AIDS progression that cannot be explained by the viral load values alone (or in the absence of CD4 cell counts).

The residuals (I_2^*) from the fitted model are included with the original HIV data as the new orthogonal variable, the orthogonal CD4 cell counts covariate (residuals). These residuals are coded as "1" for negative residuals and "0" for positive residuals. A negative CD4 cell count residual implies that the observed CD4 cell count is lower than the expected CD4 cell count, given the viral load levels of the patient, and a positive residual means having a higher CD4 cell count than expected. Instead of including the CD4 cell count at baseline as one of the covariates, this Chapter considers the inclusion of the orthogonal CD4 cell count which represents routinely collected CD4 cell counts. A continuous-time Markov model for the effects of age, gender, VLBL, non-adherence (NA), and orthogonal CD4 cell counts (I_2^*) on HIV progression based on the viral load states, is fitted. The "msm" package for multistate modelling in R software developed by Jackson (2016) is used.

9.3.1 Variable coding

The variables non-adherence to treatment (NA), age, viral load baseline and gender are defined in the previous chapters. The other variables in the model are defined as follows:

$$orthogonal\ CD4\ covariate(I_2^*) = \begin{cases} 1; & negative\ (lower\ CD4\ cell\ counts\ than\ expected) \\ 0; & otherwise. \end{cases}$$

$$Viral\ Load\ at\ Baseline\ (VLBL) = \begin{cases} 1; & > 10\,000\ copies/mL \\ 0; & \leq 10\,000\ copies/mL. \end{cases}$$

$$Viral\ load\ levels\ (X_v) = \begin{cases} 1; & VL < 50 \\ 2; & 50 \leq VL < 10\,000 \\ 3; & 10\,000 \leq VL < 100\,000 \\ 4; & 100\,000 \leq VL < 500\,000 \\ 5; & VL \geq 500\,000 \\ 6; & Dead. \end{cases}$$

9.3.2 Model Formulation

Consider a stochastic process $\{X_v(t); t \in [0; 5)years\}$ defined on a finite state space $X_v = \{1; 2; 3; 4; 5; 6\}$ based on viral load states as defined above. $X_v(t)$ represents the viral load state of an HIV/AIDS patient at time t. This process represents a Markov process if $\forall s, t \geq 0$ and for every $i, j \in V$

$$P(X_v(t+s) = j | X_v(t) = i, X_v(u) = x_v(u), 0 \leq u < s) = P(X_v(t+s) = j | X_v(t) = i)$$

The above equation implies that a Markov process is memoryless, that is, the future transitions depend on the entire history only through the present state.

HIV/AIDS progression is based on viral load states, and possible transitions between these states are shown in Figure 9.1. The transition between states is assumed to be bi-directional, that is, movement from state i to state $i \pm 2$ is always via state $i \pm 1$; where $i = 1, 2, 3, 4, 5$ define the live states based on viral load counts. The model allows for reverse transition due to the efficacy of treatment and forward due to non-adherence to treatment. Transitions between states are shown by the arrows.

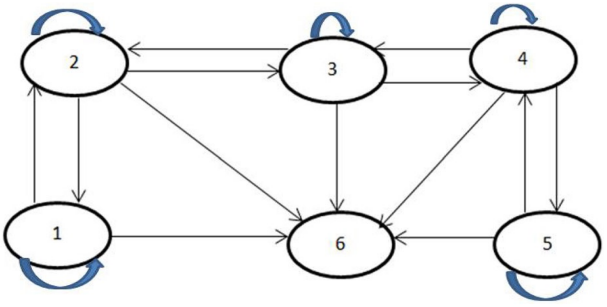

Figure 9.1 – *State diagram for the possible transitions between the first five viral load defined states and the absorbing state 6 (death).*

Based on Figure 9.1, the transition rates are defined as follows:

$$Q = \begin{pmatrix} -(q_{12}+q_{16}) & q_{12} & 0 & 0 & 0 & q_{16} \\ q_{21} & -(q_{21}+q_{23}+q_{26}) & q_{23} & 0 & 0 & q_{26} \\ 0 & q_{32} & -(q_{32}+q_{34}+q_{36}) & q_{34} & 0 & q_{36} \\ 0 & 0 & q_{43} & -(q_{43}+q_{45}+q_{46}) & q_{45} & q_{46} \\ 0 & 0 & 0 & q_{54} & -(q_{54}+q_{56}) & q_{56} \\ 0 & 0 & 0 & 0 & 0 & 0 \end{pmatrix}$$

Q is a 6×6 matrix and its elements q_{ij} are the instantaneous rates of transition from state i to state j subject to the conditions that $v = 6$ and $\sum_{j=1}^{6} q_{ij} = 0$ so that $q_{ii} = -\sum_{j \neq 1} q_{ij},\ i \neq 6$. q_{ij} is independent of time because the process is assumed to be homogeneous with respect to time. In the next section, the parameters of our models are estimated, including the transition rates.

The effect of the above explanatory variables (covariates) on the transition intensities is modelled using the proportional intensities:

$$q_{ij}(\mathbf{Z}) = q_{ij}^{(0)} exp\left(\beta_{ij}' \mathbf{Z}\right), i \neq j \tag{9.1}$$

where $\mathbf{Z}$ is a $k = 5$-dimensional vector of explanatory variables VLBL, Gender, Age, Non-adherence, and orthogonal CD4 (I_2^*). Thus, the transition intensity for a patient x in this study is given by the model:

$$q_{ij} = q_{ij}^{(0)} exp\left(\beta_{ij}^{(Age)} Age_x + \beta_{ij}^{(Gender)} Gender_x + \beta_{ij}^{(VLBL)} VLBL_x + \beta_{ij}^{(NA)} NA_x + \beta_{ij}^{(I_2^*)} I_{2x}^*\right)$$

For this model, $q_{ij}^{(0)}$ are the baseline transition intensities that refer to a patient with

age category 0 (over 45 years old), gender = 0 (female), VLBL = 0 (below 10 000 copies/mL, adherence to treatment and positive I_2^*, β_{ij} is a vector of k regression parameters relating the instantaneous rate of transitions from state i to state j to the covariates **Z**. The transition intensities, q_{ij}, are presented in rates per year. q_{ij} are the elements of a 6×6 transition intensity matrix Q from a continuous time-homogeneous Markov process. An important aspect is the inclusion of both $VLBL_x$ and I_2^* (the orthogonal CD4 covariate) derived after allowing for collinearity.

Assessment of the Fitted Models:
Based on Equation (9.1), two nested models are fitted: one of the models excludes the effect of the orthogonal CD4 cell counts covariate (nested model) and the other includes all covariates including the orthogonal CD4 cell counts covariate. These models are compared using their Akaike information criteria (AICs). According to Awad (1996) AIC is defined as follows:

$$AIC = -2 \times Log(likelihood) + 2k$$

where $-2 \times Log(likelihood)$ represents the bias, $2k$ represents the variance and k is the number of estimated parameters in the fitted model. The model with the minimum AIC is considered as the better model. Further assessment of the fitted nested models is carried out using the likelihood ratio test (LRT). The value of the
$LRT = -2log_e\left(\frac{L_s(\hat{\theta})}{L_f(\hat{\theta})}\right)$,

where $L_s(\hat{\theta})$ is the simple model (no CD4 cell count orthogonal) and $L_f(\hat{\theta})$ is the full model (with CD4 cell count orthogonal).

9.3.3 Convergence of a Time-Homogeneous Markov Model

If a Markov model fails to converge, optimisation criteria results in a failure to calculate standard errors, leading to the exclusion in the calculation of confidence intervals for the estimated parameters. After running the analysis using the 'msm' package in R, the statistical package warns if 'optimisation has probably not converged to the maximum likelihood-Hessian matrix not positive definite.' To ensure that the model converges, a scaling factor is used to normalise the likelihood and to prevent the overflow within the optimisation process.

9.4 Results

In this section, the combined effect of viral load and CD4 cell counts in the progression of HIV in patients on treatment is analysed. This is carried out by first fitting a time-homogeneous Markov model for the effects of the covariates, VLBL and NA, on HIV/AIDS progression based on viral load states. Secondly, a time-homogeneous Markov model for the effects of covariates, VLBL, NA, age and the orthogonal CD4 cell counts covariate, is fitted. Comparison of these models is based on their -2xLog-likelihood, AIC, likelihood ratio tests and also the percentage prevalence plots. The results are shown in the following subsections.

9.4.1 Time-Homogeneous Markov Model with the Effects of Orthogonal CD4 Cell Counts Covariate Excluded

A time-homogeneous Markov model is fitted for HIV/AIDS progression defined by viral load states. In this model, the effects of the covariates VLBL and NA, to the progression of HIV are considered. The relationship between these covariates and the transition intensities is defined by the following equation:

$$q_{ij}(\mathbf{Z}) = q_{ij}^{(0)} exp(\beta_{ij}' \mathbf{Z}), i \neq j$$

where $\mathbf{Z} = [VLBL,\ Gender,\ Age,\ Non-adherence]$ is a $k = 4$-dimensional vector of covariates and β_{ij} is a vector of k regression parameters relating the instantaneous rate of transitions from state i to state j to the covariates $\mathbf{Z}$ and baseline intensities $q_{ij}^{(0)}$ relating to the baseline transition from state i to state j.

When fitting the time-homogeneous Markov model, the variables; gender and age of HIV patients had no significant effects on HIV progression, hence their exclusion from the results (Table 9.1), in which the first column represents possible transitions from state i to state j, where $i = 1, \ldots, 5$ and $j = 1, \ldots, 6$. The second column represent the baseline transition intensities (with confidence intervals), the third column gives coefficients (with confidence intervals) to represents the effects of non-adherence to HIV progression, and the fourth column gives coefficients (with confidence intervals) to represent the effects of having a VLBL above 10 000 copies/mL to HIV progression. The results are given in Table 9.1.

The results from Table 9.1 show that, when a patient's viral load is above 10 000 copies/mL (states 3, 4 and 5), rates of viral load suppression are higher than rates of viral load rebound. However, from state 2 (viral load between 50 and 10 000

Table 9.1: Estimated parameters (with 95% confidence intervals) for the time homogeneous model that excludes the effects of CD4 cell counts.

	Baseline intensities ($q_{ij}^{(0)}$)	Viral load baseline	Non-adherence
State 2-1	3.395 (2.93, 3.94)	- 0.209 (- 0.63, 0.21)	- 1.002 (- 1.42,- 0.58)
State 1-2	0.495 (0.40, 0.61)	0.020 (- 0.61, 0.650)	0.418 (- 0.17, 1.00)
State 3-2	238.6 (0.08, 71,27)	2.759 (- 4.95, 10.47)	- 2.092 (- 6.00, 1.82)
State 2-3	31.57 (0.010, 10,23)	3.884 (- 3.65, 11.42)	- 0.853 (- 4.79, 3.08)
State 4-3	21.34 (3.49, 130.7)	- 1.597 (- 12.51, 9.31)	0.337 (- 2.26, 2.93)
State 3-4	2.691 (0.34, 21.61)	- 1.930 (- 13.24, 9.38)	0.966 (- 2.01, 3.94)
State 5-4	15.06 (2.41, 93.99)	- 0.457 (- 4.41, 3.50)	2.038 (- 11.57, 15.65)
State 4-5	2.495 (0.11, 56.49)	2.393 (- 12.57, 17.36)	2.263 (- 11.65, 16.17)
State 1-6	0.001 (0.00008, 5.31)	5.109 (- 7.98, 18.20)	5.469 (- 4.51, 15.45)
State 2-6	0.249 (0.05, 1.26)	0.961 (- 0.22, 2.15)	- 4.618 (- 17.76, 8.52)
State 3-6	0.007 (0.000002, 189)	0.603 (- 40.23, 41.44)	- 0.667 (- 40.81, 39.48)
State 4-6	0.002 (0.000005, 8444)	- 0.295 (- 75.48, 74.89)	- 0.055 (- 55.78, 55.67)
State 5-6	0.006 (0.000001, 2 8800)	- 0.344 (- 91.10, 90.41)	- 0.143 (- 61.44, 61.15)

-2Log-Likelihood: 2508.101

copies/mL), the rates of viral load rebound are higher than the rates of viral suppression. The rates of viral load rebound are increased for patients who had problems in adhering to treatment therapy, regardless of the original state.

Patients who started therapy with VLBL above 10 000 copies/mL experienced higher rates of viral load rebound than patients who started therapy with VLBL below 10 000 copies/mL. Having a viral load above 10 000 copies/mL also accelerates the rates of transition to death from the undetectable viral load level (state 1). The same group also experienced high risks of transition from state 2 and state 3, although the risk is lower than when the patients are in state 1.

The results from Table 9.1 also show a significant reduction in the rate of attaining an undetectable viral load level for patients who were non-adherent to treatment (state 2-1). This is indicated by the exclusion of zero in the confidence interval of the estimated parameter. Although not significant, transitions to death for patients who were non-adherent are higher compared to those of adherent patients.

The results show wide confidence intervals for transitions to death from each of the live states. This indicates a relatively poor prediction of mortality by the fitted model. To obtain a better picture of how the fitted model predicts mortality, percentage prevalences in each state are plotted to compare the observed data from the expected data. The percentage prevalence plots are shown in Figure 9.2.

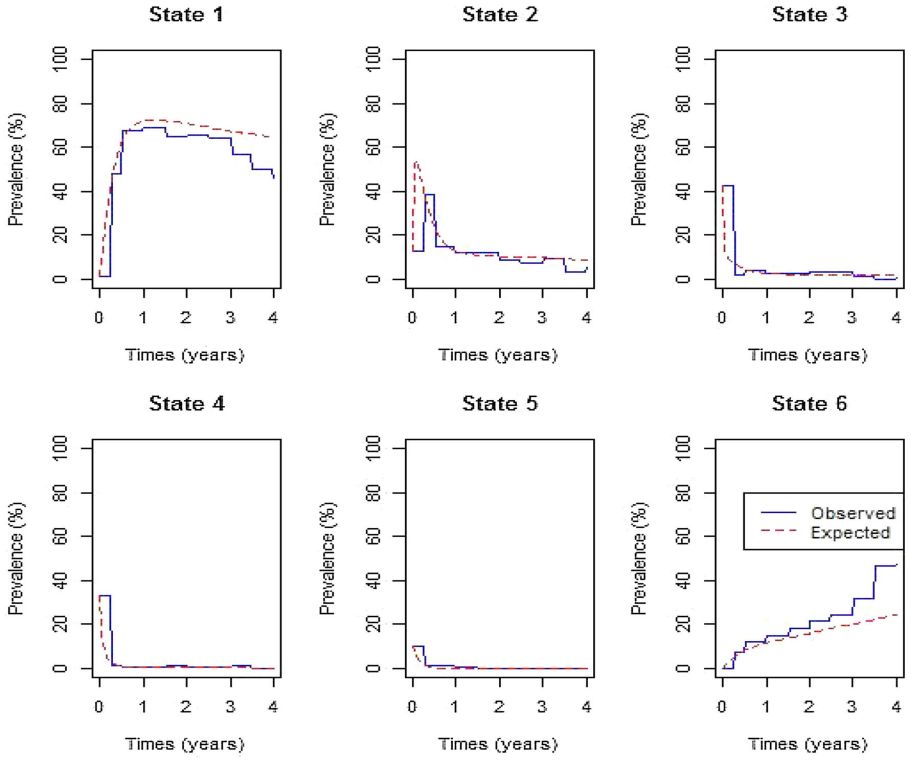

Figure 9.2 – *Percentage prevalence viral load defined state and the effects of non-adherence and age excluding CD4 orthogonal variable.*

Figure 9.2 shows that the expected percentage prevalences give a good fit of the observed percentage prevalence only for the live states, that is states 2, 3, 4 and 5. However, the expected percentage prevalences underestimates the observed prevalences for the death state and overestimate the observed prevalences for state 1. The other anomaly is that of experiencing more than 40% deaths towards the end of the study. This is a cause for concern, since these patients were receiving anti-retroviral therapy. This is a further confirmation that the model does not give a good prediction of mortality. A decision to include the orthogonal CD4 cell counts covariate in the model was made and is discussed in the next subsection.

9.4.2 Time-Homogeneous Markov Model with the Effects of Orthogonal CD4 Cell Counts Covariate Included

The orthogonal components for this model are obtained by regressing CD4 cell count on viral load, as discussed earlier. The residuals from this model are then used to represent the orthogonal covariate, CD4 cell counts, and is now incorporated in the continuous-time Markov model.

Table 9.2: Estimated parameters for the regression model for CD4 cell counts on the viral load.

	Estimate	SE	t value	Pr($>\|t\|$)	
γ_1 (intercept)	419.8	7.000	59.98	< 0.0001	***
γ_2(slope)	- 0.0008477	0.00007415	- 11.43	< 0.0001	***

Multiple R-squared: 0.06015; VIF = 1.06015 F-statistic: 130.7 on 1 and 2042 DF, p-value:< 0.0001
***Significant at 5% level

The results from Table 9.2 show a significant model confirming correlation between CD4 cell counts and the viral load. After regressing CD4 cell counts on viral load, the residuals from the model are extracted. Collinearity between viral load and the residual CD4 cell count is checked by fitting a linear regression model for these variables. The fitted model is shown below:

Table 9.3: Estimated parameters for the regression model for viral load on residual CD4 cell count.

	Estimate	SE	t value	Pr($>\|t\|$)	
γ_1 (intercept)	2.700e+04	2.002e+03	13.49	< 0.0001	***
γ_2(slope)	8.265e-06	7.595	0.00	1	

Multiple R-squared: < 0.0001; Adjusted R-squared: -0.0004897; F-statistic: < 0.0001 on 1 and 2042 Degrees of Freedom; p-value = 1; ***Significant at 5% level

Results show that the variables viral load count and orthogonal CD4 cell count are uncollinearity. Therefore, these residuals are included with the original covariates and then coded as ”1” for negative residuals and ”0” for positive residuals. A negative CD4 cell counts residual implies having lower CD4 cell counts than the expected given the viral load levels. A positive residual means having a higher CD4 cell count than the expected. The orthogonal covariate is then used together with the other covariates to determine the progression of HIV/AIDS based on the viral load states.

The relationship between these covariates and the transition intensities is defined by the following equation:

$$q_{ij}(\mathbf{Z}) = q_{ij}^{(0)} exp(\beta_{ij}' \mathbf{Z}), i \neq j$$

,

where **Z** = [VLBL, Gender, Age, Non-adherence, orthogonal CD4 cell counts covariate] is a $k = 5$-dimensional vector of the covariates and β_{ij} is a vector of k regression parameters relating the instantaneous rate of transitions from state i to state j to the covariates **Z** and baseline intensities $q_{ij}^{(0)}$ relating to the baseline transition from state i to state j. The inclusion of the orthogonal CD4 cell counts covariate has resulted in the significant effects of age on the progression of HIV, hence its inclusion in Table 9.3. However, the covariate gender is still not significant. The inclusion of the gender covariate together with the use of a scaling factor of 4000 resulted in a failure of convergence to a maximum likelihood and a non-positive Hessian matrix. The adjustment of the scaling factor to 5000 resulted in normalising the likelihood, leading to the convergence of the Markov model. Thus, the gender covariate is included after adjusting the scaling factor. The results are shown in Table 9.4.

The results from Table 9.4 show that, when the patient's viral load is above 10 000 copies/mL, represented by states 3, 4 and 5, the rates of viral load count suppression are higher than the rates of viral rebound. However, once the viral load count level is below 10 000 copies/mL (states 2 and 1), patients experience higher rates of viral load count rebound than rates of viral load count suppression. This is a cause for concern, since state 1 represents the undetectable viral load level.

Table 9.4 also shows that the risk of viral load count rebound from states 1 and 2 is higher in patients who initiated therapy with a VLBL above 10 000 copies/mL than in patients who initiated therapy with lower viral load count levels. Other factors that accelerate viral load count rebound from state 1 are negative CD4 residuals and non-adherence to treatment. From state 2, males experience higher risks of viral load count rebound than their female counterparts. However, when the viral load count level is above 10 000 copies/mL, males have increased rates of transitions to good states and reduced rates of transition to bad states than females.

The results also show increased rates of transitions to death (state 6) from state 1. This is mainly caused by non-adherence to treatment, followed by having a viral load count levels above 10 000 copies/mL, age and then orthogonal CD4 cell counts covariate. Thus, younger patients, below the age of 45 years, and patients with CD4 cell counts lower than expected, have accelerated risks of death from state 1.

Table 9.4: Parameter effects (with 95% Confidence intervals) of age, viral load baseline, non-adherence and CD4 orthogonal (I_2^*) on the transition intensities for the viral load levels based Markov model.

State	Baseline	RC	Age	VLC	NA	Gender
2-1	3.891	0.043	-0.568	-0.137	-1.179	-0.028
	(3.25, 4.66)	(-0.30,0.39)	(-1.00,-0.13)	(-0.61,0.33)	(-1.67,-0.69)	(-0.41,0.35)
1-2	0.457	0.428	-0.206	0.138	0.298	-0.298
	(0.3.52,0.59)	(-0.11,0.96)	(-0.82,0.41)	(-0.61,0.88)	(-0.40,0.99)	(-0.88,0.28)
3-2	3379	-0.285	-1.846	4.256	-3.094	1.883
	(0.00,1.5×10^6)	(-4.43,3.86)	(-27.95,24.25)	(-11.99,20.51)	(-14.99,8.81)	(-25.90,29.67)
2-3	381.9	-0.854	-1.676	6.275	-1.886	1.733
	(0.00,1.7×10^7)	(-5.02,3.31)	(-27.79,24.44)	(-10.04, 22.59)	(-13.81,10.03)	(-26.05,29.52)
4-3	0.016	-0.155	-0.170	-3.511	-0.876	5.045
	(0.00,6.4×10^5)	(-1.86,1.55)	(-3.82,3.48)	(-44.78,37.76)	(-2.66,0.91)	(-22.16,32.25)
3-4	0.087	-0.112	3.983	2.999	0.045	-6.220
	(0.00,62160)	(-2.39,2.17)	(-11.35,19.32)	(-76.00,82.00)	(-2.45,2.54)	(-31.91,19.47)
5-4	33.10	2.066	-0.747	2.262	4.474	-2.862
	(1.70,646.6)	(-2.13,6.26)	(-4.64,3.14)	(-4.60,9.13)	(-14.44,23.39)	(-6.31,0.59)
4-5	0.391	1.325	1.194	1.139	9.631	4.901
	(0.00,6.4×10^6)	(-3.72,6.37)	(-6.99,9.38)	(-104.8,107.1)	(-14.46,33.72)	(-22.64,32.44)
1-6	0.00001	3.629	4.391	5.611	7.438	-5.012
	(0.00,2250)	(-17.79,25.05)	(-20.41,29.19)	(-24.66,35.88)	(-10.67,25.55)	(-27.97,17.94)
2-6	0.0008	1.016	-7.171	3.841	-5.261	-6.132
	(0.00,13570)	(-12.27,14.30)	(-29.60,15.26)	(-25.32,33.01)	(-33.28,22.76)	(-31.85,19.58)
3-6	0.002	-5.258	0.547	2.756	-5.970	-4.659
	(0.00,78330)	(-27.28,16.77)	(-35.6,36.71)	(-23.54,29.05)	(-33.08,21.14)	(-30.09, 20.77)
4-6	0.002	-0.014	-0.830	-0.568	-1.309	0.819
	(0.00,1.9×10^7)	(-54.22,54.19)	(-58.09,56.43)	(-492.9,491.8)	(-77.77,75.15)	(-312.8,314.5)
5-6	0.008	-3.167	0.064	-0.332	-4.967	3.244
	(0.00,583500)	(-21.93,15.59)	(-27.55,27.68)	(-162.3,161.6)	(-33.53,23.59)	(-18.83,25.32)

-2Log-likelihood: 1556.29

The estimated parameters in Table 9.4 have narrow confidence intervals for transitions that took place between live states: transitions from i to j, where j is not an absorbing state. Transitions to death have wider confidence intervals. For transitions between live states, the estimated parameters for the orthogonal CD4 cell count covariate have narrow confidence intervals, indicating that the inclusion of the orthogonal CD4 cell counts covariate gives rise to more precise estimates than the first model. The model with the orthogonal CD4 cell counts covariate has a lower -2xLog-likelihood than the model without the covariate.

Figure 9.3 shows the percentage prevalence plots for each of the states given that CD4 cell count residual is included in the model. Figure 9.3 helps in assessing whether the expected percentage prevalence gives a better fit of the observed prevalence in the death state (state 6) compared to the results in Figure 9.2.
The results from Figure 9.3 show that, if HIV progression is defined by viral load states with the inclusion of the orthogonal CD4 cell counts covariate, this results in

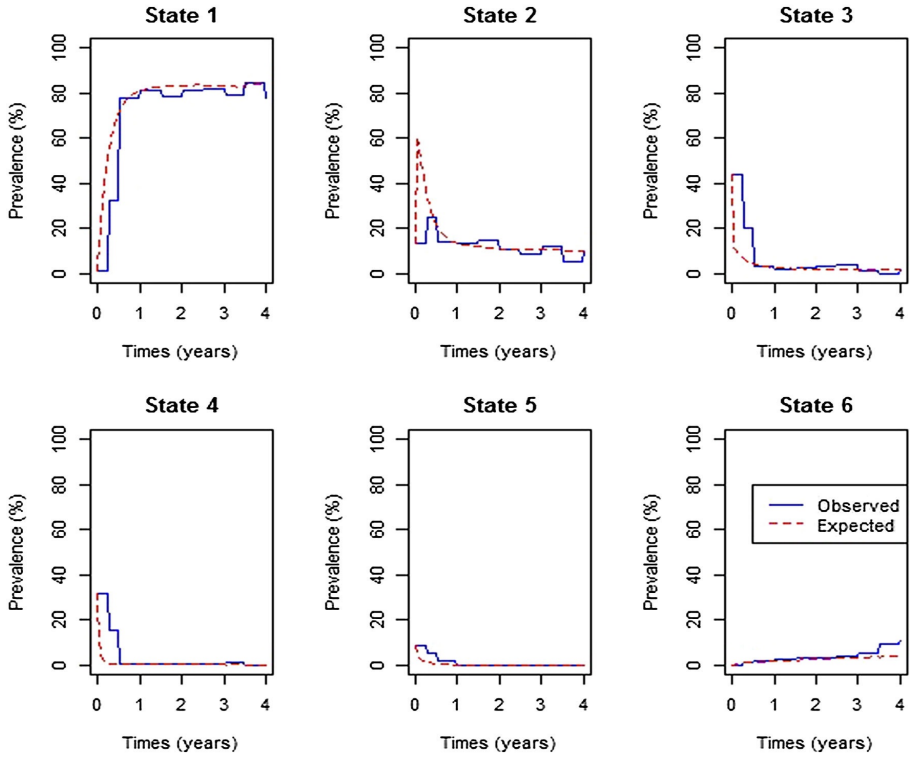

Figure 9.3 – *Percentage prevalence plots for continuous-time-homogeneous Markov model in which the CD4 cell counts orthogonal component is included as a covariate.*

a better fit of the observed prevalence. As a result, for the death state, the expected percentage prevalence state explains the observed percentage prevalence better than the model without the orthogonal CD4 cell counts covariate.
From both models represented by by plots in Figure 9.2 and Figure 9.3, cumulative deaths by the end of four years of treatment uptake had increased to close to 40% and 20%, respectively. However, from the data only 60 out of 320 deaths were recorded throughout the whole study period which is approximately equal to 18.8%. Therefore, we conclude that inclusion of the orthogonal CD4 cell count variable gives a better prediction of survival of HIV-infected patients on cART.

9.4.3 Assessment of the fitted models

The fitted models were assessed to identify the model that best describes the data. Assessment of the fitted models is carried out using the likelihood ratio test and estimates of AICs. The model with the lowest AIC is considered as the best model for the observed data. Table 9.5 shows the results.

The likelihood ratio tests from Table 9.5 show that the continuous-time-homogeneous

Table 9.5: Likelihood ratio test for the fitted models.

Likelihood ratio test for the models	**Preferred model**	**LRT statistic**	AIC	**df**	**p**
Without orthogonal CD4 versus with orthogonal CD4	With orthogonal CD4	934.425	1703.676	26	< 0.0001
With orthogonal CD4 versus with orthogonal CD4 and gender	With orthogonal CD4 and gender	951.803	1712.298	39	< 0.0001
	without orthogonal CD4		2586.101		

Markov model defined by viral load count states with the orthogonal CD4 cell counts covariate, and including the gender variable, gives the best fit to the data. However, since the interest is in the lowest AIC for our model, the model with the orthogonal CD4 cell counts covariate, while excluding the gender variable, is the best model. Thus, a gender difference was not a good predictor of HIV progression based on viral load count states together with the orthogonal CD4 cell counts covariate.

9.5 Concluding Remarks

In this chapter, a time-homogeneous Markov model has been developed to explain and predict the probability of death for HIV/AIDS patients. The states of the Markov model were based on viral load levels. A time-homogeneous model for the effects of VLBL, NA, gender and age with the orthogonal CD4 cell count covariate included, is fitted. Construction of the orthogonal CD4 cell counts covariate used the principal component approach to address the issue of collinearity of the viral load and the CD4 cell counts covariates. The orthogonal CD4 cell counts covariate was included so that HIV mortality is explained and predicted in a better way.

The findings from this chapter reveal the importance of Principal Components Approach in treating collinearity of the viral load counts and CD4 cell counts covariates when both are in the one model. As a result, it was observed that having lower CD4 cell counts than expected results in accelerated risks of viral rebound from undetectable viral load levels, and also accelerated deaths from undetectable viral load levels. Thus, higher CD4 cell counts improve the health and consequently the survival of HIV/ AIDS patients. The inclusion of both viral load counts and CD4 cell counts in the one model gives a better prediction of mortality.

The next chapter concludes the whole thesis and highlights future research directions.

Chapter 10

Conclusion

10.1 Introduction

In this thesis, different continuous-time Markov models were fitted using data from a Wellness clinic in Bela Bela, South Africa, to model the progression of HIV/AIDS in patients receiving combination anti-retroviral therapy (cART). The choice of a continuous-time model over discrete-time is based on the fact that in disease modelling, the exact time in which a patient makes a transition is not known. These states are assumed to be interval censored, so by making the intervals between these transitions relatively small, continuous-time Markov models are appropriate. Continuous-time Markov models are good at handling interval censored data. Continuous-time Markov models are based on states that define severity of the disease. Progression of HIV/AIDS is defined by transitions between states. In this thesis, transitions are bi-directional, that is, allowing forward or backward movements between states. Forward transitions define immune deterioration or virologic rebound and backward transition define immune recovery or virologic suppression, depending on whether the states are CD4 cell count based or viral load count based, respectively. Thus, backward transitions indicate effectiveness of cART. Findings from this thesis help in decision making regarding monitoring and management cART in HIV/AIDS patients for the improvement of the lifestyle of patients and ultimately reducing rates of mortality.

10.2 Summary and Concluding remarks

A continuous-time homogeneous Markov approach to the modelling of HIV/AIDS progression with states based on CD4 cell counts is important when analysing HIV/AIDS immunology when TB co-infection is of interest, as observed in Chapter 4. The fitted model was used to explore predictors of HIV/AIDS immunological progression

for patients on combination anti-retroviral therapy. Some of the predictors include age, gender, baseline viral load count, baseline CD4 cell count, developing active TB before cART initiation, and developing active TB after cART initiation. Of interest in Chapter 4, was the analysis of the effects of TB co-infection on HIV/AIDS progression.

Findings from Chapter 4 established the importance of the inclusion of the effects of covariates when fitting time-homogeneous Markov models for HIV/AIDS progression based on CD4 cell count (immunological) sates. Fitting Markov models with covariates improves the efficiency of the model (likelihood ratio test for inclusion of covariates had a $p - value < 0.0001$). Although patients who developed TB during the course of treatment have higher chances of immune deterioration than immune recovery compared to those who did not develop any TB co-infection (particularly when the immune system is still weak), the findings show that transition rates to immune recovery are generally higher than the transition rates to immune deterioration. However, findings reveal that the strongest predictor of immune deterioration from a CD4 cell count level greater than 750 to a CD4 cell count level between 500 and 750 is reaction to treatment. These patients are 4 times more likely to make transitions from a CD4 cell count level greater than 750 to a CD4 cell count level between 500 and 750 than those who did not react to treatment. Patients who had initially been diagnosed with TB before commencement of ART and received the treatment recover better from HIV/AIDS disease. However, for these patients, rates of transitions to death for patients with CD4 cell count between 350 and 500 cells/mm^3 are two times higher than that of patients who were not initially diagnosed with TB.

Another observation from Chapter 4 was that, although transitions to immune recovery are generally higher than transitions to immune deterioration, male patients had higher rates of immune deterioration than their female counterparts. This is quite pronounced in transitions from a CD4 cell count between 500 and 750 to a CD4 cell count between 350 and 500, where the hazards for males are 6 times more than that of females. This result is consistent with the findings from Maskew et al. (2012), who argued that males gain fewer CD4 cell counts than their female counterparts. An assessment of published studies by Castilho, et al., 2014 from both resource-limited and resource-rich countries, suggests an improved survival outcome for females than males. However, their study does not show a clear sex disparity in the disease progression or in treatment effects of viral suppression and immunologic recovery.

Patients who started treatment when their baseline CD4 cell count was at least 350 cells/mm^3 had higher rates of immune recovery than those who had a lower CD4 cell count at baseline. In their study, Moore and Keruly (2007), established that patients with baseline CD4 cell count above 350 cells/mm^3 returned to nearly normal CD4 cell count after 6 years. Findings from Chapter 4 further reveal that transitional probabilities to death for HIV/AIDS patients increase with decreasing CD4 cell counts of the individual at enrolment. This is supported by the findings of Biadgilign et al. (2013); Goshu et al. (2013); and Lifson et al. (2012), who also concluded that being in the AIDS defining stage leads to the highest probability of reaching the death state. The AIDS defining state is the most severe HIV/AIDS state and is normally defined by CD4 cell count below 200 cells/mm^3 (The Opportunistic Infections Project Team of the Collaboration of Observational HIV Epidemiological Research in Europe (COHERE), 2012).

Patients below the age of 45 years had higher chances of immune recovery than the older ones. This finding is supported by some previous researchers who observed lower mean CD4 cell count increases for older patients than younger patients (Maskew et al., 2012; Hasibi et al., 2014). Alioum et al. (1998) further argue that this could be caused by the fact that older subjects may have a reduced capacity to generate CD4 cells in response to the viral killing. The highest mean sojourn times were revealed in the AIDS state (CD4 cell count below 200 cell/mm^3). This means that HIV/AIDS patients receiving cART spend most of their time in the AIDS defining states before recovering to higher CD4 cell count states.

CD4 cell count has been identified to be an essential component in monitoring HIV treatment outcome. However, CD4 cell count monitoring sometimes fails to predict virologic failure, resulting in unnecessary switch of treatment lines, which causes drug resistance and limitations of treatment options (Reynolds et al., 2009). Since the goal of cART is to suppress the viral load levels to undetectable levels in HIV/AIDS patients, progression of HIV/AIDS is best monitored using viral load counts (WHO, 2018). Thus, in Chapter 5, a non-homogeneous continuous-time Markov model based on viral load states is fitted to analyse the effect of time on the progression of HIV/AIDS patients and also to investigate any possibilities of viral load rebound, as well as the time in which viral load rebound takes place. Non-homogeneous Markov models are preferred when modelling disease progression because the time-homogeneous Markov assumption of constant hazard function is frequently unrealistic (Lange et al., 2015) and puts limitations on the disease history behaviour (Saint-Pierre et al., 2003), especially on HIV/AIDS progression for patients on cART. Some studies have shown that if a patient responds well to treatment and manages to

achieve viral load suppression within the first 6 months, that patient is likely to continue responding well to treatment (Maartens et al., 2012). This goes against the Markov and memoryless properties of the models, showing a limitation in the application of time homogeneous Markov processes.

In Chapter 5, a piece-wise constant approach to non-homogeneous Markov modelling is used. The model reveals that viral load based transition intensities do not follow a constant rate, rather, two trends in the progression of HIV are shown. The first trend is in the first 6 months of treatment uptake, which shows a decline in percentage prevalences in viral load levels above 10 000 copies/mL and an increase in percentage prevalences of undetectable viral load levels. A study by Silveira et al. (2002) also indicates that most patients on cART reach the undetectable viral load in the first 6 months of treatment uptake. After 6 months of treatment uptake, percentage prevalences of the undetectable viral load states show a slightly decreasing trend, which is a sign that HIV/AIDS patients are likely to experience virologic failure.

Transitions within the 5 live states defined by viral load had narrow confidence intervals, indicating precision of the model in predicting transitions rates between live states. The results show a significant reduction of mortality from 6 months of treatment uptake onwards for patients who have achieved an undetectable viral load. This calls for the need to closely monitor HIV/AIDS patients to ensure that viral load suppression is reached within the first 6 months of treatment uptake and maintained to reduce mortality rates. Chapter 5 also reveals possibilities of viral rebound from almost every viral load state. Thus, in Chapter 6, assessment of the determinants of viral rebound on patients receiving cART is done.

Antiretroviral therapy (ART) has become the standard of care for patients with HIV infection in South Africa and has led to the reduction in AIDS-related morbidity and mortality. In developing countries, the nucleotides reverse transcriptase inhibitors (NRTIs) class are widely used because of their low production costs. However, patients treated with NRTIs develop varying degrees of toxicity after long-term therapy. For this study, patients are administered with a triple therapy of two NRTIs and one non-nucleotide reverse transcriptase inhibitor (NNRTI). In Chapter 6, the progression of HIV in vivo was divided into some viral load states and a continuous time-homogeneous model was fitted to assess the determinants of viral rebound, namely gender, age, baseline CD4 cell count, baseline viral load, lactic acidosis, peripheral neuropathy, non-adherence and resistance to treatment. Effects of different drug combinations on transition intensities were also assessed.

Four nested continuous-time homogeneous Markov models were fitted. The first one had no effects of covariates, the second one had the log-linear effects of covariates without combination therapy, the third one had the log-linear effects of different combination therapy, and the last one had the log-linear effects of all covariates including combination therapy. The fitted models were assessed using the AICs for each model, percentage prevalences in each state and pairwise likelihood ratio test for the goodness of fit. The continuous-time Markov model with all covariates including combination therapy had the lowest AIC, an indication that it gives the best fit of the data than all the other models. This was further confirmed by the likelihood ratio test which showed that the model with all covariates including combination therapy fits significantly better than any other model nested within it. Exclusion of covariates had caused some irregularities in predicting mortality, which was corrected after the inclusion of covariates effects in the fitted model.

In Chapter 6, relatively higher transition rates to viral suppression than transitions to viral rebound were observed. However, although close to 80% of the individuals had their viral load suppressed to undetectable levels in the first year of treatment uptake, some viral rebound were also notable, particularly from state 2 (viral load level between 50 and 10 000 copies/mL) to state 3 (viral load level between 10 000 and 100 000 copies/mL). Further analysis shows that this rebound was accelerated by non-adherence to treatment, lactic acidosis and resistance to treatment. However, for patients who developed peripheral neuropathy, there was an accelerated transition to viral rebound from state 2. For these patients when the viral load is above 100 000 copies/mL, there are reduced rates of viral suppression. This corroborates work done by Simpson (2002) who argued that greater incidences of peripheral neuropathy are in the strata of patients with plasma HIV RNA levels greater than 10 000 copies/ mL. Patients who initiated treatment therapy with a viral load level above 10 000 copies/mL also had some notable viral rebound from state 2 (viral load level between 50 and 10 000 copies/mL) to state 3 (viral load level between 10 000 and 100 000 copies/mL). Considering the different combination therapy administered to patients, rates of viral rebound are greater than the rates of viral suppression, especially for patients who were administered with FTC-TDF-EFV. Higher rates of mortality are recorded for patients with viral load level between 50 and 10 000 copies/mL, but from all the other viral load states, mortality rates are relatively low. In particular, for patients with viral load level between 10 000 and 500 000 copies/mL, lowest transition rates were recorded, especially for patients administered with d4T-3TC-EFV and AZT-3TC-EFV.

When the states of the Markov model are based on viral load, disease progression is

faster on patients below the age of 45 years, compared to patients over 45 years in the cohort. However, the opposite is true when the Markov model is based on CD4 cell count as shown in Chapter 4, where older patients take more time to recover than younger patients. This shows that older patients have a better understanding of the treatment therapy, resulting in a better adherence to the treatment therapy. On the other hand, young patients have substantial challenges in achieving level of adherence necessary for successful therapeutic outcomes. The results are corroborated by the findings from a study that was carried out in Tehran, Iran, which showed that mean CD4 cell count increments after initiation of anti-retroviral therapy are lower on older patients (Hasib et al., 2014). Prior to this study, a study that was carried out in Greece showed higher magnitudes of absolute CD4 cell count among patients 50 years and older (Metallidis et al., 2013). The results also reveal that although HIV/AIDS patients generally take longer to reach a normal CD4 cell count compared to the time taken to reach an undetectable viral load, for patients below the age of 45 years once the CD4 cell count is normal, mortality risks are reduced.

From a viral load level between 10 000 and 100 000 copies/mL, rates of viral suppression are higher than the rates of viral rebound, particularly for patients administered with d4T-3TC-EFV. A baseline CD4 cell count below 300 cells/mm^3 accelerates viral rebound rates from a viral load level between 10 000 and 100 000 copies/mL to a viral load level between 100 000 and 500 000 copies/mL. This is also the case with patients below the age of 45 years.

Non-adherence accelerates viral rebound for patients with viral load levels between 100 000 and 500 000 copies/mL. This is also supported by Keiser et al. (2011) who, in their findings, proposed that viral load monitoring promotes motivation to stay in care and adherence to treatment. This supports the issues raised by Chesney (2000), that without proper adherence, anti-retroviral agents are not maintained at sufficient concentration to suppress HIV replication. Hence there is need to have a proper patient-health-care provider relationship and also count check of the pills by asking patients to bring their pill packs, including the empty ones.

However, assuming that the patient was initially in the undetectable viral load state, he is expected to spend approximately 18.5 years in that state, before death. This is evidenced by the fact that throughout the 5 year study period, only 17.8% of the patients were reported dead, with 10.9 points occurring during the first 6 months.

Hence, the need to administer HIV drug regimens is better based on the viral load level of a patient. This is also supported by Keiser et al. (2011) who, in their find-

ings, observed that people living with HIV and on antiretroviral therapy with routine viral load monitoring have better health outcomes than people monitored with CD4 testing alone. Before initiation of treatment, patients should be well equipped on how anti-retroviral drugs operate, including possibilities of toxicity, in order to reduce chances of non-adherence to treatment. There should also be a good relationship between patient and health-care-giver to ensure proper adherence to treatment. Uptake of therapy by young patients should be closely monitored by adopting pill counting every time they come for review.

Although in some resource limited countries viral load count may be expensive to test, in some cases both viral load results and CD4 cell count results may be available. In Chapter 7, the use of either CD4 cell count or viral load in monitoring HIV/AIDS patients in order to examine the superiority of viral load over CD4 cell count in modelling HIV/AIDS progression for patients on anti-retroviral therapy is examined. This is done by fitting two separate continuous-time homogeneous models, one based on viral load states and the other based on CD4 cell count states. These two models are compared based on the observed and expected percentage prevalences for each model. From this study, we observed no gender effects on the progression of HIV/AIDS when viral load levels in the plasma is used as a surrogate marker. The results showed that significant gender differences are only shown when CD4 cell count is the surrogate marker of HIV progression. Previous findings by Dounelly et al (2005) also demonstrate that women had non-significant lower viral loads than men and that gender only has a significant effect when CD4 cell count is the marker of HIV/AIDS progression.

Findings from Chapter 7 also show that although both CD4 cell count and viral load are the surrogate markers of HIV progression, viral load is more powerful in monitoring progression of HIV/AIDS in patients on anti-retroviral therapy than CD4 cell count. The models for viral load with and without the inclusion of covariates give a better fit compared to the models for CD4 cell count. This point coincides with WHO recommendations that advise the use of viral load monitoring as a routine procedure in the management of HIV infection. WHO goes further and argues that in cases of treatment failure, where viral load testing is not routinely available, CD4 cell count should be used to diagnose treatment failure (WHO, 2017). Also to note from the findings is that, deaths are better explained in the model for viral load monitoring than in the model for CD4 cell count. This contradicts with findings from previous studies, that CD4 cell count is a better predictor of HIV/AIDS progression than viral load count (Miller et al., 2002; Brown et al., 2009; Ghadha et al., 2013).

Although viral load monitoring in predicting HIV/AIDS progression gives the clients a measure of understanding, control and motivation to adhere to treatment and understanding their HIV infection (WHO, 2017), basing on findings from Chapter 7 we recommend the use of both viral load monitoring and CD4 cell count monitoring since viral load determines the need for treatment change and CD4 cell count helps in monitoring the risk of opportunistic infection (OI) and treatment failure. From this study, one can also conclude that although patients take more time to achieve a normal CD4 cell count and less time to achieve an undetectable viral load, once the CD4 cell count is normal, mortality risks are reduced. Therefore, both viral load counts monitoring and CD4 cell counts monitoring can be used to contribute significantly to the improvement in the life expectancy of patients living with HIV.

The Markov models that were fitted in Chapter 7, CD4 cell count based or viral load based, show wider confidence intervals for the estimated transition rates to death. This indicates lack of efficiency of the model in explaining and predicting mortality. In Chapter 8, both CD4 cell count and viral load variables were in one model. A Principal Component Approach was used to incorporate both CD4 cell count and viral load monitoring of HIV/AIDS progression in a single continuous-time homogeneous Markov model. The model is improved by including an orthogonal viral load covariate derived from principal component analysis. Principal Component Analysis is a technique used to combine highly correlated factors into Principal Components that are much less correlated with each other, CD4 cell count and viral load in this case. This improves the efficiency of the model. Principal Component variables are created by fitting a regression model of viral load count on CD4 cell count. The new orthogonal covariate is included to represent the viral load covariate for the Markov model defined. This orthogonal viral load covariate helps to explain a component of mortality/transition, that could not be explained by the CD4 cell count alone.

Results from the likelihood ratio test show that the model with the orthogonal viral load covariate fits significantly better than the model with the exclusion of viral load. Thus, the orthogonal viral load covariate along with CD4 cell count at baseline, gender, non-adherence and age play a significant role in modelling HIV/AIDS progression based on CD4 cell counts states and viral load monitoring.

Results from the analysis show that when CD4 cell count is below 500 cells/mm^3, rates of immune recovery are higher than rates of immune deterioration, particularly for younger patients aged 45 years and below. However, when the CD4 cell counts are between 500 and 800 cells/mm^3, the rate of immune deterioration is higher than

the rate of immune recovery and this was mainly attributed to patients who were non-adherent to treatment and patients who initiated therapy with a CD4 cell count at baseline below 200 cell/mm^3. Once the CD4 cell count is above 800 cells/mm^3, the results show a possibility of immune deterioration, although the magnitude is very low, mainly due to non-adherent to treatment. This contradicts the finding from a previous study that was carried out in India, which revealed higher rates of immune recovery than immune deterioration, regardless of the HIV/AIDS state of the patient (Gurprit et al., 2013).

The results show that having a lower viral load than expected (orthogonal viral load=negative residual) results in a reduction in immune deterioration from a CD4 cell count state above 800 cells/mm^3 and an increase in the rate of immune recovery from the CD4 cell counts are between 500 and 800 cells/mm^3 to a CD4 cell count state above 800 cells/mm^3 for younger adults aged 45 years and below. Generally, these patients experienced higher rates of immune recovery than immune deterioration, compared to patients who are over 45 years. This concurs with findings from previous studies (Hogg et al., 2001). This is also in agreement with a previous study carried out in Tehran, India, that showed that mean CD4 cell count increments after initiation of combination therapy are lower on older patients (Hasibi et al., 2014).

For patients whose viral load level is lower than the expected given their CD4 cell count state, there was a reduction in transition to deaths. This means that for given levels of CD4 cell count, the patients ought to have more viral load, but they have less, resulting in reduction in mortality.

This study shows the importance of using both CD4 cell count and viral load in the same model for monitoring progression of HIV/AIDS patients on anti-retroviral therapy. By including both variables, the model reveals that, for given levels of CD4 cell count, there is the possibility of reduction of mortality for patients whose viral load is lower than expected given their CD4 cell count. Progression to death was more pronounced on patients who have achieved normal CD4 cell counts and this is experienced mainly in younger patients, non-adherent patients and also for patients whose initial CD4 cell counts were below 200 cells/mm^3. This study will help to uncover the critical areas of dealing and correcting for collinearity when including both CD4 cell count and viral load in multi-state modelling of HIV/AIDS that many researchers were not able to explore. Thus a new application of theory and better understanding of the Principal Component Approach when dealing with both CD4 cell counts and viral load counts (in the same model) to HIV/AIDS modelling may be arrived at.

In Chapter 9, the same methods as those in Chapter 8 are used, but the difference being that the orthogonal variable is the CD4 cell count and the states for the fitted model are based on viral load count. The Principal Component Approach helps in making the model more effective and also to explain the aspect of mortality which could not be explained by either CD4 cell count alone or viral load alone.

This resulted in the variable age contributing significantly to the HIV/AIDS progression. For the viral load based model, the gender variable had significant effects after adjusting the scaling factor from 4 000 to 5 000 to ensure convergence of the optimisation process. However, Randarajan et al. (2016), in their study, reveal the non-significant effects of the gender variable in viral suppression.

The results from the analysis show that, if HIV progression is defined by viral load states without including CD4 cell count in the model, the expected percentage prevalence underestimates mortality from a period of 0.5 years of treatment uptake. This resulted in a death prevalence of over 40%, which is unrealistic, considering that patients were on cART. The orthogonal CD4 cell counts covariate was then included in the continuous-time Markov model defined by viral load levels and HIV mortality is explained and predicted in a better way. The results from the fitted model show an improvement in the -2xLog-likelihood compared to the model without the orthogonal CD4 cell counts covariate. The model also has the lowest AIC. The death prevalence from this model was reduced to below 20%.

The results also show high risks of viral rebound from undetectable viral load levels, which was mainly caused by non-adherence to treatment, having negative CD4 cell count residuals and starting therapy when the VLBL was above 10 000 copies/mL. Having CD4 cell counts that are lower than expected increases the rates of viral rebound from undetectable levels. These findings are also corroborated by a study by Silveira et al. (2002) which shows that a higher prevalence of undetectable viral load levels has been associated with lower levels of VLBL at the beginning of treatment. This supports the issues raised by Chesney (2000) that, without proper adherence, anti-retroviral agents are not maintained at a sufficient concentration to suppress HIV replication. Pasternak et al. (2012), in their study, also demonstrated that incomplete ART adherence is associated with increased levels of cell-associated HIV-1 RNA.

Findings also showed high risks of mortality from the undetectable viral load for non-adherent patients, patients who initiated therapy with a viral load level above

10 000 copies/ mL, younger patients below the age of 45 years and patients whose CD4 cell counts were lower than expected. This may be explained by findings by Mujugira et al. (2016), whose study reveals delayed ART initiation, failure to achieve viral suppression, and virologic rebound among young patients.

10.3 Summary of the key findings

The key findings of this research are as follows:

1 Patients who developed active TB during the course of treatment have higher chances of immune deterioration than immune recovery, compared to those who did not develop any TB co-infection especially when the immune system is still weak (below 350 cell/mm^3. Patients who were initially diagnosed with TB have double the chances of transitions to death than patients who were not initially diagnosed with TB. This is notable for CD4 cell counts between 350 and 500 cells/mm^3. Thus, the study recommends constant screening for TB co-infection for patients on anti-retroviral drugs.

2 Although the fitted models show that viral load is superior over CD4 cell count in monitoring and management of cART in HIV infected patients, there is need to include the CD4 cell count variable in the monitoring process so that any possibility of co-infections that take advantage of the suppressed immune system is guarded against. Hence there is need to use both viral load and CD4 cell count monitoring and in the management of cART.

3 Inclusion of both CD4 cell count monitoring and viral load monitoring in one model after treating for collinearity helps in explaining the component of mortality which one variable can not explain on its on without the inclusion of the other variable.

4 Viral load rebound was notable, particularly from state 2 (viral load level between 50 and 10 000 copies/mL) to state 3 (viral load level between 10 000 and 100 000 copies/mL) and this was accelerated by non-adherence to treatment, lactic acidosis and resistance to treatment.

5 Transition intensities among viral load states change with time, thus HIV progression can best be described using non-homogeneous continuous-time Markov models. In this thesis, time inhomogeneity is addressed using the piece-wise constant approach to Markov modelling.

10.4 Limitations of the thesis

The results from this thesis are based on data collected from a Wellness clinic in Bela Bela in the Northern part of South Africa. It would have been interesting to analyse data from all provinces of South Africa. However, absence of routinely collected data on viral load monitoring caused severe limitations to the study. Viral load is more expensive to measure than CD4 cell count.

The analysis is based on a retrospective set of data. Information on other comorbidities or opportunistic infections in AIDS was not available, so the observations should be understood in the context of these limitations. The intended outcome of combination antiretroviral therapy is to suppress viral loads to undetectable levels, in the absence or presence of comorbidities.

The exponential distribution is a memoryless continuous distribution, hence a limitation in the application of Markov processes. The 'memoryless' property could be seen as a problematic assumption in this setting. It is likely the case that patients starting on ART who respond well to treatment will continue to respond well to treatment - contradicting the Markov assumption and the memoryless property.

10.5 Future research directions

The results of this thesis provide possible areas for future research. The following possible future research directions are proposed:

This thesis used a Markov model in analysing progression of HIV in vivo, that is, individual level. In future, the study recommends application of Multi-level analysis of HIV progression. This approach analyses progression of HIV between different societal clusters, for example, starting progression at individual level then village level, school level, district level, provincial level and finally national level.

References

Abner EL, Nelson PT, Schmitt FA, Browning SR, Fardo DW, Wan L, Jicha GA, Cooper GE, Smith CD, Caban-Holt AM, Van Eldik LJ, Kryscio RJ. Self-reported head injury and risk of late-life impairment and AD pathology in an AD center cohort. *Dement Geriatr Cogn Disord*, 2014; 37: 294-306.

Alioum A, Leroy V, Commenges D, et al. Effects of gender, age, transmission category, and antiretroviral therapy on the progression of human immune virus infection using multistate Markov models. *Group d'Epidemiologie clinique du SIDA en Aquitaine, Epidemiology.* 1998; 9(6): 605-12.

Alizon S. and Magnus C. Modelling the course of an HIV infection: Insights from Ecology and Evolution, *Viruses*, 2013; (4): 1984-2013, *doi: 10.3390/v4101984*.

Babinska M, Chudek J, Chelmecka E, Janik M, Klimek K and Owczarek A. Limitations of Cox Proportional Hazards Analysis in Mortality Prediction of Patients with Acute Coronary Syndrome. *Studies in Logic Grammar and Rhetoric*, 2015; 43(56): 33-48. DOI: https://doi.org/10.1515/slgr-2015-0040

Battegay M, Nesch R, Hirschel B, Kaufmann GR. Immunological recovery and antiretroviral therapy in HIV-1 infection. *Lancet Infect Dis.*, 2006; 6(5): 280-7.

Berestycki N and Sousi P. Applied Probability. March 6, 2017. Accessed from http://www.statslab.cam.ac.uk/ ps422/notes-new.pdf on 13 June 2019.

Biadgilign S, Reda AA, Digaffe T. Predictors of mortality among HIV infected patients taking antiretroviral treatment in Ethiopia: A retrospective cohort study. *AIDS Res Ther.* 2012; 9: 15 https://doi.org/10.1186/1742-6405-9-15.

Binquet C, Le Teuff G, Abrahamovicz M, Mahboubi A, Yazdanpanah Y, Rey D, Rabaud C, Chirouze C, Berger JL, Faller JP, Chavanet P, Quantin C, Piroth L, Groupe

InterCOrevih du Nord-Est (ICONE). Markov modelling of HIV infection evolution in the HAART era. *Epidemiol Infect.* 2009; 137(9): 1272-82. https://doi.org/10.1017/S0950268808001775. Epub 2009 Jan 12

Bommae K. Understanding diagnostic plots for linear regression analysis. University of Virginia library. 2015. Accessed from: https://data.library.virginia.edn

Brennan AT, Maskew M, Sanne I, and Matthew P Fox MP. The interplay between CD4 cell count, viral load suppression and duration of ART on mortality in a resource-limited setting. *Trop Med Int Health.* 2013; 18(5): 619-31. https://doi.org/10.1111/tmi.12079.

Brown ER, Otieno P, Mbori-Ngacha DA, Farquhar C, Obimbo EM, Nduati R, Overbaugh J, and John-Steward GC. Comparison of CD4 cell count, viral load and other markers for the prediction of mortality among HIV-1 - Infected Kenyan pregnant women. *The Journal of Infectious Diseases.* 2009; 199: 1292-300.

Case KK, Ghys PD, Gouws E, Eaton JW, Borquez A, Stover J. Understanding the modes of transmission model of new HIV infection and its use in prevention planning. Bull. *World Health Organ* 2012; 90: 831-838.

Cassels S, Clark SJ and Morris M. Mathematical Models for HIV Transmission Dynamics: Tools for Social and Behavioral Science Research. *J Acquir Immune Defic Syndr*. 2008 March 1; 47(1): 34-39. doi:10.1097/QAI.0b013e3181605da3.

Castilho JL, Melhekin VV, Sterling TR. Sex Differences in HIV Outcomes in the Highly Active Antiretroviral Therapy Era: A Systematic Review. *AIDS Res Hum Retroviruses.* 2014; 30(5): 446-56. https://doi.org/10.1089/aid. 2013.0203.

Chaiyachati KH, Ogbuoji O, Price M, Suthar AB, Negussie EK, Barnighausen T. Interventions to improve adherence to antiretroviral therapy: a rapid systematic review. *AIDS*. 2014; 28(2): 187-204.

Charlebois DA, Ribeiro AS, Lehmussola A, Lloyd-Price J. Effects of microarray noise on inference efficiency of a stochastic model of gene networks. *WSEAS Trans Biol Biomed*, 2007; 4: 15-21

Carr A, Samaras K, Burton S, et al. A syndrome of peripheral lipodystrophy, hyperlipidaemia and insulin resistance in patients receiving HIV protease inhibitors. AIDS 1998;12:F51-F58.

Chen H and Chen J. Tests for homogeneity in normal mixture with presence of a structural parameter statist. Sinica 13: 351-365. MR1977730
Chenand B and Zhou Xiao-Hua. Non-homogeneous Markov process models with informative observations with an application to Alzheimer's disease. *Biom J*, 2011; 53(3): 444-463.

Chesney M. Factors affecting adherence to antiretroviral therapy. *Clin Infect Dis.* 2000; 30(2): 171-6.

Chiang CL. Introduction to Stochastic Processes in Biostatistics. *New York: Wiley*, 1968.

Chifurira R, Chikobvu D. A Weighted Multiple Regression Model to Predict Rainfall Patterns: Principal Component Analysis approach. *Mediterranean Journal of Social Sciences*, 2014; 5(7). DOI: 10.5901/mjss.2014.v5n7p34.

Chinen J and Shearer WT. Molecular virology and immunology of HIV infection. *J Allergy Clin Immunol*. 2002; 110(2): 189-198.

Cichocki M. What are CD4 T-cells and why are they important. *HIV/AIDS*. Updated December 18, 2018.

Cingolani A, Lepri AC, Castagna A, Goletti D, De Luca A, Scarpellini P, Fanti I, Antinori A, d'Armino Monfarte A, Girardi E. Impaired CD4 T-cell count response to combined antiretroviral therapy in antiretroviral-naive HIVinfected patients presenting with tuberculosis as AIDS-defining condition. *CID*, 2012; 54(6): 853-61.

Clemencon S, Tran VC and Arazoza H. A stochastic SIR model with contact-tracing: large population limits and statistical inference. *Journal of Biological Dynamics*, 2008; 2(4): 392-414, DOI:10.1080/17513750801993266

Coates TJ, Linda Richter L. and Caceres C, Behavioural strategies to reduce HIV transmission: how to make them work better. *Lancet*. 2008 August 23; 372(9639): 669-684. doi:10.1016/S0140-6736(08)60886-7.

Cole SR, Hernan MA, Anastos K, et al. Determining the effect of highly active antiretroviral therapy on changes in human immunodeficiency virus type 1 RNA viral load using a marginal structural left-censored mean model. *American Journal of Epi-*

demiology. 2007; 166(2): 219-227.

Cox DR. The statistical analysis of dependencies in point processes. In Stochastic Point Processes. *Wiley*; 1972.

Cox DR and Miller HD. The Theory of Stochastic Processes. *Chapman and Hall, London*, 1965.

Currier JS. Sex differences in antiretroviral therapy toxicity; lactic acidosis, Stavudine and omen. *Clin Infect Dis.*, 2007; 45: 261-2. https://doi.org/10.1086/ 518977.

Dalakas MC. Peripheral neuropathy and antiretroviral drugs. *J Peripher Nerv Syst.* 2001; 6(1): 14-20.

Dalal, N. and Greenhalgh, D. and Mao, X. A stochastic model for internal HIV dynamics. *Journal of Mathematical Analysis and Applications*, 2008; 341 (2): 1084-1101. ISSN 0022-247X , http://dx.doi.org/10.1016/j.jmaa.2007.11.005

Dessie ZG. Modeling HIV dynamics evolution using non-homogeneous semi-Markov process. *Springer Plus.* 2014; 3: 537.

Dounelly CA, Bartley LM, Ghani AC, Le Fevre AM, Kwong GP, Cowling BJ, van Sighem AI, de Wolf F, Rode RA, and Anderson RM. Gender differences in HIV-1 RNA viral loads. *HIV medicine.* 2005; 6(3): 170-178.

DUFFIN RP and TULLIS RH. Mathematical Models of the Complete Course of HIV Infection and AIDS. *Journal of Theoretical Medicine*, 2002; 4 (4): 215-221.

Erb P, Batlegay M, Zimmerli W, et al. Effect of antiretroviral therapy on viral load, CD4 cell count, and progression to acquired immunodeficiency virus - Infected cohort. *Arch Intern Med.* 2000; 160(8): 1134-1140. Doi:10.1001/archinte.160.8.1134.

Estill J, Aubriere C, Egger M, Johnson L, Wood R. Viral load monitoring of antiretroviral therapy, cohort viral load and HIV transmission in Southern Africa: A mathematical modelling analysis. *AIDS* 2012; 26: 1403-1413.

Faria, N.R. et al. The early spread and epidemic ignition of HIV-1 in human populations. *Science*, 2014; 346(6205): 56-61

Fennell P.G., Melnik S., Gleeson J.P. The limitations of discrete-time approaches to continuous-time contagion dynamics. *Phys. Rev. E* 94, 052125 Published 16 November 2016

Ford N, Mentjes G, Victoria M, Greene G, and Chiller T. The evolving role of CD4 cell count in HIV care. *Curr Opin HIV AIDS.* 2017; 12: 123-128. Doi:10.1097/COH.0000000000000348.

Foucher Y, Mathieu E, Saint-Pierre P, Durand JF, Daures JP. A semi-Markov based on generalised Weibull distribution with an illustration for HIV disease. *Biom J*. 2005; 6: 1-9.

Frerot M, Lefebvre A, Aho S, Callier P, Astruc K, Aho Glele LS (2018) What is epidemiology? *Changing definitions of epidemiology*, 1978-2017. PLoS ONE 13(12): e0208442. https://doi.org/10.1371/journal.pone.0208442

Gentleman RC, Lawless JF, Lindsey JC, Yan P. Multi-state Markov models for analysing incomplete disease history data with illustrations for HIV disease. *Statistics in Medicine*. 1994; 13: 805-821. [PubMed: 7914028]

Ghadha S, Bhalla P, Jha AK, Gautam H, Saini S, and Aneradha S. Diseases progression and antiretroviral therapy in newly seropositive HIV subjects in a tertiary care hospital in North India. *J Infect Dev Ctries.* 2013; 7(2): 110-115.

Gibson EL. Continuous time multi-state models for survival analysis. Winston-Salem: Wake Forest University, Department of Mathematics; 2008.

Goshu AT, Getahun D. Modeling progression of HIV/AIDS disease stages using semi-Markov processes. *J Data Sci* 2013; 11: 269-280.

Gouda and Powles. The science of epidemiology and the methods needed for public health assessments: a review of epidemiology textbooks. *BMC Public Health*, 2014; 14:139. http://www.biomedcentral.com/1471-2458/14/139

Gouws E., Modelling the impact of Antiretroviral therapy on HIV transmission, Current HIV reseach, *Bentham Science Publishers limited*, 2011; 9(6).

Greene WC. A history of AIDS: Looking back to see ahead. *Eur J Immunol* (2007); 37 (Suppl. 1): S94S102.

Grover G, Gadpayle KA, Swain PK, Deka B. A multistate Markov model based on CD4 cell count for HIV/AIDS patients on antiretroviral therapy (ART). *Int J Stat Med Res.* 2013; 2: 144-51.

Gurprit G, Adesh Kumar G, Prafulla KS, Barnali D. A multistate Markov model based on CD4 cell count for HIV/AIDS patients on antiretroviral therapy (ART). *Int J Stat Med Res* 2013; 2: 144-151.

Halim D. Maximum likelihood estimation for generalized semi-Markov processes. Discrete event dynamics systems: theory and applications. *Dep Ind Eng.* 1996; 6(2): 73-104.

Hasibi M, Hajiabdolbaghi M, Hamzelou S, Sardashti S, Faroughi M, Jozani ZB, Alinaghi SAS. Impact of age on CD4 response to combination antiretroviral therapy: a study in Tahran, Iran. *Orld J AIDS.* 2014; 4: 156-62.

Heesterbeek H, Anderson R, Andreasen V, Bansal S et al. Modeling infectious disease dynamics in the complex landscape of global health. *Science*. 2015 March 13; 347(6227): aaa4339. doi:10.1126/science.aaa4339.

Herbeck JT, Mittler JE, Gottlieb GS, Mullins JI. An HIV epidemic model based on viral load dynamics: value in assessing empirical trends in HIV virulence and community viral load. *PLoS Comput Biol* 2014; 10: 1003673.

Hirchhorn L, Beattie A, Davidson D and Agins B. The role of viral load as a measure of the quality of care for people with HIV: the expert meeting report. 2005.

Hoffman RM, Black V, Technau K. Effects of highly active antiretroviral therapy duration and regimen on risk for mother-to-child transmission of HIV in Johannesburg,South Africa. *J Acquir Immune Defic Syndr* 2010; 54: 35-41.

Hogg RS, Yip B, Chan KJ, wood E. Rates of disease progression by baseline CD4 cell count and viral load after initiating triple-drug therapy. *JAMA* 2001; 286: 2568-2577.

Hubbard RA and Zhou XH. A comparison of non-homogeneous Markov regression models with application to Alzheimers disease progression. J Appl Stat. 2011 ; 38(10): 23132326. doi:10.1080/02664763.2010.547567.

Ingram R. E., Nelson T., Steidtmann D. K., Bistricky S. L. Comparative data on child

and adolescent cognitive measures associated with depression Journal of Consulting and Clinical Psychology, 75 (3) (2007), pp. 390-403

Isham V. Lecture notes for LTCC Course on Stochastic Processes. Stochastic Processes, VSI, 2008-2009.

Jackson C., Multi-state modelling with R: the msm package Version 1.6.4. *MRC Biostatistics Unit.* 02 October, 2016

Jackson CH. Multi-state models for Panel Data: The msm package for R. *J Stat Softw.* 2013; 38(8). http://www.jstatsoft.org/.

Jackson C. Multi-state modelling with R: the msm package. Version 1.6.7. *MRC Biostatistics Unit.* 18 March, 2019.

Kalbfleisch JD, Lawless JF. The analysis of panel data under a Markov assumption. *J Am Stat Assoc*. 1985; 80(392): 863-71.

Kandathil A.J., Ramalingam S., Kannangai R. and David S. and Sridharan, G.. Molecular Epidemiology of HIV. Department of Clinical Virology, Christian Medical College, Vellore, India. *Indian J Med Res*, 2005; 121: 333-344.

Kay R. A Markov model for analysis of cancer markers and diseases states in survival studies. *Biometrics* 1986; 42: 855-865.

Keiser O, Chi BH, Gsponer T, Boulle A, Orrell C, Phiri S, et al. Outcomes of antiretroviral treatment in programmes with and without routine viral load monitoring in Southern Africa. AIDS. 2011;25:1-10.

Kharsany ABM, Quarraisha A and Karim QA. HIV Infection and AIDS in Sub-Saharan Africa: Current Status, Challenges and Opportunities. *The Open AIDS Journal*, 2016; 10, 34-48. DOI: 10.2174/1874613601610010034

Kore S and Waghmare CS. Anti retroviral therapy (ART)- induced lactic acidosis: A potentially life threatening but preventable complication in HIV/AIDS patients receiving Nucleoside Reverse Transcriptase Inhibitors (NRTIs). *Biomed Res-India* 2012; 23(4): 625-27

Kranzer K, Zeinecker J, Grinsberg P, Orrel C, Kalawe NN et al. Linkage to HIV care

and antiretroviral therapy in Cape Town, South Africa. *PloS One*, 2010; 5: e13801.

Lange JM, Hubbard RA, Inoue LYT, Minin VN. A joint model for multistate disease processes and random informative observation times, with applications to electronic medical records data. *Biometrics.* 2015; 71(1):90-101.

Langford S. E., Ananworanich J. and Cooper D. A. (2007), Predictors of disease progression in HIV infection: A review, *AIDS Research Therapy*,4:11 *doi:10.1186/1742-6405-4-11*.

Lecher S, Williams J, Fonjungo PN. Progress with scaleup of HIV viral load monitoring-seven sub-Saharan African countries, January 2015-June 2016. *Morbid Mortal Week Rep* 2016; 65: 47.

Lawless JF and Rad N. Estimation and assessment of markov multistate models with intermittent observations on individuals. *Lifetime Data Analysis*, 2015; 21 (2), 160179. DOI: 10.1007/s10985-014-9310-z.

Lee S, Ko J, Tan X, Patel I, Balkrishnan R, Chang J. Markov chain modeling analysis of HIV/AIDS progression: a race-based forecast in the United States. J *Ind Pharm Sci* 2014; 76: 107-115.

Libin R., Michael A. G., Zhilan F., Alan S. P. (2007). Modeling within-host HIV-1 dynamics and the evolution of drug resistance: Trade-offs between viral enzyme function and drug susceptibility. *Journal of Theoretical Biology*. Vol.247 pp 804-818.

Lifson AR, Krantz EM. Grambsch PL. Macalino GE. Crum-Cianflone NF. Ganesan A, Okulicz JF, Eaton A, Powers JH, Eberly LE, Agan BK. Clinical, demographic and laboratory parameters at HAART initiation associated with decreased post-HAART survival in a U.S. military cohort. *AIDS Res Ther.* 2012; 9(4).

Lihana R. W., Ssemwanga D., Abimiku A and Ndembi N. (2012). Update on HIV-1 Diversity in Africa: A Decade in Review. *AIDS Rev*. 2012; 14: 83-100.

Longini I.M. Jr., and Hudgens M.G. Lecture Notes on Stochastic Processes in Biostatistics: Applications to Infectious Diseases. Department of Biostatistics, Rollins School of Public Health, Emory University Atlanta. January 2003.

Longini IM, Clark WS, Byers RH, Ward J, Darrow WW. Statistical analysis of the

stages of HIV infection using a Markov model. *Stat Med.* 1989;8:831-43. DOI: 10.1002/sim.4780080708.

Maartens G, Cotton M, Meintjes G, Mendelson M, Rabie H, Maharaj S. Clinical guidelines 9th Edition. *Copyright Aids for AIDS management (Pty)* Ltd. 2012.

Maartens G., Celum C, Lewin SR. HIV infection: epidemiology, pathogenesis, treatment, and prevention. *Lancet.* 2014; 384: 258-71. http://dx.doi.org/10.1016/s0140-6736(14) 60164-1, Accessed 11 January 2018.

Mann, J.M. (1989). AIDS: A worldwide pandemic; in Current Topics in AIDS Volume 2, edited by Gottlieb, M.S. et al. *John Wiley and Sons*

Manoto SL., Lugongolo M., Govender U. and Mthunzi-Kufa P. Point of Care Diagnostics for HIV in Resource Limited Settings: An Overview. *Medicina* 2018, 54, 3; doi:10.3390/medicina54010003

Maskew M, Brennary AT, Westreich D, McNamara L, MacPhail P, and Fox MP. Gender Differences in Mortality and CD4 Count Response Among HIVPositive Patients Virally Suppressed Within 6 Months of Antiretroviral Therapy Initiation. *J Womens Health.* 2012; 22(00). https://doi.org/10.1089/jwh. 2012.3585.

Mathieu E, Foucher Y, Dellamanica P et al. Parametric and Non Homogeneous Semi-Markov Process for HIV Control. *Methodol Comput Appl Probab.* 2007; 9: 389-397. DOI: 10.1007/s11009-007-9033-7.

Mbogo R W (2013). Intra -Host stochastic models for HIV dynamics and management. A research thesis submitted for the degree of Doctor of Philosophy in Biomathematics to Strathmore University, Nairobi, Kenya, November 2013

Meira-Machado L., de Ua-lvarez J., Cadarso-Surez C, Per K Andersen. Multi-state models for the analysis of time-to-event data. *Stat Methods Med Res*. 2009 April ; 18(2): 195-222. doi:10.1177/0962280208092301.

Metallidis, S., Tsachouridou, O., Skoura, L., Zebekakis, P., Chrysanthidis, T., Pilalas, D., Bakaimi, I., Kollaras, P., Germanidis, G., Tsiara, A., Galanos, A., Malisiovas, N. and Nikolaidis, P. (2013) Older HIV-Infected Patients-An Underestimated Population in Northern Greece: Epidemiology, Risk of Disease Progression and Death. *International Journal of Infectious Diseases*, 17, e883-e891. http://dx.doi.org/10.1016/j.ijid.2013.02.023

Miller V, Phillips AN, Clotet B, Mocroft A, Ledergerber B, Kirk O, Ormaasen V, Gargalianos-Kakolyris P, Vella S and Lundgren JD. Association of virus load, CD4 cell count and treatment with clinical progression in Human Immunodeficiency virus-infected patients with very low CD4 cell counts. *The Journal of Infectious Diseases.* 2002; 186: 189-97.

Moncivaiz A and Alexander D. CD4 vs. Viral load: What's in a number. *Healthline*. February 16, 2018. https:/www.healthline.com.

Moore RD and Keruly JC. CD4+Cell Count 6 Years after Commencement of Highly Active Antiretroviral Therapy in Persons with Sustained Virologic Suppression. *CID*, 2007; 44: 441-6.

Moorhouse M, Conradie F, Venter F. What is the role of CD4 count in a large public health antiretroviral programme? S Afr J HIV Med. 2016;17(1), Art. 446, 3 pages. http://dx.doi. org/10.4102/sajhivmed.v17i1.446

Moysis L, Kafetzisi I, and Politis M. A DYNAMIC MODEL FOR HIV INFECTION. 1st Panhellenic Conference of M.Sc. and Ph.D. *New Holders in Mathematics*, May 27-28, 2016, Special Volume, pp. 50-58.

Mujugira A, Celum C, Tappero JW, Ronald A, Mugo N, Baeten JM. Younger age predicts failure to achieve viral suppression and virologic rebound among HIV-1-infected persons in serodiscordant partnerships. *Aids Res Human Retrovir.* 2016;32(2):5. https://doi.org/10.1089/aid.2015.0296.

Mullins DC and Weisman ES. A Simplified Approach to Teaching Markov Models. *American Journal of Pharmaceutical Education*. Vol. 60, Spring 1996.

Munderi P. When to start antiretroviral therapy in adults in low-income and middle-income countries: science and practice. *Curr Opin HIV AIDS* 2010; 5:6-11

Myhre J and Sifris D. What Is the HIV Treatment Cascade? And Why It Should Be of Concern to All of Us. *Medical Review Board*. Updated February 2018.

Nachega JB, Marconi VC, van Zy GU, Gardner EM, Preiser W, Hong SY, Mills EJ, and Gross R. HIV Treatment Adherence, Drug Resistance, Virologic Failure: Evolving Concepts. Infect Disord Drug Targets. 2011; 11(2): 167-174.

Naresh R, Tripathi A, Omar S. Modelling the spread of AIDS epidemic with vertical transmission. *Appl Math Comput.* 2006;178:262-72.

Ndumbi P, Falutz J, Pai NP, Tsoukas CM, et al. *PLoS One*. 2014;9(4):e94018. https://doi.org/10.1371/journal.pone.0094018.

Nielsen SF. Continuous-time homogeneous Markov chains. University of Copenhagen, Department of Mathematical Sciences. May 11, 2009.

Ocarn-Riola R. Non-homogeneous Markov Processes for Biomedical data Analysis. *Biometrical Journal.* 2005; 47(3): 369-376. DOI:10.1002/bimj. 200310114

Osisiogu UA, Nwosu CA. A stochastic analysis of the absorption probabilities of CD4 cell counts of HIV/AIDS patients using the smoothed non-stationary Markov chain model: a case study of Anambra State. *Eur J Stat Probab* 2015; 3: 1-11.

Palella FJ, Delaney KM, Moorman AC, Loveless MO, Fuhrer J, Satten GA, Aschman DJ, Holmberg SD. Declining morbidity and mortality among patients with advanced human immunodeficiency virus infection. *N Engl J Med* 1998; 338: 853-860.

Pasternak AO, de Bruin M, Jurriaans S, Bakker M, Berkhout B, Prins JM, Lukashov VV. Modest nonadherence to antiretroviral therapy promotes residual HIV-1 replication in the absence of virological rebound in plasma. *J Infect Dis.* 2012;206:1443-52.

Paterson DL, Swindells S, Mohr J, et al. Adherence to protease inhibitor therapy and outcomes in patients with HIV infection. Ann Intern Med 2000;133:21-30. [Erratum, Ann Intern Med 2002;136:253.]

Phillips AN, Staszewski S, Weber R, Kirk O, Francidi P, Miller V, Vernazza P, Lundgren JD, and Ledergerber B. HIV viral response to antiretroviral therapy according to the baseline CD4 cell count and viral load. *JAMA.* 2001; 286: 2560-2567.

Portela M. C. and Simpson K. N. (1997). Markers, Cofactors and Staging systems in the study of HIV Disease Progression: A review. *Mem Inst Oswaldo Cruz, Rio de Janeiro*. Vol.92(4), pp.437-457.

Prosperi MCF, D'Autilia R, Incardona F, De Luca A, Zazzi M, Giovanni U. Stochastic modelling of genotypic drug-resistance for human immunodeficiency virus towards

long-term combination therapy optimization. *Bioinformatics.* 2009;25(8):1040-7.

Rambaut A., Posada D., Crandall K.A. and Holmes E.C. (2004). The causes and Consequences of HIV Evolution. Volume 5. www.nature.com/review/genetics.

Randarajan S, Colby DJ, Truong G, et al. Factors associated with HIV viral loads suppression on anti-retroviral therapy in Vietman. *J Virus Erad.* 2016;2:94-101.

Reddy T. HIV disease progression in South Africa using multistate Markov models. *SACEMA.* 2011; http://www.sacemaquarterly.com.

Reynolds SJ, Nakigozi G, Newell K, Galiwongo ANR, Boaz I, Quinn TC, Gray R, Wawer M, and Serwadda D. Failure of immunologic criteria to appropriately identify antiretroviral treatment failure in Uganda. AIDS. 2009 March 27; 23(6): 697700. doi:10.1097/QAD.0b013e3283262a78.

Richman DD, Morton SC, Wrin T, et al. The prevalence of antiretroviral drug resistance in the United States. AIDS 2004;18: 1393-401.

Rivadeneira PS, Moog CH, Stan GB. Mathematical Modeling of HIV Dynamics After Antiretroviral Therapy Initiation:A Review. *BioResearch Open Access*. Volume 3, Number 5, October 2014. DOI: 10.1089/biores.2014.0024

Rong, L. et al. Modeling Within-Host HIV-1 Dynamics and the Evolution of Drug Resistance: Trade-Offs between Viral Enzyme Function and Drug Susceptibility. *Journal of Theoretical Biology*, 2007; 247: 804-818.

Rose CE, Gardener L, Girde JCS, et al. A comparison of methods for analysing viral load data in studies of HIV patients. *PLoS ONE.* 2015;10(6):e0130090.

Saint-Pierre P, Combescure C, Daures JP, Godard P. The analysis of asthma control under a Markov assumption with use of covariates. *Statistics in Medicine*. 2003; 22(24): 3755-3770

Salazar-Vizcaya L, Keiser O, Technau K, Davies M, Haas AD, Blaser N, Cox V, Eley B, Rabie H, Moultrie H, Giddy J, Wood R, Egger M, and Estill J. Viral load versus CD4 monitoring and a 5-year outcomes of ART in HIV-positive children in Southern Africa: cohort-based modelling study. *AIDS.* 2014; 28(16): 2451-2460.

Sanchez MS, Grant RM, Porco TC, Getz WM (2006). HIV drug-resistant strains as epidemiologic sentinels. *Emerging infectious disease. www.cdc.gov/eid.* volume 12, No. 2, Feb 2006.

SCHNEIDER, H. and STEIN, J., 2001. Implementing AIDS policy in post-apartheid South Africa. *Social Science and Medicine*, 52:723-731.

Serfozo, R. Basics of Applied Stochastic Precesses. Probability and its application, Springer, 2009. DOI: 10.10007/978-3-540-89332-5.

Sharp PS and Hahn BH. Origins of HIV and the AIDS Pandemic. *Cold Spring Harb Perspect Med*. 2011;1:a006841. doi: 10.1101/cshperspect.a006841

Shiri T., 2011. In-Vivo Dynamics of HIV-1 Evolution. *Faculty of Science, University of the Witwatersrand, Johanesburg, Doctor of Philosophy*.

Shoko C. and Chikobvu D., Time-homogeneous Markov process for HIV/AIDS progression under a combination treatment therapy: cohort study, South Africa. *Theoretical Biology and Medical Modelling* (2018) 15:3. DOI 10.1186/s12976-017-0075-4

Silva JAG, Dourado I, Bristo AM, Silva CAL. Factors associated with nonadherence to antiretroviral therapy in adults with AIDS in the first six months of treatment in Salvador Bahia state, Brazil. *Cad Saude Publica*. 2015;31(6):1-11.

Silveira M.P.T., de Lourdes Draschler M., de Carvalho Leite J.C., et al. Predictors of Undetectable Plasma Viral Load in HIV-Positive Adults Receiving Antiretroviral Therapy in Southern Africa, *The Brazilian Journal of Infectious Diseases*, 2002; 6(4): 164-171.

Simon V, Ho DD. HIV-1 dynamics in vivo: implications for therapy. *Nat Rev Microbiol*, 2003;1:18190. [PubMed: 15035022]

Simpson DM. Selected peripheral neuropathies associated with human immunodeficiency virus infection and antiretroviral therapy. *J NeuroVirol.* 2002;8(2):33-41. https://doi.org/10.1080/13550280290167939.

Sonnenberg FA and Beck J. Markov Models in Medical Decision Making: A Practical Guide Article. *Med Decis Making*, 1993; 13:322-338. DOI: 10.1177/0272989X9301300409 Source: PubMed.

SRIVASTAVA P. K., BANERJEE M. and CHANDRA P (2008). MODELING THE DRUG THERAPY FOR HIV INFECTION. *Department of Mathematics and Statistics. Indian Institute of Technology, Kanpur, India*. *Journal of Biological Systems*, Vol.17, No.2 (2009) 213-223.

R.E. Ingram, T. Nelson, D.K. Steidtmann, S.L. Bistricky Comparative data on child and adolescent cognitive measures associated with depression Journal of Consulting and Clinical Psychology, 75 (3) (2007), pp. 390-403

Thaker HK, Snow MH. HIV viral suppression in the era of antiretroviral therapy. *Postgrad Med J.* 2003;79:36-42.

The Opportunistic Infections Project Team of the Collaboration of Observational HIV Epidemiological Research in Europe (COHERE) in EuroCoord (2012) CD4 Cell Count and the Risk of AIDS or Death in HIV-Infected Adults on Combination Antiretroviral Therapy with a Suppressed Viral Load: A Longitudinal Cohort Study from COHERE. PLoS Med 9(3): e1001194. doi:10.1371/journal.pmed.1001194.

Titman, A.C., Model diagnostics in multi-state models of biological systems, Department of Pure Mathematics and Mathematical Statistics, University of Cambridge, 2007.

Titus RK. Mathematical modelling of the spread of HIV/AIDS by Markov chain process. *Am J Appl Math.* 2016;4:235-46.

UNAIDS (2016). The need for routine viral load testing. Questions and answers.
UNAIDS (2013). 90-90-90: Treatment for all: AN AMBITIOUS TREATMENT TARGET TO HELP END THE AIDS EPIDEMIC. http://www.unaids.org/en/resources/909090. Last accessed: 18 February 2019.

UNAIDS 2011. Global Report. UNAIDS World AIDS Day Report (2011)

UNAIDS 2012 Global Report. UNAIDS World AIDS Day Report (2012)

UNAIDS/WHO 2003. A history of HIV/AIDS epidemic with emphasis on Africa. Population Division, Department of Economic and Social Affairs, United Nations secretariat, New York 8-13, September 2003.

Vasconcellos R, Oliveira C, Shimakura S E, Campos D P, Victoriano F P, Ribeiro S R, Veloso V G, Grinsztejn B, Carvalho M. Multistate models for defining degrees of chronicity related to HIV-infected patient therapy adherence. Cad. *Saude Publica, Rio de Janeiro*, 2013; 29(4): 801-811.

Waziri AS, Estomih S, Massawe ES, Makinde OD. Mathematical Modelling of HIV/AIDS Dynamics with Treatment and Vertical Transmission. *Applied Mathematics*, 2012. 2(3): 77-89 DOI: 10.5923/j.am.20120203.06

Williams BG, Granich R, De Cock KM, Glaziou P, Sharma A, Dye C. 2010. Antiretroviral therapy for tuberculosis control in nine African countries. Proc Natl Acad Sci 107: 1948519489

Whitt W. CONTINUOUS-TIME MARKOV CHAINS. Department of Industrial Engineering and Operations Research Columbia University New York, NY 10027-6699. Accessed from: www.columbia.edu/ww2040 December 4, 2013.

WHO. Viral suppression for HIV treatment success and prevention of sexual transmission of HIV. HIVA/IDS July 2018

WHO. What's new in treatment monitoring: Viral load and CD4 cell testing, July 2017. Geneva: World Health Organisation; Updated July 2017. WHO/HIV/2017.22

Williams B, Gupta S, Wollmers M, Granich R. Progress and prospects for the control of HIV and tuberculosis in South Africa: a dynamical modelling study. Lancet Public Health 2017; published online April 10. http://dx.doi.org/10.1016/S2468-2667(17)30066-X

Worobey M, Gemmel M, Teuwen DE, Haselkorn T, Kunstman K, Bunce M, Muyembe JJ, Kabongo JM, Kalengayi RM, Van Marck E, Gilbert MT, Wolinsky SM. Direct Evidence of Extensive Diversity of HIV-1 in Kinshasa by 1960. *Nature*. 2008 October 2; 455(7213): 661-664. doi:10.1038/nature07390.

WRIGHT ST, PETOUMENOS K, BOYD M, CARR A, DOWNING S, O'CONNOR CC, GROTOWSKI M, and LAW MG on behalf of the Australian HIV Observational Database. Ageing and long-term CD4 cell count trends in HIV-positive patients with 5 years or more combination antiretroviral therapy experience. HIV Med. 2013 April ; 14(4): 208-216. doi:10.1111/j.1468-1293.2012.01053.x.

Wu H. Introduction to Stochastic Processes, Lecture 22: Infinitesimal generator. MIT. 06 May 2015. http://ocw.mit.edu/terms

Xie T, Liu W, Anderson BD, Liu X, Gray GC. A system dynamics approach to understanding the One Health concept. *PLoS ONE*, 2017: 12(9): e0184430. https://doi.org/10.1371/journal.pone.0184430

Yadavalli, V.S.S., Labeodan, M.M.O., Udayabaskaran, S. and Mwanga, Y. A stochastic model of the dynamics of HIV under a combination therapeutic intervention. *Institute of Statistics and Economics*, 2009; 25(1):17-30.

Zhang Z. Survival analysis in the presence of competing risks. *Researchgate*. 2017; DOI: 10.21037/atm.2016.08.62. https://www.researchgate.net/publication/313790075.

Publications

Publications
Shoko and Chikobvu *Theoretical Biology and Medical Modelling* (2018) 15:3
DOI 10.1186/s12976-017-0075-4

192
Theoretical Biology and Medical Modelling

RESEARCH Open Access

Time-homogeneous Markov process for HIV/AIDS progression under a combination treatment therapy: cohort study, South Africa

Claris Shoko* and Delson Chikobvu

Abstract

Background: As HIV enters the human body, its main target is the CD4 cell which it turns into a factory that produces millions of other HIV particles. These HIV particles target new CD4 cells resulting in the progression of HIV infection to AIDS. A continuous depletion of CD4 cells results in opportunistic infections, for example tuberculosis (TB). The purpose of this study is to model and describe the progression of HIV/AIDS disease in an individual on antiretroviral therapy (ART) follow up using a continuous time homogeneous Markov process. A cohort of 319 HIV infected patients on ART follow up at a Wellness Clinic in Bela Bela, South Africa is used in this study. Though Markov models based on CD4 cell counts is a common approach in HIV/AIDS modelling, this paper is unique clinically in that tuberculosis (TB) co-infection is included as a covariate.

Methods: The method partitions the HIV infection period into five CD4-cell count intervals followed by the end points; death, and withdrawal from study. The effectiveness of treatment is analysed by comparing the forward transitions with the backward transitions. The effects of reaction to treatment, TB co-infection, gender and age on the transition rates are also examined. The developed models give very good fit to the data.

Results: The results show that the strongest predictor of transition from a state of CD4 cell count greater than 750 to a state of CD4 between 500 and 750 is a negative reaction to drug therapy. Development of TB during the course of treatment is the greatest predictor of transitions to states of lower CD4 cell count. Transitions from good states to bad states are higher on male patients than their female counterparts. Patients in the cohort spend a greater proportion of their total follow-up time in higher CD4 states.

Conclusion: From some of these findings we conclude that there is need to monitor adverse reaction to drugs more frequently, screen HIV/AIDS patients for any signs and symptoms of TB and check for factors that may explain gender differences further.

Keywords: HIV/AIDS progression, Homogeneous Markov models, Reaction to treatment

* Correspondence: claris.shoko@gmail.com
Department of Mathematical Statistics and Actuarial Sciences, University of the Free State, Box 339, Bloemfontein 9300, South Africa

Background

The life cycle of HIV starts as it enters the human body, its major target being a white blood cell called T-helper cells or CD4 cells [1]. Once these cells are infected, HIV takes over and turns them into factories that produce thousands of copies of the virus. The HIV makes use of the enzyme Reverse Transcriptase to change copies of its Ribonucleic Acid (RNA) into Deoxyribose nucleic Acid (DNA). The viral DNA then enters the nucleus of the host cell and combines with cell DNA and starts making copies of viral RNA. The enzyme protease helps in assembling the viral particles into thousands of new viruses, which will bud and destroy the host cell. These new viruses will then be ready to attack other CD4 + T cells. Hence, the importance of CD4+ T cell count in understanding the progression of HIV. Depreciation of the CD4+ T cells in the human body leads to the deterioration of the human immune system, which is why the virus is called the Human Immunodeficiency Virus (HIV).

As the immune system is compromised, the individual is now prone to opportunistic infections like tuberculosis (TB). TB may occur at any stage of HIV disease and is frequently the first recognised presentation of underlying HIV [2]. HIV and TB coinfection is characterised by challenges that include poor adherence and overlapping toxicities resulting in an impaired CD4 T-cell recovery with antiretroviral therapy (ART) due to the effect of drug-drug interaction [3].

The need to address the challenges associated with HIV/AIDS progression in the presence of TB coinfection has prompted this study and also to analyse HIV disease history based CD4 multi-states and death/loss to follow-up in a single model. However, most studies use Kaplan-Meier analysis and Cox proportional hazards regression models [3–5]. Kaplan-Meier survival methods and Cox proportional hazards regression are commonly employed tools to model mortality and time to viral suppression and/or subsequent rebound and occasionally used to model time to CD4 recovery. However, survival models are not appropriate for all studies, particularly in the presence of competing risks and when multiple or recurrent outcomes are of interest. In particular, when modelling HIV/AIDS progression, Markov models are relatively straight forward to analyse both CD4 stage and death or loss to follow-up within a single model which survival models fail to do. Markov models can accommodate censored data, competing risks (informative censoring), multiple outcomes, recurrent outcomes, frailty and non-constant survival probabilities [6]. Examination of the conditions of the stochastic processes at various points in time, categorisation of the conditions, and examination of the external influences on the stochastic processes can be done using Markov models [7]. Markov models are favourable to the modelling of diseases in particular cases where the disease is grouped into a set of exhaustive and mutually exclusive health states, thereby forming a multi-state model [8]. History is naturally generated as the multi-states evolve over time; it contains information on previous visits, time of entry into various states, and the length of stay in states.

Continuous-time homogeneous Markov models have been used since early in the epidemic to model disease progression of HIV/AIDS patients, and there has been some recent renewed interest in the use of these models. In 1989 Longini et al. used a 5-state Markov model based on the clinical indicators of the HIV disease progression [9]. In 1998 Alioum et al. estimated the effects of gender, age, mode of transmission and ART on HIV progression using a 3-state Markov model [10]. In 2011 Reddy [11] carried out a research almost similar to Alioum et al. in South Africa. However, Reddy used a 5-state Markov model with 4 CD4 based transient states followed by the absorbing state, ARV initiation. Reddy's model is characterised by high rates of immune deterioration since the study was carried out on ARV naïve patients. In 2009, Binquet et al. used a multi-state Markov model to analyse the impact of gender, intravenous drug use, weight loss, low haemoglobin, CD8 cell count and HIV viral load on HIV evolution in the era of highly active antiretroviral therapy (HAART) [12]. Recently, in 2013 Grover et al. assessed the impact of ART using a 5-staged multistate Markov model and went further to examine the effects of explanatory variables; age, sex and mode of transmission on the transition rates [13].

In this study, we use 7-staged continuous-time Markov model to assess the disease progression of HIV/AIDS patients receiving ART from a clinic in Bela-Bela, South Africa. The first 5 stages are based on CD4 cell counts and the end points are either death or withdrawal from study. In addition to the gender and age differences in HIV/AIDS progression, we further assess the effects of having TB as the initial marker of HIV/AIDS, developing TB during the course of treatment, developing some adverse effects to treatment (Reaction), CD4 baseline and viral load baseline. Though Markov models based on CD4 cell counts is a common approach in HIV/AIDS modelling, this paper is unique clinically in that tuberculosis (TB) co-infection is included as a covariate.

In medical research, the state of the patient at observation time is the only thing known with certainty. The researcher may know the time interval in which a transition has occurred, but not the exact time. Thus, homogeneous Markov models which are interval censored can handle such data [14]. The transition intensities, probabilities and the distribution functions associated with the times are the basic building blocks of the Markov processes [15]. For a continuous-time

Markov model, transitions can occur at any (real-valued) time instant. For a time-homogeneous Markov jump process, the holding time in state i are modelled using exponential distributions. The exponential distributions may be adequate for many real-life situations, for example, time until death, and waiting time before moving to another state. However, the exponential distributions are memoryless continuous distributions, hence a limitation in the application of Markov processes. The 'memoryless' property could be seen as a problematic assumption in this setting. It is likely the case that patients starting on ART who respond well to treatment will continue to respond well to treatment - contradicting the Markov assumption and memoryless property.

Transition probabilities for continuous-time homogeneous models only depend on the difference between the two observation times. That is, for all $t \geq 0$ the probability of moving from state i to state j is given by:

$$\begin{aligned} p_{ij}(s,t) &= P[X_t = j|F_t] = P(X_t = j|X_s = i) \\ &= P(X_{t-s} = j|X_0 = i), \forall t \geq 0, t > s. \end{aligned}$$

This is the Markov property, where F_t is the natural Filtration of the stochastic process. $P[X_t = j|\, F_t]$, therefore, represents the probability that the stochastic process X_t is in state j at time t given the history of the process up to time t. The Markov property implies that all the history of the process is contained in the state currently occupied, $X_s = i$. The transition probabilities of a continuous time homogeneous Markov process X_t, $t \geq 0$ is given by:

$$p_{ij}(t) = P(X_t = j|X_0 = i)$$

The equations obey the Chapman-Kolmogorov equations:

$$p_{ij}(t+s) = \sum\nolimits_{k \in X} p_{ik}(s) p_{kj}(t) \quad \forall s, t > 0 \tag{1}$$

In this paper we describe, using the theory of continuous time Markov processes, and using real data on an evolving disease such as AIDS. Also, the effects of covariates, including TB, on baseline transition rates is considered. Models with and without covariates are fitted and compared using the likelihood ratio test.

The next section explores the methods of Markov modelling and an illustrative case study on HIV progression is given. In this section, data used in the analysis is described and we explain formulation of the model based on the data. This is followed by a section on the results and discussions. The final section concludes on the findings.

Methods

A continuous-time homogeneous Markov model

Formulation of the continuous-time homogeneous model is done by considering transition probabilities over narrow interval of time Δt. In this study $\Delta t = \frac{1}{2}$ year making it appropriate to assume that transition rates over these intervals are constant. These transition rates, also known as transition intensities or forces of transition, are the fundamental concept in continuous time Markov jump processes. They can take values greater than 1, unlike probabilities. In order to differentiate the transition probabilities and avoid technical problems with mathematics, the assumption is that the functions $p_{ij}(t)$ are continuously differentiable and are subject to the initial condition:

$$p_{ij}(0) = \delta_{ij} = \begin{cases} 0 \; if \; i \neq j \\ 1 \; if \; i = j \end{cases} \tag{2}$$

δ_{ij} is a Kronecker delta, $p_{ii}(0) = 1$ means that at $t = 0$ the system maintains its original state and $p_{ij}(0) = 0$ means that there is no change of state when no time elapses. The force of transition from state i to j is defined as:

$$\alpha_{ij} = \frac{d}{dt} p_{ij}(t)\Big|_{t=0} = \lim_{\Delta t \to 0} \frac{p_{ij}(\Delta t) - \delta_{ij}}{\Delta t}$$

α_{ij}, for $i = 1, \ldots, 5$ and $j = 1, \ldots, 7$, does not vary over time and satisfies the following conditions; $\sum_{j \in X} \alpha_{ij} = 0$ and $\alpha_{ii} = -\sum_{i \neq j} \alpha_{ij}$.

Once the transition intensities are known, the transition probabilities can be obtained by solving a system of differential equations known as the Kolmogorov's forward equation subject to the initial conditions stated in eq. (2). The Kolmogorov's forward equation is as follows:

$$\frac{d}{dt} p_{ij}(t) = \sum\nolimits_{\forall k} p_{ik}(t) \alpha_{kj} \quad \forall i, j \tag{3}$$

where k is a state that the system can pass through as it makes a transition from state i to state j. The time homogeneous models are fitted for this data to assess effectiveness of the treatment by comparing the forward transition and the reverse transitions. This then lead to building of models that allow transitions in both directions.

Data description

The model is initially applied on 319 HIV patients on anti-retroviral therapy (ART) from a Wellness clinic in Bela Bela, South Africa, from year 2005 to year 2009. Two hundred and twenty-seven of these patients were females and 92 were males at treatment commencement

($t = 0$). After 3 years of treatment uptake, 173 females and 71 males were remaining in the study. Thirty-eight females had died and 16 withdrew and their status was not known after 3 years of treatment up take. Nineteen of the males died during the first three years and two had withdrawn and it was not known whether they were alive or dead. A 2-year old (subject 81) together with subject 82 were detected by the residuals plot as an outlier and it was removed from the analysis meaning that the remaining 317 patients were used for analysis. About 50 and 65% of the female and male deaths respectively occurred during the first 6 months of treatment uptake. The interquartile range of patient ages is (33; 47.5) years with a mean and median age of 39.53 and 40 years respectively. The ages were negatively skewed (skew = −0.24) which means that there were more younger patients than older patients in this cohort.

At time $t = 0$ there were 242 individuals with CD4 baseline (CD4BL) cell count below 200, 59 individuals with CD4 cell count between 200 and 350, 11 individuals with CD4 cell count between 350 and 500, 6 individuals with CD4 cell count between 500 and 750 and 1 individual with CD4 cell count above 750. At t = 0 the CD4 cell count had mean of 156 cells/mm^3, a median of 116 cell/mm^3 and the maximum CD4 cell count was 1202 cells/mm^3. The mean viral load baseline (VLBL) for these patients was 105,573.35 copies/mm^3 and it ranged from 56 to 818,600 copies/mm^3. The median viral load was 58,523.00 copies/mm^3. From these individuals 155 had a WHO stage baseline (WSBL) of 4 which is related to severe HIV symptoms. WSBL is the categorisation of HIV/AIDS at baseline basing on the clinical markers as defined by World Health Organisation (WHO).

Although some individuals developed TB (DTB) during the course of treatment, 109 patients had TB as an initial marker of HIV. From the individuals who had TB before (TBB4) commencement of antiretroviral therapy (ART), 66 had a CD4 baseline below 200cells/mm^3, 20 had a CD4 baseline between 200 and 350cells/mm^3, 2 had CD4 baseline between 350 and 500cells/mm^3, 2 between 500 and 750cells/mm^3 and 19 had unknown CD4 baseline. These patients completed their TB treatment before commencement of ART. Fifty-two patients developed TB during the treatment period and 12 of these patients had TB before commencement of treatment. During the first 6 months of treatment uptake, 35 patients died and from these deaths, only five were attributed to having TB before commencement of ART.

A combination therapy was administered to all HIV-infected individual in the cohort. The therapeutic intervention inhibits the actions of reverse transcriptase enzyme and/or protease of new infectious free HIV by the HIV-infected cell. The drug regimens at $t = 0$ were mainly a combination of d4T-3TC-EFV (administered to 207 patients) and d4T-3TC-NVP (administered to 83 patients). The second line regimens were mainly a combination of AZT-3TC-EFV/NVP and were given to patients who developed some adverse reaction. These second line regimens were frequently used from 2 to 4 years post-treatment commencement. The therapeutic intervention lowers the number of infectious free virus particles in the circulation, and in some cases to beyond detection. This results in a reduction on the density of infected cells, causing a rise on the CD4 cell count of infected individuals. So generally the CD4 cell count of an individual receiving therapeutic intervention is expected to rise to well above 500 cell/mm^3, assuming a proper adherence to treatment. Hence the use of increase in CD4 cell count as the marker of efficacy of treatment.

During the course of treatment, some individuals developed some adverse reaction (React) to treatment. For these individuals the adverse reactions were treated and drugs administered to them were changed. Change of treatment was also based on the viral load monitoring.

For the purpose of analysis, the variables are coded into the model as follows:

	WSBL	Gender	Age	CD4BL	VLBL	DTB	TBB4	React
1	4	Male	≤ 40*years*	≤ 350	≥10 000	Yes	Yes	Yes
0	other	Female	> 40*years*	> 350	< 10 000	No	No	No

Model formulation

At any time $t + \Delta t$, the state of an HIV-infected individual is defined basing on the CD4 cell count level or whether the individual is dead or has withdrawn as follows:

State 1-$CD4 \geq 750$	**State 2**–$500 \leq CD4 < 750$
State 3–$350 \leq CD4 < 500$	**State 4**–$200 \leq CD4 < 350$
State 5-$CD4 < 200$	**State 6**-Death
State 7-Withdrawal.	

Basing on these seven states, progression of HIV positive individuals on treatment is defined by the state diagram on Fig. 1 below. The arrows in the diagram show possible transitions between the seven states defined above.

The information in Fig. 1 shows that state 6 and 7 are absorbing states hence no transitions from these states. As HIV progresses in an individual's body, there is a

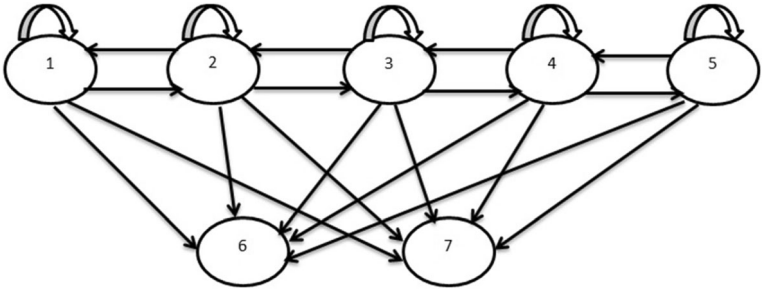

Fig. 1 The State Diagram for HIV Progression of Individuals on ART

possibility of an individual being in the same state in consecutive visit times.

Basing on the classification above, Table 1 summarises transition counts that took place for the whole period of study 2005 to 2009.

Table 1 shows that, transition counts from state i to $i \pm j$ are higher for all the values in which $j = 1$ than for $j > 1$ where $i, j \in \{1, \ldots, 5\}$. As a result a bidirectional model is proposed which defines transitions from state i to $i \pm 1$ or from i to $j = 6; 7$.

The model is formulated basing on the assumptions that between times $(t, t + \Delta t)$, where Δt is a very small value, there is a transition from any one of the states $i = 1, 2, \ldots, 5$ (transient states) to state $j = 1, 2, \ldots, 7$ defined as follows:

- CD4 cell count of an individual is expected to rise due to efficacy of treatment at a rate of α_{ij}, where $j = i - 1$;
- Some individuals fail to adhere to treatment therapy. These individuals can move to a state of lower CD4 cell count at a rate of α_{ij}, where $j = i + 1$;
- From any state $i = 1, 2, \ldots, 5$ an infected individual can die (state 6) at a rate of α_{i6};
- An individual in state $i = 1, 2, \ldots, 5$ can decide to withdraw (state 7) at a rate of α_{i7};
- An individual can remain in the same state at a rate of $\alpha_{ii} = -\lambda_i = -(\alpha_{i,\,i-1} + \alpha_{i,\,i+1} + \alpha_{i6} + \alpha_{i7})$. This is based on the fact that the sum of transition rates from any state is equal to zero.

These assumptions can be represented by the following transition rate matrix $Q(t)$:

$$Q(t) = \begin{pmatrix} -(\alpha_{12}+\alpha_{16}+\alpha_{17}) & \alpha_{12} & 0 & 0 & 0 & \alpha_{16} & \alpha_{17} \\ \alpha_{21} & -(\alpha_{21}+\alpha_{23}+\alpha_{26}+\alpha_{27}) & \alpha_{23} & 0 & 0 & \alpha_{26} & \alpha_{27} \\ 0 & \alpha_{32} & -(\alpha_{32}+\alpha_{34}+\alpha_{36}+\alpha_{37}) & \alpha_{34} & 0 & \alpha_{36} & \alpha_{37} \\ 0 & 0 & \alpha_{43} & -(\alpha_{43}+\alpha_{45}+\alpha_{56}+\alpha_{57}) & \alpha_{45} & \alpha_{56} & \alpha_{57} \\ 0 & 0 & 0 & \alpha_{54} & -(\alpha_{54}+\alpha_{56}+\alpha_{57}) & \alpha_{56} & \alpha_{57} \\ 0 & 0 & 0 & 0 & 0 & 0 & 0 \\ 0 & 0 & 0 & 0 & 0 & 0 & 0 \end{pmatrix}$$

Once the transition rate matrix has been obtained, the matrix of transition probabilities can be obtained using Kolmogorov's forward differential equations defined in (3). This yields the following differential equations for the Markov jump processes:

$$\frac{dp_{i1}(t)}{dt} = -(\alpha_{12}+\alpha_{16}+\alpha_{17})p_{i1}(t) + \alpha_{21}p_{i2}(t) \quad \text{for } i = 1, 2; \tag{4}$$

$$\frac{dp_{i2}(t)}{dt} = \alpha_{12}p_{i1}(t) - (\alpha_{21}+\alpha_{23}+\alpha_{26}+\alpha_{27})p_{i2}(t) + \alpha_{32}p_{i3}(t) \quad \text{for } i = 1, 2, 3; \tag{5}$$

$$\frac{dp_{i3}(t)}{dt} = \alpha_{23}p_{i2}(t) - (\alpha_{32}+\alpha_{34}+\alpha_{36}+\alpha_{37})p_{i3}(t) + \alpha_{43}p_{i4}(t) \quad \text{for } i = 2, 3, 4; \tag{6}$$

$$\frac{dp_{i4}(t)}{dt} = \alpha_{34}p_{i3}(t) - (\alpha_{43}+\alpha_{45}+\alpha_{46}+\alpha_{47})p_{i4}(t) + \alpha_{54}p_{i5}(t) \quad \textit{for } i = 3, 4, 5; \tag{7}$$

$$\frac{dp_{i5}(t)}{dt} = \alpha_{45}p_{i4}(t) - (\alpha_{54}+\alpha_{56}+\alpha_{57})p_{i5}(t) \quad \text{for } i = 4, 5; \tag{8}$$

$$\frac{dp_{i6}(t)}{dt} = \sum_{k=1}^{5} p_{ik}(t)\alpha_{k6} \quad \text{for } i = 1, \ldots, 5; \tag{9}$$

$$\frac{dp_{i7}(t)}{dt} = \sum_{k=1}^{5} p_{ik}(t)\alpha_{k7} \quad \text{for } i = 1, \ldots, 5. \tag{10}$$

Equations (4) to (10) represent all the possible transition probabilities from state i, for $i = 1, 2, \ldots 5$, to state $j = 1, \ldots, 7$. $p_{ij}(t)$ represents the probability that a patient in state i makes a transition to state j and its coefficients represent the transition rates. For example, in equation (4), $-(\alpha_{12} + \alpha_{16} + \alpha_{17}) = \alpha_{11}$. These states denoted by i are defined based on the CD4 cell count grouping. So there is a

Table 1 Transition Counts from 2005 to 2009

	To	1	2	3	4	5	6	7
From	1	69	34	5	1	1	1	1
	2	47	80	37	4	0	2	4
	3	21	79	193	46	9	6	5
	4	0	14	128	203	37	8	9
	5	0	3	26	117	204	42	8

possibility of a backward or forward movement transition between transient states due to failure or efficacy of treatment respectively. There is no possible transition from state $i = 6$ and state $i = 7$ because these states are absorbing states where $i = 6$ represents death of an infected individual and state $i = 7$ represents withdrawal from treatment by an infected individual. All the analysis is done using the package 'msm' for multistate modelling in R software. The package was developed by Jackson in 2011 [16].

Results and discussions

Estimation of the transition rate matrix

Estimation of the transition intensities is done using the method of maximum likelihood to estimate the transition intensities. The likelihood, L, is given by:

$$L = e^{\alpha_{11.}}t_1 + \alpha_{22.}t_2 + \ldots + \alpha_{77.}t_7 \times \alpha_{11}^{n_{11}}\alpha_{12}^{n_{12}}\ldots\alpha_{77}^{n_{77}}, \tag{11}$$

where t_i : $i = 1, 2, \ldots, 7$, is the total number of observed waiting/holding time in state i, $\alpha_{ii} = -\sum_{i \neq j}\alpha_{ij}$ and n_{ij} is the number of transitions observed from state i to state j. The estimates are obtained by taking the logarithm of the likelihood and differentiating this with respect to each of the transition intensities α_{ij}'s. This leads to the maximum likelihood estimates of the transition intensities as $\alpha_{ij} = \frac{n_{ij}}{t_i}$, where n_{ij} is the number of transitions from state i to state j, and t_i the total observed waiting/holding time in state i.

The plot of residuals for each of the individuals in the study was drawn to identify the outliers (subjects with higher influence) in the data. Once the outliers are identified they can simply be deleted and the model is re-fit. According to Titman in 2007 [17] residuals for multi-state models can be determined as follows;

If n subjects and a parameter vector $\theta \epsilon \Theta$, with maximum likelihood estimator based upon the whole data $\hat{\theta}$. Let $\hat{\theta}_{(j)}$ represent the estimate with subject j deleted. Thus the quantity $\hat{\theta}_{(j)} - \hat{\theta}$ for $j = 1, \ldots, n$ is of interest. The influence of each point on each parameter can be compared separately and to get a measure of the overall influence of a particular subject we take the scalar quantity;

$$\left(\hat{\theta}_{(j)} - \hat{\theta}\right)' I\left(\hat{\theta}\right)\left(\hat{\theta}_{(j)} - \hat{\theta}\right)$$

where $I(\theta)$ is the observed Fisher information matrix at the maximum likelihood estimates for the full data. Consider the contribution to the score function of each subject evaluated to the maximum likelihood estimate for the full model. Highly influential subjects will have scores of high magnitude. For a single subject, the score residual is given by an analogous scalar measure:

$$U_j\left(\hat{\theta}\right)' I\left(\hat{\theta}\right)^{-1} U_j\left(\hat{\theta}\right)$$

where $U_j\left(\hat{\theta}\right)$ is the vector of first derivatives of the log-likelihood for that subject at maximum likelihood estimates θ. That is, $U(\theta) = \frac{\partial l}{\partial \theta}(\theta)$, is determined using the derivative of the transition probability matrix $P(t)$ with respect to θ. These derivatives were given by Kalbfleisch and Lawless [18]. The residuals plot displays the residuals for each subject in the order labelled by subject identifiers. Subjects with a higher influence on the maximum likelihood estimates will have higher score residuals [16]. The plot helps to identify any outliers in the data. Figure 2 below shows the plot of residuals.

Results from Fig. 2 show that patients with ID numbers 81 and 82 are outliers as indicated by their positions from the rest of the patients in the cohort. The corresponding residuals for these values are 1.58315799 and 1.58315999, respectively compared to the rest of the subjects whose residuals below 1. Patient number 81 is a 2 year old enrolled whilst in state 1 and maintained the state throughout the study period. Patient number 82 was enrolled whilst in state 5 and, during the third visit, was already in state 1 and maintained it throughout the study

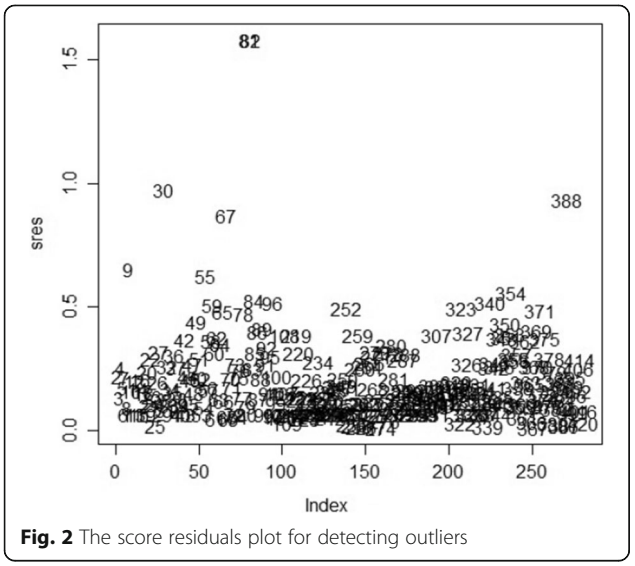

Fig. 2 The score residuals plot for detecting outliers

Table 2 Transition intensities and their corresponding confidence intervals for the model with and the model without outliers

	With outliers	Without outliers
α_{12}	0.9820 (0.6695,1.4410)	0.8872 (0.6355,1.2390)
α_{16}	0.1176 (0.0678,0.2040)	0.1016 (0.0541,0.1907)
α_{17}	0.1153 (0.0663,0.2005)	0.1418 (0.0843,0.2386)
α_{21}	0.6871 (0.4814,0.9808)	0.5183 (0.3723,0.7217)
α_{23}	0.4256 (0.3129,0.5790)	0.4959 (0.3729,0.6593)
α_{26}	0.0726 (0.0406,0.1300)	0.0811 (0.0468,0.1404)
α_{27}	0.0261 (0.0093,0.0734)	0.0377 (0.0167,0.0850)
α_{32}	0.4373 (0.3605,0.5305)	0.4231 (0.3451,0.5186)
α_{34}	0.3382 (0.2639,0.4335)	0.3324 (0.2605,0.4241)
α_{36}	0.0273 (0.0127,0.0587)	0.0145 (0.0047,0.0444)
α_{37}	0.0298 (0.0155,0.0574)	0.0311 (0.0166,0.0584)
α_{43}	0.5524 (0.4693,0.6503)	0.5183 (0.4389,0.6120)
α_{45}	0.2242 (0.1686,0.2980)	0.2523 (0.1936,0.3287)
α_{46}	0.0361 (0.0171,0.0763)	0.0033 (0.0149,0.0742)
α_{47}	0.0382 (0.0225,0.0647)	0.0541 (0.0352,0.0833)
α_{54}	0.5482 (0.4651,0.6463)	0.5164 (0.4356,0.6123)
α_{56}	0.0904 (0.0622,0.1316)	0.0906 (0.0625,0.1313)
α_{57}	0.0357 (0.0211,0.0605)	0.0288 (0.0158,0.0524)
-2xLL	3969.72	3941.971

period. These patients are excluded from the analysis leaving us with 317 subjects. Table 2 shows transition intensities α_{ij} for $i = 1, 2, \ldots, 5$ and $j = 1, 2, \ldots, 6, 7$ for the two models, one with outliers and the other one without outliers. The corresponding confidence interval is also given for each transition intensity. The state space is $X_t = \{1, 2, 3, 4, 5, 6, 7\}$.

The results from Table 2 show narrow confidence intervals which is an indication that the suggested continuous time Markov model gives a precise estimate of the data. Results from Table 2 show that transitions to better CD4 cell count states are higher than transitions to worse CD4 cell count states which is an indication of efficacy of ART. The model with outliers has got a higher log-likelihood than the model without outliers as expected since the model with outliers has got a greater dimension. A further analysis on the transition intensities was also done for each of the CD4 baseline (CD4BL) and WHO stage baseline (WHOSBL) levels coded as follows:

$$\text{CD4BL} = \begin{cases} \mathbf{1}; & & CD4 & > & 750 \\ \mathbf{2}; & 500 & < CD4 & \leq & 750 \\ \mathbf{3}; & 350 & < CD4 & \leq & 500 \\ \mathbf{4}; & 200 & < CD4 & \leq & 350 \\ 5; & & CD4 & \leq & 200 \end{cases} \text{and, WHOSBL} = \begin{cases} 1; & \textit{Asymptomatic} \\ 2; & \textit{Mild symptoms} \\ 3; & \textit{Advanced symptoms} \\ 4; & \textit{Severe symptoms} \end{cases}$$

The results are shown in Appendix 2 and 3 for CD4BL and WHOSBL respectively. The results from Appendix 2 show that transition rates to CD4 recovery (2 to 1, 3 to 2, 4 to 3 and 5 to 4) were high for patients who initiated therapy when their CD4 baseline level was well above 350 per mm^3. These rates of CD4 recovery decrease with as the CD4 cell count at treatment initiation decrease with a baseline CD4 cell count below 200 per mm^3 recording the lowest rates of CD4 recovery. The results from Appendix 3 show that regardless of the WHO stage baseline, transition rates to CD4 recovery are higher than transition rates to CD4 deterioration. The rates of CD4 recovery are the highest for transitions from state 5 to state 4. Transition rates to state 6 (death) are the highest for those individuals who had severe HIV symptoms (WHOBL = 4) and these intensities decrease as the symptoms decrease from severe to asymptomatic levels.

Expected holding times

The expected holding time in each state also known as the mean sojourn time describes the average time an individual spends in each state in a single stay before he/she makes a transition to another state. The mean sojourn time in each state i for $i = 1, 2, \ldots, 5$, is estimated as $\frac{1}{\lambda_i}$, where $\lambda_i = \sum_{i \neq j} \alpha_{ij}$ is the total force of transition out of state i. For example, the expected holding time in state 1 is $1/(0.887 + 0.1016 + 0.1418) \approx 0.8844$ as shown in Table 3 below:

Results from Table 3 show estimates of the holding time, the standard error (SE), the lower bound (L) and the upper bound (U) for each of the transient state i. From the results, if an individual is in state 5 (corresponding to a CD4 count below 200cell/mm^3) he spends more time in that state before making a transition to other states. This could be due the time taken by an individual to respond to treatment since state 5 is the worst state in HIV/AIDS progression.

The jump chain

This is when a Markov process is observed at the times it makes transitions to a new state. In other words a jump chain is a stochastic matrix R of probabilities where each row sums to one, on the state space X_t, which gives the conditional probability of the next state an individual goes to after leaving state i. If $\alpha_{ii} > 0$ then given that there is a jump to a different state, it means we never stay in state i, we make a jump out resulting in having $R_{ii} = 0$ and if $\alpha_{ii} = 0$

Table 3 Expected holding times in each state

i	Estimates	SE	L	U
1	0.8844741	0.12602569	0.6689603	1.169418
2	0.8826571	0.09158707	0.7202261	1.081721
3	1.2482706	0.09636263	1.0729973	1.452175
4	1.2077295	0.07925375	1.0201303	1.331720
5	1.5728163	0.11539878	1.3621492	1.816065

then we never leave state i meaning that $R_{ii} = 1$ (States 6 and 7). The computed matrix of probabilities of each state being next (also known as the jump chain), together with the mean sojourn times in each state, fully define a continuous-time Markov model. This is a more intuitively meaningful description of a model than the transition intensity matrix. The matrix for the probabilities that the next state after state i is state j is approximated as $p_{ij} = \frac{\alpha_{ij}}{\lambda_i}$, for each i and j such that $i \neq j$. α_{ij} is the force of transition from state i to state j and α_{ii} is the total force of transition out of state i. For example, $p_{12} = \frac{\alpha_{12}}{\lambda_1} = \frac{0.8872}{0.8872+0.1016+0.1418} = 0.7847$, as shown in the matrix below. The results are shown Table 4 below:

The results from Table 4 show that $R_{i,\ 1-1} > R_{i,\ i+1}$, which shows that the probability of jumping to a better state is higher than the probability of jumping to a worse state. This is more pronounced for individuals in state 5 where the probability of jumping to state 4 (recovery) is 0.8123 which is very high compared to probability of making a jump to state 6. This is an indication of the effectiveness of treatment. Probability of the death state being next is the highest for those patients with CD4 counts less than 500. These probabilities increase with the decreasing number of CD4 counts.

Forecast of the total length of stay in each state

We need to forecast the total time spent in the good states and the bad states by individuals who are on HIV treatment before death or withdrawal from the study. Estimates of the forecasted total lengths of time spent in each state j between two future time points t_1 and t_2 are estimated using the formula:

$$L_j = \int_{t_1}^{t_2} P_{ij}(t)dt$$

where i is the state at the start of the process, which defaults to 1. The results are shown below:

State1	State2	State3	State4	State5	State6	State7
8.988960	8.806075	7.767124	3.520485	1.153648	Inf	Inf

Table 4 Probability of each State being next (R_{ij})

	To	1	2	3	4	5	6	7
From	1	0	0.7847	0	0	0	0.0899	0.1254
	2	0.4575	0	0.4377	0	0	0.0715	0.0333
	3	0	0.5282	0	0.4149	0	0.0181	0.0388
	4	0	0	0.6041	0	0.294	0.0388	0.0631
	5	0	0	0	0.8123	0	0.1425	0.0451
	6	0	0	0	0	0	1	0
	7	0	0	0	0	0	0	1

The results show that each individual is forecasted to spend approximately 8.99 half years in state 1, 8.8 half years in state 2, 7.77 half years in state 3, 3.52 half years in state 4 and finally 1.153 half years in state 5. These results show that HIV positive individuals on treatment are expected to spend more time in good states compared to the time spent in bad states.

Percentage prevalence for the model without covariates.

Using the fitted time-homogeneous Markov model, the percentage prevalence were plotted to compare the expected values with the observed values. The results are shown in Fig. 3 below:

The results from Fig. 3 show that for the state $i = 1, \ldots, 6$ the expected prevalence fit the observed data perfectly well except for the withdrawal state where the expected prevalence overestimate the observed. The plots further show a sharp decrease on state 5 percentage prevalence with the fitted model, underestimating the model for observed data up to time = 7 half years. The percentage prevalence for the death state is increasing at a slow rate and from time = 2 half years to time = 8 half years the percentage prevalence is stable.

Effects of covariates on transition intensities

A continuous-time Markov model for the effects of covariates; Age, CD4BL, VLBL, WSBL, Reaction, DTB, TBB4 and Gender is fitted. Identification of covariates that have a significant contributory effect is done by entering each covariate one after the other and performing the likelihood ratio test in comparison to the model without covariates. All the other variables proved to be significant to the progression except for the variable gender which could not be eliminated because of its demographic importance. The baseline transition intensities $\left(\alpha_{ij}^{(0)}\right)$ relate to the transitions from state i to state j. Baseline transition intensities and linear effect of each of the covariates is estimated and the results are shown in two separate Table 5 and Appendix 1 respectively:

The fitted time homogeneous model with covariates has -2xLL = 3699.259, which represents an improvement of 242.712 compared to the model without covariates. A Likelihood ratio test is performed to compare the two nested models that were fitted, the one without covariates and the other with covariates. The value of the $LRT = -2log_e\left(\frac{L_s(\hat{\theta})}{L_g(\hat{\theta})}\right)$ where $L_s\left(\hat{\theta}\right)$ is the simple model (no covariates) and $L_g\left(\hat{\theta}\right)$ is the general model (with covariates). A likelihood ratio test statistic of 1770.618 is compared to a χ^2 distribution with 144 degrees of freedom. The test was performed and the results are shown below:

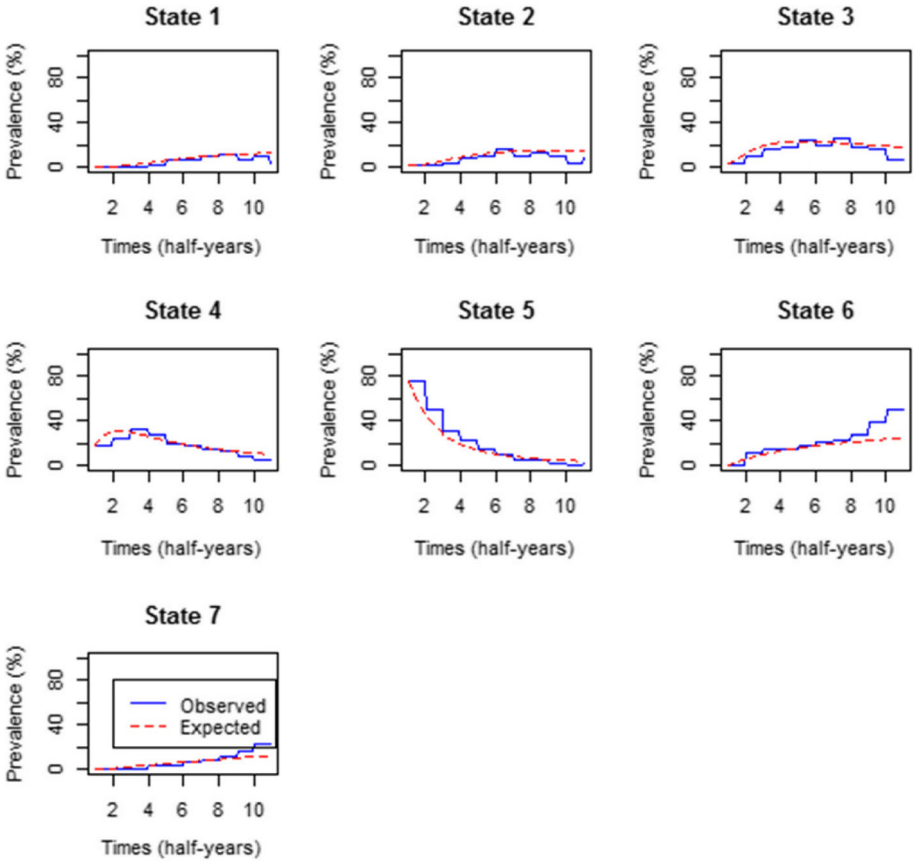

Fig. 3 Comparison of observed and expected prevalence from the time-homogeneous model without covariates

	−2logLR	Df	p-value
with.covariates	1770.186	144	10^{-4}

The results show that the model with covariates fits significantly better than the model without covariates.

Hazard ratios of covariates on transition intensities

In this section the hazard ratios for each of the covariates; VLBL-viral load baseline, DTB-develop TB during treatment period, TBB4-develop TB before treatment, Gender, React-reaction to treatment, CD4BL-CD4 baseline, WSBL-WHO stage baseline and Age are estimated. The relationship between these covariates and the transition intensities is defined by the following equation:

$$\alpha_{ij}(\boldsymbol{Z}) = \alpha_{ij}^{(0)} \exp\left(\beta_{ij'}\boldsymbol{Z}\right), \quad i \neq j,$$

where $\boldsymbol{Z}$ = [VLBL, DTB, TBB4, Gender, React, CD4BL, WSBL, Age] is a $k = 8$-dimensional vector of covariates and β_{ij} is a vector of k regression parameters relating the instantaneous rate of transitions from state i to state j to the covariates $\boldsymbol{Z}$ and baseline intensities $\alpha_{ij}^{(0)}$ relating to the transition from state i to state j as shown in Table 5 above. Estimates of β_{ij}'s, regression coefficients, were calculated and the results are shown in Appendix 1. The regression coefficients can be interpreted similarly to those in the proportional hazards regression model [19]. The results are shown in Table 6.

The -2xLL for the model fitted in Table 6 is 3699.259. The results show that the strongest predictor of transition from state 1 to 2 is a negative reaction to treatment, which has a hazard ratio of 4.715. This means that patients who developed some form of reaction were over 4 times more likely to transit from a level of CD4 ≥ 750 to a level of 500 ≤ CD4 < 750 than patients who did not react to treatment. However, from all the other states, hazard ratios for the patients who reacted to treatment are higher for immune recovery than for immune deterioration.

The strongest predictor of immune deterioration from a CD4 level between 350 and 500 to a CD4 level between 200 and 350 (3 to 4) is developing TB during treatment, with a hazard ratio of over 2. Developing TB is also the strongest predictor of immune deterioration from 4 to 5, with a hazard ratio also greater than 2. This means that TB is the major cause of further immune deterioration when the immune system is too weak. Hence the

Table 5 Baseline intensities and their corresponding confidence intervals for the covariate effects

(i, j)	Intensities (a_{ij})	B.L. Intensities $\left(a_{ij}^{(0)}\right)$
(1, 2)	0.8872 (0.6355,1.2390)	0.5030 (0.4277,0.8612)
(1, 6)	0.1016 (0.0541,0.1907)	0.0200 (0.0100,0.4641)
(1, 7)	0.1418 (0.0843,0.2386)	0.0175 (0.009,0.4934)
(2, 1)	0.5183 (0.3723,0.7217)	0.3900 (0.3846,0.6863)
(2, 3)	0.4959 (0.3729,0.6593)	0.4440 (0.2973,0.5550)
(2, 6)	0.0811 (0.0468,0.1404)	0.0111 (0.0073,0.2018)
(2, 7)	0.0377 (0.0167,0.0850)	0.0116 (0.001,0.0189)
(3, 2)	0.4231 (0.3451,0.5186)	0.3760 (0.3252,0.5010)
(3, 4)	0.3324 (0.2605,0.4241)	0.2333 (0.2076,0.3641)
(3, 6)	0.0145 (0.0047,0.0444)	0.0063 (0.00367,0.1287)
(3, 7)	0.0311 (0.0166,0.0584)	0.0095 (0.00285,0.3149)
(4, 3)	0.5183 (0.4389,0.6120)	0.5600 (0.4485,0.6284)
(4, 5)	0.2523 (0.1936,0.3287)	0.2300 (0.1522,0.2785)
(4, 6)	0.0033 (0.0149,0.0742)	0.0070 (0.0049,0.4210)
(4, 7)	0.0541 (0.0352,0.0833)	0.0084 (0.00589,0.1547)
(5, 4)	0.5164 (0.4356,0.6123)	0.5020 (0.4450,0.6297)
(5, 6)	0.0906 (0.0625,0.1313)	0.0198(0.00662,0.1456)
(5, 7)	0.0288 (0.0158,0.0524)	0.0055 (0.001280,3.936)
-2xLL	3941.971	3699.259

Table 6 Hazard ratios for the covariates on intensities

(i, j)	VLBL	DTB	TBB4	Gender	React	CD4BL	WSBL	Age
(1, 2)	0.69	2.29	0.31	2.04	4.72	1.17	0.55	1.45
(1, 6)	1.57	0.87	1.11	1.55	0.60	1.30	1.11	0.83
(1, 7)	1.01	0.96	1.00	1.26	0.68	0.92	0.56	0.40
(2, 1)	0.48	1.14	0.76	1.33	1.46	1.17	0.74	2.63
(2, 3)	0.92	1.98	0.67	6.46	0.67	1.37	0.26	0.40
(2, 6)	1.12	0.96	1.69	1.45	0.54	0.997	1.16	1.10
(2, 7)	1.30	1.19	1.92	0.93	0.73	1.33	0.79	0.70
(3, 2)	0.68	1.58	1.10	2.35	2.08	0.69	0.75	0.83
(3, 4)	0.42	2.55	0.53	1.04	0.55	1.57	1.06	0.89
(3, 6)	0.92	1.17	2.03	1.20	0.59	1.05	1.32	1.77
(3, 7)	1.34	0.86	2.34	0.72	0.20	1.20	0.54	2.06
(4, 3)	1.52	1.72	0.86	0.61	1.02	0.27	0.84	1.08
(4, 5)	0.74	2.25	1.65	1.36	0.65	1.05	0.46	0.89
(4, 6)	1.31	1.09	1.09	1.59	0.22	1.01	1.40	1.96
(4, 7)	1.56	1.17	1.88	0.58	0.36	1.02	0.52	2.18
(5, 4)	0.51	1.86	1.02	0.81	1.32	0.61	0.40	0.63
(5, 6)	0.92	0.65	0.41	2.10	0.06	1.003	2.09	2.60
(5, 7)	0.97	1.20	0.88	1.19	0.66	0.87	0.40	2.31

recommendation that HIV patients should continuously have their TB status checked. Those individuals who had TB before enrolment had the strongest predictor for the transition from state 3 to state 6. These patients had a hazard ratio of over 2 times more likely to die from state 3 than those who were enrolled without having TB. However, for these individuals, transitions to better states were generally higher than transitions to worse states for almost all states.

A hazard ratio of 6.46 for the predictor variable male shows that males were over 6 times more likely to transit from state 2 to 3 than their female counterparts. The hazard ratios of males from a bad state to a better state are less than 1, which is an indication that males are less likely to respond to treatment compared to females.

The hazard ratios for the transitions to a better state for patients who were enrolled with CD4 counts below 350 are less than one, but hazards to worse states are greater than one, an indication that starting treatment when the CD4 levels are below 350 retards immune recovery. The transitions to the death state for individuals who started treatment when they were on the WHO stage of 4 are all more than one, meaning that starting treatment with a WHO stage of 4 is a leading cause of being absorbed in the death state.

Percentage prevalence for the model with covariates

The prevalence for the model with covariates were plotted to examine areas of poor fit of the time-homogeneous model with covariates. The plots are shown in Fig. 4.

Figure 4 confirms that the inclusion of covariates on the model improves the fitness of the model since the expected prevalence is now perfectly closer to the observed prevalence for all states than the model without covariates.

Conclusion

In this paper a continuous-time homogeneous Markov model is fitted to explore predictors of HIV/AIDS progression for patients on antiretroviral therapy. A continuous-time homogeneous model is fitted with and without covariates and comparison of these two models is done using the likelihood ratio test. Parameters that define progression of HIV/AIDS were estimated and these include transition intensities, mean sojourn times and probability of each state being next or jump chains. The fitted model is used to analyse the effects of the covariates on the transition intensities. These covariates were reaction to treatment, development of TB during treatment and gender among others.

Results from the likelihood ratio test show that the model with covariates provides a better fit than the model with no covariates with a p-value $=10^{\{-4\}}$. The results show that transition rates to immune recovery are generally higher than the transition rates to immune deterioration. However, the results show that the strongest predictor of

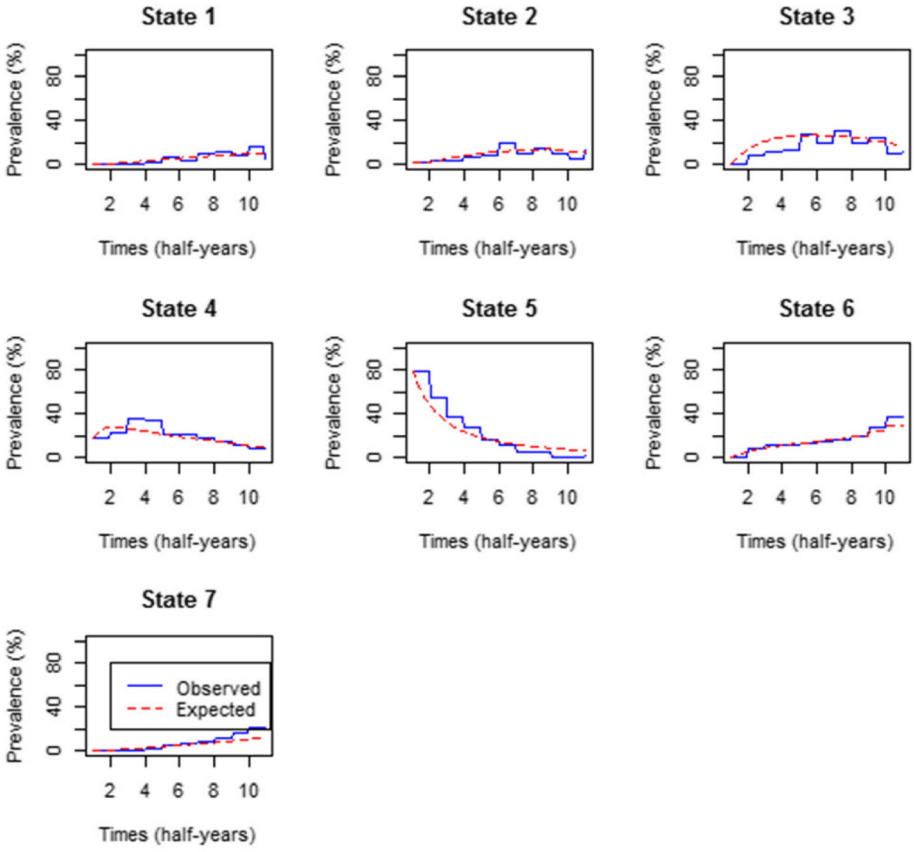

Fig. 4 Comparison of observed and expected prevalence from the time-homogeneous model with covariates

immune deterioration from state 1 (CD4 cell count greater than 750) to state 2 (CD4 cell count between 500 and 750) is reaction to treatment. These patients are 4 times more likely to transit from state 1 to state 2 than those who did not react to treatment.

Patients who developed TB during the course of treatment have higher chances of immune deterioration than immune recovery compared to those who did not develop any TB co-infection. These incidences are quite high for transition from state 4 (CD4 cell count between 200 and 350) to state 5 (CD4 cell count below 200). For these states the immune system is still weak. As a result patients on antiretroviral drugs should consistently be screened for TB co-infection. Patients who had initially been diagnosed with TB before commencement of ART recover better from HIV/AIDS disease except that transitions to death for patients with CD4 cell count between 350 and 500 cells/mm^3 are two times higher than that of patients who were not initially diagnosed with TB.

From this cohort, transitions to bad states are higher for males than for their female counterparts. This is quite pronounced on transitions from state 2 (CD4 cell count between 500 and 750) to state 3 (CD4 cell count between 350 and 500) where the hazards for males are 6 times that of females. This result is consistent with the findings from Maskew and others, they discovered that men gain fewer CD4 cell counts than did women [20]. An assessment of published studies by Castillo and others [21] from both resource-limited and resource-rich countries suggest an improved survival outcomes for females than males. However, the studies they assessed do not show a clear sex disparity in the disease progression or in treatment effects of viral suppression and immunologic recovery.

The results from the fitted model show that the rates of immune recovery were much higher than the rates of immune deterioration which is an indication of effectiveness of treatment. Patients who started treatment when their CD4 baseline was at least 350 had higher rates of immune recovery than those who had a lower CD4 baseline. This result is commensurate with the findings from Moore and Keruly who also discovered that patients with baseline CD4 cell count above 350 cells/mm^3 returned to nearly normal CD4 cell count after 6 years [22]. The probability of dying increases with decreasing CD4 count of the individual at enrolment. This is supported by the findings of [23–25], who also concluded that being in the AIDS defining stage leads to the highest probability of reaching the death state.

The mean sojourn times revealed that patients take longer time in the AIDS defining states (CD4 cell count below 200) before they move to the other states. Research has also shown that CD4 cell count rises gradually despite the suppressed viral load particularly in older patients. Hence, there is need to use both CD4 cell count and viral load in monitoring the efficacy of treatment. The younger people below the age of 40 have higher chances of immune recovery than the older ones. This finding is supported by some previous studies who concluded lower mean CD4 increases for older patients than younger patients [20, 26]. Alioum and others further argued that this could be caused by the fact that older subjects may have a reduced capacity to generate CD4 cells in response to the viral killing [10].

Although continuous time Markov models can handle multiple or recurrent outcomes compared to the Kaplan Meier analysis and Cox proportional hazards models, the assumption of constant hazard function that is frequently unrealistic [27] and puts limitations on the disease history behaviour [28], especially on HIV/AIDS progression for patients on ART. Some studies have shown that if a patient responds well to treatment and manages to achieve viral load suppression within the first 6 months, that patient is likely to continue responding well to treatment [29]. This goes against the Markov and memoryless properties of the models. Thus a limitation in the application of time homogeneous Markov processes.

Appendix 1

Table 7 Linear effects of covariates on transition intensities

Param.	VLBL	CD4BL	WSBL	React	DTB	TBB4	Gender	Age
β_{12}	−0.37	0.15	−0.59	1.55	0.83	−1.17	0.7118	0.37
β_{16}	0.45	0.27	0.101	−0.52	−0.14	0.11	0.4379	−0.18
β_{17}	0.0071	−0.088	−0.58	−0.39	−0.039	0.00086	0.23	−0.90
β_{21}	−0.73	0.156	−0.31	0.38	0.13	−0.28	0.29	0.97
β_{23}	−0.84	0.31	−1.35	−0.40	0.68	−0.39	1.87	−0.92
β_{26}	0.112	−0.0028	0.150	−0.63	−0.044	0.53	0.37	0.100
β_{27}	0.26	0.29	−0.24	−0.32	0.17	0.65	−0.077	−0.36
β_{32}	−0.39	−0.37	−0.28	0.73	0.46	0.096	0.86	−0.18
β_{34}	−0.86	0.45	0.057	−0.59	0.94	−0.63	0.036	−0.116
β_{36}	−0.085	0.047	0.28	−0.53	0.16	0.71	0.18	0.57
β_{37}	0.29	0.181	−0.24	−1.63	−0.15	0.85	−0.33	0.72
β_{43}	0.42	−1.32	−0.17	0.020	0.54	−0.15	−0.49	0.080
β_{45}	−0.305	0.049	−0.77	−0.43	0.81	0.50	0.31	−0.12
β_{46}	0.27	0.0079	0.34	−1.50	0.087	0.089	0.46	0.67
β_{47}	0.45	0.020	−0.66	−1.01	0.16	0.63	−0.55	0.78
β_{54}	−0.66	−0.501	−0.91	0.27	0.62	0.022	−0.22	−0.46
β_{56}	−0.079	0.0030	0.74	−2.83	−0.43	−0.89	0.74	0.95
β_{57}	−0.028	−0.141	−0.92	−0.41	0.19	−0.13	0.18	0.84

Appendix 2

Table 8 Transition intensities for each CD4 baseline

Transition	2	3	4	5
1 to 2	3.1280	6.3180	12.760	25.780
1 to 6	0.0125	0.0203	0.0330	0.0537
1 to 7	0.0389	0.0560	0.0807	0.1163
2 to 1	0.6644	0.5991	0.5407	0.4870
2 to 3	0.2842	0.4054	0.5783	0.8249
2 to 6	0.0176	0.0184	0.0194	0.0203
2 to 7	0.0227	0.0278	0.0341	0.0417
3 to 2	0.2450	0.1658	0.1123	0.0760
3 to 4	0.2749	0.1781	0.1153	0.0747
3 to 6	0.0079	0.0088	0.0098	0.0108
3 to 7	0.0347	0.0332	0.0318	0.0305
4 to 3	1.3990	0.8116	0.4708	0.2731
4 to 5	0.8935	0.6913	0.5348	0.4138
4 to 6	0.0110	0.0011	0.0103	0.0099
4 to 7	0.0496	0.0510	0.0524	0.0539
5 to 4	13.140	5.3300	2.1620	0.8774
5 to 6	0.0192	0.0167	0.0145	0.0126
5 to 7	0.3747	0.2259	0.1362	0.0821

Appendix 3

Table 9 Transition for the WHO Stage Baseline Line

Transition	1	2	3	4
1 to 2	0.3143	0.1289	0.0529	0.0217
1 to 6	0.0044	0.0041	0.0038	0.0035
1 to 7	0.0139	0.0103	0.0076	0.0057
2 to 1	0.8460	0.8758	0.9066	0.9384
2 to 3	0.1250	0.1119	0.1001	0.0896
2 to 6	0.0171	0.0182	0.0194	0.0207
2 to 7	0.0139	0.1286	0.0119	0.0109
3 to 2	0.8116	1.2320	1.8700	2.8390
3 to 4	0.8856	1.1970	1.6170	2.1850
3 to 6	0.0072	0.0081	0.0091	0.0102
3 to 7	0.0305	0.0245	0.0197	0.0159
4 to 3	4.5930	5.0750	5.6070	6.1950
4 to 5	1.2360	1.0240	0.8484	0.7028
4 to 6	0.0139	0.0165	0.0195	0.0232
4 to 7	0.0325	0.0226	0.0157	0.0109
5 to 4	67.220	56.630	47.710	40.190
5 to 6	0.0390	0.0596	0.0912	0.1394
5 to 7	0.5792	0.3253	0.1827	0.1026

Acknowledgements
This study would not have been a success without the assistance of the Microbiology Department at the University of Venda in providing the secondary data through Professor Pascal O. Bessong.

Funding
Not applicable

Availability of data and materials
The data are available by contacting the corresponding author and can be submitted upon request.

Authors' contributions
CS and DC drafted the manuscript. CS and DC contributed to the analysis and interpretation of the data. Both authors participated in critical revision of the manuscript drafts and approved the final version.

Authors' information
CS is a PhD student and DC is a senior lecturer at the University of the Free State.

Ethics approval and consent to participate
Not applicable

Consent for publication
The authors give their consent to publish this work.

Competing interests
The authors declare that they have no competing interests.

Publisher's Note
Springer Nature remains neutral with regard to jurisdictional claims in published maps and institutional affiliations.

Received: 25 July 2017 Accepted: 6 December 2017
Published online: 18 January 2018

References

1. Perelson AS, Nelson PW. Mathematical analysis of hiv-1 dynamics in vivo. SIAM Rev. 1999;41(1):3–44.
2. Sonnenberg P, Glynn JR, Fielding K, Murray J, Godfrey-Faussett P, Shearer S. How soon after infection with HIV does the risk of tuberculosis start to increase? A retrospective cohort study in south African gold miners. J Infect Dis. 2007;191:150–8.
3. Cingolani A, Lepri AC, Castagna A, Goletti D, De Luca A, Scarpellini P, Fanti I, Antinori A, d'Armino Monfarte A, Girardi E. Impaired CD4 T-cell count response to combined antiretroviral therapy in antiretroviral-naive HIV-infected patients presenting with tuberculosis as AIDS-defining condition. CID. 2012;54(6):853–61.
4. Ndumbi P, Falutz J, Pai NP, Tsoukas CM, et al. PLoS One. 2014;9(4):e94018. https://doi.org/10.1371/journal.pone.0094018.
5. Phillips AN, Staszewski S, Weber R, Kirk O, Francidi P, Miller V, Vernazza P, Lundgren JD, Ledergerber B. HIV viral response to antiretroviral therapy according to the baseline CD4 cell count and viral load. JAMA. 2001;286:2560–7.
6. Abner EL, Nelson PT, Schmitt FA, Browning SR, Fardo DW, Wan L, Jicha GA, Cooper GE, Smith CD, Caban-Holt AM, Van Eldik LJ, Kryscio RJ. Self-reported head injury and risk of late-life impairment and AD pathology in an AD center cohort. Dement Geriatr Cogn Disord. 2014;37:294–306.
7. Mullins LJ. Management and Organisational behaviour. 4th ed. London: Pitman Publishing; 1996.
8. Foucher Y, Mathieu E, Saint-Pierre P, Durand JF, Daures JP. A semi-Markov based on generalised Weibull distribution with an illustration for HIV disease. Biom J. 2005;6:1–9.
9. Longini IM, Clark WS, Byers RH, Ward J, Darrow WW. Statistical analysis of the stages of HIV infection using a Markov model. Stat Med. 1989;8:831–43.
10. Alioum A, Leroy V, Commenges D, et al. Effects of gender, age, transmission category, and antiretroviral therapy on the progression of human immuno virus infection using multistate Markov models. Group d'Epidemiologie clinique du SIDA en Aquitaine, Epidemiology. 1998;9(6):605–12.
11. Reddy T. HIV disease progression in South Africa using multistate Markov models. SACEMA. 2011; http://www.sacemaquarterly.com.
12. Binquet C, Le Teuff G, Abrahamovicz M, Mahboubi A, Yazdanpanah Y, Rey D, Rabaud C, Chirouze C, Berger JL, Faller JP, Chavanet P, Quantin C, Piroth L, Groupe InterCOrevih du Nord-Est (ICONE). Markov modelling of HIV infection evolution in the HAART era. Epidemiol Infect. 2009;137(9):1272–82. https://doi.org/10.1017/S0950268808001775. Epub 2009 Jan 12
13. Grover G, Gadpayle KA, Swain PK, Deka B. A multistate Markov model based on CD4 cell count for HIV/AIDS patients on antiretroviral therapy (ART). Int J Stat Med Res. 2013;2:144–51.
14. Gibson EL. Continuous time multi-state models for survival analysis. Winston-Salem: Wake Forest University, Department of Mathematics; 2008.
15. Halim D. Maximum likelihood estimation for generalized semi-Markov processes. Discrete event dynamics systems: theory and applications. Dep Ind Eng. 1996;6(2):73–104.
16. Jackson CH. Multi-state models for Panel Data: The msm package for R. J Stat Softw. 2013;38(8). http://www.jstatsoft.org/.
17. Titman, A.C., Model diagnostics in multi-state models of biological systems, Department of Pure Mathematics and Mathematical Statistics, University of Cambridge, 2007.
18. Kalbfleisch JD, Lawless JF. The analysis of panel data under a Markov assumption. J Am Stat Assoc. 1985;80:863–71.
19. Cox DR. The statistical analysis of dependencies in point processes. In Stochastic Point Processes. Wiley; 1972.
20. Maskew M, Brennary AT, Westreich D, McNamara L, MacPhail P, and Fox MP. Gender Differences in Mortality and CD4 Count Response Among HIV-Positive Patients Virally Suppressed Within 6 Months of Antiretroviral Therapy Initiation. J Womens Health. 2012; 22(00). https://doi.org/10.1089/jwh. 2012.3585.
21. Castilho JL, Melhekin VV, Sterling TR. Sex Differences in HIV Outcomes in the Highly Active Antiretroviral Therapy Era: A Systematic Review. AIDS Res Hum Retroviruses. 2014;30(5):446–56. https://doi.org/10.1089/aid. 2013.0203.
22. Moore RD and Keruly JC. CD4+Cell Count 6 Years after Commencement of Highly Active Antiretroviral Therapy in Persons with Sustained Virologic Suppression CID. 2007; 44: 441–6.

23. Biadgilign S, Reda AA, Digaffe T. Predictors of mortality among HIV infected patients taking antiretroviral treatment in Ethiopia: A retrospective cohort study. AIDS Res Ther. 2012;9:15 https://doi.org/10.1186/1742-6405-9-15.
24. Goshu TA and Dessie ZG. Modeling progression of HIV/AIDS disease stages using semi-Markov processes. 2013.
25. Lifson AR, Krantz EM. Grambsch PL. Macalino GE. Crum-Cianflone NF. Ganesan A, Okulicz JF, Eaton A, Powers JH, Eberly LE, Agan BK. Clinical, demographic and laboratory parameters at HAART initiation associated with decreased post-HAART survival in a U.S. military cohort. AIDS Res Ther. 2012; 9(4).
26. Hasibi M, Hajiabdolbaghi M, Hamzelou S, Sardashti S, Faroughi M, Jozani ZB, Alinaghi SAS. Impact of age on CD4 response to combination antiretroviral therapy: a study in Tahran, Iran. Orld J AIDS. 2014;4:156–62.
27. Lange JM, Hubbard RA, Inoue LYT, Minin VN. A joint model for multistate disease processes and random informative observation times, with applications to electronic medical records data. Biometrics. 2015; 71(1):90–101.
28. Saint-Pierre P, Combescure C, Daures JP and Godard P. The analysis of Asthma control under a Markov assumption with use of covariates. Statistics in Medicine. 2003;22(24):3755–3770.
29. Maartens G, Cotton M, Meintjes G, Mendelson M, Rabie H, Maharaj S. Clinical guidelines 9th Edition. Copyright Aids for AIDS management (Pty) Ltd. 2012.

Publications
Shoko and Chikobvu *Theoretical Biology and Medical Modelling* (2018) 15:10
https://doi.org/10.1186/s12976-018-0082-0

206
Theoretical Biology and Medical Modelling

RESEARCH Open Access

Determinants of viral load rebound on HIV/AIDS patients receiving antiretroviral therapy: results from South Africa

Claris Shoko* and Delson Chikobvu

Abstract

Background: Antiretroviral therapy (ART) has become the standard of care for patients with HIV infection in South Africa and has led to the reduction in AIDS related morbidity and mortality. In developing countries, the nucleosides reverse transcriptase inhibitors (NRTIs) class are widely used because of their low production costs. However patients treated with NRTIs develop varying degree of toxicity after long-term therapy. For this study patients are administered with a triple therapy of two NRTIs and one non-nucleoside reverse transcriptase inhibitor (NNRTI).

Method: In this study the progression of HIV in vivo is divided into some viral load states and a continuous time-homogeneous model is fitted to assess the effects of covariates namely gender, age, CD4 baseline, viral load baseline, lactic acidosis, peripheral neuropathy, non-adherence and resistance to treatment on transition intensities between the states. Effects of different drug combinations on transition intensities are also assessed.

Results: The results show no gender differences on transition intensities. The likelihood ratio test shows that the continuous time Markov model for the effects of the covariates including combination give a significantly better fit to the observed data. From almost all states, rates of viral suppression were higher than rates of viral rebound except for patients in state 2 (viral load between 50 and 10,000 copies/mL) where rates of viral rebound to state 3 (viral load between 10,000 and 100,000 copies/mL) were higher than rates of viral suppression to undetectable levels. For this transition, confidence intervals were very small. This was quite notable for patients who were administered with AZT-3TC-LPV/r and FTC-TDF-EFV. Although patients on d4T-3TC-EFV also had higher rates of viral rebound from state 2 than suppression, the difference was not significant.

Conclusion: From these findings, we can conclude that administering of any HIV drug regimen is better when based on the viral load level of an HIV+ patient. Before initiation of treatment, patients should be well equipped on how antiretroviral drugs operate including possibilities of toxicity in order to reduce chances of non-adherence to treatment. There should also be a good relationship between patient and health-care-giver to ensure proper adherence to treatment. Uptake of therapy by young patients should be closely monitored by adopting pill counting every time they come for review.

Keywords: HIV progression, Viral load, Lactic acidosis, Peripheral neuropathy, Non-adherence, Triple therapy

* Correspondence: claris.shoko@gmail.com
Department of Mathematical Statistics and Actuarial Sciences, University of the Free State, Box 339, Bloemfontein 9300, South Africa

Background

The first acquired immunodeficiency syndrome (AIDS) case emerged in the early 1980s and since then, the AIDS prevalence has been increasing [1]. Antiretroviral therapy (ART) has become the standard of care for patients with HIV infection and has led to the reduction in AIDS related morbidity and mortality [2, 3].

In South Africa, the antiretroviral therapy available at the present moment are the nucleotides reverse transcriptase inhibitors (NRTIs) class which includes among others zidovudine (AZT), didanosine (ddI), lamivudine (3TC) and stavudine (d4T) [2]. Other NRTIs include abacavir (ABC), tenofovir (TDF) and Emtricitabine (FTC) [4]. NRTIs are most preferred for HIV/AIDS patients in low income countries [5] because of their low production costs [6].

However, patients treated with NRTIs develop varying degrees of myopathy or neuropathy after long-term therapy [7]. AZT causes myopathy, ddI and 3TC cause neuropathy, d4T causes neuropathy or myopathy and lactic acidosis (LA). Studies show that d4T appears to cause lactic acidosis (LA) more frequently than ddI or AZT [8, 6]. In developed countries d4T is no longer favoured as a consequence of both short-term toxicity (lactic acidosis) and long-term toxicity (lipoatrophy and neurophathy) [6]. Neuropathy is long-term in the sense that it is usually associated with late stages of HIV disease as indicated by the presence of opportunistic infections [9]. Thus, it is highly associated with low CD4 cell count and high HIV viral load.

Science literature has successfully established the efficiency of ART in controlling HIV; however its effectiveness depends particularly on the adherence of patients to ART [1]. Adherence can be defined as the extent to which a person uses a medication according to medical recommendations, inclusive of time, dosing, and consistency [10]. Non-adherence results in antiretroviral agents not being able to maintain sufficient concentration to suppress HIV replication in infected cells and to lower the plasma viral load [11]. Poor adherence also accelerates drug-resistant HIV [11, 10].

The development of drug-resistant variants that can develop in HIV/AIDS patients under ART makes it not feasible to completely eradicate the virus [12]. This results in virological rebound and eventual disease progression [12]. But, with proper adherence to treatment, ART has the potential to suppress viral replication, often below the level of detection by commercially available tests [13]. Hirschhorn and others also identified the range of possible virologic responses which among others include failure to ever see a virologic response, decline followed by rebound, ever achieved suppression and loss of suppression after it had been achieved. This justifies the importance of viral load as a marker of treatment efficacy.

Stochastic models have proved to be the best when dealing with real life situations particularly when modelling biological phenomena such as in vivo HIV dynamics. As the HIV progresses in an individual, there is random movement between states, stochastic models are very good at handling these random variables. Stochastic processes also allow modelling the effects of covariates like stage of infection, virus subtype, presents of STIs, sexual practices, condom use, religion, education, age, gender and genes on transition intensities. In particular, time-homogeneous Markov models are usually used to model the evolution in chronic diseases [14].

Time-homogeneous Markov modelling

Consider a model consisting of $k = 6$ states belonging to the state space $S = \{1, 2, \ldots, \mathrm{k} = 6\}$. Consider the i^{th} individual being in some state at time t. Let $X(t)$ denote the state occupied by a randomly chosen individual at time t. Assuming that the individual's movements obey a continuous time-homogeneous Markov process, then for $0 \le s \le t$ the $k \times k$ transition probability matrix $P(s, t)$ with entries:

$$p_{ij}(s,t) = \Pr\{X(t) = j | X(s) = i\}, i; j = 1, \ldots, k$$

Can be specified in terms of transition intensities

$$q_{ij}(t) = \begin{cases} \lim\limits_{\Delta t \to 0} \dfrac{p_{ij}(t, t+\Delta t)}{\Delta t}, & i \neq j \\ -\sum\limits_{i \neq j} q_{ij}(t), & i = j \end{cases}$$

Here $q_{ij}(t)$ are the entries of the $k \times k$ transition intensity matrix $Q(t)$. Since our model is time-homogeneous we consider $q_{ij}(t) = q_{ij}$ independent of time. $Q = (q_{ij})$ is the transition intensity matrix. For this model, transition probabilities are stationary such that:

$$P(s, s+t) = P(0, t) = P(t)$$

For each of the individuals, covariates are measured. Interest centres on the relationship between the covariates and the transition intensities q_{ij} in the Markov model. Variables associated with the transition intensities are assumed to have a multiplicative effect of the form;

$$q_{ijh} = q_{ij}^{(0)} \exp\left(\beta_{ijs}^{T} \boldsymbol{Z}_s\right) \quad (1)$$

Where $\boldsymbol{Z}$ is the s-dimensional vector of covariates. β_{ijs} is the vector of s regression parameters relating to the instantaneous rate of transition from state i to state j. $q_{ij}^{(0)}$ is the baseline transition intensity relating to the transition from state i to state j.

Eq. (1) can be written as a log-linear model as shown below;

$$log\ q_{ij} = \beta_{ij0} + \sum_{s=1}^{p} \beta_{ijs} z_s \ \text{ for } \ i \neq j = 1, 2, \ldots \text{ and } s = 1, 2, \ldots, p \quad (2)$$

where $\exp(\beta_{ij0}) = q_{ij}^{(0)}$ the baseline transition rates for patients in which the covariates are not mentioned, z_s is a s-dimensional vector of covariates and β_{ijs} represents a vector of vector of s regression parameters relating the transition rates from state i to state j to the covariates $\bar{z}_s$.

Maximum likelihood estimates of the baseline transition intensity matrix can be obtained by maximising the likelihood function with respect to the parameter $q_{ij}^{(0)}$. We let T_{ij}, i; $j = 1, \ldots, k$, be the total time spent by all individuals in state i before making a transition to state j. we also let b_{ij}, i; $j = 1, \ldots, k$, be the total number of transitions from state i to state j. Then the maximum likelihood estimates of the baseline transition intensities are;

$$q_{ij}^{(0)} = \frac{b_{ij}}{T_{ij}}, i; j = 1, \ldots, k$$

$q_{ij}^{(0)}$ is the baseline hazard rate without (or ignoring) the effects of the covariates. In calculating $q_{ij}^{(0)}$ all β_{ij0} are chosen to be equal to zero, which means that there are no covariates effects.

Estimates of $\hat{\beta}$ obtained by maximising the partial likelihood function are given by;

$$L(\beta) = \prod_{h=1}^{n} \frac{\exp\left(\beta_{ij}^{T} z_{sh}\right)}{\sum_{l \in R\left(t_{ij,h}\right)} exp\left(\beta_{ij}^{T} z_{sh}\right)}$$

Where z_{sh} is the s-dimensional covariate vector for patient h and $R(t_{ij,\,h})$ is the risk at time t for making a transition from state i to state j.

In this study, we explore the effects of treatment toxicity (lactic acidosis (LA) and peripheral neuropathy (PN)), non-adherence (NA), treatment line, CD4 baseline, viral load baseline, age on the changes in the level of viral load in the plasma cells. The analysis is done using a time-homogeneous Markov model with covariates. In medical research, the state of the patient at observation time is the only thing known with certainty. The researcher may know the time interval in which a transition has occurred, but not the exact time. Thus, time-homogeneous Markov models which are interval censored can handle such data [15].

In the section that follow, methods used in analysing the data are explored. This is followed by a section 3 on results and discussions. Lastly in section 4 conclusion of the findings is done.

Methods

Data description

The model is applied to 320 HIV-1 infected patients on anti-retroviral therapy (ART) from a Wellness clinic in Bela Bela, South Africa, from year 2005 to year 2009. These patients were observed after 3 months of treatment uptake and every 6 months thereafter. This yielded 2259 observations. From these patients 224 were females and 96 were males. 172 patients were aged between 15 and 45 and 72 were over 45 years of age. The mean age of the patients at enrolment was 40.62 years. 267 had a viral load baseline above 10,000 copies/μL and 49 had a viral load baseline below 10,000 copies/μL. At enrolment, the mean viral load was 138,208 copies/μL with a maximum of 818,600 copies/μL. 226 patients had a CD4 baseline below 200 cells/mm^3 and 96 had a CD4 baseline above 200 cells/mm^3. Upon initiation of treatment a number of factors were considered. These include drug toxicity which results in lactic acidosis and peripheral neuropathy. Other variables include non-adherence to treatment therapy, treatment change, treatment line and resistance to treatment. 101 patients developed lactic acidosis, 43 developed peripheral neuropathy and 36 showed some signs of non-adherence to treatment.

For each and every visit time, blood samples were obtained for each patient and stored frozen until assayed. Plasma HIV RNA was measured using an amplicator HIV-1 monitor assay kit which has a lower limit of sensitivity of 50 copies/μL.

At $t = 0$ the regimens that were mostly administered to patients were the triple combination therapy, d4T-3TC-EFV (208 patients) and d4T-3TC-NVP (92 patients). d4T and 3TC represent Stavudine and Lamivudine respectively which fall under nucleoside reverse transcriptase inhibitors (NRTI) class. EFV and NVP stand for Efavirenz and Nevirapine respectively and are from the non-nucleoside reverse transcriptase inhibitors (NNRTI) class. Table 1 below gives a frequency

Table 1 Distribution of different treatment combination for the period t = 0 to $t = 3.5$ years

	Time in Years								
	0	0.25	0.5	1	1.5	2	2.5	3	3.5
D1	208	194	168	141	95	46	18	5	3
D2	2	4	21	51	81	96	90	60	32
D3	92	77	72	63	35	23	7	1	0
D4	3	6	6	14	35	38	45	36	31
D5	0	0	0	1	1	3	8	10	10
D6	0	0	0	0	0	3	5	7	3
D7	2	2	1	2	5	4	2	2	1

Key: **D1** = d4T-3TC-EFV, **D2** = AZT-3TC-EFV, **D3** = d4T-3TC-NVP, **D4** = AZT-3TC-NVP, **D5** = FTC-TDF-EFV, **D6** = AZT-3TC-LPV/r, **D7** = Other combinations

distribution for the different treatment combinations from $t = 0$ to $t = 3.5$ *years*.

In patients who showed some signs of non-adherence, d4T was substituted with AZT (Zidovudine). A switch from d4T-3TC-EFV (D1) to AZT-3TC-EFV (D2) was most common rising from 10 patients in the first 6 months to 92 patients in 30 months (2 and half years). During the same period the number of patients who switched from d4T-3TC-NVP (D3) to AZT-3TC-NVP (D4) rose from 6 to 45. After 1 year of treatment uptake one patient was introduced to FTC-TDF-EFV (D5) and after three and half years, the frequency increased to 10 patients. Another combination of FTC-TDF-NVP was also introduced to 3 patients after 2 years and the number rose to 7 after 3 years. AZT-3TC-LPV/r (D6) was also administered and at $t = 0$, 2 patients were administered with this triple combination. Other treatment combinations that were administered include FTC-TDF-NVP, AZT-ddI-LPV/r, d4T-3TC-LPV/r, ddI-d4T-3TC, FTC-TDF-LPV/r. However, these were not frequently administered and hence they were treated as other (D7) combinations for analysis purpose. The table below shows the frequencies for each of the treatment combinations;

Drug	D1	D2	D3	D4	D5	D6	D7	Total
Frequency	879	461	370	234	56	47	212	2259

The table shows that d4T-3TC-EFV was the most frequently used drug combination.

For each visit, viral load in the plasma was also measured. In this study, if the viral load was below 50 copies/μL it recorded it as undetectable. In this study, the progression of HIV/AIDS is defined by change in viral load level. The viral load levels are divided into 5 transient states and the sixth state being the absorbing state, death. The viral load states and other factors that are likely to determine change in viral load levels are defined in the next sub-section.

Variable coding

For this study, variables are coded as follows:

$$\text{Age} = \begin{cases} 1, & \leq 45\ years \\ 0, & > 45\ \text{years} \end{cases},$$

$$\text{Lactic acidosis (LA)} = \begin{cases} 1, & Yes \\ 0, & \text{No} \end{cases},$$

$$\text{Peripheral neuropathy(PN)} = \begin{cases} 1, Yes \\ 0, No \end{cases},$$

$$\text{Non-adherence (NA)} = \begin{cases} 1, Yes \\ 0, No \end{cases},$$

$$\text{CD4 baseline (CD4B)} = \begin{cases} 1, \leq 200\ \text{cells/mm}^3 \\ 0, > 200\ \text{cels/mm}^3 \end{cases},$$

$$\text{Gender} = \begin{cases} 1, & male \\ 0, & female \end{cases},$$

$$\text{viral load baseline (VLB)} = \begin{cases} 1, & > 10\,000\ copies/\mu L \\ 0, & \leq 10\,000\ copies/\mu L \end{cases},$$

$$\text{Treatment Change (TC)} = \begin{cases} 1, Yes \\ 0, No \end{cases},$$

$$\text{Treatment line (TL)} = \begin{cases} 1, TL = 1 \\ 0, TL = 2. \end{cases}$$

$$\text{Viral load levels } (X(t)) = \begin{cases} \mathbf{1;} & VL < 50 \\ \mathbf{2;} & 50 \leq VL < 10\,000 \\ \mathbf{3;} & 10\,000 \leq VL < 100\,000 \\ \mathbf{4;} & 100\,000 \leq VL < 500\,000 \\ \mathbf{5;} & VL \geq 500\,000 \\ \mathbf{6;} & Dead \end{cases},$$

$$\text{Resistance (Res)} = \begin{cases} 1\ if\ yes \\ 0\ if\ NO \end{cases}$$

The table below shows the frequency distribution of each viral load state at $t = 0$ (baseline), that is at treatment commencement; (Table 2).

Results from Table 2 show that at t=0 years most of the patients had a viral load above 10 000 copies/μL. During the first 0.25 years of treatment uptake the majority of the patients had achieved a suppressed viral load to undetectable levels. These results show possibility of transitions, from state i to state j, between the viral load states, $X(t)$. In this case $X(t) = \{1, \ldots, 6\}$. We assume that the transition rate between states for any subject is governed by some covariates identified above. The effects of the covariates; age, lactic acidosis (LA), peripheral neuron (PN), gender, CD4 baseline (CD4BL), treatment line (TL), viral load baseline (VLBL), treatment change (TC), non-adherence (NA) and resistance to treatment (Res) on transition intensities, q_{ij}, is assessed. The log-likelihood linking q_{ij} with the linear effects of covariates is given by:

$$\log q_{ij} = \beta_{ij0} + \sum_{s=1}^{p} \beta_{ijs} z_s \ \ for\ \ i \neq j, i = 1, 2.., 5\ \ and$$
$$j = 1, 2..., 6\ \ \text{and}\ \ s = 1, 2..., 10$$

As defined in Eq. (2).

Thus, the transition intensity for a patient h in this study is given by the model:

Table 2 Number of HIV/AIDS patients in each viral load state from t = 0 to t = 0.5 years

	Viral load levels ($X(t)$)					
	1	2	3	4	5	6
t = 0 years	4	43	134	106	32	0
t = 0.25 years	155	123	6	4	4	24
t = 0.5 years	214	48	13	2	3	11

$$q_{ij} = q_{ij}^{(0)} \exp(\beta_{ij}^{(Age)} Age_h + \beta_{ij}^{(LA)} LA_h + \beta_{ij}^{(PN)} PN_h + \beta_{ij}^{(Gender)} Gender_h + \beta_{ij}^{(CD4BL)} CD4BL_h + \beta_{ij}^{(TL)} TL_h + \beta_{ij}^{(VLBL)} VLBL_h + \beta_{ij}^{(TC)} TC_h + \beta_{ij}^{(NA)} NA_h + \beta_{ij}^{(Res)} Res_h) \quad (3)$$

For this model the baseline transition intensities, $q_{ij}^{(0)}$, refer to a patient with age category 0 (over 45 years old), no LA, no PN, Gender = 0 (female), CD4BL = 0 (above 200 cells/mm^3, TL = 0 (second line), VLBL = 0 (over 10,000 copies/mL), no TC, no NA and no resistance. The transition intensities, q_{ij}, are presented in rates per year. q_{ij} are the elements of a 6×6 transition intensity matrix Q from a continuous time-homogeneous Markov process. As indicated in Eqs. (2 and 3) can be represented by the log-linear model;

$$\ln q_{ij} = \ln q_{ij}^{(0)} + \beta_{ij}^{(Age)} Age_h + \beta_{ij}^{(LA)} LA_h + \beta_{ij}^{(PN)} PN_h + \beta_{ij}^{(Gender)} Gender_h + \beta_{ij}^{(CD4BL)} CD4BL_h + \beta_{ij}^{(TL)} TL_h + \beta_{ij}^{(VLBL)} VLBL_h + \beta_{ij}^{(TC)} TC_h + \beta_{ij}^{(NA)} NA_h + \beta_{ij}^{(Res)} Res_h) \quad (4)$$

Here β_{ij} represents the log-linear effects of the mentioned covariate on transition intensities from state $i = 1, 2, \ldots, 5$ to state $j = 1, 2, \ldots, 6$ for individual h. Computation of the estimated baseline transition intensities is done by setting all the covariates to their mean.

Results and discussions

Figure 1 is a Box and whiskers plot which shows the distribution of viral load states, defined in Section 2.2, for each and every visit time which is originally considered to be discrete.

Figure 1 shows that at time equal to zero, there were no cases in state 6 since the state represents the death state. On treatment initiation, the majority of the patients were in state 3 defined by a viral load level between 10,000 and 100,000 copies/μL. After 3 months (0.25 years) the majority of the patients had moved to state 2. This is an indication of viral suppression by the antiretroviral therapy. From a period of 1 year onwards, the majority of the patients had moved to state 1, a state of undetectable viral load. However patients whose viral load is not suppressed throughout the whole period are still notable. There is need to investigate further the factors that are associated with failure of viral suppression.

State table for transition counts

The results from Table 3 show that the highest number of deaths were recorded from state 3 which is defined by a viral load beteen 10,000 and 100,000 copies/μl. Also to note are the deaths from state 1 defined by suppressed/undetectable viral load (< 50 copies/μl), there is need to

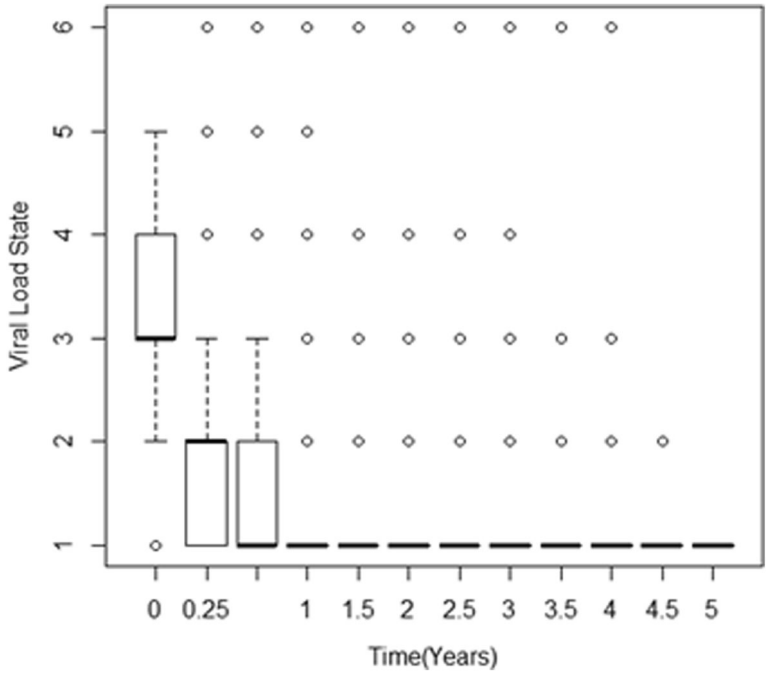

Fig. 1 Box and whiskers diagram for the distribution of viral load levels for each visit time from initiation of therapy to 5 years. Data was collected at discrete time points, that is, at $t = 0$ years, $t = 0.25$ years, $t = 0.5$ years and after every 0.5 years thereafter

Table 3 Transition counts

	To					
	1	2	3	4	5	6
From 1	1109	104	16	2	1	17
2	207	98	21	4	1	8
3	80	63	22	4	0	19
4	45	54	6	2	4	9
5	6	21	0	4	2	7

assess the determinants of deaths from this state because patients in this state have most of the virus particle cleared by the antiretroviral drug. We start off by finding estimates of the transition intensities for a continuous time Markov model without the effects of covariates. The transition intensities are estimated based on the assumption that the transition probabilities p_{ij} are known and are given as follows;

$$q_{ij}(t) = \begin{cases} \lim\limits_{\Delta t \to 0} \dfrac{p_{ij}(t, t+\Delta t)}{\Delta t}, & i \neq j \\ -\sum\limits_{i \neq j} q_{ij}(t), & i = j \end{cases}$$

Estimates of the transition intensies are given in Table 4 below;

Results from Table 4 show that antiretroviral therapy plays an important role in slowing down disease progression particularly for patients in state 3 and state 4. From state 3 transitions to a better state (state 2) is more than 8 times higher than transitions to the worse state (state 4). For patients in state 4, transition to a better state is more than 6 times than transition to the worst state (state 5). However, a patient in state 2 is about twice likely to experience disease progression than recovery. This is a cause of concern since these patients have lower levels of viral load compared to patients in state 3, 4 and 5. Although transitions to better state is lower than transition to worst state for patients initially in state 2, these patients have the least transition to death compared to deaths from all the other states. This indicates that even though viral suppression is reached, HIV/AIDS patients still experience some viral rebound as supported by Hirschhorn and others in their report [12].

Table 4 Transition intensities from a continuous time-homogeneous Markov model

Intensities	Estimated Intensities	Confidence Interval
q_{12}	0.4687	(0.3787,0.5801)
q_{16}	0.01965	(0.008817,0.04379)
q_{21}	3.446	(2.983,3.981)
q_{23}	6.195	(2.674,14.36)
q_{26}	0.0000386	(2.34 × 10^{−39},6.382 × 10^{29)
q_{32}	34	(15.22,75.93)
q_{34}	4.178	(1.551,11. 25)
q_{36}	1.203	(0.7465,1.940)
q_{43}	23.25	(11.88,45.52)
q_{45}	3.651	(1.174, 11.35)
q_{46}	0.005509	(1.84 × 10^{−45},1.64 × 10^{40}
q_{54}	10.64	(5.962,18.97)
q_{56}	1.466	(0.5114,4.202)
-2xLL	2799.465	

Results from Table 4 also show that mortality from state 4 (transition from 4 to 6) is rather too small (less than 0.05) compared to state 3 and state 5. This again is an irregularity in the fitted model which can be addressed by fitting a continuous time homogeneous Markov model with covariates effects. Thus, in the next section a continuous time Markov model with covariates is fitted.

Effects of covariates on transition intensities

Maximum likelihood estimation of the baseline transition intensities as well as the log-linear effects for the covariates; viral load baseline (VLB), CD4 baseline (CD4B), age, gender, treatment line (TL), treatment change (TC), non-adherence (NA), lactic acidosis (LA), peripheral neuropathy (PN), resistance to treatment (Res) and triple therapy (Therapy) was done using the "msm" package in R. The log-linear model as indicated in Eq. (4) is:

$$\begin{aligned} \ln q_{ij} = \ln q_{ij}^{(0)} &+ \beta_{ij}^{(Age)} Age_h + \beta_{ij}^{(LA)} LA_h \\ &+ \beta_{ij}^{(PN)} PN_h + \beta_{ij}^{(Gender)} Gender_h \\ &+ \beta_{ij}^{(CD4BL)} CD4BL_h + \beta_{ij}^{(TL)} TL_h \\ &+ \beta_{ij}^{(VLBL)} VLBL_h + \beta_{ij}^{(TC)} TC_h + \beta_{ij}^{(NA)} NA_h \\ &+ \beta_{ij}^{(Res)} Res_h + \beta_{ij}^{(Therapy)} Therapy_h) \end{aligned}$$

where β_{ij} is the log-linear effects of the mentioned covariate on the baseline transition intensities $q_{ij}^{(0)}$.

On fitting the time-homogeneous model with all the covariates, we discovered that the model did not converge to a maximum likelihood. As a result confidence interval for the estimates could not be computed. The covariates effects model was fit for each of the covariates one after the other and it was discovered that treatment line (TL), gender, resistance to treatment (Res) and treatment change (TC) had no significant effects on HIV progression based on viral load. As a result, these variables were removed from the model. Results from the model with all covariates are shown in the appendices. Table 5 shows the estimated baseline transition intensities with covariates set to their mean values in the data. These represent the average intensities for the whole

Table 5 Baseline transition intensities

	Estimated baseline transition rates	Confidence Interval
q_{12}	0.4938	(0.3849, 0.6335)
q_{16}	0.0000013	(1.7 × 10^{−39}, 9.9 × 10^{26})
q_{21}	4.008	(3.358, 4.783)
q_{23}	49.74	(6.2 × 10^{−17}, 4.0 × 10^{19})
q_{26}	0.000071	(9.0 × 10^{− 13}, 5617)
q_{32}	535.5	(6.9 × 10^{− 16}, 4.1 × 10^{20})
q_{34}	0.0090	(6.6 × 10^{−33}, 1.2 × 10^{28})
q_{36}	0.000173	(4.3 × 10^{−23}, 6.9 × 10^{14})
q_{43}	64.37	(0.000011, 3.8 × 10^8)
q_{45}	0.1553	(6.1 × 10^{−21}, 3.9 × 10^{18})
q_{46}	0.000593	(2.8 × 10^{− 103}, 1.3 × 10^{96})
q_{54}	385.0	(0.00016, 9.5 × 10^8)
q_{56}	0.00117	(8.7 × 10^{−18}, 1.6 × 10^{13})

population of given covariates. Table 6 shows estimates of log-linear effects of each covariate on transition intensities.

Table 5 above shows the baseline transition intensities for the model with covariates. Results from Table 5 now show a decreasing trend in the transition rates as the viral load becomes more and more suppressed. As a result, the undetectable viral load state (state 1) has the lowest transition rates to death. This result justifies the need to include covariates effect in Markov models. The results also show that for patients with a viral load level greater than 2, transition rates to better states are higher than transition rates to worse states. This is quite pronounced for patients initially in state 3 where transition to a better state (state 2) is 535.5 which is quite high compared to transition to the worse state (state 4) which is equal to 0.0090. However, there is a treatment challenge as patients make transitions from state 2. These patients tend to have a viral rebound resulting in transition to a worse state (state 3) being far much higher than transitions to an undetectable viral load state (state 1). This means that for HIV patients in this cohort, achieving undetectable viral load was a challenge. In the next Table are the effect age, viral load baseline (VLB), CD4 baseline (CD4B), non-adherence (NA), peripheral neuropathy (NA), Lactic acidosis (LA) and Triple therapy (Therapy). Estimates of the confidence intervals are also given. Results from Table 6 below show maximum likelihood estimates of the

Table 6 Log-linear effects of Covariate on Baseline Transition Intensities

	Age	VLB	CD4B	NA	PN	LA	Therapy
β_{12}	− 0.16633 (− 0.72,0.39)	0.2244 (− 0.548, 0.997)	− 0.07828 (− 0.621,0.464)	0.04598 (− 0.721,0.813)	− 0.22434 (1.038,0.589)	− 0.3857 (− 1.01,0.238)	− 0.16391 (− 0.291,-0.036)
β_{16}	4.90404 (− 27.45,37.25)	4.3865 (− 30.94,39.71)	4.37298 (− 29.56,38.30)	4.84416 (− 19.60,29.29)	−6.46244 (− 304.5291.5)	−5.4473 (− 132.3121.3)	− 0.62595 (− 10.66,9.409)
β_{21}	− 0.37704 (− 0.747,-0.007)	−0.3692 (− 0.958,0.219)	0.32956 (− 0.033,0.691)	− 1.37557 (− 1.941,-0.810)	0.13742 (− 0.463,0.738)	−0.2188 (− 0.664,0.227)	−0.26823 (− 0.362,-0.1743)
β_{23}	0.57497 (− 1.807,2.957)	6.9272 (− 9.54,23.39)	− 7.29998 (− 140.9126.3)	3.98173 (− 13.81, 21.77)	1.35016 (− 1.674,4.37)	6.0407 (− 10.04,22.11)	0.07194 (− 0.569, 0.714)
β_{26}	−2.30421 (− 4.149,-0.459)	4.5439 (− 29.65,38.73)	6.73053 (− 26.55,40.01)	− 7.68210 (− 42.08,26.72)	−8.15962 (− 44.34,28.01)	−8.0351 (− 38.79, 22.71)	− 0.11284 (− 0.536, 0.311)
β_{32}	0.10538 (− 2.033, 2.244)	5.5407 (− 10.91,21.99)	−7.48353 (− 141.2126.2)	2.05465 (− 15.80, 19.91)	0.90591 (− 1.60,3.41)	5.1128 (− 10.99, 21.21)	− 0.02301 (− 0.636, 0.590)
β_{34}	6.34668 (− 22.04,34.74)	0.9591 (− 364,366)	6.36080 (− 24.03,36.75)	− 0.39441 (− 5.74,4.95)	0.75615 (− 2.91, 4.43)	− 7.5396 (− 96.93, 81.85)	0.18151 (− 0.364, 0.727)
β_{36}	−0.56368 (− 91.13,90.0)	− 0.5756 (− 167.8166.7)	−0.32611 (− 100.58,99.9)	−1.74039 (− 129.,126)	−0.02814 (− 118.8118.7)	−0.5560 (− 101.8100.7)	0.17006 (− 22.594,22.93)
β_{43}	0.51266 (− 1.15,2.18)	− 5.2372 (− 101.6,91.18)	0.88887 (− 0.728,2.50)	−0.60486 (− 4.507, 3.29)	−0.17207 (− 1.94,1.59)	0.4315 (−1.64,2.50)	0.05339 (− 0.403, 0.510)
β_{45}	1.13450 (− 95.6,97.88)	1.0766 (− 182.2184.4)	−3.17689 (− 23.95,17.59)	6.33428 (− 24.76, 37.43)	−4.56027 (− 39.83, 30.71)	−1.2263 (− 28.31, 25.8)	0.12320 (− 1.479, 1.726)
β_{46}	−0.01190 (− 87.59,87.56)	−0.7223 (− 1.412,1.41)	−0.55243 (− 89.7,88.6)	−0.98022 (− 136.4134.4)	−0.33782 (− 126.7126.1)	0.7166 (− 100.7102.2)	0.16568 (− 7.369, 7.701)
β_{54}	−6.22114 (− 52.9,40.48)	−1.3299 (− 9.66,7.001)	2.39466 (− 2.147,6.94)	2.10654 (− 21.43, 25.6)	−0.578 (− 5.37,4.22)	2.3389 (− 7.64,12.31)	0.39170 (− 0.892, 1.676)
β_{56}	0.00842 (− 85.69,85.71)	3.1076 (− 29.67,35.89)	− 3.87100 (− 47.67,39.93)	−2.54236 (− 69.13, 64.0)	−0.86234 (− 68.27,66.54)	− 1.6107 (− 23.59, 20.37)	−0.01408 (− 9.110,9.082)
	−2xLL =1691.177						

log-linear effects of the variables on the baseline transition intensities.

Results from Table 6 show that for patients with non-adherence (NA) to treatment there is a reduction of transitions from a viral load level of 2 (viral load between 50 and 10,000 copies/ μL) to a viral load level of 1 (undetectable viral load). For the same group of patients, there is an accelerated rate of transition from state 2 to state 3 (between 10,000 and 100,000 copies/μL). Non-adherence to treatment also cause an accelerated rebound of viral load from state 4 (between 100,000 and 500,000 copies/μL) to state 5 (viral load over 500,000 copies/μL). From all the states, the results also show an accelerated viral rebound for patients who developed some resistance to treatment compared to those who did not. This is shown by very high positive values of β_{ij}'s for cases in which j is a worse state compared to i. Patients with peripheral neuropathy also have accelerated transition rates from state 2 to state 3. Although transition from state 2 to state 1 are accelerated, the rate is slower than that from state 2 to state 3. From the results it can also be noted that having lactic acidosis (LA) accelerates transition from state 2 to state 3 more than either having peripheral neuropathy or non-adherence. Patients who enrolled when their CD4 cell count was below 200 cells/mm^3 have higher transition rates from a viral load level between 10,000 and 100,000 copies/μL (state 3) to a viral load between 100,000 and 500,000 copies/μL (state 4). Having a viral load baseline level greater than 10,000 copies/μL at enrolment increases viral rebound from state 2 to state 3.

The different treatment combinations give precise estimates of the log-linear effects as shown by the confidence intervals that are narrow. Given the different combination therapy administered to patients, transitions to viral rebound are greater than transitions to viral suppression for patients with viral load 2 and 3 (viral load between 50 and 100,000 copies/μL).

From the different combination therapy that was administered to the patients, D4T-3TC-EFV was the most frequently administered triple therapy with 889 cases, followed by AZT-3TC-EFV and D4T-3TC-NVP and AZT-3TC-NVP with 475; 431 and 279 cases respectively. Table 7 shows the transition intensities for the different drug combinations.

Results from Table 7 shows that narrow confidence intervals for transition intensities from state 1 to 2 (rebound from an undetectable viral load to a viral load between 50 and 10,000 copies/μL), 2 to 6 (deaths from a viral load level between 50 and 10,000 copies/μL) and 2

Table 7 Transition intensities for various drug combinations on viral load states

	Baseline	D1	D2	D3	D4	D5	D6	D7
q_{12}	0.493066 (0.400,0.607)	0.607293 (0.458,0.806)	0.515483 (0.415,0.64)	0.4376 (0.353,0.543)	0.371404 (0.281,0.491)	0.3153 (0.216,0.460)	0.2676 (0.164,0.437)	0.227 (0.124,0.418)
q_{16}	0.001107 (0.00004,30.57)	0.002452 (0.0001,371)	0.001311 (0.00006,26.32)	7.013e-04 (0.00006,821)	0.000375 (8.4e-14,1.7e + 06)	2.005e-04 (4.1e-18,9.8e + 09)	1.072e-04 (1.4e − 22,8.1e + 13)	5.735e-05 (4.1e-27,7.8e + 17)
q_{21}	3.279872 (2.82,3.8122)	4.612591 (3.802,5.596)	3.527413 (3.027,4.11)	2.698 (2.289,3.180)	2.062904 (1.656,2.57)	1.578 (1.174,2.12)	1.206 (0.83,1.763)	0.9226 (0.578,1.472)
q_{23}	6.644026 (1.788,24.68)	6.063371 (1.422,25.86)	6.515630 (1.774,23.92)	7.002 (1.642,29.86)	7.523862 (1.21,46.77)	8.085 (0.792,82.53)	8.688 (0.489,154.4)	9.336 (0.293,297.6)
q_{26}	0.391710 (0.279,0.549)	0.452130 (0.259,0.79)	0.403885 (0.291,0.561)	0.3608 (0.216,0.603)	0.322291 (0.133,0.779)	0.2879 (0.0796,1.041)	0.257 (0.047,1.406)	0.2297 (0.027,1.906)
q_{32}	38.175291 (11.11,131.2)	39.308653 (10.41,148.4)	38.414356 (11.41,129.3)	37.54 (9.342,150.8)	36.686336 (6.223,216.3)	35.85 (3.737,344.0)	35.04 (2.134,575.2)	34.24 (1.187,987.3)
q_{34}	3.161374 (1.161,8.61)	2.509951 (0.829,7.60)	3.009489 (1.124,8.061)	3.608 (1.149,11.33)	4.326610 (0.968,19.33)	5.188 (0.745,36.14)	6.220 (0.549,70.43)	7.458 (0.397,140.2)
q_{36}	0.010004 (0.00005,212.1)	0.008059 (0.00001,59.72)	0.009553 (0.000001,681)	0.011 (0.00019,6700)	0.013423 (0.00011,1508)	0.016 (0.00028,8987)	0.019 (0.00053,6690)	0.02236 (0.00092,5419)
q_{43}	19.868383 (10.22,38.61)	18.564606 (10.41,33.12)	19.582706 (10.73,35.75)	20.66 (8.413,50.72)	21.789 (5.987,79.31)	22.98 (4.128,128.0)	24.24 (2.809,209.2)	25.57 (1.900,344.3)
q_{45}	4.354376 (0.513,36.90)	3.723129 (0.893, 15.53)	4.211261 (0.679,26.127)	4.763 (0.209, 108.3)	5.387908 (0.053,545.4)	6.094 (0.0013,290.2)	6.893 (0.003,1578)	7.797 (0.0007,8679)
q_{46}	0.00686 (0.00007,666.4)	0.005563 (0.00002,1335)	0.006565 (0.00006,710)	0.0077 (0.000019,3109)	0.009145 (0.00001,4305)	0.011 (0.00004,2594)	0.012 (0.00005,28,140)	0.01503 (0.00005,4004)
q_{54}	17.711355 (3.557,88.2)	10.764470 (5.385,21.52)	15.925970 (4.35,58.27)	23.56 (1.960,283.2)	34.860406 (0.829,1466)	51.58 (0.345,7711)	76.31 (0.1426,4082)	112.9 (0.0588,2168)
q_{56}	0.029928 (0.0004,2199)	0.030468 (0.00062,14,870)	0.030042 (0.00038,2347)	0.02962 (0.00004,2153)	0.029208 (0.00056,15,210)	0.02880 (0.00018,45,560)	0.02840 (0.00035,22,650)	0.02800 (0.00055,14,060)

Key: **D1** = D4T-3TC-EFV, **D2** = AZT-3TC-EFV, **D3** = D4T-3TC-NVP, **D4** = AZT-3TC-NVP, **D5** = FTC-TDF-EFV, **D6** = AZT-3TC-LPV/r, **D7** = Other combinations

to 1 (transition from a viral load between 50 and 10,000 copies/μL to an undetectable viral load). This indicates that the continuous time Markov model for the different drug combinations predicts better these transitions compared to all the other transitions. However, confidence intervals for the deaths from state 1, 3, 4 and 5 are very wide. This could be due to the smaller numbers of deaths for patients in this cohort. Highest rates of mortality are recorded for patients with viral load level between 50 and 10,000 copies/μL, but from all the other states mortality rates are very low.

Overall, the model shows higher transition rates to viral suppression compared to the transitions to viral rebound. For patients with a viral load between 10,000 and 100,000 copies/μL, drug combination d4T-3TC-EFV has the highest transition rates to recovery followed by the triple combination AZT-3TC-EFV, d4T-3TC-NVP, AZT-3TC-NVP, FTC-TDF-EFV, AZT-3TC-LPV/r respectively. When the viral load is still above 100,000 copies/μL, the triple combination AZT-3TC-LPV/r gives the best results followed by FTC-TDF-EFV, AZT-3TC -NVP, d4T-3TC-NVP, d4T-3TC-EFV, d4T-3TC-NVP, AZT-3TC-EFV in that order. However, for this cohort AZT-3TC-LPV/r as not frequently administered. For patients in state 2, viral rebound to state 3 is greater than viral suppression to undetectable levels and these rates of viral rebound are the highest for patients being administered with triple combinations AZT-3TC-LPV/r and FTC-TDF-EFV.

Below are the expected amount of time spent in each state from $t = 0$, the present time and death (absorbing state). For a patient in state r at $t = 0$, the expected total time the patient is to spend in state s before relapse to death is given by:

$$L_s = \int_0^t p_{rs}(u)du$$

where p_{rs} is the probability of transition from state r to state s. The value of state r is by default set to be 1 (the undetectable viral load state). The results are given below.

State 1	State 2	State 3	State 4	State 5	State 6
18.53012518	2.48700930	0.43269999	0.06880021	0.01688621	Infinity

Thus the patients are forecasted to spend approximately 18.5 years in a state of undetectable viral load (state 1) and in the other states patients are expected to spend less than 2.5 years since these are temporal states. This is evidenced by the fact that throughout the 5 year study period, only 17.8% of the patients were reported dead with 10.9 points occurring during the first 6 months.

Assessment of the fitted model

In order to assess the goodness of fit of the continuous time-homogeneous Markov model for the effects of covariates, the expected percentage prevalence is plotted against the observed percentage prevalence. The prevalence is averaged over the covariates observed in the data. The percentage prevalence is plotted as functions of time for each viral load state. Figures 2 and 3 show the pravalence plots for the effects of all covariates including treatment therapy and the model for the effects of treatment therapy respectively for each state.

The results from the plots in Fig. 2 show perfect fit of the model to the observed data. In addition to that, the plots show that the percentage prevalence for state 1 increase rapidly in the first year. This shows that under normal circumstances patients on antiretroviral therapy are expected to attain an undetectable viral load in less than a year post treatment commencement. For this same state it also shows that the percentage prevalence becomes stable after a year. Although at $t = 0$ state 1 had the least percentage prevalence, from 1 year onwards about 80% of the patients had attained an undetectable viral load (state 1). States 2 and 3 had the highest percentage prevalence at $t = 0$, however in less than 6 months of treatment uptake, the percentage prevalence had dropped (Fig. 3).

Results from Fig. 3 show that if we only consider the effects of treatment therapy without considering the effects of other covariates, the fitted model underestimates death prevalence as well as state 1 prevalence. We further perform a likelihood ratio test to compare the fitted models, that is, model without covariates (VLS3.msm), model with all covariates except combination therapy (VLS3.cov1.msm), model with all the covariates including the combination therapy (VLS3.cov11.msm) and the model for the combination therapy only (VLS3.cov.msm). The results from the likelihood ratio tests and the log-likelihoods of the preferred models are shown below.

Results from Table 8 show that the model with all covariates including the combination therapy, is the best model for this data. This model has got the maximum likelihood estimates leading to a lowest −2*log-likelihood and also the results from the likelihood ratio test are in favour of the model with covariates including combination therapy.

A further assessment of the fitted models is done using the Akaike Information Criteria (AIC). For each model, $AIC = -2 \times log(likelihood) + 2(k)$ where k is the number of parameters in the model. For example, the model with covariates excluding the combination therapy (VLS3.cov.msm) has got 26 degrees of freedom

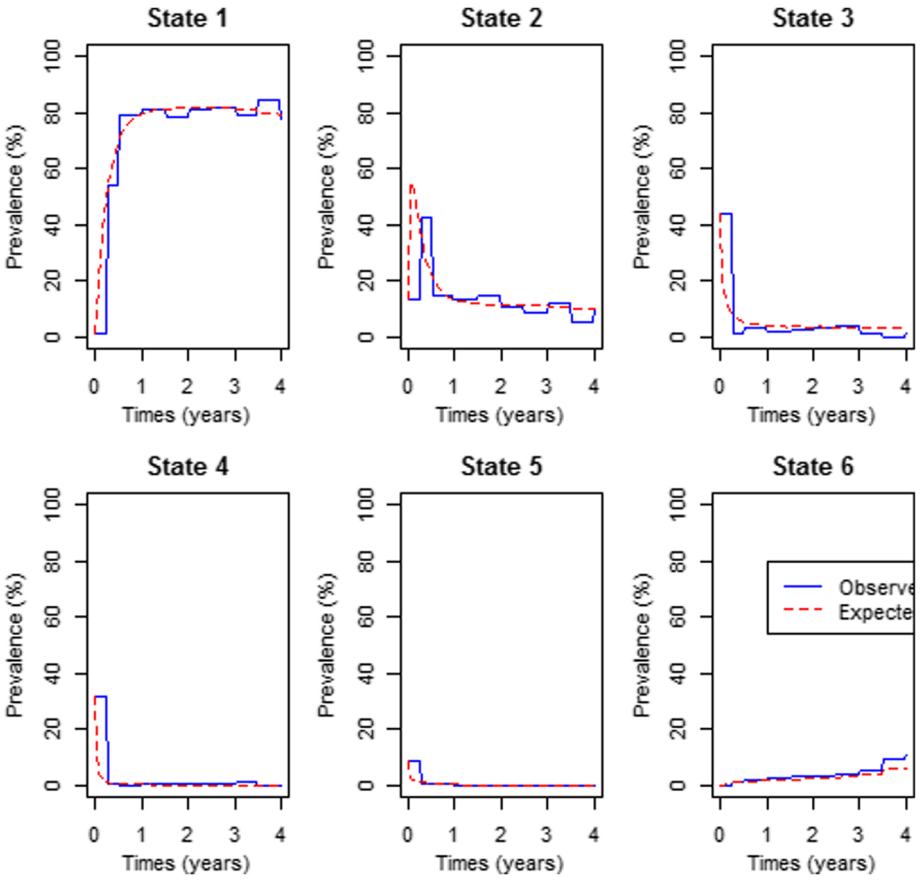

Fig. 2 A comparison of the observed and expected percentage prevalence for the effects of Covariates on Viral Load levels. Prevalence is averaged over the covariates observed in the data, that is, viral load baseline (VLB), CD4 baseline (CD4B), age, non-adherence (NA), lactic acidosis (LA), peripheral neuropathy (PN), and triple therapy (Therapy)

and $-2 \times log\,(likelihood) = 2635.207$, thus AIC = 2635.207 + 2 × 26 = 2687.207 as shown in Table 9 below. The model with the smallest AIC is considered the most effective distribution of the data. The results are shown in Table 9 below.

Results from Table 9 shows that the model with covariates has the smallest AIC. This confirms the results obtained from Table 8 that the time-homogeneous Markov model with covariates gives the most effective distribution of the data.

Conclusion

This study is carried out from a cohort of HIV+ patients receiving antiretroviral therapy in Bela Bela South Africa. Using the data, four nested continuous time homogeneous Markov models were fitted. The first one had no effects of covariates, the second one had the log-linear effects of covarites without combination therapy, the third one had the log-linear effects of different combination therapy and the last one had the log-linear effects all covariates including combination therapy. These covariates include; adherence to treatment, development of drug toxicity in the form of peripheral neuropathy and lactic acidosis, change in treatment therapy, gender, age, CD4 baseline and viral load baseline and resistance to treatment on transition intensities are assessed. From the fitted model the variables; gender difference and change of treatment do not exhibit any significant effects on the transition intensities hence they were removed from the model.

The fitted models were assessed using the AICs and pairwise likelihood ratio test. The continuous time Markov model with all covariates including combination therapy had the lowest AIC an indication that it gives the best fit of the data than all the other models and also the likelihood ratio test revealed that it fits well. This as further confirmed by the likelihood ratio test which showed that the model with all covariates including combination therapy fits significantly better than any other model nested within it. Exclusion of covariates had caused some irregularities in predicting mortality which were corrected after the inclusion of covariates effects in the fitted model.

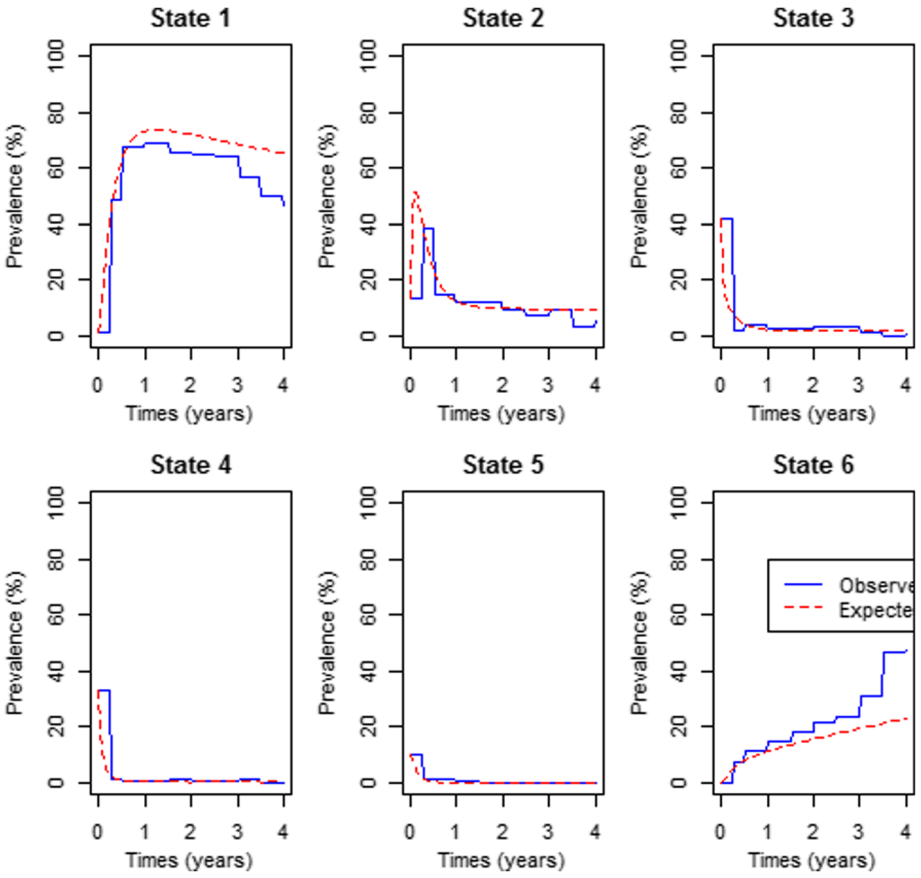

Fig. 3 A comparison of the observed and expected percentage prevalence for the model with different combination therapy. Prevalence is averaged over the different combination therapies observed in the data, that is, D1 = D4T-3TC-EFV, D2 = AZT-3TC-EFV, D3 = D4T-3TC-NVP, D4 = AZT-3TC-NVP, D5 = FTC-TDF-EFV, D6 = AZT-3TC-LPV/r, D7 = Other combinations

The results from the analysis showed that although close to 80% of the individuals had their viral load suppressed to undetectable levels in the first year of treatment uptake, some viral rebound were also notable particularly from state 2 (viral load level between 50 and 10,000 copies/μL) to state 3 (viral load level between 10,000 and 100,000 copies/μL). Further analysis showed that this rebound was accelerated by non-adherence to treatment, lactic acidosis and resistance to treatment. However, for patients who developed peripheral neuropathy, there is an accelerated transition to both viral rebound and viral suppression from state 2 although the rate of viral rebound is greater than the rate of viral suppression. For these patients when the viral load is above 100,000 copies/μL there are reduced rates of viral suppression. This corroborates work done by Simpson who argued that greater incidences of peripheral neuropathy are in the strata of patients with plasma HIV RNA levels greater than 10,000 copies/μL [9]. Patients who initiated treatment therapy with a viral load level above 10,000 copies/μL also had some notable viral rebound from state 2 (viral load level between 50 and 10,000 copies/μL) to state 3 (viral load level between 10,000 and 100,000 copies/μL). Considering the different combination therapy administered to patients, rates of viral rebound are greater than the rates of viral suppression especially for patients who were administered with FTC-TDF-EFV

Table 8 Likelihood ratio tests for the comparison of the fitted models and the −2 Log Likelihood (−2LL) for the preferred model

Models Tested	Preferred Model	-2 log LR	df	p	-2 LL
VLS3.msm & VLS3.cov.msm	VLS3.cov.msm	66.97594	13	2.9×10^{-9}	2635. 207
VLS3.msm&VLS3.cov1.msm	VLS3.cov1.msm	970.1007	78	10^{-4}	1732.082
VLS3.cov.msm&VLS3.cov1.msm	VLS3.cov1.msm	903.1247	65	10^{-4}	1732.082
VLS3.cov1.msm&VLS3.cov11.msm	VLS3.cov11.msm	40.90497	13	9.9×10^{-5}	1691.177

Table 9 AICs for the fitted models

Model	VLS3.msm	VLS3.cov.msm	VLS3.cov1.msm	VLS3.cov11.msm
AIC	2728.183	2687.207	1914.082	1899.177

and AZT-3TC-LPV/r for patients in state 2. Highest rates of mortality are also recorded for patients with viral load level between 50 and 10,000 copies/μL, but from all the other viral load states mortality rates are very low. In particular, for patients with viral load level between 10,000 and 500,000 copies/μL, lowest transition rates were recorded especially for patients administered with d4T-3TC-EFV and AZT-3TC-EFV.

Disease progression is faster on patients below the age of 45 compared to patients over 45 years in the cohort. This shows that older patients have a better understanding of the treatment therapy resulting in a better adherence to the treatment therapy. On the other hand, young patients have substantial challenges in achieving level of adherence necessary for successful therapeutic outcomes.

From state 3 (viral load level between 10,000 and 100,000 copies/μL), rates of viral suppression are higher than the rates of viral rebound particularly for patients administered with d4T-3TC-EFV. A CD4 baseline below 300 cells/mm^3 accelerates the transitions from state 3 to state 4 (between 100,000 and 500,000 copies/μL). This is also the case with younger patients below the age 40 years.

Non-adherence accelerates viral rebound for patients with viral load levels between 100,000 and 500,000 copies/μL (state 4). This supports the issues raised by Chesney [11] that without proper adherence antiretroviral agents are not maintained at sufficient concentration to suppress HIV replication. Hence the need to have a proper patient-health-care provider relationship and also count check of the pills (counts) by asking patients to bring the empty packs.

Overall, the model shows higher transition rates to viral suppression compared to the transitions to viral rebound.

This study has revealed the major attributes to viral rebound on HIV+ patients which is notable as patients attain a viral load level between 50 and 10,000 copies/μL. The major attributes were non-adherence, lactic acid, resistance to treatment, and different combination therapy like AZT-3TC-LPV/r and FTC-TDF-EFV. However, assuming that the patient was initially in state 1 (the undetectable viral load state) he is expected to spend approximately 18.5 years in state 1 before he dies. This is evidenced by the fact that throughout the 5 year study period only 17.8% of the patients were reported dead with 10.9 points occurring during the first 6 months.

Hence the need to administer HIV drug regimens is better based on the viral load level of a patient. Before initiation of treatment, patients should be well equipped on how antiretroviral drugs operate including possibilities of toxicity in order to reduce chances of non-adherence to treatment. There should also be a good relationship between patient and health-care-giver to ensure proper adherence to treatment. Uptake of therapy by young patients should be closely monitored by adopting pill counting every time they come for review.

Acknowledgements
This study would not have been a success without the assistance of the Microbiology Department at the University of Venda in providing the secondary data through Professor Pascal O. Bessong.

Availability of data and materials
The data are available by contacting the corresponding author and can be submitted upon request.

Authors' contributions
CS drafted the manuscript. CS and DC contributed to the analysis and interpretation of the data. All authors participated in critical revision of the manuscript drafts and approved the final version.

Authors' information
CS is a Ph.D student and DC is a senior lecturer at the University of the Free State.

Ethics approval and consent to participate
Not applicable. Secondary data is used in this study with participants' names removed.

Competing interests
The authors declare that they have no competing interests.

Publisher's Note

Received: 2 March 2018 Accepted: 13 June 2018
Published online: 16 July 2018

References

1. Silva JAG, Dourado I, Bristo AM, Silva CAL. Factors associated with non-adherence to antiretroviral therapy in adults with AIDS in the first six months of treatment in Salvador Bahia state, Brazil. Cad Saude Publica. 2015;31(6):1–11.
2. Thaker HK, Snow MH. HIV viral suppression in the era of antiretroviral therapy. Postgrad Med J. 2003;79:36–42.
3. Yw C, Leong CL, Chow HL, Hooi LS. Lactic acidosis in HIV patients receiving highly active antiretroviral therapy; case report. Johor Bahru: Department of Medicine, Hospital Sultanah Aminah.
4. Prosperi MCF, D'Autilia R, Incardona F, De Luca A, Zazzi M, Giovanni U. Stochastic modelling of genotypic drug-resistance for human immunodeficiency virus towards long-term combination therapy optimization. Bioinformatics. 2009;25(8):1040–7.
5. Munderi P. When to start antiretroviral therapy in adults in low-income and middle-income countries: science and practice. Curr Opin HIV AIDS 2010; 5: 6–11
6. Kore S and Waghmare CS. Anti retroviral therapy (ART)- induced lactic acidosis: A potentially life threatening but preventable complication in HIV/AIDS patients receiving Nucleoside Reverse Transcriptase Inhibitors (NRTIs). Biomed Res-India 2012; 23(4): 625–27
7. Currier JS. Sex differences in antiretroviral therapy toxicity; lactic acidosis, Stavudine and omen. Clin Infect Dis. 2007;45:261–2. https://doi.org/10.1086/518977.
8. Dalakas MC. Peripheral neuropathy and antiretroviral drugs. J Peripher Nerv Syst. 2001;6(1):14–20.

9. Simpson DM. Selected peripheral neuropathies associated with human immunodeficiency virus infection and antiretroviral therapy. J NeuroVirol. 2002;8(2):33–41. https://doi.org/10.1080/13550280290167939.
10. Chaiyachati KH, Ogbuoji O, Price M, Suthar AB, Negussie EK, Barnighausen T. Interventions to improve adherence to antiretroviral therapy: a rapid systematic review. AIDS. 2014;28(Suppl 2):S187–204.
11. Chesney M, Factors affecting adherence to antiretroviral therapy. Clin Infect Dis, 200; 30(Suppl 2): S171–S176.
12. Hirchhorn L, Beattie A, Davidson D and Agins B. The role of viral load as a measure of the quality of care for people with HIV: the expert meeting report. 2005.
13. Saint-Pierre P, Combescure C, Daures JP, Godard P. The analysis of asthma control under a Markov assumption with use of covariates. Statistics in Medicine. 2003; 22(24): 3755-3770
14. Saint-Pierre P, Combescure C, Daures JP, Godard P. The analysis of asthma control under a markov assumption with use of covariates. Stat Med. 2003; 22:3755–70.
15. Gibson EL. Continuous time multi-state models for survival analysis. Winston-Salem: Wake Forest University, Department of Mathematics; 2008.

RESEARCH ARTICLE Open Access

A superiority of viral load over CD4 cell count when predicting mortality in HIV patients on therapy

Claris Shoko* and Delson Chikobvu

Abstract

Background: CD4 cell count has been identified to be an essential component in monitoring HIV treatment outcome. However, CD4 cell count monitoring sometimes fails to predict virological failure resulting in unnecessary switch of treatment lines which causes drug resistance and limitations of treatment options. This study assesses the use of both viral load (HIV RNA) and CD4 cell count in the monitoring of HIV/AIDS progression.

Methods: Time-homogeneous Markov models were fitted, one on CD4 cell count monitoring and the other on HIV RNA monitoring. Effects of covariates; gender, age, CD4 baseline, HIV RNA baseline and adherence to treatment were assessed for each of the fitted models. Assessment of the fitted models was done using prevalence plots and the likelihood ratio tests. The analysis was done using the "msm" package in R.

Results: Results from the analysis show that viral load monitoring predicts deaths of HIV/AIDS patients better than CD4 cell count monitoring. Assessment of the fitted models shows that viral load monitoring is a better predictor of HIV/AIDS progression than CD4 cell count.

Conclusion: From this study one can conclude that although patients take more time to achieve a normal CD4 cell count and less time to achieve an undetectable viral load, once the CD4 cell count is normal, mortality risks are reduced. Therefore, both viral load monitoring and CD4 count monitoring can be used to provide useful information which can be used to improve life expectance of patients living with HIV. However, viral load monitoring is a better predictor of HIV/AIDS progression than CD4 cell count and hence viral load is deemed superior.

Keywords: CD4 cell count, Viral load, HIV/AIDS progression, Multistate modelling

Background

CD4 cell count and viral load (HIV RNA) count are the laboratory markers that are regularly used for HIV/AIDS patient management in addition to predicting disease progression and/or treatment outcomes [1]. The target of ART is to suppress the levels of HIV RNA in the plasma as this leads to increase in CD4 cell count and consequently reduces the risks of clinical events and the development of drug resistance [2].

CD4 cell count has been deemed an essential component of HIV treatment and care programmes since HIV was identified as a disease compromising the immune system [3]. Although the World Health Organisation (WHO) has recommended a shift to HIV RNA in monitoring ART, it continues to emphasise CD4 cell count's importance in evaluating disease status at baseline and appropriate care for patients with advanced stages of HIV progression [3].

HIV RNA is most useful in measuring effectiveness of ART after initiation. Some researchers argue that lack of HIV RNA monitoring leads to delayed and unnecessary switches to second line therapy resulting in development of resistance to treatment and limitations to treatment options [4]. Other researchers argue that HIV RNA appears to be the best predictor of long-term clinical outcome whereas CD4 cell count predicts clinical progression and survival in the shorter term [5]. Brennan and others, in their research to determine the interplay between CD4 cell count and viral load, further argued

* Correspondence: claris.shoko@gmail.com
Department of Mathematical Statistics and Actuarial Sciences, University of the Free State, Box 339, Bloemfontein 9300, South Africa

that long-term virological suppression plays an important role in ensuring the recovery of CD4 cell count to levels that reduce the risk of opportunistic infection and increase life expectancy [6].

In the year 2000 there were uncertainties regarding the use of either CD4 cell count or viral load markers in controlled trials [5]. Thereafter, attempts have been made by different researchers to try and address these uncertainties. Some of these studies used Cox proportional hazard models and Kaplan Meier curves [2, 7]. Another study to establish the interplay between CD4 cell count, viral load suppression and duration of ART on mortality in a resource limited setting was carried out using log-linear model with Poisson distribution [8, 6]. However, results from these studies were contradictory. Some studies show that CD4 cell count monitoring is the best for predicting HIV/AIDS progression [4, 7, 8] and other studies show that viral load monitoring is the best predictor [1].

When HIV RNA tests are done, the results cannot be reliable due to missing data as a result of limiting costs [1]. Researchers then resort to use of computer simulated data [4]. In this study, longitudinal data collected from a Wellness clinic in Bela Bela, South Africa on viral load count monitoring and CD4 cell count monitoring, is analysed. A stochastic Markov approach to multistate modelling is used in the analysis. The objective of the study is to investigate and compare the use of either CD4 cell count or viral load markers in controlled trials. The aim is to determine whether CD4 cell count or viral load count can be used to model HIV/AIDS progression. Multistate modelling is a powerful tool for studying chronic diseases and in estimating factors associated with transitions between each stage of progression [9].

In the section that follows, methods used in the analysis of the data are explained. This is followed by section 3 on results and discussions. Lastly in section 4, conclusions of the findings are highlighted.

Methods

Data description

The data used in this study was obtained as secondary data from the University of Venda in South Africa. The names of participants were removed from the data set and as such the Ethics Committee of the University of Venda approved the usage of the data in 2013 (Additional file 1).

This study includes a selection of 320 HIV patients on anti-retroviral therapy (ART) who fulfilled the entry criteria from a longitudinal cohort of 1092 HIV-infected patients followed at a Wellness clinic in Bela Bela, South Africa, from year 2005 to year 2009. Patients were eligible for inclusion if they had a routinely reported viral load count and if they were 15 years and older. Upon initiation of treatment therapy, follow up was done in the first 3 months of treatment initiation and 6 months intervals thereafter. From these patients, 224 were females and 96 were males. The ages of the patients ranged from 15 years to 77 years and the children born to HIV+ patients were not included in the study. At baseline age, the data set had a first quartile of 32 years, a median of 39 years, a mean of 39.44 years and a third quartile of 47 years. One hundred seventy-two patients were aged 45 and below, and 72 were over 45 years of age. The viral load count at baseline of the patients ranged from 45 to 818,600 copies/mL with a mean viral load of 138,208 copies/mL, a first quartile of 21,334, a median of 67,995 and a third quartile of 201,445 copies/mL. From these patients, 267 had a viral load baseline above 10,000 copies/mL and 49 had a viral load baseline below 10,000 copies/mL. The CD4 baseline of the patients ranged from 16 to 1202 cells/mm^3. The mean CD4 baseline was 156 cells/mm^3, first quartile of 38 cells/mm^3, median of 116 cells/mm^3 and a third quartile of 206 cells/mm^3. Approximately 70% of these patients had a CD4 baseline below 200 cells/mm^3 (AIDS defining stage).

For each and every visit time, blood samples were obtained for each patient and stored frozen until assayed. Plasma HIV RNA was measured using an amplicator HIV-1 monitor assay kit which has a lower limit of sensitivity of 50 copies/mL.

At $t = 0$ the ART regimens that were mostly administered to patients were the triple combination therapy, D4T-3TC-EFV (208 patients) and D4T-3TC-NVP (92 patients). D4T and 3TC represent Stavudine and Lamivudine respectively which fall under nucleoside reverse transcriptase inhibitors (NRTI) class. EFV and NVP stand for Efavirenz and Nevirapine respectively and are from the non-nucleoside reverse transcriptase inhibitors (NNRTI) class. In patients who showed some signs of non-adherence, D4T was substituted with AZT (Zidovudine). A switch from D4T-3TC-EFV to AZT-3TC-EFV was most common rising from 10 patients in the first 6 months to 92 patients in 30 months (2 and half years). During the same period the number of patients who switched from D4T-3TC-NVP to AZT-3TC-NVP rose from 6 to 45. After 1 year of treatment uptake, one patient was introduced to FTC-TDF-EFV and after three and half years the frequency increased to 10 patients. Another combination of FTC-TDF-NVP was also introduced to 3 patients after 2 years. The number for this combination rose to 7 after 3 years. The drug regimens that were mostly administered during the first three and half years are summarised in the table below; (Table 1)

During the course of the study, HIV/AIDS progression was assessed based on CD4 cell count monitoring, viral load count monitoring and also signs of non-adherence

Table 1 Treatment regimen administered to the patients i the first 3.5 years of treatment follow-up

Drug/t	0	0. 25	0.5	1	1.5	2	2.5	3	3.5
1	208	191	165	140	94	44	18	5	3
2	92	73	70	62	35	23	7	1	0
3	2	3	10	20	50	77	92	88	60
4	3	6	6	14	35	36	45	35	31
5	0	0	0	1	1	3	8	10	10
6	0	0	0	0	0	3	5	7	3
7	2	2	1	2	5	4	2	2	1

KEY: 1:-D4T-3TC-EFV, 2:-D4T-3TC-NVP, 3:-AZT-3TC-EFV, 4:-AZT-3TC-NVP, 5:-FTC-TDF-EFV, 6:-FTC-TDF-NVP, 7:-D4T-3TC-LPV/r, *t* represents time in years post treatment commencement

to treatment were noted. Patients who had problems in adherence to treatment were those patients who were intolerant to the treatment combination and those who failed to reach viral suppression. Change of treatment line was based on treatment failure, toxicity, patient intolerance to the combination therapy or inability of the patient to adhere to treatment and viral rebound. From these patients, 36 showed some signs of non-adherence to treatment. In this study, viral load below 50 copies/mL is defined as undetectable viral load and the progression of HIV/AIDS is defined either by change in viral load count level or change in CD4 count level. The viral load count levels are divided into 5 transient states and the sixth state being the absorbing state, death. The CD4 count levels are divided into 4 transient states and the fifth state is the death state. The viral load states, CD4 states as well as factors that are likely to determine change in viral load/CD4 states are defined in the next sub-section.

Variable coding

For this study, variables are coded as follows:

A. *Categorical variables*

$$\text{Age} = \begin{cases} 1, \leq 45\ years \\ 0, > 45\ years \end{cases}, \text{Non-adherence (NA)} = \begin{cases} 1, Yes \\ 0, No \end{cases},$$

$$\text{CD4 baseline (CD4BL)} = \begin{cases} 1, \leq 200\ \text{cells/mm}^3 \\ 0, > 200\ \text{cels/mm}^3 \end{cases}, \text{Gender} = \begin{cases} 1, male \\ 0, female \end{cases},$$

$$\text{viral load baseline (VLBL)} = \begin{cases} 1, > 10\,000\ copies/mL \\ 0, \leq 10\,000\ copies/mL \end{cases},$$

B. *Time-dependent variables*

$$\text{Viral load levels } (X(t)) = \begin{cases} \mathbf{1}; VL < 50 \\ \mathbf{2}; 50 \leq VL < 10\,000 \\ \mathbf{3}; 10\,000 \leq VL < 100\,000 \\ \mathbf{4}; 100\,000 \leq VL < 500\,000 \\ \mathbf{5}; VL \geq 500\,000 \\ \mathbf{6}; Dead. \end{cases}$$

$$\text{CD4 cell count levels } (X(t)) = \begin{cases} \mathbf{1}; CD4 > 800 \\ \mathbf{2}; 500 < CD4 \leq 800 \\ \mathbf{3}; 350 < CD4 \leq 500 \\ \mathbf{4}; CD4 < 350 \\ 5; Death \end{cases}$$

The effects of the categorical variables on the time-dependent variables is assessed using the Markov models:

$$q_{ij(CD4)} = q^{(0)}_{ij(CD4)} \exp\left(\beta^{(Age)}_{ij} Age_h + \beta^{(Gender)}_{ij} Gender_h + \beta^{(CD4BL)}_{ij} CD4BL_h + \beta^{(VLBL)}_{ij} VLBL_h + \beta^{(NA)}_{ij} NA_h\right)$$

and

$$q_{ij(VL)} = q^{(0)}_{ij(VL)} \exp\left(\beta^{(Age)}_{ij} Age_h + \beta^{(Gender)}_{ij} Gender_h + \beta^{(CD4BL)}_{ij} CD4BL_h + \beta^{(VLBL)}_{ij} VLBL_h + \beta^{(NA)}_{ij} NA_h\right)$$

for CD4 cell count levels and viral load levels respectively. $q^{(0)}_{ij(CD4)}$ and $q^{(0)}_{ij(VL)}$ are the baseline transition intensities for CD4 cell count states and viral load states respectively. β_{ij} is the log-linear effects of the mentioned covariate on the baseline transition intensities $q^{(0)}_{ij}$.

Results

The observed prevalence for each of the variables CD4 cell count and viral load count were computed in R using the "msm" package for multistate modelling. The observed prevalence are calculated for each CD4 cell count state and viral load count state. This is done from initiation of treatment (t = 0 years) to time t = 4 years. The comparison is based on the transient states based on either CD4 cell count or viral load levels. However, since viral load states are more than CD4 count states, viral load state 4 and state 5 are combined so that we have an equal number of transient states for both variables. The results are shown in Fig. 1 below.

Results from Fig. 1 above show an increase in the number of patients who had their viral load suppressed/undetectable in the first 6 months of treatment uptake. The plotted variables are shown at the bottom of each graph. From 6 months onwards, the number individuals with suppressed viral load started to decrease. This could be caused by loss of viral suppression or deaths.

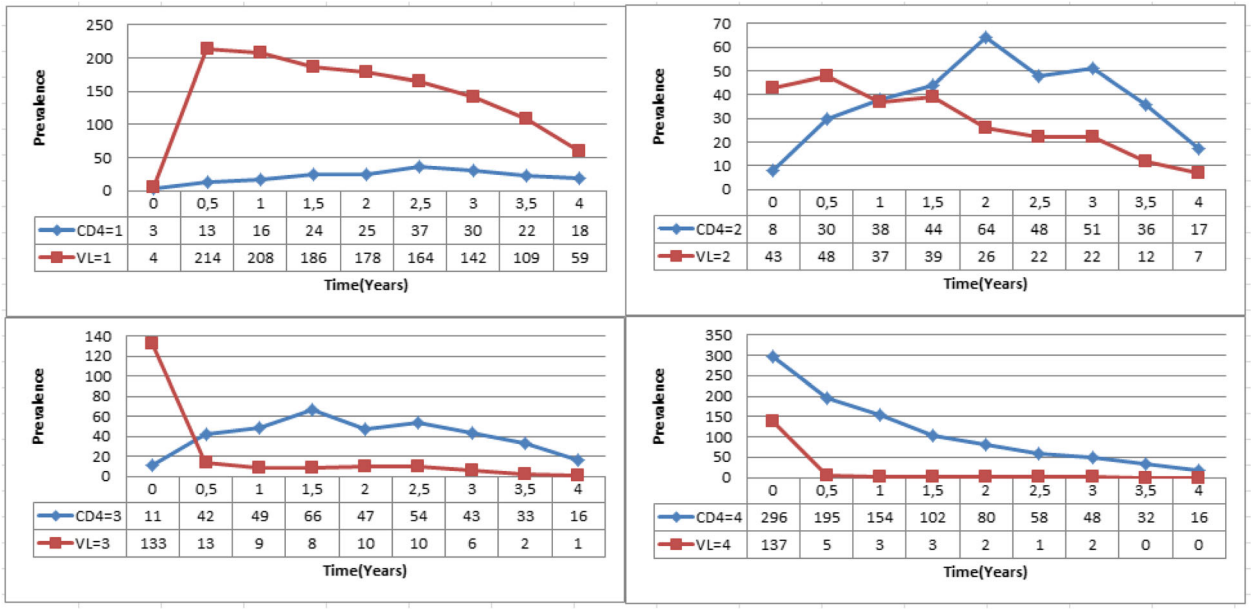

Fig. 1 Comparison of CD4 and Viral load prevalence 4 years post commencement of therapy(Original). Legend: CD4 stages:1:- CD4 > 800, **2:-** 500 < CD4 ≤ 800, **3:-** 350 < CD4 ≤ 500;4:- CD4 < 350; Viral load states:1:- VL < 50, **2:-** 50 ≤ VL < 10 000, **3:-** 10 000 ≤ VL < 100 000, **4:-** VL ≥ 100 000

The number of patients with CD4 cell count above 800 (CD4 state = 1) increased slowly with time. In 2014, Maartens and others also indicate that within 3 months of ART, the plasma viral load decreases to concentrations below the lower limit of detection of available commercial assays in most people [10]. The lower limit for this particular study is 50 copies/mL.

Upon initiation of treatment, the majority of the patients had a viral load state equal to 3, which is associated with viral load count of between 10,000 and 100,000 copies/mL. After 6 months of ART the number of patients in this category dropped from 133 to 13 and continued to decrease throughout the whole period. The highest number of patients was in the CD4 cell count category 4, which is defined by a CD4 cell count below 350 cells/mm^3. The number of patients in this state continued to decrease throughout the whole period but at a slower rate than that of viral load count levels.

Effects of CD4 levels on viral load count transition intensities

In this sub-section, we analyse the effects of CD4 cell count levels on transition intensities defined by viral load as defined by the equation:

$$\alpha_{ij(VL)} = \alpha_{ij}^{0} \exp\left(\beta_{ij} \times CD4_k\right)$$

where $\alpha_{ij(VL)}$ is the transition intensity matrix for $i = 1, \ldots, 5$ transient states defined by viral load levels in the plasma cells and $j = 1, \ldots, 6$, β_{ij} is the log-linear effect of CD4 cell count level on the transition intensity $\alpha_{ij(VL)}$ and $k = 1, \ldots, 4$ defines the different levels of CD4 cell count. For this model, transition from i to j where $i > j$ is defined as viral load count suppression and if $i < j$, it is defined as viral rebound. The values of k define the patient's immunology such that large values of k are associated with immune deterioration and smaller values of k are associated with immune recovery. α_{ij}^{0} is the baseline transition intensity from i to j . The results of the transitions are shown in Table 2 below.

Results from Table 2 above show that the rates of viral suppression are higher than the rates of viral rebound for HIV+ patients in state 3 (viral load ranging from 10,000 to below 100,000 copies/mL), state 4 (viral load level ranging from 100,000 to below 500,000 copies/mL) and state 5 (viral load level above 500,000 copies/mL). If a patient is in a viral load level suppressed to state 2 (from 50 to below 10,000 copies/mL), the rates of viral rebound to state 3 are higher than the rates further viral load suppression to state 1.

For the viral rebound from state 1 (undetectable viral load) to state 2, the log-linear effect of CD4 count level is positive. This indicates that viral rebound from the undetectable level increases as the immune system deteriorates. The increase in transition intensities from 0.2685 at $k = 1$ to 0.5595 at $k = 4$ confirms the increase in viral load as the immune system deteriorates. Although the log-linear effects of CD4 cell count levels on viral rebound and viral suppression from state 2 are both positive, the effect on viral rebound is higher and this also increases as the immune system deterioration. This means that a patient can reach a suppressed viral load

Table 2 Effects of changes in CD4 cell count levels on viral load transition intensities

	Baseline	Log-linear	Hazard	CD4Level			
α_{ij}	α_{ij}^0	β_{ij}		$k=1$	$k=2$	$k=3$	$k=4$
α_{12}	0.4679	0. 2451	1. 2778	0. 2685	0.3429	0.4380	0.5595
α_{16}	0.0170	0.0732	1.0760	0.0144	0.0155	0.0167	0.0179
α_{21}	3.1857	0.0612	1.0631	2.7644	2.9426	3.1325	3.3345
α_{23}	5.6586	0.8919	2.4397	0.7877	1.8778	4.4768	10.6725
α_{26}	0.1388	1.5639	4.7776	0.0044	0.0201	0.0921	0.4222
α_{32}	30.4528	0.8684	2.3831	4.4659	10.4049	24. 2421	56.4807
α_{34}	3.1488	−0.0002	0.9998	3.1766	3.1644	3.1521	3.1399
α_{36}	0.0072	−0.1439	0.8660	0.0126	0.0099	0.0077	0.0060
α_{43}	16.9641	0.5376	1.7119	5.0556	8.6181	14.6914	25.0443
α_{45}	2. 2611	1. 2750	3.5789	0.1182	0.4339	1.5924	5.8438
α_{46}	0.0096	−1.7277	0.1777	0.6964	0.1056	0.0160	0.0024
α_{54}	6.5317	1.0211	2.7762	0.6131	1.7387	4.9311	13.9850
α_{56}	0.0451	−2.5302	0.0796	23.7348	1.5009	0.0949	0.0060
-2xLL	2665. 285						

α_{ij}:- transition intensities, α_{ij}^0 baseline transition intensities, β_{ij}:- log-linear effects, *Hazard:*- hazard ratios, *CD4Level:*- CD4 cell count transient states, *2xLL:*- likelihood ratio test

yet the immune system is still compromised (CD4 cell count still low).

When the viral load level is 3 and above (viral load of 10,000 copies/mL and above) mortality rates decrease with immune deterioration. Mortality rates increase with immune deterioration for viral load count levels is below 10,000 copies/mL. This means that during the early phases of treatment uptake, when the viral load levels are high and the CD4 count levels are still low, there are low of transitions death rates. Deaths are mainly caused by viral rebounds due to a compromised immune system.

Effects of viral load levels on CD4 cell count transition intensities

In this sub-section we analyse the effects of viral load levels on transition intensities defined by CD4 cell count as defined by the equation:

$$\alpha_{ij(CD4)} = \alpha_{ij}^0 \exp\left(\beta_{ij} \times VL_k\right)$$

where $\alpha_{ij(CD4)}$ is the transition intensity matrix for $i = 1, \ldots, 4$ transient states defined by CD4 cell count levels and $j = 1, \ldots, 5$, β_{ij} is the log-linear effect of viral load count level on the transition intensity $\alpha_{ij(CD4)}$ and $k = 1, \ldots, 5$ defines the different levels of viral load. For this model transition where $i > j$ is defined as immune recovery and if $i < j$, it is defined as immune deterioration. The values of k define the patient's virology such that large values of k are associated with high level of viral load and smaller values of k are associated with suppressed viral load. The results are shown in Table 3 below.

The results from Table 3 show that the rates of immune deterioration are lower than the rates of immune recovery when a patient's CD4 cell count is 500 cells/mm^3 and below (state 3 and state 4). When the CD4 cell count levels are above 500 cells/mm^3 (states 1 and 2) rates of immune deterioration are higher than rates of immune recovery. This is an indication that upon reaching the safe immunological levels, there are certain factors that compromise the immune system. There is need to further investigate the cause.

The negative log-linear effect of viral load levels on the transition from state 1 (CD4 count above 800) to state 2 (CD4 count more than 500 but less or equal to 800 cells/mm^3) indicates a reduction in immune deterioration from state 1 to state 2 as the levels of viral load in the plasma increase. Mortality rates from all the states increase as the viral load levels increase. The highest transitions to death are recorded for patients with viral load levels above 500,000 copies/mL (state 5).

Effects of covariates on CD4 cell count and viral load levels

Effects of covariates; Age, Gender, VL baseline (VLBL), CD4 baseline (CD4BL), Non-adherence to treatment (NA) on HIV/AIDS progression defined by the time-dependent variables CD4 levels or viral load levels is assessed in this section. The models for the effects of covariates on transition intensities defined by CD4 cell count and viral load are:

Table 3 Effects of changes in viral load levels on CD4 cell count transition intensities

	Baseline	Log-linear	Hazard	Viral load levels				
$i;j$	α_{ij}^0	β_{ij}		1	2	3	4	5
1;2	0. 2901	−1.4148	0. 2430	0.7161	0.1740	0.0423	0.0103	0.0025
1;5	0.0240	1. 2788	3.5922	0.0106	0.0381	0.1369	0.4918	1.7665
2;1	0.6124	0.02164	1.0268	0.6021	0.6182	0.6348	0.6518	0.6692
2;3	0.8429	0. 2122	1. 2364	0.7361	0.9101	1.1252	1.3911	1.7199
2;5	0.0044	1.5472	4.6985	0.0016	0.0076	0.0358	0.1684	0.7912
3;2	1.3971	0. 2010	1. 2226	1.2287	1.5023	1.8367	2.2456	2.7454
3;4	0.7200	0. 2729	1.3138	0.6048	0.7946	1.0440	1.3716	1.8019
3;5	0.1276	1.0505	2.8591	0.0652	0.1865	0.5331	1.5241	4.3576
4;3	0.7432	0.0231	1.0233	0.7323	0.7494	0.7669	0.7847	0.8030
4;5	0.0567	0.5734	1.7743	0.0393	0.0697	0.1237	0.2195	0.3894
-2xLL	3308.126							

α_{ij}:- transition intensities from state i to state j, α_{ij}^0 baseline transition intensities, β_{ij}:- log-linear effects, *Hazard:*- hazard ratios, -2xLL:- likelihood ratio test

$$q_{ij(CD4)} = q_{ij(CD4)}^{(0)} \exp\left(\beta_{ij}^{(Age)} Age_h + \beta_{ij}^{(Gender)} Gender_h + \beta_{ij}^{(CD4BL)} CD4BL_h + \beta_{ij}^{(VLBL)} VLBL_h + \beta_{ij}^{(NA)} NA_h\right)$$

and

$$q_{ij(VL)} = q_{ij(VL)}^{(0)} \exp\left(\beta_{ij}^{(Age)} Age_h + \beta_{ij}^{(Gender)} Gender_h + \beta_{ij}^{(CD4BL)} CD4BL_h + \beta_{ij}^{(VLBL)} VLBL_h + \beta_{ij}^{(NA)} NA_h\right)$$

respectively. β_{ij} is the log-linear effects of the mentioned covariate on the baseline transition intensities $q_{ij}^{(0)}$.

The results show no gender effect on the progression of HIV based on viral load levels. This means that change in viral load levels is uniform for both males and females. However, given the time-dependent variable CD4 cell count, the effects of gender is quite significant. Thus, in Table 4 below, when the CD4 cell count is below 350 cells/mm^3, males have lower chances of immune recovery than females. The effects of gender are only indicated for CD4 cell count levels. Similar results for viral load levels are not presented since they are not significant.

Results from Table 4 above show that for patients in the disease state 2, defined either by CD4 cell count levels or viral load levels, the rates of disease progression to state 3 are higher than the rates of recovery from state 2 to state 1. However, the rate of viral rebound is higher than the rate of immune deterioration for patients in state 2.

The results also show a reduction in viral load suppression from state 2 to state 1 and an increased viral rebound from state 2 to state 3 for patients who are 45 years and below compared to those patients over 45 years. The opposite is true for changes in CD4 cell count level. These patients, 45 years and below, show an increased immune recovery from state 2 to state 1 and a reduced immune suppression from state 2 to state 3. Although young patients experience some challenges in viral load suppression, they have higher chances of cell regeneration than their older counterparts.

Patients who initiated treatment with a viral load baseline above 10,000 copies/mL experience an increase in viral rebound and also an increase in immune deterioration from state 2 to state 3 and a reduced viral suppression and immune recovery from state 2 to state 1. However, it is interesting to note that if the patient's CD4 cell count at treatment initiation is 200 cells/mm^3 and below, there is increased viral load suppression from state 2 to state 1 and a decreased viral rebound from state 2 to state 3. This emphasises the need for initiation of treatment when the CD4 cell count is low to reduce the chances of reaction to treatment that are associated with long-term treatment uptake.

Patients with non-adherence to treatment have increased viral rebound from state 2 to state 3 and a decreased viral suppression from state 2 to state 1. Non-adherence to treatment causes an increased immune deterioration from state 2 to state 3. This also leads to an increased death rate from a CD4 state of 3. In general, given that a patient is non-adherent to treatment, there are increased rates of disease progression than recovery.

The results also show that deaths from viral load state 1(undetectable viral load) are higher for patients below the age group of 45 years than their older counterparts. However, for patients whose CD4 cell count has reached normal levels, transitions to death are lower in patients below 45 years than older patients. Deaths of patients below 45 years are prominent from a CD4 cell count states 2 and 3 compared to the older patients. For these patients in viral load levels 2 and 3 the opposite is true since lower transitions to death are observed from this

Table 4 Log-linear effects of age, viral load baseline, CD4 baseline, gender and non-adherence on baseline transition intensities for CD4 and viral load stages

			Log-linear effects (β_{ij})								
	Baseline (q_{ij0})		Age		VLBL		CD4BL		Gender	Non-adherence	
i;j	CD4	VL	CD4	VL	CD4	VL	CD4	VL	CD4	CD4	VL
1;2	0.7373	0.4957	−1.3266	−0.1479	−0.1436	0.1153	−0.4644	− 0.0973	− 0.2887	− 0.2319	0.2189
1;death	0.0003	0.0001	− 0.7467	4.4953	1.1724	3.4155	0.9160	3.5811	0.5660	−0.0148	4.4320
2;1	0.5699	4.025	0.3444	−0.4369	−0.1826	− 0.3702	−0.3360	0.3262	0.1063	0.7056	−1.3054
2;3	0.7515	6.068	−0.0925	0.4862	0.4300	2.4328	−0.0483	−2.8265	0.8865	0.9685	3.2746
2;death	0.0026	0.0058	4.3919	−1.5407	4.1370	3.4727	−0.0313	5.2590	1.8332	−2.2185	−5.0841
3;2	1.2831	62.87	0.2862	0.0611	−0.1617	0.8531	−0.5877	−2.9784	0.1138	0.1224	1.9255
3;4	0.7053	0.2084	0.0226	5.5325	−0.1768	1.1270	−0.4604	5.7147	−0.5035	0.6828	−0.2225
3;death	0.0001	0.0008	3.0206	−0.2825	2.0134	−0.3685	2.2871	0.1540	−3.9785	5.1871	−1.5359
4;3	0.7923	40.77	0.0223	0.4827	0.3822	−2.6884	−1.4319	0.8024	−0.5364	−0.3456	−0.7337
4;5	0.0005	0.5795	−2.0121	1.0819	3.6009	0.7886	3.3325	−2.2219	−5.8879	−4.0417	4.8056
4;6		0.0019		0.0607		−0.5510		−0.4202			−0.7981
5;4		100.5		−5.0660		−1.1924		2.1054			1.0696
5;6		0.0398		0.2639		1.8205		−3.4286			−2.0918
−2xLL	2595.89	1767.02									

Age = 1 if ≤45 years and 0 otherwise; *VLBL*:- viral load baseline =1 if >10000copies/mL and 0 otherwise, *CD4BL*:- CD4 baseline = 1 if ≤200 cells/mm^3 and 0 otherwise; Gender = 1 if "male" and 0 if "female"; Non-adherence =1 if "yes" and 0 if "no"; −2xLL:- likelihood ratio test

data set when compared to the older patients. Thus, although HIV/AIDS patients take longer time to reach a normal CD4 cell count level than the time taken to reach a suppressed viral load count, once a normal CD4 cell count is reached mortality risks are reduced.

Patients who initially had a viral load baseline of more than 10,000 copies/mL experience higher transitions to death from almost all viral load states except state 4 and the highest transition to death are noted from state 2. For these individuals with initial viral load baseline above 10,000 copies/mL, the same trend is also notable from all the CD4 cell count states.

Patients with suppressed viral load who developed negative reaction to treatment (non-adherent to treatment) show the higher transitions to death compared to patients who did not develop any form of negative reaction to treatment.

In the next subsection prevalence plots for the two Markov models, one in which CD4 count is used as a marker of HIV/AIDS progression and the other one in which viral load count is used as the marker of the disease progression, are compared. The likelihood ratio test is also used assess the fitted models.

Assessment of the fitted models

Assessment of the fitted models is done by comparing the expected to the observed percentage prevalence. In Fig. 2 below, the comparison is based on CD4 cell count monitoring.

Figure 2 above show that at treatment initiation, more than 90% of the patients had a CD4 cell count below 200 cells/mm^3 (state 4). As the time on treatment increases, the percentage prevalence for the patients in state 4 decreases exponentially to close to 20% after 4 years of treatment initiation. For CD4 states 1, 2 and 3, the percentage prevalence at initiation were close to 0% and increased exponentially to more than 20% in state 2 and 3 after 2 years of treatment and slightly above 10% for state 1. Thereafter the percentage prevalence for all the three states started to decrease, but at a slow rate. Death prevalence increases from 0% to approximately 10% in the first 4 years of treatment uptake.

In Fig. 3 below comparison of the expected percentage prevalence with the observed percentage prevalence is based on viral load levels.

Figure 3 shows that upon initiation of treatment more than 40% of the patients were in viral load state 3. This state had the highest percentage prevalence at start of therapy administration followed by state 4 which had close to 33%. Close to 0% of the patients had undetectable viral load levels (state 1) and this increased at a fast rate to approximately 80% after 1 year of treatment up take. After 1.5 years the percentage prevalence for state 1 became stable with a slight up and down trend. This could be due to viral rebound or deaths.

The model fitted for viral load states show a perfect fit for all the states. The model for CD4 states show a perfect fit only for state 1 percentage prevalence. States 2

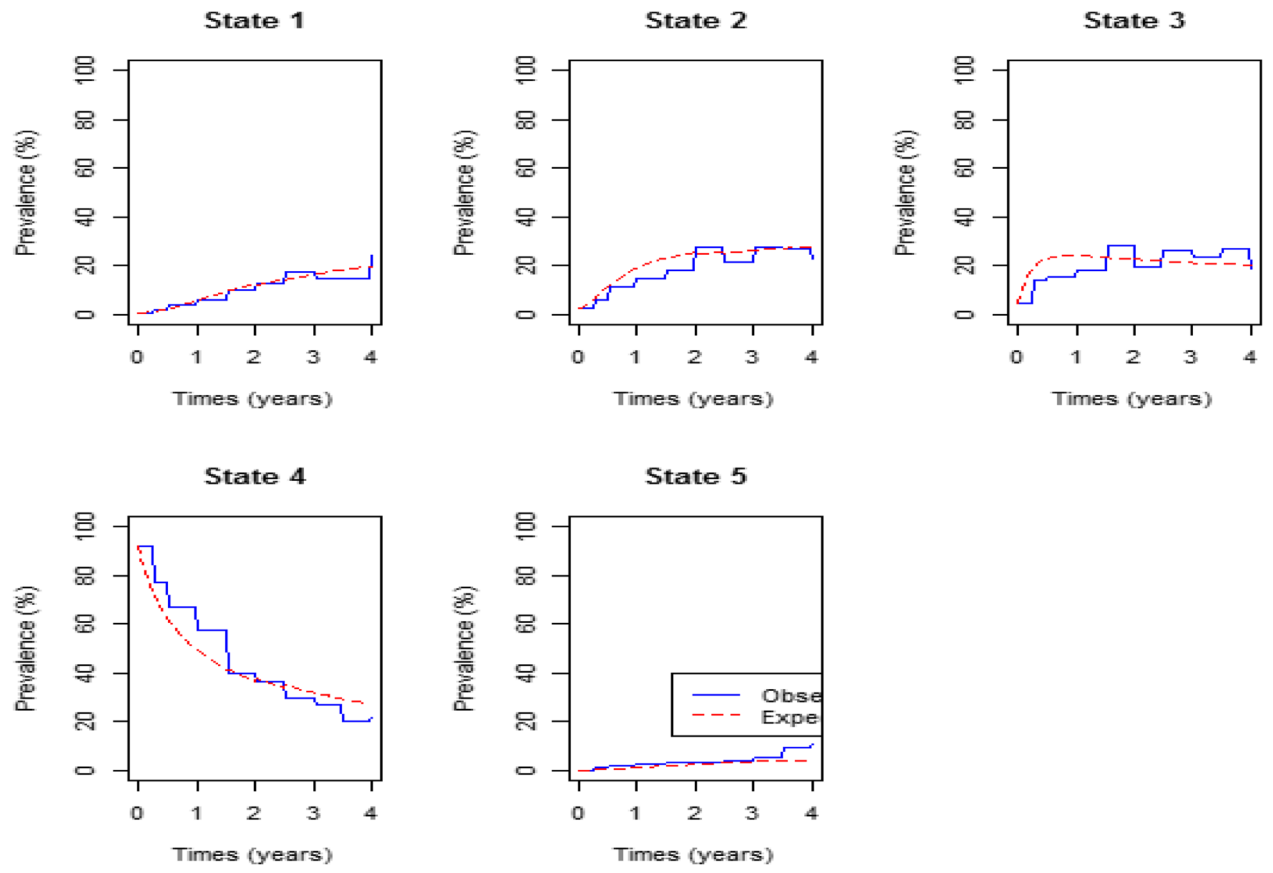

Fig. 2 Percentage prevalence plot for the covariate on HIV/AIDS progression defined by CD4 cell count (Original). Legend: State:1= CD4 > 800, State2 = 500 < CD4 ≤ 800, State3=350 < CD4 ≤ 500; State4= CD4 < 350; State5 = death

and 3 overestimate the observed prevalence in the first 2 years of treatment. State 4 underestimates the observed in the first 1.5 years of treatment up take. The fitted model for CD4 states shown in Fig. 2, underestimates the observed death percentage prevalence slightly for the first 3.5 years and the margin become wider beyond 3.5 years. In Fig. 3, the model for viral load states show a perfect fit of the expected and observed death prevalence in the first 3.5 years but underestimates the observed death prevalence beyond. Thus, the fitted model for viral load states predicts mortality better than the model for CD4 states. This shows that progression of HIV/AIDS for patients on treatment is better explained by the changes in the viral load levels than the changes in the CD4 cell count levels.

A likelihood ratio test was also performed to compare HIV/AIDS progression based on CD4 cell count monitoring with progression based on viral load monitoring. The results yield a p-value of $10^{\{-4\}}$ in favour of the Markov model based on the viral load monitoring. This again confirms that viral load monitoring is a better marker of HIV/AIDS progression than CD4 cell count. The results are shown below (Table 5).

Discussions

The major aim of this study was to assess and compare the use of the time-dependent variables; CD4 cell count and viral load level, in analysing HIV/AIDS progression on patients receiving antiretroviral therapy. Effects of covariates such as gender, age, CD4 baseline, viral load baseline, and adherence to treatment were also considered.

In this study, there are no gender effects on the progression of HIV/AIDS when viral load levels in the plasma are used as a surrogate marker. The results showed that gender effects are influenced by CD4 cell count. Previous findings by Dounelly et al. [11] demonstrate that women had non-significant lower viral loads than men and that the gender effects depended on CD4 cell count.

Patients below the age of 45 years had lower rates of viral load suppression to undetectable levels but they had faster rates of immune recovery compared to the older patients in the cohort (above 45 years of age). The results are corroborated by the findings from a study that was carried out in Tehran, Iran, which showed that mean CD4 cell count increments after initiation of antiretroviral therapy are lower on older patients (> = 50 years) [12]. Prior to the study by Hasib et al. [12], a study

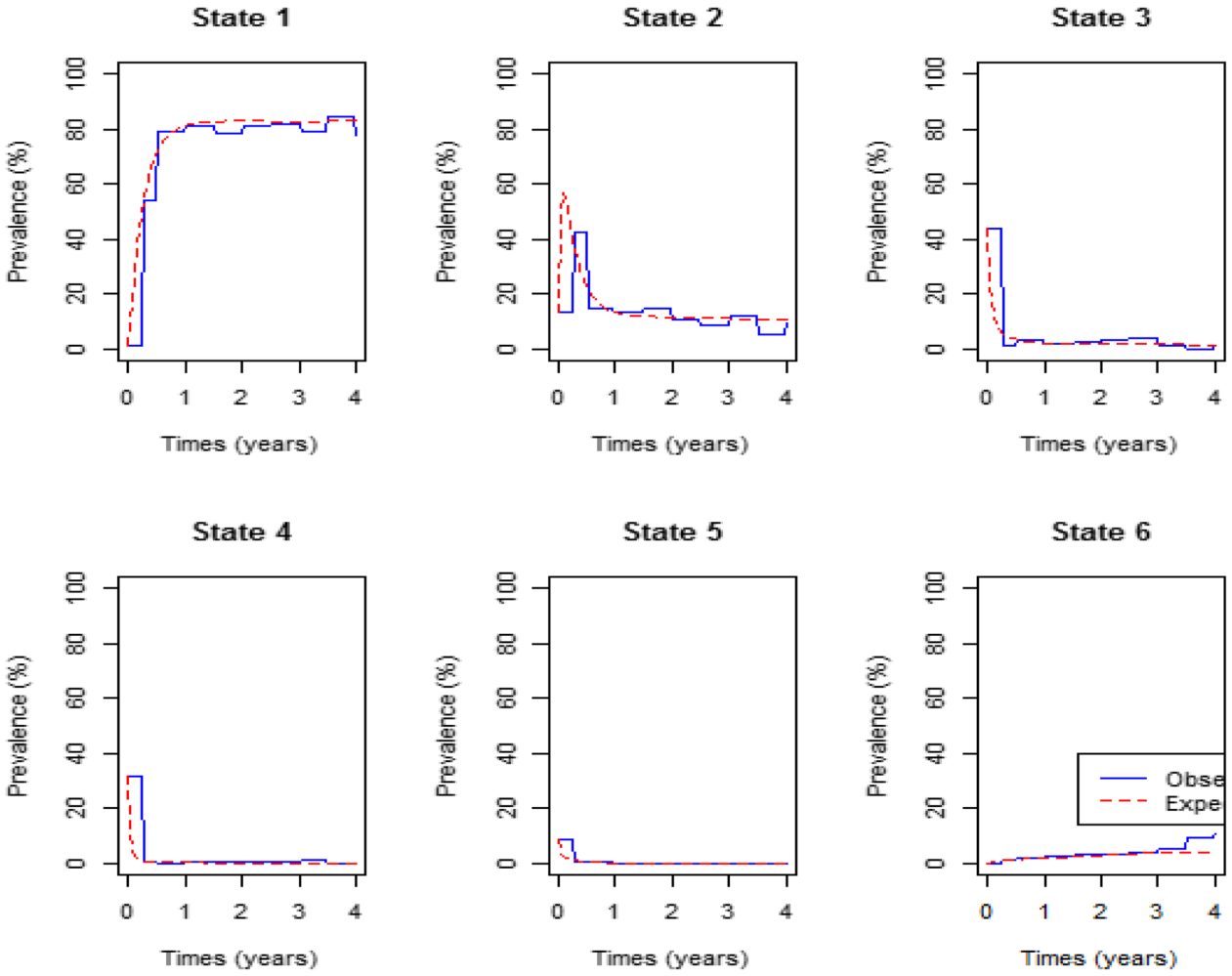

Fig. 3 Percentage prevalence plot for the covariate on HIV/AIDS progression defined by Viral load (Original). Legend: state:1 = VL < 50, State2 = 50 ≤ VL < 10 000, State3 = 10 000 ≤ VL < 100 000, State4 = 100 000 ≤ VL < 500 000; State5 = VL≥ 500,000; State6 = death

from Greece showed higher magnitudes of absolute CD4 cell count among patients 50 years and older [13]. The results reveal that, although HIV/AIDS patients generally take longer to reach a normal CD4 cell count compared to the time taken to reach an undetectable viral load, patients below the age of 45 years have reduced risks of mortality once the CD4 cell count is normal.

Overall, the results show that although both CD4 cell count and viral load are the surrogate markers of HIV progression, viral load is more powerful in monitoring progression of HIV/AIDS in patients on antiretroviral therapy than CD4 cell count. The models for viral load count with and without the inclusion of covariates give a better fit compared to the model for CD4 cell count (with and without the inclusion of covariates). This point coincides with WHO recommendations that advise the routine use of viral load monitoring as a routine procedure in the management of HIV infection. It goes further to recommend that in cases of treatment failure, where viral load testing is not routinely available, CD4 count can be used [14]. Deaths are well explained in the model for viral load monitoring than the model for CD4 cell count. This contradicts with findings from previous studies that CD4 cell count is a better predictor for HIV/AIDS progression than HIV RNA [7, 8, 15].

However, the 320 patients used in the study were selected on the basis that their viral load monitoring was routinely monitored throughout the study leading to selection bias. The limitation of this study was that although gender and age were considered in the analysis, the study disregarded the aspect of opportunistic infection.

Table 5 Log-ratio test for the superiority of viral load monitoring over CD4 cell monitoring

	-2 log LR	df	*p*-value
VL.cov1.msm	828.869	5	$10^{(-4)}$

Conclusion

Although viral load monitoring in predicting HIV/AIDS progression gives the stakeholders a measure of understanding, control and motivation to adhere to treatment and enhances understanding of HIV infection [14]. It is recommended that both viral load monitoring and CD4 cell count monitoring be used since viral load determines the need for treatment change and CD4 cell count helps in monitoring the risk of opportunistic infection (OI) and treatment failure. From this study, one can also conclude that although patients take more time to achieve a normal CD4 cell count and less time to achieve an undetectable viral load, once the CD4 cell count is normal, mortality risks are reduced. Therefore, both viral load monitoring and CD4 count monitoring can be used to contribute information which can be used to significantly improve the life expectance of patients living with HIV.

Additional file

Additional file 1: BMCID_Data. Data sheet containing all anonymised data used in this analysis. (XLSX 250 kb)

Abbreviations

AIDS: Acquired Immune deficiency Syndrome; ART: Antiretroviral Therapy; CD4BL: CD4 Baseline; HIV: Human Immunodeficiency Virus; msm: Multistate modelling; NA: Non-adherence; OI: Opportunistic Infection; RNA: Ribonucleic Acid; VL: Viral load; VLBL: Viral Load Baseline; WHO: World Health Organisation

Acknowledgements

This study would not have been a success without the assistance of the University of Venda's Department of Microbiology which provided the data through Professor Pascal O. Bessong.

Funding

Not applicable

Availability of data and materials

All data generated or analysed during this study are included in this published article and its supplementary information files.

Authors' contributions

CS drafted the manuscript. CS and DC contributed to the analysis and interpretation of the data. Both authors participated in critical revision of the manuscript drafts and approved the final version.

Ethics approval and consent to participate

Permission to use the secondary data was granted by the Ethics Committee of the University of Venda in 2013. Names of participants were not included in the data set.

Consent for publication

Not applicable.

Competing interests

The authors declare that they have no competing interests.

Publisher's Note

Received: 18 October 2017 Accepted: 5 February 2019
Published online: 15 February 2019

References

1. Hoffmann CJ, Charalambous S, Thio CL, Martin DJ, Pemba L, et al. Hepatotoxicity in an African antiretroviral therapy cohort: the effect of tuberculosis and hepatitis B. AIDS. 2010;21:1301–8. [PubMed: 17545706]
2. Phillips AN, Staszewski S, Weber R, Kirk O, Francidi P, Miller V, Vernazza P, Lundgren JD, Ledergerber B. HIV viral response to antiretroviral therapy according to the baseline CD4 cell count and viral load. JAMA. 2001;286: 2560–7.
3. Ford N, Mentjes G, Victoria M, Greene G, Chiller T. The evolving role of CD4 cell count in HIV care. Curr Opin HIV AIDS. 2017;12:123–8. https://doi.org/10.1097/COH.0000000000000348.
4. Salazar-Vizcaya L, Keiser O, Technau K, Davies M, Haas AD, Blaser N, Cox V, Eley B, Rabie H, Moultrie H, Giddy J, Wood R, Egger M, Estill J. Viral load versus CD4 monitoring and a 5-year outcomes of ART in HIV-positive children in southern Africa: cohort-based modelling study. AIDS. 2014; 28(16):2451–60.
5. Erb P, Batlegay M, Zimmerli W, et al. Effect of antiretroviral therapy on viral load, CD4 cell count, and progression to acquired immunodeficiency virus – infected cohort. Arch Intern Med. 2000;160(8):1134–40. https://doi.org/10.1001/archinte.160.8.1134.
6. Brennan AT, Maskew M, Sanne I, and Matthew P Fox MP. The interplay between CD4 cell count, viral load suppression and duration of ART on mortality in a resource-limited setting. Trop Med Int Health. 2013;18(5):619–31. https://doi.org/10.1111/tmi.12079.
7. Brown ER, Otieno P, Mbori-Ngacha DA, Farquhar C, Obimbo EM, Nduati R, Overbaugh J, John-Steward GC. Comparison of CD4 cell count, viral load and other markers for the prediction of mortality among HIV-1 – infected Kenyan pregnant women. J Infect Dis. 2009;199:1292–300.
8. Miller V, Phillips AN, Clotet B, Mocroft A, Ledergerber B, Kirk O, Ormaasen V, Gargalianos-Kakolyris P, Vella S, Lundgren JD. Association of virus load, CD4 cell count and treatment with clinical progression in human immunodeficiency virus-infected patients with very lo CD4 cell counts. J Infect Dis. 2002;186:189–97.
9. Vasconcellos R, Oliveira C, Shimakura SE, Campos DP, Victoriano FP, Ribeiro SR, Veloso VG, Grinsztejn B, Carvalho M. Multistate models for defining degrees of chronicity related to HIV-infected patient therapy adherence. CadSaude Publica, Rio de Janeiro. 2013;29(4):801–11.
10. Maartens G, Celum C, Lewin SR. HIV infection: epidemiology, pathogenesis, treatment, and prevention. Lancet. 2014;384:258–71. https://doi.org/10.1016/s0140-6736(14)60164-1 Accessed 11 Jan 2018.
11. Dounelly CA, Bartley LM, Ghani AC, Le Fevre AM, Kwong GP, Cowling BJ, van Sighem AI, de Wolf F, Rode RA, Anderson RM. Gender differences in HIV-1 RNA viral loads. HIV Med. 2005;6(3):170–8.
12. Hasibi M, Hajiabdolbaghi M, Hamzelon S, Sardashti S, Forough M, Jozani ZB, Alinaghi SAS. Impact of age on CD4 response to combination antiretroviral therapy: a study in Tehran, Iran. World J AIDS. 2014;4:156–62.
13. Metallidis S, Tsachouridou O, Skoura L, Zebekakis P, Chrysanthidis T, Pilalas D, Bakaimi I, Kollaras P, Germanidis G, Tsiara A, Galanos A, Malisiovas N, Nikolaidis P. Older HIV-infected patients—an underestimated population in northern Greece: epidemiology, risk of disease progression and death. Int J Infect Dis. 2013;17:e883–91. https://doi.org/10.1016/j.ijid.2013.02.023.
14. WHO. What's new in treatment monitoring: Viral load and CD4 cell testing, July 2017. Geneva: World Health Organisation; 2017. WHO/HIV/2017.22
15. Ghadha S, Bhalla P, Jha AK, Gautam H, Saini S, Aneradha S. Diseases progression and antiretroviral therapy in newly seropositive HIV subjects in a tertiary care hospital in North India. J Infect Dev Ctries. 2013;7(2):110–5.

Publications 229

Biomedical Research 2018; 29 (15): 3090-3098 ISSN 0970-938X
www.biomedres.info

A Markov model to estimate mortality due to HIV/AIDS using CD4 cell counts based states and viral load: a principal component analysis approach.

Delson Chikobvu, Claris Shoko*

Department of Mathematical Statistics and Actuarial Sciences, University of the Free State, Box 339, Bloemfontein (9300), South Africa

Abstract

Background: Improvement of health in HIV/AIDS patients on Highly Active Antiretroviral Therapy (HAART) is characterised by an increase in CD4 cell counts and a decrease in viral load to undetectable levels. In modelling HIV/AIDS progression in patients, researchers mostly deal with either viral load only or CD4 cell counts only as they expect these two variables to be collinear.
Methods: In this study, a cohort of 320 HIV/AIDS patients under HAART follow-up from a wellness clinic in Bela-Bela, South Africa is used. A time homogeneous Markov model is developed to explain and predict probability of death from HIV/AIDS. Principal component variables are created by fitting a regression model of viral load on CD4 cell counts.
Results: Inclusion of a viral load principal component improves the efficiency of the model. The new viral load covariate helps to explain the component of mortality/transition, which could not be explained by the CD4 cell counts alone. CD4 cell counts are categorised to define the states for the Markov model. Results show that the expected percentage prevalence gives almost a perfect fit of the observed data.
Conclusion: The orthogonal viral load covariate along with CD4 baseline, gender, non-adherence to treatment and age in years (y) variables play a significant role in modelling HIV/AIDS progression based on both CD4 cell counts and viral load monitoring.

Keywords: Principal component analysis, HIV progression, Continuous-time Markov model, Orthogonal covariate, Antiretroviral therapy.

Accepted on July 30, 2018

Introduction

The development of Highly Active Antiretroviral Therapy (HAART) has substantially reduced the death rate from HIV [1]. HAART reduces viral load of circulating HIV by blocking replication at multiple points in the virus life cycle [2] resulting in an increase in CD4 cell counts and increased life expectancy of individuals infected with HIV. This has made CD4 cell counts and viral load counts the fundamental laboratory markers regularly used for patient management [3] in addition to predicting HIV/AIDS disease progression or treatment outcomes [4].

However, although the primary predictor of HIV transmission is the HIV viral load, very few HIV modelling studies include a detailed description of the dynamics of HIV viral load along stages of HIV diseases progression [5,6]. This could be due to the unavailability of data on viral load, particularly from low and middle income countries that have historically relied on monitoring CD4 cell counts for patients on HAART because of higher costs of viral load testing [7]. However, sometimes both CD4 cell counts and viral load information is available.

Estill et al. [8] investigated the benefits of viral load count routine monitoring for reducing HIV transmission. They developed a stochastic mathematical model representing 1000 simulations for both CD4 and viral load routine monitoring. Their findings revealed that viral load routine monitoring reduces both cohort viral load and transmissions by 31%.

Goshu et al. [9] used a semi-Markov process to model the progression of HIV/AIDS. They used five CD4 cell counts classified states. They found out that transition probabilities from a given state to the next worse state increase with time, get to an optimum level at a given time and then decrease with increasing time. In a recent research Osisiogu et al. [10] also used the same states as Goshu et al. [9]. However, they used a non-stationary Markov chain approach. They examined a cohort from Nnamdi Azikiwe University Teaching Hospital with a follow-up in their CD4 cell counts of the HIV/AIDS patients. Their main finding was that low CD4 cell counts do not generally imply faster rates of patient absorption but rather the age of the patient is a relevant factor.

Lee et al. [11] investigated the most vulnerable racial minority races (African Americans) in the United States and the Caucasians in order to predict the trends of the HIV/AIDS

epidemic using a Markov chain analysis. They predicted from these races, the number of people living with HIV, and mortality count due to HIV/AIDS. They observed a stable number of deaths over the years in both races.

Gover et al. [12] assessed the effects of antiretroviral therapy on 580 AIDS patients from an ART centre in New Delhi. They used a 5-stage multistate Markov model to estimate transition intensities and transition probabilities. The states of their model were CD4 cell count based as follows; state 1 (>500), state 2 (351 to 500), state 3 (200 to 350), state 4 (<200) and state 5 (death). They further examined the effects of covariates; age, gender and mode of transmission on transition intensities using Cox proportional hazards model.

Shoko et al. [13] used a continuous time-homogeneous Markov model to analyse the effects of reaction to treatment, TB co-infection, age and gender on transmission intensities. Their model was CD4 cell counts based followed by the death state and withdrawal state.

In this study, a continuous time homogeneous Markov process is used to model the progression of HIV/AIDS patients. We classify the states by the level of sickness based on four CD4 cell counts classifications measured in cells/mm^3 followed by the end point, death. More importantly, among the determinants of HIV/AIDS, both the viral load counts and CD4 cell counts are included in the same model, thus making this research different from previous studies. The viral load count covariate was included and effects of collinearity with CD4 cell count are corrected using the principal component approach. In addition to that, effects of non-adherence to treatment on transition intensities are assessed. Transitions between the CD4 cell counts states is considered to be bi-direction using data recorded from a cohort of 320 HIV+ patients at a wellness clinic in Bela Bela, South Africa.

Continuous-time Markov processes

A stochastic process {X(t),t ϵ [0, ∞)} defined on a finite state space C={1,2,…,c} where X (t) represents the disease state of a patient at time t represents a Markov process if $\forall s, t \geq 0$ and for every i, j ϵ C.

$P(X(t+s)= j|X(t)=i,X(u)=x(u),0 \leq u <s)=P(X(t+s)=j|X(t)=i)$.

Implying that a Markov process is memory less, that is, the future transitions depend on the entire history only through the present state. Thus, the previous states once occupied by an individual do not matter. These transitions are described using the transition probabilities (p_{ij} (t)), transition intensities (q_{ij}), from state i to state j. The functions p_{ij} (t) are continuously differentiable and are subject to the initial condition:

$$p_{ij}(0) = \delta_{ij} = \begin{cases} 1, & if \quad i = j \\ 0, & if \quad i \neq j \end{cases}$$

Where δ_{ij} is a kronecker delta, p_{ij} (0)=1, i=j means the patient's state definitely does not change when no time elapses and p_{ij} (0)=0, $i \neq j$ means that when no time elapses we are sure that the patient's state cannot change with certainty. The transition intensity is defined as;

$$q_{ij}(t) = \left.\frac{d\left(p_{ij}(t)\right)}{dt}\right|_{t=0} = \lim_{s \to 0} \frac{p_{ij}(t, t+s)}{s}, \quad i, j \in C, \quad j \neq i$$

and $q_{ii}(t) = -\sum_{j \neq i} q_{ij}(t)$ for each i ϵ C. In this study, transition probabilities depend only on the elapsed time and not on the chronological time. Thus, the Markov process is time-homogeneous, implying that

p_{ij} (t, t+s)=p_{ij} (s) and q_{ij} (t)=q_{ij}

The effect of the above explanatory variables (covariates) on the transition intensities is modelled using the proportional intensities:

$$q_{ij}(Z) = q_{ij}^{(0)} \exp\left(\beta_{ij}^{'} Z\right), \quad i \neq j \rightarrow (1)$$

Where $\boldsymbol{Z}$ is a k-dimensional vector of explanatory variables, $\boldsymbol{\beta}_{ij}$ is a vector of k regression parameters relating the instantaneous rate of transitions from state i to state j to the covariates $\boldsymbol{Z}$, and $q_{ij}^{(0)}$ is the baseline transition intensities with covariates set to their means.

Materials and Methods

Data description

The model is initially applied on 320 HIV positive patients on Highly Active Anti-Retroviral Therapy (HAART) from a Wellness clinic in Bela Bela, South Africa, from year 2005 to year 2009. 224 of these patients were females and 96 were males at treatment commencement (t=0). About 50% and 65% of the female and male deaths respectively occurred during the first 6 months of treatment uptake. The interquartile range of patient ages is (33 y; 48 y) with mean and median ages of 40.62 y and 41 y respectively. The ages were negatively skewed (skew=-0.08) since there were younger patients than older patients in this cohort. At time (t=0) there were 242 individuals with CD4 baseline (CD4BL) cell counts below 200, 59 individuals with CD4 cell counts between 200 and 350, 11 individuals with CD4 cell counts between 350 and 500, 6 individuals with CD4 cell counts between 500 and 750 and 1 individual with CD4 cell count above 750. At (t=0) the CD4 cell counts had mean of 156 cells/mm^3, a median of 116 cell/mm^3 and the maximum CD4 cell counts was 1202 cells/mm^3. The mean Viral Load Count Baseline (VLBL) for these patients was 105573.35 copies/mm^3 and it ranged from 56 to 818600 copies/mm^3. The median viral load was 58523.00 copies/mm^3. From these individuals 155 had a WHO stage baseline (WSBL) of 4 which is related to severe HIV symptoms. WSBL is the categorisation of HIV/AIDS at baseline basing on the clinical markers as defined by World Health Organisation (WHO).

Statistical analysis

Principal component analysis: Principal component analysis is a technique used to combine highly correlated factors into principal components that are much less correlated with each other. This improves the efficiency of the model.

In this study, the predictive power of CD4 cell counts (I_1) and viral load (I_2) is explored. Two new, uncorrelated factors, I_1^* and I_2^*, can be constructed as follows:

Let $I_1^*=I_1$

Then, we carry out a linear regression analysis to determine the parameters γ_1 and γ_2 in the equation:

$$I_2 = \gamma_1 + \gamma_2 I_1^* + \varepsilon_1$$

γ_1 and γ_2 are the intercept and slope parameters of the regression model respectively and ε_1 is the 'error' term or residual, which by definition is independent of $I_1^*=I_1$.

We then set:

$$I_2^* = \varepsilon_1 = I_2 - (\gamma_1 + \gamma_2 I_1^*)$$

By construction I_2^* is uncorrelated with the viral load values (I_2) since $I_2^*=\varepsilon_1$ is the residual term in the equation. I_2^* in the model explains the component of mortality that cannot be explained by the CD4 cell counts alone (or in the absence of viral load counts). To deal with multi-collinearity of viral load count and CD4 cell count, the orthogonal viral load covariate (residuals) are used. This is done by regressing viral load count on CD4 cell count and doing the classification below. The residuals from the fitted model are included with the original HIV data to form the new orthogonal covariate, orthogonal viral load (residuals) (VLR). These residuals are coded as; "1" for negative residuals and "0" for positive residuals. A continuous-time Markov model for the effects of age, non-adherence (NA), CD4 baseline (CD4BL), and orthogonal viral load (I_2^*) on HIV progression based on CD4 cell counts is fitted using the "msm" package for multistate modelling in *R*. The results are presented in the next section.

The variables in the model are then defined as follows:

$$Age = \begin{cases} 1, & \leq 45 \quad years \\ 0, & > 45 \quad years \end{cases},$$

$$VLR orthogonal \text{variable}(I_2^*) = \begin{cases} 1, & negative \\ 0, & positive \end{cases}.$$

$$Non-adherence\ (NA) = \begin{cases} 1, & Yes \\ 0, & No \end{cases},$$

$$Gender = \begin{cases} 1, & male \\ 0, & female \end{cases},$$

$$CD4\ baseline\ (CD4B) = \begin{cases} 1, & \leq 200 \quad cells/mm^3 \\ 0, & > 200 \quad cels/mm^3 \end{cases},$$

$$CD4\ cell\ count\ levels\ (S) = \begin{cases} 1; & CD4 > 800 \\ 2; & 500 < CD4 \leq 800 \\ 3; & 350 < CD4 \leq 500, \\ 4; & CD4 < 350 \\ 5; & Death \end{cases}$$

Model formulation

Consider a stochastic process {X(t), t ϵ [0,5) years} defined on a finite state space C=(1,2,3,4,5) based on CD4 cell counts as defined above. X (t) represents the CD4 state of an HIV/AIDS patient at time t. This process represents a Markov process if $\forall s, t \geq 0$ and for every i, j ϵ C.

$P(X(t+s)=j|X(t)=i,X(u)=x(u),0 \leq u <s)=P(X(t+s)=j|X(t)=i)$.

The above equation implies that a Markov process is memory less, that is, the future transitions depend on the entire history only through the present state. Formulation of the model is based on the assumption that at (t=0), an HIV infected individual enters the study with an HIV state defined by CD4 cell counts levels. As the patient initiates treatment therapy, the patient is either in states 1-3 or 4 and these states are mutually exclusive. At time Δt the patient in state i is expected to either maintain his state (i=1,2,3,4), transition to state of better CD4 cell counts (i-1, $I \neq 1$) (or remain at the lowest state) or transit to a state of lower CD4 cell counts (i+1, i=1,2,3,4) (or remain at the highest state). These possible transitions are based on the assumption that not all patients initiated into HAART recover their CD4 cell counts levels. Some may fail to achieve their normal CD4 cell counts levels due to non-adherence, effect of age as younger patients may not adhere and also due to the effect of gender since the assumption is males have busy schedules. However, those who adhere to HAART respond well to treatment. Hence the bi-directional model proposed in Figure 1 below.

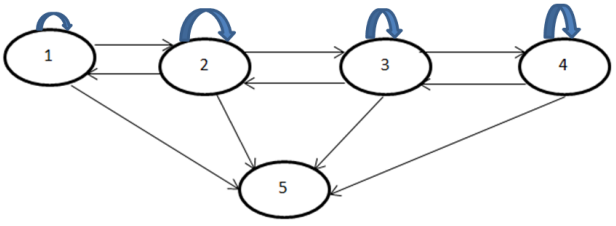

Figure 1. *Diagraph for HIV progression defined by CD4 cell count states followed by the end point, death. a) States 1-4 are transient and there is a possibility of marinating the same state in 2 or more consecutive visits. b) State 5 is the absorbing state.*

The model in Figure 1 is described by a transition intensity matrix $Q=q_{ij}$;

$$Q(t) = \begin{pmatrix} q_{11} & q_{12} & 0 & 0 & q_{15} \\ q_{21} & q_{22} & q_{23} & 0 & q_{25} \\ 0 & q_{32} & q_{33} & q_{34} & q_{35} \\ 0 & 0 & q_{43} & q_{44} & q_{45} \\ 0 & 0 & 0 & 0 & 0 \end{pmatrix}$$

The effect of the above explanatory variables on the transition intensities is modelled using the proportional intensities:

$$q_{ij}(Z) = q_{ij}^{(0)}\exp\left(\beta_{ij}^{'}Z\right), \quad i \neq j,$$

Where $\boldsymbol{Z}$ is a k=5-dimensional vector of explanatory variables "CD4BL, gender, age, non-adherence (NA), orthogonal viral load ("I_2^*")." Thus, the transition intensity for a patient h in this study is given by the model:

$$q_{ij} = q_{ij}^{(0)}\exp\left(\beta_{ij}^{(Age)}Age_h + \beta_{ij}^{(Gender)}Gender_h + \beta_{ij}^{(CD4BL)}CD4BL_h + \beta_{ij}^{(NA)}NA_h + \beta_{ij}^{\left(I_2^*\right)}I_{2h}^*\right)$$

For this model $q_{ij}^{(0)}$ are the baseline transition intensities that refer to a patient with age category 0 (over 45-y-old), gender=0 (female), CD4BL=0 (above 200 cells/mm^3, Adherent to treatment and positive I_2^*, β_{ij} is a regression parameter relating the instantaneous rate of transitions from state i to state j to the covariate Z. The transition intensities, q_{ij}, are presented in rates per year. q_{ij} are the elements of a 5 × 5 transition intensity matrix Q from a continuous time-homogeneous Markov process.

An important aspect is the inclusion of both $CD4BL_h$ and I_2^* (the orthogonal viral load covariate) derived after curing for collinearity.

Assessment of the fitted models: Based on Equation (1) two nested models are fitted, one of the models excludes the effect of the orthogonal viral load and the other includes all covariates including the orthogonal viral load. These models are compared using their Akaike information criteria (AICs) defined as:

AIC=-2 × Log (likelihood)+2k

where *-2 × Log (likelihood)* represents the bias, *2k* represents the variance and *k* is the number of estimated parameters in the fitted model. The model with the minimum AIC is considered as the better model. Further assessment of the fitted nested models is done using the likelihood ratio test (LRT). The value of the LRT=$-2log_e((L_s(\theta))/(L_f\theta))$, where $L_s(\theta\hat{})$ is the simple model (no viral load orthogonal in the model) and $L_f(\theta\hat{})$ is the full model (with the orthogonal viral load covariate in the model).

Results

In this section, the combination effect of viral load and CD4 cell counts in the progression of HIV in patients on treatment is analysed. This is done by first fitting a time-homogeneous Markov model for the effects of the covariates; CD4 cell count baseline (CD4BL), Gender, Age and non-adherence to treatment (NA) on HIV/AIDS progression based on CD4 cell count states. Notable is the exclusion of the viral load count covariate in this model. Secondly, a time-homogeneous Markov model for the effects of covariates; CD4 cell count baseline (CD4BL), gender, age, non-adherence to treatment (NA) and the orthogonal viral load covariate is then included in the model. Comparison of these two models is based on their -2 × log (likelihood), Akaike Information Criteria (AIC), likelihood ratio tests and also the percentage prevalence plots. The results are shown in the following subsections.

CD4 cell counts model and other variables excluding viral load: In this subsection we fit a continuous-time homogeneous Markov model for the effects of non-adherence (NA), CD4 baseline (CD4BL), age and gender on the progression of HIV defined by the CD4 cell counts states as defined in the model below:

$$q_{ij}(Z) = q_{ij}^{(0)}\exp\left(\beta_{ij}^{'}Z\right), \quad i \neq j,$$

where $\boldsymbol{Z}$=(CD4BL, gender, age, NA) is a k=4-dimensional vector of covariates and $\boldsymbol{\beta}_{ij}$ is a vector of k regression parameters relating the instantaneous rate of transitions from state i to state j to the covariates $\boldsymbol{Z}$ and baseline intensities $q_{ij}^{(0)}$ relating to the baseline transition from state i to state j. These states are defined by CD4 cell count and an absorbing state, death. The results are shown in Table 1 below.

From Table 1, the first column represents possible transitions from state i to state j, where i=1,..,4 and j=1,..,5. The second column represents the baseline transition intensities (with confidence intervals), the third column gives coefficients (with confidence intervals) to represents the effects of non-adherence to treatment, the fourth column gives coefficients (with confidence intervals) to represent the effects of having a CD4 baseline above 200 copies/mm^3 to HIV progression, the fifth column gives coefficients (with confidence intervals) to represent the effects of having age below 45 years and lastly the sixth column gives coefficients (with confidence intervals) to represent the effects of gender to HIV progression. The results are as follows:

Table 1. *Estimated parameters (with 95% confidence intervals in brackets) for the time homogeneous model that excludes the effects of viral loads.*

State *i-j*	Baseline ($q_{ij}^{(0)}$)	NA	CD4BL	Age	Gender
State 2-1	0.561 (0.410, 0.7677)*	0.786 (0.0081, 1.57)*	-0.411 (-0.938, 0.116)	0.37 (-0.51, 1.25)	0.106 (-0.51, 0.72)
State 1-2	0.751 (0.486, 1.159)*	0.145 (-1.29, 1.003)	-0.491 (-1.232, 0.25)	-1.309 (-2.57, -0.05)*	-0.0618 (-0.94, 0.817)

State 3-2	1.27 (1.048, 1.537)*	0.0501 (-0.74, 0.84)	-0.613 (-0.99, -0.23)*	0.277 (-0.15, 0.71)	0.117 (-0.30, 0.54)
State 2-3	0.711 (0.526, 0.964)*	0.757 (-0.42, 1.94)	-0.0338 (-0.71, 0.64)	0.188 (-0.92, 0.55)	0.737 (0.084, 1.39)*
State 4-3	0.798 (0.686, 0.929) [8]	0.389 (-0.92, 0.15)	-1.329 (-1.67, -0.99)*	0.0508 (-0.277, 0.38)	-0.463 (-0.79, -0.13)*
State 3-4	0.691 (0.528, 0.906)*	0.751 (-0.049, 1.55)	-0.522 (-1.15, 0.11)	0.0671 (-0.51, 0.65)	0.516 (-1.13, 0.09)
State 1-5	0.0005 (0.000006, 4696)	0.058 (-39.9, 39.75)	0.621 (-42.3, 43.6)	-0.607 (-36.1, 34.85)	0.714 (-42.2, 43.6)
State 2-5	0.00492 (0.00007, 0.330)*	1.629 (-14.36, 11.1)	0.0683 (-2.93, 3.07)	3.702 (-9.11, 16.51)	1.509 (-1.48, 4.50)
State 3-5	0.00036 (0.000005, 2.44)*	4.48 (-4.15, 13.11)	2.878 (-8.16, 13.9)	2.39 (-9.12, 13.90)	-3.194 (-14.1, 7.7)
State 4-5	0.0010 (0.00004, 0.276)*	3.35 (-16.4, 9.67)	3.164 (-9.80, 16.1)	-2.065 (-4.31, 0.181)	-5.271 (-18.3, 7.78)
-2log-likelihood: 2646.165; *significant.					

In Table 1 (model that excludes the viral load count), results from the baseline transition intensities show that patients in state 1 (CD4 cell counts above 800 cells/mm^3) are 1502 times more likely to experience immune deterioration to state 2 than being absorbed into the death state. When CD4 cell counts are below 500 cells/mm^3 (states 3 and 4), transitions to better states are more likely to occur than transitions to worse states. However, when CD4 cell counts are above 500 cells/mm^3 the rates of immune deterioration are higher than the rates of immune recovery.

For patients who experienced non-adherence to treatment, transitions from state 2 to state 1, state 3 to state 4, state 3 to state 2 and state 4 to state 3 estimates are relatively precise as shown by the narrower confidence intervals. The only transition that is significant, is from state 2 to state 1. This is shown by the confidence interval that is narrower (zero excluded in the interval) compared to the other transitions. For these non-adherent patient, there is a significant increase on the rate of immune recovery from state 2 to state 1. Although not significant, there is an increase in immune deterioration from state 3 to state 4 and reduction on the rate of immune recovery from state 4.

For the age variable, transitions from state 2 to state 3, state 3 to state 2, state 3 to state 4 and state 4 to state 3 estimates are relatively precise as revealed by the smaller confidence intervals. The only transition that is significant (zero excluded in the interval) is from state 2 to state 1. The results show a significant reduction in immune deterioration once a normal CD4 cell counts above 800 cell/mm^3 (state 1) are achieved for the younger patients aged 45 years and below. These younger patients experience reduced immune deterioration from state 2 to state 3 and increased immune deterioration from state 3 to state 4 although these transitions are not statistically significant.

For the other variables, gender and CD4 baseline, all the estimated transitions between live states estimates are relatively precise since they have narrow confidence intervals. However, for CD4 baseline, only transitions from state 3 to state 2 and from state 4 to state 3 are significant (zero excluded in the interval). These transitions show a significant reduction in immune deterioration. Males experienced significantly increased immune deterioration from state 2 to state 3 compared to their female counterparts. They also experience a significant reduction in immune recovery from state 4 to state 3.

Overall, the fitted model shows relatively wider confidence intervals for the transitions to the death state.

The expected and observed percentage prevalence in each CD4 cell count state and the death state are shown in Figure 2 below.

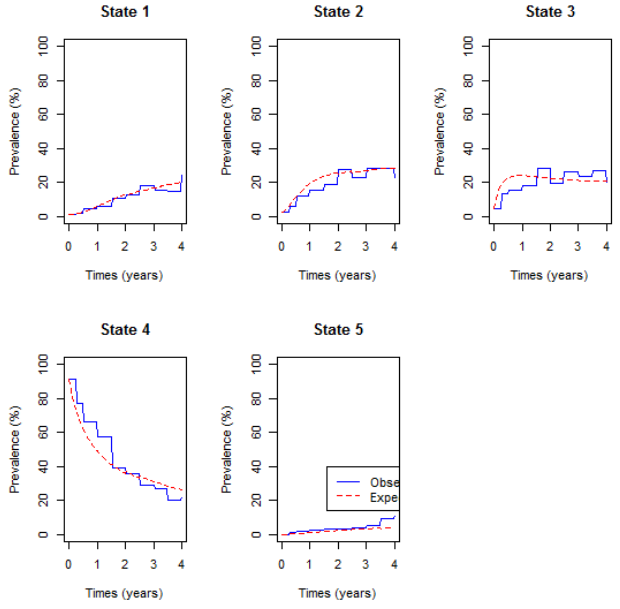

Figure 2. *Observed and expected percentage prevalence in each state for the model with CD4 states without viral load orthogonal. The expected model slightly underestimate motel after 3 years.*

Results from Figure 2 show that the expected percentage prevalence give almost a perfect fit of the observed percentage prevalence for state 1 and state 5 (death) up to 3 years. Thereafter deaths are slightly underestimated and state 1 prevalence's are slightly overestimated. In the first 2 years observed percentage prevalence in state 2 and 3 are slightly overestimated by the expected percentage prevalence. Percentage prevalence in state 4 are slightly underestimated in

the first 2 years and slightly overestimated thereafter by the fitted model.

CD4 model for the viral load principal component: since the variables CD4 cell count and viral load are expected to be collinear, orthogonality between these variables is achieved by regressing viral load on CD4 cell count as shown in Table 2 below.

The results show a highly significant regression line suggesting correlation between viral load and CD4 cell count as indicated by a p-value below 2.2e-16. The residuals from the regression model are then taken to represent another viral load covariate, which is orthogonal to the CD4 cell count covariate. The orthogonal viral load covariate is coded as follows.

$$orthogonal\ \ viral\ \ load\ \ \left(I_2^*\right) = \begin{cases} 1, & if\ \ viral\ \ load\ \ residual\ \ is\ \ negative \\ 0, & if\ \ viral\ \ load\ \ residual\ \ is\ \ positive \end{cases}$$

The orthogonal viral load covariate and other variables; age, non-adherence, gender and CD4 baseline are then used as covariates for the continuous-time Markov model with states defined by CD4 cell count. The results are shown in Table 3 below.

Table 2. *Regression of viral load on CD4 cell counts.*

	Estimate	Std. error	t value	Pr(>|t|)	
γ_1 intercept)	55166.91	3136.54	17.59	<2e-16	***
γ_2 slope	-70.963	6.207	-11.43	<2e-16	***
Multiple R-squared: 0.06015; F-statistic: 130.7 on 1 and 2042 DF, p-value<2.2e-16					

Table 3. *Parameter effects (with 95% confidence intervals) of age, CD4 baseline, non-adherence, gender and viral load residuals on the transition intensities for the CD4 based Markov model.*

	Baseline	NA	CD4BL	Age	Gender	I_2^*
State 2-1	0.545 (0.40, 0.74)	0.765 (0.034,1.496)*	-0.28255 (-0.78,0.21)	0.61259 (-0.146,1.37)	-0.03339 (-0.6273, 0.5605)	-1.17330 (-1.9536,-0.39301)*
State 1- 2	0.0401 (0.00004, 4242)	0.1483 (-1.11922, 1.4159)	-0.51969 (-1.3044, 0.26501)	-1.32263 (-2.6596, 0.01434)	-0.08131 (-1.0383, 0.8757)	-4.01482 (-18.5900,10.56033)
State 3- 2	1.398 (1.135, 1.722)	0.3269 (-0.60065,1.2544)	-0.54526 (-0.9359,-0.15463)*	0.30917 (-0.1229, 0.74129)	0.16951 (-0.2711, 0.6101)	-0.50199 (-1.0694, 0.06537)
State 2-3	0.669 (0.474, 0.943)	1.1211 (-0.19695, 2.4392)	0.03985 (-0.6460, 0.72567)	-0.08423 (-0.8219, 0.65347)	0.87997 (0.2023, 1.5577)*	0.70471 (-0.4375, 1.84694)
State 4-3	0.831 (0.710, 0.973)	-0.3759 (-0.94136,0.1896)	-1.40333 (-1.7733,-1.03333)*	0.05320 (-0.2799, 0.38628)	-0.48246 (-0.8212,-0.1437)*	-0.07262 (-0.4884, 0.34321)
State 3-4	0.697 (0.478, 1.018)	0.8527 (0.01718, 1.6883)*	-0.61048 (-1.2898, 0.06881)	0.10324 (-0.4845, 0.69097)	-0.50671 (-1.1252, 0.1118)	0.24935 (-1.3065, 1.80515)
State 1-5	0.00166 (0.00001, 17.1)	4.3732 (-1.99613,10.7425)	7.38286 (-9.1511,23.91685)	2.64846 (-14.0315,19.32845)	-2.76023 (-21.6692,16.1487)	7.96834 (-8.9552,24.89188)
State 2-5	0.0001 (0.00003, 131)	-1.7120 (-28.32334,24.8994)	-2.54389 (-18.2331,13.14536)	2.06138 (-15.1219,19.24463)	4.65693 (-8.0486,17.3625)	-5.06520 (-17.1554, 7.02498)
State 3-5	0.0001 (0.00003, 2768)	1.7018 (-36.23359,39.6373)	1.06855 (-45.1581,47.29522)	0.37856 (-48.2596,49.01677)	-1.37134 (-48.1259,45.3832)	-1.09413 (-55.9253,53.73707)
State 4-5	0.0006 (0.00004, 1.05)	-3.9372 (-22.01985,14.1455)	3.75843 (-13.5309,21.04776)	-2.06766 (-4.3237, 0.18839)	-5.76054 (-22.9616,11.4405)	-1.18026 (-2.9828, 0.62225)

-2Log-likelihood: 2554.25; *significant

The results from Table 3 (model that includes the viral load count) show that for all the covariates the model gives more precise estimates (narrower confidence intervals) of parameters for transitions between live states than the model without the orthogonal viral load covariate (I_2^*). Just like the model without the orthogonal viral load, non-adherent patients experienced a significant increase in immune recovery from state 2 to state 1. In addition, there is a significant increase in immune deterioration from state 3 to state 4. Although not significant, the inclusion of the orthogonal viral load covariate results in non-adherence to treatment accelerating death from state 3 although the magnitude is lower than when the orthogonal viral load covariate is excluded.

The covariate age results in a more precise estimate of the transition from state 4 to state 5 compared to the other covariates except the orthogonal viral load. The results reveal a reduction of deaths from state 4 for patients aged 45 y and below. Though not significant, the results now show a reduction on immune deterioration from state 1 (CD4 state above 800 cells/mm^3) and an increase on the rate of immune

recovery from state 2 to state 1 for younger patients aged 45 y and below.

The results generally show a reduction in mortality in cases where the observed viral load is lower than the expected (i.e., negative orthogonal viral load count).

For patients who initiated therapy with a CD4 cell counts below 200 cells/mm^3, the rates of immune recovery are reduced. There is a significant reduction in the rates of immune recovery from state 3 to state 2 and from state 4 to state 3.

The continuous-time homogeneous Markov model with the orthogonal viral load component has lower -2log-likelihood than that of the model that excludes the orthogonal viral load component. Next we plot percentage prevalence in each state for the fitted model.

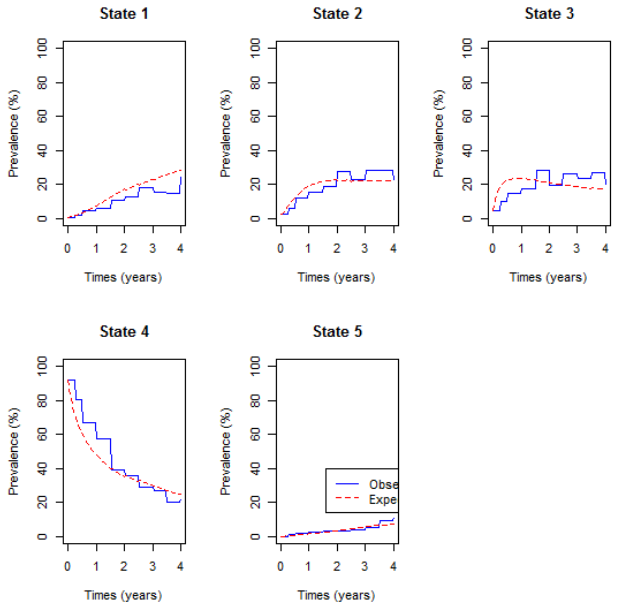

Figure 3. *Percentage prevalence for the continuous-time Markov model defined by CD4 cell count and the orthogonal variable, viral load, included. It shows an improvement in estimating mortality compared to the model without the orthogonal variable.*

Figure 3 above shows that if the orthogonal viral load covariate is included, the expected percentage prevalence gives a better estimate of the observed percentage prevalence for the mortality state (state 5), better than the Markov model in which the orthogonal viral load covariate is excluded.

Assessment of the fitted models: In this section we further assess the fitted models by performing a likelihood ratio test and calculation of the Akaike Information Criteria (AIC) for each of the fitted model (Table 4).

Table 4. *Likelihood ratio test for the model with no viral load orthogonal and the model with viral load orthogonal.*

lrtest.msm (No orthogonal viral load covariate, with the orthogonal viral load covariate)	-2loLR	df	p
with viral load orthogonal	91.91497	10	2.22E-15
AIC (No viral load orthogonal)=2746.165; AIC (with viral load orthogonal)=2674.25			

A likelihood ratio test for the two nested models has shown that the model with the orthogonal viral load covariate fits the data significantly better than the model with no orthogonal viral load covariate. This is further confirmed by the estimated AICs which is lower for the model with the orthogonal viral load covariate than that of the model with no orthogonal viral load covariate.

Discussions

In this study, a time homogeneous Markov model based on CD4 cell count states is developed to explain and predict probability of death from HIV/AIDS. The model is improved by including an orthogonal viral load covariate derived from principal component analysis. Principal component analysis is a technique used to combine highly correlated factors into principal components that are much less correlated with each other. This improves the efficiency of the model. Principal component variables are created by fitting a regression model of viral load count on CD4 cell count. The new orthogonal covariate is included to represent the viral load covariate for the Markov model defined. This viral load covariate helped to explain a component of mortality/transition, which could not be explained by the CD4 cell count alone.

Results from the likelihood ratio test show that the model with the orthogonal viral load covariate fits significantly better than the model with exclusion of viral load. Thus, the orthogonal viral load covariate along with CD4 baseline, gender, non-adherence and age play a significant role in modelling HIV/AIDS progression based on CD4 cell counts and viral load monitoring.

Results from the analysis show that when CD4 cell count is below 500 cells/mm^3 rates of immune recovery are higher than rates of immune deterioration particularly for younger patients aged 45 y and below. However, when the CD4 cell counts are between 500 and 800 cells/mm^3 the rate of immune deterioration is higher than the rate of immune recovery and this was mainly attributed to patients who were non-adherent to treatment and patients who initiated therapy with a CD4 baseline below 200 cell/mm^3. Once the CD4 cell count is above 800 cells/mm^3, the results show a possibility of immune deterioration, although the magnitude is very low, mainly due to non-adherent to treatment. This contradicts the finding from the previous study that was carried out in India which revealed higher rates of immune recovery than immune deterioration regardless of the HIV/AIDS state of the patient [12].

Progression to death is more pronounced on HIV/AIDS patients who are below the age of 45 y and with a CD4 cell count of 200 cells/mm^3 at treatment initiation. Previous studies [12,13] also reported more pronounced risk of death for patients with CD4 baseline of 200 cells/mm^3 which concurs with our findings. For this study, progression to death was also

more pronounced from the CD4 cell count above 800 cells/mm^3 for patients whose CD4 baseline was below 200 cells/mm^3 and for patients who were non-adherent to treatment.

The results show that inclusion of the orthogonal viral load covariate results in a reduction in immune deterioration from state 1 (CD4 state above 800 cells/mm^3) and an increase in the rate of immune recovery from state 2 to state 1 for younger patients aged 45 y and below. Generally younger patients experienced higher rates of immune recovery than immune deterioration compared to patients who are over 45 y and this concurs with findings from previous studies [14]. This is in agreement with previous study carried out in Tehran, India that showed that mean CD4 cell count increments after initiation of combination therapy are lower on older patients [15].

For patients whose viral load is lower than the expected given the CD4 cell count, there was a reduction in transition to deaths. This means that for given levels of CD4 cell count, the patients ought to have more viral load, but they have less resulting in reduction in mortality.

This study discovers the importance of using both CD4 cell count and viral load in the same model for monitoring progression of HIV/AIDS patients on antiretroviral therapy. By including both variables, the model has revealed that for given levels of CD4 cell count, there is the possibility of reduction of mortality for patients whose viral load is lower than expected given their CD4 count. Progression to death was more pronounced on patients who have achieved normal CD4 cell counts and this is experienced mainly in younger patients, non-adherent patients and also for patients whose initial CD4 cell counts were below 200 cells/mm^3. This study will help the researcher to uncover the critical areas of dealing and correcting for collinearity when including both CD4 cell count and viral load in multistate modelling of HIV/AIDS that many researchers were not able to explore. Thus a new application of theory and better understanding of the Principal component approach when dealing with both CD4 and viral load (in the same model) to HIV/AIDS modelling may be arrived at.

Acknowledgements

This study would not have been a success without the assistance of the Microbiology Department at the University of Venda in providing the secondary data through Professor Pascal O. Bessong.

References

1. Palella FJ, Delaney KM, Moorman AC, Loveless MO, Fuhrer J, Satten GA, Aschman DJ, Holmberg SD. Declining morbidity and mortality among patients with advanced human immunodeficiency virus infection. N Engl J Med 1998; 338: 853-860.
2. Cole SR, Hernan MA, Anastos K, Jamieson BD, Robins JM. Determining the effects of highly active antiretroviral therapy on change in human immunodeficiency virus type 1 RNA viral load using a marginal structural left-censored mean model. Am J Epidemiol 2007; 166: 219-227.
3. Mathieu E, Foucher Y, Dellamanica P, Doures JP. Parametric and non-homogeneous semi-Markov process for HIV control. Methodol Comput Appl Probab 2007; 9: 389-397.
4. Hoffman RM, Black V, Technau K. Effects of highly active antiretroviral therapy duration and regimen on risk for mother-to-child transmission of HIV in Johannesburg, South Africa. J Acquir Immune Defic Syndr 2010; 54: 35-41.
5. Case KK, Ghys PD, Gouws E, Eaton JW, Borquez A, Stover J. Understanding the modes of transmission model of new HIV infection and its use in prevention planning. Bull. World Health Organ 2012; 90: 831-838.
6. Herbeck JT, Mittler JE, Gottlieb GS, Mullins JI. An HIV epidemic model based on viral load dynamics: value in assessing empirical trends in HIV virulence and community viral load. PLoS Comput Biol 2014; 10: 1003673.
7. Lecher S, Williams J, Fonjungo PN. Progress with scale-up of HIV viral load monitoring-seven sub-Saharan African countries, January 2015-June 2016. Morbid Mortal Week Rep 2016; 65: 47.
8. Estill J, Aubriere C, Egger M, Johnson L, Wood R. Viral load monitoring of antiretroviral therapy, cohort viral load and HIV transmission in Southern Africa: A mathematical modelling analysis. AIDS 2012; 26: 1403-1413.
9. Goshu AT, Getahun D. Modeling progression of HIV/AIDS disease stages using semi-Markov processes. J Data Sci 2013; 11: 269-280.
10. Osisiogu UA, Nwosu CA. A stochastic analysis of the absorption probabilities of CD4 cell counts of HIV/AIDS patients using the smoothed non-stationary Markov chain model: a case study of Anambra State. Eur J Stat Probab 2015; 3: 1-11.
11. Lee S, Ko J, Tan X, Patel I, Balkrishnan R, Chang J. Markov chain modeling analysis of HIV/AIDS progression: a race-based forecast in the United States. J Ind Pharm Sci 2014; 76: 107-115.
12. Gurprit G, Adesh Kumar G, Prafulla KS, Barnali D. A multistate Markov model based on CD4 cell count for HIV/AIDS patients on antiretroviral therapy (ART). Int J Stat Med Res 2013; 2: 144-151.
13. Shoko C, Chikobvu D. Time-homogeneous Markov process for HIV/AIDS progression under a combination treatment therapy: cohort study, South Africa .Theor Biol Med Model 2018; 15: 3.
14. Hogg RS, Yip B, Chan KJ, wood E. Rates of disease progression by baseline CD4 cell count and viral load after initiating triple-drug therapy. JAMA 2001; 286: 2568-2577.
15. Hasibi M, Hajiabdolbaghi M, Hamzelom S, Sardashti S, Foroughi M, Jozani ZB, Alinaghi SAS. Impact of age on CD4 response to combination antiretroviral therapy: study in Tehran, Iran. World J AIDS 2014; 4: 156-160.

***Correspondence to**

Claris Shoko

Department of Mathematical Statistics and Actuarial Sciences

University of the Free State

South Africa

Publications

Infect Dis Ther
https://doi.org/10.1007/s40121-018-0217-y

ORIGINAL RESEARCH

A Markov Model to Estimate Mortality Due to HIV/AIDS Using Viral Load Levels-Based States and CD4 Cell Counts: A Principal Component Analysis Approach

Claris Shoko · Delson Chikobvu · Pascal O. Bessong

Received: August 8, 2018

ABSTRACT

Introduction: Improvement of health in human immunodeficiency virus/acquired immunodeficiency syndrome (HIV/AIDS) patients on antiretroviral therapy (ART) is characterised by an increase in CD4 cell counts and a decrease in viral load to undetectable levels. In modelling HIV/AIDS progression in patients, researchers mostly deal with either viral load levels only or CD4 cell counts only, as they expect these two variables to be collinear. In this study, both variables will be in one model.

Methods: Principal component variables are created by fitting a regression model of CD4 cell counts on viral load levels to improve the efficiency of the model. The new orthogonal covariate is included to represent the CD4 cell counts covariate for the continuous time-homogeneous Markov model defined. Viral load levels are categorised to define the states for the Markov model.

Results: The likelihood ratio test and the estimated AICs show that the model with the orthogonal CD4 cell counts covariate gives a better prediction of mortality than the model in which the covariate is excluded. The study further revealed high accelerated mortality rates from undetectable viral load levels as well as accelerated risks of viral rebound from undetectable viral level for patients with lower CD4 cell counts than expected.

Conclusion: Inclusion of both viral load levels and CD4 cell counts, monitoring and management in time homogeneous Markov models help in the prediction of mortality in HIV/AIDS patients on ART. Higher CD4 cell counts improve the health and consequently survival of HIV/AIDS patients.

Keywords: Continuous-time Markov model; HIV progression; Orthogonal CD4; Principal component analysis

INTRODUCTION

The development of highly active antiretroviral therapy (HAART) has substantially reduced morbidity and mortality in the human immunodeficiency virus/acquired immunodeficiency syndrome (HIV/AIDS) population [1]. HAART reduces the viral load of circulating HIV

Enhanced Digital Features To view enhanced digital features for this article go to https://doi.org/10.6084/m9.figshare.7172264.

C. Shoko (✉) · D. Chikobvu
Department of Mathematical Statistics and Actuarial Sciences, University of the Free State, Bloemfontein, South Africa
e-mail: claris.shoko@gmail.com

P. O. Bessong
Department of Microbiology, University of Venda, Thohoyandou, South Africa

Published online: 02 November 2018

by blocking replication at multiple points in the virus life cycle [2], resulting in an increase in CD4 cell counts and increased life expectancy of individuals infected with HIV. Thus, making CD4 cell counts and viral load the fundamental laboratory markers regularly used for patient monitoring and management [3], in addition to predicting HIV/AIDS disease progression or treatment outcomes [4].

However, although the primary predictor of HIV transmission is HIV viral load, relatively fewer HIV modelling studies include a detailed description of the dynamics of HIV viral load along stages of HIV disease progression. This could be due to the unavailability of data on viral load, particularly from low- and middle-income countries that have historically relied on monitoring CD4 cell counts for patients on ART because of higher costs of viral load testing [5]. However, sometimes, both CD4 cell counts and viral load covariates information is available.

Estill et al. [6] investigated the benefits of viral load routine monitoring for reducing HIV transmission. They developed a stochastic mathematical model representing 1000 simulations for both CD4 cell counts monitoring and viral load routine monitoring. Their findings revealed that viral load routine monitoring and managing in patients reduce both cohort viral load and transmissions by 31%. Rose et al. [7] investigated frameworks for the analysis of viral load. They came up with two frameworks: the single measure viral load and the repeated measure viral load. Their findings indicated that the repeated measure viral load has more precision than the single measure viral load because it utilises all available viral load data, has more statistical power, and also avoids subjectivity of defining a "window". Thus, in this study, we propose a repeated measure viral load monitoring and management using a Markov stochastic model.

Mathematical models have been extensively used in research into the epidemiology of HIV/AIDS, because they play an important role in improving our understanding of major factors contributing to the spread of this virus. It has also been argued that multi-state stochastic models are useful tools for studying complex dynamics such as chronic disease and also in determining factors associated with the progression between different stages of the disease [8, 9]. A Markov process is defined as a type of stochastic process in which a system changes in a random manner between different states. However, for most of these studies, states of the Markov processes are based on CD4 cell counts. For example, Titus analysed HIV dynamics using a discrete-time Markov chain mathematical model based on simulated CD4 states [10]. Dessie [9] used a CD4-based Markov model to determine the factors associated with the progression between different stages of the disease for individuals on antiretroviral therapy (ART).

In this study, a continuous-time-homogeneous Markov process is used to model the progression of HIV/AIDS patients. We define HIV/AIDS progression based on five viral load states, measured in copies/μL, followed by the end point, death. More importantly, among the determinants of HIV/AIDS, both the viral load counts and CD4 cell counts are included in the same model, thus making this research different from previous studies. The CD4 cell count covariate is included and the effect of collinearity with viral load is corrected for using the principal component approach. In addition to that, effects of non-adherence to treatment, viral load baseline (VLBL), age and gender on transition intensities is assessed. Transitions between the viral load states is considered to be bi-directional using data recorded from a cohort of 320 HIV+ patients from a wellness clinic in Bela Bela, South Africa.

Continuous-Time Markov Processes

Transitions between states are assumed to follow a stochastic Markov process, that is, transitions to the next state depend only on the current state occupied by a patient. The previous states occupied by an individual do not matter; that is, the memoryless property of the Markov models. These transitions are described using the transition probabilities ($p_{ij}(t)$), transition intensities (α_{ij}), from state i to state j. The functions $p_{ij}(t)$ are continuously differentiable and are subject to the initial condition:

$$p_{ij}(0) = \delta_{ij} = \begin{cases} 1, & \text{if } i = j \\ 0, & \text{if } i \neq j \end{cases}$$

where δ_{ij} is a kronecker delta, $p_{ij}(0) = 1, \ i = j$ means the patient's state definitely does not change when no time elapses and $p_{ij}(0) = 0, \ i \neq j$ means that, when no time elapses, we are sure that the patient's state cannot change with certainty. The transition intensity is defined as;

$$\alpha_{ij} = \left.\frac{\mathrm{d}(p_{ij}(t))}{\mathrm{d}t}\right|_{t=0} = \lim_{\Delta t \to 0} \frac{p_{ij}(\Delta t) - \alpha_{ij}}{\Delta t}, \ \ i, j \in C, j \neq i$$

and $\alpha_{ii}(t) = -\sum_{j \neq i} \alpha_{ij}(t)$ for each $i \in C$. In this study, transition probabilities depend only on the elapsed time and not on the chronological time. Thus, the Markov process is time-homogeneous, implying that $p_{ij}(t, t+s) = p_{ij}(s)$ and $\alpha_{ij}(t) = \alpha_{ij}$.

The effect of the above explanatory variables (covariates) on the transition intensities is modelled using the proportional intensities:

$$\alpha_{ij}(\boldsymbol{Z}) = \alpha_{ij}^{(0)} \exp(\beta_{ij}' \boldsymbol{Z}), \ i \neq j, \qquad (1)$$

where $\boldsymbol{Z}$ is a k-dimensional vector of explanatory variables, β_{ij} is a vector of k regression parameters relating to the instantaneous rate of transitions from state i to state j to the covariates $\boldsymbol{Z}$, and $\alpha_{ij}^{(0)}$ is the baseline transition intensities with covariates set to their means.

METHODS

Data Description

The model is applied to data from a heterosexual group of 320 HIV patients on HAART from a Wellness clinic in Bela Bela, South Africa, from 2005 to 2010. These patients were observed after 3 months of treatment uptake and every 6 months thereafter. This yielded 2259 observations. Of these patients, 224 were females and 96 were males, 172 were aged between 15 and 45 years and 72 were over 45 years. The mean age of the patients at enrolment was 40.62 years. A total of 267 had a VLBL above 10,000 copies/μL and 49 had a VLBL below 10,000 copies/μL. At enrolment, the mean viral load was 138 208 copies/μL with a maximum of 818,600 copies/μL. A total of 226 patients had a CD4 baseline below 200 cells/mm^3 and 96 had a CD4 baseline above 200 cells/mm^3. During the course of treatment, a number of factors were considered. These include non-adherence to treatment therapy, treatment change, treatment line and resistance to treatment, with 36 showing some signs of non-adherence to treatment which influenced the need for treatment change.

For each and every assessment time point, blood samples were obtained from each patient, and the plasma HIV RNA was measured using an Amplicor HIV-1 monitor assay kit which has a lower limit of sensitivity of 50 copies/μL. Thus, HIV RNA below 50 copies/μL is undetectable.

At $t = 0$, the regimens that were mostly administered to patients were the triple combination therapy, d4T-3TC-EFV (208 patients) and d4T-3TC-NVP (92 patients). d4T and 3TC represent Stavudine and Lamivudine, respectively, which fall into the nucleoside reverse transcriptase inhibitors (NRTI) class. EFV and NVP stand for Efavirenz and Nevirapine, respectively, and are from the non-nucleoside reverse transcriptase inhibitors (NNRTI) class.

In patients who showed some signs of non-adherence, d4T was substituted by AZT (Zidovudine). A switch from d4T-3TC-EFV to AZT-3TC-EFV was most common, rising from 10 patients in the first 6 months to 92 patients at 30 months. During the same period, the number of patients who switched from d4T-3TC-NVP to AZT-3TC-NVP rose from 6 to 45. After 1 year of treatment uptake, 1 patient was introduced to FTC-TDF-EFV and, after 3.5 years, the frequency increased to 10 patients. Another combination of FTC-TDF-NVP was also introduced to 3 patients after 2 years, and the number rose to 7 after 3 years. AZT-3TC-LPV/r was also administered, and at t = 0, 2 patients were administered with this triple combination. Other treatment combinations that were administered include FTC-TDF-NVP, AZT-ddI-LPV/r, d4T-3TC-LPV/r, ddI-d4T-3TC, and FTC-TDF-LPV/r. However, these were not administered frequently.

Compliance with Ethics Guidelines

The procedures used in this study were approved by the Research Ethics Committee of the University of Venda, South Africa (Protocol number SMNS/13/MBY/01/0625), in accordance with the 1964 Helsinki declaration and its subsequent amendments. Additionally, permission to access health facilities was obtained from the Limpopo Provincial Department of Health, South Africa, and the collaborating health facilities. Informed consent was obtained from the study participants prior to their involvement, and the data obtained were stripped of personal identifiers to ensure the confidentiality of the participants.

Principal Component Analysis

Principal component analysis is a technique used to combine highly correlated factors into principal components that are much less highly correlated with each other, which improves the efficiency of the model.

In this study, the predictive power of viral load values (I_1) and CD4 values (I_2) is explored. Two new, uncorrelated factors, I_1^* and I_2^*, can be constructed as follows:

$$\text{Let } \; I_1^* = I_1$$

Then, we carry out a linear regression analysis to determine the parameters γ_1 and γ_2 in the equation:

$$I_2 = \gamma_1 + \gamma_2 I_1^* + \varepsilon_1$$

γ_1 and γ_2 are the intercept and slope parameters of the regression model, respectively, and ε_1 is the 'error' term or residual, which by definition is independent of $I_1^* = I_1$.

We then set:

$$I_2^* = \varepsilon_1 = I_2 - (\gamma_1 + \gamma_2 I_1^*)$$

By construction, I_2^* is uncorrelated with the viral load values (I_1), since $I_2^* = \varepsilon_1$, the residual term in the equation. I_2^* in the model explains the component of mortality or HIV/AIDS progression that cannot be explained by the viral load values alone (or in the absence of CD4 cell counts).

The residuals (I_2^*) from the fitted model are included with the original HIV data as the new orthogonal variable, the orthogonal CD4 cell counts covariate (residuals). These residuals are coded as "1" for negative residuals and "0" for positive residuals. A continuous-time Markov model for the effects of age, gender, VLBL, non-adherence (NA), and orthogonal CD4 cell counts (I_2^*) on HIV progression based on the viral load is fitted using the "msm" package for multistate modelling in R. The variables in the model are coded as follows:

$$\text{Age } = \begin{cases} 1, \leq 45 \text{ years} \\ 0, > 45 \text{ years} \end{cases},$$

$$\text{orthogonal CD4 covariate } (I_2^*) = \begin{cases} 1, & \text{if CD4 residual is negative} \\ 0, & \text{if CD4 residual is positive,} \end{cases}$$

$$\text{Non-adherence (NA)} = \begin{cases} 1, \text{ Yes} \\ 0, \text{ No} \end{cases},$$

$$\text{Gender } = \begin{cases} 1, & \text{male} \\ 0, & \text{female,} \end{cases}$$

$$\text{Viral load baseline (VLBL)} = \begin{cases} 1, & > 10,000 \text{ copies}/\mu\text{L} \\ 0, & \leq 10,000 \text{ copies}/\mu\text{L,} \end{cases}$$

$$\text{Viral load levels } (V) = \begin{cases} \textbf{1;} & VL < 50 \\ \textbf{2;} & 50 \leq VL < 10,000 \\ \textbf{3;} & 10,000 \leq VL < 100,000 \\ \textbf{4;} & 100,000 \leq VL < 500,000 \\ \textbf{5;} & VL \geq 500,000 \\ \textbf{6;} & \text{Dead} \end{cases}$$

A negative CD4 cell count residual implies that the observed CD4 cell count is lower than the expected CD4 cell count, given the viral load levels of the patient, and a positive residual means having a higher CD4 cell count than expected.

Model Formulation

Consider a stochastic process $\{V(t), t \in [0, 5)\text{years}\}$ defined on a finite state space $V =$

$\{1,2,3,4,5,6\}$ based on viral load states as defined above. $V(t)$ represents the viral load state of an HIV/AIDS patient at time t. This process represents a Markov process if $\forall s,t \geq 0$ and for every $i,j \in V$

$$P(V(t+s)=j|V(t)=i,V(u)=v(u),0\leq u<s) = P(V(t+s)=j|V(t)=i)$$

The above equation implies that a Markov process is memoryless, that is, the future transitions depend on the entire history only through the present state.

HIV/AIDS progression is based on viral load states, and possible transitions between these states are shown in Fig. 1. The transition between states is assumed to be bi-directional, that is, movement from state i to state $i \pm 2$ is always via state $i \pm 1$, where $i = 1,2,3,4,5$ define the live states based on viral load. The model allows for reverse transition due to the efficacy of treatment and forward due to non-adherence to treatment. Transitions between states are shown by the arrows.

Based on Fig. 1, the transition rates are defined as follows:

$$Q = \begin{pmatrix} -(\alpha_{12}+\alpha_{16}) & \alpha_{12} & 0 & 0 & 0 & \alpha_{16} \\ \alpha_{21} & -(\alpha_{21}+\alpha_{23}+\alpha_{26}) & \alpha_{23} & 0 & 0 & \alpha_{26} \\ 0 & \alpha_{32} & -(\alpha_{32}+\alpha_{34}+\alpha_{36}) & 0 & 0 & \alpha_{36} \\ 0 & 0 & \alpha_{43} & -(\alpha_{43}+\alpha_{45}+\alpha_{46}) & \alpha_{46} & \alpha_{46} \\ 0 & 0 & 0 & \alpha_{54} & -(\alpha_{54}+\alpha_{56}) & \alpha_{56} \\ 0 & 0 & 0 & 0 & 0 & 0 \end{pmatrix}$$

Q is a 6×6 matrix and its elements α_{ij} are the instantaneous rates of transition from one state to another subject to the conditions that $\alpha_{ij} = 0, i \neq j$ and $\sum_{j=1}^{6} \alpha_{ij} = 0$ so that $\alpha_{ii} = -\sum_{i\neq j} \alpha_{ij}, \quad i \in V\backslash 6$. α_{ij} is independent of time because the process is assumed to be homogeneous with respect to time. In the next section, the parameters of our models are estimated including the transition rates.

The effect of the above explanatory variables (covariates) on the transition intensities is modelled using the proportional intensities:

$$\alpha_{ij}(\mathbf{Z}) = \alpha_{ij}^{(0)} \exp\left(\beta_{ij}'\mathbf{Z}\right), \quad i \neq j, \tag{2}$$

where $\boldsymbol{Z}$ is a $k = 5$-dimensional vector of explanatory variables VLBL, Gender, Age, Non-adherence, CD4orthogonal (I_2^*). Thus, the transition intensity for a patient h in this study is given by the model:

$$\alpha_{ij} = \alpha_{ij}^{(0)} \exp(\beta_{ij}^{(\text{Age})}\text{Age}_h + \beta_{ij}^{(\text{Gender})}\text{Gender}_h + \beta_{ij}^{(\text{CD4BL})}\text{VLBL}_h + \beta_{ij}^{(\text{NA})}\text{NA}_h + \beta_{ij}^{(I_2^*))}I_{2h}^*)$$

For this model, $\alpha_{ij}^{(0)}$ are the baseline transition intensities that refer to a patient with age category 0 (over 45 years old), gender = 0 (female), VLBL = 0 (below 10,000 copies/μL, adherence to treatment and positive I_2^*, β_{ij} is a vector of k regression parameters relating the instantaneous rate of transitions from state i to state j to the covariates $\boldsymbol{Z}$. The transition intensities, α_{ij}, are presented in rates per year. α_{ij} are the elements of a 6×6 transition intensity matrix Q from a continuous time-homogeneous Markov process.

An important aspect is the inclusion of both VLBL_h and I_2^* (the orthogonal CD4 covariate) derived after allowing for collinearity.

Assessment of the Fitted Models

Based on Eq. (1), two nested models are fitted: one of the models excludes the effect of the

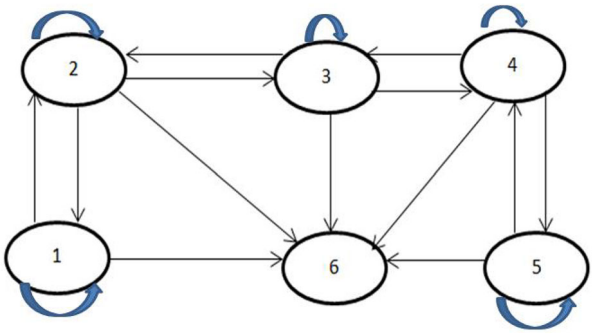

Fig. 1 State diagram for the possible transitions between the first five viral load defined states and the absorbing state 6 (death)

orthogonal CD4 cell counts covariate (nested model) and the other includes all covariates including the orthogonal CD4 cell counts covariate. These models are compared using their Akaike information criteria (AICs) defined as follows:

$$\text{AIC} = -2 \times \text{Log(likelihood)} + 2k,$$

where $-2 \times \text{Log(likelihood)}$ represents the bias, $2k$ represents the variance and k is the number of estimated parameters in the fitted model. The model with the minimum AIC is considered as the better model. Further assessment of the fitted nested models is carried out using the likelihood ratio test (LRT). The value of the $\text{LRT} = -2\log_e\left(\frac{L_s(\hat{\theta})}{L_f(\hat{\theta})}\right)$, where $L_s(\hat{\theta})$ is the simple model (no CD4 cell count orthogonal) and $L_f(\hat{\theta})$ is the full model (with CD4 cell count orthogonal).

Convergence of a Time-Homogeneous Markov Model

If a Markov model fails to converge, optimisation criteria result in a failure to calculate standard errors leading to the exclusion in the calculation of confidence intervals for the estimated parameters. After running the analysis using the 'msm' package in R, the statistical package warns if 'optimisation has probably not converged to the maximum likelihood—Hessian matrix not positive definite.' To ensure that the model converges, a scaling factor is used to normalise the likelihood and to prevent the overflow within the optimisation process.

RESULTS

In this section, the combined effect of viral load and CD4 cell counts in the progression of HIV in patients on treatment is analysed. This is carried out by first fitting a time-homogeneous Markov model for the effects of the covariates, VLBL and NA, on HIV/AIDS progression based on viral load states. Secondly, a time-homogeneous Markov model for the effects of covariates, VLBL, NA, age and the orthogonal CD4 cell counts covariate is fitted. Comparison of these models is based on their $-2 \times$ Log-likelihood, AIC, likelihood ratio tests and also the percentage prevalence plots. The results are shown in the following subsections.

Time-Homogeneous Markov Model with the Effects of Orthogonal CD4 Cell Counts Covariate Excluded

A time-homogeneous Markov model is fitted for HIV/AIDS progression defined by viral load states. In this model, the effects of the covariates VLBL and NA, to the progression of HIV are considered. The relationship between these covariates and the transition intensities is defined by the following equation:

$$\alpha_{ij}(\boldsymbol{Z}) = \alpha_{ij}^{(0)} \exp\left(\beta_{ij}'\boldsymbol{Z}\right), i \neq j,$$

where $\boldsymbol{Z}$=[VLBL,Gender,Age,Non-adherence] is a k=4-dimensional vector of covariates and β_{ij} is a vector of k regression parameters relating the instantaneous rate of transitions from state i to state j to the covariates $\boldsymbol{Z}$ and baseline intensities $\alpha_{ij}^{(0)}$ relating to the baseline transition from state i to state j.

When fitting the time-homogeneous Markov model, the gender and age of HIV patients have no significant effects to HIV progression, hence their exclusion from the results (Table 1), in which the first column represents possible transitions from state i to state j, where

Table 1 Estimated parameters (with 95% confidence intervals) for the time homogeneous model that excludes the effects of CD4 cell counts

	Baseline intensities ($\alpha_{ij}^{(0)}$)	Viral load baseline	Non-adherence
State 2–1	3.395 (2.928, 3.935)	− 0.209 (− 0.631, 0.213)	− 1.002 (− 1.422,− 0.583)
State 1–2	0.495 (0.401, 0.609)	0.020 (− 0.609, 0.649)	0.418 (− 0.167, 1.003)
State 3–2	238.6 (0.079, 71,270)	2.759 (− 4.952, 10.470)	− 2.092 (− 6.001, 1.817)
State 2–3	31.57 (0.0097, 10,230)	3.884 (− 3.652, 11.42)	− 0.853 (− 4.788, 3.082)
State 4–3	21.34 (3.485, 130.7)	− 1.597 (− 12.506, 9.311)	0.337 (− 2.255, 2.930)
State 3–4	2.691 (0.335, 21.61)	− 1.930 (− 13.240, 9.379)	0.966 (− 2.010, 3.942)
State 5–4	15.06 (2.413, 93.99)	− 0.457 (− 4.413, 3.500)	2.038 (− 11.574, 15.651)
State 4–5	2.495 (0.110, 56.49)	2.393 (− 12.574, 17.360)	2.263 (− 11.646, 16.173)
State 1–6	0.001 (0.00008, 5.306)	5.109 (− 7.984, 18.204)	5.469 (− 4.508, 15.447)
State 2–6	0.249 (0.049, 1.263)	0.961 (− 0.223, 2.145)	− 4.618 (− 17.757, 8.522)
State 3–6	0.007 (0.000002, 189,000,000)	0.603 (− 40.234, 41.441)	− 0.667 (− 40.809, 39.475)
State 4–6	0.002 (0.000005, 84,440)	− 0.295 (− 75.482, 74.893)	− 0.055 (− 55.779, 55.669)
State 5–6	0.006 (0.000001, 2,880,000)	− 0.344 (− 91.100, 90.411)	− 0.143 (− 61.439, 61.152)

−2Log-Likelihood: 2508.101

$i = 1,\ldots,5$ and $j = 1,\ldots,6$. The second column represents the baseline transition intensities (with confidence intervals), the third column gives coefficients (with confidence intervals) to represents the effects of non-adherence to HIV progression, and the fourth column gives coefficients (with confidence intervals) to represent the effects of having a VLBL above 10,000 copies/μL to HIV progression. The results are given in Table 1.

The results from Table 1 show that, when a patient's viral load is above 10,000 copies/μL (states 3, 4 and 5), rates of viral load suppression are higher than rates of viral load rebound. However, from state 2 (viral load between 50 and 10,000 copies/μL), the rates of viral rebound are higher than the rates of viral suppression. The rates of viral rebound are increased for patients who had problems in adhering to treatment therapy regardless of the original state.

Patients who started therapy with VLBL above 10,000 copies/μL experienced higher rates of viral rebound than patients who started therapy with VLBL below 10,000 copies/μL. Having a viral load above 10,000 copies/μL also accelerates the rates of transition to death from the undetectable viral load (state 1). The same group also experienced high risks of transition from state 2 and state 3, although the risk is lower than when the patients are in state 1.

The results from Table 1 also show a significant reduction in the rate of attaining an undetectable viral load for patients who were non-adherent to treatment (state 2-1). This is indicated by the exclusion of zero in the confidence interval of the estimated parameter. Although not significant, transitions to death for patients who were non-adherent are higher compared to that of adherent patients.

The results show wide confidence intervals for transitions to death from each of the live states. This indicates a relatively poor prediction of mortality by the fitted model. To obtain a better picture of how the fitted model predicts mortality, percentage prevalence in each state are plotted to compare the observed data from

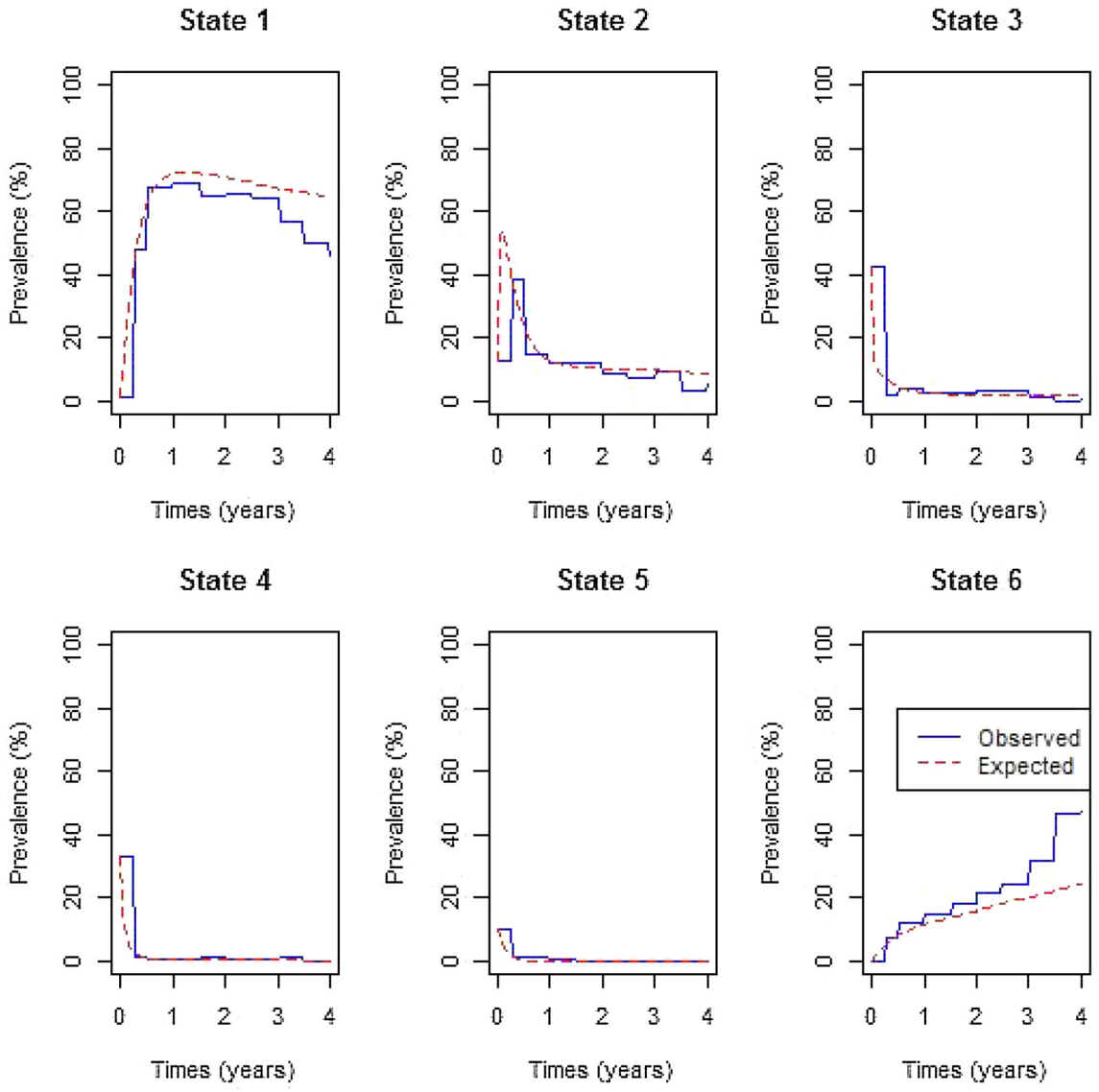

Fig. 2 Percentage prevalence viral load defined state and the effects of non-adherence and age excluding CD4 orthogonal variable

the expected data. The percentage prevalence plots are shown in Fig. 2.

Figure 2 shows that the expected percentage prevalence give a good fit of the observed percentage prevalence only for the live states, that is states 2, 3, 4 and 5. However, the expected percentage prevalence underestimates the observed prevalence for the death state and overestimates the observed prevalence for state 1. The other anomaly is that of experiencing more than 40% deaths towards the end of the study. This is a cause for concern since these patients were receiving antiretroviral therapy. This is a further confirmation that the model does not give a good prediction of mortality. A decision to include the orthogonal CD4 cell counts covariate in our model was made and is discussed in the next subsection.

Table 2 Estimated parameters for the regression model for CD4 cell counts on the viral load

	Estimate	SE	*t* value	*Pr*(> |*t*|)	
γ_1 (intercept)	419.8	7.000	59.98	< 2e−16	***
γ_2(slope)	− 0.0008477	0.00007415	− 11.43	< 2e−16	***

Multiple *R*-squared: 0.06015; VIF = 1.06015
F-statistic: 130.7 on 1 and 2042 DF, *p* value: < 2.2e−16
***Significant at $p < 0.001$

Time-Homogeneous Markov Model with the Effects of Orthogonal CD4 Cell Counts Covariate Included

The orthogonal components for this model are obtained by regressing CD4 cell count on viral load as discussed earlier. The residuals from this model are then used to represent the orthogonal covariate, CD4 cell counts, and is now incorporated in the continuous-time Markov model.

The results from Table 2 show a significant model confirming correlation between CD4 cell counts and the viral load. After regressing CD4 cell counts on viral load, the residuals from the model are taken to represent the orthogonal CD4 cell counts covariate. These residuals are included with the original covariates and then coded as "1" for negative residuals and "0" for positive residuals. A negative CD4 residual implies having lower CD4 cell count than the expected given the viral load levels. A positive residual means having a higher CD4 cell count than the expected. The orthogonal covariate is then used together with the other covariates to determine the progression of HIV/AIDS based on the viral load states.

The relationship between these covariates and the transition intensities is defined by the following equation:

$$\alpha_{ij}(\boldsymbol{Z}) = \alpha_{ij}^{(0)} \exp(\beta_{ij}'\boldsymbol{Z}),\ i \neq j,$$

where $\boldsymbol{Z} = [\text{VLBL}, \text{Gender}, \text{Age}, \text{Non-adherence}, \text{orthogonal CD4cell counts covariate}]$ is a $k = 5$-dimensional vector of the covariates and β_{ij} is a vector of k regression parameters relating the instantaneous rate of transitions from state i to state j to the covariates $\boldsymbol{Z}$ and baseline intensities $\alpha_{ij}^{(0)}$ relating to the baseline transition from state i to state j. The inclusion of the orthogonal CD4 cell counts covariate has resulted in the significant effects of age on the progression of HIV, hence its inclusion in Table 3. However, the covariate gender is still not significant. The inclusion of the gender covariate together with the use of a scaling factor of 4000 resulted in a failure of convergence to a maximum likelihood and a non-positive Hessian matrix. The adjustment of the scaling factor to 5000 resulted in normalising the likelihood, leading to the convergence of the Markov model. Thus, the gender covariate is included after adjusting the scaling factor. The results are shown in Table 3.

The results from Table 3 show that, when the patient's viral load is above 10,000 copies/μL, represented by states 3, 4 and 5, the rates of viral suppression are higher than the rates of viral rebound. However, once the viral load is below 10,000 copies/μL (states 2 and 1), patients experience higher rates of viral rebound than rates of viral suppression. This is a cause for concern, since state 1 represents the undetectable viral load level.

Table 3 shows that the risk of viral rebound from states 1 and 2 is higher in patients who initiated therapy with a VLBL above 10,000 copies/μL than in patients who initiated therapy with lower viral loads. Other factors that accelerate viral rebound from state 1 are negative CD4 residuals and non-adherence to treatment. From state 2, males experience higher risks of viral rebound than their female counterparts. However, when viral load is above 10,000 copies/μL, males have increased rates of transitions to good states and reduced rates of transition to bad states than females.

Table 3 Parameter effects (with 95% confidence intervals) of age, viral load baseline (*VLBL*), non-adherence (*NA*) and CD4 orthogonal (I_2^*) on the transition intensities for the viral load-based Markov model

	Baseline	I_2^*	Age	VLBL	NA	Gender
State 2–1	3.891 (3.247, 4.663)	0.043 (− 0.299, 0.385)	− 0.568 (− 1.003, − 0.133)	− 0.137 (− 0.607, 0.333)	− 1.179 (− 1.673, − 0.685)	− 0.028 (− 0.409, 0.354)
State 1–2	0.457 (0.3.519, 0.593)	0.428 (− 0.105, 0.961)	− 0.206 (− 0.820, 0.409)	0.138 (− 0.606, 0.883)	0.298 (− 0.395, 0.992)	− 0.298 (− 0.877, 0.280)
State 3–2	3379 (0.001, 1,51,200)	− 0.285 (− 4.434, 3.864)	− 1.846 (− 27.95, 24.25)	4.256 (− 11.99, 20.51)	− 3.094 (− 14.99, 8.810)	1.883 (− 25.90, 29.67)
State 2–3	381.9 (0.000, 1,733,000)	− 0.854 (− 5.016, 3.309)	− 1.676 (− 27.79, 24.44)	6.275 (− 10.04, 22.59)	− 1.886 (− 13.81, 10.03)	1.733 (− 26.05, 29.52)
State 4–3	0.016 (0.004, 644,800)	− 0.155 (− 1.855, 1.545)	− 0.170 (− 3.818, 3.477)	− 3.511 (− 44.78, 37.76)	− 0.876 (− 2.657, 0.906)	5.045 (− 22.16, 32.25)
State 3–4	0.087 (0.0001, 62,160)	− 0.112 (− 2.389, 2.166)	3.983 (− 11.35, 19.32)	2.999 (− 76.00, 82.00)	0.044 (− 2.449, 2.538)	− 6.220 (− 31.91, 19.47)
State 5–4	33.10 (1.695, 646.6)	2.066 (− 2.129, 6.262)	− 0.747 (− 4.636, 3.143)	2.262 (− 4.604, 9.127)	4.474 (− 14.44, 23.39)	− 2.862 (− 6.309, 0.586)
State 4–5	0.3907 (0.000, 6,446,000)	1.325 (− 3.718, 6.378)	1.194 (− 6.990, 9.379)	1.139 (− 104.8, 107.1)	9.631 (− 14.46, 33.72)	4.901 (− 22.64, 32.44)
State 1–6	0.00001 (0.000, 2250)	3.629 (− 17.79, 25.05)	4.391 (− 20.41, 29.19)	5.611 (− 24.66, 35.88)	7.438 (− 10.67, 25.55)	− 5.012 (− 27.97, 17.94)
State 2–6	0.001 (0.000, 13,570)	1.016 (− 12.27, 14.30)	− 7.171 (− 29.60, 15.26)	3.841 (− 25.32, 33.01)	− 5.261 (− 33.28, 22.76)	− 6.132 (− 31.85, 19.58)
State 3–6	0.002 (0.000, 78,330)	− 5.258 (− 27.28, 16.77)	0.547 (− 35.6, 36.71)	2.756 (− 23.54, 29.05)	− 5.969 (− 33.08, 21.14)	− 4.659 (− 30.09, 20.77)
State 4–6	0.002 (0.000, 1,972,000)	− 0.014 (− 54.22, 54.19)	− 0.830 (− 58.09, 56.43)	− 0.568 (− 492.9, 491.8)	− 1.309 (− 77.77, 75.15)	0.819 (− 312.8, 314.5)
State 5–6	0.008 (0.000, 583,500)	− 3.167 (− 21.93, 15.59)	0.064 (− 27.55, 27.68)	− 0.332 (− 162.3, 161.6)	− 4.967 (− 33.53, 23.59)	3.244 (− 18.83, 25.32)

− 2 Log-likelihood: 1556.298

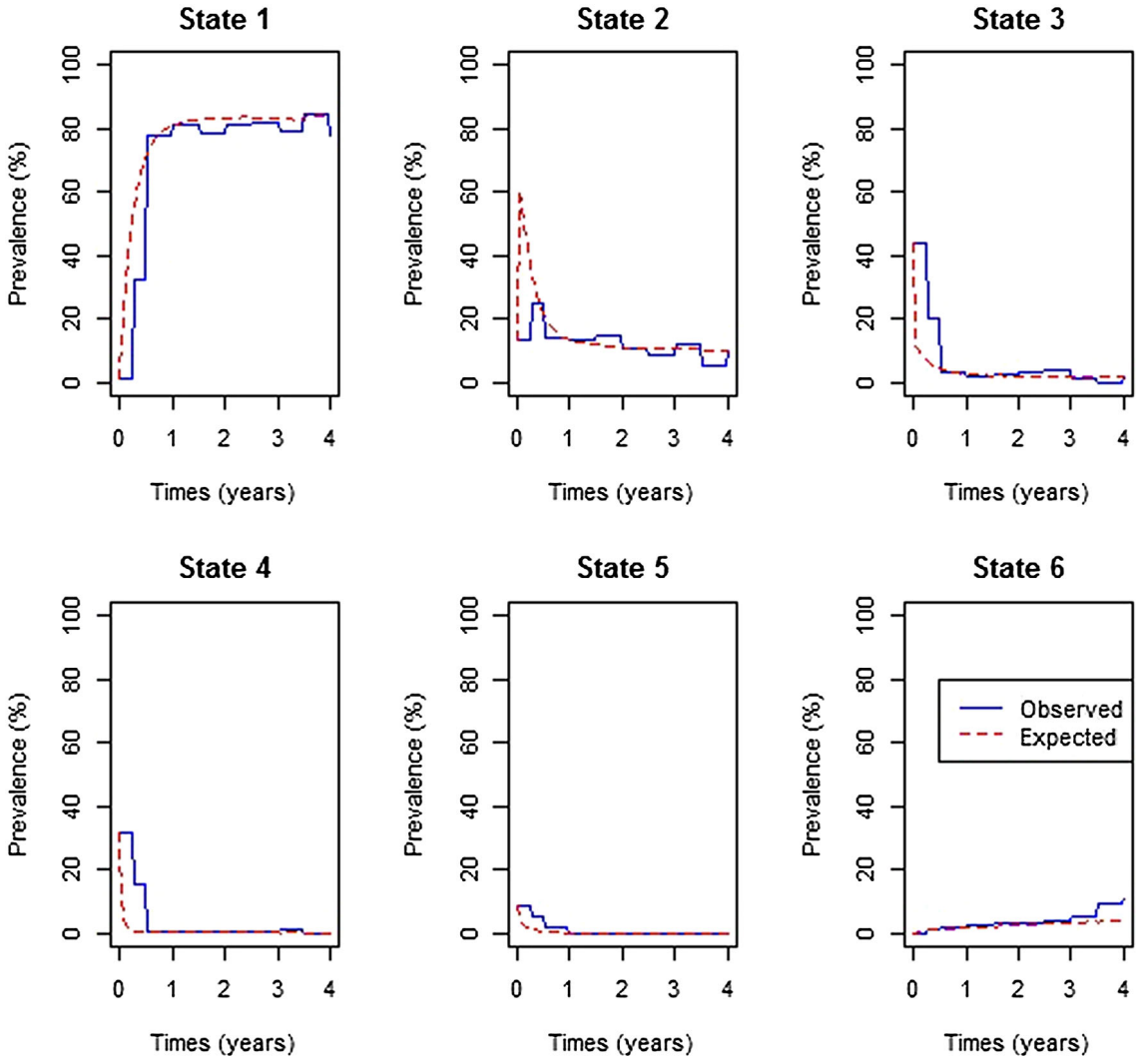

Fig. 3 Percentage prevalence plots for continuous-time-homogeneous Markov model in which the CD4 cell counts orthogonal component is included as a covariate

The results also show increased rates of transitions to death (state 6) from state 1. This is mainly caused by non-adherence to treatment followed by having a viral load above 10,000 copies/μL, age and then orthogonal CD4 cell counts covariate. Thus, younger patients, below the age of 45 years, and patients with CD4 cell counts lower than expected have accelerated risks of death from state 1.

The estimated parameters in Table 3 have narrow confidence intervals for transitions that took place between live states: transitions from i to j, where j is not an absorbing state. Transitions to death have wider confidence intervals. For transitions between live states, the estimated parameters for the variable CD4 cell counts orthogonal have narrow confidence intervals, indicating that the inclusion of the orthogonal CD4 cell counts covariate gives rise to more precise estimates than the first model. The model with the orthogonal CD4 cell counts covariate has a lower $-2 \times$ Log-likelihood than the model without the covariate.

Figure 3 shows the percentage prevalence plots for each of the states given that CD4 residual is included in the model. Figure 3 helps

Table 4 Likelihood ratio test for the fitted models

Likelihood ratio test for the models	Preferred model	− 2 log LR	*df*	*p*
Without CD4 orthogonal covariate versus with CD4 orthogonal covariate	With CD4 orthogonal covariate	934.425	26	10^{-4}
With CD4 orthogonal covariate versus with CD4 orthogonal covariate including gender	With CD4 orthogonal covariate including gender	951.803	39	10^{-4}

AIC for the Markov model without CD4 orthogonal covariate = 2586.101. AIC for the Markov model with CD4 orthogonal covariate = 1703.676. AIC for the Markov model with CD4 orthogonal covariate and gender variable = 1712.298

in assessing whether the expected percentage prevalence gives a better fit of the observed prevalence in the death state (state 6) compared to the results in Fig. 2.

The results from Fig. 3 show that, if HIV progression is defined by viral load states with the inclusion of the orthogonal CD4 cell counts covariate, this results in a better fit of the observed prevalence. As a result, for the death state, the expected percentage prevalence state explains the observed percentage prevalence better than the model without the orthogonal CD4 cell counts covariate .

Assessment of the fitted models

The fitted models were assessed to identify the model that best describes the data. Assessment of the fitted models is carried using the likelihood ratio test and estimates of AICs. The model with the lowest AIC is considered as the best model for the observed data. Table 4 shows the results.

The likelihood ratio tests from Table 4 show that the continuous-time-homogeneous Markov model defined by viral load states with the orthogonal CD4 cell counts covariate, and including the gender variable, gives the best fit to the data. However, since the interest is in the lowest AIC for our model, the model with the orthogonal CD4 cell counts covariate, while excluding the gender variable, is the best model. Thus, a gender difference was not a good predictor of HIV progression based on viral load states together with the orthogonal CD4 cell counts covariate.

DISCUSSION

In this study, a time-homogeneous Markov model has been developed to explain and predict the probability of death for HIV/AIDS patients. The states of the Markov model are based on viral load levels. A model for HIV/AIDS progression for the effects of VLBL, NA, gender and age is fitted first. From this model, the covariates age and gender were excluded, since they failed to predict HIV/AIDS progression based on viral load levels since their coefficients were insignificant. Next, we used a time-homogeneous model for the effects of the same covariates with the orthogonal CD4 covariate included. This resulted in the variable age contributing significantly to the HIV/AIDS progression. The variable gender had significant effects after adjusting the scaling factor from 4000 to 5000 to ensure convergence of the optimisation process. Randarajan et al. [11], in their study, also revealed the non-significant effects of the variable gender in viral suppression. However, this may not be comparable to our studies because they used a logistic regression model, while our findings are based on a continuous-time-homogeneous Markov model. Construction of the orthogonal CD4 cell counts covariate used the principal component approach to address the issue of collinearity of the viral load and the CD4 cell counts covariates. Most researchers deal with either of the two variables when developing models

The results from the analysis showed that, if HIV progression is defined by viral load states and the variable CD4 cell count is excluded

from the model, the expected percentage prevalence underestimates mortality from a period of 0.5 years of treatment uptake. This resulted in a death prevalence of over 40% which is unrealistic considering patients were on ART.

The orthogonal CD4 cell counts covariate was included in the continuous-time Markov model defined by viral load levels so that HIV mortality is explained and predicted in a better way. The results from the fitted model showed an improvement in the −2 Log-likelihood compared to the model without the orthogonal CD4 cell counts covariate. The model also had the lowest AIC. The death prevalence from this model was lower than 20%.

The results also show high risks of viral rebound from undetectable viral load levels which was mainly caused by non-adherence to treatment, having negative CD4 residuals and starting therapy when the VLBL was above 10,000 copies/μL. Having CD4 cell counts that are lower than expected increases the rates of viral rebound from undetectable levels. These findings are also corroborated by the studies of Silveira et al. [12] which showed that a higher prevalence of undetectable viral load levels have been associated with lower levels of VLBL at the beginning of treatment. This supports the issues raised by Chesney [13] that, without proper adherence, antiretroviral agents are not maintained at a sufficient concentration to suppress HIV replication. Pasternak et al. [14], in their study, also demonstrated that incomplete ART adherence is associated with increased levels of cell-associated HIV-1 RNA.

Our findings also showed high risks of mortality from the undetectable viral load for non-adherent patients, patients who initiated therapy with a viral load level above 10,000 copies/μL, younger patients below the age of 45 years and patients whose CD4 cell counts were lower than expected. This could be due to the findings by Mujugira et al. [15], whose study revealed delayed ART initiation, failure to achieve viral suppression, and virologic rebound among young patients.

Continuous-time-homogeneous Markov models have the ability to handle multiple outcomes compared to the Kaplan–Meier and Cox proportional hazards models. However, its memoryless property places limitations on the disease history behaviour, especially when dealing with HIV patients on ART whose adherence to treatment is likely to improve with time.

The other limitation is that the study was limited to one centre.

CONCLUSIONS

In conclusion, the findings reveal the importance of Principal components approach in treating collinearity of the viral load and CD4 cell counts covariates when both are in the one model. As a result, we have discovered that having lower CD4 cell counts than expected results in accelerated risks of viral rebound from undetectable viral load levels,and also accelerated deaths from undetectable viral load levels. Thus, higher CD4 cell counts improve the health and consequently the survival of HIV/AIDS patients. The inclusion of both viral load and CD4 cell count in the one model give a better prediction of mortality.

ACKNOWLEDGEMENTS

We thank the participants of the study.

Funding. No funding or sponsorship was received for this study or publication of this article.

Authorship. All named authors meet the International Committee of Medical Journal Editors (ICMJE) criteria for authorship for this article, take responsibility for the integrity of the work as a whole, and have given their approval for this version to be published.

Authorship Contributions. Claris Shoko devised the initial idea and drafted the first manuscript. Delson Chikobvu finalised and proofread the article. Claris Shoko and Delson Chikobvu contributed to the analysis and interpretation of the data. Pascal O. Bessong collected the data used in the current study and

aided with both revisions to and proofreading of the final manuscript. All authors participated in critical revision of the manuscript drafts and approved the final version.

Disclosures. Claris Shoko, Delson Chikobvu and Pascal O. Bessong have nothing to disclose.

Compliance with Ethics Guidelines. The procedures used in this study were as approved by the Research Ethics Committee of the University of Venda, South Africa (Protocol number SMNS/13/MBY/01/0625), in accordance with the 1964 Helsinki declaration and its subsequent amendments. Additionally, permission to access health facilities was obtained from the Limpopo Provincial Department of Health, South Africa, and the collaborating health facilities. Informed consent was obtained from study participants prior to their involvement; and data obtained was stripped of personal identifiers to ensure the confidentiality of the participants.

Data Availability. The datasets during and/or analyzed during the current study are available from the corresponding author on reasonable request.

REFERENCES

1. Palella FJ Jr, Delaney KM, Moorman AC, Loveless MO, Fuhrer J, Satten GA, Aschman DJ, Holmberg SD. Declining morbidity and mortality among patients with advanced human immunodeficiency virus infection. N Engl J Med. 1998;338:853–60.

2. Cole SR, Hernan MA, Anastos K, Jamieson BD, Robins JM. Determining the effects of hghly actictive antiretroviral therapy on change in human immunodeficiency virus type 1 RNA viral koad using a marginal structural left-censored mean model. Am J Epidemiol. 2007;166(2):219–27.

3. Mathieu E, Foucher Y, Dellamanica P, Doures JP. Parametric and non homogeneous semi-Markov process for HIV control. Methodol Comput Appl Probab. 2007;9:389–97. https://doi.org/10.1007/s11009-007-9033-7.

4. Hoffman RM, Black V, Technau K, et al. Effects of highly active antiretroviral therapy duration and regimen on risk for mother-to-child transmission of HIV in Johannesburg, South Africa. J Acquir Immune Defic Syndr. 2010;54(1):35–41.

5. Lecher S, Williams J, Fonjungo PN (2016) Progress with scale-up of HIV viral load monitoring—seven Sub-Saharan African Countries, January 2015–June 2016. Morbid Mortal Week Rep 65(47).

6. Estill J, Aubrière C, Egger M, Johnson L, Wood R, et al. Viral load monitoring of antiretroviral therapy, cohort viral load and HIV transmission in Southern Africa: a mathematical modelling analysis. AIDS. 2012;26:1403–13.

7. Rose CE, Gardener L, Girde JCS, et al. A comparison of methods for analysing viral load data in studies of HIV patients. PLoS ONE. 2015;10(6):e0130090.

8. Naresh R, Tripathi A, Omar S. Modelling the spread of AIDS epidemic with vertical transmission. Appl Math Comput. 2006;178:262–72.

9. Dessie ZG. Modeling HIV dynamics evolution using non-homogeneous semi-Markov pr0cess. Springer Plus. 2014;3:537.

10. Titus RK. Mathematical modeling of the spread of HIV/AIDS by Markov chain process. Am J Appl Math. 2016;4:235–46.

11. Randarajan S, Colby DJ, Truong G, et al. Factors associated ith HIV viral loads suppression on antiretroviral therapy in Vietman. J Virus Erad. 2016;2:94–101.

12. Silveira MPT, de Lourdes Draschler M, de Carvalho Leite J C, Pinheiro CAT, da Silveira VL. Predictors of undetectable plasma viral load in HIV-positive adults receiving antiretroviral therapy in Southern Brazil. Braz J Infect Dis. 2002;6(4):164–71.

13. Chesney M. Factors affecting adherence to antiretroviral therapy. Clin Infect Dis. 2000;30(Suppl 2):S171–6.

14. Pasternak AO, de Bruin M, Jurriaans S, Bakker M, Berkhout B, Prins JM, Lukashov VV. Modest non-adherence to antiretroviral therapy promotes

residual HIV-1 replication in the absence of virological rebound in plasma. J Infect Dis. 2012;206:1443–52.

15. Mujugira A, Celum C, Tappero JW, Ronald A, Mugo N, Baeten JM. Younger age predicts failure to achieve viral suppression and virologic rebound among HIV-1-infected persons in serodiscordant partnerships. Aids Res Human Retrovir. 2016;32(2):5. https://doi.org/10.1089/aid.2015.0296.

Biomedical Research 2019; 30 (5): 786-795 *ISSN 0970-938X*
www.biomedres.info

A comparison of the time homogeneous and time non-homogeneous markov models for monitoring HIV/AIDS disease progression: Results from patients on ART.

Claris Shoko[1]*, Delson Chikobvu[1], Pascal O. Bessong[2]

[1]Department of Mathematical Statistics and Actuarial Sciences, University of the Free State, Bloemfontein, South Africa
[2]HIV/AIDS & Global Health Research Programme, University of Venda, Thohoyandou 0950, South Africa

Abstract

Background: Markov models are widely used in studying progression of chronic diseases using the time homogeneity approach. Relatively few studies use the time non-homogeneous approach to model the progression of HIV/AIDS based particularly in the use of viral load monitoring mainly due to fact that that viral load is expensive to measure frequently hence not readily available in the format required. Non-homogeneous models reveal the interval in which viral rebound occurs.

Methods: This study compares the time-homogeneous Markov approach to the time non-homogeneous approach in predicting HIV/AIDS progression. A piece-wise constant approach to non-homogeneous modelling is used.

Results: This study reveals that a piece-wise constant Markov approach to non-homogeneous modelling which allows variation in transition rates within intervals [0,0.5) years and [0.5,∞) years is better for predicting HIV/AIDS progression compared to the time-homogeneous approach. Failure to combination antiretroviral therapy (cART) increases significantly the rate of viral rebound and deaths 6 months post treatment initiation.

Conclusion: Hence, there is need to closely monitor the uptake of antiretroviral drugs in the first six months of treatment to increase the chances of survival for HIV/AIDS patients.

Keywords: Non-homogeneous Markov model, Time-homogeneous Markov model, HIV/AIDS progression, Viral load.

Accepted April 03, 2019

Introduction

Combination antiretroviral therapy (cART) reduces HIV viral load by blocking replication of the virus [1-3]. Hence, constant monitoring of viral load counts is beneficial over routine monitoring of $CD4^+$ cell count since immunodeficiency can be prevented by early detection of virologic failure thereby enabling proper management of HIV/AIDS patients by interested stakeholders [4].

The suppression of HIV viral load from very high levels, greater than 500 000 copies/mL, to suppressed levels due to the effects of cART can be considered as a multi-state process based on the viral load including the endpoint, death state. Patients are then monitored only at visit times resulting in the exact time the transition occurred to be unknown [5]. Homogeneous and non-homogeneous Markov processes are an important field of research when dealing with interval censored data in which the exact time of transition is not known. A Markov process is a stochastic process in which the probability of transition to a future state given the current state is independent of the past history. Thus, a Markov model possesses the memoryless property involving random movements between states that occur at regular or irregular intervals [6].

The constant hazard assumption of the time-homogeneous models is unrealistic when modelling evolution in chronic diseases [7] because they put severe limitations on the previous behaviour of the disease [8]. However, most applications to HIV/AIDS disease assumed a homogeneous process where transition probabilities only depend on the elapsed time between observations [6,9-11].

Application of non-homogeneous Markov models to study the evolution of HIV allows computations of estimates of the time in which HIV patients spend in each state but also the randomness of different states in which the states can evolve known as a stochastic process [12]. Saint-Pierre et al. used a piece-wise approach to non-homogeneous Markov modelling on asthma patients. They argued that piece-wise constant transition intensities help in preserving the tractability of

constant intensities [8]. However, non-homogeneity is not treated in survival analysis as extensively as homogeneous models and in particular for HIV/AIDS disease progression when based on viral load monitoring [13].

This paper models the virology of HIV using a piece-wise constant approach to form a time non-homogeneous Markov process. The virology of HIV is split into mutually exclusive states defined by viral load including the absorbing state, death. The use of Markov models with piece-wise constant transition intensities helps in preserving the tractability of constant intensities [8].

In the next section we describe the HIV/AIDS data that is used in this study and also how the model is formulated basing on the data. In section 3, we have results and analysis where three different models are fitted and their appropriateness is assessed using the Akaike Information Criteria (AIC), likelihood ratio tests as well as the plots of percentage prevalence in each state. The last section discusses and concludes the findings.

Materials and Methods

Data description

The data set used in this study has been described in previous studies [14-17]. At treatment initiation the variables age, Viral Load Baseline (VLBL) and CD4 baseline (CD4BL) are described in Table 1.

For each and every visit, blood samples were obtained for each patient and stored frozen until assayed. Plasma HIV RNA was measured using an amplicator HIV-1 monitor assay kit which has a limit of sensitivity ranging from 50 copies/µL to 500 000 copies/µL.

Table 2 shows the possible transitions between the defined states from t=0 to t=1.5 years of treatment uptake.

At enrolment, most patients were in state 3 followed by state 4. State 1 had the least number of patients but during the first 0.25 years, it had the highest number of patients followed by state 2. From t=0.25 to t=0.5 years, the number of patients in state 3 increased from 6 to 13, an indication of viral rebound since the number of patients with higher viral loads (state 3 and state 4) reduced collectively only by 3. There is need to investigate the causes of viral rebound for HIV/AIDS patients since they are on treatment.

Table 1. *Descriptive Statistics for variables age, baseline viral load and baseline CD4+ cell count.*

Variables	Age (years)	VLBL (copies/µL)	CD4BL (copies/mm3)
Minimum	15	<50 (undetectable)	16
First Quartile	32	21 334	38
Median	39	67 995	116
Mean	40.62	138208	156
Third Quartile	47	201 445	206
Maximum	77	>500 000	1202

Table 2. *Number of HIV/AIDS patients in each viral load state from t=0 to t=0.5 years.*

Variables	Viral load States $(X(t))$					
	1	2	3	4	5	6
t=0 years	4	43	134	106	32	0
t=0.25 years	155	123	6	4	4	24
t=0.5years	214	48	13	2	3	11

Model formulation

The non-homogeneous continuous time Markov model is formulated by splitting HIV/AIDS progression into 5 viral load defined states followed by the end point, death, which is state 6. The HIV/AIDS progression states are:

$$Viral\ load\ levels\left(X(t)\right) = \begin{Bmatrix} 1; & VL < 50 \\ 2; & 50 \le VL < 10000 \\ 3; & 10000 \le VL < 100000 \\ 4; & 100000 \le VL < 500000 \\ 5; & VL \ge 500000 \\ 6; & Dead \end{Bmatrix}$$

These 6 states define the HIV/AIDS disease process is denoted by $X(t)$ as shown above. The machine that is used to detect the viral load used thresholds of [50; 500 000) such that viral load below 50 copies /mL is classified as undetectable. The other covariates included in the model are.

$$Non-adherence\ (NA) = \begin{cases} 1, Yes \\ 0, No \end{cases}, \quad Viral\ load\ baseline\ (VLBL) = \begin{cases} 1, \ge 10000\, copies/\mu L \\ 0, < 10000\, copies/\mu L \end{cases}$$

$$Gender = \begin{cases} 1, & male \\ 0, female \end{cases}$$

$$CD4baseline(CD4BL) = \begin{cases} 1, \le 200\, cells/\mathrm{mm}^3 \\ 0, > 200\, cels/\mathrm{mm}^3 \end{cases}$$

Formulation of the model is based on the approach by Saint-Pierre and others [8] where the study period $[\tau_{(l-1)}, \tau_l)$ for, $l=1,....,r+1$, and considering a vector of artificial time-varying covariates

$$z^*(t) = \left\{ z_1^*(t), z_2^*(t), \ldots, z_r^*(t) \right\}$$

such that:

$$z_0^*(t) = 0; \forall t \text{ And} \qquad z_l^*(t) = \begin{cases} 0; \tau_0 \le t < \tau_l \\ 1; t \ge \tau_l \end{cases} \text{ for}$$

$$l = 1, \ldots, r \rightarrow \tag{1}$$

And the model with transition intensities;

$$q_{ij}\left(t | z^*(t)\right) = q_{ij0} \exp\left\{ \left(\beta_{ij}^*\right)' z^*(t) \right\} \rightarrow \tag{2}$$

q_{ij0} is the baseline transition intensity corresponding to the interval $[\tau_0, \tau_l]$, β_{ij}^* is a vector of regression coefficients associated with the artificial time-varying covariates. For this model the transition intensities are step-functions of time

defined for each interval as follows:

$$q_{ij}\left(t|z^*(t)\right)=\begin{cases} q_{ij0}, & if\ \tau_0 \le t < \tau_1 \\ q_{ij1} = q_{ij0}\exp\left\{\beta^*_{ij,1}\right\}, & if\ \tau_1 \le t < \tau_2 \\ \vdots & \\ q_{ijr} = q_{ij0}\exp\left\{\beta^*_{ij,1}+\beta^*_{ij,2}+\ldots+\beta^*_{ij,r}\right\} & if\ t \ge \tau_r \end{cases}$$

Incorporating the effects of covariates, the model becomes

$$q_{ij}\left(t|z^*(t),z\right)=q_{ij0}\exp\left\{\left(\beta^*_{ij}\right)' z^*(t)+\left(\beta_{ij}\right)'z\right\}\rightarrow \quad (3)$$

Where q_{ij0} is the baseline transition intensities for the interval $0 \le t < 0.5$ with covariates set to their means, r is the log-linear effect of the r interval on the baseline transition intensity and Z^*t is the artificial time-dependent covariate, β_{ij} is the log-linear effect of the relating the instantaneous rate of transitions from state i to state j to the covariates

$$z=\left\{CD4\,baseline\left(CD4BL\right),nonadherence\left(NA\right),Gender,Viral\,load\,baseline\left(VLBL\right)\right\}$$

$$q_{ij}\left(t|z^*(t),z\right)=\begin{cases} q_{ij0}, & if\ \tau_0 \le t < \tau_1 \\ q_{ij1} = q_{ij0}\exp\left\{\beta^*_{ij,1}+\beta_{ij,2}+\ldots+\beta_{ij,k}\right\}, & if\ \tau_1 \le t < \tau_2 \\ q_{ijr} = q_{ij0}\exp\left\{\beta^*_{ij,1}+\beta^*_{ij,2}+\ldots+\beta^*_{ij,r}+\beta_{ij,1}+\beta_{ij,2}+\ldots+\beta_{ij,k}\right\}, & if\ t \ge \tau_t \end{cases}$$

Statistical analysis

All the analysis is done using the Multi-State Modelling [MSM] package for multistate modelling in R software developed by Jackson [18]. The process of identifying the appropriate model started off by fitting time homogeneous Markov model for the data. The time homogeneous model converges and has -2Log-likelihood of 2799.465. From this time homogeneous model, percentage in each state are estimated and plotted as shown in Figure 1.

A comparison of the expected prevalence and observed percentages in each state from Figure 1 show that the predicted number of HIV infected individuals who die (State 6) is underestimated by the model from about 1 year onwards. The number of individuals alive and in state 1 is overestimated by the model from 1 year onwards. Such discrepancies, according to Jackson, indicate a possibility that the transition rates vary with time since the beginning of the process. In this particular case, it could be the time on treatment therapy [19,20]. This calls for the need to fit a Markov process that is non-homogeneous which can be handled by fitting a piece-wise constant function.

Individuals in this study were followed up after every 6 months, thus we start off with a 9-segment non-homogeneous Markov model with 0.5 year intervals. Although the 9-segment model did not converge to maximum likelihood, the prevalence plots for each state in the model helped in revealing intervals with constant transition intensities.

We further investigated the best piece-wise constant function for the data by considering different change points. Most of the models did not converge to a maximum likelihood except

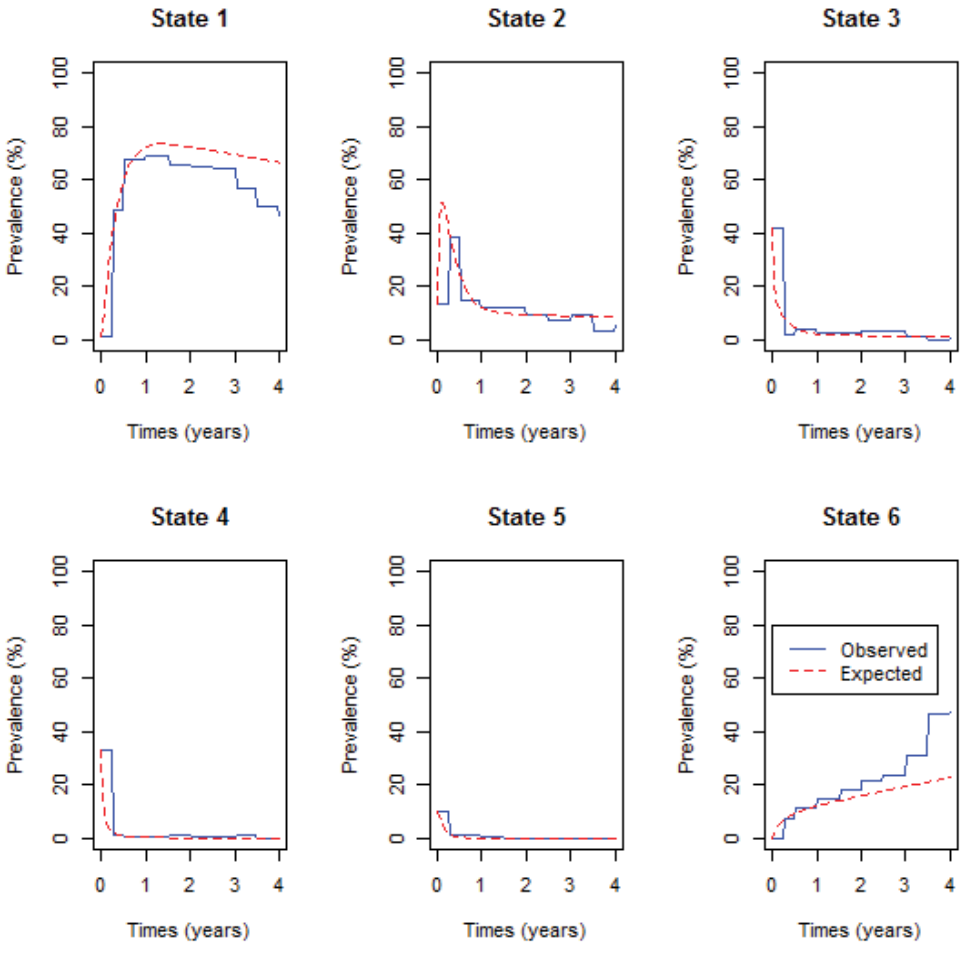

Figure 1. *Prevalence plot for the time homogeneous Markov model.*

for the models;

1. With 2-segments and having a change point at 0.5 years.
2. With 2-segments and having a change point at 1 year.
3. With 3-segments and having change points at 0.5 and 1 year.

In the next section, we base our analysis on these three models and also the time homogeneous model. We further investigate the effects of covariates; gender, non-adherence and CD4 baseline on the chosen model.

Results

For the 2-segment model, the transition intensities are defined for the following intervals.

$$q_{ij}\left(t|z^{*}(t)\right)=\begin{cases} q_{ij,0}, & 0\le t<0.5 \\ q_{ij,1}=q_{ij,0}exp\left\{\beta_{ij1}^{*}\right\}, & t\ge 0.5 \end{cases}$$

Where $q_{ij,0}$ is the baseline transition and $q_{ij,1}$ is the transition intensity matrix for the interval $t \geq 0.5$years and β^{*}_{ij1} is the regression coefficient associated with the artificial time-dependent covariate$Z_1^{*}(t)$. The point estimates of parameters and their corresponding confidence intervals are shown in Table 3.

The results from Table 3 also narrow confidence intervals for transitions from state 1 and from state 2 except for the transition from state 2 to 6 (death). This shows that estimates of transitions from these states are statistically significant. However, most of the point estimates have wide confidence intervals and therefore are not statistically significant. This could be due to the fact that within 6 months of treatment uptake, most patients had made transitions to either state 1 or state 2 as shown by the prevalence plots in Figure 1.

Next we compute estimates of parameters for the 3-segment non-homogeneous Markov model with half-year and one-year change points, with transition intensities defined for each interval as follows:

$$q_{ij}\left(t|z^{*}(t)\right)=\begin{Bmatrix} q_{ij,0}, & 0\le t<0.5 \\ q_{ij,1}=q_{ij,0}\exp\left\{\beta_{ij1}^{*}\right\}, & t\ge 0.5\le t<1 \\ q_{ij2}=q_{ij0}\exp\left\{\beta_{ij,1}^{*}+\beta_{ij,2}^{*}\right\}, & if\ t\ge 1 \end{Bmatrix}$$

is the baseline transition intensities for the interval, $0 \leq t < 0.5$, β^{*}_{ijr} tis the log-linear effect of the r^{th} interval on the baseline transition intensity and $Z^{*}(t)$ is the artificial time-dependent covariate. The estimated parameters are shown in Table 4.

Table 3. *Baseline transition intensities for the 2-segment non-homogeneous model and the time varying log-linear effects.*

Variables	Baseline $\left[q_{ij,0}\right]$	Log-linear effect $\left[\beta_{ij1}\right]$	Hazard Ratios [0.5,Inf)
q_{12}	0.445 (0.360, 0.550)	-1.295 (-1.814, -0.777)*	0.274 (0.163,0.460)
q_{16}	0.053 (0.031, 0.091)	-3.170 (-4.011, -2.330)*	0.041 (0.018,0.097)
q_{21}	2.640 (2.244, 3.107)	-1.133 (-1.426,-0.841) *	0.322 (0.240,0.431)
q_{23}	1.585 (0. 486, 5.168)	-2.660 (-6.353, 1.033)	0.070 (0.0017, 2.810)
q_{26}	0.002 (0.0000003742, 727)	1.220 (-25.055, 27.495)	3.387 (0.0000000013,870000000)
q_{32}	6.635 (2.158, 20.40)	-3.854 (-7.347, -0.361)*	0.021 (0.0006,0.697)
q_{34}	6.110 (0.015, 2428)	3.010 (-5.893, 11.91)	20.28 (0.0028,149100)
q_{36}	0.144 (0.0018, 11.64)	4.071 (-8.064, 16.21)	58.63 (0.0003,11000000)
q_{43}	47.116 (0.137, 16160)	1.387 (-7.123, 9.897)	4.004 (0.0008,19870)
q_{45}	3.772 (0.010, 1356)	-0.849 (-9.605, 7.907)	0.428 (0.000067,2717)
q_{46}	0.02 (0.0000000000, 680000000000)	2.426 (-194.2,199.1)	11.316 (0.0000000000046,28000000000)
q_{54}	23.825 (0.089, 6378)	0.649 (-7.528, 8.825)	1.913 (0.0005,6804)
q_{56}	0.035 (0.0000000013, 934000)	2.707 (-26.46, 31.87)	14.99 (0.00000000032,6950000000)
-2xLL		2495.898	

Results from Table 4 show an improvement on the estimated parameter values. This is shown by the confidence intervals that are narrower compared to the confidence intervals shown in Table 3 for the 2-segment model. However, transitions to death from states 2, 3, 4 and 5 have got very wide confidence interval. Only mortality rates from state 1 (undetectable viral load) decrease significantly with time as indicated by the narrow confidence intervals and exclusion of zero in the confidence intervals.

Next we present the results from a 2-segment piece-wise Markov model together with the effects of covariates. The model is given as follows:

$$q_{ij}\left(t|z^*(t),z\right)=q_{ij0}\exp\left\{\left(\beta_{ij}^*\right)' z^*(t)+\left(\beta_{ij}\right)'z\right\}$$

$q_{ij0}$is the baseline transition intensities for the interval $0 \le t < 0.5$ with covariates set to their means, β^*_{ijk} is the log-linear effect of the k^{th} interval on the baseline transition intensity and $Z^*(t)$ is the artificial time-dependent covariate, β^*_{ij} is the log-linear effect of the relating the instantaneous rate of transitions from state i to state j to the covariates.

$$z=\{CD4\ baseline(CD4BL),\ nonadherence(NA),\ Gender,\ Viral\ load\ baseline(VLBL)\}$$

The results are shown in Table 5.

The results from Table 5 show that during the first 0.5 years of treatment uptake (baseline) the rates of viral load suppression are higher than the rates of viral rebound regardless of the state. The highest transition rates are noted from a viral load above 500 000 copies/µL to a viral load between 100 000 and 499 999 copies/µL. During the first six months most transitions to death occurred from a viral load state between

Table 4. *Effects of half-year and one-year changes in time on the baseline transition*

Variables		Hazard Ratios		Log-linear Effects $[\hat{a}_{ij}]$	
No.	Baseline $(q_{ij,0})$	[0.5,1)	[1,Inf)	[0.5,1)	[1,Inf)
q_{12}	0.441 (0.357, 0.546)	0.393 (0.198,0.781)	0.246 (0.145,0.419)	-0.933 (-1.619,-0.248)*	-1.401 (-1.932, -0.870)*
q_{16}	0.0572 (0.0349, 0.0937)	0.0396 (0.0067,0.233)	0.0482 (0.0209,0.111)	-3.230 (-5.002,-1.458)*	-3.032 (-3.866, -2.198)*
q_{21}	2.607 (2.208, 3.079)	0.447 (0.275,0.725)	0.289 (0.210,0.400)	-0.806 (-1.289,-0.321)*	-1.240 (-1.562, -0.917)*
q_{23}	1.588 (0.501, 5.036)	0.0836 (0.00205,3.404)	0.0692 (0.00189,2.540)	-2.482 (-6.188, 1.225)	-2.670 (-6.273, 0.932)
q_{26}	0.00138 (0.00084, 2.268)	0.293 (0.0484,1.773)	2.111 (0.653,6.827)	-1.227 (-83.617,81.163)	0.747 (-34.965, 36.460)
q_{32}	6.775 (2.264, 10.027)	0.0342 (0.0104,1.120)	0.0203 (0.0067,0.61)	-3.376 (-6.866, 0.114)	-3.900 (-7.306, -0.493)*
q_{34}	4.832 (3.571, 6.540)	4.364 (3.462,13.487)	20.097 (2.418, 26.70)	1.474 (-2.907, 5.854)	3.001 (-6.025, 12.026)
q_{36}	0.0585 (0.0108, 3.182)	0.79946 (0.402,1.589)	61.1451 (60.93,61.36)	-0.224 (-35.450,35.002)	4.113 (-9.706, 17.932)
q_{43}	36.307 (2.900, 45.46)	0.688 (0.0691,6.851)	3.951 (0.653,23.91)	-0.374 (-4.975, 4.227)	1.374 (-7.334, 10.082)
q_{45}	0.638 (0.165, 2.467)	0.754 (0.518,10.96)	0.0174 (0.0028,1.084)	-0.282 (-2.959, 2.395)	-4.054 (-5.820, 7.712)
q_{46}	0.00965 (0.00183, 5.081)	2.063 (0.345,12.35)	5.745 (0.997,33.12)	0.724 (-74.748,76.196)	1.748 (-214.14,217.64)
q_{54}	26.276 (18.65, 37.02)	0.0899 (0.0474,1.703)	5.151 (3.504,7.572)	-2.409 (-5.35, 0.533)	1.639 (-24.07, 27.353)
q_{56}	0.0464 (0.0109, 1.960)	180.816 (3.766,868.2)	2.298 (0.00019,27.51)	5.198 (-5.582,15.976)	0.832 (-98.36,100.02)
-2xLL			2485.745		

Table 5. *Estimated parameters for the half-year piece-wise Markov model with the effects of covariates included.*

	Variables	**Log-linear effects** $[\beta_{ij1}]$				
	Baseline $(q_{ij,0})$	**CD4BL**	**NA.**	**Gender**	**VLBL**	**[0.5,Inf)**
q_{21}	3.021 (2.539,3.593)	0.315 (0.022,0.609)*	-0.978 (-1.395,-0.562)*	-0.0339 (-0.330,0.262)	-0.074 (-0.436, 0.288)	-0.994 (-1.295,-0.69)*
q_{12}	0.515 (0.412,0.643)	0.201 (-0.240,0.642)	0.565 (0.042, 1.088)*	-0.198 (-0.629,0.232)	0.321 (-0.238, 0.879)	-1.163 (-1.69,-0.633)*
q_{32}	7.724 (4.081,14.62)	-1.422 (-3.546,0.703)	0.0656 (-0.956,1.087)	0.236 (-0.830,1.302)	-1.476 (-3.788, 0.837)	-2.725 (-3.94,-1.512)*
q_{23}	1.277 (0.633,2.575)	-0.731 (-2.821,1.358)	0.956 (-0.034,1.947)	0.221 (-0.854,1.295)	-0.212 (-2.554, 2.130)	-1.728 (-3.11,-0.349)*
q_{43}	11.297 (3.569,35.77)	2.047 (0.190,3.903)*	0.530 (-2.012,3.073)	-0.332 (-1.293,0.629)	-0.249 (-3.018, 2.520)	-2.046 (-3.69,-0.398)*
q_{34}	0.963 (0.253,3.664)	1.714 (-0.749,4.177)	0.882 (-1.430,3.195)	-0.786 (-2.635,1.063)	-0.590 (-4.192, 3.012)	1.023 (-1.659,3.705)
q_{54}	44.854 (0.0969,2077)	0.492 (-1.963,2.948)	2.911 (-8.605,14.428)	-2.156 (-11.58,7.266)	-0.078 (-3.581, 3.426)	-1.067 (-3.716,1.581)
q_{45}	4.325 (0.0054,3489)	3.834 (-0.574,8.243)	3.591 (-8.322,15.505)	-2.742 (-12.91,7.427)	3.102 (-15.335, 21.54)	-5.474 (-9.55,-1.402)*
q_{16}	0.00391 (0.000003,48.1)	0.923 (-0.039,1.884)	-5.245 (-22.225,11.73)	-0.386 (-1.185,0.412)	1.144 (-0.065, 2.353)	-6.079 (-19.38,7.222)
q_{26}	0.0127 (0.00001,0.114)	1.221 (-1.022,3.463)	-0.909 (-3.657,1.839)	-3.554 (-18.26,11.15)	3.836 (-9.691,17.36)	5.279 (-11.01,21.57)
q_{36}	0.0218 (0.00008,58.94)	-0.0216 (-3.035,2.992)	-1.477 (-4.606,1.653)	3.454 (-9.17,16.08)	3.362 (-20.82, 27.55)	5.131 (-12.62,22.88)
q_{46}	0.166 (0.0004,64.23)	-0.327 (-4.853, 4.199)	-1.186 (-7.007,4.635)	0.587 (-2.433,3.61)	0.360 (-127.3,128.0)	6.455 (-11.13,24.04)
q_{56}	0.00899 (0.00009,82100)	0.216 (-58.05,58.48)	-0.0998 (-77.39,77.19)	-0.175 (-53.28,52.93)	-0.305 (-154.9,154.2)	3.530 (-49.91,56.97)

-2Log-likelihood: 2390.415; *Significant

100 000 and 500 000 copies/μL. This is mainly attributed to initiating treatment with a CD4 baseline below 200 cells/m^3.

Having a CD4 baseline below 200 cells/m^3 at treatment initiation contribute significantly to the increase in viral suppression to undetectable level as shown by a narrow confidence interval and exclusion of zero in the confidence interval. For these patients, there is also a significant increase in viral suppression from state 4 to state 3. Though not significant, there is reduction in viral suppression from state 3 to state 2.

For non-adherent patients, the results reveal a significant reduction in viral suppression to undetectable levels (state 2 to state 1). Thus, adherence to treatment increases significantly the transition rates to undetectable levels. Non-adherence increases transitions to viral rebound from undetectable viral load (state 1 to state 2). Although some of the estimated parameters are not significant, the results show that non-adherence to treatment contribute more to the increased rates of viral rebound than viral suppression.

Males in the study experience a reduction in the rates of viral suppression to undetectable levels, but once the undetectable viral load is reached they have reduced rates of viral rebound. This means that for their female counterparts, rates of viral suppression to undetectable levels are higher than that of males. Deaths of males are more likely to occur from viral load states between 10 000 and 500 000 copies/μL compared to their female counterparts.

The results also show reduction in the rates of transition to better states (viral suppression) for patients who initiated

treatment with a viral load level above 10 000 copies/μL. These patients experienced increased transitions to death regardless of the viral load state. Thus, starting treatment with a viral load above 10 000 copies/μL increases the mortality rates and also accelerates diseases progression.

From 6 months (0.5 years) of treatment uptake onwards, most of the transitions between live states are significant except for the transition from state 3 to state 4 and state 5 to state 4. The results show a significant reduction in viral suppression to undetectable levels from 6 months onwards but once the undetectable viral load is reached there is reduction in viral rebound and also reduction in death occurrences. However, if the viral load is still detectable after 6 months, it increases the occurrence of deaths.

Assessment of the fitted models

In this subsection, we assess the fitted models using several techniques: prevalence plots, contour plots and estimates of log-likelihoods and Akaikie Information Criteria (AIC). Prevalence plots give a rough indication of the goodness of the fitted models and contours plot the likelihood surface with respect to 2 parameters default to plus or minus 2 standard errors obtained from the Hessian matrix at the maximum likelihood estimate.

In Figure 2 we compare the percentage prevalence plots for each of the states for the a two-segment non-homogeneous Markov model with change point at 0.5 years, 3-segment non-homogeneous Markov model and the 2-segment model with change point at 1 year respectively.

Results from the percentage prevalence plots show that the fitted model gives a perfect fit of the observed data for patients in state 2,3,4 and 5. However, the expected percentage prevalence plot for the 2-segment non-homogeneous model with change point at 1 year overestimates the observed plot for patients in state 1. From 3 years onwards, expected percentage prevalence for mortality (state 6) underestimate the observed mortality from all fitted models although the 2-segment model with change point at 1 year underestimates mortality from 2 years onwards. Compared to the prevalence plot for the time homogeneous model shown in Figure 1, these plots show an improved fit to the observed data.

The prevalence of State 1 is down sloping from half a year on. This is due to non-adherence to treatment as shown by the results in Table 4.

Before computing estimates of AICs we plot the contours for the fitted models. These contours help to diagnose any irregularities in the likelihood surface. Thus, they present a graphical visualisation of the fitted surface. For biological data, these contours are expected to be elliptical. Figure 3 shows contours for the fitted models.

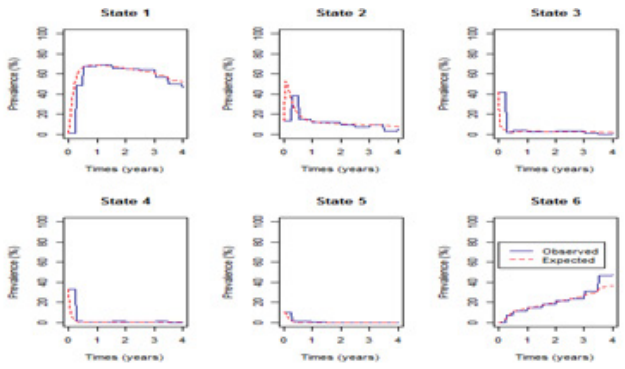

a. 0.5-year change point

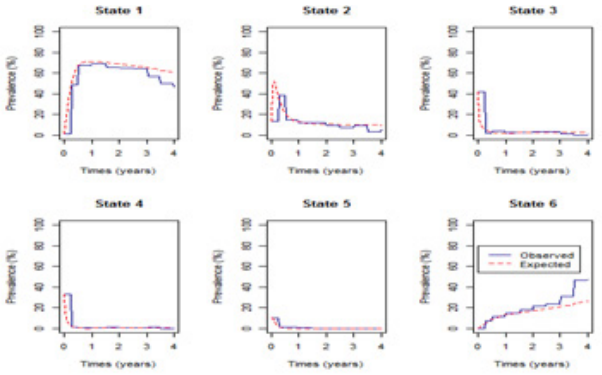

c. 1-year change point

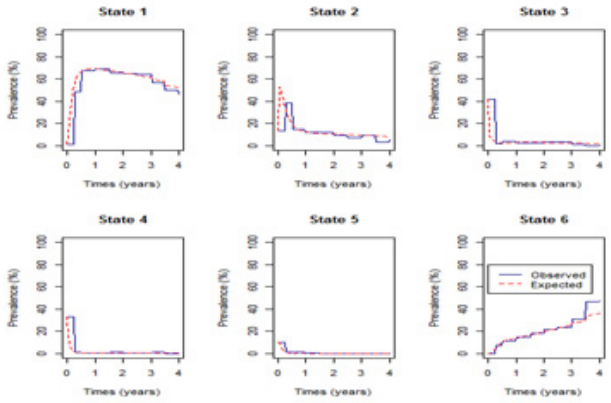

b.0.5 and 1-year change points

Figure 2. *Percentage Prevalence plots for: (a) the 2-segment model with change point at 0.5 years, (b) the 3-segment model with change points at 0.5 and 1 year and (c) the 2-segment model with change point at 1 year.*

Figure 3 shows that contours for the time homogeneous Markov (top left) are not elliptical but the contour for the three non-homogeneous models are elliptical. So the non-homogeneous model give a better fit the data compared to the homogeneous model. However, the contours for the time homogeneous model (top left) and the contours for the 2-segment with change point at 1 year (top right) are not symmetric; hence the models cannot explain this data fully. The contours for the non-homogeneous models; 2-segment with change point at 0.5 years (bottom left) and 3-segment with change points at 0.5 and 1 year (bottom right) are both elliptical and evenly distributed contours plots with symmetrical surfaces that peak at the centre (indicated by the white region). Hence these models give an adequate explanation of the data.

Table 6 shows estimates of the -2xlog-likelihood (-2 × LL), log-likelihoods (LL) are shown in brackets, the degrees of freedom for each of the fitted models and the Akaike information criteria (AIC). The AICs are calculated using the formula;

$$AIC = -2\log(likelihood) + 2 \times df$$

For example, for the homogeneous model *AIC=2799.465+2x13=2825.465* as shown in the Table 6.

The results show that the time homogeneous Markov model has the highest AIC and log-likelihood compared to the non-homogeneous Markov models. From the fitted non-homogeneous Markov model, the 3-segment model, with change points at 0.5 and 1 year, has the highest log-likelihood compared to all the other fitted models followed by the 2-segment model with change points at 0.5 years. However, a further assessment basing on the AICs reveal that a 2-segment model with change points at 0.5 years fits the data better than the 3-segment model since it has the lowest AIC. Effects of the covariates were included in the 2-segment non-homogeneous model and the model yielded the lowest AIC.

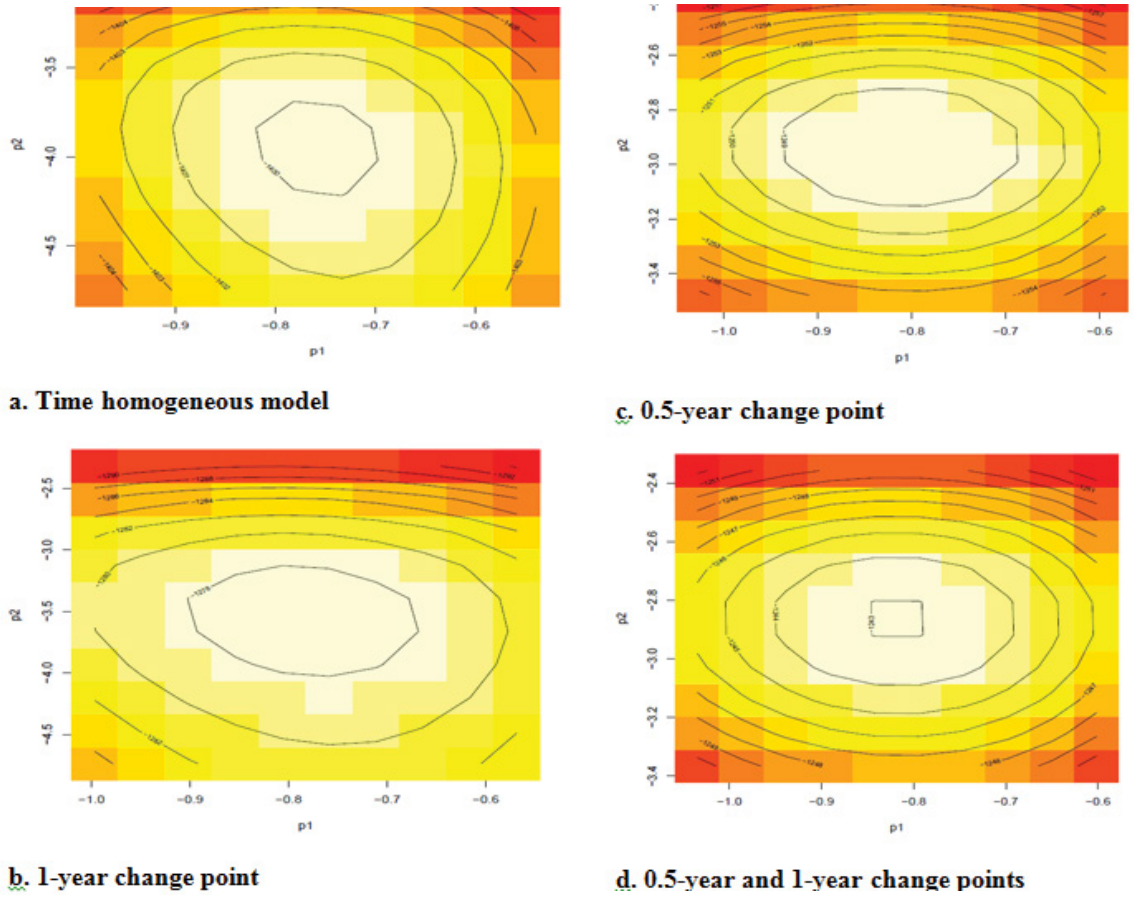

Figure 3. *Contour plots for: (a) the time homogeneous Markov model, (b) the 2-segment model with change point at 1 year, (c) the 2-segment model with change point at 0.5 years and (d) the 3-segment model with change points at 0.5 and 1 year.*

Table 6. *Estimated AICs and Log-likelihoods for the fitted models.*

Variables	Homogeneous Model	2-segment (1-year change point)	2-segments (0.5-year change point)	3-segments (0.5 and 1-year change points)	0.5-year change point and covariates
-2 × LL (LL)	2799.465 (-1399.73)	2554.177 (-1277.09)	2495.898 (-1247.95)	2485.745 (-1242.87)	2520.415 (-1260.21)
df	13	26	26	39	65
AIC	2825.465	2606.177	2547.898	2563.745	2390.415

Discussion

In this study, a comparison of the time-homogeneous Markov model and the non-homogeneous Markov model to estimate the progression of HIV/AIDS on viral load monitoring is done. For this model, the expected percentages in state 1 overestimated the observed percentages and the predicted number of individuals who died was underestimated by the model from 1 year of treatment uptake onwards. This indicated the need to fit a non-homogeneous model in which transition intensities are piece-wise constant. Non-homogeneous models with different change points were fitted. However, most of these models did not converge to a maximum likelihood except for the 2-segment model with change point at 0.5 years, 2-segment model with change point at 1 year and 3-segment model with change points at 0.5 and 1 year. From these models, non-homogeneous models and the time homogeneous model, assessment of the best model was done using the percentage prevalence plots, contour plots, perspective plots, CIs, log-likelihoods and the AICs. The model with the lowest AIC, the 2-segment model with change point at 0.5 years, was considered as the model that best explains HIV progression in patient on treatment under viral load monitoring for this data set.

This means that HIV progression is best described by a non-homogeneous Markov model with a change point at 0.5 years. This is mainly influenced by the results from viral load monitoring which are that, most of the patients on antiretroviral therapy reach the undetectable viral load within the first six months of treatment uptake (14,16). Thus, when monitoring HIV/AIDS patients, one should ensure that viral load suppression is reached as this reduces mortality rates.

Results from the fitted models show wider confidence intervals for the estimated transition rates to death. However, transitions within the 5 live states defined by viral load had narrow confidence intervals indicating significance in the estimated parameters, particularly the 2-segment model with change point at 0.5 years and covariates, in predicting transitions between live states.

The results also revealed a slower response to treatment when patients start treatment when viral load levels are above 10 000 copies/μL than when treatment is initiated when the viral load levels are below 10 000 copies/μL in the first 6 months [17]. Patients who initiated therapy with a viral load level above 10 000 copies/μL experienced accelerated rates of transition to death [14]. In 2018, Shoko et al. observed the same finding although they used a time homogeneous Markov modelling approach [17].

The results from this study revealed reduction with time in viral suppression to undetectable levels for males and patients who were non-adherent to treatment [14]. For males, once the undetectable viral load is reached, there is reduction in viral rebound particularly from 0.5 years onwards.

This study shows a significant reduction in transitions to death from 0.5 years onwards for patients who have achieved an undetectable viral load despite the challenges of non-adherence. Thus, time non-homogeneity is the best approach to modelling HIV/AIDS progression for patients receiving cART.

Ethics and Consent to Participate

The procedures used in this study were as approved by the Research Ethics Committee of the University of Venda, South Africa (Protocol number SMNS/13/MBY/01/0625), in accordance with the 1964 Helsinki declaration and its subsequent amendments. Additionally, permission to access health facilities was obtained from the Limpopo Provincial Department of Health, South Africa, and the collaborating health facilities. Informed consent was obtained from study participants prior to their involvement; and data obtained was stripped of personal identifiers to ensure the confidentiality of the participants.

Funding

The dataset used was generated from funding awards to POB by the South African Medical Research Council (RCDI) through funding received from the South African National Treasury, the South African National Research Foundation (GUN109312), and the University of Venda. The contents are solely the responsibility of the authors and do not necessarily represent the official views of the South African Medical Research Council , the National Research Foundation, or the University of Venda.

Availability of Data and Materials

The data is available upon a submitted request.

Author Contributions

CS drafted the manuscript. POB provided the data used for the analysis. CS, DC and POB contributed to the analysis and interpretation of the data. All authors participated in critical revision of the manuscript drafts and approved the final version.

Competing Interests

The authors declare that they have no competing interests.

Consent for Publication

Not applicable.

References

1. Brennan AT, Maskew M, Sanne I, Fox MP. The Interplay between CD4 Cell Count, Viral Load Suppression and Duration of Antiretroviral Therapy on Mortality in a Resource-Limited Setting. Trop Med Int Health 2013; 18: 619-631.
2. Cohen MS, Chen YQ, McCauley M, Gamble T, Hosseinipour MC, Kumarasamy N, Hakim JG, Kumwenda J, Grinsztejn B, Pilotto JHS, Godbole SV, Mehendale S, Chariyalertsak S, Santos BR, Mayer KH, Hoffman IF, Eshleman SH, Piwowar-Manning E, Wang L, Makhema J, Mills LA, Bruyn GD, Sanne I, Eron J, Gallant J, Havlir D, Swindells S, Ribaudo H, Elharrar, Burns D, Taha TE, Nielsen-Saines K, Celentano D, Essex M, Fleming TR. Prevention of HIV-1 infection with early antiretroviral therapy. N Engl J Med 2011; 365: 493-505.

3. Cole SR, Hernan MA, Anastos K, Jamieson BD, Robins JM. Determining the effect of highly active antiretroviral therapy on changes in human immunodeficiency virus type 1 RNA viral load using a marginal structural left-censored mean model. Am J Epidemiol. 2007; 166: 219-227.
4. Lecher S, Williams J, Fonjungo PN, Kim AA, Ellenberger D, Zhang G, Toure CA, Agolory S, Appiah-Pippim G, Beard S, Borget MY, Carmona S, Chipungu G, Diallo K, Downer M, Edgil D, Haberman H, Hurlston M, Jadzak S, Kiyaga C, MacLeod W, Makumb B, Muttai H, Mwangi C, Mwangi JW, Mwasekaga M, Naluguza M, NgAngA LW, Nguyen S, Sawadogo S, Sleeman K, Stevens W, Kuritsky J, Hader S, Nkengasong J. Progress with Scale-Up of HIV Viral Load Monitoring — Seven Sub-Saharan African Countries, January 2015–June 2016. R Morb Mortal Wkly Rep 2016; 65: 1332-1335.
5. Chenand B, Zhou XH. Non-homogeneous Markov process models with informative observations with an application to Alzheimer's disease. Biom J 2011; 53: 444-463.
6. Lee S, Ko J, Tan X, patel I, Balakrishnan R, Chang J. Markov Chain Modelling Analysis of HIV/AIDS Progression: A Race Based Forecast in the United States. Indian J Pharm Sci 2014; 76: 107-115
7. Lange JM, Hubbard RA, Inoue LYT, Minin V. A joint model for multistate disease processes and random informative observation times, with applications to electronic medical records Data. UW Biostatistics Working Paper Series, 2014: 401.
8. Saint-Pierre P, Combescure C, Daures JP, Godard P. The analysis of asthma control under a Markov assumption with use of covariates. Stat Med. 2003; 22: 3755-3770.
9. Shoko C, Chikobvu D. Time-homogeneous Markov process for HIV/AIDS progression under a combination treatment therapy: cohort study, South Africa. Theor Biol Med Model 2018; 15: 3.
10. Grover G, Gadpayle KA, Swain PK, Deka B. A Multistate Markov Model Based on CD4 cell count for HIV/AIDS Patients on Antiretroviral Therapy (ART). Int J Stat Med Res 2013; 2: 144-151.
11. Mathieu E, Foucher Y, Dellamanica P, Daures JP. Parametric and non homogeneous Semi-Markov process for HIV control. Methodol Comput Appl Probab 2007; 9: 389-397.
12. Ocarn-Riola R. Non-homogeneous Markov Processes for Biomedical data Analysis. Biom J 2005; 47: 369-376.
13. Dessie ZG. Modeling of HIV/AIDS dynamics evolution using non-homogeneous semi-Markov process. SpringerPlus 2014; 3: 537.
14. Shoko C and Chikobvu D. Determinants of viral load rebound on HIV/AIDS patients receiving antiretroviral therapy: Results from South Africa. Theor Biol Med Model 2018; 15: 10.
15. Shoko C, Chikobvu D. A superiority of viral load over CD4 cell count when predicting mortality in HIV patients on therapy. BMC Infectious Disease. 2019; 19: 169.
16. Chikobvu D and Shoko C. A Markov Model to estimate Mortality due to HIV/AIDS using CD4 cell counts based states and viral load: A Principal Component Analysis approach. Biomedical Research. 2018; 29 (15): 3090-3098
17. Shoko C, Chikobvu D, Pascal O. Bessong. A Markov Model to estimate Mortality due to HIV/AIDS using viral load levels based states and CD4 cell counts: A Principal Component Analysis approach. Infect Dis Ther 2018; 4: 457-471.
18. Jackson C, Multi-state modelling with R: the msm package Version 1.6.4. MRC Biostatistics Unit. 2016
19. Silveira MP, De Lourdes DM, Leite JC, Pinheiro CA, Da Silveira VL. Predictors of undetectable plasma viral load in HIV-positive adults receiving antiretroviral therapy in Southern Africa, Braz J Infect Dis 2002; 6: 164-171.
20. Azia IN, Mukumbang FC, Van Wyk, B. Barriers to adherence to antiretroviral treatment in a regional hospital in Vredenburg, Western Cape, South Africa. South Afr J HIV Med 2016; 17: 476.

***Correspondence to**

Claris Shoko,
University of the Free State,
Bloemfontein,
South Africa.

Accepted Manuscripts

South African Medical Journal

A Markov model for the effects of virologic failure on HIV/AIDS progression in TB co-infected patients receiving antiretroviral therapy in a rural clinic in northern South Africa

--Manuscript Draft--

Manuscript Number:	SAMJ13934
Article Type:	Original Research
Keywords:	Virologic failure; Viral rebound; tuberculosis; non-homogeneous Markov model; combination antiretroviral therapy (cART).
Corresponding Author:	Claris Shoko, Ph.D University of the Free State SOUTH AFRICA
First Author:	Claris Shoko, Ph.D
Order of Authors:	Claris Shoko, Ph.D
	Delson Chikobvu, Ph.D
	Pascal O. Bessong, Ph.D
Manuscript Region of Origin:	SOUTH AFRICA
Abstract:	Background The goal of antiretroviral therapy (ART) is to suppress viral replication to undetectable levels. In some patients, these low viral load levels may not be attained and therefore represent potential virologic failure. This study presents the results of a Markov model, exploring how virologic failure and active TB affect the progression of HIV in people on ART. Method A continuous time non-homogeneous Markov model is used to model the progression of HIV/AIDS in patients on combination antiretroviral therapy (cART). We define seven states in our model. The first five states are based on viral load levels and the other two are absorbing states; death and withdrawal from study. The effects of TB co-infection, viral load baseline, lactic acidosis and treatment failure on transition intensities is assessed. Results The model shows that viral load based transition intensities do not follow a constant rate; rather, two different trends in HIV/AIDS progression. The first type of trend is an increase in the prevalence in state 1 (undetectable viral load levels) in the first 0.5 years of treatment. The second trend follows thereafter and shows a slowly decreasing trend. Thus, within the first 0.5 years of therapeutic intervention, the undetectable viral load state is attained from any viral load state. However, in cases where virologic failure is mentioned, there is increased risk of death. Developing TB whilst on cART increases the risks of viral rebound from undetectable levels to viral loads between 50 and 10 000 copies/mL by 1.03 folds. From a viral load between 10 000 and 100 000, developing active TB whilst on cART increases the rate of viral rebound by approximately 2.5 folds. However, if TB is detected and treated at enrolment, the rates of viral rebound from undetectable levels are reduced. Conclusion The model confirms that virologic failure, coupled with developing active TB whilst on ART, increase rates of mortality irrespective of the patient's HIV state. It also suggests that whilst TB at the time of cART initiation does not increase the risk of viral rebound, the development of active TB after cART initiation does increase the risk of viral rebound. These highlight the importance of strengthening viral load monitoring, every two months, especially in people with TB, and to appropriately address unsuppressed

	viral loads once detected.

A Markov model for the effects of virologic failure on HIV/AIDS progression in TB co-infected patients receiving antiretroviral therapy in a rural clinic in northern South Africa

Abstract

Background: The goal of antiretroviral therapy (ART) is to suppress viral replication to undetectable levels. In some patients, these low viral load levels may not be attained and therefore represent potential virologic failure. This study presents the results of a Markov model, exploring how virologic failure and active TB affect the progression of HIV in people on ART.

Method: A continuous time non-homogeneous Markov model is used to model the progression of HIV/AIDS in patients on combination antiretroviral therapy (cART). We define seven states in our model. The first five states are based on viral load levels and the other two are absorbing states; death and withdrawal from study. The effects of TB co-infection, viral load baseline, lactic acidosis and treatment failure on transition intensities is assessed.

Results: The model shows that viral load based transition intensities do not follow a constant rate; rather, two different trends in HIV/AIDS progression. The first type of trend is an increase in the prevalence in state 1 (undetectable viral load levels) in the first 0.5 years of treatment. The second trend follows thereafter and shows a slowly decreasing trend. Thus, within the first 0.5 years of therapeutic intervention, the undetectable viral load state is attained from any viral load state. However, in cases where virologic failure is mentioned, there is increased risk of death. Developing TB whilst on cART increases the risks of viral rebound from undetectable levels to viral loads between 50 and 10 000 copies/mL by 1.03 folds. From a viral load between 10 000 and 100 000, developing active TB whilst on cART increases the rate of viral rebound by approximately 2.5 folds. However, if TB is detected and treated at enrolment, the rates of viral rebound from undetectable levels are reduced.

Conclusion: The model confirms that virologic failure, coupled with developing active TB whilst on ART, increase rates of mortality irrespective of the patient's HIV state. It also suggests that whilst TB at the time of cART initiation does not increase the risk of viral rebound, the development of active TB after cART initiation does increase the risk of viral rebound. These highlight the importance of strengthening viral load monitoring, every two

months, especially in people with TB, and to appropriately address unsuppressed viral loads once detected.

Background

The Joint United Nations Programme on AIDS (UNAIDS) reported that about 37 million people were living with HIV globally, with an estimated 17 million accessing antiretroviral therapy (ART) in 2017 (UNAIDS, 2018). South Africa has one of the highest burdens of HIV in the world. In 2017, UNAIDS reported that there were an estimated 7.1 million people living with HIV, 270 000 new HIV infections, and about 110 000 AIDS related deaths. Of those living with HIV, only about 45% had suppressed viral loads (UNAIDS, 2018). The South African comprehensive treatment plan is an approach to ensure that 90% of those infected with HIV are detected, 90% of those diagnosed are treated, and viral suppression is attained in 90% of all those under treatment (The 90-90-90 objective).

HIV infection is characterised by a progressive depletion of the CD4+ T-cell populations. This increases the risk of latent tuberculosis (TB) reactivation 20-fold (Pawlowski et al., 2012); and the risk of developing active TB has been shown to be significantly greater shortly after HIV infection (Bulage et al., 2017). Martinson et al. (2011b), showed that between 60-80% of people with TB in Southern Africa are HIV positive, emphasizing TB as an important common opportunistic infection among HIV infected individuals.

The use of cART in HIV/AIDS patients is characterised by an increase in CD4+ cell counts and a decrease in viral load to undetectable levels (Bruisker et al., 2015). However, management of HIV infections in TB co-infected patients has been a challenge due in part to drug interactions between rifampicin and non-nucleosides reverse transcriptase inhibitors (NNRTIs) and protease inhibitors (PIs), and concerns about adherence and virologic failure (Cohen and Meintjes, 2010). The World Health Organisation (WHO) (2001) emphasised the need to further strengthen TB control between 2002 and 2020 otherwise a billion people will be newly infected with *Mycobacterium tuberculosis*, more than 150 million would develop active TB disease and 36 million would die of TB. Day et al. (2004) suggested that active TB accelerates HIV disease progression, but not much data are available to confirm or refute this hypothesis. Day et al. (2004) argued that although antiretroviral therapy is required for a major effect on survival in HIV-infected individuals, prevention of TB is important for the reduction of HIV-related morbidity and mortality. Hence, there is need to consider virologic

failure and TB control in tandem to minimise the consequences of partial or incomplete viral suppression.

Virologic failure is due to patient-factors like non-adherence to treatment or due to ART regimen factors like peripheral neuropathy and lactic acidosis, drug resistance or drug-drug interactions. Constant monitoring of viral load levels (states) helps in avoiding unnecessary switching to second line therapy that could have happened with clinical (WHO stage) and immunologic criterion (CD4+ cell counts). Routine viral load monitoring helps in early detection of virologic failure (Sigaloff et al., 2011) as patients are observed making random transitions from one viral load state to another.

The random movement from one viral load state to the other is regarded as a stochastic process. HIV/AIDS progression is split into various states of the disease based on the viral load measurement including the endpoints, death state and withdrawal from study (loss to follow-up). Stochastic processes allow random movements between viral load states before an HIV/AIDS patient is finally absorbed into the death state (Lee et al., 2014). Patients are monitored only at visit times resulting in the exact time the transition has occurred not known (Chenand and Zhou, 2011). When transition times are not known and interval censored observations are present, homogeneous and non-homogeneous Markov processes are an important field of research into stochastic processes (Kalbfleisch and Lawless, 1985). Non-homogeneous models are particularly important when transitions rates between diseases states are not constant but allowed to change with time to mimic better, observed reality.

The Markov model is an appropriate stochastic approach when the present state of the patient summarises all previous information (known as the history or natural filtration of the process). Time-homogeneous Markov models have been widely used in the modelling of different disease progressions such as cancer (Duffy et al., 1995, Yen and Chen, 2007), stroke (Pan and Kastin, 2007) and diabetic retinopathy (Marshall and Jones, 1995). However, the assumption of time-homogeneity is unrealistic in the sense that over long periods the diseases evolve resulting in changes in transition intensities. The use of time-homogeneous models then puts severe limitations on disease history behaviour. In particular, when dealing with HIV, it is more realistic to assume that science and medicine evolve, hence the rate at which patients change in severity of the disease is likely to change as newer medications will improve the quality of their lives (Pan and Kastin, 2007). This justifies the need for

continuous-time non-homogeneous models in analysing disease progressions. The problem can be addressed by using piecewise constant transition rate Markov models that preserve the tractability of the constant rates (Lindsay and Ryan, 1993).

In this study, a non-homogeneous Markov process, using a piecewise constant transition rate model approach, is used to model the progression of HIV/AIDS in patients with TB co-infection. The states of the Markov process are based on viral load measurements followed by absorbing states, death or withdrawal from study. The viral load (VL) states are defined as follows; **1**: VL<50 copies/mL; **2**: $50 \leq VL < 10\,000$; **3**: $10\,000 \leq VL < 100\,000$; **4**: $100\,000 \leq VL < 500\,000$; and **5**: $VL \geq 500\,000$. State 1 is accessible from any VL state. The effects of virologic failure and TB, among others, on HIV/AIDS progression are assessed. The inclusion of the effects of virologic failure on HIV progression in patients with TB co-infection prompted the current analysis research and also the use of a continuous-time non-homogeneous Markov model in which the undetectable viral load is accessed from any of the five viral load states.

The South African description of virologic failure is as follows: (i) two consecutive VL greater than 1000 copies/ml after previous suppression (ii) one VL > 1000 copies/ml after previous suppression followed by a change in treatment (iii) one VL > 1000 copies/ml after 6 months on ART without suppression. This is in line with the Adult Guideline from the South African Department of Health which proposed a virologic failure threshold of 1000 copies/mL (Stead, 2017).

Although in resource limited areas, viral load levels monitoring may not be routinely available, viral load levels monitoring helps in detection of treatment failure and in avoiding unnecessary switching to second line treatment that could happen when clinical and immunological criteria are used (Gunda et al., 2017). Treatment failure is defined clinically as a new or recurrent event indicating severe immunodeficiency or immunological failure as persistent CD4+ T-cell count levels are below 100 cells/mm^3 after 6 months of treatment. In this paper, a continuous-time non-homogeneous Markov model with states based on viral load is developed to assess the progression of HIV/AIDS in patients on cART.

A cohort of HIV/AIDS patients from a rural clinic in northern South Africa was used. TB tests were carried out at enrolment and also at every follow up time for the cohort subjects.

Methods

Ethical considerations

The data collection procedures used in this study were as approved by the Research Ethics Committee of the University of Venda, South Africa (Protocol number SMNS/13/ MBY/01/0625), in accordance with the 1964 Helsinki declaration and its subsequent amendments. Additionally, permission to access health facilities was obtained from the Limpopo Provincial Department of Health, South Africa, and the collaborating health facilities. Informed consent was obtained from study participants prior to their involvement; and data obtained was stripped of personal identifiers to ensure the anonymity and confidentiality of the participants.

Data Description

The study cohort comprised 399 patients undergoing treatment follow up at a wellness clinic in Bela Bela, South Africa. The data was collected from 2004 to 2009. At the time of data extraction, patients with TB were on TB treatment. At enrolment, the baseline viral load, baseline CD4 cell count, and data on the presence of active TB was retrieved. TB cases, in this study, was the outcome of a diagnostic process comprising a combination of laboratory (microscopy and culture) and clinical investigations.

From these patients, 338 had a viral load at baseline above 10 000 copies/mL and 55 had a viral load at baseline of 10 000 copies/mL or below. 353 patients had a baseline CD4 cell count of 350cells/mm^3 or below and 46 had a baseline CD4 cell count above 350 cells/mm^3. Females comprised 69.1% (n=276) of the cohort. The variable age had a skew value of -0.44 at baseline, an indication that the majority of the patients were young adults. The variables; age at baseline, viral load at baseline and CD4 at baseline, are further described in Table 1.

Table 1: Descriptive summary for Age, viral load at baseline and CD4 cell count at baseline

	Age	VLBL (copies/mL	CD4BL(cells/mm^3)
Minimum	15	<50 (undetectable)	16
First Quartile	32	21 334	38
Mean	38.3	138 208	163
Median	39	67 995	116

Third Quartile	47	201 445	206
Maximum	77	>500 000	1 202

From the 399 patients, 292 (73.18%) had TB co-infection. 261 (65%) of the HIV/TB co-infected patients were enrolled at the clinic when they already had active TB. However, 89 (22%) patients developed active TB whilst on treatment. Post treatment, 58 (22%) of the patients who were once cured of TB became actively infected with TB. 168 of the HIV/TB co-infected at enrolment were mostly administered with an initial combination therapy of D4T-3TC-EFV, 76 received an initial combination therapy of D4T-3TC-NVP, and 6 received AZT-3TC-LPV/r, 5 received ABC-AZT-3TC and 4 received D4T-3TC-LPV/r. These drugs belong to the nucleoside reverse transcriptase inhibitors (NRTIs) class.

However, although NRTIs are relatively affordable, they cause varying degrees of myopathy and neuropathy after long-term therapy (Currier, 2007). AZT causes myopathy, ddI and 3TC cause neuropathy, d4T causes neuropathy or myopathy and lactic acidosis (LA), and studies suggest that d4T causes lactic acidosis (LA) more frequently than ddI or AZT. Patients under treatment may experience virologic failure. In this paper, treatment failure is defined clinically and immunologically. Thus, the effect of lactic acidosis and peripheral neuropathy, together with other covariates, to the progression of HIV is analysed.

Limitations of the data

This is a retrospective set of data. Information on other comorbidities or opportunistic infections in AIDS were not available, so the observations should be understood in the context of these limitations. The intended outcome of combination antiretroviral therapy is to suppress viral loads to undetectable levels, in the absence or presence of comorbidities.

Piece-wise constant transition rate Markov model (PWC)

Modelling the non-homogeneous Markov model can easily be done using a piecewise constant intensities approach. This approach, according to Saint-Pierre et al. (2003) in the analysis of cancer, involves the inclusion of time-dependent covariates in a Markov model, making it easier to deal with non-homogeneous Markov models. This approach partitions the time axis into r continuous and disjoint intervals, $[\tau_{l-1}, \tau_l)$ where $l = 1, \dots, r+1$ and $\tau_{r+1} =$

∞ and assumes constant transition intensities in different time intervals. Consider a vector $z^*(t) = (z_0^*(t), z_1^*(t), \dots, z_r^*(t))'$ of artificially time-dependent covariates defined as:

$$z_0^*(t) = 0, \forall t$$

$$z_l^*(t) = \begin{cases} 0; if\ \tau_0 \le t < \tau_l, \\ 1; if t \ge \tau_l \end{cases}$$

Where $l = 1, \dots, r+1$. The model with transition intensities is as follows:

$$q_{ij}\left(t \middle| z^*(t)\right) = q_{ij}^{(0)} \exp\left\{\left(\beta_{ij}^*\right)' z^*(t)\right\}, i \ne j \qquad (1)$$

This approach to non-homogeneity in a Markov process is a step-wise method that assumes constant transition intensities in different time intervals. The parameters of this model are the baseline transition intensities $q_{ij}^{(0)}$, which represent transition intensities in the interval $[\tau_0, \tau_1)$ and the vector of regression coefficient β_{ij}^* associated with artificially time-dependent covariates. For this model, transition intensities are step-functions of time and defined for each interval as follows:

$$q_{ij}\left(t \middle| z_l{}^*(t)\right) = \begin{cases} q_{ij}^{(0)} & if\ \tau_0 \le t < \tau_1 \\ q_{ij}^{(1)} = q_{ij}^{(0)} exp\{\beta_{ij,1}^*\}; & if\ \tau_1 \le t < \tau_2 \\ \vdots & \\ q_{ij}^{(l)} = q_{ij}^{(0)} exp\{\beta_{ij,1}^* z_1^* + \beta_{ij,2}^* z_2^* + \cdots + \beta_{ij,l}^* z_l^*\}; & if\ if\ t \ge \tau_l \end{cases}$$

for $l = 1,2, \dots, r$

Incorporating the effects of covariates, represented by the vector $\boldsymbol{z}$, the model becomes:

$$q_{ij}(t|\boldsymbol{z}_l{}^*(t), \boldsymbol{z}) = q_{ij}^{(0)} exp\{\beta_{ij,l}{}^* \boldsymbol{z}_l{}^*(t) + \beta_{ij}{}' \boldsymbol{z}\}$$

Where β_{ij} is the log-linear effect relating to the instantaneous rate of transition from state 1 to state j to the covariate $\boldsymbol{z}$.

Computing $P(0, t_i)$ for a t_i in segment τ_l entails multiplying all the transition matrices across the various intervals as shown below;

$$P(0, t_i) = \left[\pi_{l=1}^{l-1} P^{(b)}(\pi_b)\right] P^{(l)}(t_{(l-1)}, t_j)$$

where $P^{(b)}$ is the transition probability matrix obtained using q_{ijb} for the b^{th} segment denoted by τ_b. If subjects are observed on an equal spaced grid and segments are divided up along these time points, then $p_{ij}(0, t_i)$ would simply be the $(ij)^{th}$ element of the matrix in the above equation. When data is not equally spaced, then observations would be considered missing at the breakpoints. To resolve this, a model that accounts for all possible pathways between the last observed state in the segment b_{l-1} and the first observation in segment b_0

was suggested. For example, if a breakpoint t' is created between two points t_j and t_k, then via Chapman-Kolmogorov equations, the likelihood contribution from interval (t_j, t_k) for individual x can be found as;

$$L_x = \sum_{l=1}^{k} P_{il}^{(1)}(t_j, t') P_{lj}^{(2)}(t', t_k)$$

for states i, j.

Model formulation

Patients were put on combination antiretroviral therapy (cART) at time t=0. The patients were monitored after 3 months (0.25 years) of cART and thereafter in follow up intervals of 6 months (0.5 years). Follow up was done for a maximum of 5 years but due to some deaths and withdrawal cases associated with the data, the average follow up time for each patient in this study is 3.5 years. At follow up times, the effectiveness of cART was assessed by changes in the HIV viral load level. Attainment of a suppressed viral load below level of detection within the first 6 months indicated good adherence to treatment and effectiveness of cART. In this study, the level of detection is 50 viral RNA copies/mL.

The viral load levels during the course of treatment for each individual were classified into states based on the severity of the patient's condition as follows:

$$Viral\ load\ state\ (VLS) = \begin{cases} 1, & if\ VL < 50 \\ 2, & if 50 \leq VL < 10\,000 \\ 3, & if\ 10\,000 \leq VL < 100\,000 \\ 4, & if\ 100\,000 \leq VL < 500\,000 \\ 5, & if\ VL \geq 500\,000 \\ 6, & if\ dead \\ 7, & if\ loss\ to\ follow\ up \end{cases}$$

States $i = 1,2,3,4,5$ are the live/transient states and states 6 and 7 are the absorbing states. Transitions from state i to $i + c$, for $c > 0$, represent disease progression to worse states and transitions from state i to state $i - c$, for $c > 0$, represent disease progression to better states. At t=0 there were 2 patients in viral load state **1**; 42 in state **2**; 174 in state **3**; 135 in state **4**; and 45 in state **5**. This confirms that at treatment initiation, most patients had viral load between 10 000 and 100 000 copies/mL (state 3).

Table 2 below is a state table that shows the possible transitions, from state i to state j, $j = i \pm c$, that occurred during the study period:

Table 2: State Table

	To(*j*)						
From(*i*)	**1**	**2**	**3**	**4**	**5**	**6**	**7**
1	1185	94	22	2	0	22	53
2	198	105	27	4	2	14	24
3	105	71	34	2	0	27	14
4	55	70	8	2	4	17	0
5	13	22	0	8	0	3	2

Table 2 shows that most states are accessible from each other. Of interest is the undetectable viral load state (state 1), which is accessible from all transient states. Thus, basing on these transitions, the following transition diagram is proposed:

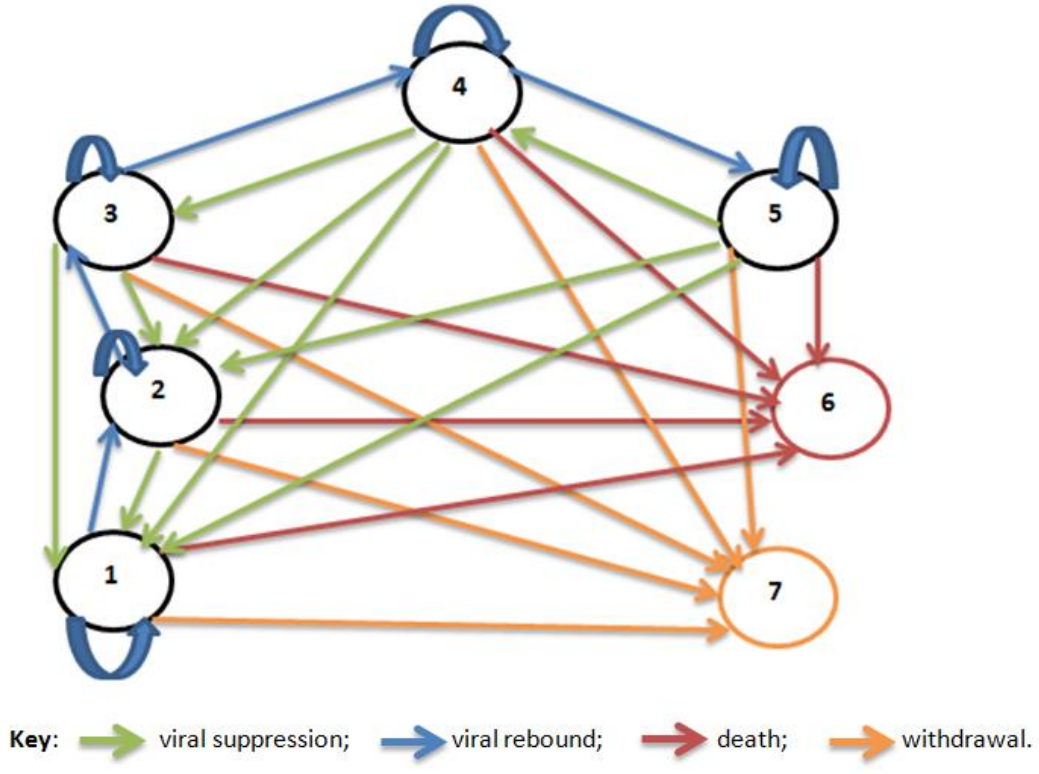

Figure 1: Transition Diagram

The arrows in the diagram represent possible transitions between states. Green arrows represent viral suppression. Blue arrows represent viral rebound and red arrows represent

absorption into the death state. Orange arrows represent loss to follow-up. Transitions between states can be represented by the transition matrix below:

$$Q(t) = \begin{pmatrix} q_{11} & q_{12} & 0 & 0 & 0 & q_{16} & q_{17} \\ q_{21} & q_{22} & q_{23} & 0 & 0 & q_{26} & q_{27} \\ q_{31} & q_{32} & q_{33} & q_{34} & 0 & q_{36} & q_{37} \\ q_{41} & q_{42} & q_{43} & q_{44} & q_{45} & q_{46} & q_{47} \\ q_{51} & q_{52} & 0 & q_{54} & q_{55} & q_{56} & q_{57} \\ 0 & 0 & 0 & 0 & 0 & 0 & 0 \\ 0 & 0 & 0 & 0 & 0 & 0 & 0 \end{pmatrix}$$

The force of transition from state i to j is defined as:

$$q_{ij}(t) = \frac{d}{dt} p_{ij}(t)|_{t=0} = \lim_{\Delta t \to 0} \frac{p_{ij}(\Delta t) - \delta_{ij}}{\Delta t}$$

q_{ij}, for $i = 1, \ldots, 5$ and $j = 1, \ldots, 7$, vary over time and satisfies the following conditions; $\sum_{j \in X} q_{ij}(t) = 0$ and $q_{ii}(t) = -\sum_{i \neq j} q_{ij}(t)$. Once the transition intensities are estimated, the probabilities that state j is next subject in the long run, on condition that the patient was in state i, is given as $p_{ij} = \frac{q_{ij}}{\lambda_i}$, for each i and j where $\lambda_i = \sum_{j \in X} q_{ij}(t)$, such that $i \neq j$, is the total time spent in state *i* before a jump to state *j*. For example $p_{12} = \frac{q_{12}}{q_{12}+q_{16}+q_{17}}$.

The effects of the covariates gender, age, virologic failure (VF), treatment failure (TF), viral load level baseline (VLBL), peripheral neuropathy (PN), having TB before enrolment (TBB4), developing TB whilst on ART (TBEN), lactic acidosis (LA) and the effect of time on transition intensities is assessed. Peripheral neuropathy and lactic acidosis are long-term effects of the NRTI class. Virologic failure is defined as having a viral load of at least 1000 copies/mL in two consecutive visits or having a viral load above 1000 copies/mL in the first 6

months of cART initiation. In this paper, treatment failure is defined immunologically and clinically. These covariates are coded as follows:

$$\text{Age} = \begin{cases} 1, & \leq 45\ years \\ 0, & > 45\ \text{years} \end{cases}, \quad \text{VF} = \begin{cases} 1, & Yes \\ 0, & \text{No} \end{cases}, \quad \text{TBB4} = \begin{cases} 1, & Yes \\ 0, & \text{No} \end{cases}, \quad \text{LA} = \begin{cases} 1, & Yes \\ 0, & \text{No} \end{cases}$$

$$\text{TBEN} = \begin{cases} 1, & Yes \\ 0, & \text{No} \end{cases}, \quad \text{Gender} = \begin{cases} 1, & male \\ 0, & female \end{cases}, \quad \text{TF} = \begin{cases} 1, & Yes \\ 0, & \text{No} \end{cases}, \quad \text{PN} = \begin{cases} 1, & Yes \\ 0, & \text{No} \end{cases}$$

$$\text{VLBL} = \begin{cases} 1, & > 10\,000\ copies/\mu L \\ 0, & \leq 10\,000\ copies/\mu L \end{cases}, \quad \text{Time} = \begin{cases} 0; & if\ 0 \leq t < 0.5 \\ 1; & if\ t \geq 0.5\ years \end{cases}$$

$$\text{CD4BL} = \begin{cases} 1, & \leq 350 cells/mm^3 \\ 0, & > 350\ cells/mm^3 \end{cases}$$

So that the piecewise constant Markov model becomes:

$$q_{ij}(t|\boldsymbol{z}_l^*(t), \boldsymbol{z}) = q_{ij}^{(0)} exp\{\beta_{ij,l}^{*\prime} \boldsymbol{z}_l^*(t) + \beta_{ij}{}' \boldsymbol{z}\}$$

$$\text{where } \boldsymbol{z} = \left\{ \begin{array}{c} Age, virologic\ failuer\ (VL), TB\ before\ \ treatment\ (TBB4),, \\ Lactic\ Acidosis\ (LA) TB\ whilst\ on\ cART(TBEN), Gender, \\ Treatment\ Failure\ (TF), Peripheral\ neuropathy\ (PN), \\ Viral\ load\ at\ baseline\ (VLBL), Time, CD4\ at\ baseline\ (CD4BL) \end{array} \right\}$$

Results

In this section, a continuous time non-homogeneous Markov model for the effects of time $t \geq 0.5\ years$, viral load baseline , gender, having TB co-infection, having active TB before enrolment, developing active TB on treatment , peripheral neuropathy, lactic acidosis, virologic failure and treatment failure on virology is defined by the equation;

$$q_{ij}(t|z^*(t), \boldsymbol{z}) = q_{ij}^{(0)} \exp\{\boldsymbol{\beta}_{ijl}^{*\prime} \boldsymbol{z}_l^*(t) + \boldsymbol{\beta}_{ij}{}' \boldsymbol{z}]\}, i \neq j$$

The parameters $q_{ij}^{(0)}$ are the baseline transition intensities for intervals $[0, 0.5 year)$, $\boldsymbol{\beta}_{ijl}^*$ is the vector of regression coefficients associated with the artificial time-dependent covariates $\boldsymbol{z}_l^* = [1, 0]'$ as defined earlier on, $\boldsymbol{\beta}_{ij}$ is the vector of regression coefficients associated with

covariates $\boldsymbol{z}$=[VLBL, Gender, TB, TBEN, TBB4, PN, LA, VF, TF]′. The results from the fitted model are shown in the Table 3 below;

Table 3: Effects of different variables on transition intensities based on viral load states

State i - j	**Baseline** $q_{ij}^{(0)}$	**VLBL**	**Gender**	**TB**	**TBEN**	**TBB4**	**PN**	**LA**	**VF**	**TF**	**Time [0.5,Inf)**
State 2-1	2.333	-0.063	0.191	-1.624	0.216	0.973	0.767	-0.038	-1.337	-0.353	-1.003
State 3-1	0.966	0.424	0.479	0.419	-0.504	-0.121	1.523	1.346	-1.091	-0.585	-2.719
State 4-1	0.545	0.145	0.259	0.137	0.413	0.576	-0.014	0.517	-0.124	-0.119	-0.778
State 5-1	0.427	0.222	-0.203	-0.201	0.532	-0.008	-0.229	0.244	-0.055	-0.039	-0.879
State 1-2	0.410	0.017	-0.016	-0.539	0.032	-0.139	0.116	0.18	1.985	-0.08	-1.394
State 3-2	2.775	-0.022	-0.660	0.460	-0.625	-0.832	-0.601	-0.298	-0.232	-1.046	-2.041
State 4-2	4.978	0.159	-0.583	-0.375	-0.355	1.219	-0.503	0.069	-0.049	0.229	-1.626
State 5-2	2.428	0.129	-0.338	0.621	0.441	1.080	0.200	-0.077	0.289	-0.076	-1.432
State 2-3	0.852	1.403	-0.789	-1.530	0.493	1.010	-0.132	0.685	1.265	0.879	-0.660
State 4-3	0.148	0.082	-0.068	-0.131	-0.026	-0.071	0.147	-0.057	-0.010	-0.006	-0.132
State 3-4	0.439	0.315	-0.195	0.516	0.896	0.590	0.452	-0.803	0.339	-0.522	-0.023
State 5-4	1.108	0.315	0.272	-0.521	1.004	-1.475	-0.223	-0.759	-0.069	-0.064	-1.578
State 4-5	0.456	0.253	0.695	-0.953	-0.429	-0.775	-0.315	-0.852	0.748	-0.044	-1.222
State 1-6	0.010	0.809	-0.742	-1.451	0.560	-2.716	-1.120	-1.316	0.024	-0.103	-2.345
State 2-6	0.032	0.453	0.572	-0.316	1.151	-2.083	-0.232	-1.001	-0.333	-0.153	-0.396
State 3-6	0.040	0.064	0.116	-0.163	0.280	-0.915	0.006	-0.404	-0.290	-0.201	-0.434
State 4-6	0.138	0.092	0.014	-0.101	0.459	-0.423	-0.188	-0.133	-0.034	-0.029	0.398
State 5-6	0.106	0.018	0.185	-0.078	0.041	-0.157	-0.032	-0.050	-0.032	-0.002	-0.053
State 1-7	0.037	0.564	-0.577	-0.990	-0.081	-1.572	-1.518	-1.733	0.087	0.235	0.776
State 2-7	0.103	-0.524	-0.036	0.010	0.161	0.303	-0.448	-1.556	0.007	-0.126	-0.139
State 3-7	0.080	-0.018	0.016	-0.176	-0.005	-0.218	-0.077	-0.217	-0.005	-0.171	0.141
State 4-7	0.056	-0.048	0.034	0.014	-0.099	0.069	-0.005	0.037	0.015	0.004	0.214
State 5-7	0.101	0.009	0.157	-0.163	-0.084	-0.118	-0.0222	-0.036	-0.027	-0.001	0.248
-2LL	2869.38										

Key: VLBL=Viral load at baseline; TB=Tuberculosis either at entry or whilst on cART; TBEN=Developing Tuberculosis during cART; TBB4=Tuberculosis before cART initiation; PN=Peripheral neuropathy; LA=Lactic Acidosis; VF= virologic failure; TF=Treatment failure.

Results show that when the viral load of a patient is below 100 000 copies/mL, rates of viral suppression are higher than rates of viral rebound. The undetectable viral load (state 1) is accessible from all the states. The rate of attainment of an undetectable viral load depends with the condition of a patient. Patients with the highest viral copies/mL (state 5) have the lowest risk of attaining an undetectable viral load whereas patients with the lowest viral copies/mL (state 2) have the highest chance of attaining an undetectable viral load.

Developing active TB whilst on ART (TBEN) increases the rates of viral rebound from an undetectable level (state 1) to a viral load measurement above 50 copies/mL and below 10 000 copies/mL (state 2). If the TB is detected at enrolment (TBB4), there are reduced rates of viral rebound from state 1 to state 2. However, detecting TB co-infection, be it at enrolment or during the course of treatment, reduces viral rebound from state 1 to state 2. Virologic failure is experienced from state 1 to state 2. Other factors that contribute to viral failure from undetectable levels are peripheral neuropathy and lactic acidosis. From 0.5 years of treatment and beyond, there is reduced viral rebound from undetectable levels. Thus, more time on cART reduces rates of viral rebound.

Table 3 shows virologic rebound from a viral load state between 50 and 10 000 copies/mL (state 2) to a viral load state between 10 000 copies/mL and 100 000 copies/mL (state 3). The virologic failure is due to effects of developing TB on treatment (TBEN), having TB at enrolment (TBB4), Lactic acidosis, treatment failure and having a viral load baseline above 10 000 copies/mL at enrolment.

Patients mostly experience virologic failure in state 4 (viral load baseline between 100 000 and 500 000 copies/mL). These patients experience a viral rebound back to a viral load level above 500 000 copies/mL (state 5). Males are also at higher risk of experiencing a rebound from state 4 to state 5 compared to their female counterparts.

Results show an increased rate of mortality (state 6) from an undetectable viral load (state 1) for patients who enrolled with a viral load baseline above 10 000 copies/mL, patients who developed active TB whilst on cART and for patients who experienced virologic failure. Patients who developed active TB whilst on cART have accelerated rates to mortality regardless of the state of a patient.

Next we estimate long run probabilities of state j being the next state given the condition that the patient was initially in state i, referred to as the jump process. This is when a Markov process is observed at the times it makes transitions to a new state. In other words, a jump process is a stochastic matrix R of probabilities where each row sums to one on the state space X_t, which gives the conditional probability of the next state an individual goes to, after leaving state i. If $q_{ii} > 0$, then given that there is a jump to a different state, implies the patient will not stay in state i, the patient makes a jump out of state i resulting in $R_{ii} = 0$ and if $q_{ii} = 0$, then the patient will never leave state i, implying that $R_{ii} = 1$ (in States 6 and 7).

The computed matrix of probabilities of each state being next (also known as the jump process), together with the mean sojourn times in each state, fully define a continuous-time Markov model. This is a more intuitively meaningful description of a model than the transition intensity matrix. The matrix for the probabilities that the next state after state i is state j is approximated as $p_{ij} = \frac{q_{ij}}{\lambda_i}$, for each i and j such that $i \neq j$. q_{ij} is the force of transition from state i to state j and q_{ii} is the total force of transition out of state i. For example, the probability that state 2 is next given that the patient is initially in state 1 is given by $p_{12} = \frac{q_{12}}{\lambda_1} = \frac{0.410}{0.410+0.010+0.037} \approx 0.897$, as shown in the matrix below. The results are shown in Table 4 below:

Table 4: Probability of each state being next (jump chain)

From (*i*)	**To (*j*)**						
	State 1	**State 2**	**State 3**	**State 4**	**State 5**	**State 6**	**State 7**
State 1	0	0.897	0	0	0	0.022	0.081
State 2	0.703	0	0.257	0	0	0.010	0.031
State 3	0.225	0.645	0	0.102	0	0.009	0.019
State 4	0.086	0.787	0.023	0	0.072	0.022	0.009
State 5	0.102	0.582	0	0.266	0	0.025	0.024
State 6	0	0	0	0	0	1	0
State 7	0	0	0	0	0	0	1

Results from Table 4 show an increase in the probabilities of transition to death with increasing viral load states resulting in patients with viral load levels above 500 000 copies/µL having highest chances of transitions to death. For patients with viral load above 10 000 copies/µL (state 3, state 4, and state 5), probabilities of viral suppression to levels between 50 and 10 000 copies/µL (state 2) are higher compared to transitions to any other states. The results generally show higher chances of transitions to viral suppression than viral rebound, an indication of treatment efficacy.

Figure 2 below, shows the plots of percentage prevalence in each state from time of treatment commencement to the end of the study period.

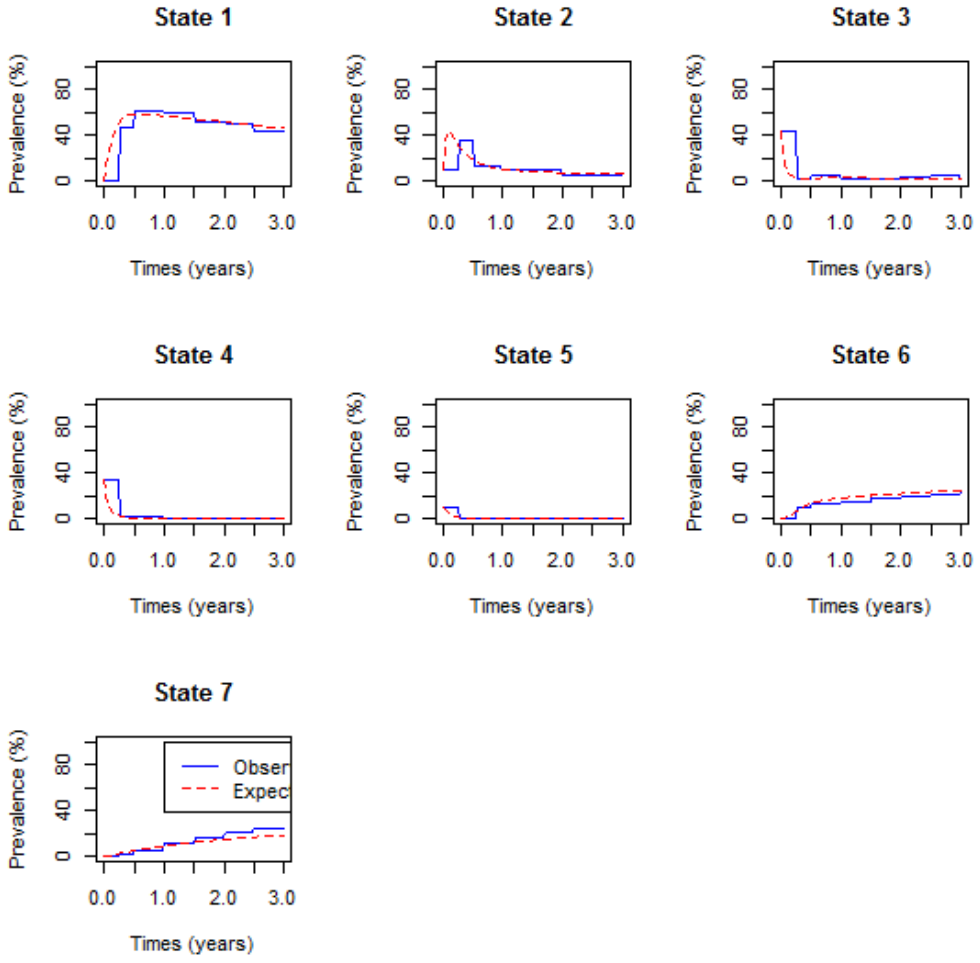

Figure 2: Percentage prevalence in each state from time of treatment commencement to 3 years post-treatment commencement

The model gives almost a perfect fit of the observed data. The plots show an increase in percentage prevalence during the first 0.5 years for state 1 or the undetectable viral load state. After 1.5 years, there is a slight drop in percentage prevalence from state 1. This could be attributed to factors such as developing active TB on cART, virologic failure, peripheral neuropathy and lactic acidosis as revealed in Table 3.

Discussion

In this study, a continuous-time non-homogeneous Markov model is used to model the progression of HIV/TB co-infected patients receiving cART at a South African rural clinic. Non-homogeneity of transition intensities is approached using a piecewise constant model, thus, allowing transitions to vary between different time segments. The effects of viral load prior to treatment initiation, gender, developing active TB whilst on cART, having TB at

enrolment, peripheral neuropathy, lactic acidosis, virologic failure and treatment failure on HIV/AIDS progression defined by transition intensities is assessed.

Results from the analysis show a bi-directional movement between HIV states, thus revealing a possibility of viral rebound and viral suppression. However, transitions to suppressed viral loads are higher than transitions to viral rebound. This is quite encouraging since it shows efficacy of ART in reducing viral load as expected. Results also show that, from any viral load state, undetectable viral load state can be attained. This varies from state to state with patients in lower viral load levels having better chances of attaining undetectable viral loads than patients in higher viral load levels. This takes place during the first 0.5 years of treatment uptake, according to our findings, which shows a rapid increase in state 1 (undetectable viral load) prevalence within the first 0.5 years.

Findings from this study reveal that, although the undetectable viral load state can be attained from any HIV state, there are some factors that increase the rate of viral rebound from undetectable levels to viral loads between 50 and 10 000 copies/mL. The results reveal increased rates (by more than 7 folds) of virologic failure from undetectable viral load levels to viral loads between 50 and 10 000 copies/mL. This is attributed to the development of active TB whilst on ART, lactic acidosis and peripheral neuropathy, with the development of active TB on cART the major cause. However, if TB is detected at enrolment, the rates of viral rebound from undetectable levels are reduced. This is corroborated by the studies by WHO (2017) which suggested early diagnosis and timely treatment of TB to reduce the risks of virologic rebound.

The risk of virologic failure from between 50 and 10 000 copies/mL to a state between 10 000 and 100 000 copies/mL increases by approximately 3.5 times. This happens for patients who had TB at enrolment, developed some or all of TB on ART, lactic acidosis, treatment failure and having a viral load baseline above 10 000 copies/mL at enrolment. In this case, developing active TB before initiation of cART is the major player.

Our findings generally reveal that patients mostly experience virologic failure in state 4 (that is, viral load baseline between 100 000 and 500 000 copies/mL). These patients experience a viral rebound to a viral load level above 500 000 copies/mL (state 5). Virologic failure coupled with development of active TB whilst on ART increase rates of HIV/AIDS progression as well as mortality from HIV/AIDS after achieving an undetectable viral load. Bulage et al. (2017), in their findings, suggested that having active TB increases the odds of

virologic non-suppression. Patients who developed active TB whilst on cART experienced increased rates of transitions to death irrespective of their HIV/AIDS state. The highest rates are experienced when viral load levels are between 50 and 10 000 copies/mL where patients who developed active TB on cART are 3.2 times more likely to experience death than patients who did not develop active TB. Our findings are in congruence with the findings by Bekker et al. (2011) and von Reyn et al. (2010) which show higher rates of mortality in HIV patients with virologic failure and co-infected with TB. Bekker et al. 2011 also observed that onset of tuberculosis in HIV-infected patients is associated with an increased risk of AIDS and death. Hence, it is proposed that virologic failure be regularly monitored in HIV patients coinfected with TB. This should be done every two months and decisions made on alternative treatment approaches to prevent potential mortality.

Conclusion

In conclusion, the findings reveal the importance of time in monitoring HIV/AIDS progression for patients with virologic failure as well as TB co-infection. A piecewise constant approach to non-homogeneous Markov modelling is used and shows two different trends in HIV/AIDS progression, that is, a sharp increase in state 1 (undetectable viral load level) prevalence in the first 0.5 years of treatment followed by a slowly decreasing prevalence trend thereafter. The model, not surprisingly, confirms that virologic failure increases the risk of death. However, it suggests that whilst TB at the time of ART initiation does not increase the risk of viral rebound, the development of active TB after initiation of ART does increase the risk of viral rebound. This highlights the importance of strengthening viral load monitoring, especially in people at risk of TB, and addressing unsuppressed viral loads in this category of patients.

Acknowledgements

Pascal Bessong's research is supported by the South African Medical Research Council (RCDI) through funding received from the South African National Treasury; and the South African National Research Foundation (GUN109312, GUN86037). The views expressed here are solely the responsibility of the authors and do not necessarily represent the official views of the South African Medical Research Council or the National Research Foundation.

References

1. Badri M, Ehrlich R, Wood R, Pulerwitz T, Maartens G.Association between tuberculosis and HIV disease progression in a high tuberculosis prevalence area. Int JTuberc Lung Dis. 2001;5:225–32
2. Bekker LG and Wood R. TB and HIV co-infection: when to start antiretroviral therapy: Guidelines on when to start therapy in TB and HIV co-infection. CME, 2011 Vol 29, No 10.
3. Bruisker T, Dufour MK, MPH, PhD, and Myers JJ. Recall of Nadir CD4 Cell Count and Most Recent HIV Viral Load Among HIV-Infected, Socially Marginalized Adults. AIDS Behav, 2015; 19(11): 2108–2116. doi:10.1007/s10461-015-1018-x
4. Bulage L, Ssewanyana I , Nankabirwa V, Nsubuga F, Kihembo C et al. Factors Associated with Virological Nonsuppression among HIV-Positive Patients on Antiretroviral Therapy in Uganda, August 2014–July 2015. BMC Infectious Diseases (2017) 17:326 DOI 10.1186/s12879-017-2428-3
5. Chenand B and Zhou Xiao-Hua. Non-homogeneous Markov process models with informative observations with an application to Alzheimer's disease. Biom J. 2011; 53(3):444-463.
6. Cohen K and Meintjes G. Management of individuals requiring ART and TB treatment. Curr Opin HIV AIDS. 2010 January; 5(1): 61–69. doi:10.1097/COH.0b013e3283339309
7. Day JH, Alison D. Grant, Katherine L. Fielding, Lynn Morris, Victoria Moloi, Salome Charalambous, Adrian J. Puren, Richard E. Chaisson, Kevin M. De Cock, Richard J. Hayes,1 and Gavin J. Churchyard. Does Tuberculosis Increase HIV Load? The Journal of Infectious Diseases 2004; 190:1677–84
8. Duffy MJ, Blaser J, Duggan C, Mcdermott E, O'higgens N, Fen-Nelly JJ and Tschesche H. Assay of metalloproteases types 8 and 9 by ELISA in human breast cancer. Br. J. Cancer, 71:1025-1028, 1995.
9. Gunda D W, Kidenya BR, Mshana SE, Kilonzo SB and Mpondo BCT. Accuracy of WHO immunological criteria in identifying virological failure among HIV‑infected adults on First line antiretroviral therapy in Mwanza, North‑western Tanzania. *BMC Res Notes (2017) 10:45* DOI 10.1186/s13104-016-2334-6
10. Kalbfleisch JD, Lawless JF. The analysis of panel data under a Markov assumption. J Am Stat Assoc. 1985; 80(392): 863-71.

11. Lee S, Ko J, Tan X, et al. Markov Chain Modelling Analysis of HIV/AIDS Progression: A Race Based Forecast in the United States. Indian J Pharm Sci. 2014; 76(2): 107-115
12. Lindsay JC and Ryan LM, A three-state multiplicative model for rodent tumorigenicity experiments, Applied Statistics, 42: 283-300, 1993.
13. Marshall G, and Jones R.H., Multi-state Markov models and diabetic retinopathy. Statist. Med., 14:19751983, 1995.
14. Martinson NA, Hoffmann CJ, Chaisson RE. Epidemiology of tuberculosis and HIV: Recent advances in understanding and responses. Proc Am Thorac Soc, 2011b; 8: 288–293.
15. Pan W, and Kastin AJ, Tumor necrosis factor and stroke: role of the blood-brain barrier, Progress in neurobiology 83:363-374, 2007.
16. Pawlowski A, Jansson M, Skold M, Rottenberg ME, Kallenius G. Tuberculosis and HIV Co-Infection. PLoS Pathog, 2012; 8(2): e1002464.doi:10.1371/journal. ppat.1002464
17. Saint-Pierre P, Combescure C, Daurès JP, et al. The analysis of asthma control under a Markov assumption with use of covariates. Statistics in Medicine. 2003; 22, 3755–3770.
18. Sigaloff KCE, Hamers RL, Wallis CL, Kityo C, Siwale M, Ive P, et al. Unnecessary antiretroviral treatment switches and accumulation of HIV resistance mutations; two arguments for viral load monitoring in Africa. J Acquir Immune Defic Syndr. 2011;58:23–31. http://www.ncbi.nlm.nih.gov/pubmed/21694603.
19. Stead D. Southern African HIV clinicians society. Guidelines. HIV clinicians adult guideline 2017 CME. East London CME: 25 November 2017.
20. UNAIDS Data. 2018. https://www.unaids.org/sites/default/files/media_asset/unaids-data-2018_en.pdf
21. von Reyn CF, Mtei L, Arbeit RD, et al. Prevention of tuberculosis in bacille Calmette-Guerin-primed, HIV-infected adults boosted with an inactivated whole-cell mycobacterial vaccine. AIDS 2010; 24:675–85.
22. World Health Organization (WHO). Global tuberculosis control [WHO/CDS/TB/2001.287.2001]. Geneva: WHO, 2001.
23. Yen A. M. F, Chen T. H. H, Mixture Multi-State Markov Regression Model, J Appl Stat, 34: 11-21,2007.

A Markov model for the effects of virologic failure on HIV/AIDS progression in TB co-infected patients receiving antiretroviral therapy in a rural clinic in northern South Africa

Claris Shoko[1*](claris.shoko@gmail.com), Delson Chikobvu[1] (Chikobvu@ufs.ac.za) and Pascal O. Bessong[2] (pascal.bessong@univen.ac.za)

Authors' affiliation:

[1]Department of Mathematical Statistics and Actuarial Sciences, University of the Free State, P.O. Box 339, Bloemfontein, 9300, South Africa.

[2]HIV/AIDS & Global Health Research Programme, University of Venda, PMB X5050 Thohoyandou, 0950, South Africa.

[*]**Correspondence:** claris.shoko@gmail.com, Department of Mathematical Statistics and Actuarial Sciences, University of the Free State, Bloemfontein, South Africa.

Abstract

Background: The goal of antiretroviral therapy (ART) is to suppress viral replication to undetectable levels. In some patients, these low viral load levels may not be attained and therefore represent potential virologic failure. This study presents the results of a Markov model, exploring how virologic failure and active TB affect the progression of HIV in people on ART.

Method: A continuous time non-homogeneous Markov model is used to model the progression of HIV/AIDS in patients on combination antiretroviral therapy (cART). We define seven states in our model. The first five states are based on viral load levels and the other two are absorbing states; death and withdrawal from study. The effects of TB co-infection, viral load baseline, lactic acidosis and treatment failure on transition intensities is assessed.

Results: The model shows that viral load based transition intensities do not follow a constant rate; rather, two different trends in HIV/AIDS progression. The first type of trend is an increase in the prevalence in state 1 (undetectable viral load levels) in the first 0.5 years of treatment. The second trend follows thereafter and shows a slowly decreasing trend. Thus,

within the first 0.5 years of therapeutic intervention, the undetectable viral load state is attained from any viral load state. However, in cases where virologic failure is mentioned, there is increased risk of death. Developing TB whilst on cART increases the risks of viral rebound from undetectable levels to viral loads between 50 and 10 000 copies/mL by 1.03 folds. From a viral load between 10 000 and 100 000, developing active TB whilst on cART increases the rate of viral rebound by approximately 2.5 folds. However, if TB is detected and treated at enrolment, the rates of viral rebound from undetectable levels are reduced.

Conclusion: The model confirms that virologic failure, coupled with developing active TB whilst on ART, increase rates of mortality irrespective of the patient's HIV state. It also suggests that whilst TB at the time of cART initiation does not increase the risk of viral rebound, the development of active TB after cART initiation does increase the risk of viral rebound. These highlight the importance of strengthening viral load monitoring, every two months, especially in people with TB, and to appropriately address unsuppressed viral loads once detected.

Background

The Joint United Nations Programme on AIDS (UNAIDS) reported that about 37 million people were living with HIV globally, with an estimated 17 million accessing antiretroviral therapy (ART) in 2017 (UNAIDS, 2018). South Africa has one of the highest burdens of HIV in the world. In 2017, UNAIDS reported that there were an estimated 7.1 million people living with HIV, 270 000 new HIV infections, and about 110 000 AIDS related deaths. Of those living with HIV, only about 45% had suppressed viral loads (UNAIDS, 2018). The South African comprehensive treatment plan is an approach to ensure that 90% of those infected with HIV are detected, 90% of those diagnosed are treated, and viral suppression is attained in 90% of all those under treatment (The 90-90-90 objective).

HIV infection is characterised by a progressive depletion of the CD4+ T-cell populations. This increases the risk of latent tuberculosis (TB) reactivation 20-fold (Pawlowski et al., 2012); and the risk of developing active TB has been shown to be significantly greater shortly after HIV infection (Bulage et al., 2017). Martinson et al. (2011b), showed that between 60-80% of people with TB in Southern Africa are HIV positive, emphasizing TB as an important common opportunistic infection among HIV infected individuals.

The use of cART in HIV/AIDS patients is characterised by an increase in CD4+ cell counts and a decrease in viral load to undetectable levels (Bruisker et al., 2015). However, management of HIV infections in TB co-infected patients has been a challenge due in part to drug interactions between rifampicin and non-nucleosides reverse transcriptase inhibitors (NNRTIs) and protease inhibitors (PIs), and concerns about adherence and virologic failure (Cohen and Meintjes, 2010). The World Health Organisation (WHO) (2001) emphasised the need to further strengthen TB control between 2002 and 2020 otherwise a billion people will be newly infected with *Mycobacterium tuberculosis*, more than 150 million would develop active TB disease and 36 million would die of TB. Day et al. (2004) suggested that active TB accelerates HIV disease progression, but not much data are available to confirm or refute this hypothesis. Day et al. (2004) argued that although antiretroviral therapy is required for a major effect on survival in HIV-infected individuals, prevention of TB is important for the reduction of HIV-related morbidity and mortality. Hence, there is need to consider virologic failure and TB control in tandem to minimise the consequences of partial or incomplete viral suppression.

Virologic failure is due to patient-factors like non-adherence to treatment or due to ART regimen factors like peripheral neuropathy and lactic acidosis, drug resistance or drug-drug interactions. Constant monitoring of viral load levels (states) helps in avoiding unnecessary switching to second line therapy that could have happened with clinical (WHO stage) and immunologic criterion (CD4+ cell counts). Routine viral load monitoring helps in early detection of virologic failure (Sigaloff et al., 2011) as patients are observed making random transitions from one viral load state to another.

The random movement from one viral load state to the other is regarded as a stochastic process. HIV/AIDS progression is split into various states of the disease based on the viral load measurement including the endpoints, death state and withdrawal from study (loss to follow-up). Stochastic processes allow random movements between viral load states before an HIV/AIDS patient is finally absorbed into the death state (Lee et al., 2014). Patients are monitored only at visit times resulting in the exact time the transition has occurred not known (Chenand and Zhou, 2011). When transition times are not known and interval censored observations are present, homogeneous and non-homogeneous Markov processes are an important field of research into stochastic processes (Kalbfleisch and Lawless, 1985). Non-

homogeneous models are particularly important when transitions rates between diseases states are not constant but allowed to change with time to mimic better, observed reality.

The Markov model is an appropriate stochastic approach when the present state of the patient summarises all previous information (known as the history or natural filtration of the process). Time-homogeneous Markov models have been widely used in the modelling of different disease progressions such as cancer (Duffy et al., 1995, Yen and Chen, 2007), stroke (Pan and Kastin, 2007) and diabetic retinopathy (Marshall and Jones, 1995). However, the assumption of time-homogeneity is unrealistic in the sense that over long periods the diseases evolve resulting in changes in transition intensities. The use of time-homogeneous models then puts severe limitations on disease history behaviour. In particular, when dealing with HIV, it is more realistic to assume that science and medicine evolve, hence the rate at which patients change in severity of the disease is likely to change as newer medications will improve the quality of their lives (Pan and Kastin, 2007). This justifies the need for continuous-time non-homogeneous models in analysing disease progressions. The problem can be addressed by using piecewise constant transition rate Markov models that preserve the tractability of the constant rates (Lindsay and Ryan, 1993).

In this study, a non-homogeneous Markov process, using a piecewise constant transition rate model approach, is used to model the progression of HIV/AIDS in patients with TB co-infection. The states of the Markov process are based on viral load measurements followed by absorbing states, death or withdrawal from study. The viral load (VL) states are defined as follows; **1**: VL<50 copies/mL; **2**: $50 \leq VL < 10\,000$; **3**: $10\,000 \leq VL < 100\,000$; **4**: $100\,000 \leq VL < 500\,000$; and **5**: $VL \geq 500\,000$. State 1 is accessible from any VL state. The effects of virologic failure and TB, among others, on HIV/AIDS progression are assessed. The inclusion of the effects of virologic failure on HIV progression in patients with TB co-infection prompted the current analysis research and also the use of a continuous-time non-homogeneous Markov model in which the undetectable viral load is accessed from any of the five viral load states.

The South African description of virologic failure is as follows: (i) two consecutive VL greater than 1000 copies/ml after previous suppression (ii) one VL > 1000 copies/ml after previous suppression followed by a change in treatment (iii) one VL > 1000 copies/ml after 6 months on ART without suppression. This is in line with the Adult Guideline from the

South African Department of Health which proposed a virologic failure threshold of 1000 copies/mL (Stead, 2017).

Although in resource limited areas, viral load levels monitoring may not be routinely available, viral load levels monitoring helps in detection of treatment failure and in avoiding unnecessary switching to second line treatment that could happen when clinical and immunological criteria are used (Gunda et al., 2017). Treatment failure is defined clinically as a new or recurrent event indicating severe immunodeficiency or immunological failure as persistent CD4+ T-cell count levels are below 100 cells/mm^3 after 6 months of treatment. In this paper, a continuous-time non-homogeneous Markov model with states based on viral load is developed to assess the progression of HIV/AIDS in patients on cART.

A cohort of HIV/AIDS patients from a rural clinic in northern South Africa was used. TB tests were carried out at enrolment and also at every follow up time for the cohort subjects.

Methods

Ethical considerations

The data collection procedures used in this study were as approved by the Research Ethics Committee of the University of Venda, South Africa (Protocol number SMNS/13/ MBY/01/0625), in accordance with the 1964 Helsinki declaration and its subsequent amendments. Additionally, permission to access health facilities was obtained from the Limpopo Provincial Department of Health, South Africa, and the collaborating health facilities. Informed consent was obtained from study participants prior to their involvement; and data obtained was stripped of personal identifiers to ensure the anonymity and confidentiality of the participants.

Data Description

The study cohort comprised 399 patients undergoing treatment follow up at a wellness clinic in Bela Bela, South Africa. The data was collected from 2004 to 2009. At the time of data extraction, patients with TB were on TB treatment. At enrolment, the baseline viral load, baseline CD4 cell count, and data on the presence of active TB was retrieved. TB cases, in this study, was the outcome of a diagnostic process comprising a combination of laboratory (microscopy and culture) and clinical investigations.

From these patients, 338 had a viral load at baseline above 10 000 copies/mL and 55 had a viral load at baseline of 10 000 copies/mL or below. 353 patients had a baseline CD4 cell count of 350cells/mm^3 or below and 46 had a baseline CD4 cell count above 350 cells/mm^3. Females comprised 69.1% (n=276) of the cohort. The variable age had a skew value of -0.44 at baseline, an indication that the majority of the patients were young adults. The variables; age at baseline, viral load at baseline and CD4 at baseline, are further described in Table 1.

Table 1: Descriptive summary for Age, viral load at baseline and CD4 cell count at baseline

	Age	VLBL (copies/mL	CD4BL(cells/mm^3)
Minimum	15	<50 (undetectable)	16
First Quartile	32	21 334	38
Mean	38.3	138 208	163
Median	39	67 995	116
Third Quartile	47	201 445	206
Maximum	77	>500 000	1 202

From the 399 patients, 292 (73.18%) had TB co-infection. 261 (65%) of the HIV/TB co-infected patients were enrolled at the clinic when they already had active TB. However, 89 (22%) patients developed active TB whilst on treatment. Post treatment, 58 (22%) of the patients who were once cured of TB became actively infected with TB. 168 of the HIV/TB co-infected at enrolment were mostly administered with an initial combination therapy of D4T-3TC-EFV, 76 received an initial combination therapy of D4T-3TC-NVP, and 6 received AZT-3TC-LPV/r, 5 received ABC-AZT-3TC and 4 received D4T-3TC-LPV/r. These drugs belong to the nucleoside reverse transcriptase inhibitors (NRTIs) class.

However, although NRTIs are relatively affordable, they cause varying degrees of myopathy and neuropathy after long-term therapy (Currier, 2007). AZT causes myopathy, ddI and 3TC cause neuropathy, d4T causes neuropathy or myopathy and lactic acidosis (LA), and studies suggest that d4T causes lactic acidosis (LA) more frequently than ddI or AZT. Patients under treatment may experience virologic failure. In this paper, treatment failure is defined clinically and immunologically. Thus, the effect of lactic acidosis and peripheral neuropathy, together with other covariates, to the progression of HIV is analysed.

Limitations of the data

This is a retrospective set of data. Information on other comorbidities or opportunistic infections in AIDS were not available, so the observations should be understood in the context of these limitations. The intended outcome of combination antiretroviral therapy is to suppress viral loads to undetectable levels, in the absence or presence of comorbidities.

Piece-wise constant transition rate Markov model (PWC)

Modelling the non-homogeneous Markov model can easily be done using a piecewise constant intensities approach. This approach, according to Saint-Pierre et al. (2003) in the analysis of cancer, involves the inclusion of time-dependent covariates in a Markov model, making it easier to deal with non-homogeneous Markov models. This approach partitions the time axis into r continuous and disjoint intervals, $[\tau_{l-1}, \tau_l)$ where $l = 1, \dots, r+1$ and $\tau_{r+1} = \infty$ and assumes constant transition intensities in different time intervals. Consider a vector $z^*(t) = (z_0^*(t), z_1^*(t), \dots, z_r^*(t))'$ of artificially time-dependent covariates defined as:

$$z_0^*(t) = 0, \forall t$$

$$z_l^*(t) = \begin{cases} 0; if\ \tau_0 \le t < \tau_l, \\ 1; if t \ge \tau_l \end{cases}$$

Where $l = 1, \dots, r+1$. The model with transition intensities is as follows:

$$q_{ij}\left(t \middle| z^*(t)\right) = q_{ij}^{(0)} \exp\left\{\left(\beta_{ij}^*\right)' z^*(t)\right\}, i \ne j \qquad (1)$$

This approach to non-homogeneity in a Markov process is a step-wise method that assumes constant transition intensities in different time intervals. The parameters of this model are the baseline transition intensities $q_{ij}^{(0)}$, which represent transition intensities in the interval $[\tau_0, \tau_1)$ and the vector of regression coefficient β_{ij}^* associated with artificially time-dependent covariates. For this model, transition intensities are step-functions of time and defined for each interval as follows:

$$q_{ij}\left(t \middle| z_l{}^*(t)\right) = \begin{cases} q_{ij}^{(0)} & if\ \tau_0 \le t < \tau_1 \\ q_{ij}^{(1)} = q_{ij}^{(0)} exp\{\beta_{ij,1}^*\}; & if\ \tau_1 \le t < \tau_2 \\ \vdots & \\ q_{ij}^{(l)} = q_{ij}^{(0)} exp\{\beta_{ij,1}^* z_1^* + \beta_{ij,2}^* z_2^* + \cdots + \beta_{ij,l}^* z_l^*\}; & if\ if\ t \ge \tau_l \end{cases}$$

for $l = 1,2, \dots, r$

Incorporating the effects of covariates, represented by the vector $\boldsymbol{z}$, the model becomes:

$$q_{ij}(t|\boldsymbol{z}_l^*(t), \boldsymbol{z}) = q_{ij}^{(0)} exp\{\beta_{ij,l}^{*\prime} \boldsymbol{z}_l^*(t) + \beta_{ij}' \boldsymbol{z}\}$$

Where β_{ij} is the log-linear effect relating to the instantaneous rate of transition from state 1 to state j to the covariate $\boldsymbol{z}$.

Computing $P(0, t_i)$ for a t_i in segment τ_l entails multiplying all the transition matrices across the various intervals as shown below;

$$P(0, t_i) = \left[\pi_{l=1}^{l-1} P^{(b)}(\pi_b)\right] P^{(l)}(t_{(l-1)}, t_j)$$

where $P^{(b)}$ is the transition probability matrix obtained using q_{ijb} for the b^{th} segment denoted by τ_b. If subjects are observed on an equal spaced grid and segments are divided up along these time points, then $p_{ij}(0, t_i)$ would simply be the $(ij)^{th}$ element of the matrix in the above equation. When data is not equally spaced, then observations would be considered missing at the breakpoints. To resolve this, a model that accounts for all possible pathways between the last observed state in the segment b_{l-1} and the first observation in segment b_0 was suggested. For example, if a breakpoint t' is created between two points t_j and t_k, then via Chapman-Kolmogorov equations, the likelihood contribution from interval (t_j, t_k) for individual x can be found as;

$$L_x = \sum_{l=1}^{k} P_{il}^{(1)}(t_j, t') P_{lj}^{(2)}(t', t_k)$$

for states i, j.

Model formulation

Patients were put on combination antiretroviral therapy (cART) at time t=0. The patients were monitored after 3 months (0.25 years) of cART and thereafter in follow up intervals of 6 months (0.5 years). Follow up was done for a maximum of 5 years but due to some deaths and withdrawal cases associated with the data, the average follow up time for each patient in this study is 3.5 years. At follow up times, the effectiveness of cART was assessed by changes in the HIV viral load level. Attainment of a suppressed viral load below level of detection within the first 6 months indicated good adherence to treatment and effectiveness of cART. In this study, the level of detection is 50 viral RNA copies/mL.

The viral load levels during the course of treatment for each individual were classified into states based on the severity of the patient's condition as follows:

$$Viral\ load\ state\ (VLS) = \begin{cases} 1, & if\ VL < 50 \\ 2, & if 50 \leq VL < 10\ 000 \\ 3, & if\ 10\ 000 \leq VL < 100\ 000 \\ 4, & if\ 100\ 000 \leq VL < 500\ 000 \\ 5, & if\ VL \geq 500\ 000 \\ 6, & if\ dead \\ 7, & if\ loss\ to\ follow\ up \end{cases}$$

States $i = 1,2,3,4,5$ are the live/transient states and states 6 and 7 are the absorbing states. Transitions from state i to $i + c$, for $c > 0$, represent disease progression to worse states and transitions from state i to state $i - c$, for $c > 0$, represent disease progression to better states. At t=0 there were 2 patients in viral load state **1**; 42 in state **2**; 174 in state **3**; 135 in state **4**; and 45 in state **5**. This confirms that at treatment initiation, most patients had viral load between 10 000 and 100 000 copies/mL (state 3).

Table 2 below is a state table that shows the possible transitions, from state *i* to state *j*, $j = i \pm c$, that occurred during the study period:

Table 2: State Table

	To(*j*)						
From(*i*)	**1**	**2**	**3**	**4**	**5**	**6**	**7**
1	1185	94	22	2	0	22	53
2	198	105	27	4	2	14	24
3	105	71	34	2	0	27	14
4	55	70	8	2	4	17	0
5	13	22	0	8	0	3	2

Table 2 shows that most states are accessible from each other. Of interest is the undetectable viral load state (state 1), which is accessible from all transient states. Thus, basing on these transitions, the following transition diagram is proposed:

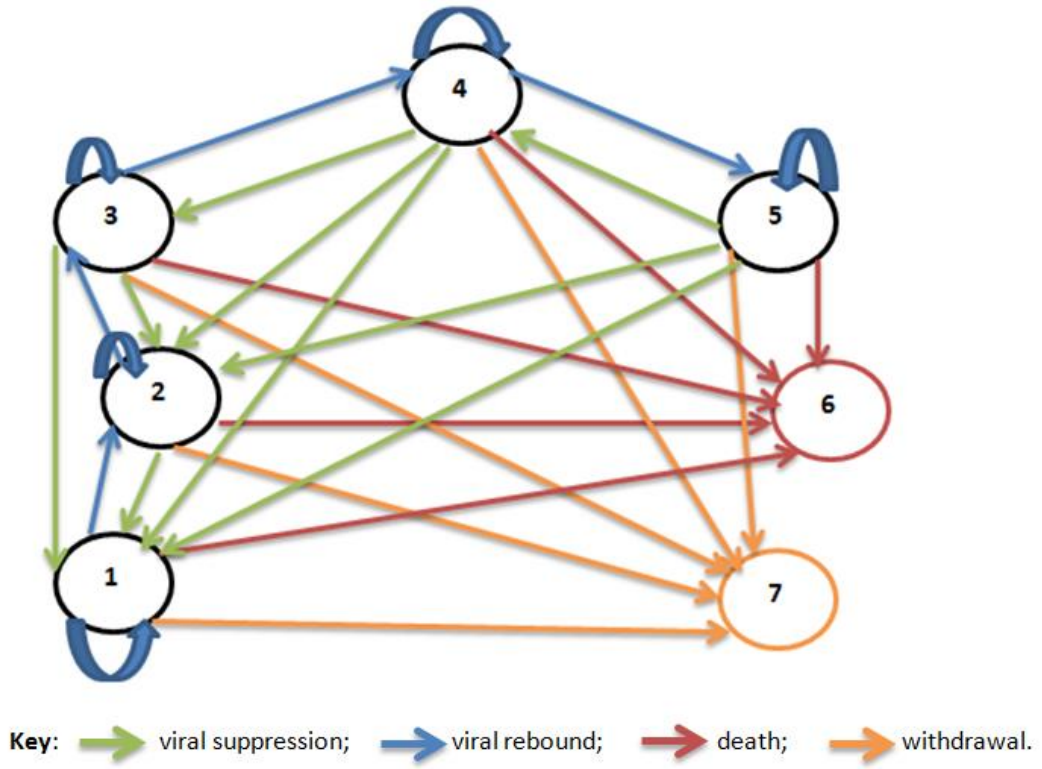

Figure 1: Transition Diagram

The arrows in the diagram represent possible transitions between states. Green arrows represent viral suppression. Blue arrows represent viral rebound and red arrows represent absorption into the death state. Orange arrows represent loss to follow-up. Transitions between states can be represented by the transition matrix below:

$$Q(t) = \begin{pmatrix} q_{11} & q_{12} & 0 & 0 & 0 & q_{16} & q_{17} \\ q_{21} & q_{22} & q_{23} & 0 & 0 & q_{26} & q_{27} \\ q_{31} & q_{32} & q_{33} & q_{34} & 0 & q_{36} & q_{37} \\ q_{41} & q_{42} & q_{43} & q_{44} & q_{45} & q_{46} & q_{47} \\ q_{51} & q_{52} & 0 & q_{54} & q_{55} & q_{56} & q_{57} \\ 0 & 0 & 0 & 0 & 0 & 0 & 0 \\ 0 & 0 & 0 & 0 & 0 & 0 & 0 \end{pmatrix}$$

The force of transition from state i to j is defined as:

$$q_{ij}(t) = \frac{d}{dt} p_{ij}(t)|_{t=0} = \lim_{\Delta t \to 0} \frac{p_{ij}(\Delta t) - \delta_{ij}}{\Delta t}$$

q_{ij}, for $i = 1, \ldots, 5$ and $j = 1, \ldots, 7$, vary over time and satisfies the following conditions; $\sum_{j \in X} q_{ij}(t) = 0$ and $q_{ii}(t) = -\sum_{i \neq j} q_{ij}(t)$. Once the transition intensities are estimated, the probabilities that state j is next subject in the long run, on condition that the patient was in state i, is given as $p_{ij} = \frac{q_{ij}}{\lambda_i}$, for each i and j where $\lambda_i = \sum_{j \in X} q_{ij}(t)$, such that $i \neq j$, is the total time spent in state *i* before a jump to state *j*. For example $p_{12} = \frac{q_{12}}{q_{12}+q_{16}+q_{17}}$.

The effects of the covariates gender, age, virologic failure (VF), treatment failure (TF), viral load level baseline (VLBL), peripheral neuropathy (PN), having TB before enrolment (TBB4), developing TB whilst on ART (TBEN), lactic acidosis (LA) and the effect of time on transition intensities is assessed. Peripheral neuropathy and lactic acidosis are long-term effects of the NRTI class. Virologic failure is defined as having a viral load of at least 1000 copies/mL in two consecutive visits or having a viral load above 1000 copies/mL in the first 6 months of cART initiation. In this paper, treatment failure is defined immunologically and clinically. These covariates are coded as follows:

Age = $\begin{cases} 1, & \leq 45\ years \\ 0, & > 45\ \text{years} \end{cases}$, VF = $\begin{cases} 1, & Yes \\ 0, & \text{No} \end{cases}$, TBB4 = $\begin{cases} 1, & Yes \\ 0, & \text{No} \end{cases}$, LA = $\begin{cases} 1, & Yes \\ 0, & \text{No} \end{cases}$

TBEN = $\begin{cases} 1, & Yes \\ 0, & \text{No} \end{cases}$, Gender = $\begin{cases} 1, & male \\ 0, & female \end{cases}$, TF = $\begin{cases} 1, & Yes \\ 0, & \text{No} \end{cases}$, PN = $\begin{cases} 1, & Yes \\ 0, & \text{No} \end{cases}$

VLBL = $\begin{cases} 1, & > 10\ 000\ copies/\mu L \\ 0, & \leq 10\ 000\ copies/\mu L \end{cases}$, Time = $\begin{cases} 0; & if\ 0 \leq t < 0.5 \\ 1; & if\ t \geq 0.5\ years \end{cases}$

CD4BL=$\begin{cases} 1, & \leq 350 cells/mm^3 \\ 0, & > 350\ cells/mm^3 \end{cases}$

So that the piecewise constant Markov model becomes:

$$q_{ij}(t|\boldsymbol{z}_l{}^*(t), \boldsymbol{z}) = q_{ij}^{(0)} exp\{\beta_{ij,l}^*{}' \boldsymbol{z}_l{}^*(t) + \beta_{ij}{}' \boldsymbol{z}\}$$

where $\boldsymbol{z} = \begin{Bmatrix} Age, virologic\ failuer\ (VL), TB\ before\ \ treatment\ (TBB4),, \\ Lactic\ Acidosis\ (LA) TB\ whilst\ on\ cART(TBEN), Gender, \\ Treatment\ Failure\ (TF), Peripheral\ neuropathy\ (PN), \\ Viral\ load\ at\ baseline\ (VLBL), Time, CD4\ at\ baseline\ (CD4BL) \end{Bmatrix}$

Results

In this section, a continuous time non-homogeneous Markov model for the effects of time $t \geq 0.5\ years$, viral load baseline , gender, having TB co-infection, having active TB before enrolment, developing active TB on treatment , peripheral neuropathy, lactic acidosis, virologic failure and treatment failure on virology is defined by the equation;

$$q_{ij}(t|z^*(t), \boldsymbol{z}) = q_{ij}^{(0)} \exp\{\boldsymbol{\beta}_{ijl}^{*\prime}\, \boldsymbol{z}_l^*(t) + \boldsymbol{\beta}_{ij}{}'\boldsymbol{z}]\}, i \neq j$$

The parameters $q_{ij}^{(0)}$ are the baseline transition intensities for intervals $[0, 0.5 year)$, $\boldsymbol{\beta}_{ijl}^*$ is the vector of regression coefficients associated with the artificial time-dependent covariates $\boldsymbol{z}_l^* = [1, 0]'$ as defined earlier on, $\boldsymbol{\beta}_{ij}$ is the vector of regression coefficients associated with covariates $\boldsymbol{z}$=**[**VLBL, Gender, TB, TBEN, TBB4, PN, LA, VF, TF]′. The results from the fitted model are shown in the Table 3 below;

Table 3: Effects of different variables on transition intensities based on viral load states

State $\boldsymbol{i - j}$	**Baseline** $\boldsymbol{q_{ij}^{(0)}}$	**VLBL**	**Gender**	**TB**	**TBEN**	**TBB4**	**PN**	**LA**	**VF**	**TF**	**Time [0.5,Inf)**
State 2-1	2.333	-0.063	0.191	-1.624	0.216	0.973	0.767	-0.038	-1.337	-0.353	-1.003
State 3-1	0.966	0.424	0.479	0.419	-0.504	-0.121	1.523	1.346	-1.091	-0.585	-2.719
State 4-1	0.545	0.145	0.259	0.137	0.413	0.576	-0.014	0.517	-0.124	-0.119	-0.778
State 5-1	0.427	0.222	-0.203	-0.201	0.532	-0.008	-0.229	0.244	-0.055	-0.039	-0.879
State 1-2	0.410	0.017	-0.016	-0.539	0.032	-0.139	0.116	0.18	1.985	-0.08	-1.394
State 3-2	2.775	-0.022	-0.660	0.460	-0.625	-0.832	-0.601	-0.298	-0.232	-1.046	-2.041
State 4-2	4.978	0.159	-0.583	-0.375	-0.355	1.219	-0.503	0.069	-0.049	0.229	-1.626
State 5-2	2.428	0.129	-0.338	0.621	0.441	1.080	0.200	-0.077	0.289	-0.076	-1.432
State 2-3	0.852	1.403	-0.789	-1.530	0.493	1.010	-0.132	0.685	1.265	0.879	-0.660
State 4-3	0.148	0.082	-0.068	-0.131	-0.026	-0.071	0.147	-0.057	-0.010	-0.006	-0.132
State 3-4	0.439	0.315	-0.195	0.516	0.896	0.590	0.452	-0.803	0.339	-0.522	-0.023
State 5-4	1.108	0.315	0.272	-0.521	1.004	-1.475	-0.223	-0.759	-0.069	-0.064	-1.578
State 4-5	0.456	0.253	0.695	-0.953	-0.429	-0.775	-0.315	-0.852	0.748	-0.044	-1.222
State 1-6	0.010	0.809	-0.742	-1.451	0.560	-2.716	-1.120	-1.316	0.024	-0.103	-2.345
State 2-6	0.032	0.453	0.572	-0.316	1.151	-2.083	-0.232	-1.001	-0.333	-0.153	-0.396
State 3-6	0.040	0.064	0.116	-0.163	0.280	-0.915	0.006	-0.404	-0.290	-0.201	-0.434
State 4-6	0.138	0.092	0.014	-0.101	0.459	-0.423	-0.188	-0.133	-0.034	-0.029	0.398

State 5-6	0.106	0.018	0.185	-0.078	0.041	-0.157	-0.032	-0.050	-0.032	-0.002	-0.053
State 1-7	0.037	0.564	-0.577	-0.990	-0.081	-1.572	-1.518	-1.733	0.087	0.235	0.776
State 2-7	0.103	-0.524	-0.036	0.010	0.161	0.303	-0.448	-1.556	0.007	-0.126	-0.139
State 3-7	0.080	-0.018	0.016	-0.176	-0.005	-0.218	-0.077	-0.217	-0.005	-0.171	0.141
State 4-7	0.056	-0.048	0.034	0.014	-0.099	0.069	-0.005	0.037	0.015	0.004	0.214
State 5-7	0.101	0.009	0.157	-0.163	-0.084	-0.118	-0.0222	-0.036	-0.027	-0.001	0.248
-2LL	2869.38										

Key: VLBL=Viral load at baseline; TB=Tuberculosis either at entry or whilst on cART; TBEN=Developing Tuberculosis during cART; TBB4=Tuberculosis before cART initiation; PN=Peripheral neuropathy; LA=Lactic Acidosis; VF= virologic failure; TF=Treatment failure.

Results show that when the viral load of a patient is below 100 000 copies/mL, rates of viral suppression are higher than rates of viral rebound. The undetectable viral load (state 1) is accessible from all the states. The rate of attainment of an undetectable viral load depends with the condition of a patient. Patients with the highest viral copies/mL (state 5) have the lowest risk of attaining an undetectable viral load whereas patients with the lowest viral copies/mL (state 2) have the highest chance of attaining an undetectable viral load.

Developing active TB whilst on ART (TBEN) increases the rates of viral rebound from an undetectable level (state 1) to a viral load measurement above 50 copies/mL and below 10 000 copies/mL (state 2). If the TB is detected at enrolment (TBB4), there are reduced rates of viral rebound from state 1 to state 2. However, detecting TB co-infection, be it at enrolment or during the course of treatment, reduces viral rebound from state 1 to state 2. Virologic failure is experienced from state 1 to state 2. Other factors that contribute to viral failure from undetectable levels are peripheral neuropathy and lactic acidosis. From 0.5 years of treatment and beyond, there is reduced viral rebound from undetectable levels. Thus, more time on cART reduces rates of viral rebound.

Table 3 shows virologic rebound from a viral load state between 50 and 10 000 copies/mL (state 2) to a viral load state between 10 000 copies/mL and 100 000 copies/mL (state 3). The virologic failure is due to effects of developing TB on treatment (TBEN), having TB at enrolment (TBB4), Lactic acidosis, treatment failure and having a viral load baseline above 10 000 copies/mL at enrolment.

Patients mostly experience virologic failure in state 4 (viral load baseline between 100 000 and 500 000 copies/mL). These patients experience a viral rebound back to a viral load level above 500 000 copies/mL (state 5). Males are also at higher risk of experiencing a rebound from state 4 to state 5 compared to their female counterparts.

Results show an increased rate of mortality (state 6) from an undetectable viral load (state 1) for patients who enrolled with a viral load baseline above 10 000 copies/mL, patients who developed active TB whilst on cART and for patients who experienced virologic failure. Patients who developed active TB whilst on cART have accelerated rates to mortality regardless of the state of a patient.

Next we estimate long run probabilities of state j being the next state given the condition that the patient was initially in state i, referred to as the jump process. This is when a Markov process is observed at the times it makes transitions to a new state. In other words, a jump process is a stochastic matrix R of probabilities where each row sums to one on the state space X_t, which gives the conditional probability of the next state an individual goes to, after leaving state i. If $q_{ii} > 0$, then given that there is a jump to a different state, implies the patient will not stay in state i, the patient makes a jump out of state i resulting in $R_{ii} = 0$ and if $q_{ii} = 0$, then the patient will never leave state i, implying that $R_{ii} = 1$ (in States 6 and 7). The computed matrix of probabilities of each state being next (also known as the jump process), together with the mean sojourn times in each state, fully define a continuous-time Markov model. This is a more intuitively meaningful description of a model than the transition intensity matrix. The matrix for the probabilities that the next state after state i is state j is approximated as $p_{ij} = \frac{q_{ij}}{\lambda_i}$, for each i and j such that $i \neq j$. q_{ij} is the force of transition from state i to state j and q_{ii} is the total force of transition out of state i. For example, the probability that state 2 is next given that the patient is initially in state 1 is given by $p_{12} = \frac{q_{12}}{\lambda_1} = \frac{0.410}{0.410+0.010+0.037} \approx 0.897$, as shown in the matrix below. The results are shown in Table 4 below:

Table 4: Probability of each state being next (jump chain)

From (*i*)	**To (*j*)**						
	State 1	**State 2**	**State 3**	**State 4**	**State 5**	**State 6**	**State 7**
State 1	0	0.897	0	0	0	0.022	0.081
State 2	0.703	0	0.257	0	0	0.010	0.031
State 3	0.225	0.645	0	0.102	0	0.009	0.019
State 4	0.086	0.787	0.023	0	0.072	0.022	0.009
State 5	0.102	0.582	0	0.266	0	0.025	0.024

State 6	0	0	0	0	0	1	0
State 7	0	0	0	0	0	0	1

Results from Table 4 show an increase in the probabilities of transition to death with increasing viral load states resulting in patients with viral load levels above 500 000 copies/µL having highest chances of transitions to death. For patients with viral load above 10 000 copies/µL (state 3, state 4, and state 5), probabilities of viral suppression to levels between 50 and 10 000 copies/µL (state 2) are higher compared to transitions to any other states. The results generally show higher chances of transitions to viral suppression than viral rebound, an indication of treatment efficacy.

Figure 2 below, shows the plots of percentage prevalence in each state from time of treatment commencement to the end of the study period.

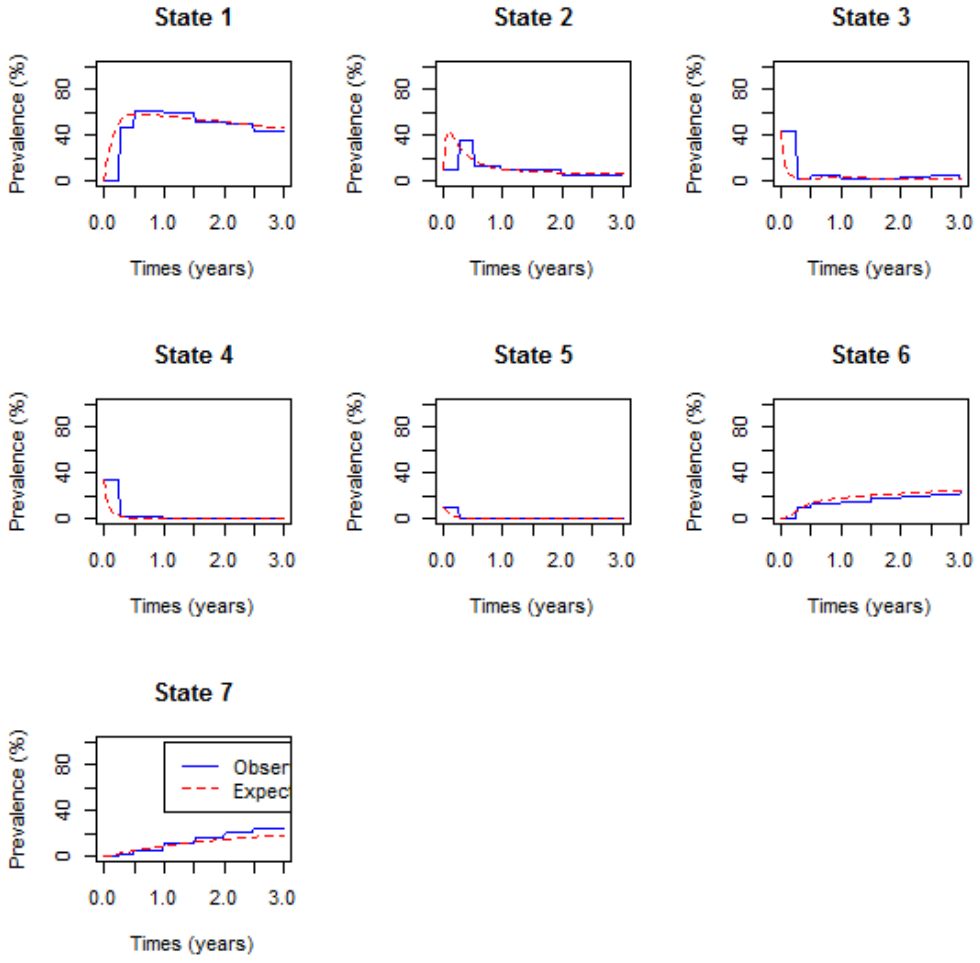

Figure 2: Percentage prevalence in each state from time of treatment commencement to 3 years post-treatment commencement

The model gives almost a perfect fit of the observed data. The plots show an increase in percentage prevalence during the first 0.5 years for state 1 or the undetectable viral load state. After 1.5 years, there is a slight drop in percentage prevalence from state 1. This could be attributed to factors such as developing active TB on cART, virologic failure, peripheral neuropathy and lactic acidosis as revealed in Table 3.

Discussion

In this study, a continuous-time non-homogeneous Markov model is used to model the progression of HIV/TB co-infected patients receiving cART at a South African rural clinic. Non-homogeneity of transition intensities is approached using a piecewise constant model, thus, allowing transitions to vary between different time segments. The effects of viral load prior to treatment initiation, gender, developing active TB whilst on cART, having TB at

enrolment, peripheral neuropathy, lactic acidosis, virologic failure and treatment failure on HIV/AIDS progression defined by transition intensities is assessed.

Results from the analysis show a bi-directional movement between HIV states, thus revealing a possibility of viral rebound and viral suppression. However, transitions to suppressed viral loads are higher than transitions to viral rebound. This is quite encouraging since it shows efficacy of ART in reducing viral load as expected. Results also show that, from any viral load state, undetectable viral load state can be attained. This varies from state to state with patients in lower viral load levels having better chances of attaining undetectable viral loads than patients in higher viral load levels. This takes place during the first 0.5 years of treatment uptake, according to our findings, which shows a rapid increase in state 1 (undetectable viral load) prevalence within the first 0.5 years.

Findings from this study reveal that, although the undetectable viral load state can be attained from any HIV state, there are some factors that increase the rate of viral rebound from undetectable levels to viral loads between 50 and 10 000 copies/mL. The results reveal increased rates (by more than 7 folds) of virologic failure from undetectable viral load levels to viral loads between 50 and 10 000 copies/mL. This is attributed to the development of active TB whilst on ART, lactic acidosis and peripheral neuropathy, with the development of active TB on cART the major cause. However, if TB is detected at enrolment, the rates of viral rebound from undetectable levels are reduced. This is corroborated by the studies by WHO (2017) which suggested early diagnosis and timely treatment of TB to reduce the risks of virologic rebound.

The risk of virologic failure from between 50 and 10 000 copies/mL to a state between 10 000 and 100 000 copies/mL increases by approximately 3.5 times. This happens for patients who had TB at enrolment, developed some or all of TB on ART, lactic acidosis, treatment failure and having a viral load baseline above 10 000 copies/mL at enrolment. In this case, developing active TB before initiation of cART is the major player.

Our findings generally reveal that patients mostly experience virologic failure in state 4 (that is, viral load baseline between 100 000 and 500 000 copies/mL). These patients experience a viral rebound to a viral load level above 500 000 copies/mL (state 5). Virologic failure coupled with development of active TB whilst on ART increase rates of HIV/AIDS progression as well as mortality from HIV/AIDS after achieving an undetectable viral load. Bulage et al. (2017), in their findings, suggested that having active TB increases the odds of

virologic non-suppression. Patients who developed active TB whilst on cART experienced increased rates of transitions to death irrespective of their HIV/AIDS state. The highest rates are experienced when viral load levels are between 50 and 10 000 copies/mL where patients who developed active TB on cART are 3.2 times more likely to experience death than patients who did not develop active TB. Our findings are in congruence with the findings by Bekker et al. (2011) and von Reyn et al. (2010) which show higher rates of mortality in HIV patients with virologic failure and co-infected with TB. Bekker et al. 2011 also observed that onset of tuberculosis in HIV-infected patients is associated with an increased risk of AIDS and death. Hence, it is proposed that virologic failure be regularly monitored in HIV patients coinfected with TB. This should be done every two months and decisions made on alternative treatment approaches to prevent potential mortality.

Conclusion

In conclusion, the findings reveal the importance of time in monitoring HIV/AIDS progression for patients with virologic failure as well as TB co-infection. A piecewise constant approach to non-homogeneous Markov modelling is used and shows two different trends in HIV/AIDS progression, that is, a sharp increase in state 1 (undetectable viral load level) prevalence in the first 0.5 years of treatment followed by a slowly decreasing prevalence trend thereafter. The model, not surprisingly, confirms that virologic failure increases the risk of death. However, it suggests that whilst TB at the time of ART initiation does not increase the risk of viral rebound, the development of active TB after initiation of ART does increase the risk of viral rebound. This highlights the importance of strengthening viral load monitoring, especially in people at risk of TB, and addressing unsuppressed viral loads in this category of patients.

Acknowledgements

Pascal Bessong's research is supported by the South African Medical Research Council (RCDI) through funding received from the South African National Treasury; and the South African National Research Foundation (GUN109312, GUN86037). The views expressed here are solely the responsibility of the authors and do not necessarily represent the official views of the South African Medical Research Council or the National Research Foundation.

References

1. Badri M, Ehrlich R, Wood R, Pulerwitz T, Maartens G.Association between tuberculosis and HIV disease progression in a high tuberculosis prevalence area. Int JTuberc Lung Dis. 2001;5:225–32
2. Bekker LG and Wood R. TB and HIV co-infection: when to start antiretroviral therapy: Guidelines on when to start therapy in TB and HIV co-infection. CME, 2011 Vol 29, No 10.
3. Bruisker T, Dufour MK, MPH, PhD, and Myers JJ. Recall of Nadir CD4 Cell Count and Most Recent HIV Viral Load Among HIV-Infected, Socially Marginalized Adults. AIDS Behav, 2015; 19(11): 2108–2116. doi:10.1007/s10461-015-1018-x
4. Bulage L, Ssewanyana I , Nankabirwa V, Nsubuga F, Kihembo C et al. Factors Associated with Virological Nonsuppression among HIV-Positive Patients on Antiretroviral Therapy in Uganda, August 2014–July 2015. BMC Infectious Diseases (2017) 17:326 DOI 10.1186/s12879-017-2428-3
5. Chenand B and Zhou Xiao-Hua. Non-homogeneous Markov process models with informative observations with an application to Alzheimer's disease. Biom J. 2011; 53(3):444-463.
6. Cohen K and Meintjes G. Management of individuals requiring ART and TB treatment. Curr Opin HIV AIDS. 2010 January; 5(1): 61–69. doi:10.1097/COH.0b013e3283339309
7. Day JH, Alison D. Grant, Katherine L. Fielding, Lynn Morris, Victoria Moloi, Salome Charalambous, Adrian J. Puren, Richard E. Chaisson, Kevin M. De Cock, Richard J. Hayes,1 and Gavin J. Churchyard. Does Tuberculosis Increase HIV Load? The Journal of Infectious Diseases 2004; 190:1677–84
8. Duffy MJ, Blaser J, Duggan C, Mcdermott E, O'higgens N, Fen-Nelly JJ and Tschesche H. Assay of metalloproteases types 8 and 9 by ELISA in human breast cancer. Br. J. Cancer, 71:1025-1028, 1995.
9. Gunda D W, Kidenya BR, Mshana SE, Kilonzo SB and Mpondo BCT. Accuracy of WHO immunological criteria in identifying virological failure among HIV‑infected adults on First line antiretroviral therapy in Mwanza, North‑western Tanzania. *BMC Res Notes (2017) 10:45* DOI 10.1186/s13104-016-2334-6
10. Kalbfleisch JD, Lawless JF. The analysis of panel data under a Markov assumption. J Am Stat Assoc. 1985; 80(392): 863-71.

11. Lee S, Ko J, Tan X, et al. Markov Chain Modelling Analysis of HIV/AIDS Progression: A Race Based Forecast in the United States. Indian J Pharm Sci. 2014; 76(2): 107-115
12. Lindsay JC and Ryan LM, A three-state multiplicative model for rodent tumorigenicity experiments, Applied Statistics, 42: 283-300, 1993.
13. Marshall G, and Jones R.H., Multi-state Markov models and diabetic retinopathy. Statist. Med., 14:19751983, 1995.
14. Martinson NA, Hoffmann CJ, Chaisson RE. Epidemiology of tuberculosis and HIV: Recent advances in understanding and responses. Proc Am Thorac Soc, 2011b; 8: 288–293.
15. Pan W, and Kastin AJ, Tumor necrosis factor and stroke: role of the blood-brain barrier, Progress in neurobiology 83:363-374, 2007.
16. Pawlowski A, Jansson M, Skold M, Rottenberg ME, Kallenius G. Tuberculosis and HIV Co-Infection. PLoS Pathog, 2012; 8(2): e1002464.doi:10.1371/journal. ppat.1002464
17. Saint-Pierre P, Combescure C, Daurès JP, et al. The analysis of asthma control under a Markov assumption with use of covariates. Statistics in Medicine. 2003; 22, 3755–3770.
18. Sigaloff KCE, Hamers RL, Wallis CL, Kityo C, Siwale M, Ive P, et al. Unnecessary antiretroviral treatment switches and accumulation of HIV resistance mutations; two arguments for viral load monitoring in Africa. J Acquir Immune Defic Syndr. 2011;58:23–31. http://www.ncbi.nlm.nih.gov/pubmed/21694603.
19. Stead D. Southern African HIV clinicians society. Guidelines. HIV clinicians adult guideline 2017 CME. East London CME: 25 November 2017.
20. UNAIDS Data. 2018. https://www.unaids.org/sites/default/files/media_asset/unaids-data-2018_en.pdf
21. von Reyn CF, Mtei L, Arbeit RD, et al. Prevention of tuberculosis in bacille Calmette-Guerin-primed, HIV-infected adults boosted with an inactivated whole-cell mycobacterial vaccine. AIDS 2010; 24:675–85.
22. World Health Organization (WHO). Global tuberculosis control [WHO/CDS/TB/2001.287.2001]. Geneva: WHO, 2001.
23. Yen A. M. F, Chen T. H. H, Mixture Multi-State Markov Regression Model, J Appl Stat, 34: 11-21,2007.